Workshop on Squeezed States and Uncertainty Relations

NASA

Workshop on Squeezed States and Uncertainty Relations

Edited by
D. Han
NASA Goddard Space Flight Center
Greenbelt, Maryland

Y. S. Kim
University of Maryland
College Park, Maryland

W. W. Zachary
COMSERC
Howard University
Washington, D.C.

NASA

Principal Organizers:

D. Han (NASA - Goddard Space Flight Center)
Y. S. Kim (University of Maryland at College Park)
W. W. Zachary (Howard University)

Local Organizing Committee:

D. R. Brill (Univ. of Maryland at College Park)
J. D. Franson (Johns Hopkins University Applied Physics Lab.)
M. Kafatos (George Mason University)
P. McGrath (Laboratory for Physical Sciences)
H. S. Pilloff (Office of Naval Research)
A. K. Rajagopal (Naval Research Laboratory)
Y. H. Shih (Univ. of Maryland at Baltimore County)

PREFACE

The Workshop on Squeezed States and Uncertainty Relations was held at the University of Maryland at College Park on March 28 - 30, 1991. This Workshop was largely supported by the Goddard Space Flight Center of the National Aeronautics and Space Administration. The idea to hold the Workshop of this nature was initiated by the Office of Naval Research.

The purpose of this Workshop was to study possible applications of squeezed states of light. Specifically, the Workshop will be concerned with the following questions.

(1) What physics can we do with squeezed-state lasers?
(2) What impact does the squeezed state give to other branches of physics?

The Workshop brought together active researchers in squeezed states of light and those who may find the concept of squeezed states useful in their research efforts, particularly in the foundations of quantum mechanics.

The effort made for this meeting will be continued by the Second International Workshop on Squeezed States and Uncertainty Relations to be held in Moscow on May 25 - 29, 1992. The principal organizers for this Moscow meeting are V. I. Man'ko (Lebedev Physical Insitute) and Y. S. Kim (Univ. of Maryland at College Park). We expect that the Moscow meeting will attract many researchers from Europe as well as those from the United States.

Registered Participants

Alley, Carroll O., Dept. of Physics, Univ. of Maryland, College Park, MD 20742

Alsing, Paul M., Dept. of Physics, Univ. of Oregon, Eugene, OR 97403

Aragone, Carlos, Dept. of Physics, Universidad Simon Bolivar, Caracas 1080A, Venezuela

Aravind, P. K., Dept. of Physics, Worcester Polytechnic Institute, Worcester, MA 01609

Artoni, Maurizio, Dept. of Physics, City College of CUNY, New York, NY 10031

Ashrafi, Solyman, Computer Science Co, 10110 Aerospace Building, Lanham, MD 20706

Bergrman, Keren, Dept. of Electrical Engineering, Massachusetts Inst. of Tech., Cambridge, MA 02139

Bernstein, Herbert J., School of Natural Science, Hampshire College, Amherst, MA 01002

Birman, Joseph L., Dept. of Physics, City College of CUNY, New York, NY 10031

Boyd, Derek, Dept. of Physics, Univ. of Maryland, College Park, MD 20742

Brandt, Howard, Harry Diamond Laboratories, Adelphi, MD 20783

Brill, Dieter R., Dept. of Physics, Univ. of Maryland, College Park, MD 20742

Brooke, James A., Dept. of Mathematics, Univ. of Saskatchewan, Saskatoon, SAS, S7N 0W0, Canada

Buzek, Vladimir, Optics Section, Blackett Lab., Imperial College, London SW7 2BZ, United Kingdom

Campos, Richard A., Dept. of Applied Physics, Columbia University, New York, NY 10027

Carmichael, Howard J., Dept. of Physics, Univ. of Oregon, Eugene, OR 97403

Caves, Carlton M., Center for Laser Studies, Univ. of Southern California, Los Angeles, CA 90089

Cha, Boyoung, Dept. of Physics, Univ. of Maryland, College Park, MD 20742

Chang, Chung Yun, Dept. of Physics, Univ. of Maryland, College Park, MD 20742

Chiao, Raymond Y., Dept. of Physics, Univ. of California, Berkeley, CA 94720

Choi, Hyung Sup, Dept. of Physics, City College of CUNY, New York, NY 10031

Cruze, Stephen P., TASC, 12107 Maple Forest Ct., Apt. L, Fairfax, VA 22030

D'Ariano, Giacomo Mauro, Dipto. di Fisica, Univ. di Pavia, I-27100 Pavia, Italy

Dattoli, Giuseppe, INN.SVIL, ENEA, Box 65, I-0044 Frascati, Italy

DeFacio, Brian, Dept. of Physics, Univ. of Missouri, Columbia, MO 65211

Debergh, Natalie, Dept. of Theoretical Physics, Univ. of Liege, B-4000 Liege, Belgium

Deutch, Ivan, Dept. of Physics, Univ. of California, Berkeley, CA 94720

Dodonov, V. V., Dept. of Physics, Moscow Physical Technical Institute, 140160 Zhukovsky, Moscow Region, U.S.S.R.

Dowling, Jonathan P., AMSMI-WS, U.S. Army Missile Command, Weapons Science Directorate, Redstone Arsenal, AL 35898

Ford, Lawrence, Dept. of Physics, Tufts University, Medford, MA 02155

Fortini, Pierluigi, Dept. of Physics, Univ. of Ferrara, I-44100 Ferrara, Italy

Franson, J. D., Applied Physics Lab., Johns Hopkins University, Laurel, MD 20723

Fuchs, Christopher, Dept. of Physics, Univ. of North Carolina, Chapel Hill, NC 27599

Gallis, Michael, Dept. of Physics, Pennsylvania State University, Schuylkill Haven, PA 17972

Garrison, John C., Dept. of Physics, L-297, Lawrence Livermore, Lab., Livermore, CA 94550

Greenberg, O. W., Dept. of Physics, Univ. of Maryland, College Park, MD 20742

Greenberger, Daniel, Dept. of Physics, City College of CUNY, New York, NY 10031

Griffin, James J., Dept. of Physics, Univ. of Maryland, College Park, MD 20742

Grishchuck, Leonid, Sternberg Astronomical Inst., Moscow State University, 119899 Moscow, U.S.S.R.

Han, Daesoo, Code 936, Goddard Space Flight Center, National Aeronautics and Space Administration, Greenbelt, MD 20771

Hartle, James B., Dept. of Physics, Univ. of California, Santa Barbara, CA 93108

Haus, Hermann A., Dept. of Electrical Engineering, Massachusetts Inst. of Tech., Cambridge, MA 02139

Henry, Richard W., Dept. of Physics, Bucknell University, Lewisville, PA 17837

Hillery, Mark, Dept. of Physics, Hunter College of CUNY, New York, NY 10021

Hochberg, David, Dept. of Physics, Vanderbilt University, Nashville, TN 37235

Hope, Deborah, Dept. of Physics, Australian National University, Canberra, ACT 2601, Australia

Horne, Michael, Dept. of Physics, Stonehill College, North Easton, MA 02357

Hu, Bei-Lak, Dept. of Physics, Univ. of Maryland, College Park, MD 20742

Hwang, Euyheon, Dept. of Physics, Hampton University, Hampton, VA 23668

Jacobs, Verne L., Naval Research Lab., Code 4694, Washington, DC 20375

Jin, Insik, Dept. of Physics, Univ. of Maryland, College Park, MD 20742

Joneckis, Lance, Research Lab. of Electronics, Massachusetts Inst. of Technology, Cambridge, MA 02139

Kafatos, Minas, Dept. of Physics, George Mason University, Fairfax, VA 22030

Kennedy, T. A. Brian, School of Physics, Georgia Inst. of Tech., Atlanta, GA 30332

Ketov, Sergay V., Dept. of Physics, Univ. of Maryland, College Park, MD 20742

Kiess, Thomas, E., Dept. of Physics, Univ. of Maryland, College Park, MD 20742

Kim, Myung Shik, Dept. of Physics, Sogang University, Box 1142, Seoul 100-611, S. Korea

Kim, Shoon K., Dept. of Chemistry, Temple University, Philadelphia, PA 19122

Kim, Y. S., Dept. of Physics, Univ. of Maryland, College Park, MD 20742

Klauder, John R., Dept. of Physics, Univ. of Florida, Gainesville, FL 32612

Kostelecky, Alan, Dept. of Physics, Indiana University, Bloomington, IN 47405

Kuo, Chung-I, Dept. of Physics, Tufts University, Medford, MA 02155

Larchuk, Todd, 218 Wellington Place, Matawan, NJ 07747

Lee, C. T., Dept. of Physics, Alabama A\& M University, Normal, AL 35762

Lee, Seung-Hee, Dept. of Electrical Engineering, Northwestern University, Evanston, IL 60208

Ma, Xin, Dept. of Chemistry, Univ. of Houston, Houston, TX 77204

Mandel, Leonard, Dept. of Physics, Univ. of Rochester, Rochester, NY 14627

Man'ko, Margarita A., Lebedev Physical Institute, 53 Leninsky Prospect, 117924 Moscow, U.S.S.R.

Man'ko, Vladimir I., Lebedev Physical Institute, 53 Leninsky Prospect, 117924 Moscow, U.S.S.R.

Maguire, Gerald Q., Dept. of Computer Science, Columbia University, New York, NY 10027

Mari, Carlo, INN.SVIL, ENEA, Box 65, I-00044 Frascati, Italy

McGrath, Paul, Lab. for Physical Sciences, 4928 College Ave., College Park, MD 20740

Misner, Charles, Dept. of Physics, Univ. of Maryland, College Park, MD 20742

Morris, Randall, Gov. Electronics Div., General Electric Co., Moorestown, NJ 08057

Movshovich, Roman, AT\& T Bell Labs., 1C-247, 600 Mountain Ave., Murray Hill, NJ 07974

Mufti, Asif Ali, Dept. of Physics, Univ. of Arizona, Tucson, AZ 85721

Nikitin, S., Lebedev Physical Institute, 53 Leninsky Prospect, 117924 Moscow, U.S.S.R.

Noz, Marilyn E., Dept. of Radiology, New York University, New York, NY 10016

Oneda, Sadao, Dept. of Physics, Univ. of Maryland, College Park, MD 20742

Ortolan, Antonello, Dept. of Physics, Univ. of Ferrara, I-44100 Ferrara, Italy

Park, Shim C., Dept. of Physics, Baylor University, Waco, TX 76798

Paz, Juan Pablo, Dept. of Physics, Univ. of Maryland, College Park, MD 20742

Pedrotti, Leno, Dept. of Physics, Univ. of Dayton, Dayton, OH 45469

Pilloff, Herschell, Div. of Physics, Office of Naval Research, 800 North Quincy Street, Arlington, VA 22217

Rajagopal, A. K., Naval Research Laboratory, Code 6830R, Washington, DC 20375

Rajalakshmi, R., 511 Hampton Court, Blacksburg, VA 24060

Ralph, Timothy, Dept. of Physics, Australian National Univ., Canberra, ACT 2601, Australia

Raymer, Michael G., Dept. of Physics, Univ. of Oregon, Eugene, OR 97403

Reifler, Frank, Gov. Electronics Div., General Electric Co., Moorestown, NJ 08057

Reiss, Howard, Dept. of Physics, American University, Washington, DC 20016

Renaud, Rocio Jauregui, Inst. de Fisica, Univ. Nacional Autonoma de Mexico, Mexico 01000, Mexico

Rice, Perry, Dept. of Physics, Miami University, Oxford, OH 45056

Richard, Jean-Paul, Dept. of Physics, Univ. of Maryland, College Park, MD 20742

Rubin, Morton H., Dept. of Physics, Univ. of Maryland at Baltimore County, Baltimore, MD 21228

Saif, Babak V., NASA - Goddard Space Flight Center, Code 726, Greenbelt, MD 20771

Sarty, Gordon E., Dept. of Mathematics, Univ. of Saskatchewan, Saskatoon, SAS, S7N 0W0, Canada

Schleich, Wolfgang, Abteilung f. Theoretische Physik III, Universitat Ulm, W-7900 Ulm, Germany

Schmitt, Harry A., Naval Weapons Station, Code 063, Seal Beach, CA 90740

Scully, Marlan O., Dept. of Physics, Univ. of New Mexico, Albuquerque, NM 87131

Sergienko, Alexandr V., Dept. of Physics, Moscow State University, 119899 Moscow, U.S.S.R.

Shapiro, Jeffrey, Dept. of Electrical Engineering, Massachusetts Inst. of Tech., Cambrdige, MA 02139

Shepard, Scott, Dept. of Electrical Engineering, Massachusetts Inst. of Tech., Cambrdige, MA 02139

Shevy, Yaakov, Dept. of Applied Physics, California Inst. of Tech., Pasadena, CA 91125

Shih, Yan-Hua, Dept. of Physics, Univ. of Maryland at Baltimore Campus, Baltimore, MD 21228

Sica, Louis, Applied Optics Branch, Naval Research Lab., Code 6530, Washington, DC 20375

Singer, Faige, Dept. of Electrical Engineering, Columbia University, New York, NY 10027

Stoler, David, Research Center, Kearfott Guidance and Navigation Corp., Little Falls, NJ 07424

Svensmark, Henrik, NORDITA, Blegdemsvej 17, DK-2100 Copenhagen 0, Denmark

Suzuki, Norikazu, Max-Plank-Institut f. Kernphysik, W-6900 Heidelberg, Germany

Teich, Malvin C., Dept. of Electrical Engineering, Columbia University, New York, NY 10027

Toll, John S., Dept. of Physics, Univ. of Maryland, College Park, MD 20742

Um, Chung-In, Dept. of Physics, Korea University, Seoul 131-701, S. Korea

Van Hine, Christopher, Naval Surface Weapons Center, Silver Spring, MD 20903

Villarreal, Carlos, Inst. de Fisica, Univ. Nacional Autonoma de Mexico, Mexico 01000, Mexico

Vinogradov, A. V., Lebedev Physical Institute, 53 Leninsky Prospect, 117924 Moscow, U.S.S.R.

Vyas, Reeta, Dept. of Physics, Univ. of Arkansas, Fayetteville, AR 72701

Weiner, Brian, Dept. of Physics, Pennsylvania State University, DuBois, PA 15801

Wheeler, John A., Dept. of Physics, Princeton University, Princeton, NJ 08544

Xiao, Min, Dept. of Physics, Univ. of Arkansas, Fayetteville, AR 72701

Yeon, Kyu Hwang, Dept. of Physics, Chungbuk National University, Cheongju 360-763, S. Korea

Yi, Pang, Dept. of Physics, Univ. of Maryland, College Park, MD 20742

Yilmaz, H., Hammamatzu Photonics K.K., 105 Church Street, Winchester, MA 01890

Yin, Xiaosong, Dept. of Physics, Miami University, Oxford, OH 45056

Yuen, Horace P., Dept. of Electrical Engineering, Northwestern University, Evanston, IL 60208

Zachary, W. W., COMSERC, Howard University, Washington, DC 20059

Zaidi, H. R., Dept. of Physics, Univ. of New Brunswick, Fredericton, NBK, E3B 5A3, Canada

Zeilinger, Anton, Dept. of Experimental Physics, Univ. of Innsbruck, A-6020 Innsbruck, Austria

Zhu, Chengjun, Dept. of Physics, Univ. of Florida, Gainesville, FL 32612

Zorn, Gus T., Dept. of Physics, Univ. of Maryland, College Park, MD 20742

TABLE OF CONTENTS

INTRODUCTION

Squeezed states were predicted theoretically in the 1970's. They became a physical reality during the period 1985-1988. Efforts are being made to produce more efficient squeezed-state lasers. More refined theoretical tools are being developed for this new physical phenomenon. One of the pressing questions during the 1990's will be: What should we do with squeezed states? This is the main question we wanted to address in this Workshop.

There are many who say that the potential for industrial applications is enormous, as the history of the conventional laser suggests. There are also those who say that the squeezed state is only a fad and will disappear within two years. In order to find a more accurate answer to the question, let us make the following observations.

(1)   All those who worked so hard to produce squeezed states of light are continuing their efforts to construct more efficient squeezed-state lasers. Quite naturally, they are looking for new experiments using these lasers. New experiments often require new ideas from branches of physics somewhat removed from their own. For instance, the concept of squeezed states arose in part from the desire to detect gravitational waves.

(2)   The physical basis of squeezed states is the uncertainty relation in Fock space, which is also the basis for the creation and annihilation of particles in quantum field theory. Indeed, squeezed states provide a unique opportunity for field theoreticians to develop a measurement theory for quantum field theory. The precondition for formulating field theoretic measurement theory is a correct understanding of the conventional measurement theory and related experiments.

(3)   The theory of squeezed states shares a common mathematical language with many other branches of physics. The basic language is the Lorentz group, which plays important roles in quantum field theory, the phase- space picture of quantum mechanics, relativity, elementary particle physics, condensed matter physics, canonical transformations in classical mechanics, and crystal and polarization optics. It is possible for the physicists in these fields to learn new lessons from the physics of squeezed states.

The Workshop was attended by many of the originators of squeezed states of light as well as those who spent many years studying the foundations of quantum mechanics and related problems. There were also many students. The Editors are very happy to present the papers by those active researchers on squeezed states and related subjects.

I. Measurement Problems and the Einstein-Podolsky-Rosen Paradox

NONCLASSICAL AND NONLOCAL EFFECTS IN THE INTERFERENCE OF LIGHT[*]

L. Mandel

Department of Physics and Astronomy
University of Rochester
Rochester, New York 14627

INTRODUCTION

Although we tend to think of optical interference as a classical wave phenomenon, recent experiments have revealed a number of effects that are not describable in classical terms. This is particularly true of interference effects involving the detection of a photon pair. We shall refer to them as fourth order interference, on the grounds that the joint probability density for the detection of one photon at r_1 at time t and another at r_2 at time t is proportional to the fourth order correlation function of the field (Ref. 1)

$$\Gamma^{(2,2)}(\underline{r}_1 t, \underline{r}_2 t) = \langle \hat{E}_i^{(-)}(\underline{r}_1 t)\hat{E}_j^{(-)}(\underline{r}_2 t) \times \hat{E}_j^{(+)}(\underline{r}_2 t)\hat{E}_i^{(-)}(\underline{r}_1 t)\rangle . \quad (1)$$

This probability is readily measured when two photodetectors are positioned at r_1 and r_2 and the signals from the two detectors are fed to a coincidence counter that registers 'simultaneous' detections by the two detectors in coincidence.

4'th ORDER INTERFERENCE MEASUREMENTS

In the special case in which the two points x_1, x_2 lie on a line, and

the light is produced by two sources A,B on a parallel line such that A emits one photon and B emits one photon, it can be shown that (Refs. 2,3)

$$\Gamma^{(2,2)} \propto [1+\cos \frac{2\pi(x_1-x_2)}{L}] , \quad (2)$$

where $L = \lambda/\theta$. θ is the small angle subtended by the two points A,B at x_1 or x_2 and λ is the wavelength. L is the same fringe spacing that is encountered in the more usual second order interference. According to Eq. (2) the visibility of the fourth order interference effect can be 100%, despite the absence of phase correlation between the two sources. By contrast a classical field that exhibits 4'th order interference cannot achieve a visibility higher than 50%. (Refs. 2-4)
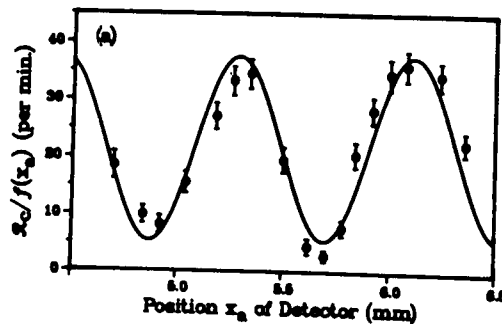
Fig. 1 Experimental results showing 4'th order interference. [Reproduced from Ref. 6.]

5

We have observed greater than 50% visibility in several recent interference experiments,(Refs. 5,6) in which the two photons were generated together in the process of spontaneous parametric down-conversion in a nonlinear crystal.(Ref. 7) It is convenient to produce the interference pattern by mixing the two incoming photons with the help of a 50%:50% beam splitter with a photodetector at each output port. Figure 1 shows the experimental results when the rate of coincidence counting, after some corrections are applied, is plotted against the position of one detector, while the other detector remains fixed. The interference pattern has the expected periodicity L, and the observed 75% visibility shows that we are dealing with a quantum phenomenon, because there is no classical field that can give rise to more than 50% visibility.

The same mixing technique has been applied to the measurement of the time separation between the two photons on a femtosecond time scale, and to study violations of locality. In order to understand the principle of the method, let us consider the symmetric beam splitter with intensity transmissivity T and reflecticity R ($R+T = 1$), shown in Fig. 2. Let α,β label the two input ports and μ,ν the two output ports. Suppose that the two photons enter in the state $|1\alpha,1\beta\rangle$, in which each photon is in the form of a
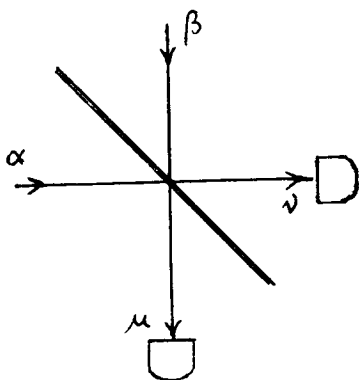
short wave packet and the two wave packets are identical and overlap completely in time. In order to arrive at the output state $|\psi_{out}\rangle$ we first note that there are three possibilities: (a) one photon appears at each output $(|1_\mu,1_\nu\rangle)$; (b) both photons appear at output port μ $(|2_\mu,0_\nu\rangle)$; (c) both photons appear at output port ν $(|0_\mu,2_\nu\rangle)$. It can be shown (Ref. 8) that $|\psi_{out}\rangle$ is given by the linear superposition

$$|\psi_{out}\rangle = (T-R)|1_\mu,1_\nu\rangle + i\sqrt{2RT}$$
$$\times \left(|2_\mu,0_\nu\rangle + |0_\mu,2_\nu\rangle\right) , \qquad (3)$$

from which it follows that when $T = 1/2 = R$, both photons always appear together at one or the other output. If there is a photodetector at each output, there will be no coincidence detections (other than accidentals), because the corresponding two-photon probability amplitude vanishes by destructive interference. But if one photon is delayed slightly relative to the other one by some amount τ, the destructive interference is no longer complete, and the coincidence probability $P(\tau)$ rises from zero with increasing τ. When τ exceeds the duration of the wave packet and the two wave packets no longer overlap, $P(\tau)$ becomes constant and independent of τ.

Fig. 2 The beam splitter.
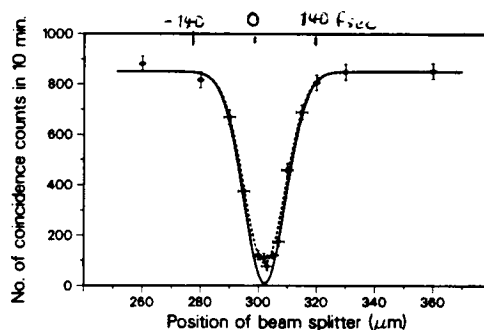
Fig. 3 Measured coincidence rate as a function of time delay in fsec between the two photons. [Reproduced from Ref. 9.]

Figure 3 shows the result of such a coincidence counting experiment (Ref. 9) in which each photon wave packet had a length of about 100 fsec. It can be seen that the observed probability $P(\tau)$ is close to zero for $\tau = 0$, and rises to become constant when $\pm\tau$ equals or exceeds about 100 fsec. We therefore have a technique for measuring the time separation between two pulses of light and the length of the pulse, when each pulse consists of a single photon. The time resolution achieved in this experiment was about 3 fsec, which is about a million times shorter than the resolving time of the detectors and the associated electronics. In some later experiments (Ref. 10) the resolution was further measured to about 1 fsec, which is less than half an optical period.

THE FRANSON EXPERIMENT

A number of experiments have also been performed for which there is no adequate classical model to explain the 4'th order interference.(Refs. 11-14) Let us consider the experimental situation illustrated in Fig. 4, which
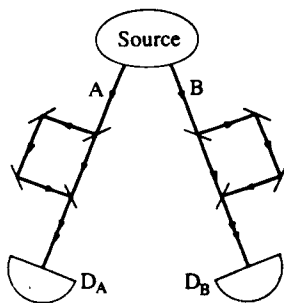
Fig. 4 The principle of the Franson 4'th order interference experiment. [Reproduced from Ref. 13.]

was first proposed and discussed by Franson.(Ref. 15) A source emits two photons A and B simultaneously, each with some center frequency ω_A, ω_B and

bandwidth $\Delta\omega$. The photons emerge in two different directions and fall on two photodetectors D_A and D_B without ever coming together. Some beam splitters and mirrors forming two similar interferometers are introduced, so as to provide two alternative paths for each photon, as shown: a direct path and a longer indirect path. Let the propagation time difference between the two paths be $T+\tau_A$ in channel A and $T+\tau_B$ in channel B, with $T \gg 1/\Delta\omega$, $\tau_A, \tau_B \ll 1/\Delta\omega$.

Because the path difference in each of the two interferometers greatly exceeds the coherence length $c/\Delta\omega$ of the light, no second order interference is expected. The probability that a photon is detected by D_A does not change significantly when τ_A is changed slightly, and similarly for D_B. However, if we calculate the joint probability P_{AB} that a photon is detected by D_A and by D_B in coincidence, which can be measured with a coincidence counter, we find that it exhibits interference of the form

$$P_{AB} \propto \left[1+\eta \cos\left(\omega_A\tau_A+\omega_B\tau_B+\text{const.}\right)\right]. \quad (4)$$

η can be 100% if the coincidence resolving time T_R is sufficiently short, and it is about 50% when $T_R \gg T \gg 1/\Delta\omega$.

This result is best understood as an interference of a photon pair. There are several different ways in which a coincidence can occur: (a)both photons follow the short interferometer paths and arrive simultaneously at the two detectors; (b)both photons follow the long interferometer paths and arrive simultaneously at the detectors; (c)one photon follows the long path and one follows the short path but the

time difference $T+\tau_A$ (say) lies within the coincidence resolving time T_R, so that the photons are deemed to arrive 'simultaneously'. As these probabilities are intrinsically indistinguishable, we have to add the corresponding probability amplitudes and then square in order to arrive at the probability P_{AB}. This leads to the result in Eq. (4). The interference exhibits non-local features, because the outcome of a measurement registered by D_A depends not only on τ_A but also on τ_B, even though the interferometer in channel B cannot influence what happens in channel A.

This interference effect has recently been observed (Refs. 13,14) in experiments in which the two photons were produced by down-conversion in a non-linear crystal. Figure 5 shows the results of such an experiment in which one mirror was moved piezoelectrically and the two-photon coincidence rate was measured. Evidently there is interference despite the fact that the two photons never mix and the path difference exceeds the coherence length of the light more than 100-fold.

Optical Phase Difference
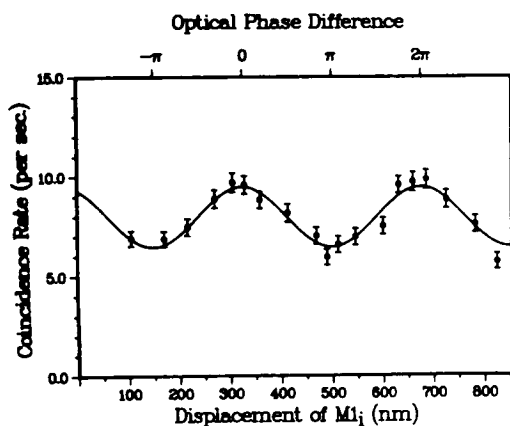
Fig. 5 Results of the Franson-type interference experiment. [Reproduced from Ref. 13.]

The question whether a classical field can give rise to this kind of behavior has been discussed.(Refs. 16-

18) Let us attempt to describe the experimental situation in Fig. 4 in terms of classical waves. Let $V_A(t), V_B(t)$ be the complex analytic signals representing the stationary light field leaving the source. Then the fields at the two detectors D_A, D_B can be expressed in the form

$$W_A(t) = \alpha V_A(t) + \beta V_A(t+T+\tau_A)$$
$$W_B(t) = \alpha V_B(t) + \beta V_B(t+T+\tau_B) \ , \tag{5}$$

where α, β are constants characteristic of the beam splitters and mirrors. The joint probability that a photoemission occurs at D_A at time t and at D_B at time $t+\tau$ is proportional to the two-time correlation

$$P_{AB}(\tau) = \langle |W_A(t)|^2 |W_B(t+\tau)|^2 \rangle \ . \tag{6}$$

The integral of $P_{AB}(\tau)$ with respect to τ over the resolving time T_R of the coincidence counter yields the coincidence counting rate, which is proportional to

$$\mathcal{R}_C = \int_{-T_R/2}^{T_R/2} d\tau \langle |W_A(t)|^2 |W_B(t+\tau)|^2 \rangle. \tag{7}$$

With the help of Eqs. (5) it may be shown (Ref. 16) that $\mathcal{R}_C$ contains an interference term of the form

$$\mathcal{J}_{\text{interfer.}} = \alpha^{*2}\beta^2 \int_{-T_R/2}^{T_R/2} d\tau$$
$$\times \langle V_A^*(t)V_A(t+T)V_B^*(t+\tau)V_B(t+\tau+T) \rangle$$
$$\times e^{-i(\omega_A\tau_A+\omega_B\tau_B)} + \text{c.c.}, \tag{8}$$

together with a somewhat similar interference term involving $\exp[i(\omega_B\tau_B-\omega_A\tau_A)]$. But $\mathcal{R}_C$ also contains a non-oscillatory or background contribution

$$\mathcal{J}_{background} = \int_{-T_R/2}^{T_R/2} d\tau (|\alpha|^4 + |\beta|^4)$$

$$\times \langle I_A(t) I_B(t+\tau) \rangle + |\alpha|^2 |\beta|^2$$

$$\times (\langle I_A(t) I_B(t+\tau+T) \rangle$$

$$+ \langle I_A(t) I_B(t+\tau-T) \rangle) , \quad (9)$$

which represents light background for the interference. Here $I_A(t) = |V_A(t)|^2$, etc. The presence of the interference terms suggests that certain classical fields can exhibit the observed interference effect.

Let us now examine the magnitudes. Whereas the integrand in Eq. (8) tends to zero with increasing τ, that in Eq. (9) does not. We recall that for any ergodic process correlations must eventually die out. It follows that for sufficiently long τ the terms in τ are no longer correlated with those without τ, and therefore for a stationary field,

$$\langle V_A^*(t) V_A(t+T) V_B^*(t+\tau) V_B(t+\tau+T) \rangle$$

$$\to \langle V_A^*(t) V_A(t+T) \rangle \langle V_B^*(t) V_B(t+T) \rangle$$

$$\approx 0 , \quad (10)$$

because $T \gg 1/\Delta\omega$. The integrand in Eq. (9), on the other hand, tends to the constant value $(|\alpha|^2 + |\beta|^2)^2 \langle I_A \rangle \langle I_B \rangle$ as $\tau \to \infty$. Therefore if we integrate with respect to τ over a sufficiently long resolving time T_R, the background term will greatly exceed the interference terms, and the visibility of the interference will become negligibly small. In ref. 16 it was argued that the integrand in Eq. (8) has a range in τ of order $1/\Delta\omega$. But even if it has a longer range, so long as T_R is much longer than this range, the visibility of the interference given by Eqs. (8) and (9) would be very small.

Actually, a classical model of the light from a parametric down-converter fails for other, more compelling reasons. It can be shown (Ref. 19) that for any classical field whose correlation time is much shorter than T_R,

$$\mathcal{R}_{AB} - \mathcal{R}_{AB\ accid.} \leq \mathcal{R}_{AA} - \mathcal{R}_{AA\ accid.} , \quad (11)$$

where $\mathcal{R}_{AB}$ is the coincidence counting rate when signal light falls on one detector and idler light on the other, and $\mathcal{R}_{AA}$ is the self-coincidence rate for the signal. Accidental coincidence contributions are subtracted on both sides. In practice, classical inequality (11) is, however, found to be violated by down-converted light by several hundred standard deviations.(Ref. 19)

EXPERIMENTAL TEST OF THE DE BROGLIE GUIDED WAVE THEORY

Finally, we describe a recent experiment to test a prediction of the de Broglie guided wave theory relating to interference.(Refs. 20,21) According to this theory, which is a hybrid of classical and quantum concepts, there exist both photons and electromagnetic waves, with the latter acting as guides for the former. But, in addition to yielding the probability for detecting a photon, the electromagnetic wave is supposed to have a physical reality that extends beyond being a probability wave.

Figure 6 shows the essential features of the experiment.(Ref. 22) Three 50%:50% beam splitters BS_1, BS_2, BS_3 form a Michelson type of interferometer, and BS_2 can be adjusted piezoelectrically to move through one or two microns. Any light that penetrates BS_1 and BS_2 falls on detector D_1 and D_2, respectively. The counting rates R_1, R_2 of the two detec-
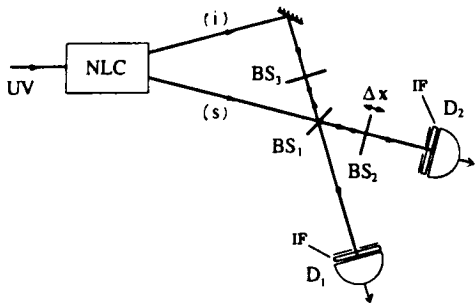
Fig. 6 Outline of the interference experiment to test the de Broglie guided wave theory. [Reproduced from Ref. 22.]

tors are measured as a function of beam splitter BS_2 displacement Δx, together with the coincidence counting rate R_{12}. The interferometer is fed with the signal (s) and idler (i) light produced by down-conversion in the non-linear crystal NLC, as shown, and it is balanced so that the paths of i from NLC to BS_3 and of s from NLC to BS_1 to BS_3 are equal.

Reference to Fig. 6 shows that the idler can only reach detector D_1. On the other hand, the signal can reach both detector D_2 and detector D_1, and moreover it can reach D_1 via the two different paths NLC to BS_1 to BS_3 to BS_1 to D_1 and NLC to BS_1 to BS_2 to BS_1 to D_1. If the distances BS_1 to BS_3 and BS_1 to BS_2 are nearly equal, these two paths interfere, so that counting rate R_1 of D_1, which is given by the expectation of the square of the wave function ψ_1 at D_1, depends on Δx. On the other hand, the counting rate R_2 of D_2, which is given by $\langle|\psi_2|^2\rangle$ is independent of Δx. According to the guided wave theory, (Ref. 21) the counting rate R_{12} of D_1 and D_2 in coincidence is proportional to the expectation $\langle|\psi_1|^2|\psi_2|^2\rangle$, and since $|\psi_2|^2$ is constant and independent of Δx, whereas $|\psi_1|^2$ shows interference, this would be expected to exhibit much the same interference as R_1.

Let us compare that prediction with the quantum mechanical one. As there is only one signal and one idler photon emitted at one time, and because the idler can only reach D_1, it follows that whenever a coincidence is registered, D_1 must have detected the idler photon and D_2 the signal photon. But reference to Fig. 6 shows that, in that case, there is no ambiguity in the photon paths, because the wave function ψ_1 collapses along the two paths s to BS_1 to BS_3 to BS_1 and s to BS_1 to BS_2 to BS_1 that interfere. Therefore R_{12} should exhibit no interference or dependence on Δx. A similar conclusion is reached by a mathematical treatment of the problem.(Ref. 22)

The results of the experiment are shown in Figs. 7 and 8. Figure 7 gives
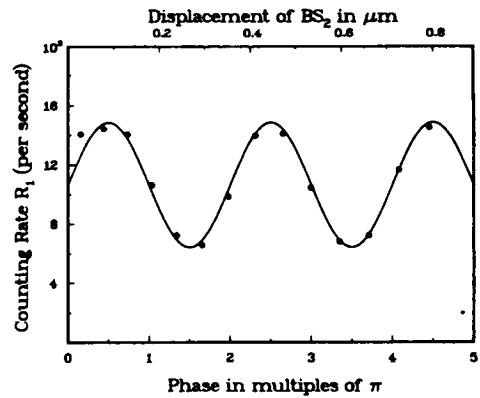
Fig. 7 The measured photon counting rate R_1 as a function of the displacement of BS_2. [Reproduced from Ref. 22.]
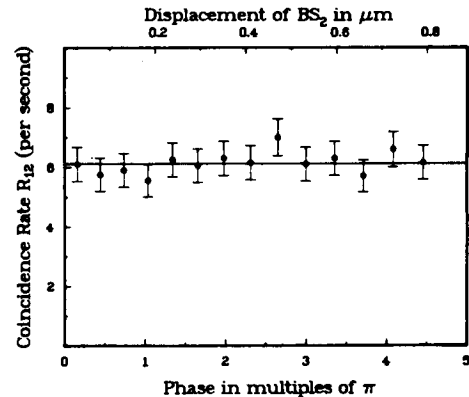
Fig. 8 The measured two-photon coincidence counting rate as a function of BS_2 displacement. [Reproduced from Ref. 22.]

10

the measured photon counting rate R_1 as a function of the displacement Δx of BS_2. As expected, this exhibits interference attributable to the two alternative paths of s to D_1. But this is predicted by all theories, by quantum mechanics, by classical wave theory and by the guided wave theory.

Figure 8 gives the measured two-photon coincidence rate R_{12}, after subtraction of accidental counts, as a function of BS_2 displacement. This time there is no evidence of any interference, in agreement with quantum mechanics, but in violation of the guided wave theory. We have therefore disproved one prediction of the guided wave theory. Needless to say, this conclusion applies only to the particular form of the theory described above, in which probabilities are calculated very much as in semiclassical radiation theory.

The fourth order interference technique is capable not only of very high accuracy, such as the measurement of the time separation between two photons to 1 fsec accuracy, but it also lends itself to the exploration of quite fundamental questions about our quantum world.

REFERENCES

1. Glauber, R.J., Phys. Rev. 130, p. 2529 and 131, p. 2766 (1963).

2. Mandel, L., Phys. Rev. A 28, p. 929 (1983).

3. Ghosh, R., C.K. Hong, Z.Y. Ou and L. Mandel, Phys. Rev. A 34, p. 3962 (1986).

4. Richter, Th., Ann. Phys. (Leipzig) 36, p. 266 (1979).

5. Ghosh, R. and L. Mandel, Phys. Rev. Lett. 59, p. 1903 (1987).

6. Ou, Z.Y. and L. Mandel, Phys. Rev. Lett. 62, p. 2941 (1989).

7. Burnham, D.C. and D.L. Weinberg, Phys. Rev. Lett. 25, p. 84 (1970).

8. Ou, Z.Y., C.K. Hong and L. Mandel, Opt. Commun. 63, p. 118 (1987).

9. Hong, C.K., Z.Y. Ou and L. Mandel, Phys. Rev. Lett. 59, p. 2044 (1987).

10. Ou, Z.Y. and L. Mandel, Phys. Rev. Lett. 61, p. 54 (1988).

11. Ou, Z.Y., X.Y. Zou, L.J. Wang and L. Mandel, Phys. Rev. A 42, p. 2957 (1990).

12. Rarity, J.G., P.R. Tapster, E. Jakeman, T. Larchuk, R.A. Campos, M.C. Teich and B.E.A. Saleh, Phys. Rev. Lett. 65, p. 1348 (1990).

13. Ou, Z.Y., X.Y. Zou, L.J. Wang and L. Mandel, Phys. Rev. Lett. 65, p. 321 (1990).

14. Kwiat, P.G., W.A. Vareka, C.K. Hong, H. Nathel and R.Y. Chiao, Phys. Rev. A 41, p. 2910 (1990).

15. Franson, J.D., Phys. Rev. Lett. 62, p. 2205 (1989).

16. Ou, Z.Y. and L. Mandel, J. Opt. Soc. Am. B 7, p. 2127 (1990).

17. Carmichael, H., private communication (1991).

18. Franson, J.D., to be published.

19. Ou, Z.Y., L.J. Wang and L. Mandel, to be published (1991).

20. de Broglie, L., The Current Interpretation of Wave Mechanics, Elsevier, Amsterdam, 1969.

21. Croca, J.R., A. Garuccio, V.L.

Lepore and R.N. Moreira, Found.
Phys. Lett. 3, p. 557 (1990).

22.   Wang, L.J., X.Y. Zou and L.
Mandel, Phys. Rev. Lett. 66, p.
1111 (1991).

THE ULTIMATE QUANTUM LIMITS ON THE ACCURACY OF MEASUREMENTS†

Horace P. Yuen
Department of Electrical Engineering and Computer Science
Department of Physics and Astronomy
Northwestern University
Evanston, IL 60208

ABSTRACT

A quantum generalization of rate-distortion theory from standard communication and information theory is developed for application to determining the ultimate performance limit of measurement systems in physics. For the estimation of a real or a phase parameter, it is shown that the root-mean-square error obtained in a measurement with a single-mode photon level N cannot do better than $\sim N^{-1}$, while $\sim exp\{-N\}$ may be obtained for multi-mode fields with the same photon level N. Possible ways to achieve the remarkable exponential performance are indicated.

INTRODUCTION

Given whatever physical constraints one has to operate with, what is the best possible system one can build for the measurement or estimation of a physical parameter of interest? It is evident that a systematic approach to the answer of this class of questions is of great interest in physics, which is so much concerned with the detection and accurate measurement of various quantities, from routine temperature gauging to the detection of very weak gravitational radiation. In this paper, I will describe a systematic theory for answering these questions. Conceptually, this theory is directly transplanted from ordinary (classical) information and communication theory, although technically the new quantum issues may greatly complicate the actual workout of a solution. As illustrations, I will provide the ultimate quantum limits on the accuracy of estimating a phase parameter, and also an arbitrary real parameter, when an optical field of a given power level is employed. Let N be the available number of photons of a narrowband optical field. For both the estimation of a phase parameter and a real amplitude parameter, the following results will be proved. For a single-mode field, the best root-mean-square error one may obtain is

$$\delta\phi \sim \frac{1}{N}, \quad \delta r \sim \frac{1}{N} \tag{1}$$

whereas for a multimode field with sufficiently many modes one may achieve

$$\delta\phi \sim e^{-N}, \quad \delta r \sim e^{-N}. \tag{2}$$

Moreover, the theory provides various indications on how one may actually approach the problem of realizing a multimode system that would yield the remarkable exponential performance given by (2). In the following, the underlying information theoretic results will first be explained before the quantum situation is discussed. Due to limitations in space-time, everything can only be briefly outlined. Nevertheless, I hope the discussion is self-contained and comprehensible.

RATE-DISTORTION LIMIT

The theory of information transmission pioneered by Shannon (refs. 1-3) can be immediately adapted to provide a systematic answer to the above class of questions. For a system described by classical physics, the solution goes as follows. First, we assign an a priori probability distribution $p(u)$ on the parameter u we are interested in estimating. This parameter would modulate a physical variable in whatever physical system we pick for extracting information about this parameter. For example, if u is the amplitude of a gravitational wave, the system may be a Michelson interferometer with the physical variable a certain optical phase of an electromagnetic field mode. Some measurement is to be made on the system, such as a determination of the field strengths of the mode, to extract information on the physical variable through which an estimate of u is to be obtained. Let x be the physical variable, and y the measurement variable which is in general random with conditional probability $p(y|x)$, with x itself a function of u depending on the specific scheme. Both the cases of discrete and continuous variables will be included throughout with proper interpretation of the probabilities as a distribution or a density function of the random quantities under discussion.

The condition probability $p(y|x)$ defines a *channel* in information theory, with x the channel *input* and y the channel *output*. For any input probability $p(x)$, the joint probability $p(y,x) = p(y|x)p(x)$ is specified from which one can evaluate the *average mutual information* between x and y,

$$I(\text{x;y}) \equiv \int p(x,y) \log \frac{p(x|y)}{p(x)} dx dy. \tag{3}$$

The entropy of a single random variable can be defined as average self-information

$$H(\text{v}) \equiv I(\text{v;v}) \tag{4}$$

in which $p(v|v)$ is to be interpreted as a Kronecker or Dirac delta. The units in (3) and (4) are given as bits per channel use (per channel input) and bits per source symbol if the log is taken to be of base 2, and as nats per use if the log is of base e. Shannon's channel coding theorem and its converse (ref. 1) state that successive independent samples of a random variable v can be transmitted over a channel $p(y|x)$ with zero probability of error if and only if $H(\text{v}) \leq I(\text{x;y})$. However, for a noisy channel, i.e., when y does not specify x uniquely, channel encoding and decoding are required to get zero error probability which is only obtained in the limit of arbitrarily long codes. Note that we have deviated somewhat from the standard notations in information theory to avoid conflict with later quantum notations. Also, the coding theorem is usually stated in terms of the *capacity* of the channel, which is defined to be the $I(\text{x;y})$ obtained by maximizing over $p(x)$ under whatever further constraints one may impose on x. Typically, one assigns a cost function $\beta(x)$ and constraint the average cost to be under a given level B. The capacity $C(B)$ will then be an increasing function of B. *Roughly speaking, $C(B)$ is the maximum number of information bits one can transmit error-free over a channel with an average resource level B.*

The *rate-distortion function* $R(D)$ of a random variable u is defined to be the minimum $I(\text{u;v})$ between u and any another random variable v such that the *average distortion* between u and v

$$E[d(u,v)] \equiv \int d(u,v)p(u)p(v|u) du dv \tag{5}$$

is at or below a given level D, where the distortion function $d(u,v)$ is a given measure of the difference between u and v. When u is a continuous real parameter, $d(u,v)$ is often chosen to be $|u-v|^2$ or $|u-v|$. The minimization of $I(\text{u;v})$ is carried over $p(v|u)$ subject to the constraint

$$E[d(u,v)] \leq D. \tag{6}$$

One may think of v as a data-compressed version of the source variable u —— v represents u with an average distortion D but it requires less bits to represent v than u. Shannon's source coding theorem with a fidelity criterion and its converse (ref. 3) state that a source can be asymptotically represented with an average distortion D if and only if at least $R(D)$ bits per source symbol is provided. Again, source encoding and decoding are in general required to achieve such minimum distortion in the limit of long codes. Nevertheless, this result shows that *roughly speaking, $R(D)$ is the minimum number of information bits required to represent a source with an average distortion level D.*

What is the minimum average distortion D one can get for transmitting a source variable u over a channel with resource B? The answer is provided by Shannon's joint source-channel coding theorem (refs. 4-5) in what is often called the *rate-distortion limit* or *rate-distortion bound.* By combining the source and the channel coding theorems, the bound is

$$D \geq R^{-1}C(B) \tag{7}$$

where R^{-1} is the inverse of the monotone function $R(D)$. It is important to emphasize that the *Shannon theorem and its converse state that* (7) *is the ultimate limit and can be approached by an actual system that employs source coding and channel coding separately. It does not say that it can only be approached by separate source and channel coding.* In fact, the following example illustrating the power of the rate-distortion bound also shows that it is sometimes possible to achieve it (to get the actual minimum) without any coding or nonlinear modulation at all.

Let u be a zero-mean Gaussian random variable with variance σ_u^2, and distortion measure the squared error $d(u,v) = |u-v|^2$. The rate distortion function in this case is well known [refs. 3-5],

$$\begin{aligned} R(D) &= \tfrac{1}{2}log\tfrac{\sigma_u^2}{D} & 0 \leq D \leq \sigma^2 \\ &= 0 & D \geq \sigma^2 \end{aligned} \tag{8}$$

Consider an additive Gaussian noise channel

$$y = x + n \tag{9}$$

where n is a zero-mean Gaussian noise variable with variance $\mathcal{N}_0$ statistically independent of x. With a given power level, $E[x^2] \leq S$, it is wellknown [refs. 1-2, 4-5] that the capacity is

$$C(S) = \frac{1}{2}log(1 + \frac{S}{\mathcal{N}_0}). \tag{10}$$

The rate-distortion bound solves the following problem which cannot be solved in any other way, to my knowledge. Suppose each sample of u matches each use of x, i.e., the rate that u is generated is equal to the rate that x can be transmitted over the Gaussian channel. We are interested in finding the best signal processing scheme before transmission over the channel and after transmission in receiver processing that would yield an estimate of u with minimum mean-square error. From (7),(8) and (10) one gets

$$D \geq \sigma_u^2 \left(1 + \frac{S}{\mathcal{N}_0}\right)^{-1}. \tag{11}$$

It turns out that the right side of (11) can be obtained by simply letting $x = \sigma_u^{-1}S^{1/2}u$ and estimating $\hat{u}(y) = \sigma_u S^{-1/2}y$, i.e., direct linear transmission and estimation without coding or nonlinear modulation is already optimal as verified from the rate-distortion limit. On the other hand, a direct optimization approach to this or most other comunication problems is very difficult to just formulate, not to mention writing down the optimization conditions.

Despite the power of rate-distortion theory, we are faced with two complications in its application to measurement problems in physics. The first is derived from the fact that in a measurement

system, one may have very little or no room at all for source coding, basically because the parameter u in this case may be entirely out of one's control for further processing before modulating onto the physical variable x. Thus, while the bound (7) still remains a limit, one is *no longer sure that the limit can be achieved arbitrarily closely.* This problem can be overcome by replacing $R(D)$ by $\mathcal{R}(D)$, which is defined to be the number of bits required to represnet u to a distortion level D given a specific simple source coding scheme such as uniform quantization, or no coding at all. The second problem is similarly derived from the fact that no channel coding may be employed. In the same way, one can replace $C(B)$ by an average mutual information $\mathcal{I}(B)$ which incorporates whatever constraint one must face, including perhaps some modulation but no coding. In contrast to the source case $\mathcal{R}(D)$, in the evaluation of $\mathcal{I}(B)$ it may be difficult to actually take into account precisely the constraints one operates with. Anyhow, in a way exactly parallel to the Shannon joint source-channel coding theorem, the following generalized rate-distortion limit applies with whatever additional constraints in the present measurement situation,

$$D \geq \mathcal{R}^{-1}\mathcal{I}(B). \tag{12}$$

Depending on the specific case, the limit (12) may be much higher than (7).

In addition to providing an answer on how accurately one may actually perform a measurement through (7) or (12), this theory also indicates a way to approach the best performance, namely, through channel coding or modulation to achieve $C(B)$ or $\mathcal{I}(B)$, assuming source coding cannot be carried out. Illustrations will be given in the following quantum problems.

MEASUREMENT WITH A QUANTUM SYSTEM

The development of squeezed and nonclassical lights [ref. 6-7] has been strongly motivated by their possible applications to precision measurements. It is logical, in fact imperative, to ask for the ultimate limit of measurements in quantum physics; quantum fluctuations, being an intrinsic feature of nature as we understand it, would have to be taken into account in assessing such ultimate limits. Contrary to what one may first think, the uncertainty principle does not provide the answer either by itself or in conjuction with other additional considerations as discussed in the following two prime cases of continuous parameter estimation. Consider first the case of a real parameter λ defined over the whole real line $\Re$. For simplicity, let λ be a Gaussian random variable and N be the average available number of photons in a single-mode field that one can use to capture λ. That is, we wish to design the best measurement system, which is represented by the way λ modulates the quantum state ρ_λ of the mode and the quantum measurement one chooses to make on the mode, subject to the constraint

$$\int tr[\rho_\lambda a^\dagger a] p(\lambda) d\lambda \leq N \tag{13}$$

where $p(\lambda)$ is the probability of λ, a the model photon annihilation operator, and ρ_λ a density operator on the Hilbert space of quantum states $\mathcal{H}$. To include all possible quantum measurements such as heterodyning, a general quantum measurement on the system $\mathcal{H}$ is represented, as far as the measurement probability is concerned, by a *positive operator-valued measure* (POM) [ref. 8-10] generalizing the usual selfadjoint operator description. In a notation including possible operator-valued distributions, a POM X with measurement value $x \in \Re^n$ is a function $x \longmapsto X(x)$ such that each $X(x)$ is a bounded positive semidefinite selfadjoint operator and all the $X(x)$ sum to the identity operator, i.e.,

$$X(x) \geq 0, \tag{14}$$

$$\int X(x) dx = I. \tag{15}$$

When $X(x) = |x><x|$ are *orthogonal* projectors, the POM X can be desribed by a unique selfadjoint operator obeying the functional calculus

$$f(X) = \int f(x)X(x)dx. \tag{16}$$

For a general POM, (16) does *not* hold. When X is measured on a system in state ρ, the probability that x is obtained is given by $tr[\rho X(x)]$. Mathematically, the problem is to find a mapping $\lambda \mapsto \rho_\lambda, \lambda \in \Re$, a quantum measurement X, an estimate $\hat{\lambda}(x)$ of λ, such that the resulting mean-squared error between $\hat{\lambda}$ and λ is as small as possible subject to the constraint (13). It should be clear that the uncertainty principle is of little help in solving this problem, although some weaker conclusion may be obtained with its help [refs. 11-14]. Thus, if one assumes that X is to be a single field-quadrature operator, and the criterion is changed to average signal-to-noise ratio, then the uncertainty relation between conjugate quadratures

$$< \Delta a_1^2 >< \Delta a_2^2 >\geq \frac{1}{16} \tag{17}$$

can be used to show that the use of two-photon coherent states (TCS) or squeezed states in the narrow sense [refs. 6,15] is optimum. In fact, it yields a mean-square error given by, from (11),

$$D_0 = (\frac{\sigma_\lambda}{1 + 2N})^2. \tag{18}$$

As will be shown in the next section, this turns out to be very close to the best one can do.

In the second case, consider the estimation a real parameter defined over a finite interval, which for simplicity we take to be a phase parameter $\phi \in (-\pi, \pi]$. Mathematically, the problem is exactly the same as above except that $p(\lambda)$ is changed. The number-phase uncertainty relation in whatever form or interpretation,

$$\Delta N \Delta \Phi > \frac{1}{4} \tag{19}$$

is of no help at all here. In contrast to (17), (19) does not even place a limit on how small $\Delta \Phi$ may get under an average photon number constraint because ΔN may still be arbitrarily large. *More significantly*, in an actual measurement problem it is not the quantum fluctuation alone that is important in determining the limit. The total quantum state (the full statistics) and the way energy is distributed could be just as important. We now show how the rate-distortion theory can be generalized to provide the answers.

ULTIMATE QUANTUM LIMITS

To obtain the ultimate possible performance for the above two problems, we note that with the mean-square error criterion the rate distortion function $R(D)$ for a Gaussian random variable λ with variance σ^2 is given by (8) while that for a uniformly distributed $\phi \in (-\pi, \pi]$ is difficult to evaluate exactly. However, the wellknown Shannon upper and lower bounds [ref. 3] on $R(D)$ gives a very accurate estimate in this case: in nats per symbol

$$0.419 - log\sqrt{D} \leq R_\phi(D) \leq 0.595 - log\sqrt{D} \tag{20}$$

If the magnitude distortion function $d(u, v) = |u - v|$ is employed instead, the $R(D)$ for the uniform phase parameter is known exactly while that of a Gaussian random variable is known parametrically [ref. 16]. In both cases, they are quite close to that given by the Shannon lower bound, and are approximately the same as the mean-square case with the natural replacement of D by $\sqrt{D}$. Moreover, for the uniform phase variable the $\mathcal{R}(D)$ function obtained from a *uniform quantizer* (digitizer) can be easily evaluated. For the mean-square-criterion,

17

$$\mathcal{R}_\phi(D) \sim 0.595 - log\sqrt{D} \tag{21}$$

which is exactly the upper bound part of (20)! Thus, uniform digitization without coding is quite close to optimum in this case. For the Gaussian case, uniform quantization also leads to a $\mathcal{R}(D)$ with a similar functional form to $R(D)$, but with a further fixed constant difference. In fact, it is well known that for a large class of memoyylas sources and distortion measures simple quantization already leads to a performance close to the rate-distortion limit. The upshot of our discussion is that independently of the exact distortion criterion one chooses and without the need of coding, the $\mathcal{R}(D)$ functions for our two cases can be accurately estimated and they are close to the rate-distortion limit $R(D)$.

Given $\mathcal{R}(D)$ or $R(D)$, the quantum limitation on communication or measurement is determined by substituting the ultimate quantum information transmission capacity C into $C(B)$ in the bound (7). For a given system, the *ultimate quantum capacity* C is the maximum average mutual information $I(x;j)$ one may obtain by picking an input alphabet J, discrete or continuous, probability p_j on J, a map $j \mapsto \rho_j, j \in J, \rho_j$ density operators on the system state space $\mathcal{H}$, and a POM $X(x)$ subject to whatever constraints one may have. It is clear that the channel coding theorem and its converse hold for this capacity C. The actual evaluation of C can be very complicated due to the added optimization over ρ_j and X which are entirely of quantum mechanical origin. However, for certain cases including the following ones, the evaluation can be carried out with the help of an entropy bound [ref. 10]. Thus, for a single-mode optical field with average photon number constraint N,

$$\sum_j p_j tr[\rho_j a^\dagger a] \le N, \tag{22}$$

the ultimate quantum capacity is achieved by photon number eigenstates with the result [ref. 10]

$$C(N) = (N + 1)log(N + 1) - NlogN. \tag{23}$$

For a narrowband optical field with m modes of approximately the same frequency and a constraint N on the *total* number of average photons in all m modes, the ultimate capacity is [ref. 10]

$$C(N) = mlog(\frac{N}{m} + 1) + \frac{N}{m}log(\frac{m}{N} + 1). \tag{24}$$

We may also be interested in the capacity of TCS with homodyne detection [ref.17]

$$C_{TCS}^{HOM}(N) = mlog(2\frac{N}{m} + 1) \tag{25}$$

and the capacity of coherent states with heterodyne detection

$$C_{CS}^{HET}(N) = mlog(\frac{N}{m} + 1). \tag{26}$$

Going back to our single-mode optimal measurement problem, it follows from (8) and (23) that for a Gaussian parameter r with variance σ^2, the best root-mean-square error $\delta r \equiv \sqrt{D}$ one may obtain is

$$\delta r = \frac{\sigma}{N + 1}(1 + \frac{1}{N})^{-N} \sim \frac{\sigma}{eN} \quad , N >> 1 \tag{27}$$

The suboptimum TCS and CS performance are close to the optimum (27); from (25)-(26) with $m = 1$,

$$\delta r^{TCS} = \frac{\sigma}{2N+1}, \quad \delta r^{CS} = \frac{\sigma}{N+1} \quad . \tag{28}$$

Note that δr^{TCS} can be achieved *without* coding or nonlinear modulation from (18) as discussed in the previous section, while $\delta r^{CS} = \frac{\sigma}{\sqrt{N+1}}$ without coding or modulation. Thus, *the use of TCS can be viewed as an alternative to coding or nonlinear modulation* in at least the single-mode case. For the phase parameter ϕ with uniform distribution, it follows from (21) and (23) that the ultimate limit is

$$\delta\phi \sim \frac{1}{eN}, \quad N \gg 1 \tag{29}$$

while with TCS and coherent states

$$\delta\phi^{TCS} \sim \frac{1}{2N}, \quad \delta\phi^{CS} \sim \frac{1}{N}, \quad N \gg 1. \tag{30}$$

Again, it is known that the use of TCS or other phased-squeezed states would lead directly to $\delta\phi \sim \frac{1}{N}$ [ref. 18], while the use of coherant states without coding or modulation yields only $\delta\phi^{CS} \sim \frac{1}{\sqrt{N}}$.

Consider now the multimode limit under the constraint of the *same* number of photons N. From (8) and (24), we have

$$\delta r = \sigma \left(\frac{N}{m}\right)^{-m} \left(1 + \frac{m}{N}\right)^{-N} \tag{31}$$

which implies that δr would go to zero at least as quickly as e^{-N} for $m \geq 0.1N$. For TCS and coherent states,

$$\delta r^{TCS} = \sigma \left(1 + \frac{2N}{m}\right)^{-m}, \quad \delta r^{CS} = \sigma \left(1 + \frac{N}{m}\right)^{-m} \tag{32}$$

which implies that they would go to zero as e^{-N} for $m \geq N$. Similarly for the phase parameter ϕ,

$$\delta\phi \sim \left(\frac{N}{m}\right)^{-m} \left(1 + \frac{m}{N}\right)^{-N} \tag{33}$$

$$\delta\phi^{TCS} \sim \left(1 + \frac{2N}{m}\right)^{-m}, \quad \delta r^{CS} \sim \left(1 + \frac{N}{m}\right)^{-m} . \tag{34}$$

This multimode behavior as indicated by equ (2) is not unexpected from communication theory, as a larger number of modes is equivalent to signal space of higher dimension which means that the different messages can be placed farther apart in signal space to combat the effect of noise [refs. 2,19]. This is familiar in what is called FM quieting in frequency modulation, and is commonly referred to as the exchange of bandwidth with signal-to-noise ratio. The remarkable feature is that a large number of modes moves the N^{-1} dependence of the ultimate limit to $\exp\{-N\}$ which is so much more accelerated!

There are several approaches one may consider for obtaining such exponential performance, although in a measurement rather than a communication situation one cannot be sure that the above capacities can be actually obtained. Since the number-states channel is noise-free, its capacity can be achieved *without* coding. Indeed it is achieved by a rather simple modulation scheme and the effect of a small nonideal residue noise is not expected to affect the resulting performance too much. The problem remains to find a scheme which, for a measurement system,

would naturally capture the parameter λ (either r or ϕ) of interest in such a modulation scheme or another one which is nearly as good. On the other hand, one may consider the use of nonlinear modulation on TCS or coherent states; different nonlinear modulation schemes are known to get quite close to the rate-distortion limit in many classical communication situations [ref. 20]. In particular, if nonlinear modulation or coding is to be employed, one may consider dispensing with the use of TCS and staying with coherent states, with the resulting loss of a factor of 2 in the exponent but a tremendous gain in practicality. Many different nonlinear modulation schemes may be employed. For example, it is wellknown that a simple pulse frequency modulation in which the modulated signal is given by

$$s(t,\lambda) = \sqrt{\frac{2E}{T}} sin(\omega_0 + \beta\lambda)t, \quad 0 \le t \le T \tag{35}$$

where β is a known constant and E the energy of the signal, could lead to an increase in the signal-to-noise ratio for the estimation of a phase parameter in the presence of additive Gaussian noise by a fact m^2, where $m = WT$ is the total number of modes in $s(t,\lambda)$ with W the frequency bandwidth of the signal. While such a simple scheme may not lead to exactly an exponential performance (2), it may still be a large improvement as the N^{-1} performance of (1) becomes $(mN)^{-1}$.

In conclusion, the quantum generalized rate-distortion theory and the possible actual systems it may suggest seem to hold much promise for greatly improved precision measurements in physics, as our two important examples discussed in this paper amply demonstrate.

REFERENCES

1. Shannon, C.E., 1948, "A Mathematical Theory of Communication", *Bell Sys. Tech. J.* 27, pp. 379-423, 623-656.

2. Shannon, C.E., 1949, "Communication in the Presence of Noise", *Proc. IRE* 37, pp. 10-21.

3. Shannon, C.E., 1959, "Coding Theorems for a Discrete Source with a Fidelity Criterion", *IRE Nat. Cov. Rec.*, Part 4, pp. 142-163.

4. Gallager, R.G., 1968, *Information Theory and Reliable Communication*, Wiley, New York.

5. Blahut, R.E., 1987, *Principles and Practice of Information Theory*, Addison-Wesley, Reading, Mass.

6. Loudon, R. and Knight, P.L. 1987, "Squeezed Light", *J. Modern Opt.* 34, pp. 709-759.

7. Teich, M.C. and Saleh, B.E. A., 1988, "Photon Bunching and Anti-Bunching", *Progress in Optics* XXVI, ed. by E. Wolf, Elsevier, New York, pp. 1-104.

8. Davies, E.B., 1976, *Quantum Theory of Open Systems*, Academic Press, New York.

9. Yuen, H.P. 1982, "Generalized Quantum Measurements and Approximate Simultaneous Measurements of Noncommuting Observables", *Phys. Lett.* 91A, pp. 101-104.

10. Yuen, H.P., and Ozawa, M., 1991, "The Ultimate Information Carrying Limit of Quantum Systems", submitted to *Phys. Rev. Letters*.

11. Yuen, H.P., 1976, "States that Give the Maximum Signal-to-Quantum Noise Ratio for a Fixed Energy", *Phys. Lett.* 56A, pp. 105-106.

12. Yuen, H.P., and Shapiro, J.H., 1978, "Optical Communication with Two-Photon Coherent States Part I: Quantum-State Propagation and Quantum-Noise Reduction", *IEEE Trans. Inform. Theory*, vol. IT-24, pp. 657-668.

13. Shapiro, J.H., Yuen, H.P., and Machado Mata, J.A., 1979, "Optical Communication with Two-Photon Coherent States – Part II: Photoemissive Detection and Structured Receiver Performance", *IEEE Trans. Inform. Theory*, vol. IT-25, pp. 179-192.

14. Yuen, H.P. and Shapiro, J.H., 1980, "Optical Communication with Two-Photon Coherent States Part III: Quantum Measurements Realizable with Photoemissive Detectors", *IEEE Trans. Inform. Theory*, vol. IT-26, pp. 78-92.

15. Yuen, H.P., 1976, "Two-Photon Coherent States of the Radiation Field", *Phys. Rev. A*, vol. 13, pp. 2226-2232.

16. Viterbi, A.J., and Omura, J.K., 1979, *Principles of Digital Communication and Coding*, McGraw Hill, New York.

17. Yuen, H.P., 1975, "Generalized Coherent States and Optical Communications", *Proc. 1975 Conf. Information Sciences and Systems*, John Hopkins Univ., Baltimore, MD, pp. 171-177.

18. Shapiro, J.H., and Shepard, S.R., 1991, "Quantum Phase Measurement: A System-Theory Perspective", *Phys. Rev. A*, vol. 43, pp. 3795-3818.

19. Wozencraft, J.M., and Jacobs, I.M., 1965, *Principles of Communication Engineering*, Wiley, New York.

20. Van Trees, H.L., 1971, *Detection, Estimation and Modulation Theory, Part II, Nonlinear Modulation Theory*, Wiley, New York.

VIOLATIONS OF A NEW INEQUALITY FOR CLASSICAL FIELDS

J.D. Franson
The Johns Hopkins University
Applied Physics Laboratory
Laurel, MD 20723

ABSTRACT

Two entangled photons incident upon two distant interferometers can give a coincidence counting rate that depends nonlocally on the sum of the phases of the two interferometers. It has recently been shown that experiments of this kind may violate a simple inequality that must be satisfied by any classical or semi-classical field theory. The inequality provides a graphic illustration of the lack of objective realism of the electric field. The results of a recent experiment which violates this inequality and in which the optical path length between the two interferometers was greater than 100 m are briefly described.

INTRODUCTION

It has been shown[1,2] that two-photon interferometer experiments can violate Bell's inequality[3] and a number of experiments[4-7] have demonstrated effects of that kind. Several experiments[4,6] based upon the two-photon interferometer of Ref. 1 have not, however, violated Bell's inequality due to the limited visibility (50%) of the interference fringes that results when the resolving time of the photon detectors and electronics is not sufficiently fast.

Those experiments may[8], however, violate a surprisingly simple inequality that must be satisfied by any classical or semi-classical field theory. The inequality follows directly from the assumption that the classical field has some well-defined value and thus illustrates the lack of objective realism exhibited by the quantum-mechanical field.

This paper will briefly review the nature of two-photon interferometry and then derive the new inequality; the derivation closely follows that of Ref. 8. Some additional details of the derivation that are not contained in Ref. 8 but are required for applications to actual experiments are presented in the Appendix. The results of a recent two-photon interferometer experiment performed over a distance of 100 meters will be briefly described. Finally, some comments will be made with regard to the connection between uncertainty relations and inequalities of this type.

TWO-PHOTON INTERFEROMETRY

The experiments of interest[4,6,7] are outlined in Figure 1. Two coincident photons are emitted by parametric down-conversion and travel in different directions toward two identical interferometers. Each interferometer contains a shorter and a longer path, and the difference ΔT in transit times over the two paths is taken to be much larger than the coherence time of the photons. Nevertheless, interference between the quantum-mechanical amplitudes for the photons to have both traveled the shorter paths or the longer paths produces a modulation in the coincidence counting rate R_c given[1] by

$$R_c = \frac{1}{4} R_{c0} \cos^2\left(\frac{\theta_1 + \theta_2 + \omega_0 \Delta T}{2}\right) \tag{1}$$

Here R_{c0} is the coincidence rate with the beam splitters removed, θ_1 and θ_2 are phase-shifts introduced into the two longer paths, and ω_0 is the frequency of the pump laser. Eq. (1) violates Bell's inequality but is only valid if the resolution of the coincidence measurements is better than ΔT. The maximum visibility is 50% for time resolutions much worse than ΔT.

There has been some question as to whether or not the experiments with visibilities of 50% or less are nevertheless inconsistent with any semi-classical field theory. Ou and Mandel[9] have suggested that that is the case but counter-examples to their argument have been given by Carmichael[10] and by Chiao and Kwiat[11]. Although their semi-classical models are able to reproduce the modulation in the coincidence rate, they are not able to represent the fact that the photons are known from other experiments[12] to be coincident to within a time interval much smaller than ΔT. That provides the physical basis for the inequalities derived below.

BASIC INEQUALITY

The basic inequality that must be satisfied by any classical field is based on Cauchy's inequality[13], which follows from the fact that

$$(a - b)^2 \geq 0 \tag{2}$$

where a and b are any two real numbers. Multiplying the two factors and rearranging gives Cauchy's inequality:

$$2ab \leq a^2 + b^2 \tag{3}$$

When a and b are complex it is still the case that

$$|ab| = |a| \, |b| \leq \frac{|a|^2 + |b|^2}{2} \tag{4}$$

The modulation of the coincidence rate will be found to be proportional to the quantity Q defined by

$$Q \equiv \langle |E_1^*(t) \, E_2^*(t) \, E_2(t - \Delta T) \, E_1(t - \Delta T)| \rangle \tag{5}$$

Here E_1 and E_2 refer to the fields at the positions of detectors 1 and 2 (which will be assumed to be equidistant from the source) with the beam splitters removed and $\langle \rangle$ denotes an average over a long time interval.

It should be emphasized from the start that the angular brackets denote an average over time and not an ensemble average. That is what the experiments actually measure, since the results from a single system are simply averaged over time. In addition, no assumption of ergodicity is required in the proof that follows; the average over an ensemble is not considered and it therefore makes no difference whether or not the time average is equivalent to an ensemble average. It will also be found that the proof does not assume stationarity, either.

The basic inequality can be obtained by choosing

$$a = E_1^*(t) E_2(t - \Delta T) \qquad\qquad (6)$$

$$b = E_2^*(t) E_1(t - \Delta T) \qquad\qquad (7)$$

Inserting eqs. (6) and (7) into eq. (4) gives

$$
\begin{aligned}
&\langle |E_1^*(t) E_2^*(t) E_2(t - \Delta T) E_1(t - \Delta T)| \rangle \\
&\leq \langle E_1^*(t) E_2^*(t - \Delta T) E_2(t - \Delta T) E_1(t) \rangle / 2 \qquad (8) \\
&+ \langle E_2^*(t) E_1^*(t - \Delta T) E_1(t - \Delta T) E_2(t) \rangle / 2
\end{aligned}
$$

The physical significance of the above inequality can be seen in Figure 2, in which both fields $E_1(t)$ and $E_2(t)$ correspond to narrow pulses emitted at the same time. If E_1 is evaluated at time t and E_2 is evaluated at time $t \pm \Delta T$, as illustrated by the arrows in the figure, then one or the other of the fields must be zero and their product vanishes. The right-hand-side of eq. (8) is then zero, which requires that the left-hand-side also vanish. Although this inequality may seem trivial in nature, it is a consequence of the fact that the classical fields are well-defined (complex) numbers and the inequality is violated by quantum fields, as will be discussed below.

INEQUALITY FOR THE VISIBILITY

The inequality of eq. (8) can be used to set a limit on the amount of modulation that can occur in a classical treatment of the two-photon interferometer experiments. Once again, let $E_1(t)$ be the classical field that would arrive at detector 1 in the absence of the two beam splitters and assume for the moment that the half-width w of the coincidence window is negligibly small. The corresponding coincidence rate as a function of the time offset τ is then

$$
\begin{aligned}
R_{co}(\tau) &= \eta \langle I_1(t) I_2(t + \tau) \rangle \qquad\qquad (9) \\
&= \eta \langle E_1^*(t) E_2^*(t + \tau) E_2(t + \tau) E_1(t) \rangle
\end{aligned}
$$

where I_1 and I_2 are the intensities of the two beams and the constant η is related to the detection efficiencies and w. With the insertion of the two beam splitters, the total electric field $E_{T1}(t)$ at detector 1 becomes

$$E_{T1} = \frac{1}{2}[E_1(t) + e^{i\theta_1}E_1(t - \Delta T)] \qquad\qquad (10)$$

A similar expression exists for the total field at detector 2 and the classical coincidence rate R_c with the beam splitters inserted and $\tau = 0$ is given by

$$R_c = \frac{1}{16}\eta \langle |[E_1(t) + e^{i\theta_1}E_1(t - \Delta T)][E_2(t) + e^{i\theta_2}E_2(t - \Delta T)]|^2 \rangle \qquad (11)$$

Multiplying out all the factors in eq.(11) gives a total of sixteen terms:

$$R_c = \frac{1}{16}\eta \langle E_1^*(t) E_2^*(t) E_1(t) E_2(t)$$

$$+ e^{i\theta_2} E_1^*(t) E_2^*(t) E_1(t) E_2(t - \Delta T)$$

$$+ e^{i\theta_1} E_1^*(t) E_2^*(t) E_1(t - \Delta T) E_2(t)$$

$$+ e^{i[\theta_1 + \theta_2]} E_1^*(t) E_2^*(t) E_1(t - \Delta T) E_2(t - \Delta T)$$

$$+ e^{-i\theta_2} E_1^*(t) E_2^*(t - \Delta T) E_1(t) E_2(t)$$

$$+ E_1^*(t) E_2^*(t - \Delta T) E_1(t) E_2(t - \Delta T)$$

$$+ e^{i[\theta_1 - \theta_2]} E_1^*(t) E_2^*(t - \Delta T) E_1(t - \Delta T) E_2(t)$$

$$+ e^{i\theta_1} E_1^*(t) E_2^*(t - \Delta T) E_1(t - \Delta T) E_2(t - \Delta T) \qquad (12)$$

$$+ e^{-i\theta_1} E_1^*(t - \Delta T) E_2^*(t) E_1(t) E_2(t)$$

$$+ e^{i[\theta_2 - \theta_1]} E_1^*(t - \Delta T) E_2^*(t) E_1(t) E_2(t - \Delta T)$$

$$+ E_1^*(t - \Delta T) E_2^*(t) E_1(t - \Delta T) E_2(t)$$

$$+ e^{i\theta_2} E_1^*(t - \Delta T) E_2^*(t) E_1(t - \Delta T) E_2(t - \Delta T)$$

$$+ e^{i[-\theta_1 - \theta_2]} E_1^*(t - \Delta T) E_2^*(t - \Delta T) E_1(t) E_2(t)$$

$$+ e^{-i\theta_1} E_1^*(t - \Delta T) E_2^*(t - \Delta T) E_1(t) E_2(t - \Delta T)$$

$$+ e^{-i\theta_2} E_1^*(t - \Delta T) E_2^*(t - \Delta T) E_1(t - \Delta T) E_2(t)$$

$$+ E_1^*(t - \Delta T) E_2^*(t - \Delta T) E_1(t - \Delta T) E_2(t - \Delta T) \rangle$$

As suggested by eq. (1), the experiments can be performed in such a way as to measure the averaged coincidence rate as a function of $\theta_T = \theta_1 + \theta_2$:

$$\overline{R}_c(\theta_T) = \frac{1}{2\pi} \int_0^{2\pi} d\theta_1 \int_0^{2\pi} d\theta_2 R_c(\theta_1, \theta_2) \delta(\theta_1 + \theta_2 - \theta_T) \qquad (13)$$

The averages over θ_1 and θ_2 were explicitly performed in one of the experiments[6]. In the remaining experiments the individual phases were not directly measured and had essentially random values from one run to the next, since variations in the temperature of the laboratory would have shifted the phase of both interferometers by several fringes from one day to the next. Thermal drifts during the course of an experimental run would have a similar effect on the individual phases while leaving the modulation of the coincidence rate unaltered.

In any event, the terms in eq. (12) with phase factors of $\exp(i\theta_1)$, $\exp(i\theta_2)$, $\exp[i(\theta_1 - \theta_2)]$, etc., average to zero, leaving only those terms with no phase dependence or a dependence on $\theta_1 + \theta_2$. The remaining terms can be written as

$$\overline{R}_c = \frac{1}{8}\eta \langle E_1^*(t) E_2^*(t) E_2(t) E_1(t) \rangle$$

$$+ \frac{1}{8}\eta \langle E_1^*(t) E_2^*(t - \Delta T) E_2(t - \Delta T) E_1(t) \rangle \qquad (14)$$

$$+ \frac{1}{16}\eta [e^{i\theta_T} \langle E_1^*(t) E_2^*(t) E_2(t - \Delta T) E_1(t - \Delta T) \rangle + c.c.]$$

where the average over a long time interval ensures that

$$\langle E_1^*(t - \Delta T) E_2^*(t - \Delta T) E_2(t - \Delta T) E_1(t - \Delta T) \rangle$$
$$= \langle E_1^*(t) E_2^*(t) E_2(t) E_1(t) \rangle \qquad (15)$$

and the symmetry of the two beams gives

$$\langle E_1^*(t) E_2^*(t - \Delta T) E_2(t - \Delta T) E_1(t) \rangle \tag{16}$$
$$= \langle E_2^*(t) E_1^*(t - \Delta T) E_1(t - \Delta T) E_2(t) \rangle$$

The assumption inherent in eq. (16) is not essential and can be avoided by simply replacing $R_{co}(\Delta T)$ with $[R_{co}(\Delta T) + R_{co}(-\Delta T)]/2$ in what follows.

The maximum and minimum coincidence rates from eq. (14) satisfy

$$R_{max} \leq \frac{1}{8}\eta \langle E_1^*(t) E_2^*(t) E_2(t) E_1(t) \rangle$$
$$+ \frac{1}{8}\eta \langle E_1^*(t) E_2^*(t - \Delta T) E_2(t - \Delta T) E_1(t) \rangle \tag{17}$$
$$+ \frac{1}{8}\eta \langle |E_1^*(t) E_2^*(t) E_2(t - \Delta T) E_1(t - \Delta T)| \rangle$$

$$R_{min} \geq \frac{1}{8}\eta \langle E_1^*(t) E_2^*(t) E_2(t) E_1(t) \rangle$$
$$+ \frac{1}{8}\eta \langle E_1^*(t) E_2^*(t - \Delta T) E_2(t - \Delta T) E_1(t) \rangle \tag{18}$$
$$- \frac{1}{8}\eta \langle |E_1^*(t) E_2^*(t) E_2(t - \Delta T) E_1(t - \Delta T)| \rangle$$

The visibility is defined as usual by

$$V = \frac{R_{max} - R_{min}}{R_{max} + R_{min}} \tag{19}$$

Using the inequality of eq. (8) and expressing the right-hand-side in terms of $R_{co}(\Delta T)$ gives

$$V \leq \frac{R_{co}(\Delta T)}{R_{co}(0) + R_{co}(\Delta T)} \tag{20}$$

Eq. (20) gives the maximum visibility that can occur in any classical field theory and gives zero modulation for the case in which the fields correspond to coincident pulses.

If the experiments are performed using detectors with limited time responses and large coincidence windows, as is often the case, then the above inequality can be generalized to

$$V \leq \frac{\int_{\Delta T/2}^{\infty} R_{co}(\tau)\, d\tau + \frac{1}{2}\int_{\Delta T/2}^{3\Delta T/2} R_{co}(\tau)\, d\tau}{2\int_{0}^{\infty} R_{co}(\tau)\, d\tau} \tag{21}$$

as is shown in the Appendix. R_{co} is again the coincidence rate that would be obtained using detectors with a negligible time response and a negligibly-small window.

COMPARISON WITH EXPERIMENT

Earlier experiments[12] have shown that the down-converted photons are coincident to within a time interval much less than the value of ΔT in at least three[4,6,7] of the two-photon interferometer experiments, in which case the inequalities of eqs. (20) or (21) show that there is no classical or semi-

classical field theory consistent with all of the available observations.

The author has recently completed an experiment [6] in which the optical path length between the two interferometers was larger than 100 meters. The main goal of the experiment was to investigate these effects in the limit of large distances. Furry has suggested that the collapse of the wavefunction may be degraded in some way when it occurs over sufficiently large distances, leading to an eventual modification of the quantum-theory predictions. The visibility of the interference pattern observed agreed with that expected from the quantum theory to within the experimental uncertainty of 4% and violated the inequality of eq. (21) by four standard deviations. This provides some indication that the collapse of the wavefunction is unaffected even when it occurs over relatively large optical path lengths.

CLASSICAL MODELS

In the classical models suggested by Carmichael[9] and by Chiao and Kwiat[10], the fields E_1 and E_2 have well-defined frequencies that sum to the pump laser frequency for a time interval larger than ΔT or the time resolution of the coincidence circuits. In that case the coincidence rate of eq. (14) simplifies to

$$\overline{R_c} = \frac{1}{4} R_{c0} \left[\cos^2 \left(\frac{\theta_T + \omega_0 \Delta T}{2} \right) + 1/2 \right] \tag{22}$$

This differs from the quantum-mechanical result by the additional factor of 1/2 and corresponds to a visibility of 50%.

Such models cannot simultaneously localize the fields into coincident pulses whose widths are less than ΔT, however. Any classical model that does would have the visibility reduced accordingly as required by the inequalities of eqs. (20) or (21).

VIOLATION OF THE INEQUALITY IN QUANTUM OPTICS

The intensity operator is given by $I(t) = E^-(t) E^+(t)$, where E^+ and E^- are the positive and negative-frequency components of the electric field operator[13]. As a result, the quantum-mechanical equivalent of eq. (8) is

$$\left| \langle E_1^-(t) E_2^-(t) E_2^+(t - \Delta T) E_1^+(t - \Delta T) \rangle \right|$$
$$\leq \langle E_1^-(t) E_2^-(t - \Delta T) E_2^+(t - \Delta T) E_1^+(t) \rangle / 2 \tag{23}$$
$$+ \langle E_2^-(t) E_1^-(t - \Delta T) E_1^+(t - \Delta T) E_2^+(t) \rangle / 2$$

It has already been noted[1] that in experiments of this kind the coincidence of the photons requires

$$E_1^+(t) E_2^+(t \pm \Delta T) = 0 \tag{24}$$

while conservation of energy in the parametric down-conversion process requires that

$$E_1^+(t - \Delta T) E_2^+(t - \Delta T) = e^{i(\omega_1 + \omega_2)\Delta T} E_1^+(t) E_2^+(t) \tag{25}$$

where the sum of the two photon frequencies ω_1 and ω_2 is equal to ω_0. (Eq. (24) is only valid when ΔT is small compared to the pump laser coherence time.) Inserting eq. (24) into the right-hand-side of eq. (23) gives zero, whereas inserting eq. (25) into the left-hand-side gives
$\langle E_1^-(t) E_2^-(t) E_2^+(t) E_1^+(t) \rangle$, which is the product of the individual beam

intensities and a nonzero quantity. Thus the inequality is violated in quantum optics.

The quantum-mechanical situation is shown in Figure 3. The field corresponds to an entangled state in which there is a superposition of times at which the pair of photons may have been emitted, as indicated by the existence of both the solid and dotted curves. Although the product of E_1^+ and E_2^+ at two different times is zero, that does not imply that the left-hand-side of eq. (22) must vanish. Equations (24) and (25) would be logically inconsistent if the fields were well-defined complex numbers and the violation of this inequality provides a graphic demonstration of the lack of objective realism of the electric field.

CONNECTION WITH UNCERTAINTY RELATIONS

The main topics of this conference are squeezing and uncertainty relations. It may thus be useful to make some general comments about the connection between the inequality derived above and the uncertainty relations associated with the quantized field.

The inequality derived above is a result of the fact that the fields are not just complex numbers and thus have no well-defined value. In particular, the field operators are non-commuting and satisfy

$$[A_\mu(x), A_\nu(x')] = -ich\delta_{\mu\nu}D(x - x') \tag{26}$$

A variety of uncertainty relations can be derived from this commutation relation, which illustrates the fact that the quantized field has no well-defined value. As a result, there is an unavoidable uncertainty in the left-hand-side of the classical inequality and this uncertainty is evidently large enough that the left-hand-side can exceed the right-hand-side. Thus it seems apparent that the violations of these classical inequalities in quantum optics are related to the uncertainty relations for the quantized fields. More detailed uncertainty relations for the actual quantities involved in the classical inequality could be derived, if desired.

SUMMARY

Two-photon interferometer experiments with a sufficiently large visibility will violate Bell's inequality and are thus inconsistent with any local hidden-variable theory. Those experiments with smaller visibilities may nevertheless violate an inequality for classical fields if the degree of coincidence of the photon counts is taken into account. A recent two-photon interferometer experiment with a large optical path length between the two interferometers gave a visibility in good agreement with the quantum theory and also violated the classical inequality, indicating that the effects observed were quantum-mechanical in nature.

APPENDIX

When finite coincidence windows are used, Eq. (9) must be replaced by

$$R_{co}' = \eta' \int_{-w}^{w} \langle I_1(t) I_2(t + \tau) \rangle \, d\tau \tag{27}$$

The modulation in the coincidence rate then involves

$$Q' = \frac{1}{8}\eta' \int_{-w}^{w} d\tau < |E_1^*(t) E_2^*(t+\tau) E_2(t - \Delta T + \tau) E_1(t - \Delta T)| > \qquad \textbf{(28)}$$

The range of the integral can be divided into two regions depending on the value of $|\tau|$. For $|\tau| \leq \Delta T/2$, a and b can be chosen as

$$a = E_1^*(t) E_2(t - \Delta T + \tau)$$
$$b = E_2^*(t + \tau) E_1(t - \Delta T) \qquad \textbf{(29)}$$

and the analysis proceeds as in the text. For $|\tau| \geq \Delta T/2$, a and b are chosen instead as

$$a = E_1^*(t) E_2^*(t + \tau) \qquad \textbf{(30)}$$
$$b = E_2(t - \Delta T + \tau) E_1(t - \Delta T)$$

The inequality of eq. (21) then results from the use of eq. (8) in the limit that w is much larger than ΔT.

REFERENCES

1. Franson, J. D., 1989, "Bell Inequality for Position and Time", Phys. Rev. Lett. 62, pp. 2205-2208.

2. Horne, M. A., Shimony, A., and Zeilinger, A., 1989, "Two-Particle Interferometry", Phys. Rev. Lett. 62, pp. 2209-2212.

3. Bell, J. S., 1964, "On the Einstein Podolsky Rosen Paradox", Physics 1, pp. 195-200.

4. Kwiat, P. G., Vareka, W. A., Hong, C. K., Nathel, H., and Chiao, R. Y., 1990, "Correlated Two-Photon Interference in a Dual-Beam Michelson Interferometer", Phys. Rev. A 41, pp. 2910-2913; Ou, Z. Y., Zou, X. Y., Wang, L. J., and Mandel, L, 1990, "Observation of Nonlocal Interference in Separated Photon Channels", Phys. Rev. Lett. 65, pp. 321-324.

5. Rarity, J. G., and Tapster, P. R., 1990, "Experimental Violation of Bell's Inequality Based on Phase and Momentum", Phys. Rev. Lett. 64, pp. 2495-2498; Rarity, J. G., Tapster, P. R., Jakeman, E., Larchuk, T., Campos, R. A., Teich, M. C., and Saleh, B. E. A., 1990, "Two-Photon Interference in a Mach-Zehnder Interferometer", Phys. Rev. Lett. 65, pp. 1348-1351.

6. Franson, J. D., 1991, "Two-Photon Interferometry Over Large Distances", submitted to Phys. Rev. A.

7. Brendel, J., Mohler, E., and Martienssen, W., 1991, "Time-Resolved Dual-Beam Two-Photon Interferences with High Visibility", Phys. Rev. Lett. 66, pp. 1142-1145.

8. Franson, J. D., 1991, "Violations of a Simple Inequality for Classical Fields", submitted to Phys. Rev. Lett.

9. Ou, Z. Y., and Mandel, L., 1990, "Classical Treatment of the Franson Two-Photon Correlation Experiment", J. Opt. Soc. Am. B 7, pp. 2127-2131.

10. Carmichael, H. J., 1990, private communication; and to be published.

11. Chiao, R. Y., and Kwiat, P. G., 1990, private communication.

12. Friberg, S., Hong, C. K., and Mandel, L., 1985, "Measurement of Time Delays in the Parametric Production of Photon Pairs", Phys. Rev. Lett. 54, pp. 2011-2013; Ou, Z. Y., and Mandel, L., 1988, "Observation of Spatial Quantum Beating with Separated Photodetectors", Phys. Rev. Lett. 61, pp. 54-57.

13. Loudon, R., 1983, The Quantum Theory of Light, Oxford University Press, New York.
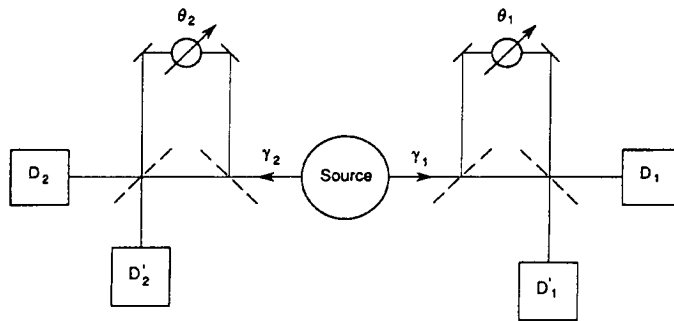
Figure 1   Two-photon interferometer.
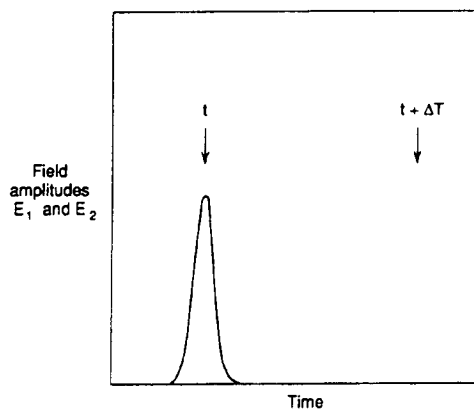
Figure 2   A pair of classical coincident pulses.
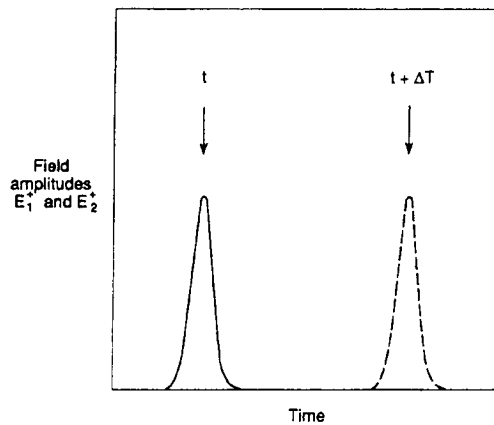
Figure 3   Quantum-mechanical field corresponding to an entangled pair of coincident photons, with a superposition of times at which the pair may have been emitted.

USE OF ENTANGLEMENT IN QUANTUM OPTICS*

Michael A. Horne
Stonehill College, North Easton, Massachusetts 02357

Herbert J. Bernstein
Hampshire College, Amherst, Massachusetts 01002

Daniel M. Greenberger
City College of the City University of New York, New York, New York 10031

Anton Zeilinger
Atominstitut der Österreichischen Universitäten
Schüttelstrasse 115, A-1020 Vienna, Austria

Abstract

Several recent demonstrations of two-particle interferometry are reviewed and shown to be examples of either color entanglement or beam entanglement. A device, called a number filter, is described and shown to be of value in preparing beam entanglements. Finally we note that all three concepts (color and beam entanglement, and number filtering) may be extended to three or more particles.

Introduction

In recent years there has been a variety of demonstrations of two-particle interferometry. By a two-particle interferometer we mean an arrangement without polarizers whereby the coincident count rate in a pair of detectors exhibits sinusoidal oscillations (two-particle fringes) as some apparatus parameter is uniformly varied, but the singles rate in each detector is constant. Whereas the earliest demonstrations[1,2] of two-particle fringes employed pairs of photons from atomic cascades and employed polarizer orientation as the parameter, the new experiments employ photon pairs produced by down-conversion and usually employ mirror translation as the parameter.

Two-particle interference fringes occur only when the quantum mechanical state of the particles is entangled. By entanglement we mean that the two-particle state does not factor into a product of single particle states, but is a sum of at least two terms, each of which is a product. Note that when two-particles are so entangled, neither particle separately has a state. Because particles in an entanglement do not have states or even some properties, independently of each other, we will often refer to them not as two particles, but simply as a two-particle, i. e., a single entity.

The present paper reviews a selection of the recent demonstrations of two-particle interferometry, in order to point out the central role of entanglement. The experiments are selected so as to especially emphasize two important types of entanglement: *color entanglement* and *beam entanglement*. Although each of these types of entanglement have previously been separately discussed (but without these names) in earlier papers and conference proceedings, we thought this an appropriate place for a review. In the course of the review of existing experiments, we also describe a device, which we call a *number filter*, that may be of use in experimentally preparing entanglements in the future. Finally, we note that all three ideas discussed here (color

entanglement, beam entanglement, and number-filtering) also apply to a three-particle, a four-particle, etc.

Before starting the review, we emphasize two other aspects of our point of view, both essential to the way we use entanglement. First, we distinguish beams or paths (labelled A, B, C,...) from particles or detectors (labelled 1,2,3,...). Second, we apply elementary quantum-mechanical concepts as follows. Amplitudes and kets will be assigned to the particles and not to the beams. Total amplitude is the sum over all contributing amplitudes (i.e., the Feynman-Wheeler rule). Note then that our approach is unorthodox in that quantum optics usually employs a quantum field theory in which states (e.g., kets) are assigned not to the particles, (i.e., the photons) but to the beams (i.e., the field modes).

A Color-Entangled Two-Photon

When a single particle decays into two, as for example in a down-conversion of an ultraviolet photon into a pair of red photons, energy conservation, together with a suitable apparatus, produce entanglement. Fig. (1) depicts an arrangement for producing entanglement in this way during down conversion.[3,4] Suppose, for simplicity that the incident photon is ideally monochromatic with wavenumber $2k_0$, so that its state is

$$\Phi(k) = \delta(k - 2k_0) \tag{1}$$

Suppose that the outgoing pair, 1 and 2, are selected as to direction by the symmetrically placed slits and as to color by filters of wavenumber width σ, centered at k_0, and that σ is narrower than any feature in the down-conversion spectrum. Then from eq. (1) and energy conservation, the state of the down-conversion photons after the filters is

$$\Phi(k_1, k_2) = \delta(k_1 + k_2 - 2k_0)\, e^{-(k_1 - k_0)^2/2\sigma^2}\, e^{-(k_2 - k_0)^2/2\sigma^2}. \tag{2}$$

Because of the δ-function, this state cannot be factored, i. e., the two red photons are actually a *color-entangled two-photon*.

In general, a state entangled in k-space is also entangled in x-space. For example, eq. (2) in x-space, with the time dependence included, becomes

$$\psi(x_1, x_2, t_1, t_2) = e^{ik_0(x_1 - ct_1)} e^{ik_0(x_2 - ct_2)} e^{-\frac{\sigma^2}{4}[(x_1 - ct_1) - (x_2 - ct_2)]^2}, \tag{3}$$

along the outgoing beams. Here it is the real exponential that does not factor, i. e., the photons are still entangled and with spectacular consequences. If detectors are placed in the beams equally far from the source ($x_1 = x_2$),the joint probability density is, from eq. (3),

$$\psi^*\psi = e^{-\sigma^2(c\tau)^2/2}, \tag{4}$$

where $\tau \equiv t_2 - t_1$ is the time difference in the arrival of the photons. In short, the color entanglement implies that the distribution in time separation of the photons is dictated by the filter width.[4]

For even more spectacular consequences, consider the expanded arrangement first proposed by Franson[5] and shown in Fig. (2). Here each beam of Fig. (1) has been fed into a single particle interferometer. Kwiat, et al.,[6] and Ou, et al.,[7] have confirmed Franson's prediction that two-particle fringes can be exhibited with this arrangement. These Franson fringes follow easily from the color-entangled two-photon state (2) and (3), as has been shown in an earlier conference proceedings.[8] The argument is as follows. For simplicity, suppose that the path lengths are adjusted so that the two interferometers are identical, with the long path longer by Δ than the short path . Place detectors in the corresponding output beams of the interferometer and monitor for coincidences. From Fig. (2), the state falling on these detectors is

$$\psi(0, 0, t_1, t_2) + \psi(\Delta, \Delta, t_1, t_2) + \psi(\Delta, 0, t_1, t_2) + \psi(0, \Delta, t_1, t_2), \tag{5}$$

where ψ is given by eq. (3).

It follows from the state (5) that the coincident count rate is
$$A(1 + \cos 2k_0\Delta) + B\cos k_0\Delta + C,$$ (6)
where A, B, and C are elementary (error) functions of σ, Δ, and the coincidence "window" T. In the ideal limit that
$$\sigma\Delta >> 1$$ (7a)
and
$$cT << \Delta,$$ (7b)
the third and fourth terms of the state (5) do not contribute and as a consequence, B=C=0 in expression (6). That is, (6) reveals that under ideal conditions two-particle fringes of visibility unity can be exhibited by varying Δ or k_0. Although experiments cannot achieve such ideal contrast, several groups at the present conference report continuing investigation of fringe contrast in Franson interferometry. We propose that some of the relationships in (6) be compared with experimental data.

A Beam-entangled Two-photon

The collapse of the state (5) to just two terms, when the conditions of the inequalities (7) are satisfied, has already produced an example of *beam entanglement*. That is, the beams taken by the detected pair of photons were either both short or both long, the other two cases being impossible because of the choices of filter width σ, path difference Δ, and coincidence window T. Beam entanglement may also be produced by directly exploiting momentum conservation[9] during the decay process, instead of the energy conservation that was built into the color entanglement of eq. (2). In general, this approach requires that the two beams of Fig. (1) be brought together. Fringes were first produced in this way by Alley and Shih,[10,11] but since their arrangement involved polarization manipulation, we will review instead the simpler arrangement of Ghosh and Mandel,[12] shown in Fig. (3).

As indicated in that figure, Ghosh and Mandel uncovered some of the fun of two-particle quantum mechanics in the small region of beam overlap. Consider, as shown in the Fig. (3) insert, two small detectors placed in this region. When coincident counts occur in these detectors, the count in detector 1 could have been caused by a photon 1 that took route A, in which case, by momentum conservation at the source, photon 2 took route B. Equally likely, the routes taken could have been reversed. Consequently, the state falling on the detectors is the beam-entangled two-photon state
$$\frac{1}{\sqrt{2}}\left[|A\rangle_1|B\rangle_2 + |B\rangle_1|A\rangle_2\right]$$ (8)
where ket $|A\rangle_1$ denotes particle 1 in beam A, etc.

Assume, for simplicity, that each beam is monochromatic and monodirectional. Then, from state (8), the stationary two-particle amplitude at the detectors is proportional to
$$e^{i k_A \cdot r_1}e^{i k_B \cdot r_2} + e^{i k_B \cdot r_1}e^{i k_A \cdot r_2},$$ (9)
where k_A and k_B are the wave-vectors of the beams and r_1 and r_2 are the positions of the detectors. It follows from the amplitude (9) that the probability of joint detection is proportional to
$$1 + \cos[(k_A - k_B)\cdot(r_2 - r_1)],$$ (10)
as confirmed by Ghosh and Mandel, who varied the separation of the detectors in Fig. (3).

Note that manipulation of the phases of beams A and B, either by changing their geometrical lengths with mirror motion or their optical lengths with phase plates, has no effect on the fringes (10). This is because each term of the entangled state (8) has both an A-beam and a B-beam factor, and hence the phase manipulations introduce only an unobservable overall phase in the amplitude (9).

Fig. (4) depicts an extended arrangement of Rarity et al[13] that is responsive to such phase manipulations. Here, by simply relabeling the kets in (8), the state before the first beam splitters is

$$\tfrac{1}{\sqrt{2}}\Big[|C\rangle_1 |D\rangle_2 + |D\rangle_1 |C\rangle_2 \Big],$$
(11)

which evolves into

$$\tfrac{1}{\sqrt{2}}\Big[|A\rangle_1 |A\rangle_2 + e^{2i\varphi} |B\rangle_1 |B\rangle_2 \Big]$$
(12)

after the phase plate and before the final beamsplitter. That is, now both particles either take route A, or both take route B, and hence the phase 2φ enters. The derivation of (12) from (11) uses only the elementary rules for transmission and reflection at beam splitters, i. e.,

$$|C\rangle_1 \rightarrow \tfrac{1}{\sqrt{2}}\big(i|A\rangle_1 + |B\rangle_1 \big),$$
(13)

etc. Applying this rule again at the last beam splitter, the state (12) evolves into four terms, but two of these describe both particles going into the same detector, and hence are of no interest in a coincidence counting experiment. From either of the other amplitudes, the coincident count rate is proportional to

$$1 + \cos 2\varphi$$
(14)

i. e., two particle fringes appear when φ is varied, as was indeed observed by Rarity et al.[13]

Fig. (5) proposes another arrangement for preparing the entangled state (12). Here a beam of wave number k impinges on a beam splitter. Outgoing beam A contains two non-linear crystals separated by a 2k filter. Clearly the only way k radiation can pass this three-element device is for an incident two-photon to up-convert in the first crystal to a single 2k photon which , after passing the filter, downconverts back to a two photon in the second crystal. Consequently, we call the device a *number filter*, since only a two-photon can pass. Of course, the two-photon could avoid the device entirely and take route B, which contains phase shifter φ. Thus the state (12) is prepared and the two-particle fringes of (14) can be observed. Although this experiment has not been performed, we note the similarity of Fig. (5) to an arrangement of Wu, et al.[14] It seems that the only significant difference is that we assume the discrete counting of photons in coincidence, whereas they continuously monitored the current difference of two photo-diodes. Clearly there must exist interesting relationships between our point of view (i.e., entanglement of particles) and theirs (i.e., field quantization with "squeezing").

A Two-Photon in Four-Beam Entanglement

Figs. (6) through (10) depict various performed or proposed experiments for exhibiting two-particle fringes by manipulating four beams of down-conversion radiation. Fig. (6) is a proposal of Horne, et al.[15] and an actual experiment of Rarity and Tapster[16] in which the four beams are taken directly from the down-conversion crystal. Fig. (7) is a proposal of Reid and Walls,[17] in which only two beams are taken directly from the crystal and each of these is split before suitable recombining. Fig. (8) is an experiment of Ou et al.[18], in which the splitting is done before the down-conversion. Fig. (9) is a proposal for a four-beam experiment employing number-filtering. Fig. (10) is (the completion of) a figure in a recent proposal of Tan et al.[19]

The main point we wish to make here is that, from an elementary entanglement point of view, these five experiments are, essentially, identical. That is, in each case, the arrangement prepares the four-beam two-photon entangled state

$$\frac{1}{\sqrt{2}}\left[|A\rangle_1|B\rangle_2 + |A'\rangle_1|B'\rangle_2\right]$$

(15)

which, in an appropriate pair of the four detectors, produces fringes, as in (14), when the phases are manipulated. For figs. (6) and (7), the state (15) is an immediate consequence of momentum conservation at the decay. In Fig. (8), a single photon has its amplitude split at the beam splitter and then each of these amplitudes down-converts (in different crystals) to produce the state (15). Note that our description does not employ the "entanglement with the vacuum" description of Ou et al.[18] In Fig. (9), the state (15) is an immediate consequence of the number filter, and Fig. (10), if one ignores the extra detector marked 3, is identical to Fig. (9).

In Fig. (10), only the portion below and to the right of the dash-dot line appeared in the figure of Tan, et al.[19] The remainder of Fig. (10) is drawn from their verbal description, i.e., their text. It isn't clear from their text whether they propose to monitor for two particles or for three particles in coincidence. Consequently, we have included the (optional) detector 3 in order to discuss both cases here. If detector 3 is ignored, and coincidence counts are monitored in various pairs of detectors at stations 1 and 2, then the state is given by (15), since, just as in Fig. (9), the particles must either both come through the number filter, or both avoid it. Thus the phases φ_1 and φ_2 both enter in the second term of (15), and the joint probability of coincidence counts in appropriate detectors at stations 1 and 2 is proportional to

$$1 + \cos(\varphi_2 + \varphi_1).$$

(16)

On the other hand, if one does record a particle at 3, the other particle coming through the number filter can either be 1 or 2, but not both. Consequently, the phases φ_1 and φ_2 enter into different terms and in fact the state approaching the final beam splitters is now

$$e^{i\varphi_2}|A\rangle_1|B'\rangle_2 + e^{i\varphi_1}|A'\rangle_1|B\rangle_2,$$

(17)

instead of (15). Then the fringe pattern

$$1 + \cos(\varphi_2 - \varphi_1).$$

(18)

will occur in an appropriate pair of the detectors at 1 and 2. Since the fringes in (18) depend on the phase *difference*, as in the fringe equations exhibited by Tan, et al., it appears that they are proposing a three-particle coincidence experiment. In either case, it is clear that our elementary entanglement description is not compatible with their talk of a "single photon": their arrangement studies at least a two-photon and, if detector 3 is used, a three-photon.

A Three-Photon

Clearly the concepts of color-entanglement, beam entanglement, and number filtering may be applied to three or more particles. Fig. (11) depicts an arrangement producing a color-entangled three-photon, i.e., the generalization of Fig. (1). Here, the analogs to eqs. (1) through (3) are

$$\Phi(k) = \delta(k - 3k_0),$$

(19)

$$\Phi(k_1, k_2, k_3) = \delta(k_1 + k_2 + k_3 - 2k_0)\, e^{-(k_1-k_0)^2/2\sigma^2}\, e^{-(k_2-k_0)^2/2\sigma^2}\, e^{-(k_3-k_0)^2/2\sigma^2}.$$

(20)

and

$$\psi(x_1, x_2, x_3, t_1, t_2, t_3) = e^{ik_0(x_1-ct_1)}e^{ik_0(x_2-ct_2)}e^{ik_0(x_3-ct_3)}e^{-\frac{\sigma^2}{6}[\{2,1\}+\{3,2\}+\{1,3\}]},$$

$$where\ \{2,1\} \equiv \{(x_2 - ct_2) - (x_1 - ct_1)\}^2,\ etc.$$

(21)

Note that the real exponential in this last equation implies remarkable space-time correlations among the three photons.

Fig. (12) depicts a three particle generalization of the Franson interferometer of Fig. (2). From eq. (21) and the eight-term three-photon analog of the state (5), one easily finds that the three photon equivalent of the counting rate (6), in the limit of ideal filters and detectors, is

$$1 + \cos 3k_0\Delta. \tag{22}$$

In another paper in these proceedings[20], we also consider other higher-order entanglements: the three photon generalization of the direct-beam interferometer of fig. (6) and of the number filter interferometer of Fig. (9).

Some aspects of three particle interferometry have also been explored by Choi.[21]

Comments

We conclude with two comments. First, we have not attempted here a comprehensive review of all of the recent demonstrations of two-particle interferometry but have selected enough examples to exhibit the usefulness of entanglement. Consequently many beautiful experiments (and theoretical papers) have not been discussed. However, we have found that our point of view does provide simple, direct, and yet complete descriptions of all the experiments, either via color entanglement, beam entanglement, or a combination of the two. For example, one may imagine that the beams of Fig. (1) are brought together at a beam splitter, that the two filters are not inserted until downstream of the beam splitter and, moreover, that the filters are now centered on different colors, k_{10} and k_{20}. This is the arrangement of the "quantum beating" experiment of Ou and Mandel.[22] Our description consists of two steps. First, generalize state (3) to include two different filter colors. Second, superpose two of these generalized states to accommodate the beam entanglement aspect of the arrangement. In this way, one reproduces the key result of Ou and Mandel (their eq. (10)).

Second, note that a single quantum mechanical particle in an elementary plane-wave state has only three adjustable properties: wavenumber, propagation direction, and polarization. Consequently we claim that for two or more particles there are only three basic types of entanglement: wavenumber, propagation direction, and polarization. Clearly color entanglement is just the optical realization of wavenumber entanglement and our beam entanglement is intimately related to propagation direction entanglement. We say "intimately related to" instead of "is" because one must be on guard when idealizing a beam as monodirectional. A beam, unlike a spatially unlimited plane wave, has a finite transverse width and hence can't ever be strictly monodirectional, because of diffraction.

References

*   This work was supported in part by grants from the National Science Foundation, and (for DMG) the City University of New York CUNY-FRAP program .

1.   Kocher, C. A., and E. D. Commins, 1967, "Polarization Correlation of Photons Emitted in an Atomic Cascade," Phys. Rev. Lett. 18, pp. 575-577.

2.   Freedman, S. J., and J. F. Clauser, 1972, "Experimental Test of Local Hidden-Variable Theories," Phys. Rev. Lett. 28, pp. 938-941.

3.   Burnham, D. C., and D. L. Weinberg, 1970, "Observation of Simultaneity in Parametric Production of Optical Photon Pairs," Phys. Rev. Lett. 25, pp. 84-87.

4.   Friberg, S., C. K. Hong, and Ll. Mandel, 1985, "Measurement of Time Delays in the Parametric Production of Photon Pairs," Phys. Rev. Lett. 54, pp. 2011-2013.

5.   Franson, J. D., 1989, "Bell Inequality for Position and Time," Phys. Rev. Lett. 62, pp. 2205-2208.

6.   Kwait, P. G., W. A. Vareka, C. K. Hong, H. Nathel, and R. Y. Chiao, 1990, "Observation of Nonlocal Two-Photon Interference in a Dual-Beam Michelson Interferometer," Phys. Rev. A41, pp. 2910-2913.

7.   Ou, Z. Y., X. Y. Zou, L. J. Wang, and L. Mandel, 1990, Obsevation of Nonlocal Interference in Separated Photon Channels," Phys. Rev. Lett. 65, pp. 321-324.

8.   Horne, M., A. Shimony, and A. Zeilinger, 1990, "Down-Conversion Photon Pairs: A New Chapter in the History of Quantum-Mechanical Entanglement," in *Quantum Coherence*, Jeeva F. Anandan, ed., World Scientific, Singapore, pp. 356-372.

9.   Horne, M. A., and A. Zeilinger, 1985, "A Bell-Type EPR Experiment Using Linear Momenta," in *Symposium on the Foundations of Modern Physics*, P. Lahti and P. Mittelstaedt, eds., World Scientific, Singapore, pp. 435-439.

10.   Alley, C. O., and Y. H. Shih, 1986, "A New Type of EPR Experiment," in *Proceedings of the Second International Symposium on Foundations of Quantum Mechanics in the Light of New Technology*, M. Namiki, et al., eds., Physical Soc. of Japan, Tokyo, pp. 47-52.

11.   Shih, Y. H., and C. O. Alley, 1988, "New Type of Einstein-Podolsky-Rosen-Bohm Experiment Using Pairs of Light Quanta Produced by Optical Parametric Down Conversion," Phys. Rev. Lett. 61, pp. 2921-2924.

12.   Ghosh, R., and L. Mandel, 1987, Observation of Nonclassical Effects in the Interference of Two Photons," Phys. Rev. Lett. 59, 1903-1905.

13.   Rarity, J. G., P. R. Tapster, E. Jakeman, T. Larchuk, R. A. Campos, M. C. Teich, B. E. A. Saleh, 1990, "Two Photon Interferometry in a Mach-Zehnder Interferometer," Phys. Rev. Lett. 65, pp. 1348-1351.

14.   Wu, Ling-An, H. J. Kimble, J. L. Hall, and Huifa Wu, 1986, "Generation of Squeezed States by Parametric Down Conversion," Phys. Rev. Lett. 57, pp. 2520-2523.

15.   Horne, M. A., A. Shimony, and A. Zeilinger, 1989, "Two-Particle Interferometry," Phys. Rev. Lett., 62, pp. 2209-2212.

16.   Rarity, J. G., and P. R. Tapster, 1990, "Experimental Violation of Bell's Inequality Based on Phase and Momentum,," Phys. Rev. Lett.64, 2495-2498.

17.   Reid, M. D., and D. F. Walls, 1986, "Violations of Classical Inequalities in Quantum Optics," Phys. Rev. A34, pp. 1260-1276.

18.   Ou, Z. Y., L. J. Wang, X. Y. Zou, and L. Mandel, 1990, "Evidence for Phase Memory in Two-Photon Down Conversion Through Entanglement With the Vacuum," Phys. Rev. A41, pp. 566-568.

19.   Tan, S. M., D. F. Walls, and M. J. Collett,1991, "Non-Locality of a Single Photon," Phys. Rev. Lett. 66,pp. 252-255.

20. Zeilinger, A., M. A. Horne, and D. M. Greenberger, "Higher Order Quantum Entanglement," in *Squeezed States and Uncertainty Relations*, NASA CP-   , 1991. (Paper   of this compilation.)

21. Choi, H. S., "Bell's Theorem Without Inequalities," 1991, thesis, City College of the City University of New York, unpublished.

22. Ou, Z. Y., and L. Mandel, 1988, "Observation of Spatial Quantum Beating With Separated Photo-Detectors", Phys. Rev. Lett. 61,pp. 54-57.
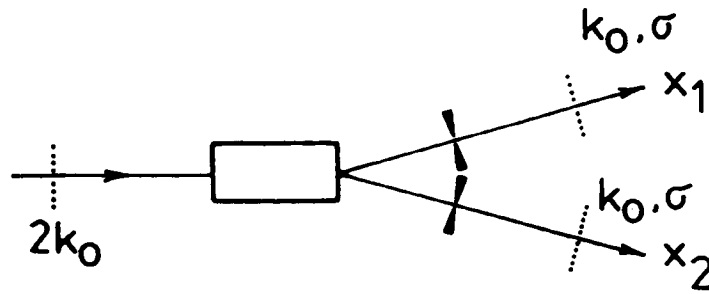
Fig. (1). An incident monochromatic UV photon of wavenumber $2k_0$ downconverts in a crystal. Two beams of the downconversion radiation are selected by slits and by filters of center k_0 and width σ, thereby preparing the color-entangled two-photon state of eqs. (2) and (3). Consequently, the distribution in time separation, τ, of the two photons is given by eq. (4).
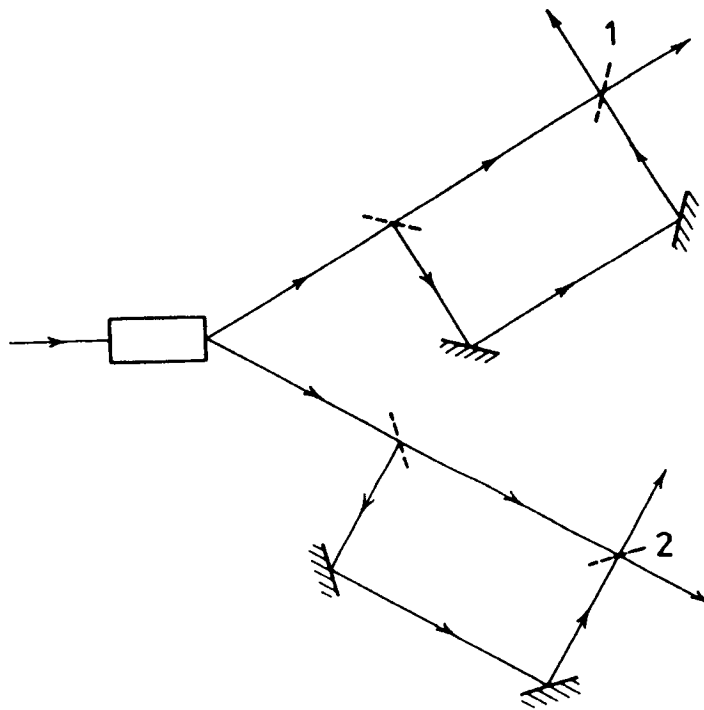
Fig. (2). Franson's two particle interferometer. The two beams of Fig. (1) are each fed into a single-particle interferometer in which one path is Δ longer than the other and adjustable. As Δ is varied in both interferometers, the coincident count rate in two corresponding outgoing beams (one at station 1 and one at station 2) exhibits the oscillations (two-particle fringes) given by (6).
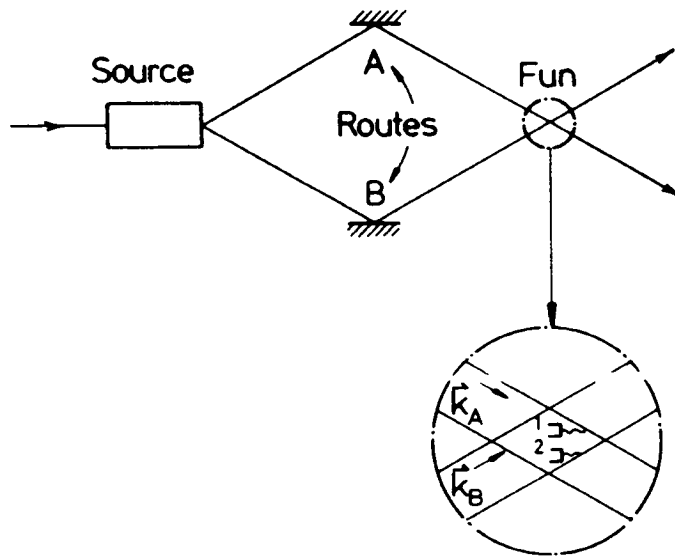
Fig. (3). The crossed-beam two-particle interferometer of Ghosh and Mandel, ref. (12). The beams of Fig. (1) here intersect so that the two-photon falling on the pair of small detectors, 1 and 2, is the beam-entangled state (8), i. e., a superposition of particle (1) in beam A and particle 2 in beam B, and vice-versa. Consequently, the coincident count rate exhibits the two-particle fringes (10); r_2 and r_1 are the positions of the detectors.
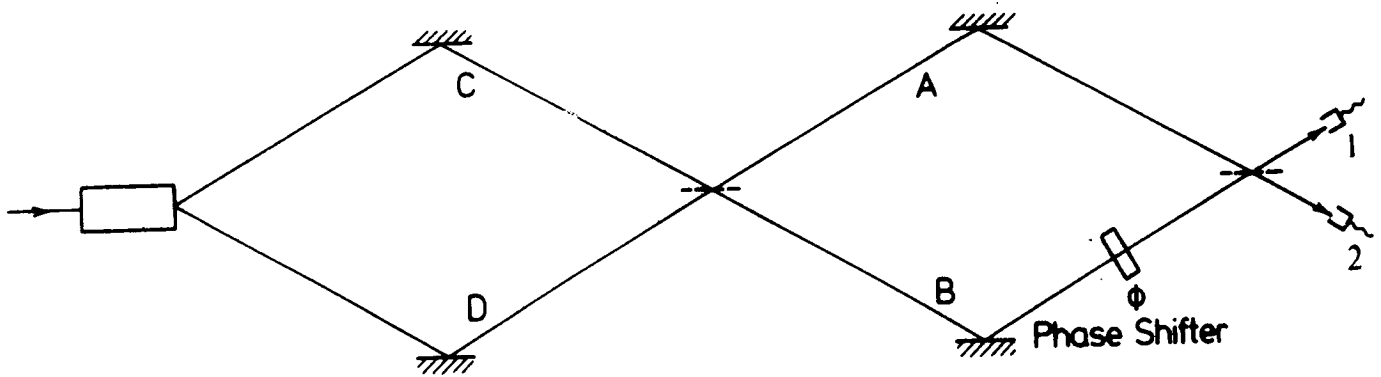
Fig. (4). A two-beam two-particle interferometer of Rarity et al., ref. (13). The beams C and D intersect on the central beam splitter and thereby prepare the beam-entangled state (12). Consequently, the coincident count rate exhibits the two-particle fringes (14), where φ is the phase shift imparted by the glass plate in beam B.

42
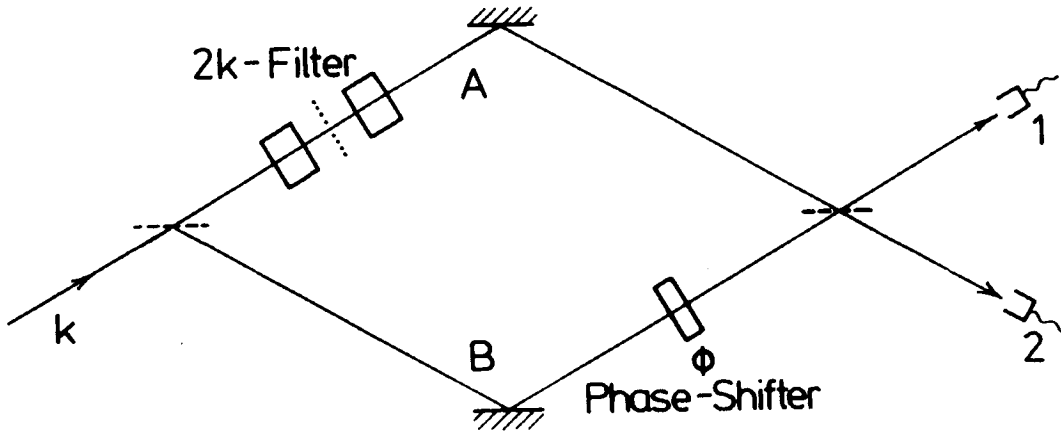
Fig. (5). A two-beam two-particle interferometer employing a number filter. Incident radiation of wavenumber k can transit beam A only if a two-photon upconverts in the first crystal, passes the filter as a 2k single photon, and then downconverts in the second crystal. Alternatively, the two-photon can take route B. Consequently the state 12 is prepared.
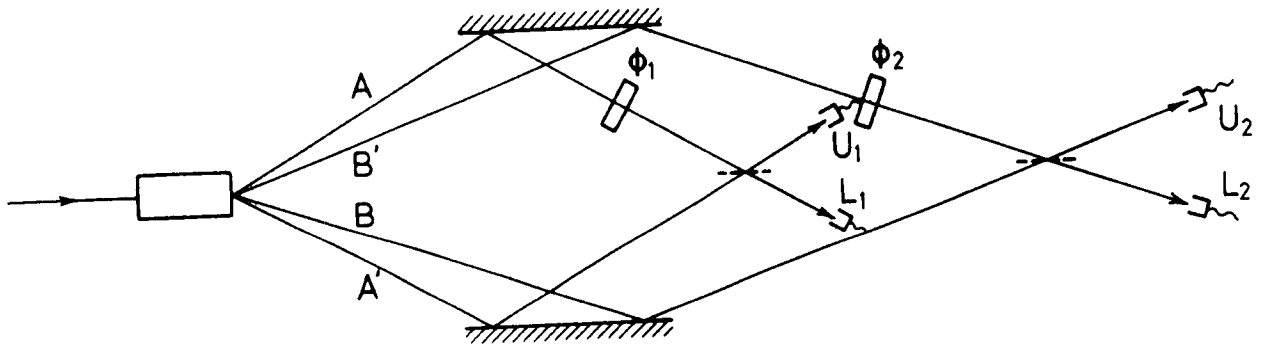
Fig. (6). Preparation of the two-particle beam-entangled state (15) by selecting four direct beams of downconversion radiation.
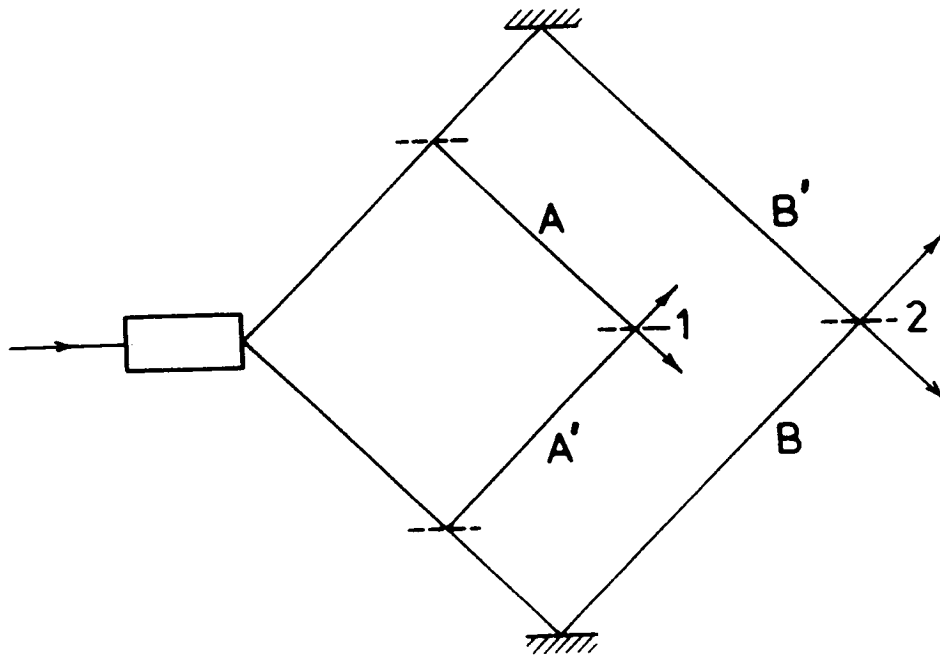
Fig. (7). Preparation of state (15) by first downconverting and then beam splitting.
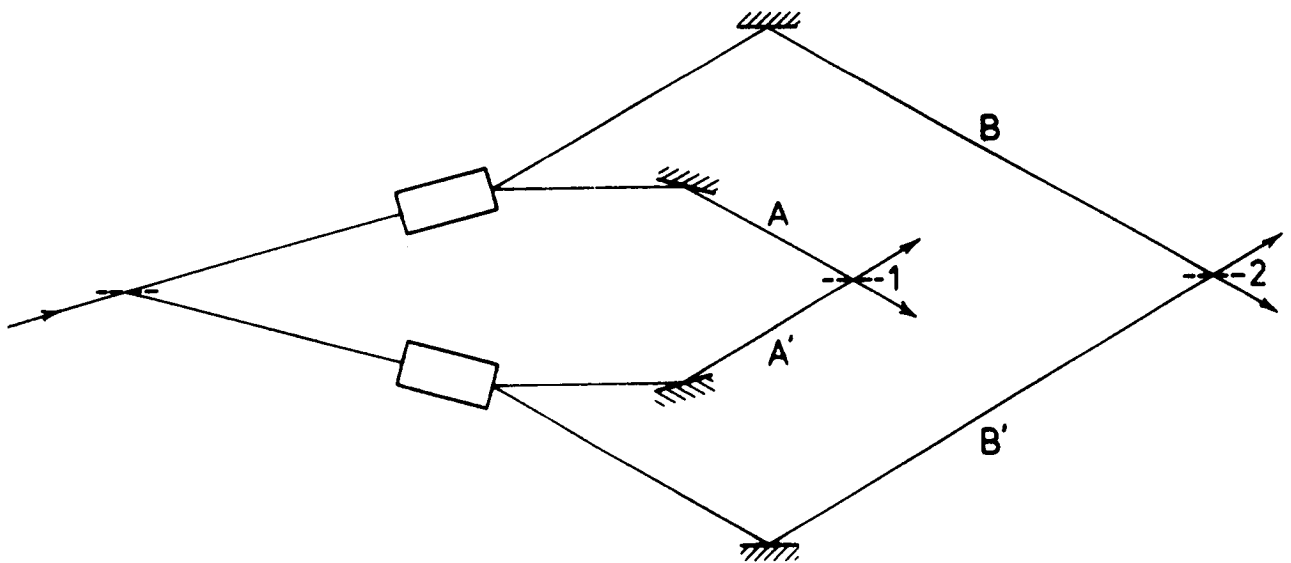
Fig. (8). Preparation of state (15) by first beam splitting and then downconverting.

44
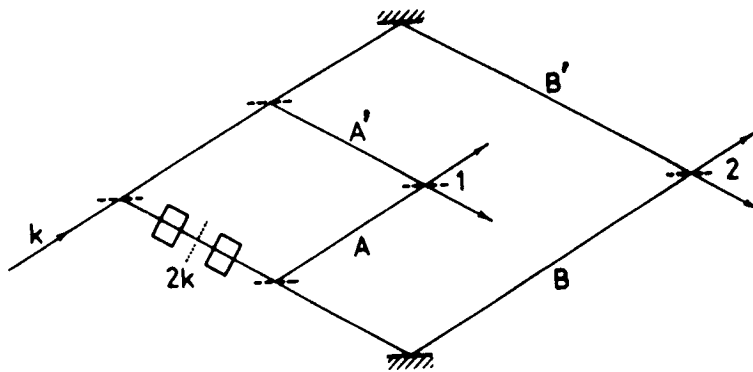
Fig. (9). Preparation of state (15) by using a number filter.
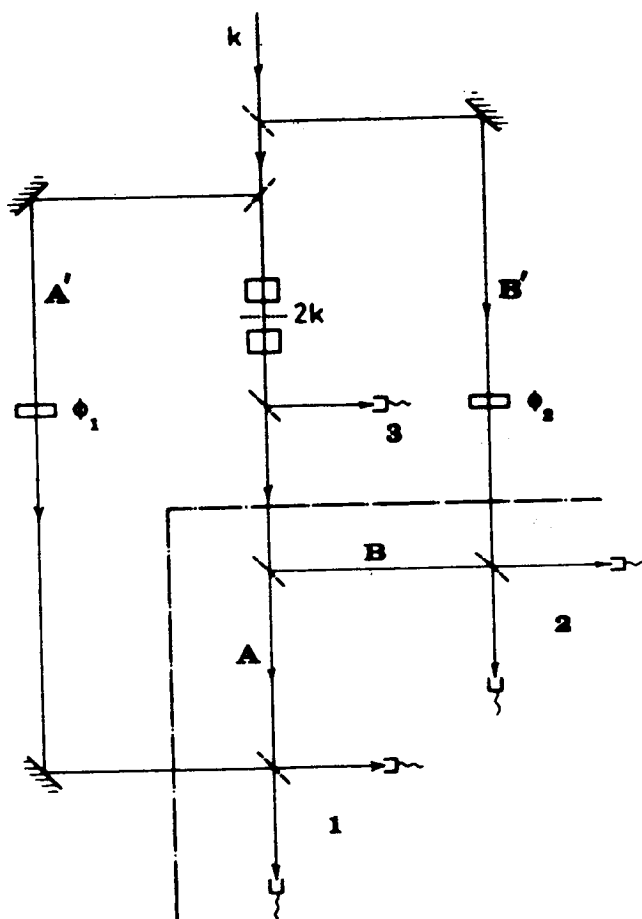
Fig. (10). An arrangement proposed by Tan, et al., ref. (19). If detector 3 is ignored, the state (15) is prepared. If detector 3 is monitored for coincidences with detectors at 1 and 2, the state (17) is prepared.
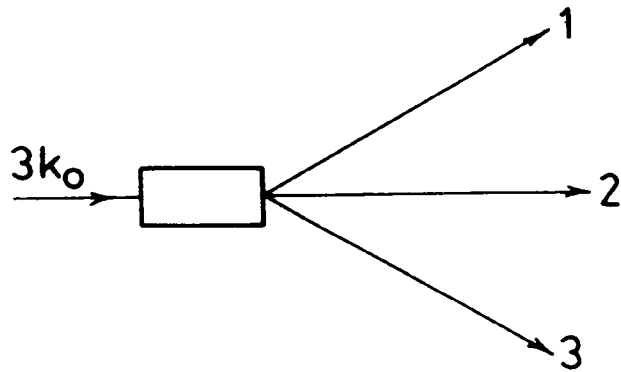
Fig. (11). Three particle downconversion to produce the color-entangled three-photon state (20) and (21). Each outgoing beam contains a filter (not shown) of width σ and centered at k_0.
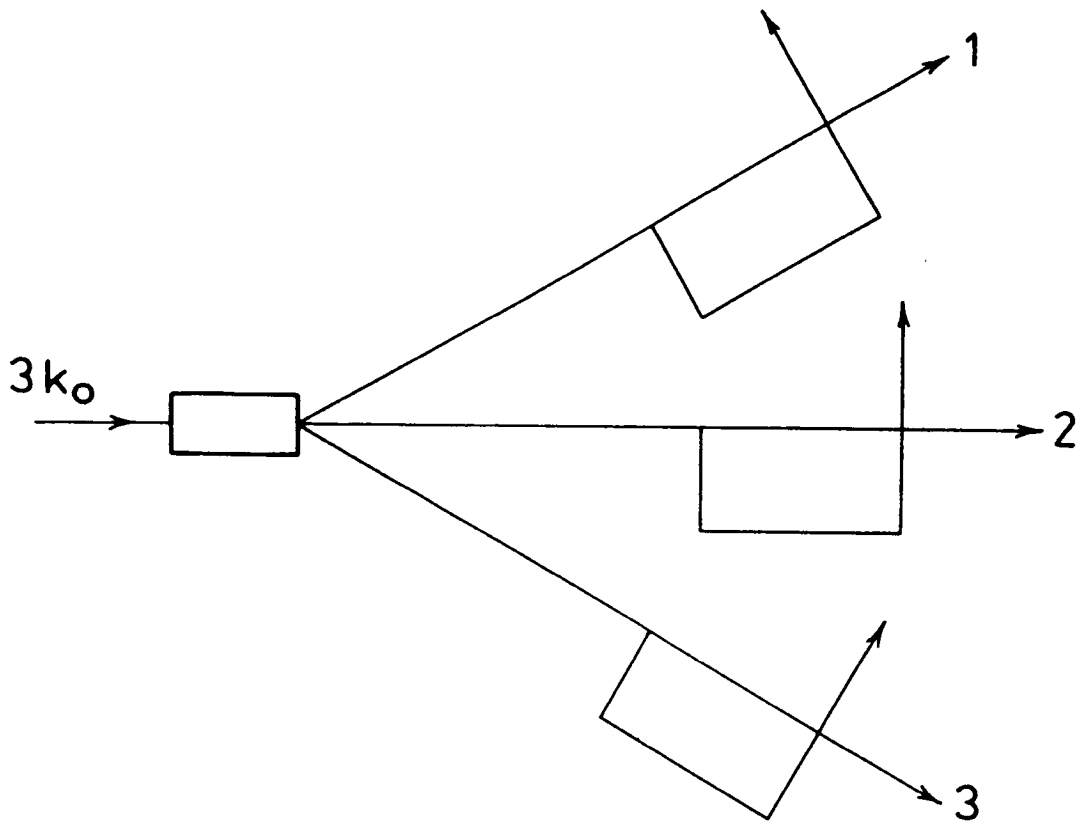
Fig. (12). A three-particle Franson type interferometer. Under ideal conditions the triple coincident count rate at corresponding outgoing beams is given by (22), where Δ is the path difference in each of the three branches.

46

EPR Experiment and Two-Photon Interferometry
— Report of A Two-Photon Interference Experiment —

Y. H. Shih, M. H. Rubin and A. V. Sergienko
Department of Physics
University of Maryland at Baltimore County
Baltimore, MD 21228

ABSTRACT

After a very brief review of the historical EPR experiments, this paper reports a new two-photon interference type EPR experiment. A two-photon state was generated by optical parametric down conversion. Pairs of light quanta with degenerate frequency but divergent directions of propagation were sent to two independent Michelson interferometers. First and second order interference effects were studied. Different than other reports, we observed that the second order interference visibility vanished when the optical path difference of the interferometers were much less then the coherence length of the pumping laser beam. However, we also observed that the second order interference behaved differently depending on whether the interferometers were set at equal or different optical path differences.

1. Historical EPR Experiments

In May 1935, Einstein, Podolsky and Rosen published a paper in the form of a paradox to show quantum mechanics fails to provide a complete description of physical reality. They put a question as the title of the paper: "Can Quantum-Mechanical Description of Physical Reality Be Considered Complete? "[1]

It seemed to EPR that a necessary requirement for a complete physical theory was the following:
(1) Every element of physical reality must have a counterpart in a complete physical theory.

EPR also suggested the following criterion for recognizing an element of reality, which seemed to them a sufficient criterion:
(2) If, without in any way disturbing the system, we can predict with certainty (i.e., with probability equal to unity) the value of a physical quantity, then there exists an element of reality corresponding to this physical quantity.

What EPR wished to do with their criteria for reality was to show that the quantum mechanics wavefunction cannot provide a complete description of all physically significant factors (or "elements of reality") existing within a system.

A clear example of such system was proposed by David Bohm in 1951.[2] Bohm's *gedankenexperiment* concerned a pair of spatially separated spin-1/2 particles produced somehow in a singlet state, for example, by disassociation of the spin-0 system. The spin part of the state may be written as:

$$| \Psi > = \frac{1}{\sqrt{2}} [\ | \hat{n}_1^+ > \otimes | \hat{n}_2^- >$$
$$- | \hat{n}_1^- > \otimes | \hat{n}_2^+ >] \quad (1)$$

where $| \hat{n}_1^\pm >$ quantum mechanically describes a state in which particle 1 or 2 has spin "up" or "down" respectively along the direction $\hat{n}$. Since the singlet state $| \Psi >$ is spherically symmetric, $\hat{n}$ can be specified to be any direction. Suppose one can set up his

experiment to measure the spin of the particles in any direction and he wants to measure the spin of particle 1 along the $\hat{x}$ axis. What he can measure is not predetermined by the quantum state $|\Psi\rangle$. However from $|\Psi\rangle$ one can predict with certainty that if particle 1 is found to have its spin parallel to the $\hat{x}$ axis, then particle 2 will immediately be found to have its spin antiparallel to the $\hat{x}$ axis if the $\hat{x}$ component of its spin is also measured. Thus one can arrange his experimental apparatus in such a way that he can predict the value of the $\hat{x}$ component of spin of particle 2 presumably without any way disturbing it. According to the criterion, the $\hat{x}$ component of spin of particle 2 is an element of reality. Likewise, one can also arrange his apparatus so that he can predict any other component of the spin of particle 2 without interacting with it. The conclusion would be all the $\hat{x}$, $\hat{y}$, $\hat{z}$ components of the spin of each particle are the elements of physical reality, and of course all the σ_x, σ_y, σ_z, must exist without considering which component is being measured. But this is not true in quantum mechanics, the wavefunction can specify, at most, only one of the components at a time with complete precision. The conclusion is that the wavefunction does not provide a complete description of all elements of physical reality.

The existence of an entangled quantum state is the heart of the E.P.R. argument. It must be a entangled pure state . There must be a definite phase relation among the amplitudes of the state. Does any such quantum state exist ? Yes, experiments have demonstrated the existence of such quantum states.

(1). Positronium Annihilation

The existence of the pure two photon singlet state of the positronium annihilation was predicted by J. A. Wheeler in late 40's and experimentally proved by C. S. Wu and I. Shaknov in 1950.[3]

(2). Atomic Cascade Decay

Atomic cascade decay were introduced to EPR experiments in 1970's. Several groups of researchers have demonstrated the existence of the pure two photon EPR state from the atomic cascade decay. Since 1965, when J. Bell provided a theory to show that the local deterministic hidden variable theory has different predictions from those of quantum mechanics in some special experimental situations, experiments have been performed to test his inequalities using the light quanta pair prepared from the atomic cascade decay.[4] Even though it is hard to believe that the photon pair emitted from the atomic cascade decay are phase correlated when considering the rather long life time intermediate state of the atom, the experimental results seemed to show that the phase correlation is really there. Bell's inequalities are violated in most of the experiments.

However, none of the above experiments has completely satisfied the serious physics community. One of the problems is the efficiency "loophole". The emission of the photon pairs do not have a defined K vector direction in both the positronium annihilation and atomic cascade decay experiments. The emission is symmetric in 4π solid angle and the collection angle can not be very large. The low collection efficiency in these experiments has been criticized by dozens of physicists and philosophers. It was concluded that none of these experiments was a compelling test of Bell's inequality, or in other words that none of these experiments has really demonstrated the phase correlation of the EPR state.

(3). Parametric Down Conversion

The first EPR experiment using light quanta pair generated by optical parametric down conversion[5] is illustrated in figure 1. The two quanta polarization pure quantum state is prepared with the help of beam splitter.

Parametric down conversion generates photon pairs with definite **K** vectors. The collection efficiency could be 100%. It is also different than all the other EPR experiments in that the entangled pure quantum state is "made" by people instead of God. The down conversion state starts from a circular or linear polarized eigenstate depending on whether quarter wave plate or half wave plate are used. It seems like "nothing hidden" in this experiment. With the help of a 50-50 beam splitter, the following quantum states can be "made",

$$| \Psi > = \frac{1}{2} e^{i(\alpha+\beta)} [| R_1 > \otimes | R_2 >$$
$$- | L_1 > \otimes | L_2 >]$$
$$+ \frac{1}{2} e^{i(\alpha_1+\beta_1)} | R_1 > \otimes | L_1 >$$
$$- \frac{1}{2} e^{i(\alpha_2+\beta_2)} | R_2 > \otimes | L_2 >$$

or,

$$| \Psi > = \frac{1}{2} e^{i(\alpha+\beta)} [| X_1 > \otimes | Y_2 >$$
$$+ | Y_1 > \otimes | X_2 >]$$
$$+ \frac{1}{2} e^{i(\alpha_1+\beta_1)} | X_1 > \otimes | Y_1 >$$
$$+ \frac{1}{2} e^{i(\alpha_2+\beta_2)} | Y_2 > \otimes | X_2 >$$

respectively. For the coincidence measurement, only the first two terms contribute. They are the singlet states needed for the EPR experiments. For the coincidence measurements, one would have:

$$|< X_1 Y_2 | \Psi >|^2 = |< Y_1 X_2 | \Psi >|^2 = 50\%$$

$$|< X_1 X_2 | \Psi >|^2 = |< Y_1 Y_2 | \Psi >|^2 = 0.$$

and

$$| < X_1(\theta_1) X_2(\theta_2) | \Psi >^2 |$$
$$= \frac{1}{2} \sin^2(\theta_1+\theta_2) = \frac{1}{2} \sin^2\varphi$$

The experimental results agreed with the quantum mechanics prediction very well.[5],[6]

2. Two Photon Interference Experiment

All the above historical EPR experiments are concerned polarization correlation measurements. J. D. Franson proposed a new type EPR experiment[7] for measurement of position and time correlation in contrast to the historical measurement of polarization correlation. This proposed experiment is also concerned to be a two-photon interference experiment. This experiment may be simply illustrated in Fig. 2: a pair of time and frequency correlated photons is generated. One travels to the left, another travels to the right and both goes through a independent interferometer. The optical path difference $\Delta L_1 = L_1 - S_1$ and $\Delta L_2 = L_2 - S_2$ can be arranged to be shorter or longer then the coherence length of the down converted field.

Case 1. $\Delta L_1 <$ coherence length

Both interferometer I and II (or one of them, if only one interferometer satisfy the condition) will have independent first order interference,

$$R_i = R_{oi} \cos^2(\delta_i/2), \qquad (2)$$

where R_i is the counting rate of the ith detector, δ_i is the phase difference between the L_i and S_i optical paths of the independent interferometer. The classical coincidence rate is expected to be,

$$R_c = R_{oc} \cos^2(\delta_1/2)\cos^2(\delta_2/2). \qquad (3)$$

The same result comes from quantum calculation.

49

Case 2. $\Delta L_i >$ coherence length

The first order interference disappears from both interferometers. It was suggested by Franson that the following coincidence detection probability amplitudes can be treated coherently,

(photon #1 travel from path S_1)

⊗ (photon #2 travel from path S_2)

and

(photon #1 travel from path L_1)

⊗ (photon #2 travel from path L_2),

if the travel time difference between the long and short paths of the two interferometers are equal.

The amplitudes:

(photon #1 travel from path S_1)

⊗ (photon #2 travel from path L_2)

and

(photon #1 travel from path L_1)

⊗ (photon #2 travel from path S_2)

will be cut off by the time window of the coincidence circuit if the travel time difference between the long and short paths is larger then the time window or will contribute to the noise if the time window of the coincidence circuit is not short enough.

The coincidence counting rate was predicted to be

$$R_c = \frac{1}{4} R_o \cos^2\left\{[(\omega_1 + \omega_2)\cdot\Delta T + \phi_1 + \phi_2]/2\right\}$$

$$= \frac{1}{4} R_o \cos^2\left\{\delta_1/2 + \delta_2/2\right\} \qquad (4)$$

where ΔT is the travel time difference

between the long and short paths of the two independent interferometers and ϕ_i, any other phase shift. Eq. (4) shows a 100% interference modulation for an arbitrary time difference of ΔT, in other words, the interference pattern will be the same even when the optical path difference of the interferometer is much longer (infinite) then the coherence length of the field. It was suggested that this prediction leads to a violation of Bell's inequality and a quantum non-local effect. Compared to the historical E.P.R. experiments, which used polarization as a measured quantity, this experiment is looking at the direct phase correlation between the long-long and short-short path amplitude. Unlike the other second order interference experiments which superpose the two photons at a beamsplitter, the photon pair never "come" together in this proposed experiment. The "interference" can not be explained by the idea of definite field phase relation at the beamsplitter as usually do. The experiment simply counts the timing of the detections and through the timing analyzer to distinguish the coincidence detection and the noncoincidence detection, i.e., the phase relation will be explored through the timing of detection and the width of the time window of the timing analyzer.

Since then, two experiments have reported the observation of the quantum mechanical effect.[8],[9] However, it seems that these two experiments did not provide enough data and information to support the conclusion that the quantum non-local effect was detected. Both experiments reported only one visibility measurement for one setting of the optical path difference of the interferometers. More measurements are required to test Franson's calculation. We report a similar two-photon interference experiment with more measurements and different results.

The experimental arrangement is shown in Fig. 3. A 351 nm CW Argon laser line was used to pump a 50 mm long

potassium dihydrogen phosphate (KDP) nonlinear crystal for optical parametric down conversion. Nonlinear optical parametric down conversion produces correlated pairs of photons which satisfy the phase-matching condition:

$$\omega = \omega_1 + \omega_2, \qquad k = k_1 + k_2, \qquad (5)$$

where ω and k are the frequency and the wave vector of the pumping beam, ω_1, ω_2 and k_1, k_2 are the frequencies and the wave vectors of the generated light quanta. The KDP crystal was cut at TYPE I phase-matching angle for degenerate frequency but divergent propagation direction of signal and idler light quanta. The 702 nm photon pair was selected by pinholes and traveled to two independent Michelson interferometers (I and II). Two detectors D_1 and D_2 with 10 Å spectral filters (centered at 702 nm) were placed after the interferometers. The detectors were avalanche photodiodes operated in Geiger mode with less then 1 nonasecond rise time and less then 50 picosecond time jitter. The output pulses from D_1 and D_2 were sent to a coincidence counting circuit which had a 100 picosecond time window to record R_c, the counting rate of coincidence and R_1, the counting rate of single detector.

Before the experiment, we first measured the coherence length of the down converted field by using our Michelson interferometer. It was concluded by direct observation with out any spectral filter that the first order interference pattern disappeared at about 50 μ from the white light condition. The coherence length of the pump laser beam was measured to be much much longer than 50 mm (limited by the interferometer).

The experiment was done by two steps:

First, interferometer II was set with $\Delta L_1 = 5$ mm from white light condition and interferometer II was scanned from the white light condition to 5 mm. 96% second order and 82% first order interference visibilities were observed at the beginning of the scanning (near white light condition), see Fig. 4 and Fig. 5. The fist order interference visibility dropped to 0 at 400 μ (with 10 Å spectral filter). The second order interference visibility is reported in Fig. 6. It is important to mention that the noise counting rate was not subtracted from the visibility calculation (the same as the other reports)

$$V = \frac{R_{max} - R_{min}}{R_{max} + R_{min}}. \qquad (6)$$

Because the short time window of the coincidence measurement, the noise counting rate for the second order interference measurement was almost zero. On the other hand, the noise counting rate from single detector (first order interference measurement) was significant. It is clear from Eq. (6) that the contribution of the noise counting rate will result a lower visibility. It can not be concluded that the "second order coherence length is longer than the first order coherence length", or "the visibility of second order interference is better than that of the first order interference" as in some of the early reports.

The second order visibility was measured to be zero at $\Delta L_2 = \Delta L_1 = 5$ mm, this is different than Franson's prediction.

Second step of the experiment, interferometer II was moved 400 μ at a time from $\Delta L_2 = 400$ μ to $\Delta L_2 = 6$ mm and interferometer I was scanned around the position of equal path difference,

$\Delta L_2 \simeq \Delta L_1$, for 50 μ and the visibility of the second order interference was measured. Fig. (7) reports this measurement. It is clear that the second order interference visibility (for $\Delta L_2 \simeq \Delta L_1$) did drop to zero at about 4 mm from the white light condition which is much shorter than the coherence length of the pumping laser beam. However, it is also true that the visibility for equal optical path difference measurement did not drop to zero as quick as that for non-equal optical path difference measurement which was reported at step one. It takes six to seven times longer distance to approach 10% visibility when the optical path difference are equal (compare Fig. (6) and Fig. (7)).

The alignment of the optical system is important. The alignment of the interferometers were checked before taking of date. We use He-Ne laser and sodium discharge light to check the alignment for ΔL from white light condition to 10 mm.

A classical model predicts that the visibility of second order interference in the case of long coincidence time compared to the coherence time of the down converted beam approaches

$$V = \frac{1}{2} \exp -(\Delta L / L) \qquad (7)$$

where $\Delta L = \Delta L_1 = \Delta L_2$, and L is a constant in length which expresses the precision to which the phase matching condition in Eq. (5) is satisfied. The same result may be obtained from a quantum mechanical model. The details of these models will be presented later elsewhere.

Reference

1. A. Einstein, B. Podolsky and N. Rosen, Phys. Rev. **47**, 777 (1935).

2. D. Bohm, "Quantum Theory", Prentice Hall Englewood Cliffs, (1951).

3. C. S. Wu and I. Shaknov, Phys. Rev. **77**, 136 (1950).

4. For a review, see J. F. Clauser and A. Shimony, Rep. Prog. Phys. **41**, 1881, (1976).

   A. Aspect, P. Grangier and G. Roger, Phys. Rev. Lett. **47**, 460 (1981).

   A. Aspect, P. Grangier and G. Roger, Phys. Rev. Lett. **49**, 91 (1982).

   A. Aspect, J. Dalibard and G. Roger, Phys. Rev. Lett. **49**, 1804 (1982).

5. Y. H. Shih and C. O. Alley, Phys. Rev. Lett. **61**, 2921 (1988).

6. Z. Y. Ou and L. Mandel, Phys. Rev. Lett. **61**, 50 (1988).

7. J. D. Franson, Phys. Rev. Lett. **62**, 2205, (1989).

8. P. G. Kwiat, W. A. Vareka, C. K. Hong, H. Nathel, R. Y. Chiao, Phys. Rev. A, **41**, 2910 (1990).

9. Z. Y. Ou, X. Y. Zou, L. J. Wang L. Mandel, Phys. Rev. Lett. **65**, 321 (1990).
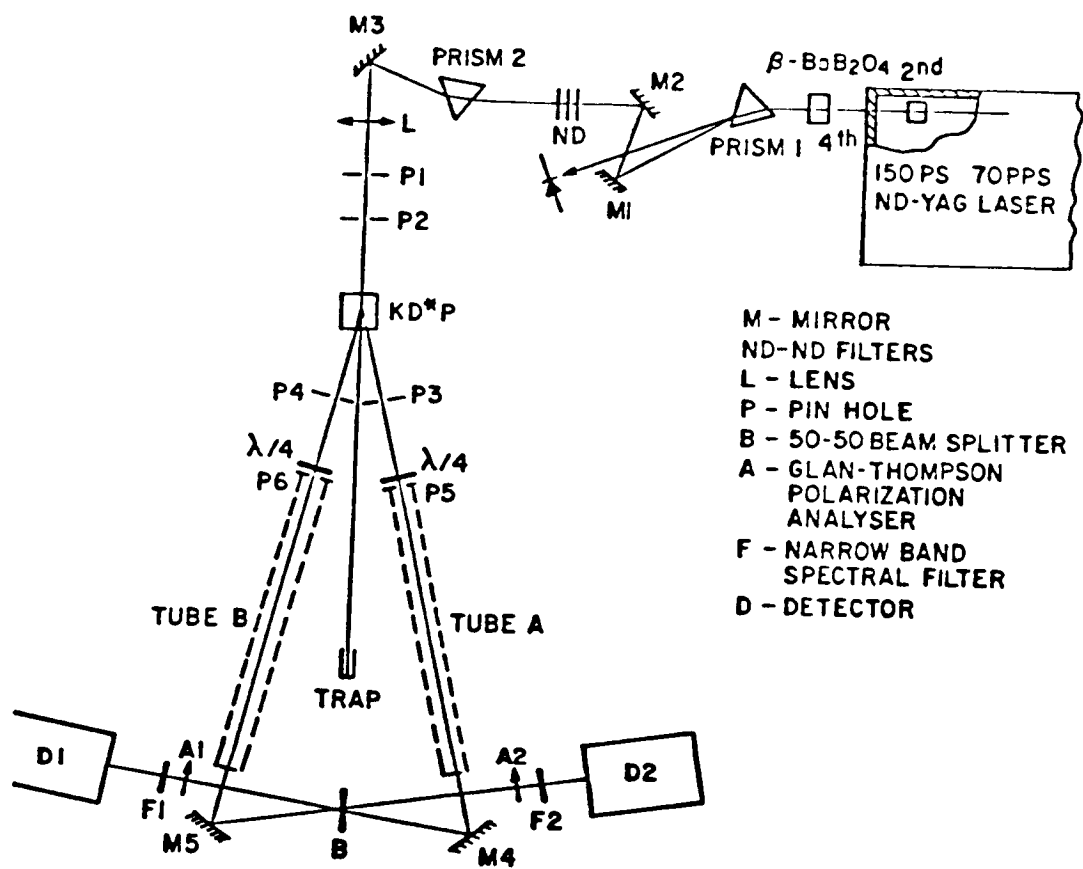
Figure 1. First EPR experiment using parametric down conversion.
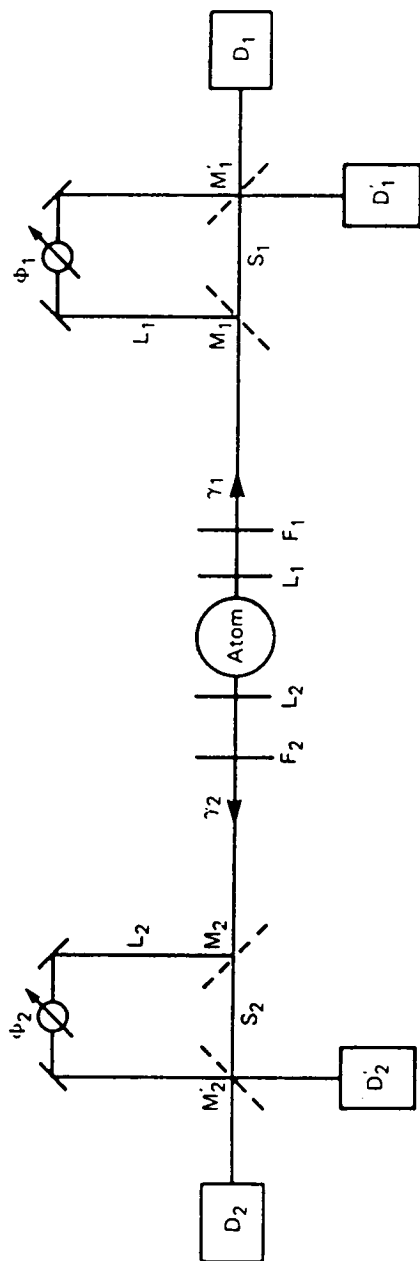
Figure 2. Proposed Franson's experiment.

351 nm

KDP

Interferometer II

702 nm   Interferometer I

step motor

L_2 S_2

S_1 L_1

S.F.

S.F.

D_2

D_1

Coincidence
100 ps window

N_2

N_1

N_C
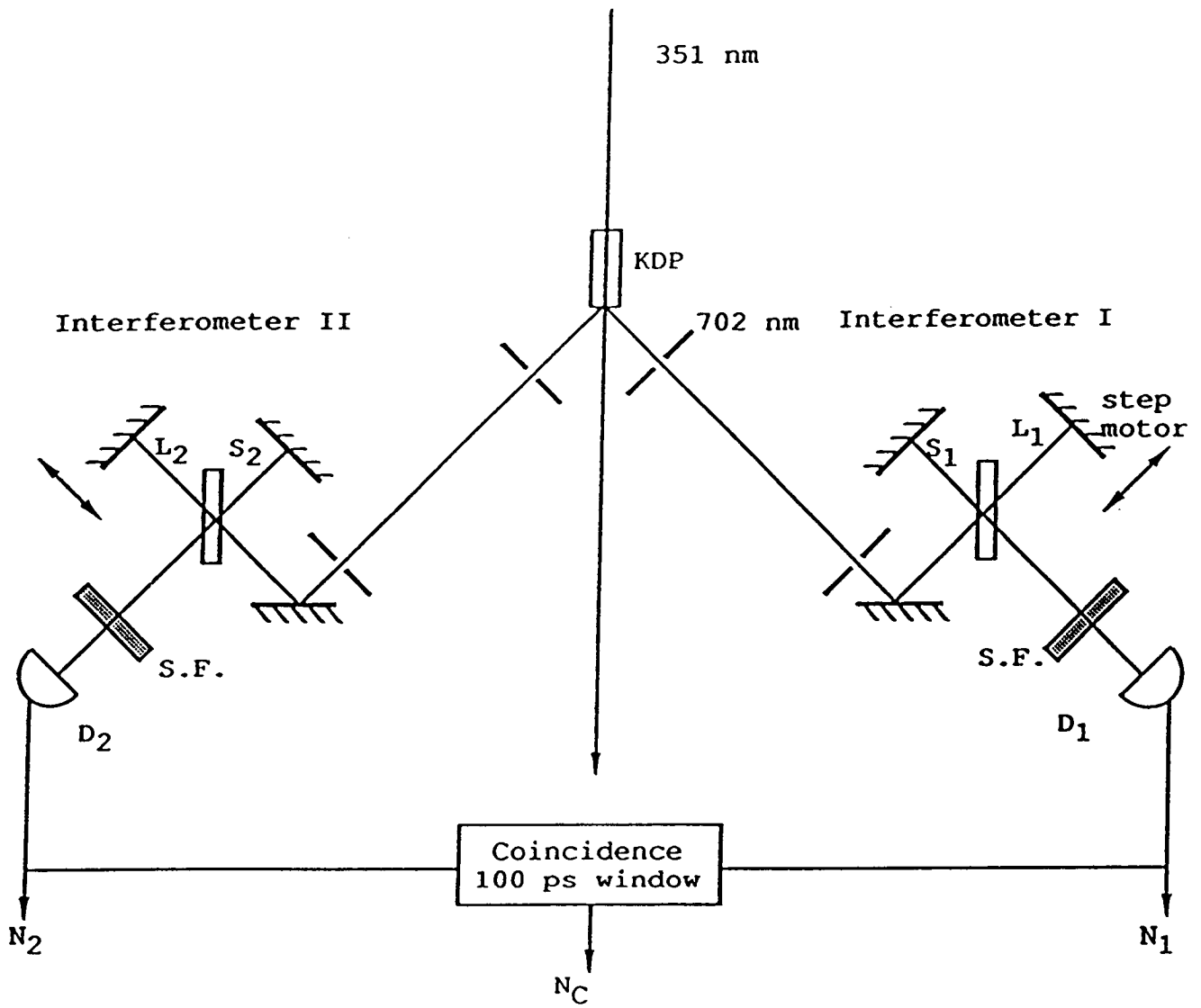
Figure 3.   Schematic diagram of the experiment.
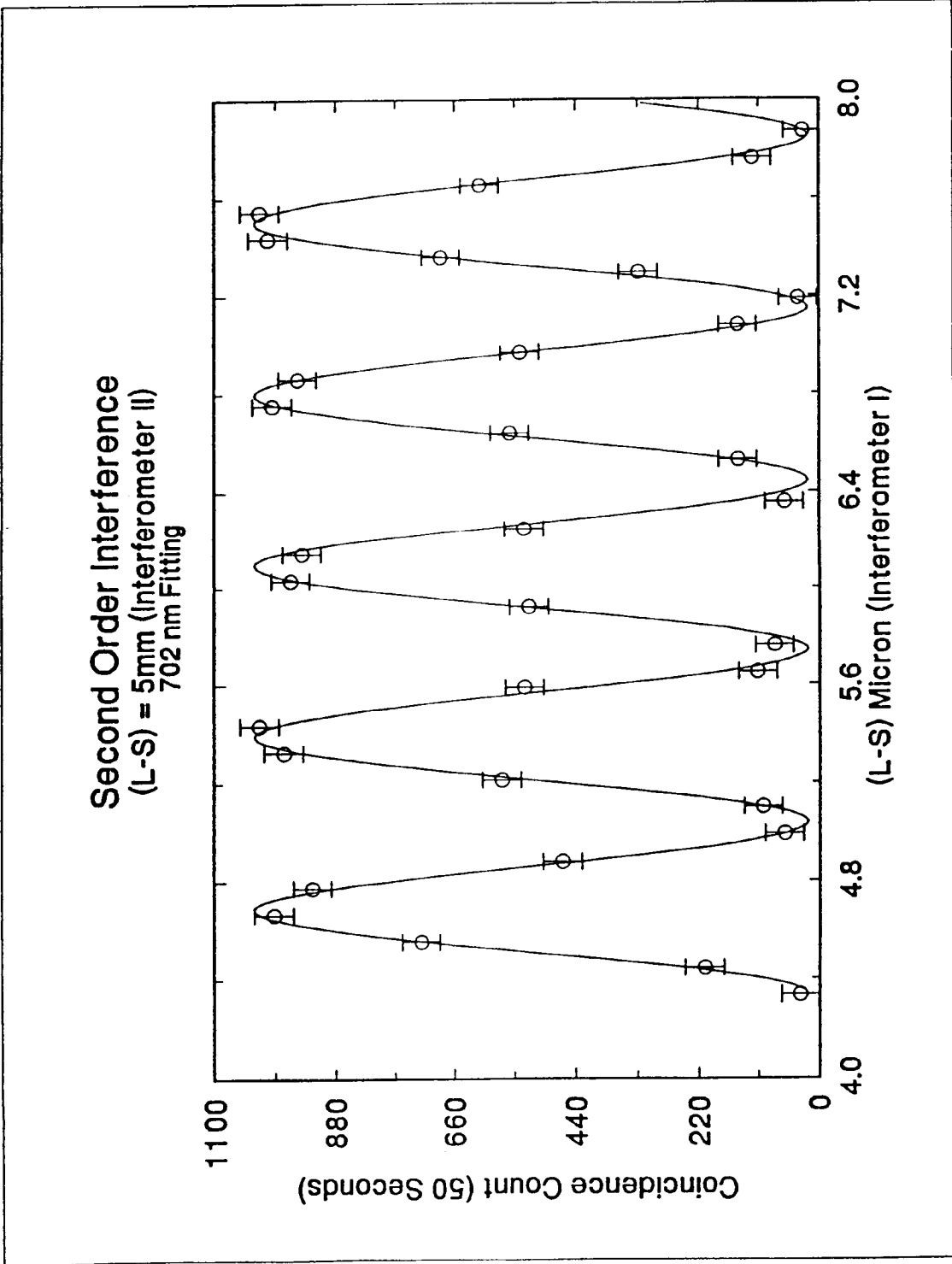
Figure 4. Second order interference (near white light condition).
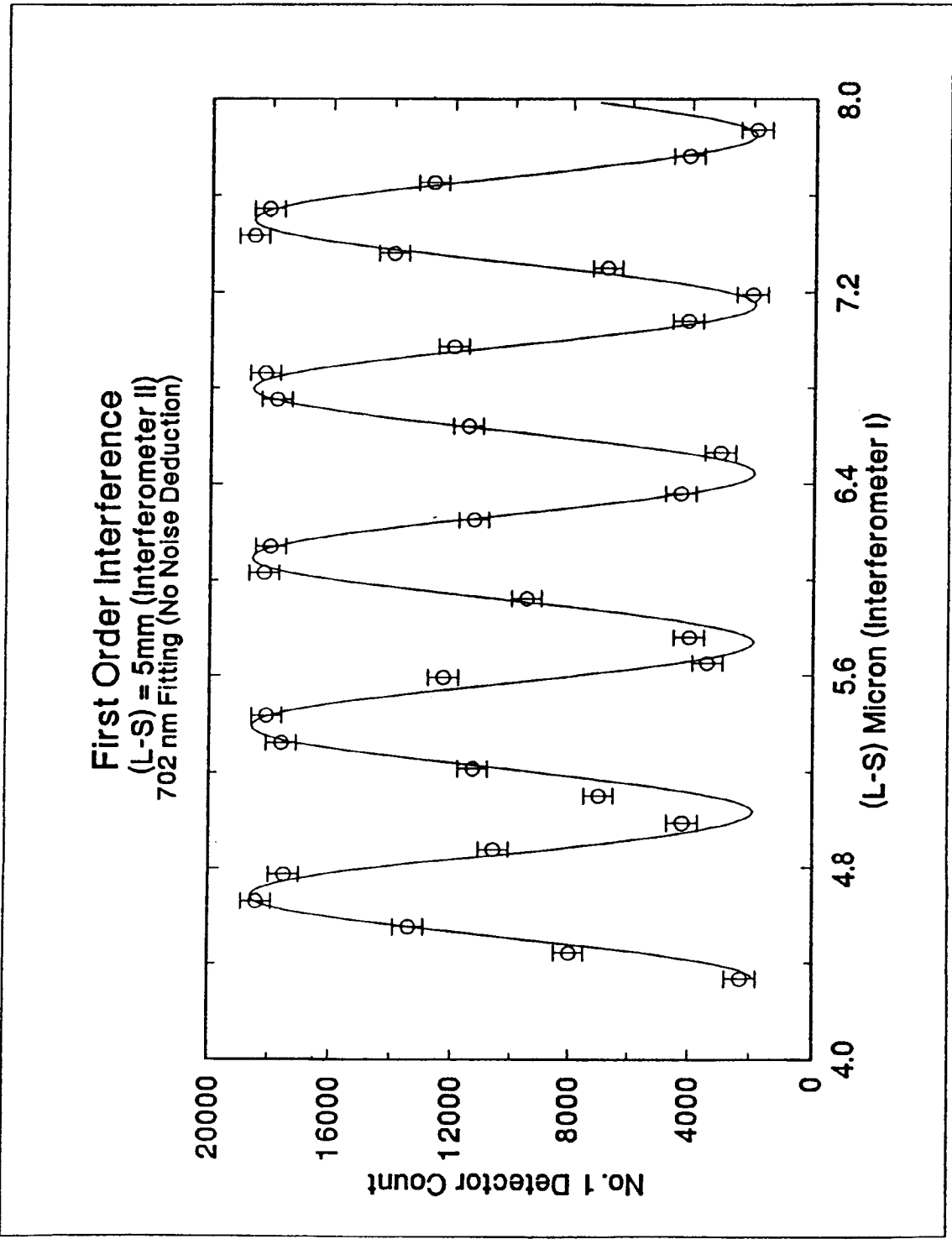
Figure 5. First order interference (near white light condition).
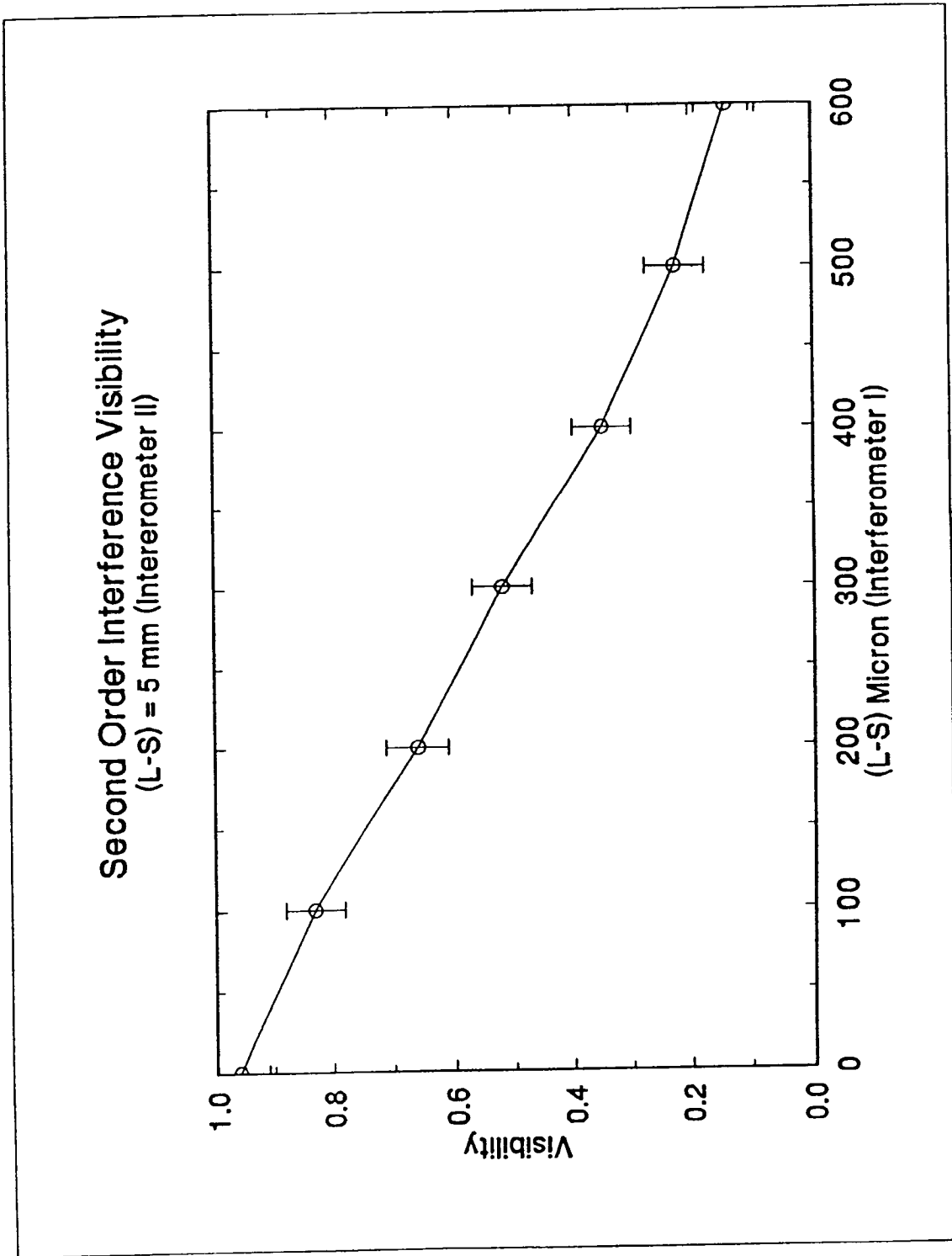
Figure 6. Second order interference visibility (non-equal optical path differences).
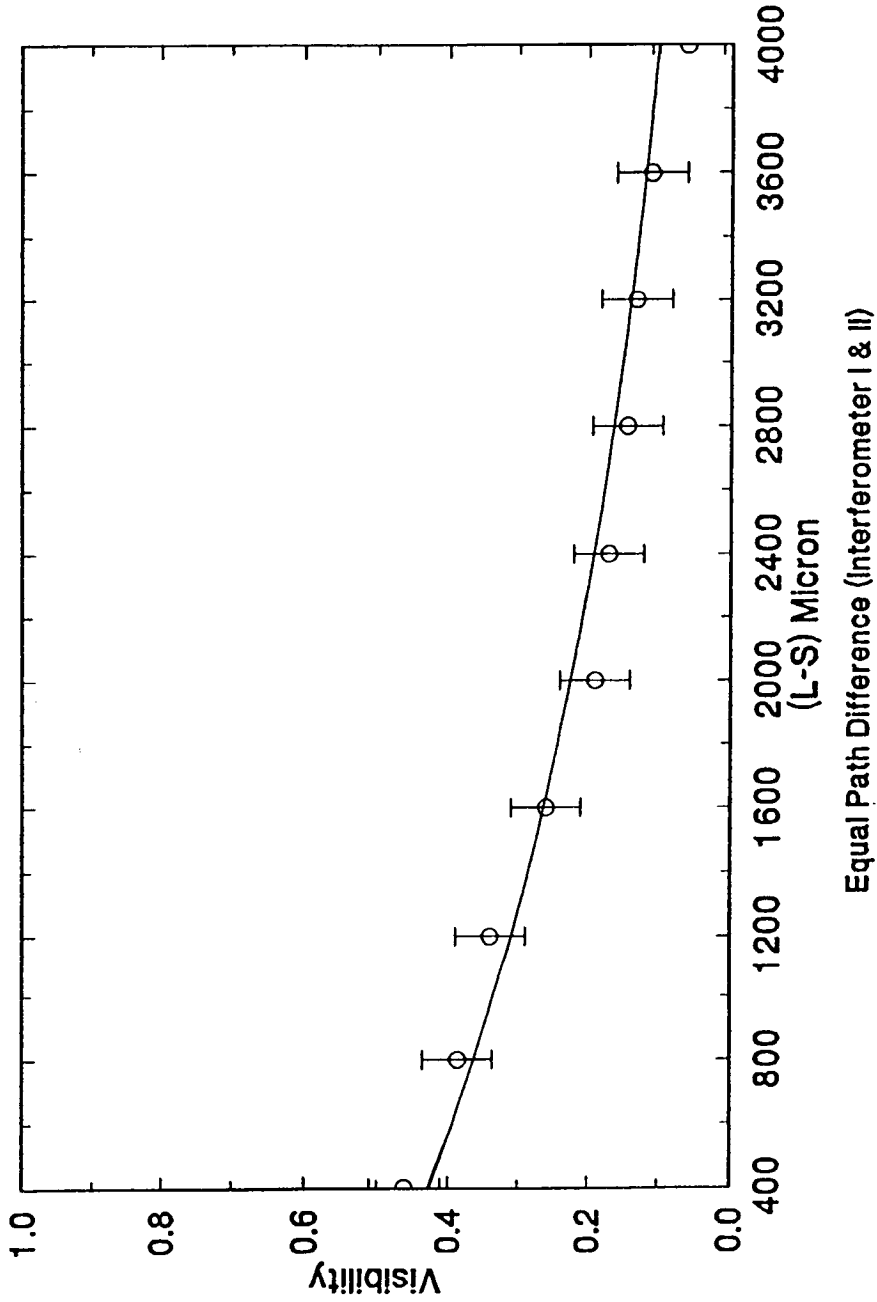
Figure 7. Second order interference visibility (equal optical path differences).

The Energy-Time Uncertainty Principle and the EPR Paradox:
Experiments involving Correlated Two-Photon Emission
in Parametric Down-Conversion*

Raymond Y. Chiao, Paul G. Kwiat, and Aephraim M. Steinberg

Department of Physics, University of California, Berkeley, CA 94720

ABSTRACT

The energy-time uncertainty principle is on a different footing than the momentum-position uncertainty principle: In contrast to position, time is a c-number parameter, and not an operator. As Aharonov and Bohm have pointed out, this leads to different interpretations of the two uncertainty principles. In particular, one must distinguish between an *inner* and an *outer* time in the definition of the spread in time Δt. It is the *inner* time which enters the energy-time uncertainty principle. We have checked this by means of a correlated two-photon light source in which the individual energies of the two photons are broad in spectra, but in which their sum is sharp. In other words the pair of photons is in an *entangled state* of energy. By passing one member of the photon pair through a filter with width ΔE, it is observed that the other member's wave packet collapses upon coincidence detection to a duration Δt, such that $\Delta E \Delta t \approx \hbar$, where this duration Δt is an *inner* time, in the sense of Aharonov and Bohm. We have measured Δt by means of a Michelson interferometer by monitoring the visibility of the fringes seen in coincidence detection. This is a nonlocal effect, in the sense that the two photons are far away from each other when the collapse occurs. We have excluded classical-wave explanations of this effect by means of triple coincidence measurements in conjunction with a beam splitter which follows the Michelson interferometer. Since Bell's inequalities are known to be violated, we believe that it is also incorrect to interpret this experimental outcome as if *energy* were a local hidden variable, i.e., as if each photon, viewed as a particle, possessed some definite but unknown energy before its detection.

PRECEDING PAGE BLANK NOT FILMED

INTRODUCTION

The momentum-position and the energy-time uncertainty principles have very similar forms:

$$\Delta p \Delta x \geq \hbar/2 \ , \tag{1}$$

$$\Delta E \Delta t \geq \hbar/2 \ . \tag{2}$$

One expects this on the basis of relativistic considerations, since both momentum-energy and position-time form four-vectors. However, in the usual formulation of quantum mechanics, there is an important difference between the two uncertainty principles, since time is not an operator but a c-number parameter, in contrast to position. Hence the standard method of derivation of the uncertainty principle for momentum and position from the fundamental commutator of quantum mechanics,

$$[p, x] = \hbar/i \ , \tag{3}$$

does not work for energy and time. Furthermore, in contrast to momentum, energy is a physical quantity with a definite *lower* bound. These difficulties are not merely mathematical ones, as pointed out by Aharonov and Bohm [Ref. 1]. There have also been many recent papers on this subject [Ref. 2].

Aharonov and Bohm made a distinction between *inner* and *outer* times. Inner time refers to an intrinsic time defined by the system itself, whereas outer time refers to a duration of measurement made by some external apparatus. They showed by construction of an explicit counterexample that the "usual" statement of the energy-time uncertainty principle in terms of an outer time, such as, "if the duration of a measurement by an external apparatus on a system is restricted to Δt, then there exists an uncontrollable amount of energy $\Delta E \approx \hbar/\Delta t$ imparted to the system by the apparatus," is incorrect. However, the standard example of the energy-time uncertainty principle in terms of energy broadening ΔE of an atomic energy level due to its finite lifetime τ, such that $\Delta E \approx \hbar/\tau$, is correct, but here the lifetime τ refers to an *inner* time of the system. The latter example of the energy-time uncertainty principle can be understood in terms of a *classical* Fourier analysis of a finite wave train of duration τ, i.e., $\Delta \omega \approx 1/\tau$.

Here we point out a *nonclassical* aspect of this uncertainty principle, which arises from the nonlocal collapse of the wave packet upon coincidence detection of a correlated pair of photons. The two correlated photons (conventionally called "signal" and "idler" photons) are prepared by spontaneous parametric down-conversion of a uv photon in a $\chi^{(2)}$ nonlinear crystal. When one member of this pair (the "remote" one) is detected through a filter with width $\Delta \omega$, the other member (the "nearby" one) immediately collapses into a wave packet of duration $\tau \approx 1/\Delta \omega$. If the remote filter is broad, the nearby photon wave packet becomes narrow upon collapse; if the remote filter is narrow, the

nearby wave packet becomes broad, upon coincidence detection. In this sense, there exists a nonlocal action at a distance. Hence it is closely related to the Einstein-Podolsky-Rosen paradox. The way we measured τ is to pass the nearby wave packet through a Michelson interferometer. If this wave packet overlaps with itself after reflection from the mirrors of the Michelson onto the recombining beam splitter, then there will be interference fringes detected in coincidence with the remote photon; otherwise interference fringes will not be visible. The wave packet duration thus measured is clearly an *inner* time of the system, since it is self-referential.

EXPERIMENT

In our experiment the incident light was prepared in an entangled state consisting of a pair of photons whose energies, $E_s = \hbar\omega_s$ and $E_i = \hbar\omega_i$, although individually broad in spectrum, sum up to a sharp quantity $E_p = \hbar\omega_p$ because they were produced from a single pump photon whose frequency ω_p was sharp. This entangled state is given by

$$\left| \psi \right\rangle = \int d\omega_s \, A(\omega_s) \left| 1 \right\rangle_{\omega_s} \left| 1 \right\rangle_{\omega_p - \omega_s} \tag{4}$$

where $A(\omega_s) = A(\omega_p - \omega_s)$ is the complex probability amplitude for finding one photon with a frequency ω_s, i.e., in the n=1 Fock state $\left| 1 \right\rangle_{\omega_s}$, and one photon with a frequency $\omega_p - \omega_s$, i.e., in the n=1 Fock state $\left| 1 \right\rangle_{\omega_p - \omega_s}$. According to the standard Copenhagen interpretation, the meaning of this entangled state is that when a measurement of the energy of one photon results in a sharp value E_s, there is a sudden collapse of the wavefunction such that instantly at a distance, the other photon, no matter how remote, also possesses a sharp value of energy $E_p - E_s$. Thus energy is conserved. Entangled states, i.e., coherent sums of product states, such as the one given by Eq. (4), result in Einstein-Podolsky-Rosen-like effects which are nonclassical and nonlocal [Refs. 3-4].

We prepared the entangled state of energy, Eq. (4), by means of parametric fluorescence in the $\chi^{(2)}$ nonlinear optical crystal potassium dihydrogen phosphate (KDP), excited by a single mode ultraviolet (uv) argon ion laser operating at λ=351.1 nm [Ref. 4]. The uv laser beam was normally incident on the KDP input face. In this fluorescence process, a single uv photon with a sharp spectrum is spontaneously converted inside the crystal into two photons with broad, conjugate spectra centered at half the uv frequency, conserving energy and momentum. We employed type I phase matching, so that both signal and idler beams were horizontally polarized. The KDP crystal was 10 cm long and cut such that the c-axis was 50.3° to the normal of its input face. We selected for study idler and signal beams both centered at λ=702.2 nm which emerged at +1.5° and −1.5°, respectively, with respect to the uv beam. Coincidences in the detection of conjugate photons were then observed.

In Fig. 1, we show a schematic of the experiment. The idler photon (upper beam) was transmitted through the "remote" filter F1 to the detector D1, which was a cooled RCA C31034A-02 photomultiplier. The signal photon (lower beam) entered a Michelson interferometer, inside one arm of

which were sequentially placed two zero-order quarter waveplates Q1 and Q2. The fast axis of the first waveplate Q1 was fixed at 45° to the horizontal, while the fast axis of the second waveplate Q2 was slowly rotated by a computer-controlled stepping motor. After leaving the Michelson the signal beam impinged on a second beamsplitter B2, where it was either transmitted to detector D2 through filter F2, or reflected to detector D3 through filter F3. Filters F2 and F3 were identical: They both had a broad bandwidth of 10 nm centered at 702 nm. Detectors D2 and D3 were essentially identical to D1. Coincidences between D1 and D2 and between D1 and D3 were detected by feeding their outputs into constant fraction discriminators and coincidence detectors after appropriate delay lines. We used EGG C102B coincidence detectors with coincidence window resolutions of 1.0 ns and 2.5 ns, respectively. Also, triple coincidences between D1, D2 and D3 were detected by feeding the outputs of the two coincidence counters into a third coincidence detector (a Tektronix 11302 oscilloscope used in a counter mode). The various count rates were stored on computer every second.

Our arrangement of quarter waveplates inside the Michelson interferometer generates a geometrical (Berry-Pancharatnam) phase, proportional to the angle θ between the fast axes of the quarter wave plates. We shall not go into detail concerning this phase here, except to say that it affords a convenient way to see interference fringes without changing the difference in arm lengths of the interferometer [Ref. 5].

We took data both outside and inside the white light fringe region where the usual interference in singles detection occurs. We report here only on data taken outside this region, where the optical path length difference was at a fixed value much greater than the coherence length of the signal photons determined by the filters F2 and F3. Hence the fringe visibility seen by detectors D2 and D3 in singles detection was essentially zero.

THEORY

First we present a simplified quantum analysis of this experiment. In the Appendix, we will present a more comprehensive analysis based on Glauber's correlation functions. The state of the light after the Michelson interferometer is given by

$$|\psi\rangle_{out} = \int d\omega_s \, A(\omega_s) \, |1\rangle_{\omega_s} \, |1\rangle_{\omega_p - \omega_s} \frac{1}{\sqrt{2}}\{1 + e^{i\phi(\omega_p - \omega_s)}\} \qquad (5)$$

where $\phi(\omega_p - \omega_s) = 2\pi\Delta L/\lambda_{\omega_p - \omega_s} + \phi_{Berry}$ is the phase shift arising from the optical path length difference ΔL of the Michelson for the photon with frequency $\omega_p - \omega_s$, plus the Berry's phase contribution for this photon. The coincidence rate N_{12} (N_{13}) between detectors D1 and D2 (D1 and D3) is proportional to the probability of finding at the same time t one photon at detector D1 placed at r_1, and one photon at detector D2 (D3) placed at r_2 (r_3). When a narrowband filter F1 centered at frequency ω_s is placed in front of the detector D1, N_{12} becomes proportional to

$$|\psi'_{out}(r_1, r_2, t)|^2 = |\langle r_1, r_2, t|\psi\rangle'_{out}|^2 \propto 1 + \cos\phi, \qquad (6)$$

where the prime denotes the output state after a von Neumann projection onto the eigenstate associated with the sharp frequency ω_s upon measurement. Therefore, the phase ϕ is determined at the sharp frequency $\omega_p - \omega_s$, or equivalently, the sharp energy $E_p - E_s$. In practice, the energy width depends on the bandwidth of the filter F1 in front of D1, so that the visibility of the fringes seen in coincidences should depend on the width of this *remote* filter. This fringe visibility will be high, provided that the optical path length difference of the Michelson does not exceed the coherence length of the *collapsed* signal photon wave packet, determined by F1. If a sufficiently broadband remote filter F1 is used instead, such that the optical path length difference is much greater than the coherence length of the collapsed wave packet, then the coincidence fringes should disappear.

RESULTS

In Fig. 2, we show data which confirm these predictions. In the lower trace (squares) we display the coincidence count rate between detectors D1 and D3, as a function of the angle θ between the fast axes of waveplates Q1 and Q2, when the remote filter F1 was narrow, i.e., with a bandwidth of 0.86 nm. The calculated coherence length of the collapsed signal photon wave packet (570 μm) was greater than the optical path length difference at which the Michelson was set (220 μm). The visibility of the coincidence fringes was quite high, viz., 60%±5%.[*] This is in contrast to the low visibility, viz., less than 2%, of the singles fringes detected by D3 alone (not shown). For comparison, in the upper trace (triangles) we display the coincidence count rate versus θ when a broad remote filter F1, i.e., one with a bandwidth of 10 nm, was substituted for the narrow one. The coherence length of the collapsed signal photon wave packet was thus only 50 μm. The coincidence fringes in this case have indeed disappeared, as predicted.

DISCUSSION

In light of the observed violations of Bell's inequalities [Ref. 6], it is incorrect to interpret these results in terms of an ensemble of conjugate signal and idler photons which possess definite, but unknown, conjugate energies before filtering and detection. Any observable, e.g., energy or momentum, should not be viewed as a local, realistic property carried by the photon *before it is actually measured.*

The function of the second beamsplitter B2 was to verify that the signal beam was composed of photons in an n=1 Fock state. In such a state, the photon, due to its indivisibility, will be either transmitted or reflected at the beamsplitter, but not both. Thus coincidences between D2 and D3 should never occur, except for rare accidental occurrences of two pairs of conjugate photons within the coincidence window. However, if the signal beam were a classical wave, then one would expect an equal division of the wave amplitude at the 50% beamsplitter, and hence frequent occurrences of

---

*The slightly nonsinusoidal component in Fig. 3 (lower trace) can be explained by a slight wedge in Q2, in conjunction with the fact the signal beam was incident on Q2 off center.

coincidences. An inequality, which was strongly violated in our experiment, places a lower bound on this coincidence rate for classical light (see below). This verifies the essentially n=1 Fock state nature of the light, and confirms the previous result of Hong and Mandel [Ref. 7].

The vertical arrows in Fig. 2 indicate the points at which triple coincidences were measured. Let us define the anticorrelation parameter [Ref. 8]

$$a \equiv N_{123} \, N_1 \, / \, N_{12} \, N_{13} \, ,$$
(7)

where N_{123} is the rate of triple coincidences between detectors D1, D2 and D3, N_{12} is the rate of double coincidences between D1 and D2, N_{13} is the rate of double coincidences between D1 and D3, and N_1 is the rate of singles detections by D1 alone. The inequality $a \geq 1$ has been shown to hold for any classical wave theory [Ref. 8]. The equality $a=1$ holds for coherent states $|\alpha\rangle$, independent of their amplitude α. Since in our experiment the amplitude fluctuations in the double coincidence pulses led to a triple coincidence detection efficiency η less than unity, we should reduce the expected value of a accordingly. The modified classical inequality is $a \geq \eta$. We calibrated our triple coincidence counting system by replacing the two-photon light source by an attenuated light bulb, and measured $\eta = 0.70 \pm 0.07$. During the data run of Fig. 2 (lower trace), we measured values of a shown at the vertical arrows. The average value of a is 0.08 ± 0.04, which violates by more than thirteen standard deviations the predictions based on any classical wave theory. It is therefore incorrect to interpret these results in terms of a stochastic ensemble of classical waves, in a semiclassical theory of photoelectric detection [Ref. 9]. Classical waves with conjugate, but random, frequencies could conceivably yield the observed interference pattern, but they would also yield many more triple coincidences than were observed.

We have therefore verified the energy-time uncertainty principle for pairs of photons in essentially n=1 Fock states, in a way which excludes with very high probability any possible classical explanation. These results can be understood in terms of the nonlocal collapse of the wavefunction.

ACKNOWLEDGMENTS

APPENDIX

A more rigorous theoretical description of the experiment can be carried out within the Glauber correlation function formalism [Ref. 10]. We start with the entangled state of the down-converted light

$$|\psi\rangle = \int d\omega_s \, A(\omega_s) \, |1\rangle_{\omega_s} \, |1\rangle_{\omega_p - \omega_s}$$
(A.1)

where $A(\omega_s) = A(\omega_p - \omega_s)$ is the complex probability amplitude for finding one photon with a frequency ω_s and one photon with a frequency $\omega_p - \omega_s$. For simplicity we have assumed that the pump photon is monochromatic. The second order correlation function relating the field amplitudes for the signal and idler modes at the times t_s and t_i, respectively, is defined as

$$G^{(2)}(t_s, t_i; t_i, t_s) = \langle \psi | \, \hat{E}_s^{(-)}(t_s) \, \hat{E}_i^{(-)}(t_i) \, \hat{E}_i^{(+)}(t_i) \, \hat{E}_s^{(+)}(t_s) \, | \psi \rangle. \tag{A.2}$$

In this expression, $\hat{E}_{s(i)}^{(-)}(t_{s(i)})$ and $\hat{E}_{s(i)}^{(+)}(t_{s(i)})$ are the negative- and positive-frequency parts of the electric field for the signal (idler) mode. Assuming, as in Fig.1, that the idler photon is directed to detector D1, the field operators for this mode at the time t_i may simply be Fourier expanded in terms of a frequency-dependent detection efficiency $|\eta_1(\omega_i)|^2$, and creation and destruction operators $\hat{a}_i^\dagger(\omega_i)$ and $\hat{a}_i(\omega_i)$:

$$\hat{E}_i^{(+)}(t_i) = \int d\omega_i \, \eta_1^*(\omega_i) \, \hat{a}_i(\omega_i) \, e^{-i\omega_i t_i} \tag{A.2a}$$

$$\hat{E}_i^{(-)}(t_i) = \left(\hat{E}_i^{(+)}(t_i) \right)^\dagger. \tag{A.2b}$$

The effects of filter F1 are included in the factor η. Similarly, the signal mode field operators may be expanded, but these require an additional factor to account for the interferometer:

$$\hat{E}_s^{(+)}(t_s) = \int d\omega_s \, \eta_2^*(\omega_s) \, \hat{a}_s(\omega_s) \, e^{-i\omega_s t_s} \frac{1}{\sqrt{2}} \left\{ 1 - e^{i\omega_s \tau} e^{i\phi_B} \right\} \tag{A.3a}$$

$$\hat{E}_s^{(-)}(t_s) = \left(\hat{E}_s^{(+)}(t_s) \right)^\dagger, \tag{A.3b}$$

where $\tau = \Delta L/c$ is the optical delay time between the arms of the interferometer, and ϕ_B is the geometrical/Berry phase.

The probability of joint detection of a signal-idler pair within the detector resolution window ΔT, after a total time $\mathcal{T}$, is then given by

$$P = \int_{-\mathcal{T}/2}^{\mathcal{T}/2} dt_s \int_{t_s - \frac{\Delta T}{2}}^{t_s + \frac{\Delta T}{2}} dt_i \, G^{(2)}(t_s, t_i; t_i, t_s) \tag{A.4}$$

In practice, the duration time $\mathcal{T}$ of any data point is essentially infinite (with respect to all relevant time-scales in the problem). In addition, for our experiment ΔT (≈ 1ns) was much greater than τ (≈ 730fs, for $\Delta L = 220 \mu$m) and the reciprocal bandwidths, $1/\Delta\omega_i$ and $1/\Delta\omega_s$, of the filters F1 and F2.

Hence, we are justified in setting the limits of integration to infinity:

$$P \approx \int_{-\infty}^{\infty} dt_s \int_{-\infty}^{\infty} dt_i \int d\omega \int d\omega' \, A(\omega) A^*(\omega') \int d\omega_s \int d\omega'_s \int d\omega_i \int d\omega'_i$$

$$\times \, \eta_1(\omega_i) \, \eta_1^*(\omega'_i) \, \eta_2(\omega_s) \, \eta_2^*(\omega'_s) \; e^{i(\omega_i - \omega'_i)t_i} \; e^{i(\omega_s - \omega'_s)t_s}$$

$$\times \, \frac{1}{2}\left(1 - e^{-i\omega_s\tau} e^{-i\phi_B}\right)\left(1 - e^{i\omega'_s\tau} e^{i\phi_B}\right)$$

$$\times \, _{\omega', \, \omega_p - \omega'}\langle 1, 1 \mid \hat{a}_s^\dagger(\omega_s) \, \hat{a}_i^\dagger(\omega_i) \, \hat{a}_i(\omega'_i) \, \hat{a}_s(\omega'_s) \mid 1, 1 \rangle_{\omega, \, \omega_p - \omega} \qquad\qquad (A.5)$$

If we assume that the probability amplitude is essentially constant $(A(\omega) \approx A_0)$ over the filter bandwidths $\Delta\omega_i$ and $\Delta\omega_s$, and that $\eta_2(\omega_s) \approx \eta_{20}$ over the bandwidth $\Delta\omega_s \gg 1/\tau$ (i.e. a broad square bandpass filter F2 in front of detector D2), then (A.5) simplifies considerably:

$$P \approx |A_0|^2 \, |\eta_{20}|^2 \int d\omega_i \, |\eta_1(\omega_i)|^2 \left\{1 - \cos\left((\omega_p - \omega_i)\tau + \phi_B\right)\right\}. \qquad\qquad (A.6)$$

We now examine the behavior of this detection probability in two limiting cases of filter F1:

1. If $|\eta_1(\omega_i)|^2 \approx |\eta_{10}|^2 \, \delta(\omega_i - \omega_{i0})$ (i.e. a very narrow filter in front of detector D1), then

$$P \approx |A_0|^2 \, |\eta_{20}|^2 \, |\eta_{10}|^2 \left\{1 - \cos\left((\omega_p - \omega_{i0})\tau + \phi_B\right)\right\}. \qquad\qquad (A.7)$$

It should be clear from (A.6) that in order to observe these fringes, it suffices to have $\Delta\omega_i \ll 1/\tau$. This is the situation in the lower trace of Fig. 2.

2. If $|\eta_1(\omega_i)|^2 \approx |\eta_{10}|^2 \, e^{-(\omega_i - \omega_{i0})^2/\Delta\omega_i^2}$, where $\Delta\omega_i \gg 1/\tau$ (we have previously stipulated the experimental condition $\Delta\omega_s \gg 1/\tau$), then

$$P \approx |A_0|^2 \, |\eta_{20}|^2 \, |\eta_{10}|^2 \, , \qquad\qquad (A.8)$$

a constant, with no fringes. The experimental results (top trace, Fig. 2) corresponding to a broad filter F1 are in agreement with these predictions.

Note that since the filter F2 is relatively broadband (i.e. $\Delta\omega_s \gg 1/\tau$), there are no fringes visible in the singles rate of detector D2, even though fringes in coincidence may be present.

REFERENCES

1. Y. Aharonov and D. Bohm, Phys. Rev. **122**, 1649 (1961).

2. P. E. Hussar, Y. S. Kim, and M. E. Noz, Am. J. Phys. **53**, 142 (1985), and references contained therein; B. A. Orfanopoulos, Phys. Essays **3**, 368 (1990).

3. M. A. Horne, A. Shimony, and A. Zeilinger, Phys. Rev. Lett. **62**, 2209 (1989).

4. P. G. Kwiat, W. A. Vareka, C. K. Hong, H. Nathel, and R. Y. Chiao, Phys. Rev. **A41**, 2910 (1990), and references therein.

5. P. G. Kwiat and R. Y. Chiao, Phys. Rev. Lett. **66**, 588 (1991).

6. J. G. Rarity and P. R. Tapster, Phys. Rev. Lett. **64**, 2495 (1990), and references therein.

7. C. K. Hong and L. Mandel, Phys. Rev. Lett. **56**, 58 (1986).

8   P. Grangier, G. Roger, and A. Aspect, Europhys. Lett. **1**, 173 (1986).

9   J. F. Clauser, Phys. Rev. **D9**, 853 (1974).

10 R. J. Glauber, Phys. Rev. **130**, 2529 (1963).
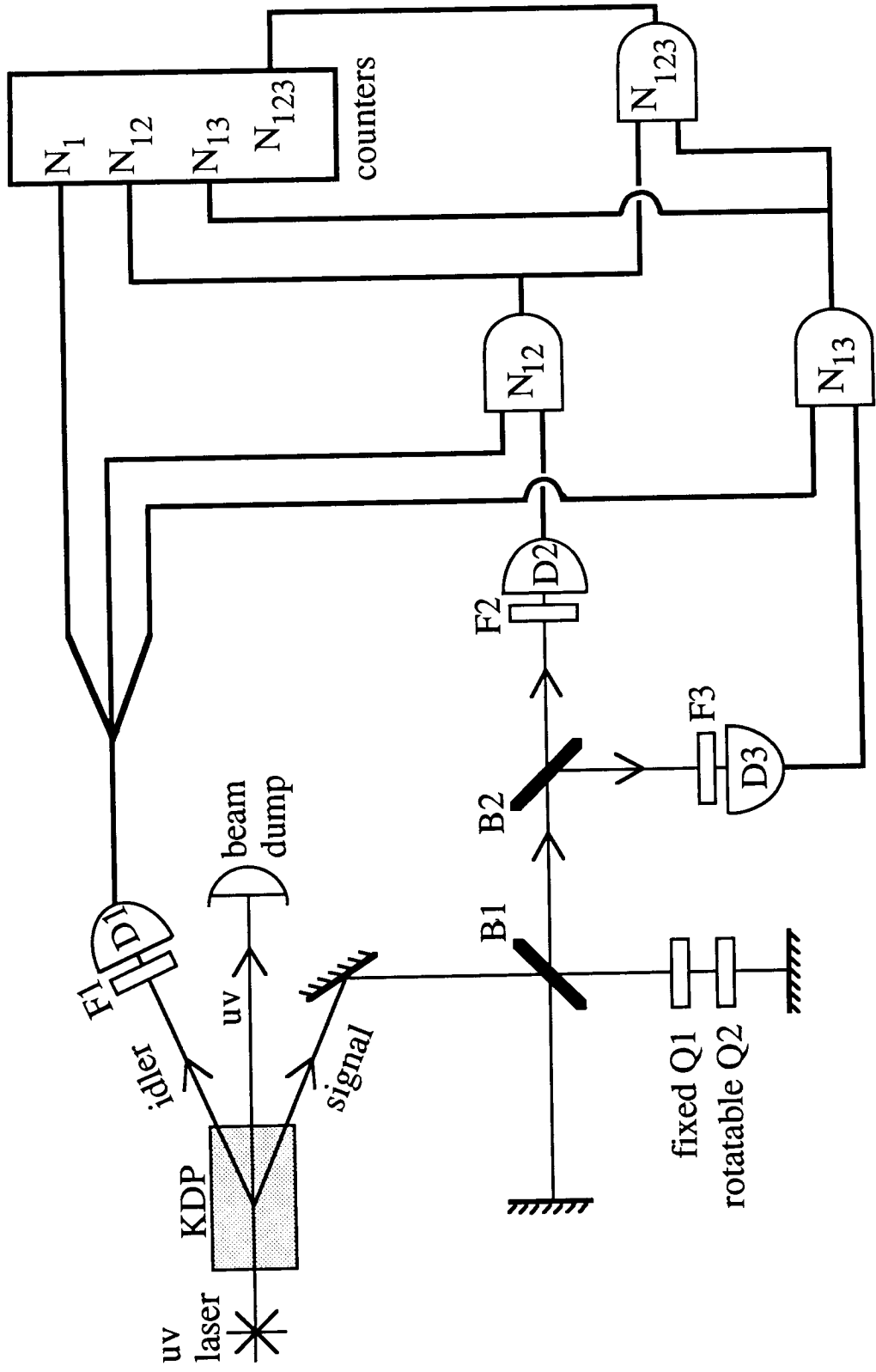
Fig. 1: Schematic of experiment to verify the energy-time uncertainty principle for correlated pairs of photons. D1, D2, and D3 are photomultipliers, Q1 and Q2 quarter waveplates, and B1 and B2 beamsplitters. Logical "AND" symbols denote coincidence detectors.
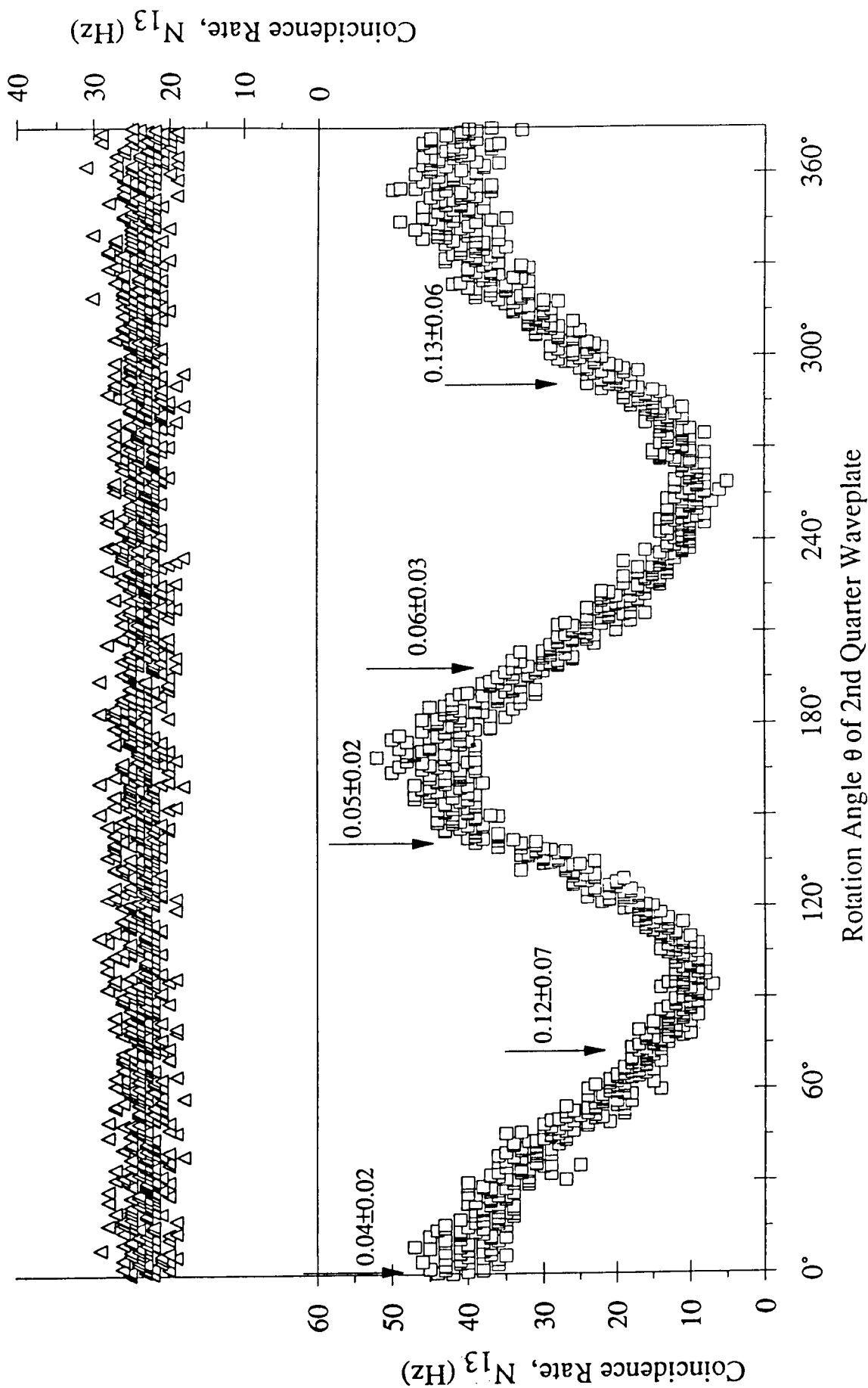
Fig. 2: Interference fringes (lower trace, squares) for an unbalanced Michelson with a slowly varying Berry's phase, observed in coincidences between D3 and D1 with a narrow remote filter F1. With a broad F1, these fringes disappear (upper trace, triangles). They also disappear when detected by D3 alone. Vertical arrows indicate where the anti-correlation parameter *a* was measured (see text).

HIGHER-ORDER QUANTUM ENTANGLEMENT

Anton Zeilinger
Institut für Experimentalphysik
Universität Innsbruck
Technikerstrasse 25
A-6020 Innsbruck, Austria

Michael A. Horne
Stonehill College
North Easton, MA 02357

Daniel M. Greenberger
Department of Physics
City College of the City University of New York
New York, NY 10031

ABSTRACT

In quantum mechanics the general state describing two or more particles is a linear superposition of product states. Such a superposition is called entangled if it cannot be factored into just one product. When only two particles are entangled the stage is set for Einstein-Podolsky-Rosen discussions and Bell's proof that the EPR viewpoint contradicts quantum mechanics. If more than two particles are involved new possibilities and phenomena arise. For example the GHZ disproof of EPR applies. Furthermore, as we point out in this paper, with three or more particles even entanglement itself can be an entangled property.

INTRODUCTION

Of the many conceptual innovations of quantum mechanics the notion of *entanglement* is gaining increasing attention over the last few years. This is because entanglement implies the quantum nonlocality as discussed by Einstein, Podolsky, and Rosen (Ref. 1) and Bell (Ref. 2). The increased attention has also led to a somewhat loose discussion of these topics, quite often lacking care with respect to the fundamental issues involved. It is therefore one of the purposes of the present paper to give a detailed discussion of the notion of entanglement.

The term "Entanglement" (in Schrödinger's original German "Verschränkung") in quantum mechanics goes back to Schrödinger's famous 1935 paper (Ref. 3) where he gives a general confession, as he calls it, of his understanding of the situation of quantum mechanics at that time. Most of the analysis of the

measurement problem presented in Schrödinger's paper rests on the properties of nonfactorizable states of two-particle systems as first discussed in the same year by Einstein, Podolsky and Rosen (EPR). Here we shall first briefly review entanglement for the case of two particles. Then, focussing on situations where three particles are entangled, we will see that entanglement itself can be an entangled property.

TWO PARTICLES

For two-particle systems the best known entangled states are those which exhibit entanglement of spin variables, e.g. in the case of two spin-1/2 particles with total spin zero this is the singlet state (Ref. 4)

$$|\psi> = \sqrt{1/2} \ [\ |+>_1|->_2 \ - \ |->_1|+>_2].$$

(1)

Here, $|+>_1$ describes particle one with spin up etc. Because of the rotational symmetry of the singlet state the direction along which the spins are defined in Eq. (1) need not be specified.

As can easily be seen, the state of Eq. (1) does not make any specific predictions for spin measurement results on either particle, but it makes the definite prediction that, as soon as the spin of one particle is found to be oriented along one direction, the spin of the other one will be found to be oriented along the opposite direction should it be measured along that direction. Schrödinger calls this property "entanglement of predictions" or "entanglement of our knowledge of the two bodies". As in classical physics, one might draw up before the measurement an expectation catalog which gives the possible measurement results together with the probabilities of these various results. In quantum mechanics, the expectation catalog has to be calculated from the quantum state of the system.

While in classical mechanics the combined expectation catalog for two objects (bodies, particles, pieces...) can always be written as the logical sum of the expectation catalogs of the individual systems, this is not possible anymore in quantum mechanics for the case of entangled states. Or, in other words, while in classical physics (and certainly in the case of factorizable quantum states) disjoint catalogs for two bodies that once did interact exist, in quantum mechanics this is generally not true anymore. Or, in Schrödinger's original words: *Maximal knowledge of a total system does not necessarily include total knowledge of all its parts, not even when these are fully separated from each other and at the moment are not influencing each other at all.* This results in the interesting nonlocality questions in quantum mechanics.

Consider a measurement on particle 1 along some direction. The experimenter is certainly free to choose this direction at will, call it direction **n**. The experimental result for particle 1 along that

direction can either be + ("up") or - ("down"). The entangled state (Eq. 1) implies that particle 2 is then either in the state $|-n>_2$ if particle 1 was found to be up along n, or particle 2 is in the state $|+n>_2$ if particle 1 was found to be down along n. This is simply a consequence of the von Neumann reduction of the state vector which is equivalent to the property that, upon measurement of particle 1, the expectation catalog for particle 2 changes to be in agreement with the result for particle 1 and the predictions obtained from the entangled state (Eq. 1).

In the case of two particle-entanglement just discussed it is the experimenter's choice of the direction along which she measures the spin of particle 1 which determines that particle 2 will be in an eigenstate along that direction. Which specific eigenstate of the two possible ones it will be is completely random and outside the influence of the experimenter, it is "Nature's choice". We might also express this as the property that after measurement of particle 1, the expectation catalog for particle 2 gives a definite prediction for measurement along the same direction, the specific result being objectively undefined until the measurement on particle 1 is actually performed.

To summarize, for two particles, entanglement implies that no disjoint catalogs for all observable properties of the two particles exist and that the specific result of the measurement of an entangled quantity instantly permits prediction with certainty of the result of a measurement of the related quantity on the other particle.

THREE PARTICLES, TWO TERMS

All the discussion on entanglement in quantum mechanics until recently exclusively focused on two-particle states only. Yet it is evident that correlations between three and more particles provide a richer abundance of new quantum phenomena. For example, while any entangled state of two particles can always be written as a sum of just two terms (see e.g. Eq. 1) this in general is not true anymore for three particles. Specifically, there may be experimental situations where the state of the three-particle system consists of two terms or maybe even one term only, while in other situations three or more product terms are necessary for a complete description. Here we shall first analyze a specific case of a three-particle experiment where the state contains two terms.

The introduction of three-particle correlations into discussions of the EPR-paradox (Refs. 5 - 7) and related questions not only did lead to more stringent contradictions between local realistic models and quantum mechanics than in two-particle situations, it also provides qualitatively new entanglement phenomena. Let us consider a three-particle interferometer experiment of the type recently proposed (Ref. 7). A suitable source, say a nonlinear crystal exploiting a second-order nonlinearity of the

electric polarizability, emits three photons in the entangled state

$$|\psi\rangle = \sqrt{1/2} \, [|A\rangle_1 |B\rangle_2 |C\rangle_3 + |A'\rangle_1 |B'\rangle_2 |C'\rangle_3]. \tag{2}$$

Here, e.g., $|A\rangle_1$ describes photon one in beam A etc. (see Figure 1). We now consider two possible choices the experimenter has:

(a) She might determine which path photon 1 takes by placing detectors into beam path A and beam path A'. As soon as one of these detectors fires, the state of the system collapses due to von Neumann wave packet reduction. This implies that depending on whether the detector in beam path A fires or the one in beam path A' the state of the remaining two particles is different. If detector A registers photon 1 (we assume, as is customary in photon experiments, that the photon is absorbed by a detector registering it) that state is

$$|\psi\rangle' = |B\rangle_2 |C\rangle_3. \tag{3}$$

But, if detector A' registers photon 1 the state of the remaining two photons is

$$|\psi\rangle' = |B'\rangle_2 |C'\rangle_3. \tag{4}$$

In either case, after registration of photon 1 the remaining two photons are left in a product state, i.e. they are not entangled. In other words, registering photon 1 in either beam A or A' did untangle the other two photons. From a complementarity point of view this might readily be understood on basis of the fact that registering any of the photons in a beam path before it encounters the recombining beam splitter instantaneously provides information not only in this photon's path but, because of the momentum correlations implied in state (2), also on the paths taken by the other two photons.

(b) The experimenter might alternatively decide not to insert detectors into any of the beam paths before the recombining beam splitter but measure the interference fringes instead. In order to simplify the analysis we assume that the phase shifter phases (Fig. 1) are all chosen to obey the condition

$$\phi_1 + \phi_2 + \phi_3 = \pi/2. \tag{5}$$

Let us now call D (E) the beam path of particle 1 leading to detector R_1 (L_1) and likewise F (G) and H (J) the beam paths of particles 2 and 3 leading to their detectors. Without loss of generality we assume that photon 1 is registered in detector D: The state of the remaining 2 photons is then (see Ref. 7)

$$|\psi\rangle = \sqrt{1/2} \, [|E\rangle_2 |F\rangle_3 - |E'\rangle_2 |F'\rangle_3]. \tag{6}$$

Thus photon 2 and photon 3 are clearly in an entangled state now. This holds always for the remaining two photons if a photon was registered after any of the other beam splitters. In other words, registering a photon in a detector behind its recombining beam splitter does not untangle the other two photons.

Clearly, the experiment can be set up in such a way that the detection events for the three photons occur at spacelike separation. Nevertheless, the experimenter's decision as to which measurement is to be performed at one of the photons determines - upon registration of the measurement result - whether or not the other two photons are left in an entangled state.

In Schrödinger's terms this means that the experimenter, simply by deciding whether to measure photon 1 before or after its recombining beam splitter, also decides whether or not the other two photons each enjoy their own disjoint expectation catalog, no matter how far these other photons might be away at the time that decision is made or at the instant of registration of photon 1. For completeness we simply remark here that, as in two-particle entanglement, the detection events of the three photons might be arranged in any time order.

A THREE-TERM STATE

For three or more particles with each particle enjoying its own two-dimensional Hilbert space there are evidently a number of different three-term states. Clearly the details of the experimental situation determine which state is present. To be specific, let us analyze the experiment represented in Figure 2. There, the incident beam A bearing radiation with wave number $k = 2\pi/\lambda$ is split by a series of successive partially reflecting mirrors into the beams B, C, and D and a through going beam. This latter one is assumed to enter a nonlinear crystal where it is upconverted into radiation with wavenumber 3k and then passes a filter set at the wavelength $\lambda' = 2\pi/3k$. Afterwards it is downconverted again. We shall call such a device consisting of an upconverter, a monochromatic filter and a downconverter a "number filter" because it lets only pass states with a certain number of photons, in our case three. This beam subsequently encounters a partially reflecting mirror again where some of it is deflected into a beam which we call A' towards a detector set to count a particle, call it particle 1. Registration of particle 1 in that detector acts as a trigger signal to indicate that a three-particle state has passed the number filter.

The transmitted beam again encounters some mirrors such that the beams B', C', and D' result as indicated in Figure 2. These latter beams are then superposed at a set of three semireflecting mirrors with the corresponding beams B, C, and D and we assume that detectors are placed into the outgoing beams of these semireflecting mirrors. We arrange the experiment such that the amplitudes incident on either port of any recombining mirror are equal and we look only for such events where in one and only one of the outgoing beams of each semireflecting mirror a photon is found (assuming 100% efficient detectors). Let us call these photons by their numbers 2, 3, and 4 respectively and let us agree to look only at the detectors if particle 1 has been registered in its detector.

The state of these photon quadruples is

$$|\psi\rangle = \sqrt{1/3} \; |A'\rangle_1 \left[|B'\rangle_2|C'\rangle_3|D\rangle_4 + |B'\rangle_2|C\rangle_3|D'\rangle_4 + |B\rangle_2|C'\rangle_3|D'\rangle_4 \right] \tag{7}$$

because this describes exactly the situation where photon 1 triggers the detector in beam path A' thus indicating that a three-photon has passed the number filter and one of these is photon 1. The other two photons coming through the filter might either be photon 2 and 3, or photon 2 and 4, or photon 3 and 4 as indicated by the primes in the terms above. For each term one other photon must have used the unprimed beam completing the quadruple.

We immediately note that in the state (7) photons 2, 3, and 4 are entangled with each other, while photon 1 is not entangled with any of the others, it enjoys its own disjoint catalog of predictions. More importantly, let us now consider what happens if we place a detector into any of the primed beam paths of photon 2, 3, or 4. Suppose explicitly and without loss of generality that a detector is placed into path B' of photon 2. Still we assume that we only look at such cases where the detector in beam A' has registered photon 1. Then two different possibilities arise: Either the detector in beam path B' fires or it does not fire. If it fires, the state of the remaining two photons, the photons 3 and 4, is

$$|\psi'\rangle = \sqrt{1/2} \; [|C'\rangle_3|D\rangle_4 + |C\rangle_3|D'\rangle_4] \tag{8}$$

which is clearly an entangled state for these two photons. On the other hand detector B' might not fire. In that case the predictions for the quadruple of photons can be described by the last term of Eq. (8)

$$|\psi'\rangle = |A'\rangle_1|B\rangle_2|C'\rangle_3|D'\rangle_4 \tag{9}$$

which now implies that none of the photons is entangled with any of the other photons. Most remarkably, if the detector inserted into the beam path B' of photon 2 fires, photon 3 and 4 are entangled. If that detector does not fire, photon 3 and 4 are not entangled anymore! The absence of a registration event of the detector in beam B' untangles the other two photons. Whether or not such a registration event happens is completely and objectively random, at least within the standard interpretation of quantum probabilities. In this situation it is therefore a totally random event happening to photon 2 which determines whether or not photons 3 and 4 are entangled.

We point out here too that the apparatus might easily be arranged in such a way that the detection events on particles 2, 3 and 4 are spacelike separated from each other. Again we might call the specific random event "Nature's choice" and we find it quite remarkable that a spacelike separated random event happening to particle 2 decides whether or not particle 3 and 4 are entangled with each other.

CONCLUDING COMMENTS

Several comments might be in order. Firstly we remark that the analysis given above is not restricted to multiparticle interferometry. In fact, it is rather straightforward to give an example in terms of spin correlations. We might also point out that such experiments, though they have not been performed yet, should be feasible given further development in our knowledge of the nonlinear conversion processes in quantum optics. Furthermore, it was implicitly assumed that the incident radiation is rich enough to contain the multiparticle states exploited in the various experiments. Finally, entangled entanglement also is consistent with special relativity in the sense that it does not permit information to be transmitted with a speed larger than that of light.

REFERENCES

1. Einstein, A., Podolsky, B., and N. Rosen, 1935, "Can Quantum Mechanical Description of Physical Reality Be Considered Complete?" *Phys. Rev.*, 47, p. 777.

2. Bell, J.S., 1964, "On the Einstein-Podolsky-Rosen Paradox" *Physics*, 1, p. 195. Reprinted, 1983, in *Quantum Theory and Measurement*, J.A. Wheeler and W.H. Zurek, eds., Princeton, p. 403.

3. Schrödinger E., 1935, "Die gegenwärtige Situation in der Quantenmechanik," *Naturwissenschaften*, 23, pp. 807-812, 823-828, 844-849. English Translation, 1980, "The Present Situation in Quantum Mechanics," *Proceedings of the American Philosophical Society*, 124, p. 323; reprinted, 1983, in *Quantum Theory and Measurement*, J.A. Wheeler and W.H. Zurek, eds., Princeton, p. 153.

4. Bohm, D., 1951, *Quantum Theory*, Prentice-Hall, Englewood Cliffs, NJ, pp. 614-623.

5. Greenberger, D., Horne, M. A., and A. Zeilinger, 1989, "Going beyond Bell's Theorem," in *Bell's Theorem, Quantum Theory, and Conceptions of the Universe*, M. Kafatos, ed., Kluwer Academic, Dordrecht, The Netherlands, p. 73.

6. Mermin, N. D., 1990, "Quantum Mysteries Revisited," *Am. J. Phys.*, 58, p. 731; and "What's Wrong with these Elements of Reality?," *Physics Today*, 43(6), p. 9.

7. Greenberger, D. M., Horne, M. A., Shimony, A., and A. Zeilinger, 1990, "Bell's Theorem without Inequalities," *Am. J. Phys.*, 58, p. 1131.
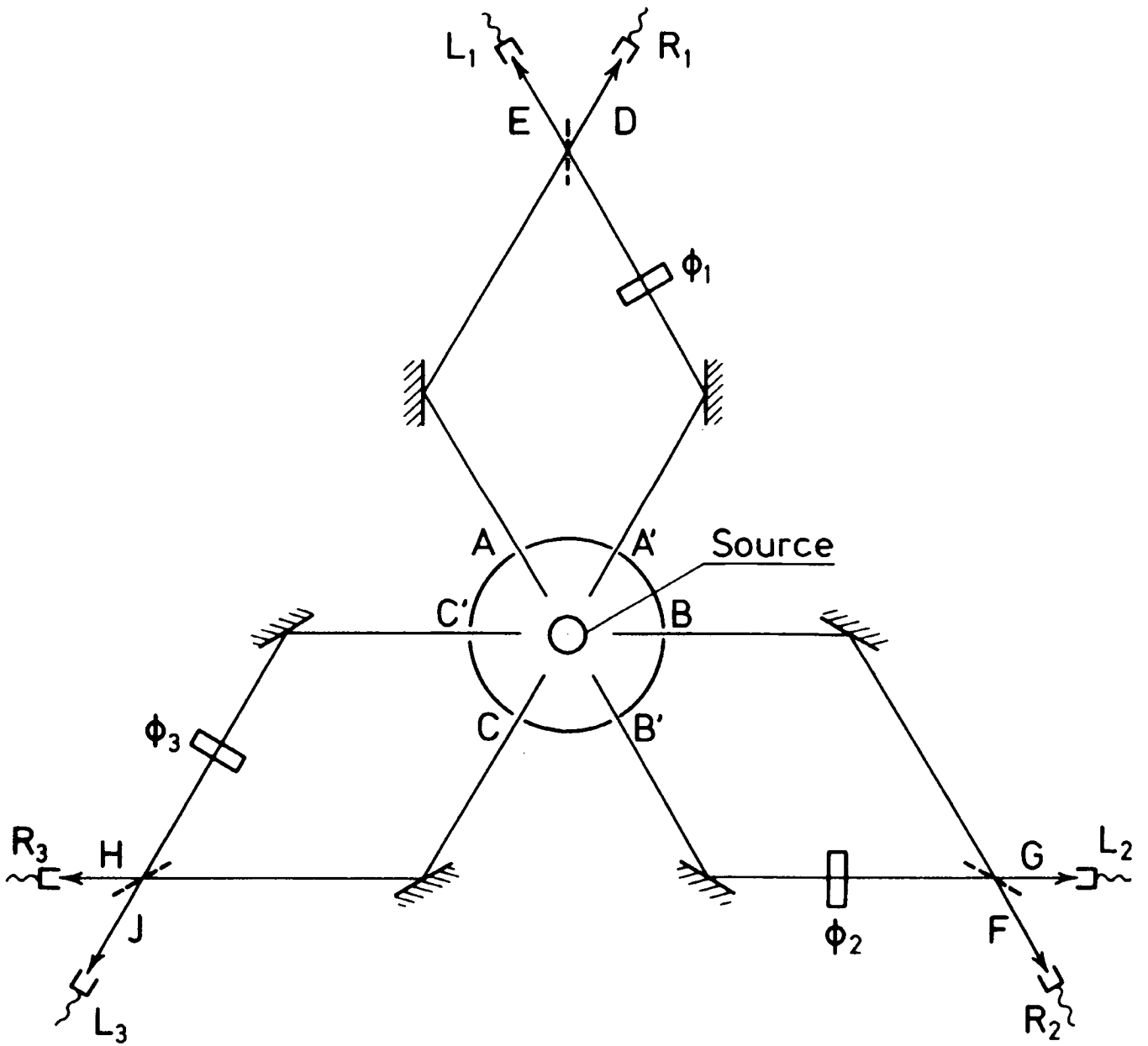
Fig. 1: Principle of a 3-particle interferometer experiment.
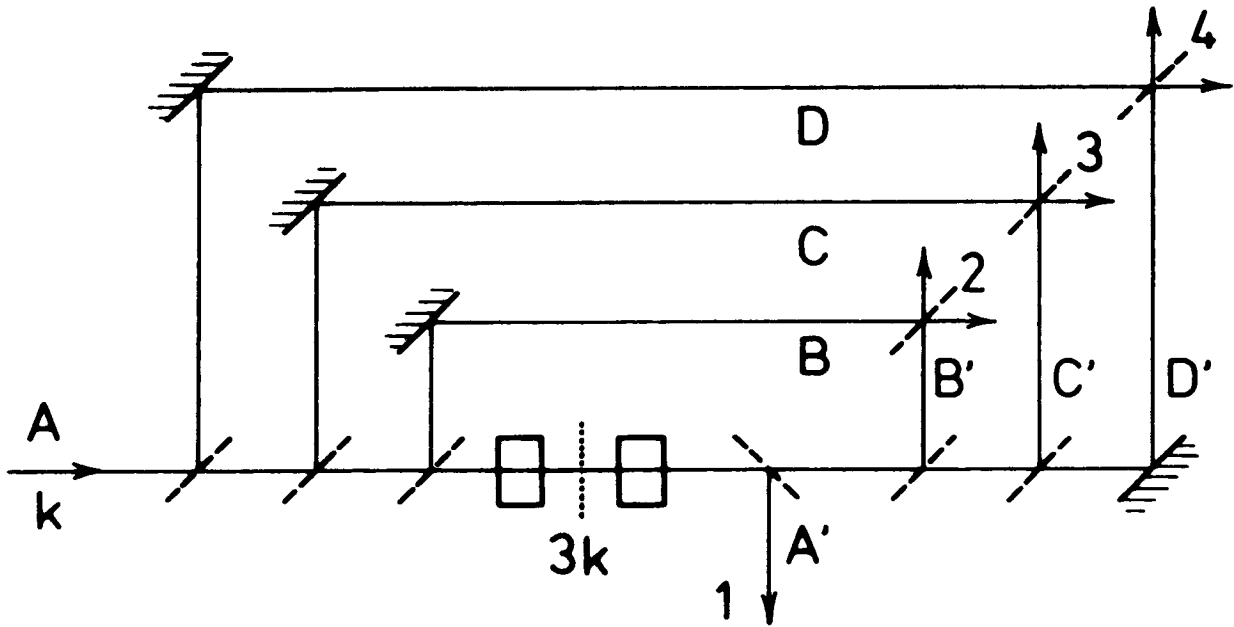
Fig. 2: Principle of an interferometer experiment exhibiting entanglement of more than two terms.

C-2

Algorithmic Information Theory and the Hidden Variable Question

Christopher Fuchs

Dept. of Physics & Astronomy, University of North Carolina

Chapel Hill, NC 27599

Abstract

This note explores, via information theory, the admissibility of certain <u>nonlocal</u> hidden-variable theories. Consider a pair of Stern-Gerlach devices with fixed nonparallel orientations that periodically perform spin measurements on identically prepared pairs of electrons in the singlet spin state. Suppose the outcomes are recorded as binary strings l and r (with l_n and r_n denoting their n-length prefixes). The hidden-variable theories considered here require that there exists a recursive function which may be used to transform l_n into r_n for any n. This note demonstrates that such a theory cannot reproduce all the statistical predictions of quantum mechanics. Specifically, consider an ensemble of outcome pairs (l,r). From the associated probability measure, the Shannon entropies H_n and $\bar{H}_n$ for strings l_n and pairs (l_n, r_n) may be formed. It is shown that such a theory requires that $|\bar{H}_n - H_n|$ be bounded — contrasting the quantum mechanical prediction that it grow with n.

I. Introduction

The class of inequalities initiated by Bell[1] do not absolutely exclude the possibility of hidden variables underlying the phenomena statistically described by quantum mechanics. Hidden-variable theories of the so-called *nonlocal* variety are not constrained by Bell's theorem. Although there is no pressing theoretical reason for taking the existence of such a theory seriously, it is clear that one can only truly begin to understand quantum mechanics when one first understands what it is *not*. This note will attempt to make a contribution to this end. Here a seemingly not- *a priori* unreasonable class of nonlocal hidden-variable theories called the "computable hidden-variable theories" (CHV's) will first be defined for a particular thought experiment and then shown to be inconsistent with certain statistical requirements of quantum mechanics. The reason for this procedure is to make explicit, through the language of *algorithmic information theory*,[2,3] an aspect of quantum theory hitherto seldom discussed and then demonstrate the practical use of this aspect in answering foundational questions. This aspect is that the data obtained from identical measurements performed on identically prepared systems is generally "algorithmically incompressible."

II. The Thought Experiment and the Result

The thought experiment described is a modification of the standard one used for discussions of Bell's theorem. Consider a pair of distantly separated Stern-Gerlach (SG) devices situated so to (flawlessly) measure the spins of a pair of correlated electrons. These are called the left and right devices, respectively. For definiteness, suppose that the correlated electrons are in the singlet spin state

$$|\psi\rangle = \frac{1}{\sqrt{2}}\Big(|\uparrow\rangle_L|\downarrow\rangle_R - |\downarrow\rangle_L|\uparrow\rangle_R\Big). \quad (1)$$

Assume that the left and right SG devices, respectively, are oriented so that they invariably measure spin along $\hat{z}$ and an axis that differs from $\hat{z}$ by a computable angle θ. "θ computable" simply means that there is an algorithm for generating the decimal expansion of θ. E.g., $\theta = \pi/6$ is clearly computable. Suppose that at <u>periodic</u> time intervals these devices are supplied with identically prepared pairs of correlated electrons. (This would allow the measurement outcomes to serve as a "window" into the "hidden" dynamics of the devices, if such a dynamics did indeed exist.) Finally, imagine that each SG device is endowed with the capability of recording its measurement outcomes as a string of binary digits — 0 and 1 denoting down and up outcomes, respectively. Denote the left and right strings, respectively, by l and r, and their n-length prefixes by l_n and r_n. E.g., a typical run of the devices might give $l = 01101011\ldots$ and $r = 10110100\ldots$; the length-4 prefixes for these strings are $l_4 = 0110$ and $r_4 = 1011$. To cap off the description of the thought experiment, assume that there is in fact an ensemble of such devices: each macroscopically identical to the next, each with its own supply of electrons, and each performing the operation described. Associated with this ensemble will be an ensemble of ordered pairs (l,r) and consequently ensembles of pairs (l_n, r_n).

With this as a scaffold, the CHV notion can be formalized. Simply put, a CHV is said to be responsible for the measurement outcomes if for every pair (l,r) in the ensemble, there is at least one of a finite set of computer programs (more formally recursive functions) that, for any n, produces the string r_n as output whenever given l_n as input. Note that each string l can have as its origin any process whatsoever:

deterministic or indeterministic. This definition only requires that a rigid, mechanistic relation between l and r be maintained. Furthermore, such a theory is inherently nonlocal; the program provides the "medium" for the instantaneous action of the one string on the other. The finiteness of the set of programs is meant to allow for the possibility that the SG devices in the ensemble might have differing microscopic initial conditions.

The main result may now be stated. Because a CHV provides a compression scheme for the measurement data, it must contradict the statistical predictions of quantum mechanics. Suppose the probability distributions for the ensembles of strings l_n and pairs (l_n, r_n) are $p_n(l_n)$ and $q_n(l_n, r_n)$, respectively. The Shannon entropies for these distributions are:

$$H_n = - \sum_{l_n} p_n(l_n) \log[p_n(l_n)]$$
$$\text{and} \qquad (2)$$
$$\overline{H}_n = - \sum_{l_n} \sum_{r_n} q_n(l_n, r_n) \log[q_n(l_n, r_n)],$$

where $\log$ denotes the base-2 logarithm. Consider the quantity $|\overline{H}_n - H_n|$. Standard quantum theory requires that this be proportional to n. For CHV's, however, this quantity is necessarily bound by a constant independent of n. The remainder of this section will be devoted to justifying the quantum mechanical result; the corresponding result for a CHV will be derived in the next two sections.

Suppose that standard quantum theory does indeed hold in the thought experiment. In that case, the required Shannon entropies are straightforward to derive. The essential ingredient in this derivation is simply noted: quantum theory declares that the only condition determining the measurement outcomes is the probability distribution derivable from (1). Hence, the probability of a 0 or a 1 occurring in the k'th place of a string l_n must be independent of k. Furthermore, this probability is independent of which left-hand SG device in the ensemble produced l_n. Analogous results hold for any string r_n and for the correlation probabilities between the k'th places of l_n and r_n. With these considerations, it is a simple exercise in quantum mechanics to show that

$$|\overline{H}_n - H_n| = -f(\theta)n, \quad \text{where}$$

$$f(\theta) = \left(\sin^2 \frac{\theta}{2} \log[\sin^2 \frac{\theta}{2}] + \cos^2 \frac{\theta}{2} \log[\cos^2 \frac{\theta}{2}] \right).$$

Therefore, for any θ other than $\theta = 0$ or $\theta = \pi$,

$$|\overline{H}_n - H_n| \propto n. \qquad (3)$$

IV. Algorithmic Information Theory

This section introduces enough of the appara-

tus of algorithmic information theory that the main result can be proven. It does not purport to be a general introduction to the subject. The notion of a "recursive function" is taken as primitive. For the most part, this section follows the development of algorithmic information theory found in Ref. 3.

Notation and Definitions:

Let $\mathbf{X} = \{\Lambda, 0, 1, 00, 01, \ldots\}$ be the set of finite binary strings in lexicographic order, where Λ is the empty string. Elements of $\mathbf{X}$ may be thought of dually as strings and natural numbers. Let $\mathbf{X}_n$ be the set of n-length strings. $\mathcal{O}(1)$ denotes a bounded function. The variables s, t, v, x, and y denote elements of $\mathbf{X}$. The length, n-length prefix, and k'th digit of s are denoted by $|s|$, s_n, and $s(k)$, respectively. A set $\mathbf{S} \subset \mathbf{X}$ is called an *instantaneous code* if for any x, y in $\mathbf{S}$, neither x nor y is a prefix of the other. Elements of $\mathbf{S}$ (denoted generally by r) are called *programs*. A *computer* C is a recursive function $C : \mathbf{S} \times \mathbf{X} \to \mathbf{X}$. A computer U is said to be *universal* iff for each computer C there is a constant k_C such that: if $C(r, v)$ is defined, then there exists a program $r' \in \mathbf{S}$ such that $U(r', v) = C(r, v)$ and $|r'| \leq |r| + k_C$. Let a particular countably infinite instantaneous code $\mathbf{S}$ and universal computer U be chosen as standard. Finally, let $\langle , \rangle : \mathbf{X} \times \mathbf{X} \to \mathbf{X}$ be a recursive bijection with the property that if $|s| = |t|$, then $\langle s, t \rangle = s(1)t(1)s(2)t(2)\ldots$. E.g., if $s = 011$ and $t = 101$, then $\langle s, t \rangle = 011011$.

The *algorithmic complexities* are defined by:

$$K_C(s/t) = \min\{|r| : C(r, t) = s\}$$
$$K_C(s) = K_C(s/\Lambda)$$
$$K_C(s, t) = K_C(\langle s, t \rangle)$$
$$K(s/t) = K_U(s/t)$$

The *canonical program* s^* for s is defined by $s^* = \min\{r : U(r, \Lambda) = s\}$. Clearly $|s^*| = K(s)$.

Now let $p : \mathbf{X} \to [0, 1]$ and let p_n denote the restriction of p to $\mathbf{X}_n$. p is said to be a *probability measure for a stochastic process* if it satisfies:

$$\sum_{|x| = n} p_n(x) = 1 \quad \& \quad p_{n-1}(y) = p_n(y0) + p_n(y1)$$

for any n and any $y \in \mathbf{X}_{n-1}$. If p is recursive, then p is said to be a *computable* measure. In this section, only computable measures are considered. The *Shannon entropy* H_n for p over n-length strings is:

$$H_n = - \sum_{|x| = n} p_n(x) \log[p_n(x)].$$

Finally, with the measure p, the *average complexities* $\langle K/y \rangle_p^n$ and $\langle K \rangle_p^n$ for n-length strings are defined by:

$$\langle K/y \rangle_p^n = \sum_{|x| = n} p_n(x) K(x/y) \quad \& \quad \langle K \rangle_p^n = \langle K/\Lambda \rangle_p^n.$$

Theorems:

Theorems (a)-(f), from Ref. 3, are listed so that the present treatment will be self-contained. Theorem (i), from Ref. 4, provides the link relating complexity to entropy. Theorems (g), (h), and (j) are simple results due to the author. When crucial, rather than relegating bounded terms to a term written as $\mathcal{O}(1)$, a constant written in the form $D_{...}$, where the ellipsis symbolizes a set of subscripts, will be used so that all dependencies are clear. (E.g., D_p denotes a constant that depends only on the measure p.)

(a) For any computer C, $K(s/t) \leq K_C(s/t) + k_C$.

(b) $K(s) \leq K(s,t) + \mathcal{O}(1)$.

(c) $K(s/t) \leq K(s) + \mathcal{O}(1)$.

(d) $K(s,t) = K(t,s) + \mathcal{O}(1)$.

(e) $K(s,t) = K(s) + K(t/s^*) + \mathcal{O}(1)$. (To make the $\mathcal{O}(1)$ term's dependence on U explicit, this can be written as $|K(s,t) - K(s) - K(t/s^*)| \leq D_U$.)

(f) If $f: \mathbf{N} \rightarrow \mathbf{N}$ is a recursive function and $\sum \left(\frac{1}{2}\right)^{f(n)}$ converges, then $K(n) \leq f(n) + \mathcal{O}(1)$.

(g) $K(t/s^*) \leq K(t/s) + \mathcal{O}(1)$.

Proof: Consider a computer C such that $C(r,v) = U(r, U(v, \Lambda))$. Then $C(r,s^*) = U(r,s)$. Hence it must be the case that $K_C(t/s^*) = K(t/s)$ for any t. By (a) then, $K(t/s^*) \leq K(t/s) + \mathcal{O}(1)$. □

(h) $-D_U \leq K(s) - K(s/|s|^*) \leq 2\log|s| + D_U$.

Proof: A similar result is derived in Ref. 4. The left-hand inequality is a consequence of (c). By (f), there is a constant D_U such that $K(n) \leq 2\log(n) + D_U$ for all n. The right-hand inequality then follows from successive applications of (b), (d), and (e). □

(i) There is a constant $D_{U,p}$ such that, for all n, $0 \leq \langle K/n^* \rangle_p^n - H_n \leq D_{U,p}$.

(j) There are constants D_U and $D_{U,p}$ such that, for all n, $-D_U \leq \langle K \rangle_p^n - H_n \leq 2\log n + D_{U,p}$.

Proof: This is a simple consequence of (h) and (i). □

V. Computable Hidden-Variable Theories

Armed with the last section's tools, a precise definition of a CHV can now be formed. Let $\mathcal{H}$ denote the set of all possible pairs (l,r) in the ensemble of strings produced by the thought experiment.

Def: A <u>CHV</u> V is said to be responsible for the measurement outcomes if there is a finite subset $\mathbf{V} \subset \mathbf{S}$ such that for each $(l,r) \in \mathcal{H}$ there exists a $v \in \mathbf{V}$ for which it is the case that $U(v, l_n) = r_n$ for every n.

Notice immediately that if V is responsible for the outcome strings, then for each $(l,r) \in \mathcal{H}$ it follows that $K(r_n/l_n) \leq \max\{|v| : v \in \mathbf{V}\}$ for all n. But then by (g), $K(r_n/l_n^*) \leq D_{U,\mathbf{V}}$ for all n. This, coupled with (e), leads to the following conclusion.

Thm 1: If V is responsible for the measurement outcomes, then for each $(l,r) \in \mathcal{H}$, it follows that $|K(l_n, r_n) - K(l_n)| \leq D_{U,\mathbf{V}}$ for all n.

Now consider the probability measures for the outcome strings using the notation introduced in Section II. It is assumed that these measures are computable. (This will be the case if standard quantum theory is valid since θ is required to be computable. If it were not the case here, by being noncomputable, p and q would trivially differ from the values predicted by quantum mechanics and there would be no need for further discussion.) For these measures: $\sum_{r_n} q_n(l_n, r_n) = p_n(l_n)$ for all n. An important fact to note is that $q_n(s_n, t_n)$ vanishes iff $(s,t) \notin \mathcal{H}$. Hence from Theorem 1 it follows that, if V generates the measurement outcomes, for all n, the quantity

$$\left| \sum_{l_n, r_n} q_n(l_n, r_n) K(l_n, r_n) - \sum_{l_n} p_n(l_n) K(l_n) \right|$$

will be bounded by a constant $D_{U,\mathbf{V}}$. Now because of the form of the bijection $\langle l_n, r_n \rangle$, the double sum in this expression may be construed as a single sum over strings of length $2n$. This fact leads to the following:

Thm 2: If V is responsible for the outcome strings, $|\langle K \rangle_q^{2n} - \langle K \rangle_p^n| \leq D_{U,\mathbf{V}}$ for all n.

Combining Theorems 2 and (j), the following emerges:

Thm 3: If V is responsible for the outcome strings, $|\bar{H}_n - H_n| \leq D_{U,\mathbf{V},p,q}$ for all n.

This is the sought after identity; for, although $D_{U,\mathbf{V},p,q}$ depends on the the CHV explicitly (through V and possibly p and q), it is independent of n.

References

[1] For a more recent effort see S. L. Braunstein and C. M. Caves, Phys. Rev. Lett. **61**, 662 (1988).

[2] G. J. Chaitin, *Information, Randomness & Incompleteness* (World Scientific, Singapore, 1987); W. H. Zurek, Phys. Rev. A **40**, 4731 (1989).

[3] G. J. Chaitin, J. ACM **22**, 329 (1975).

[4] S. K. Leung-Yan-Cheong and T. M. Cover, IEEE Trans. Inf. Theory **IT-24**, 331 (1978).

Photon Polarization Version of the GHZ-Mermin Gedanken

Thomas E. Kiess
Department of Physics
University of Maryland
College Park, MD 20742

ABSTRACT

We have defined a photon polarization analog of the GHZ experiment that was initially proposed for spin-1/2 quanta. Analogs of the ket states and Pauli spin matrix operators are presented.

DISCUSSION

We have developed an explicit photon polarization version of the three-quanta GHZ experiment (Ref. 1) discussed by Mermin (Ref. 2). We define operators, eigenkets, and measurements in the two-dimensional space of photon polarization that map directly onto the Pauli spin matrix representation of a spin-1/2 system. This construction enables us to represent the GHZ experiment in terms of photon polarization measurements on a three-photon quantum state.

This photon analog of the spin-1/2 counterparts is developed by using retardation plates, which rotate the polarization of an incident photon by producing an associated change of phase. A $\lambda/4$ retardation plate with optic axis at $45°$ to an imposed X-Y coordinate system will act analogously to σ_x, up to a phase representing a polarization-independent translation. A $\lambda/4$ plate with optic axis parallel to one of the X-Y axes produces the σ_z operation, again up to an inessential phase factor. The product operation defined by both retardation plates accomplishes the operation $\sigma_y = i\sigma_z \cdot \sigma_x$.

The polarization states that represent eigenkets of σ_z are $|X\rangle$ and $|Y\rangle$, measured by using a birefringent polarization analyzer (e. g. a Wollaston prism) oriented to send each of these polarizations into a distinct direction, en route to one of two separate photomultiplier tube detectors. The polarization states that represent eigenkets of σ_x are defined similarly, to be light linearly polarized at $45°$ and $135°$ to the X-axis. These polarizations are measured by rotating the analyzer at $45°$ to its σ_z orientation, and recording which of the two phototubes generated an output pulse. Finally, the eigenkets of σ_y are found to be left- and right-circularly polarized light in this representation. These are measured (i. e. ±1 is determined) by inserting a quarter-wave plate in front of the previously-defined analyzer, to generate in one output direction light that was originally left circular polarized, and in the other direction the originally right circular polarization.

The experiment consists of first verifying that the three-photon state being studied is a +1 eigenstate of each of the operators $A = \sigma_y^1 \cdot \sigma_x^2 \cdot \sigma_x^3$, $B = \sigma_x^1 \cdot \sigma_y^2 \cdot \sigma_x^3$, and $C = \sigma_x^1 \cdot \sigma_x^2 \cdot \sigma_y^3$. A measurement of

PRECEDING PAGE BLANK NOT FILMED

operator $O = A \cdot B \cdot C$ represents the decisive test between quantum mechanics and local reality theories. The quantum mechanical prediction for the observed eigenvalue of O is -1, whereas the local reality prediction can be easily shown to be $+1$.

The most difficult element of any non-gedanken experiment similar to the one presented here is the construction of the three-photon quantum state. The requisite state vector is a perfectly anti-ferromagnetic "entangled" ket proportional to $[|X\rangle_1|X\rangle_2|X\rangle_3 - |Y\rangle_1|Y\rangle_2|Y\rangle_3]$ which is difficult to manufacture (Ref. 3) by any physical process, such as a three-photon emission of an excited species. We have proposed a method of creating this state by hand, a task not obviously possible because most operators on optical photons do not restrict themselves to the Hilbert space of any one photon exclusive of the others.

We assemble the needed three-photon ket by sending a product $|X\rangle_1|X\rangle_2|X\rangle_3$ of three one-photon number states (obtainable by using an attenuated Glauber state for each one) onto an array of beam splitters and interferometers (either Mach-Zehnder or Michelson will work here) to achieve a summation of correlated amplitudes at the end of the apparatus (see Figure). The total apparatus is a three-tiered structure, with one tier for each photon. For clarity, only one tier is shown in the figure. The boxed interferometers are specific to each tier; all other optical components (beamsplitters and mirrors) are common to all three tiers, a requirement that can be satisfied for sufficiently large components. The entangled state is obtained by using phases in the apparatus to cause the amplitudes of some components of the total ket to sum to zero. This cancellation of undesired "cross terms" produces the anti-ferromagnetic state needed in the GHZ test.

REFERENCES

1. Greenberger, D. M., M. Horne, and A. Zeilinger, 1989, "Going Beyond Bell's Theorem," in *Bell's Theorem, Quantum Theory, and Conceptions of the Universe*, M. Kafatos, ed., Dordrecht, The Netherlands, p. 73.

2. Mermin, N. D., 1990, "What's Wrong with These Elements of Reality?," *Physics Today* (June 1990), p. 9.

3. Greenberger, D. M., M. A. Horne, and A. Zeilinger, 1990, "Bell's Theorem Without Inequalities," *Am. J. Phys.*, 58(12), p. 1131.

| = beamsplitter

| = half wave plate

| = mirror

D2 = phototube

pump

KDP crystal

D2
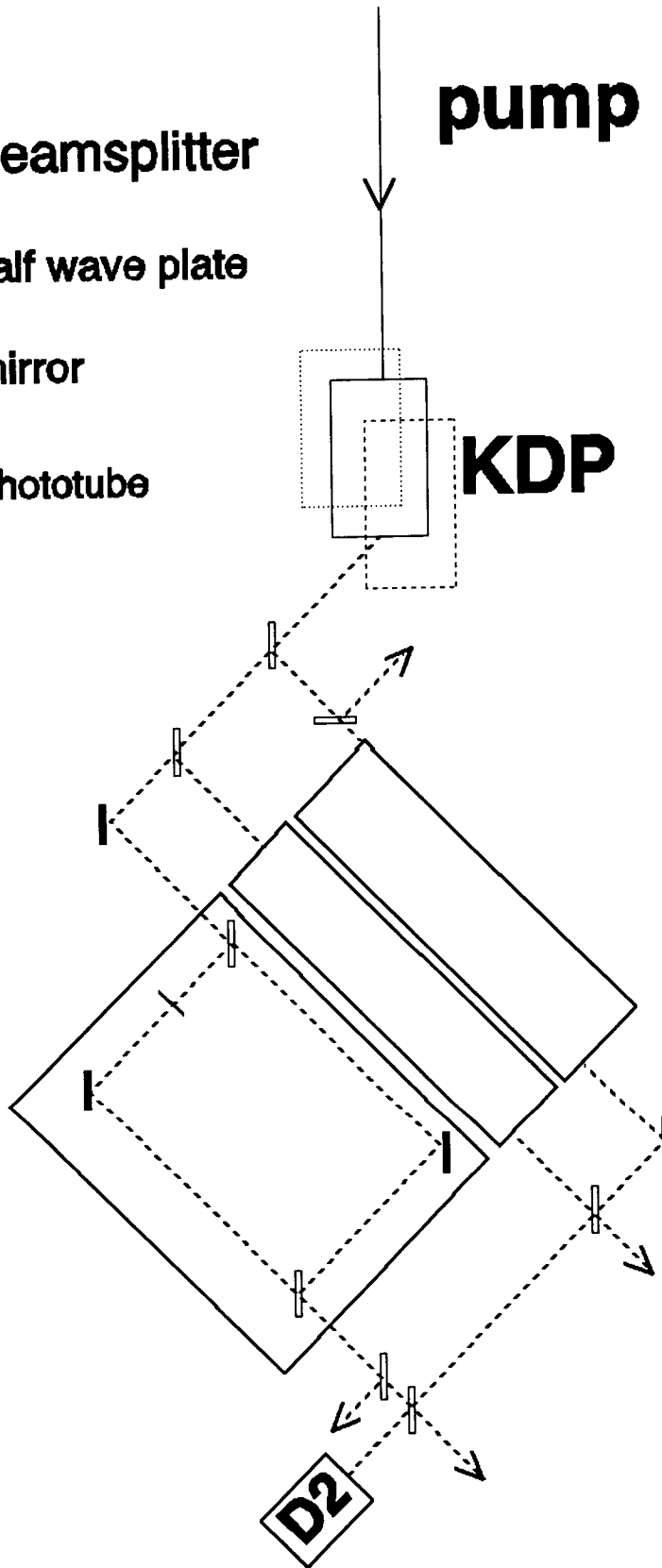
Apparatus Defining the Three-Photon State

PROPOSAL FOR A QND WHICH-PATH MEASUREMENT USING PHOTONS*

M. G. Raymer and S. Yang
Department of Physics and Chemical Physics Institute
University of Oregon, Eugene, OR 97403

A scheme is proposed for experimentally realizing the famous two-slit gedänken experiment using photons. As elegantly discussed for electrons by Feynman, a particle's quantum pathways interfere to produce fringes in the probability density for the particle to be found at a particular location. If the path taken by the particle is experimentally determined, the complementarity principle says that the fringes must disappear. To carry out this experiment with photons is difficult because normally the act of determining a photon's location destroys it.

We propose to overcome this difficulty by putting a type-II optical parametric amplifier (OPA) in each arm of a Mach-Zehnder interferometer, and observing fringes at the output, as shown in Fig.1. An OPA responds to an input photon by increasing its probability to produce a pair of photons, one having (vertical) polarization orthogonal to the (horizontal) polarization of the input photon. A polarizing beam splitter is used to eject only those photons with polarization orthogonal to the input, the detection of which allows partial inference about the path taken by the input photon without destroying it. The measurement is thus of the quantum nondemolition (QND) type.
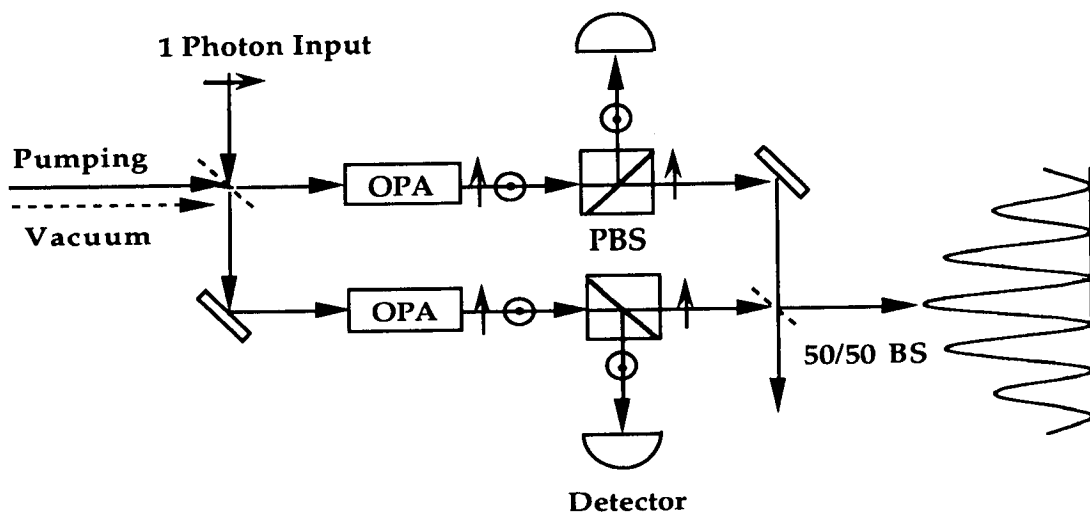
Fig.1   Apparatus for which-path measurement.

The price paid for this inference is at least one noise photon in the interferometer, which degrades the fringe visibility, in accordance with the complementarity principle. Information theory is used to show that the visibility is connected to the amount of information available to be collected, regardless of whether or not anyone looks at it. In this sense information should perhaps be regarded as a physical quantity, rather than a subjective concept.

The calculation treats the signal (horizontal polarization) and idler (vertical polarization) modes of the OPA quantum mechanically and the pump mode as a given classical field. The one-photon input state is transformed on the 50/50 beam splitter by a unitary transformation (Ref.1), and then is acted upon by a factorized two-mode squeezing operator (Ref.2) for each OPA crystal. From the resulting probabilities for mode occupation, Bayes theorem is used to infer the probabilities $P(\text{upper} \mid n_v, m_v)$ and $P(\text{lower} \mid n_v, m_v)$ for each path (upper or lower) that the input photon may have taken. This inference is possible because the probability distributions for numbers of generated idler photons, n_v, m_v, depend on the number of photons (0 or 1) entering each OPA.

Information gain is defined in the following way knowing the prior probabilities (1/2,1/2) and the final probabilities inferred from Bayes theorem: $\Delta I = I_{prior} - I_{final}$, where $I_{prior} = 1$ bit is the initially missing information, and the final information after the measurement is

$$I_{final} = P(upper|n_v, m_v) \log_2 P(upper|n_v, m_v) +$$

$$P(lower|n_v, m_v) \log_2 P(lower|n_v, m_v).$$

For a given sub-ensemble of trials in which n_v (m_v) idler photons are generated in the upper (lower) arm, the fringe visibility is found to be

$$V_{n_v, m_v} = 2(m_v + 1)(n_v + 1) / [(m_v + n_v + 1)(m_v + n_v + 2)].$$

The sub-ensemble fringe visibility and information gain are plotted in Fig.2 for different values of n_v and m_v. When $n_v = m_v$ the information gain is zero, and the visibility approaches unity for small n_v and m_v. For larger values of n_v and m_v the noise in the OPA degrades the visibility even though no information is imparted. For $n_v = 0$ and $m_v \gg 1$, the information increases and the visibility decreases, in accordance with the complementarity principle. See related discussions (Refs.3-5).
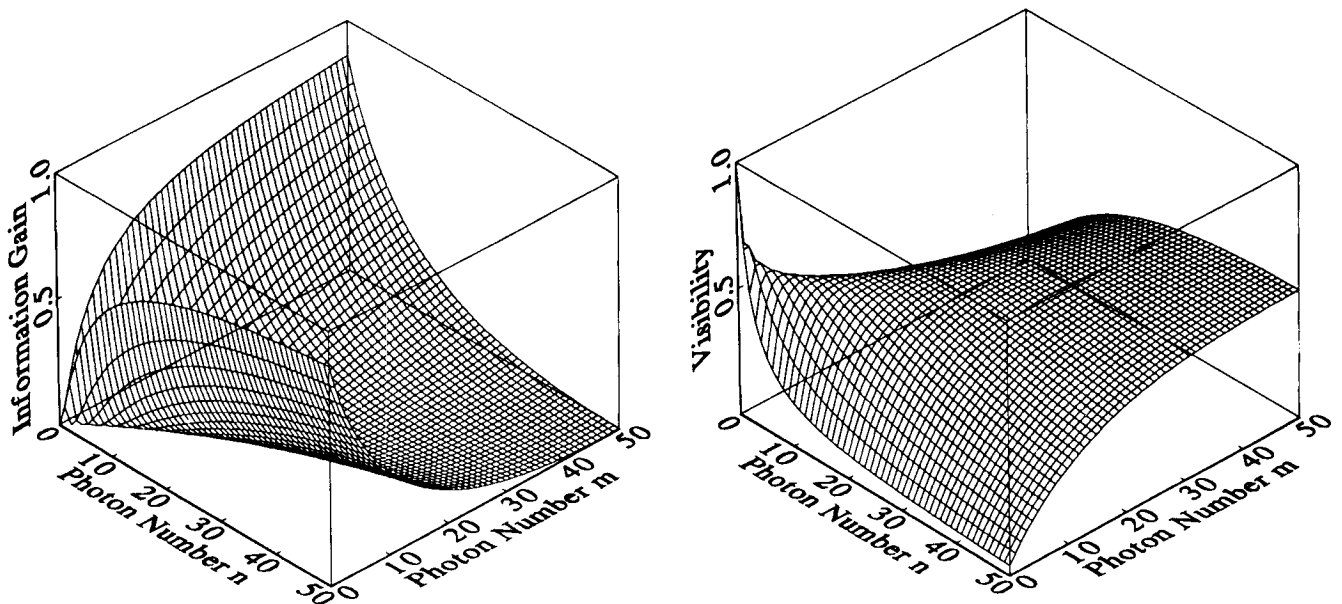
Fig.2 Information gain and fringe visibility versus measured photon numbers.

Thus, partial measurements of the photon path can be made, but noise is added, degrading the visibility, and thereby enforcing the complementarity principle. If n_V and m_V are not measured, and the total ensemble is used to calculate visibility, it can be shown that there is still an inverse relation between average information gain and visibility. Thus, it is not necessary to collect the information, only that it be "out there" available to be collected. This suggests that information has an objective, rather than a subjective, physical reality. It should be considered whether information plays an unrecognized role in physical processes, and as such should be incorporated in a more explicit, dynamical way into the theory of quantum mechanics.

1. Prasad, S., M. O. Scully, and W. Martienssen, 1987,*Opt. Commun.*62, p.139.
2. Schumaker, B. L., and C. M. Caves, 1985, *Phys. Rev. A* 31, p. 3093.
3. Glauber, R. J., 1986, "Amplifiers, Attenuators and the Quantum Theory of Measurement," *Frontiers In Quantum Optics*, E R Pike and S. Sarkar, eds., Malvern, pp 534.
4. Sanders, B. C. ,and G. J. Milburn, 1989,*Phys. Rev. A*39, p. 694 .
5. Scully, M. O., and H. Walther, and B. G. Englert, and J. Schwinger,1990, "Observation" And.Complementarity In Quantum Mechanics: New Tests And Insights," *Proceedings of the Matter Wave Interferometry Workshop* , Santa Fe, New Mexico, Jan. 15-16.

628/03

6 p

LOCALIZATION OF ONE-PHOTON STATE IN SPACE AND EINSTEIN-PODOLSKY-ROSEN PARADOX IN SPONTANEOUS PARAMETRIC DOWN CONVERSION

A.N.Penin, T.A.Reutova, *)A.V.Sergienko

Department of Physics, Moscow State University,
Moscow 119899, USSR
*)Present address: Department of Physics and Astronomy,
University of Maryland, College Park, MD   20742

An experiment on one-photon state localization in space using a correlation technique in Spontaneous Parametric Down Conversion (SPDC) process is discussed. Results of measurements demonstrate an idea of the Einstein-Podolsky-Rosen (EPR) paradox for coordinate and momentum variables of photon states. Results of the experiment can be explaned with the help of the advanced wave technique developed by D.N.Klyshko /1,2/.

The experiment is based on the idea that two-photon states of optical electromagnetic fields arising in the nonlinear process of the spontaneous parametric down conversion (spontaneous parametric light scattering) can be explained by quantum mechanical theory with the help of a single wave function. The interaction of monochromatic laser radiation with a nonlinear crystal without a center of symmetry results in the spontaneous emergance of two-photon states with a broad set of different coordinate-momentum and energy-time pairs of variables. The radiation after the nonlinear crystal has a continuous distribution of wavevectors in space depending on the nonlinear properties of crystal and phase matching conditions $\omega_1+\omega_2=\omega_L$, $k_1+k_2=k_L$. This forms the main reason why we can easily measure coordinates or wavevectors of photons. The typical experimental setup for the measurement of the distribution of scattered radiation in space as a function frequency that have being used in our earlier works /3-5/ is illustrated in Fig.1. Ultraviolet radiation at $\lambda=325$ nm from a He-Cd laser interacted with a 2 cm long nonlinear LiIO$_3$ crystal and created broad band scattered radiation centered at $\lambda=650$ nm. The radii of rings in the focal plane of the collecting lens are defined by phase matching conditions. The

PRECEDING PAGE BLANK NOT FILMED
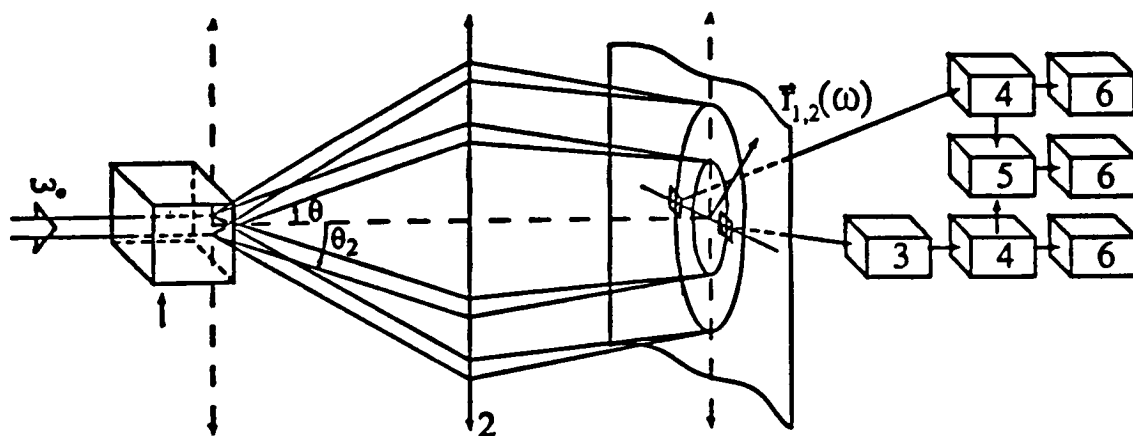
Fig.1. Outline of the experimental setup for the investigation of correlation properties of radiation in the spontaneous parametric down conversion process. 1- nonlinear LiIO$_3$ crystal, 2- collecting lens, 3-spectral device, 4- photodetectors, 5- coincident circuit, 6-counters.
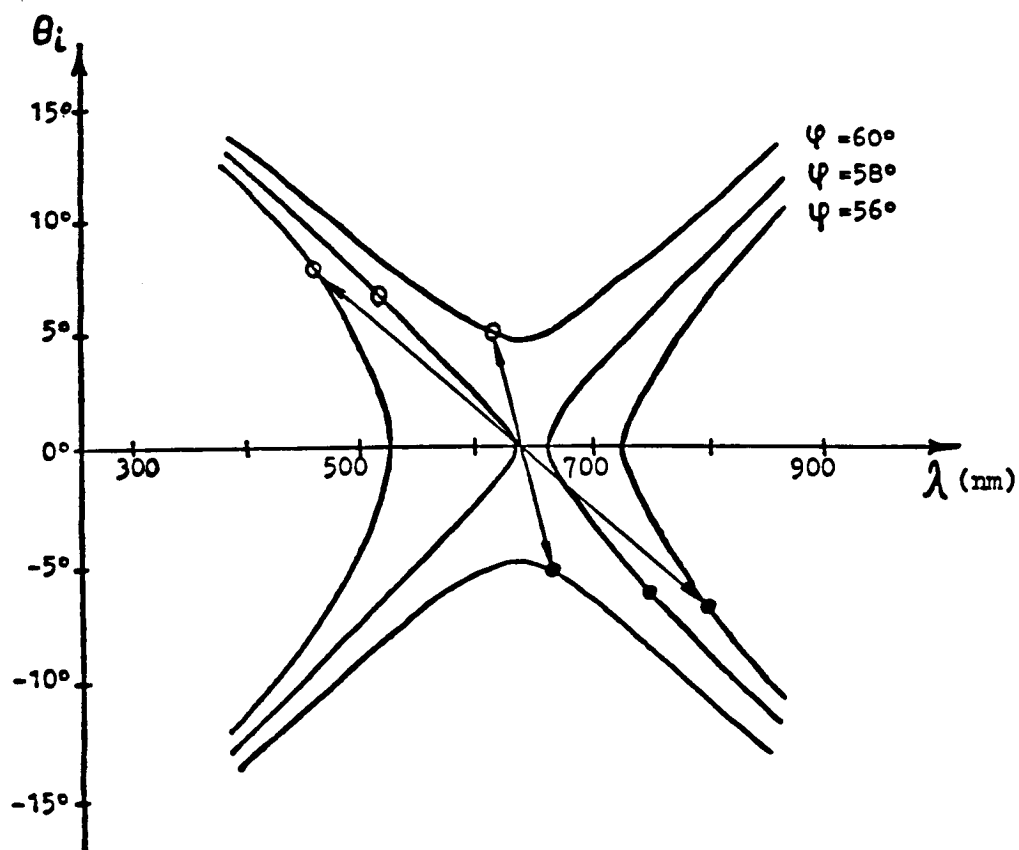
Fig.2. Frequency-angular dependence of scattered radiation. the symbols ● and o denote the photons conjugated by phase matching conditions.

thickness of rings of different frequency depends on the parameters of spacial coherency and the focal length of collecting lens 2.

The frequency-angular dependence of scattered radiation for the different orientations of the optical axis (z) of the crystal with respect to the laser beam wavevector k_L is shown in Fig.2. This dependence was measured with the help of a spectral device placed in the focal plane of the collecting lens.

The region of one-photon state localization was determined from measurements of the fourth-order space correlation function $G^{(2)}(E^{(-)}(r_1)E^{(-)}(r_2)E^{(+)}(r_1)E^{(+)}(r_2))$. The three-dimentional shape of that function was measured by scanning in space using micro holes (see Fig.3). The micro holes had a diameter much smaller than the space coherence area of radiation and were connected with photodetectors by fibers. The point of maximum probability of one-photon state localization along the z-direction was calculated by using a Gaussian approximation to the shape of the space correlation function and projecting the half-width dependence onto the x-z coordinate plane (see Fig.4).

It was found in our first experiment that the location of the point giving the maximum probability of one-photon state localization dependeds on the location of the reference photodetector in space. This result demonstrates the EPR paradox conditions for coordinate and momentum variables. We note here that the indirect measurement technique used here gave only a qualitative result. The accuracy of the first experiments was about 30-40%. We had to use a method of interpolation of the space correlation function shape because the time resolution of our electronics correlation circuit ($\tau \approx$ 1ns) could not allow us to make a direct measurement of the precise space point of photon localisation.

The result of the experiment could be easily interpreted with the help of the theory of hypothetical advanced Green functions /1,2/ and classical lens equations if the nonlinear crystal is considered as a mirror. However, it does not mean that real advanced electromagnetic waves exist.

We look forward to improvements of time parameters of our experimental apparatus to provide a quantitive result in the measurement of coordinate and momentum variables of optical fields generated in the SPDC process. Such work is in progress.
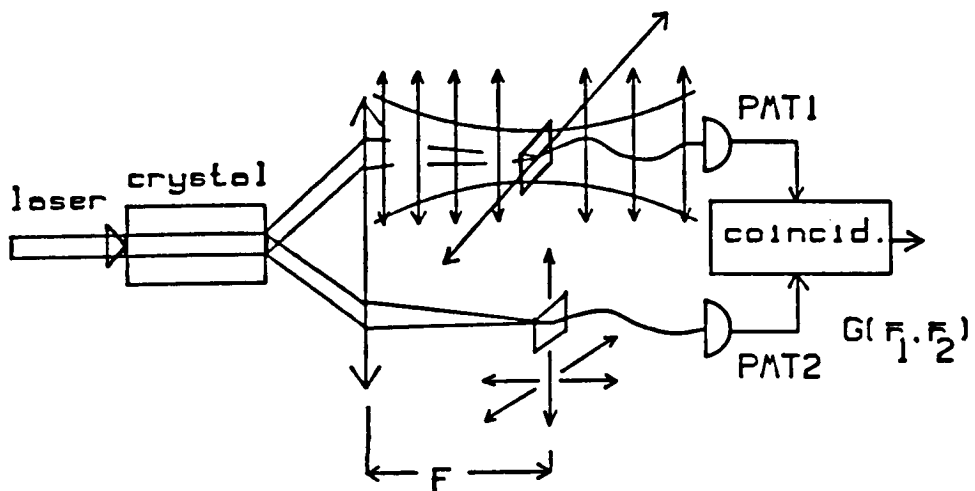
Fig.3. Outline of measurement of fourth-order space correlation function $G^{(2)}(r_1, r_2)$.
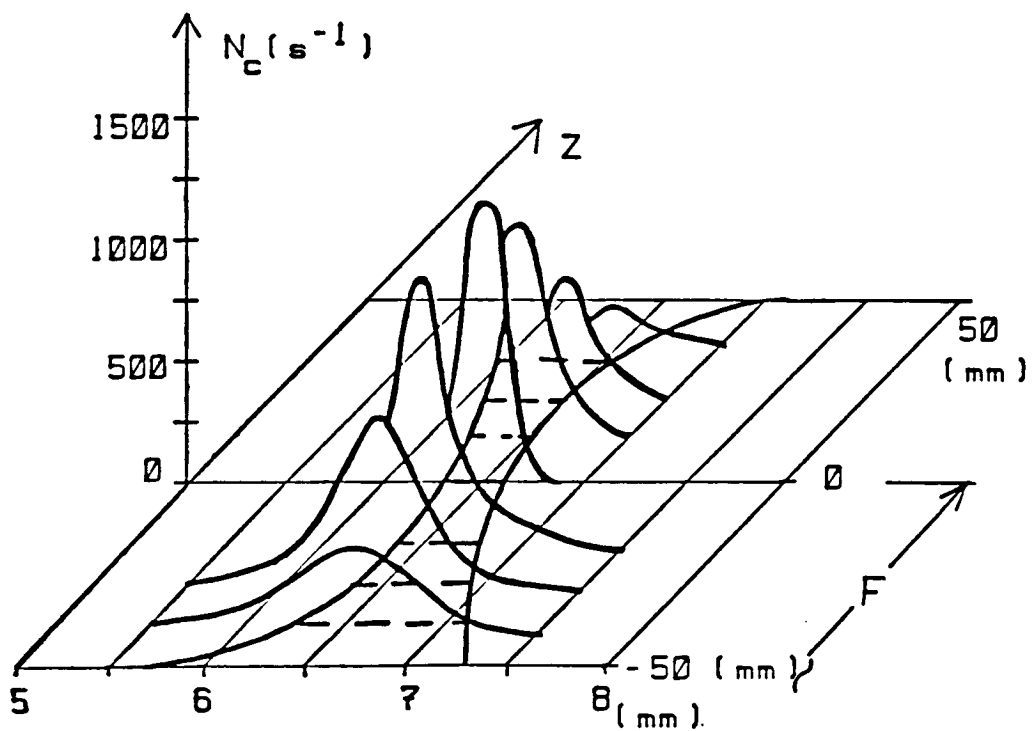
Fig.4. Result of the $G^{(2)}(r_1, r_2)$ space distribution measurement. The point of maximum probability of photon localization was calculated by interpolation of projection of half-width of correlation function value in a Gaussian shape approach on the x-z- plane.

1.Klyshko, D.N., 1988, "Combined EPR and Two-Slit Experiments: Interference of Advanced waves", Phys.Lett.A v.132, p.299 (1988).

2.Klyshko, D.N., 1988, "Effect of Focusing on Photon Correlation in Parametric Light Scattering", Sov.Phys.JETP, v.94, p.82 (1988).

3.Malygin, A.A., A.N.Penin and A.V.Sergienko, "Efficient Generator of Two-Photon Field of Visible Radiation," 1981, Sov.J.Quantum Electron., v.11(7), p.939.

4.Malygin, A.A., A.N.Penin and A.V.Sergienko, "Absolute Calibration of Sensitivity of Photodetectors Using a Biphotonic Field," 1981, Sov.Phys.JETP Lett., v.33, p.477.

5.Malygin, A.A., A.N.Penin and A.V.Sergienko, "Spatiotemporal Grouping of Photons in Spontaneous Parametric Scattering of Light," 1985, Sov.Phys.Dokl., v.30(3), p.227.

628/07
4 Pgs

GENERALIZED PARAMETRIC DOWN CONVERSION, MANY PARTICLE INTERFEROMETRY, AND BELL'S THEOREM

Hyung Sup Choi

The City College of The City University of New York
New York, NY 10031

ABSTRACT

A new field of multi-particle interferometry is introduced using a nonlinear optical spontaneous parametric down conversion (SPDC) of a photon into more than two photons. The study of SPDC using a realistic Hamiltonian in a multi-mode shows that at least low conversion rate limit is possible. The down converted field exhibits many stronger nonclassical phenomena than the usual two photon parametric down conversion. Application of the multi-particle interferometry to a recently proposed many particle Bell's theorem on Einstein-Podolsky-Rosen problem is given.

INTRODUCTION

A two photon *spontaneous* parametric down conversion (SPDC)[1] has been known to be an effective source of highly correlated photon pairs that exhibit many interesting nonclassical properties, such as squeezed states, antibunching, violation of classical inequalities, etc. Our study, which starts with a realistic Hamiltonian not only shows that the divergence problem[2,3], which occured in the usual parametric approximation, does not occur when the pump is quantized, but also shows that the phase matching problem, in principle, doesn't prohibit the phenomena to occur.

It is possible[4] to have the phenomenon at least in the low conversion rate limit. Since we know that quantum interferometers do not require a high coversion rate (indeed we like to have only one set of photons in the entire setup at any time), we can introduce a multi-particle quantum optical interferometry in which one measures the quantum correlation properties among more than two particles. One can construct three-photon coherent state interferometers in the form of a generalized momentum-position interferometry, a generalized form of a Franson-type position-time interferometry, and a generalized polarization correlation experiments, and look for their nonclassical behaviors.

I. GENERALIZED PARAMETRIC DOWN CONVERSION

Starting with an interaction Hamiltonian for three photon SPDC in the parametric approximation which allows multiple mode down conversion from the pump with wavevector k_0 and frequency ω_0:

$$H_I = \int dv \, \Sigma \Sigma \Sigma \, K \, \{\hat{a}_1 \hat{a}_2 \hat{a}_3 e^{-i\Lambda \, k \cdot r + i\omega_0 t}$$
$$+ \, \hat{a}_1^+ \hat{a}_2^+ \hat{a}_3^+ e^{i\Lambda \, k \cdot r - i\omega_0 t}\}, \tag{1}$$

we obtain the expressions for the time development of the operators $\hat{a}$, $\hat{a}^+$:

$$\dot{\hat{a}}_{ka} = -i\omega_k \, \hat{a}_{ka} - i \, \Sigma \Sigma K \, \hat{a}_1^+ \hat{a}_2^+ e^{-i\omega_0 t}$$
$$\cdot \delta(k_0 - k - k_1 - k_2) \tag{2a}$$

$$\dot{\hat{a}}^+_{ka} = i\omega_k \, \hat{a}^+_{ka} + i \, \Sigma \Sigma K \, \hat{a}_1 \hat{a}_2 e^{i\omega_0 t}$$
$$\cdot \delta(k_0 - k - k_1 - k_2) \tag{2b}$$

A major difference between Eqs.(2) and the equivalent two photon case is that in this case the δ function at the end of Eqs.(2) cannot eliminate the summations (or integrals, for a continuum) over k_1, k_2 unless we have a special selection mechanism such as ideal phase matching, or photon resonances, for the specific down converted frequencies.

But in any case, the equations can be solved and yield the same type of curves for the photon number, although in non-ideal phase matched cases, we have much smaller values. For example, for the 3 photon degenerate case we have

$$\ddot{N} = 18K^2 \cdot (3N^2 + 3N + 2) \qquad , \text{ etc.} \tag{3}$$

Except for the two photon case, which has a well known analytic solution $N = \sinh^2 Kt$ that diverges

at infinity, it can be shown that in all higher order cases the photon number diverges at a finite time. On the other hand, if we quantize the pump field, the interaction Hamiltonian H_{IQ} becomes

$$H_{IQ} = \int dv \ \Sigma \Sigma \Sigma \Sigma \ K_Q \{a_1 a_2 a_3 a_0^+ e^{-i\triangle k \cdot r}$$

$$+ \ a_1^+ a_2^+ a_3^+ a_0 e^{i\triangle k \cdot r}\}, \quad (4)$$

where K_Q is a quantum pump equivalent to K in parametric approximation.

From this we have a time development of the down converted photon number for the three photon degenerate SPDC:

$$N = 18 K_Q^2 \{(3N^2+3N+2)N_0(t)-N^3+5N+2)\}, \quad (5)$$

where $N_0(t)$ gives the expression for the depleted pump beam and is related to the down converted beam as $\langle N_0(t)\rangle = \langle N_0(0)\rangle - \langle N(t)\rangle$. The extra term with a negative sign in Eq.(5) will slow down the change of the slope of the curve when the pump depletion becomes significant. Notice that the expression in the quantum pump reduces to the parametric approximation for $N_0(t)>>N$. The photon number will eventually oscillate greatly for large Kt. This is true even in the case when we don't have an ideal phase matching.

II. MULTIPARTICLE INTERFEROMETRY

Two fundamental relations for a multi-photon spontaneous parametric down conversion, i.e.

$$k_0 = k_1 + k_2 + \cdots + k_n, \quad (6)$$

$$\omega_0 = \omega_1 + \omega_2 + \cdots + \omega_n, \quad (7)$$

along with the facts that the pump beam with k_0 and ω_0 is a coherent one and that the n-photon down converted state is represented by the *product* of the individual photon states, tell us that each individual down converted photon doesn't have a definite phase, while the total system carries the phase information. This n-photon correlation property opens a new field of multi-photon interferometry in which one measures the joint detection probability of n photons.

Our scheme for multi-photon interferometry starts with forming a quantum mechanically entangled state.

$$|\Psi\rangle = 2^{-1/2} \{ |+_1+_2\cdots+_n\rangle +$$

$$e^{i(\Phi_1+\Phi_2+\cdots+\Phi_n)} |-_1-_2\cdots-_n\rangle \}, \quad (8)$$

where $|+_i\rangle$ and $|-_i\rangle$ refer to the two different possible states of photon i and Φ_i represents

the phase difference between those two states. It is a matter of indifference whether $|+_i\rangle$ and $|-_i\rangle$ states are switched for any particle(s) i.

Now if our measurement M on the system involves off-diagonal matrix elements, i.e., a mixing of the two possible states, then the quantum mechanical expectation value $\langle\Psi| M |\Psi\rangle$ for the measurement will generally contain terms that oscillate sinusoidally with $\Phi_1+\Phi_2+\cdots+\Phi_n$. These off diagonal elements or the mixing of the states may be achieved by making use of beam splitters or a polarization analyzer whose axis lies in between the two orthogonal polarization axes. We stay with three particle systems because we would have an extremely small chance of getting a right set of correlated photons in higher order.

(1) Generalized Horne-Shimony-Zeilinger[5] interferometer: This two-photon momentum-position interferometer was implemented by Rarity and Tabster[6]. Recently, a three-particle version of the experiment was proposed by Greenberger et.al[7] to test against a family of local realism. Their gedanken three particle setup can be realized through the three photon SPDC which we described in the previous section. One would have an expectation value for the three photon joint detection that oscillates sinusoidally with $\Phi_1+\Phi_2+\Phi_3$.

(2) Generalized Franson Interferometer:
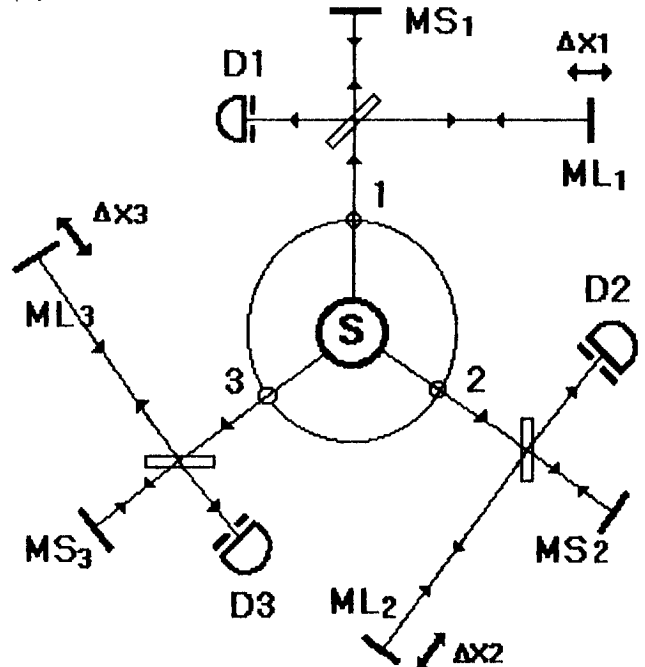
Fig.1 Three arm Franson interferometer

Franson[8] devised a two particle gedanken interferometor that uses the interference between two possible states each of which belongs to a different emission time.

The experiment was implemented by Ou et al.[9] and by Kwiat et al.[10] A generalized three-photon Franson interferometry may use the Ou et al.-type of setup with three Michelson interferometers as in Fig.1. The same analysis should go through as in the two photon case and the expectation value for the coincidence counting rate of three photons will exhibit a sinusoidal oscillation that depends upon the accumulated optical path differences between two possible paths.

(3) Polarization Interferometer: Finally, we construct a third type of entangled state formed by two orthogonal polarizations of photons for a three photon polarization interferometer. Suppose all three down converted photons are x-polarized. (one can in principle enforce this by placing x-filters after the apertures) In one set of paths (primed ones) we place half wave plates and in the other set of paths (unprimed ones) we place compensators and the variable phase shifters Φ_i.

Then we combine the beams on the beam splitters so that the polarization states may be mixed before they are registered by two channel linear polarization analyzers. If we count a detection of an x-polarized photon as +1 and a y-polarized photon as -1, using two channel analyzers, then we would have a three-photon joint detection probability:[11]

$$E(\Phi_1,\Phi_2,\Phi_3) = \eta^3 \cos(\Phi_1+\Phi_2+\Phi_3). \quad (9)$$

III.   BELL'S THEOREM   AND MORE

In general, the many particle correlated system we discussed here is not a mere generalization of two particle correlated system. It exhibits much stronger nonclassical effects than the usual two particle correlated system through its additional degree of freedom. Some found a stronger squeezing[3] and a more prominent antibunching[12]. We found a stronger violation of classical generalized Cauchy-Schwartz inequality by a

factor of (n-1)/n in a simple higher order system which can be easily generalized to other systems. We also found that in a Franson-type time-energy interferometer classical stochastic electrodynamics fails rapidly to reproduce quantum mechanical result in visibility by a factor of 1/2 for each additional order.

Finally, we saw the dramatic breakdown of local realism in many particle system due to Greenberger et.al (GHZ)[7]. It has shown that any local theories that is based on EPR type realism faces contradiction as it tries to immitate quantum mechanical results in a many particle correlated system. This theorem can be implemented by multiphoton interferometries which we discribed in Section II. Mermin[13] also has shown that the violation of Bell type inequality in a many particle system increases exponentially as it goes to a higher order. This is just an another example of a strong violation of classical limits by a many particle system through its additional quantum degree of freedom.

REFERENCES

1. C.Hong, L.Mandel, Phys.Rev.A 31, 2409 (1985)
2. M.Hillery, Phys.Rev.A 42, 498 (1990)
    R.Fisher et.al Phys.Rev.D 29, 1107 (1984);
3. S.Braunstein, R.McLachlan, Phys.Rev.A 35, 1659 (1987)
4. H.S.Choi, Submitted for publication
5. M.Horne et.al, Phys.Rev.Lett. 62, 2209 (1989)
6. J.Rarity, P.Tapster, Phys.Rev.Lett.64, 2495 (1990)
7. D.M.Greenberger et.al Am.J.Phys. 58, 1131 (1990)
8. J.D.Franson, Phys.Rev.Lett.62, 2205 (1989)
9. Z.Ou et.al, Phys.Rev.Lett.65, 321 (1990)
10. P.Kwiat et.al, Phys.Rev.A 41, 2910 (1990)
11. H.S.Choi, Phys.Lett.A 153, 285 (1991)
12. C.T.Lee, Phys.Rev.A 41, 1721 (1990)
13. N.D.Mermin, Phys.Rev.Lett. 65, 1838 (1990)

II. Squeezed States of Light

GOING THROUGH A QUANTUM PHASE

Jeffrey H. Shapiro
Department of Electrical Engineering and Computer Science
Massachusetts Institute of Technology
Cambridge, Massachusetts 02139-4307

Abstract

Phase measurements on a single-mode radiation field are examined from a system-theoretic viewpoint. Quantum estimation theory is used to establish the primacy of the Susskind-Glogower (SG) phase operator; its phase eigenkets generate the probability operator measure (POM) for maximum-likelihood phase estimation. A commuting observables description for the SG-POM on a signal×apparatus state space is derived. It is analogous to the signal-band×image-band formulation for optical heterodyne detection. Because heterodyning realizes the annihilation operator POM, this analogy may help realize the SG-POM. The wave function representation associated with the SG-POM is then used to prove the duality between the phase measurement and the number operator measurement, from which a number-phase uncertainty principle is obtained, via Fourier theory, without recourse to linearization. Fourier theory is also employed to establish the principle of number-ket causality, leading to a Paley-Wiener condition that must be satisfied by the phase-measurement probability density function (PDF) for a single-mode field in an *arbitrary* quantum state. Finally, a *two-mode* phase measurement is shown to afford phase-conjugate quantum communication at zero error probability with finite average photon number. Application of this construct to interferometric precision measurements is briefly discussed.

1. INTRODUCTION

A *classical* single-mode radiation field is characterized by a spatial-mode pattern $\vec{\xi}(\vec{r})$, an oscillation frequency ω in rad/s, and a c-number phasor a. The latter specifies both the energy and the initial phase

shift of the field—we can take $H = N\hbar\omega$ to be the mode energy, and ϕ to be the mode phase, where

$$a = \sqrt{N}e^{i\phi}, \qquad (1)$$

is the polar decomposition of a. When the single-mode classical field is quantized, its mode pattern and frequency are unchanged, but a is replaced by the annihilation operator $\hat{a}$. The phase problem, for this single-mode quantum field, has long been taken to mean finding a satisfactory quantum version of Eq. 1.[1] However, owing to the noncommutative nature of the quantum theory's operator algebra, no such decomposition exists, i.e., there is no observable $\hat{\phi}$ such that[2]

$$\hat{a} = \sqrt{\hat{N}}e^{i\hat{\phi}}. \qquad (2)$$

One may quibble about the order of the amplitude and phase terms on the right-side of Eq. 2, or prefer the use of $\hat{N} + \hat{I} = \hat{a}\hat{a}^\dagger$ in lieu of $\hat{N} = \hat{a}^\dagger\hat{a}$, etc., but the essential issue is the nonexistence of the observable $\hat{\phi}$.

Until recently the Susskind-Glogower (SG) phase operator,[2]

$$\widehat{e^{i\phi}} \equiv (\hat{a}\hat{a}^\dagger)^{-1/2}\hat{a}, \qquad (3)$$

has seemed to provide the best quantum description of phase. The SG operator is non-Hermitian, and its quadratures,

$$\widehat{\cos(\phi)} \equiv \mathrm{Re}(\widehat{e^{i\phi}}), \quad \text{and} \quad (4)$$

$$\widehat{\sin(\phi)} \equiv \mathrm{Im}(\widehat{e^{i\phi}}), \qquad (5)$$

are *non*commuting observables which *fail* certain reasonable conditions that the cosine and sine of a phase should meet. For example, it turns out that

$$\langle\psi|\widehat{\cos(\phi)}^2|\psi\rangle + \langle\psi|\widehat{\sin(\phi)}^2|\psi\rangle < 1, \qquad (6)$$

107

unless the state $|\psi\rangle$ is orthogonal to the vacuum, $|0\rangle$. On the other hand, the SG-based commutator

$$\left[\hat{N}, \widehat{\sin(\phi)}\right] = i\widehat{\cos(\phi)}, \qquad (7)$$

does lead to the oft-employed number phase uncertainty principle, $\Delta N \Delta\phi \geq 1/2$, under a high-mean-field linearization.

Lately, there has been intense renewed interest in the quantum phase problem. In what follows we will review some of the recent quantum phase work of Shapiro, Shepard, and Wong,[3, 4] and present some new results. Because the effort of Shapiro et al. originates from a quantum estimation theory viewpoint, that tack will taken here as well. Because the formalism of Shapiro et al. relies on the probability operator measure (POM) description of quantum measurement—a generalization of observables not well known in the physics literature—we will begin with a brief tutorial on POM's.

2. POM REVIEW

The textbook approach to quantum measurement is through *observables*.[5] For example, consider the quadrature components of the single-mode field's annihilation operator, i.e.,

$$\hat{a}_1 \equiv \mathrm{Re}(\hat{a}), \quad \text{and} \qquad (8)$$
$$\hat{a}_2 \equiv \mathrm{Im}(\hat{a}). \qquad (9)$$

These are *continuous-spectrum* observables. In other words, they are Hermitian operators

$$\hat{a}_j^\dagger = \hat{a}_j, \quad \text{for } j = 1, 2, \qquad (10)$$

with complete orthonormal (CON) eigenkets,

$$\hat{a}_j|\alpha_j\rangle_j = \alpha_j|\alpha_j\rangle_j,$$
$$\text{for } -\infty < \alpha_j < \infty, (11)$$
$$_j\langle\alpha_j'|\alpha_j\rangle_j = \delta(\alpha_j' - \alpha_j), \qquad (12)$$
$$\hat{I} = \int_{-\infty}^{\infty} d\alpha_j \, |\alpha_j\rangle_{jj}\langle\alpha_j|, (13)$$

where $\hat{I}$ is the identity operator, and $\delta(\cdot)$ is the Dirac delta function.

Measurement of a quadrature operator, when the system is in state $|\psi\rangle$, gives a continuous-valued, *classical* random variable with PDF

$$p(\alpha_j \mid |\psi\rangle) \equiv |_j\langle\alpha_j|\psi\rangle|^2,$$
$$\text{for } -\infty < \alpha_j < \infty, j = 1, 2. (14)$$

For this classical probability density to be correct, for all possible $|\psi\rangle$, it must satisfy

$$p(\alpha_j \mid |\psi\rangle) \geq 0,$$
$$\text{for } -\infty < \alpha_j < \infty, j = 1, 2, (15)$$

and

$$\int_{-\infty}^{\infty} d\alpha_j \, p(\alpha_j \mid |\psi\rangle) = 1,$$
$$\text{for } j = 1, 2. \qquad (16)$$

These conditions are ensured by Eq. 13, which leads to the familiar quadrature representations—essentially the position and momentum wave functions—given by

$$|\psi\rangle = \hat{I}|\psi\rangle = \int_{-\infty}^{\infty} d\alpha_1 \, |\alpha_1\rangle_{11}\langle\alpha_1|\psi\rangle$$
$$= \int_{-\infty}^{\infty} d\alpha_1 \, \psi(\alpha_1)|\alpha_1\rangle_1, \qquad (17)$$

and

$$|\psi\rangle = \hat{I}|\psi\rangle = \int_{-\infty}^{\infty} d\alpha_2 \, |\alpha_2\rangle_{22}\langle\alpha_2|\psi\rangle$$
$$= \int_{-\infty}^{\infty} d\alpha_2 \, \Psi(\alpha_2)|\alpha_2\rangle_2, \qquad (18)$$

with the obvious identifications for $\psi(\alpha_1)$ and $\Psi(\alpha_2)$. Of course, the quadratures are *noncommuting* observables,

$$[\hat{a}_1, \hat{a}_2] = \frac{i}{2}\hat{I}, \qquad (19)$$

so they cannot be measured *simultaneously*.[5]

The preceding review demonstrates that the full specification of observables, i.e., Hermitian operators with CON eigenkets, is *not* needed to produce a consistent statistical characterization of a quantum measurement. For an arbitrary quantum state, a *resolution of the identity*—an outer-product sum like Eq. 13—generates a proper classical-probability description of a quantum measurement. This is the

108

essence of the POM concept. Our principal purpose for introducing POM's is to accommodate measurements that are *not* observables on the state space, $\mathcal{H}$, of the $\hat{a}$-mode. The best way to introduce such nonobservable POM's is through an example. It is well known that the annihilation operator, $\hat{a}$, is *not* an observable—it is non-Hermitian,

$$\hat{a}^\dagger \neq \hat{a}. \tag{20}$$

Furthermore, its real and imaginary parts, $\hat{a}_1$ and $\hat{a}_2$, are *noncommuting* observables—$\hat{a}$ cannot be measured in the usual textbook sense. However, the annihilation operator *does* have eigenkets—the coherent states,[6]

$$\hat{a}|\alpha\rangle = \alpha|\alpha\rangle,$$
$$\text{for } \alpha \in \mathcal{C}, \tag{21}$$

where $\mathcal{C}$ is the complex plane. These states are *not* orthonormal, i.e.,

$$\langle\alpha'|\alpha\rangle =$$
$$\exp\left(-\frac{1}{2}|\alpha'|^2 - \frac{1}{2}|\alpha|^2 + \alpha'^*\alpha\right), \tag{22}$$

which is a consequence of the nonvanishing commutator

$$\left[\hat{a}, \hat{a}^\dagger\right] = \hat{I}, \tag{23}$$

implied by Eq. 19. Nevertheless, the coherent states are complete, in fact overcomplete—they form a resolution of the identity

$$\hat{I} = \frac{1}{\pi} \int_{\alpha \in \mathcal{C}} d^2\alpha \, |\alpha\rangle\langle\alpha|, \tag{24}$$

which defines the $\hat{a}$-POM. The outcome of the $\hat{a}$-POM is a complex-valued, continuous classical random variable with PDF

$$p(\alpha \mid |\psi\rangle) = \frac{1}{\pi}|\langle\alpha|\psi\rangle|^2,$$
$$\text{for } \alpha \in \mathcal{C}, \tag{25}$$

when the field state is $|\psi\rangle$. Because of Eq. 24, it follows that

$$p(\alpha \mid |\psi\rangle) \geq 0, \quad \text{for } \alpha \in \mathcal{C}, \tag{26}$$

and

$$\int_{\alpha \in \mathcal{C}} d^2\alpha \, p(\alpha \mid |\psi\rangle) = 1, \tag{27}$$

hold, for all $|\psi\rangle$.

The preceding POM has long been known.[7, 8, 9] It represents a measurement, in the POM sense, of the annihilation operator $\hat{a}$: the $\hat{a}$-eigenkets generate the measurement statistics, and the $\hat{a}$-eigenvalues are the resulting observation values. This parallels the usual observables description: the observable's eigenkets generate the measurement statistics, and the associated eigenvalues are the observation values, cf. Eq. 14.

The POM formulation is *not* in conflict with the conventional dictum that only observables can be measured. Any nonobservable POM on $\mathcal{H}$ can be represented as a collection of commuting observables on some *larger* state space which describes the original system interacting with an appropriate apparatus.[7] The most familiar example of this genre is optical heterodyne detection of a single-mode signal field, which provides *both* a commuting-observables description *and* a physical realization for the $\hat{a}$-POM.

In optical heterodyne detection,[8, 9, 10] a signal field of frequency ν is mixed with a strong local-oscillator (LO) field of frequency $\nu - \nu_{IF}$ on the surface of a photodetector. With a unity-quantum efficiency detector, and two-channel lock-in amplification at the intermediate frequency (ν_{IF}), this arrangement produces a complex-valued, classical random variable, y, whose measurement statistics are identical to those of the operator[9]

$$\hat{y} \equiv \left(\hat{a}_S \otimes \hat{I}_I\right) + \left(\hat{I}_S \otimes \hat{a}_I^\dagger\right). \tag{28}$$

Here $\hat{a}_j$ and $\hat{I}_j$, for $j = S, I$, are the annihilation and identity operators for the *signal* mode (frequency ν), and the *image* mode (frequency $\nu - 2\nu_{IF}$), respectively. Both of these modes beat with the LO to produce IF waveforms, just as is the case in classical superheterodyne radio reception. It is easily verified that the real and imaginary parts of $\hat{y}$ are *commuting* observables on the *joint* state space, $\mathcal{H}_S \otimes \mathcal{H}_I$, and so are simultaneously measurable in the usual sense. Ordinarily, only the signal mode carries information, i.e., the image mode is unexcited. Under these circumstances, the PDF for the observed y-value

reduces to[8, 9]

$$p(y \mid \mid\psi\rangle_S) = \frac{1}{\pi}|_S\langle y|\psi\rangle_S|^2,$$
$$\text{for } y \in \mathcal{C}, \qquad (29)$$

where $|y\rangle_S$ is the signal-mode coherent state with eigenvalue y, and $|\psi\rangle_S$ is an arbitrary signal-mode state. Comparison of Eqs. 29 and 25 completes the demonstration that heterodyning—a pair of commuting observables on an extended state space with an unexcited image mode—realizes the $\hat{a}_S$-POM.

3. PHASE ESTIMATION

Rather than seeking a quantum formalism for phase by pursuing a quantum version of Eq. 1, Shapiro, Shepard, and Wong[3, 4] approached the problem from the estimation theory viewpoint. Consider the following abstract quantum estimation problem. A single-mode input field of annihilation operator $\hat{a}_{IN}$ and quantum state $|\psi\rangle_{IN}$ undergoes an unknown, nonrandom, c-number phase shift Φ, yielding a single-mode output field of annihilation operator

$$\hat{a} = e^{i\Phi}\hat{a}_{IN}, \qquad (30)$$

in state

$$|\psi\rangle = \exp\left(i\Phi\hat{a}_{IN}^{\dagger}\hat{a}_{IN}\right)|\psi\rangle_{IN}. \qquad (31)$$

By making an appropriate quantum measurement on the $\hat{a}$ mode, and knowing the input state $|\psi\rangle_{IN}$, we are to estimate the phase shift Φ. An interferometric phase measurement can be embedded into this scheme by placing appropriate constraints on the allowable quantum measurement. Optimizing a phase measurement within this more restricted environment *cannot* outperform the behavior obtained from an unfettered measurement optimization. Indeed, we should expect that *joint* optimization of the quantum measurement *and* the input state will yield superior phase estimation performance.

Without loss of generality, we can confine the phase shift to a 2π-rad interval, i.e., we can assume that $-\pi < \Phi \leq \pi$. The class of POM's we must optimize over, in order to find the best phase measurement,

can be taken to be $\{d\hat{\Pi}(\phi) : -\pi < \phi \leq \pi\}$, where

$$d\hat{\Pi}(\phi) = d\hat{\Pi}(\phi)^{\dagger}, \qquad (32)$$

and

$$\hat{I} = \int_{-\pi}^{\pi} d\hat{\Pi}(\phi), \qquad (33)$$

on the state space of the output mode, $\hat{a}$. The conditional probability density, given Φ, for obtaining a phase value ϕ from this POM is

$$p(\phi \mid \Phi) = \frac{\langle\psi|d\hat{\Pi}(\phi)|\psi\rangle}{d\phi},$$
$$\text{for } -\pi < \phi, \Phi \leq \pi, \qquad (34)$$

where $|\psi\rangle$ is the state of the $\hat{a}$-mode.

In *classical* estimation theory, the maximum-likelihood (ML) estimate Φ_{ML} of an unknown, nonrandom, phase shift Φ, based on a noisy phase-shift observation ϕ, of known PDF $p(\phi \mid \Phi)$, is the phase shift which maximizes the likelihood of getting the observed datum, i.e.,

$$\Phi_{ML}(\phi) = \arg \max_{-\pi < \theta \leq \pi} p(\phi \mid \theta). \qquad (35)$$

Often, the ML phase estimate equals the observed phase shift, because $p(\phi \mid \theta)$ has its peak at $\theta = \phi$, for $-\pi < \phi \leq \pi$. Such is the case for phase estimation in additive white Gaussian noise.[11] It then follows the $p(\phi \mid \phi)$, the *peak* likelihood, is a simple, but meaningful, performance measure for Φ_{ML}. Indeed, its reciprocal,

$$\delta\phi \equiv \frac{1}{p(\phi \mid \phi)}, \qquad (36)$$

is the PDF's width for the case of a uniform distribution; if the distribution is Gaussian, then we have $\delta\phi = \sqrt{2\pi}\Delta\phi$, where $\Delta\phi$ is the root-mean-square (RMS) error.

Our problem is one of *quantum* estimation theory, namely, choosing the POM, $d\hat{\Pi}(\phi)$, and the input state, $|\psi\rangle_{IN}$, to optimize our estimate of the phase shift Φ. For a *given* POM *and* input state, Eq. 34 supplies the PDF needed to perform classical ML estimation. In this quantum setting, however, the observed phase value ϕ is, by presumption, our estimate of Φ. Thus, in

order for this estimate to be one of maximum likelihood, we can restrict our attention to POM's satisfying

$$\phi = \arg \max_{-\pi < \theta \le \pi} p(\phi \mid \theta),$$
$$\text{for } -\pi < \phi \le \pi, \qquad (37)$$

and optimize our estimate over $d\widehat{\Pi}$ and $|\psi\rangle_{IN}$ by maximizing the peak likelihood—minimizing $\delta\phi$—averaged over all possible Φ values. Here it is known that, for the *input* state whose number representation, $\psi_n \equiv \langle n|\psi\rangle$, is

$$\psi_n = |\psi_n|e^{i\chi_n}, \quad \text{for } n = 0,1,2,\ldots, \quad (38)$$

$\delta\phi$ is minimized by the following POM,[7]

$$d\widehat{\Pi}(\phi) = |e^{i\phi}, \psi\rangle\langle e^{i\phi}, \psi|\frac{d\phi}{2\pi},$$
$$\text{for } -\pi < \phi \le \pi, \quad (39)$$

where

$$|e^{i\phi}, \psi\rangle \equiv \sum_{n=0}^{\infty} e^{i(n\phi+\chi_n)}|n\rangle. \qquad (40)$$

Moreover, the reciprocal peak-likelihood that results when we use this optimum POM to estimate Φ is easily shown to be

$$\delta\phi = 2\pi \left|\langle e^{i\phi}, \psi|\psi\rangle\right|^{-2}$$
$$= 2\pi \left(\sum_{n=0}^{\infty} |\psi_n|\right)^{-2}, \qquad (41)$$

which is *independent* of the phases $\{\chi_n\}$. In fact, $p(\phi \mid \Phi)$ is independent of the $\{\chi_n\}$.

We can exploit the $\{\chi_n\}$ independence to good purposes by assuming, without loss of generality, that the input state has positive real ψ_n. Equation 40 then reduces to

$$|e^{i\phi}, \psi\rangle = |e^{i\phi}\rangle \equiv \sum_{n=0}^{\infty} e^{in\phi}|n\rangle,$$
$$\text{for } -\pi < \phi \le \pi, \quad (42)$$

which is the number-ket expansion of the SG phase operator's (infinite-energy) eigenkets, viz.

$$\widehat{e^{i\phi}}|e^{i\phi}\rangle = e^{i\phi}|e^{i\phi}\rangle,$$
$$\text{for } -\pi < \phi \le \pi. \quad (43)$$

This says that the SG-POM is the quantum measurement for ML phase estimation in the general measurement configuration when the input state has a positive real number representation. In other words, the phase eigenkets of the SG operator generate the resolution of the identity,

$$\hat{I} = \frac{1}{2\pi}\int_{-\pi}^{\pi} d\phi\, |e^{i\phi}\rangle\langle e^{i\phi}|, \qquad (44)$$

needed for ML quantum phase estimation in this case. For an *arbitrary* input state, the optimum POM from Eq. 39 is equivalent to performing the unitary state transformation

$$\hat{U} \equiv \sum_{n=0}^{\infty} e^{-i\chi_n}|n\rangle\langle n|, \qquad (45)$$

followed by the SG-POM.

To achieve the goal of *jointly* optimizing phase-estimation performance over *both* the measurement *and* the input state, it only remains for us to minimize $\delta\phi$, from Eq. 41, by appropriate choice of $|\psi\rangle_{IN}$. This problem has been addressed,[3, 4] and the state

$$\psi_n = \frac{A}{1+n},$$
$$\text{for } n = 0,1,2,\ldots,M < \infty, \quad (46)$$

where A is a normalization constant and M is a truncation parameter, has been shown to achieve

$$\delta\phi \sim 1/N^2, \qquad (47)$$

in terms of its average photon number, $N = \langle\hat{a}^\dagger\hat{a}\rangle$. This performance is far superior to the $\delta\phi \sim 1/N$ reciprocal peak likelihood capability of optimized squeezed-state interferometry. However, the phase measurement PDF for the Eq. 46 state is a heavy-tailed distribution, viz., its RMS phase error, $\Delta\phi$, is essentially independent of N. Thus, the degree to which this reciprocal peak likelihood advantage can be usefully exploited has yet to be established.[12] In what follows, therefore, we will concentrate on the SG-POM, in that it constitutes the maximum-likelihood quantum phase measurement for *all* quantum states.

4. SG POM

The Susskind-Glogower operator,[2, 13]

$$\widehat{e^{i\phi}} \equiv (\hat{a}\hat{a}^\dagger)^{-1/2}\hat{a}, \qquad (48)$$

affords a well-defined polar decomposition of $\hat{a}$,

$$\hat{a} = \sqrt{\hat{N} + \hat{I}}\,\widehat{e^{i\phi}}, \qquad (49)$$

in terms of energy (number) and phase operators. Using the number-ket expansions of $\hat{N}$ and $\hat{a}$ we have that

$$\widehat{e^{i\phi}} = \sum_{n=0}^{\infty} |n\rangle\langle n+1|, \qquad (50)$$

from which it follows that

$$
\begin{aligned}
\widehat{e^{-i\phi}} &\equiv \widehat{e^{i\phi}}^\dagger \\
&= \sum_{n=0}^{\infty} |n+1\rangle\langle n| \neq \widehat{e^{i\phi}}, \quad (51)
\end{aligned}
$$

and

$$\left[\widehat{e^{i\phi}}, \widehat{e^{-i\phi}}\right] = |0\rangle\langle 0|. \qquad (52)$$

In words, the SG phase operator is *not* Hermitian, and does *not* commute with its adjoint. Thus, as was seen earlier for $\hat{a}$ itself, the quadrature components of the SG operator,

$$\widehat{\cos(\phi)} \equiv \mathrm{Re}(\widehat{e^{i\phi}}), \quad \text{and} \quad (53)$$

$$\widehat{\sin(\phi)} \equiv \mathrm{Im}(\widehat{e^{i\phi}}), \qquad (54)$$

are *noncommuting* observables,

$$\left[\widehat{\cos(\phi)}, \widehat{\sin(\phi)}\right] = \frac{i}{2}|0\rangle\langle 0|. \qquad (55)$$

The SG-POM derives from the fact that $\widehat{e^{i\phi}}$ has an *overcomplete* set of eigenkets, cf. the Sect. 2 discussion of the $\hat{a}$-POM. By direct substitution of Eq. 50, we can verify that

$$
\begin{aligned}
\widehat{e^{i\phi}}|e^{i\phi}\rangle &= e^{i\phi}|e^{i\phi}\rangle, \\
&\text{for } -\pi < \phi \leq \pi, \quad (56)
\end{aligned}
$$

where $|e^{i\phi}\rangle$ has the number-ket representation given in Eq. 42. That these kets

resolve the identity is also easily shown,

$$
\begin{aligned}
&\int_{-\pi}^{\pi} d\phi\, |e^{i\phi}\rangle\langle e^{i\phi}| \\
&= \sum_{n=0}^{\infty}\sum_{m=0}^{\infty}\int_{-\pi}^{\pi} d\phi\, e^{i(n-m)\phi}|n\rangle\langle m| \\
&= 2\pi \sum_{n=0}^{\infty} |n\rangle\langle n| = 2\pi \hat{I}. \qquad (57)
\end{aligned}
$$

That they are *not* orthonormal can be demonstrated from some simple Fourier transform manipulations,[14]

$$
\begin{aligned}
\langle e^{i\phi'}|e^{i\phi}\rangle &= \sum_{n=0}^{\infty} e^{-in(\phi'-\phi)} \\
&= \frac{1}{2}\left(\sum_{n=-\infty}^{\infty} e^{-in(\phi'-\phi)}\right. \\
&\quad \left. + \sum_{n=-\infty}^{\infty}\mathrm{sgn}(n)e^{-in(\phi'-\phi)} + 1\right) \\
&= \pi\delta(\phi'-\phi) \\
&\quad - \frac{i}{2}\cot\left(\frac{\phi'-\phi}{2}\right) + \frac{1}{2} \qquad (58)
\end{aligned}
$$

Here, $\delta(\cdot)$ is the Dirac delta function, and

$$\mathrm{sgn}(n) \equiv \begin{cases} -1, & n < 0, \\ 0, & n = 0, \\ 1, & n > 0, \end{cases} \qquad (59)$$

is the signum function.

5. COMMUTING OBSERVABLES

Recall that a POM on $\mathcal{H}$ which is *not* an observable on that space can be represented as a collection of commuting observables on a larger, signal×apparatus state space, $\mathcal{H} \otimes \mathcal{H}_A$, with the apparatus placed in some appropriate state. We now develop such a representation for the SG-POM. Aside from alleviating the qualms of those who believe only in observables, this representation may guide us to a realization of the SG-POM—the commuting-observables description of the $\hat{a}$-POM is intimately connected with its heterodyne-detection realization.

Let $\hat{a}_A$ be the annihilation operator of an apparatus mode, whose state space,

$\mathcal{H}_A$, is spanned by its number kets, $\{ |n\rangle_A : n = 0, 1, 2, \dots \}$. The non-Hermitian operator

$$\hat{Y} \equiv \left(\widehat{e^{i\phi}} \otimes |0\rangle_{AA}\langle 0| \right) + \left(|0\rangle\langle 0| \otimes \widehat{e^{-i\phi}}_A \right), \quad (60)$$

where

$$\widehat{e^{-i\phi}}_A \equiv \hat{a}_A^\dagger (\hat{a}_A \hat{a}_A^\dagger)^{-1/2}, \quad (61)$$

is easily shown to commute with its adjoint. Here, $\hat{Y}$ is an operator on the joint state space $\mathcal{H} \otimes \mathcal{H}_A$, and $\widehat{e^{i\phi}}_A$ is the apparatus mode's SG phase operator.

Because $[\hat{Y}, \hat{Y}^\dagger] = 0$, the quadrature components of $\hat{Y}$—denoted $\hat{Y}_1$ and $\hat{Y}_2$—are commuting observables, which can be measured *simultaneously*, i.e., $\hat{Y} = \hat{Y}_1 + \hat{Y}_2$ can be measured in the usual sense. Solving for the eigenkets and eigenvalues of $\hat{Y}$ we find that signal×apparatus number ket

$$|Y\rangle \equiv |n\rangle|m\rangle_A, \quad \text{for } nm > 0, \quad (62)$$

is a $\hat{Y}$-eigenket with zero eigenvalue, and

$$|Y\rangle \equiv \frac{1}{\sqrt{2\pi}} \Bigg(|0\rangle|0\rangle_A$$
$$+ \sum_{n=1}^{\infty} \left(e^{in\phi}|n\rangle|0\rangle_A + e^{-in\phi}|0\rangle|n\rangle_A \right) \Bigg),$$
$$\text{for } -\pi < \phi \le \pi, \quad (63)$$

is a $\hat{Y}$-eigenket whose associated eigenvalue is $e^{i\phi}$. Collectively, these comprise a CON set from which we have that measurement of $\hat{Y}$, when the signal×apparatus state is $|\psi\rangle_{S\times A} \in \mathcal{H} \otimes \mathcal{H}_A$, yields a *mixed* classical random variable, Y, which takes on *either* the *discrete* value 0, *or* a value from the *continuum* $\{ e^{i\phi} : -\pi < \phi \le \pi \}$. The former occurs with discrete probability

$$\Pr(0 \mid |\psi\rangle_{S\times A}) = \sum_{n=1}^{\infty} \sum_{m=1}^{\infty} |\psi_{nm}|^2; \quad (64)$$

the probability density for the latter is

$$p(\phi \mid |\psi\rangle_{S\times A}) = \frac{1}{2\pi} \Bigg| \psi_{00} +$$
$$\sum_{n=1}^{\infty} \left(e^{-in\phi}\psi_{n0} + e^{in\phi}\psi_{0n} \right) \Bigg|^2,$$
$$\text{for } -\pi < \phi \le \pi, \quad (65)$$

where $\psi_{nm} \equiv {}_A\langle m|\langle n|\psi\rangle_{S\times A}$. These two are properly normalized in that for *all* $|\psi\rangle_{S\times A}$ we have that

$$\Pr(0 \mid |\psi\rangle_{S\times A})$$
$$+ \int_{-\pi}^{\pi} d\phi \, p(\phi \mid |\psi\rangle_{S\times A}) = 1, \quad (66)$$

as required by classical probability theory.

Now, the commuting-observables representation of the SG-POM is at hand. Suppose we measure $\hat{Y}$ when the apparatus mode is unexcited, i.e., $|\psi\rangle_{S\times A} = |\psi\rangle|0\rangle_A$, where $|\psi\rangle \in \mathcal{H}$ is an *arbitrary* signal-mode state and $|0\rangle_A$ is the apparatus mode's vacuum state. Then the discrete value zero is *never* obtained, and the PDF for obtaining $Y = e^{i\phi}$ reduces to

$$p(\phi \mid |\psi\rangle|0\rangle_A)$$
$$= \frac{1}{2\pi} \left| \sum_{n=0}^{\infty} e^{-in\phi}\psi_n \right|^2$$
$$= \frac{1}{2\pi} |\langle e^{i\phi}|\psi\rangle|^2,$$
$$\text{for } -\pi < \phi \le \pi, \quad (67)$$

realizing the SG-POM statistics for an *arbitrary* state of the $\hat{a}$-mode.

The equivalence of the SG-POM to the $\hat{Y}$ measurement with an unexcited apparatus mode allows us to clarify some basic points. First, because the SG operator does not commute with its adjoint, it is really the operator analog of the c-number $e^{i\phi}$ from the classical single-mode field. In other words, there is *no* Hermitian phase operator, $\hat{\phi}$, on $\mathcal{H}$ such that $\exp(i\hat{\phi}) = (\hat{a}\hat{a}^\dagger)^{-1/2}\hat{a}$. Restated in terms of the quadratures of the SG operator, this means that $\widehat{\cos(\phi)} \ne \cos(\hat{\phi})$, and $\widehat{\sin(\phi)} \ne \sin(\hat{\phi})$. As a result, the classical trigonometric identity,

$$\cos(\phi)^2 + \sin(\phi)^2 = 1,$$
$$\text{for } -\pi < \phi \le \pi, \quad (68)$$

does *not* apply to the quadratures of the SG phase operator, e.g., because

$$\widehat{\cos(\phi)}^2 + \widehat{\sin(\phi)}^2 = \hat{I} - \frac{|0\rangle\langle 0|}{2}, \quad (69)$$

113

any $|\psi\rangle$ with $\psi_0 \neq 0$ gives

$$\langle\psi|\widehat{\cos(\phi)}^2|\psi\rangle + \langle\psi|\widehat{\sin(\phi)}^2|\psi\rangle < 1. \quad (70)$$

However, the outcome of the SG-POM *is* a phasor $e^{i\phi}$—the $\hat{Y}$ measurement with a vacuum-state apparatus mode yields a complex-valued, continuous classical random variable $Y = e^{i\phi}$, where $-\pi < \phi \leq \pi$. Thus, we have that $|Y|^2 = 1$, *with probability one.*

The second point to note regarding the SG-POM is the relation of its mean value to those of the SG quadratures. Using

$$\begin{aligned}
\hat{Y}_1 &= \left(\widehat{\cos(\phi)} \otimes |0\rangle_{AA}\langle 0|\right) \\
&+ \left(|0\rangle\langle 0| \otimes \widehat{\cos(\phi)}_A\right), \quad (71)
\end{aligned}$$

and

$$\begin{aligned}
\hat{Y}_2 &= \left(\widehat{\sin(\phi)} \otimes |0\rangle_{AA}\langle 0|\right) \\
&- \left(|0\rangle\langle 0| \otimes \widehat{\sin(\phi)}_A\right), \quad (72)
\end{aligned}$$

and assuming an unexcited apparatus mode, we find that

$$_A\langle 0|\langle\psi|\hat{Y}_1|\psi\rangle|0\rangle_A = \langle\psi|\widehat{\cos(\phi)}|\psi\rangle, \quad (73)$$

and

$$_A\langle 0|\langle\psi|\hat{Y}_2|\psi\rangle|0\rangle_A = \langle\psi|\widehat{\sin(\phi)}|\psi\rangle, \quad (74)$$

for *all* $\hat{a}$-mode states, $|\psi\rangle$. What this says is that *averages* of the *classical* $\cos(\phi)$ and $\sin(\phi)$ random variables obtained from the SG-POM coincide with *averages* of the SG phase operator's quadratures. To the extent that the quadrature mean values comprise the information of interest, we can conclude that the SG-POM provides a proper quantum measurement description for simultaneous extraction of this information from both quadratures.

6. UNCERTAINTY PRINCIPLE

Number-ket expansions of the quadrature operators $\widehat{\cos(\phi)}$ and $\widehat{\sin(\phi)}$ lead to the commutator

$$\left[\hat{N}, \widehat{\sin(\phi)}\right] = i\widehat{\cos(\phi)}, \quad (75)$$

and the associated uncertainty principle

$$\langle\Delta\hat{N}^2\rangle\langle\Delta\widehat{\sin(\phi)}^2\rangle \geq \frac{1}{4}\left|\langle\widehat{\cos(\phi)}\rangle\right|^2. \quad (76)$$

Equation 76 is valid for arbitrary states, but its utility, in this general form, is somewhat limited. First, the minimum uncertainty product is state dependent— a consequence of Eq. 75 not being a c-number commutator. Second, the principle does not directly address the variance of a *phase* measurement—it is the $\widehat{\sin(\phi)}$ operator whose variance appears.

It is common practice to use the linearized form of Eq. 76,

$$\Delta N \Delta\phi \geq \frac{1}{2}, \quad (77)$$

which applies for states meeting the high-mean-field condition,

$$\langle\hat{N}\rangle \approx |\langle\hat{a}\rangle|^2 \gg 1. \quad (78)$$

The linearized result, while useful, can be abused. Number kets have zero number-measurement uncertainty, and $\langle\hat{a}\rangle = 0$, $\langle\widehat{\cos(\phi)}\rangle = 0$, hence the general result leads to the correct number-ket limit,

$$\langle\Delta\hat{N}^2\rangle\langle\Delta\widehat{\sin(\phi)}^2\rangle \geq 0, \quad (79)$$

whereas the linearized form is inapplicable.

Although the SG-POM does *not* alleviate the state-dependent nature of number-phase uncertainty limits, it *does* lead to an uncertainty principle which directly addresses phase variance. Our route to this principle—through Fourier theory— has the following motivation. The time-bandwidth uncertainty principle for the continuous-time Fourier transform (CTFT)[14] can be applied to the normalized position and momentum wave functions, $\psi(\alpha_1)$, and $\Psi(\alpha_2)$, because they satisfy the Fourier transform relations[5]

$$\Psi(\alpha_2) = \int_{-\infty}^{\infty} \frac{d\alpha_1}{\sqrt{\pi}} \psi(\alpha_1) e^{-i2\alpha_1\alpha_2}, \quad (80)$$

and

$$\psi(\alpha_1) = \int_{-\infty}^{\infty} \frac{d\alpha_2}{\sqrt{\pi}} \Psi(\alpha_2) e^{i2\alpha_1\alpha_2}. \quad (81)$$

The result of this procedure can be reduced to

$$\langle \Delta \hat{a}_1^2 \rangle \langle \Delta \hat{a}_2^2 \rangle \geq \frac{1}{16}, \qquad (82)$$

which is the Heisenberg uncertainty principle for the annihilation operator's quadratures.

Because of Eq. 44, any state $|\psi\rangle$ has a *phase* representation

$$\Psi(e^{i\phi}) \equiv \langle e^{i\phi} | \psi \rangle,$$
$$\text{for } -\pi < \phi \leq \pi, \quad (83)$$

such that

$$|\psi\rangle = \hat{I}|\psi\rangle$$
$$= \frac{1}{2\pi} \int_{-\pi}^{\pi} d\phi \, \Psi(e^{i\phi}) |e^{i\phi}\rangle. \quad (84)$$

The phase representation of $|\psi\rangle$ is intimately related to its number-ket representation, $\psi_n \equiv \langle n|\psi \rangle$—they are a Fourier transform pair

$$\Psi(e^{i\phi}) = \sum_{n=0}^{\infty} \psi_n e^{-in\phi} \qquad (85)$$

and

$$\psi_n = \frac{1}{2\pi} \int_{-\pi}^{\pi} d\phi \, \Psi(e^{i\phi}) e^{in\phi}, \quad (86)$$

as can be seen from Eqs. 83 and 42. In other words, $\Psi(e^{i\phi})$ and ψ_n constitute phase and number *wave functions*, which are capable of representing arbitrary states. The complementarity of the number operator measurement—whose probability distribution is $\Pr(\hat{N} = n) = |\psi_n|^2$—and the SG POM—whose probability density function is $p(\phi) = |\Psi(e^{i\phi})|^2 / 2\pi$—then follows from the Fourier relations, Eq. 85 and 86. Thus, to obtain a number-phase uncertainty principle for the product of the number-operator variance and the SG-POM variance, we shall exploit this complementarity by paralleling the standard Fourier derivation of Eq. 82.

With $\langle \Delta \hat{N}^2 \rangle$ denoting the number-measurement variance and $\langle \Delta \phi^2 \rangle$ the SG-POM variance, when the field is in an *arbitrary* state $|\psi\rangle$, we have that

$$\langle \Delta \hat{N}^2 \rangle \langle \Delta \phi^2 \rangle$$

$$= \sum_{n=0}^{\infty} (n - \bar{n})^2 |\psi_n|^2$$
$$\times \int_{-\pi}^{\pi} \frac{d\phi}{2\pi} (\phi - \bar{\phi})^2 |\Psi(e^{i\phi})|^2 \quad (87)$$

$$= \int_{-\pi}^{\pi} \frac{d\phi}{2\pi} \left| \frac{d\Psi'(e^{i\phi})}{d\phi} \right|^2$$
$$\times \int_{-\pi}^{\pi} \frac{d\phi}{2\pi} (\phi - \bar{\phi})^2 |\Psi'(e^{i\phi})|^2 \quad (88)$$

$$\geq \left| \int_{-\pi}^{\pi} \frac{d\phi}{2\pi} (\phi - \bar{\phi}) \Psi'(e^{i\phi})^* \right.$$
$$\left. \times \frac{d\Psi'(e^{i\phi})}{d\phi} \right|^2 \qquad (89)$$

$$\geq \left\{ \text{Re} \left[\int_{-\pi}^{\pi} \frac{d\phi}{2\pi} (\phi - \bar{\phi}) \Psi'(e^{i\phi})^* \right. \right.$$
$$\left. \left. \times \frac{d\Psi'(e^{i\phi})}{d\phi} \right] \right\}^2 \qquad (90)$$

$$= \frac{1}{2\pi} [p(\pi \mid |\psi\rangle) - 1]^2. \qquad (91)$$

In this development: $\bar{n}$ and $\bar{\phi}$ are the mean values of the number and SG-POM measurements, respectively, on the state $|\psi\rangle$; $\Psi'(e^{i\phi}) \equiv \Psi(e^{i\phi}) e^{i\bar{n}\phi}$; the Schwarz inequality has been used in Eq. 89; and the integration necessary to obtain Eq. 91 follows from the SG-POM's PDF, $p(\phi \mid |\psi\rangle) = |\Psi(e^{i\phi})|^2 / 2\pi$.

Unlike the usual number-phase uncertainty principle, i.e., Eq. 76, our result does *not* require any linearization before it can be applied to phase variance. Equation 91 is *still* state dependent, but this is unavoidable. When $|\psi\rangle$ is a number state, we have

$$p(\phi \mid |n\rangle) = \frac{1}{2\pi}, \quad \text{for } -\pi < \phi \leq \pi, \quad (92)$$

a uniform distribution, which is maximally random, but still has finite variance. There is no contradiction with Eq. 91 in this case, even though $\Delta N = 0$ for a number ket; the uniform PDF causes the right member of Eq. 91 to vanish. On the other hand, when $|\psi\rangle$ is a high-mean-field state, we will have $p(\pi \mid |\psi\rangle) \ll 1$, so that Eq. 91 reproduces the standard linearized formula, Eq. 77. Indeed, for *any* state satisfying $p(\pi \mid |\psi\rangle) \ll 1$, we have that Eq. 77 holds. This makes the SG-POM

115

derivation of Eq. 77 more robust than linearization of Eq. 76.

7. Number-Ket Causality

The SG-POM underlies maximum-likelihood quantum phase measurement for *all* quantum states. Given the problems associated with minimizing the SG-POM's reciprocal peak-likelihood $\delta\phi$, by choice of input state,[3, 4, 12] a different state-selection criterion may be worth considering. In this vein, it is germane to ask the following question. What SG-POM phase PDF's can be realized by choice of input state $|\psi\rangle$? It turns out that linear system theory has the answer.

The Susskind-Glogower probability operator measurement on a state $|\psi\rangle$ results in a classical random variable ϕ with probability density function

$$p(\phi \mid |\psi\rangle) = \frac{|\Psi(e^{i\phi})|^2}{2\pi},$$
$$\text{for } -\pi < \phi \leq \pi. \quad (93)$$

Here, $\Psi(e^{i\phi})$ is the phase representation of the state $|\psi\rangle$. According to Eq. 86, the phase representation is the Fourier transform of the number representation. The latter is a *one-sided*, discrete-parameter sequence that is the inverse Fourier transform of $\Psi(e^{i\phi})$, i.e.,

$$\psi_n = \frac{1}{2\pi} \int_{-\pi}^{\pi} d\phi \, \Psi(e^{i\phi}) e^{in\phi}$$
$$= \begin{cases} \langle n|\psi\rangle, & \text{for integer } n \geq 0, \\ 0, & \text{for integer } n < 0. \end{cases} \quad (94)$$

In system-theory parlance, the Fourier pair $\psi_n \longleftrightarrow \Psi(e^{i\phi})$ is analogous to that for a discrete-time waveform on an unbounded interval and its periodic, continuous-frequency Fourier transform, i.e., the discrete-time Fourier transform (DTFT).[14] More importantly, saying that ψ_n is one-sided is equivalent to saying that a discrete-time waveform is *causal*, viz. it could be the impulse response of a causal, linear time-invariant system. Determining what $p(\phi \mid |\psi\rangle)$ are possible from Eq. 93 is then the same as determining what $|\Psi(e^{i\phi})|$ are Fourier-transform magnitudes of one-sided $\{\psi_n\}$. To emphasize

the connection with causal waveforms, we introduce the term *number-ket causality* for the condition Eq. 94. This is a well-studied problem in linear systems, so results are immediately available.[14, 15]

From Eq. 93 and the Paley-Wiener theorem[15] we have that $p(\phi \mid |\psi\rangle)$ must satisfy

$$\int_{-\pi}^{\pi} d\phi \, |\ln[p(\phi \mid |\psi\rangle)]| < \infty, \quad (95)$$

for all number-ket causal $\Psi(e^{i\phi})$. From this condition, it follows that *no* state can confine the phase-measurement PDF to a subinterval of $(-\pi, \pi]$, e.g., the uniform density,

$$p(\phi \mid |\psi\rangle) = \frac{1}{\delta\phi},$$
$$\text{for } |\phi| \leq \delta\phi/2 < \pi, \quad (96)$$

is *impossible*. The Paley-Wiener condition is *both* necessary *and* sufficient, i.e., if a PDF obeys Eq. 95, then there *is* a state which gives this density through Eq. 93. Indeed, there are an *infinite* number of such states, because Eq. 93 only constrains the *magnitude* of the phase representation. One such state can be obtained explicitly via the discrete-parameter Hilbert transform. The procedure is as follows. For a PDF obeying Eq. 95, set

$$|\Psi(e^{i\phi})| = \sqrt{2\pi p(\phi \mid |\psi\rangle)},$$
$$\text{for } -\pi < \phi \leq \pi. \quad (97)$$

Next, find the discrete-parameter Hilbert transform,[14]

$$\arg[\Psi(e^{i\phi})] = \mathcal{P} \int_{-\pi}^{\pi} \frac{d\phi'}{2\pi} \ln[|\Psi(e^{i\phi'})|]$$
$$\times \cot\left(\frac{\phi' - \phi}{2}\right),$$
$$\text{for } -\pi < \phi \leq \pi, \quad (98)$$

where $\mathcal{P}$ denotes Cauchy principal value. Equations 97 and 98 then comprise the magnitude and phase—the polar form—of a properly-normalized phase representation $\Psi(e^{i\phi})$ *with* the prescribed phase-measurement statistics *and* a number-ket causal inverse Fourier transform.

116

The preceding phase representation construction for a state with prescribed SG-POM statistics is by no means unique. Equation 97 constrains $|\Psi(e^{i\phi})|$, but no restriction is placed on $\arg[\Psi(e^{i\phi})]$. Consider a number-ket causal function, $\{ h_n : n = 0, 1, 2, \ldots \}$, whose Fourier transform has unity magnitude, viz.

$$H(e^{i\phi}) \equiv \sum_{n=0}^{\infty} h_n e^{-in\phi},$$
$$\text{for } -\pi < \phi \leq \pi, \quad (99)$$

obeys

$$|H(e^{i\phi})| = 1, \quad \text{for } -\pi < \phi \leq \pi. \quad (100)$$

Such a function is known in digital-filter theory as an all-pass filter; were $\{ h_n : n = 0, 1, 2, \ldots \}$ the impulse response of a discrete-time, linear, time-invariant filter, the associated frequency response would pass all frequencies with neither attenuation nor gain. The prototypical example of an all-pass filter is obtained—in the z-transform domain—by balancing $H(z)$-poles within the unit circle with $H(z)$-zeros outside the unit circle to achieve[14]

$$H(e^{i\phi}) = \prod_{k=1}^{K} \frac{e^{-i\phi} - p_k^*}{1 - p_k e^{-i\phi}},$$
$$\text{for } -\pi < \phi \leq \pi,$$
$$\text{where } |p_k| < 1,$$
$$\text{for } k = 1, 2, \ldots K. \quad (101)$$

Now, suppose we assemble the phase representation

$$\Psi'(e^{i\phi}) \equiv \Psi(e^{i\phi}) H(e^{i\phi}),$$
$$\text{for } -\pi < \phi \leq \pi, \quad (102)$$

where $\Psi(e^{i\phi})$ is constructed according to Eqs. 97 and 98 for a desired phase-measurement PDF, and $H(e^{i\phi})$ is an all-pass phase representation from Eq. 101. The convolution-multiplication theorem of Fourier analysis, plus the fact that convolving two causal functions produces a causal function,[14] guarantees that $\Psi'(e^{i\phi})$ is a properly normalized, number-ket causal phase representation; the all-pass nature of $H(e^{i\phi})$ implies that $\Psi'(e^{i\phi})$ has the desired SG-POM statistics. Because this process holds for all $K \geq 1$ and for all pole locations within the unit circle,

there is an uncountable infinity of states which have the same SG-POM statistics. Nevertheless, the state constructed via the discrete-parameter Hilbert transform has a unique advantage—it is the minimum average photon-number state with the prescribed phase-measurement PDF.

The proof of the minimum average photon-number property follows almost immediately from available linear-system results. Let $\{ \Psi(e^{i\phi}) : -\pi < \phi \leq \pi \}$ and $\{ \psi_n : n = 0, 1, 2, \ldots \}$ be the phase and number representations of the state $|\psi\rangle$, obtained via Eqs. 97, 98, and 94, that realizes a particular phase PDF. Similarly, let $\{ \Psi'(e^{i\phi}) : -\pi < \phi \leq \pi \}$ and $\{ \psi'_n : n = 0, 1, 2, \ldots \}$ be the phase and number representations of any *other* state, $|\psi'\rangle$, with the *same* SG-POM statistics. Then, we have that[14]

$$\sum_{n=0}^{M-1} \left(|\psi_n|^2 - |\psi'_n|^2 \right) \geq 0,$$
$$\text{for } M = 1, 2, 3, \ldots \quad (103)$$

Physically, this says that, of all states with the desired phase behavior, the Hilbert-transform generated state concentrates its number-ket content closest to the vacuum. Because both $|\psi\rangle$ and $|\psi'\rangle$ are normalized, i.e., unit-length, states, Eq. 103 is equivalent to

$$\Delta_M \equiv \sum_{n=M}^{\infty} \left(|\psi_n|^2 - |\psi'_n|^2 \right) \leq 0,$$
$$\text{for } M = 0, 1, 2, \ldots \quad (104)$$

Proving the minimum average photon-number property is now straightforward:

$$\langle \psi | \hat{N} | \psi \rangle - \langle \psi' | \hat{N} | \psi' \rangle$$
$$= \sum_{n=0}^{\infty} n \left(|\psi_n|^2 - |\psi'_n|^2 \right)$$
$$= \sum_{M=1}^{\infty} \Delta_M \leq 0. \quad (105)$$

Thus, Eqs. 97 and 98 provide the means for choosing a state of minimum average energy and prescribed phase-measurement PDF.

8. PHASE COMMUNICATION

Sections 1–7 constitute an abridged version of Shapiro and Shepard.[4] That paper presents additional details regarding the state that achieves $\delta\phi \sim 1/N^2$, as well as substantial material on new classes of quantum states—coherent phase states, squeezed phase states, rational phase states—that are closely associated with the SG-POM. Furthermore, it proves that the Pegg-Barnett Hermitian phase operator[16, 17]—which exists on a truncated state space and provides phase-measurement statistics on the full state space through a limiting procedure—is included within the SG-POM formalism, i.e., these two schema produce *identical* phase measurement statistics for *all* quantum states. Neither of these topics will be considered herein. Instead, we shall move away from the *single-mode* case and develop new results for *two*-mode quantum phase measurement. Our objective will be to exploit the $\hat{Y}$-measurement—developed en route to the commuting observables form of the SG-POM—when the signal and apparatus modes are quantum-mechanically correlated and a phase-conjugate modulation is applied to them.

Consider the phase-conjugate quantum measurement setup shown in Fig. 1. This is a phase-conjugate system because whatever c-number phase shift Φ is applied to the signal mode, leading to the annihilation operator transformation

$$\hat{a}_S^{IN} \longrightarrow e^{i\Phi}\hat{a}_S^{IN}, \qquad (106)$$

the *conjugate* phase shift, $-\Phi$ is applied to the apparatus mode, viz.

$$\hat{a}_A^{IN} \longrightarrow e^{-i\Phi}\hat{a}_A^{IN}, \qquad (107)$$

cf. Eq. 30. If we take the signal and apparatus modes to be the appropriate linear polarizations, a transverse electro-optic modulator can be used to induce the necessary conjugate phase shifts.[18] Phase-conjugate shifts also appear, prototypically, in gravity-wave detecting interferometers. In fact, there are fundamental advantages to operating a phase-sensing interferometer in phase-conjugate fashion.[19] Our work does *not* depend explicitly on the means by which this modulation is accomplished. Its principal

motivation is to circumvent the Paley-Wiener restriction that encumbers phase-measurement PDF's for single-mode fields. As we shall see, some startling new possibilities arise with two modes.

The Paley-Wiener condition applies to a single-mode phase PDF because this density is proportional to the squared magnitude of the Fourier transform, $\{\Psi(e^{i\phi}) : -\pi < \phi \leq \pi\}$, of a one-sided sequence, $\{\psi_n : n = 0, 1, 2, \ldots, \}$. We shall break out of this limit, in the two-mode case, through quantum correlation. On $\mathcal{H}_S \otimes \mathcal{H}_A$, the joint state space of the signal and apparatus input modes, we can construct *number-product vacuum* states of the form

$$|\psi\rangle_{IN} = \psi_0|0\rangle_S|0\rangle_A + \sum_{n=1}^{\infty}(\psi_n|n\rangle_S|0\rangle_A$$
$$+ \ \psi_{-n}|0\rangle_S|n\rangle_A), \qquad (108)$$

where

$$\sum_{n=-\infty}^{\infty}|\psi_n|^2 = 1. \qquad (109)$$

The term number-product vacuum is appropriate for such $|\psi\rangle_{IN}$ because, when the signal×apparatus state is of this class, a measurement of the number-operator product—$\hat{N}_S \otimes \hat{N}_A$—yields outcome zero with probability one. Thus, for $|\psi\rangle_{IN}$ a number-product vacuum state, Eqs. 62 and 63 imply that measurement of $\hat{Y}$ yields a classical phasor $e^{i\phi}$, with $-\pi < \phi \leq \pi$. Moreover, ϕ in this case has PDF

$$p(\phi \mid \Phi) = \frac{\left|\Psi(e^{i(\phi-\Phi)})\right|^2}{2\pi},$$
$$\text{for } -\pi < \phi, \Phi \leq \pi, \qquad (110)$$

in terms of

$$\Psi(e^{i\phi}) \equiv \sum_{n=-\infty}^{\infty} \psi_n e^{-in\phi},$$
$$\text{for } -\pi < \phi \leq \pi. \qquad (111)$$

Note that $\{\psi_n : |n| = 0, 1, 2, \ldots, \}$ and $\{\Psi(e^{i\phi}) : -\pi < \phi \leq \pi\}$ are *not* the number and phase representations, respectively, of *any* single-mode field state. They *are*, however, the number and phase representations, respectively, for a two-mode, number-product vacuum

118

state. The $\{\psi_n, \Psi(e^{i\phi})\}$ notation is convenient because, as shown by Eq. 111 and its inverse,

$$\psi_n = \int_{-\pi}^{\pi} \frac{d\phi}{2\pi} \Psi(e^{i\phi}) e^{in\phi},$$
$$\text{for } |n| = 0, 1, 2, \ldots, \quad (112)$$

these functions are a Fourier transform pair. More importantly, this notation makes clear the fact that number-ket causality does *not* restrict the possible two-mode phase PDF's. In particular, there are number-product vacuum states that satisfy

$$\left| \Psi(e^{i\phi}) \right| = 0, \text{ for } |\phi| \geq \phi_c,$$
$$\text{with } \phi_c < \pi. \quad (113)$$

i.e., two-mode phase PDF's can be confined to subintervals of $(-\pi, \pi]$, a situation that is forbidden to the single-mode case, cf. Eq. 96. This possibility is of great significance for phase-based digital communication and phase-based precision measurement, as we shall see.

To cast the Fig. 1 structure into a digital communication mold, let us assume that transverse electro-optic modulation is used to transmit a randomly-selected digit k, satisfying $1 \leq k \leq K$, by using $\Phi = \Phi_k$, where

$$\Phi_k \equiv -\pi + \frac{(2k-1)\pi}{K}. \quad (114)$$

Our objective is to make a minimum error probability decision as to which Φ_k was sent, based on the result of the $\hat{Y}$-measurement when the signal×apparatus state is a number-product vacuum, characterized by $\{\psi_n, \Psi(e^{i\phi})\}$.

Hall and Fuss have considered the *single-mode* version of this K-ary digital communication problem[20]. They optimized a single-mode state—in conjunction with the SG-POM—to obtain a phase-based quantum communication setup whose error probability vs. average photon number is significantly better than that for optical heterodyne detection. Hall and Fuss found a *nonzero* error probability at *finite* average photon number, N, which approached zero as $N \rightarrow \infty$. Surprisingly, in our two-mode problem, *zero* error

probability can be achieved at *finite* root-mean-square (RMS) photon number.[21]

In order to achieve zero error probability in phase-conjugate quantum communication, we need only use a number-product vacuum state which enforces Eq. 96, with $\phi_c \leq \pi/K$. Under this condition, we have that the *observed* phase, ϕ, satisfies

$$\Pr\left(|\phi - \Phi_k| < \frac{\pi}{K} \mid \Phi = \Phi_k \right) = 1. \quad (115)$$

We also have that $|\Phi_k - \Phi_j| \geq 2\pi/K$, for $j \neq k$. So, for any observed ϕ in the interval $(-\pi, \pi]$, we know that

$$\Pr\left(\Phi = \Phi_j \mid |\phi - \Phi_k| < \frac{\pi}{K} \right) = 0,$$
$$\text{for all } j \neq k. \quad (116)$$

This means we can *unambiguously* determine which digit was sent by choosing the index associated with the *unique* Φ-value that is within π/K rad of the observed phase. Via this procedure we decode k from ϕ with zero probability of being incorrect.

To make this technique for zero error probability communication more explicit, we shall introduce a specific input state which has the desired property. The number representation we shall presume is

$$\psi_n = \sqrt{\frac{2}{K}} \frac{1}{\left(1 + \frac{2|n|}{K} \right)}$$
$$\times \frac{\sin\left[\frac{\pi}{2} \left(1 - \frac{2|n|}{K} \right) \right]}{\frac{\pi}{2} \left(1 - \frac{2|n|}{K} \right)},$$
$$\text{for } |n| = 0, 1, 2, \ldots,$$
$$\text{and } K = 2, 3, 4, \ldots \quad (117)$$

The associated phase representation for this state is easily computed to be

$$\Psi(e^{i\phi}) =$$
$$\begin{cases} \sqrt{2K} \cos\left(\frac{K\phi}{2} \right), & \text{for } |\phi| \leq \frac{\pi}{K} \\ 0, & \text{for } \frac{\pi}{K} < |\phi| \leq \pi. \end{cases} \quad (118)$$

In Fig. 2 we have plotted $p(\phi \mid \Phi = 0)$ vs. ϕ for this state when $K = 4$; we see that

the nonzero support of this PDF is the interval $(-\pi/4, \pi/4)$. In Fig. 3 we indicate how this PDF leads to zero error probability phase-conjugate communication; this figure plots the four conditional PDF's, $\{p(\phi \mid \Phi_k) : 1 \leq k \leq 4\}$, which apply when $K = 4$. For any *observed* ϕ-value we must have that $p(\phi \mid \Phi) > 0$, otherwise that ϕ-value could not have occurred. Figure 3 shows that, for any given ϕ, there is only *one* possible Φ_k-value which satisfies the nonzero PDF requirement—zero error probability communication results from deciding that this value was the transmitted phase.

The next question to address is the photon number statistics associated with our phase-conjugate communication scheme. For the general number-product vacuum state we have that the *total*—signal plus apparatus—photon number measurement has the following probability distribution,

$$\Pr\left(\hat{N}_S + \hat{N}_A = n\right) =$$
$$\begin{cases} |\psi_0|^2, & \text{for } n = 0, \\ |\psi_{-n}|^2 + |\psi_n|^2, & \text{for } n = 1, 2, 3, \ldots \end{cases} \quad (119)$$

For the particular state given by Eq. 117, it is then a simple matter to show that

$$\langle \hat{N}_S + \hat{N}_A \rangle < \sqrt{\langle (\hat{N}_S + \hat{N}_A)^2 \rangle}$$
$$= \frac{K}{2}. \quad (120)$$

In other words, we can achieve zero error probability K-ary phase-conjugate quantum communication with an RMS *total* photon number of $K/2$. Figure 4 is a plot of Eq. 119 for the $K = 4$ case.

The preceding quantum communication result is, of course, idealized. We have presumed a state generator—to produce a specific number-product vacuum state—that as yet has no explicit realization. Likewise, our scheme uses the $\hat{Y}$-measurement; again, no explicit realization is yet available. At least we can say that electro-optic modulation will impress the phase information on the input state, once that state can be produced. On the other hand, we have implicitly assumed lossless transmission; inclusion of loss will inevitably lead to nonzero error probability.

Our main purpose in going to the two-mode construct was to develop *potential* quantum-phase measurement schemes that promise substantial benefits, i.e., benefits that warrant the effort to bring them to fruition. This motivation is very much in line with the starting point for squeezed-state research.[22] In this regard, it is instructive to compare our phase-based scheme for zero error probability quantum communication with a more well-known approach based on number kets. For a single-mode field with annihilation operator $\hat{a}$, lossless transmission of one of the number kets $\{ |k - 1\rangle : 1 \leq k \leq K \}$ followed by ideal direct detection, viz. the $\hat{N} = \hat{a}^\dagger \hat{a}$ measurement, also yields K-ary digital communication without error. For k equally likely to be any digit between 1 and K, the *average*-energy efficiency of such a single-mode, number-ket system is roughly the same as that of our two-mode, phase-conjugate system, i.e., both need slightly less than $K/2$ photons on average. The number-ket system has the advantage that its state generator may be approximated via feed-forward control using photon-twin beams, and its measurement only requires a high quantum-efficiency photon counter. Also, the number-ket approach uses less bandwidth; only one mode is needed. Alternatively, number-ket direct detection on a two-mode field can be used for error-free K-ary communication at significantly less than $K/2$ photons on average. However, if we shift our attention from phase-based *communication*, to phase-based *precision measurements*, the Fig. 1 arrangement has a capability that number kets cannot match—phase sensing with controlled precision.

Suppose that we use the Fig. 1 arrangement for phase-conjugate precision measurement. Specifically, let us use the number-product vacuum state Eq. 117 in conjunction with a phase-conjugate interferometer (see, e.g., Bondurant and Shapiro[19]) and the $\hat{Y}$ measurement. Now, the phase shift Φ takes on any value from the continuum $(-\pi, \pi]$. Nevertheless, except for 2π-modularity effects which come into play when Φ is within π/K of $\pm\pi$, the observed phase will lie within π/K rad of the true phase *with probability one*. Thus, using less than $K/2$ photons on average, we can guarantee a phase measure-

ment which is within π/K rad of the exact value. In other words, unlike more conventional schemes—which only ensure an acceptable RMS phase-estimation error—our phase-conjugate interferometer provides *exact* phase determination to a *prescribed* number of decimal places.

9. REFERENCES

1. P.A.M. Dirac, Proc. R. Soc. Lond. Ser. A **114**, 243 (1927).

2. L. Susskind and J. Glogower, Physics **1**, 49 (1964).

3. J.H. Shapiro, S.R. Shepard, and N.C. Wong, Phys. Rev. Lett. **62**, 2377 (1989).

4. J.H. Shapiro and S.R. Shepard, Phys. Rev. A **43**, 3795 (1991).

5. W.H. Louisell, *Radiation and Noise in Quantum Electronics* (McGraw-Hill, New York, 1964).

6. R.J. Glauber, Phys. Rev. **131**, 2766 (1963).

7. C.W. Helstrom, *Quantum Detection and Estimation Theory* (Academic, New York, 1976).

8. H.P. Yuen and J.H. Shapiro, IEEE Trans. Inform. Theory **IT-26**, 78 (1980).

9. J.H. Shapiro and S.S. Wagner, IEEE J. Quantum Electron. **QE-20**, 803 (1984).

10. J.H. Shapiro, IEEE J. Quantum Electron. **QE-21**, 237 (1985).

11. J.J. Stiffler, *Theory of Synchronous Communications* (Prentice Hall, Englewood Cliffs, 1971).

12. S.L. Braunstein, C.M. Caves, and A.S. Lane, "Maximum Likelihood Statistics of Multiple Quantum Phase Measurements," *Technical Digest Opt. Soc. Am. 1990 Annual Meeting*, (Opt. Soc. Am., Washington, D.C., 1990) p. 114.

13. P. Carruthers and M.M. Nieto, Rev. Mod. Phys. **40**, 411 (1968).

14. A.V. Oppenheim and R.W. Schafer, *Digital Signal Processing* (Prentice-Hall, Englewood Cliffs, 1975).

15. A. Papoulis, *Signal Analysis* (McGraw-Hill, New York, 1977).

16. D.T. Pegg and S.M. Barnett, Phys. Rev. A **39**, 1665 (1989).

17. S.M. Barnett and D.T. Pegg, J. Mod. Opt. **36**, 7 (1989).

18. A. Yariv, *Optical Electronics, Third Edition* (Holt, Rinehart, Winston, New York, 1985).

19. R.S. Bondurant and J.H. Shapiro, Phys. Rev. D **30**, 2548 (1984).

20. M.J.W. Hall and I.G. Fuss, "Quantum Phase Detection and Digital Communication," Quant. Opt. to appear.

21. J.H. Shapiro, "Phase Conjugate Quantum Communication with Zero Error Probability at Finite Average Photon Number," in preparation.

22. H.P. Yuen, Phys. Rev. A **13**, 2226 (1976).
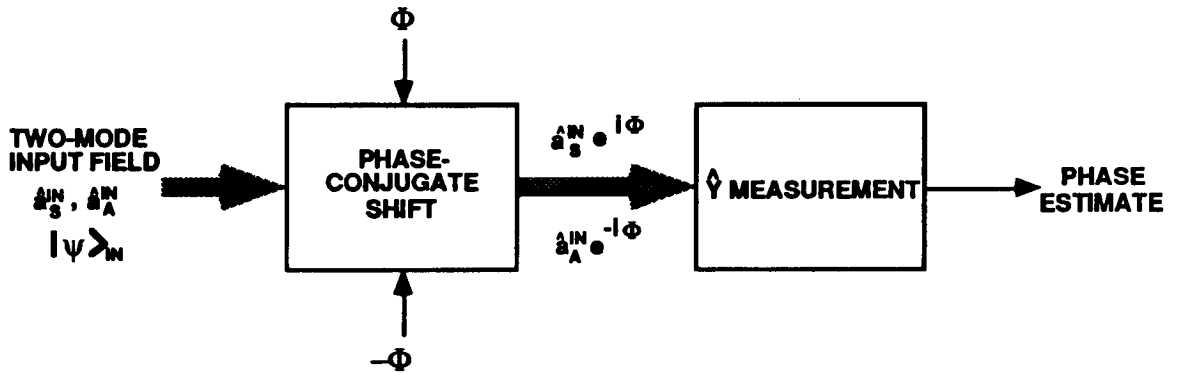
Figure 1: Phase-conjugate quantum communication system.
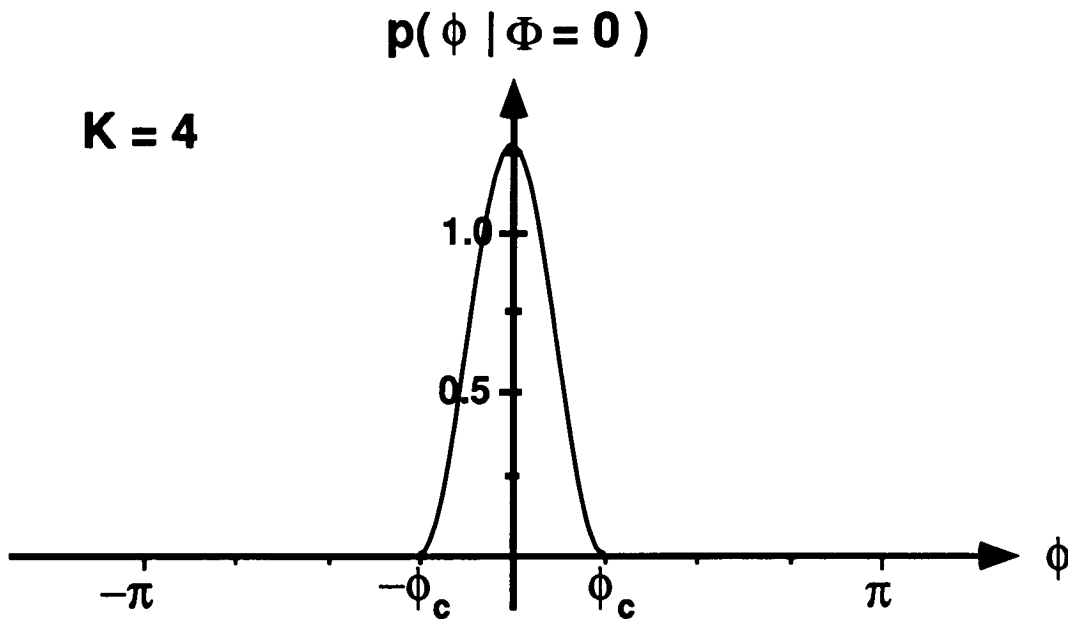
Figure 2: Conditional phase-measurement PDF, given $\Phi = 0$, for the state Eq. 118 when $K = 4$.
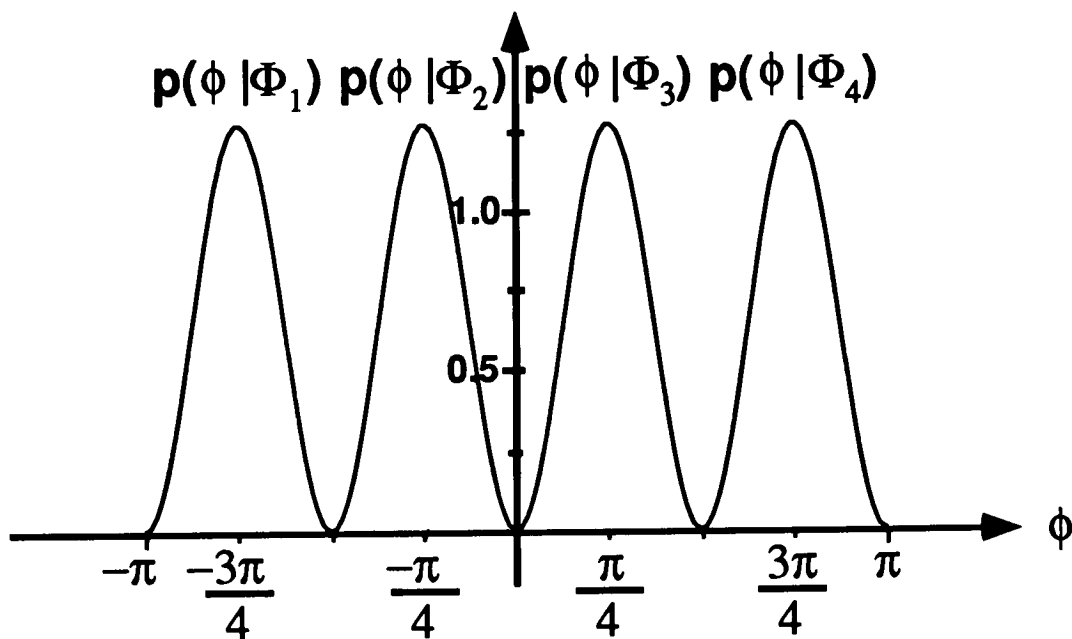
Figure 3: *Conditional phase-measurement PDF's for the state Eq. 118 when $K = 4$.*
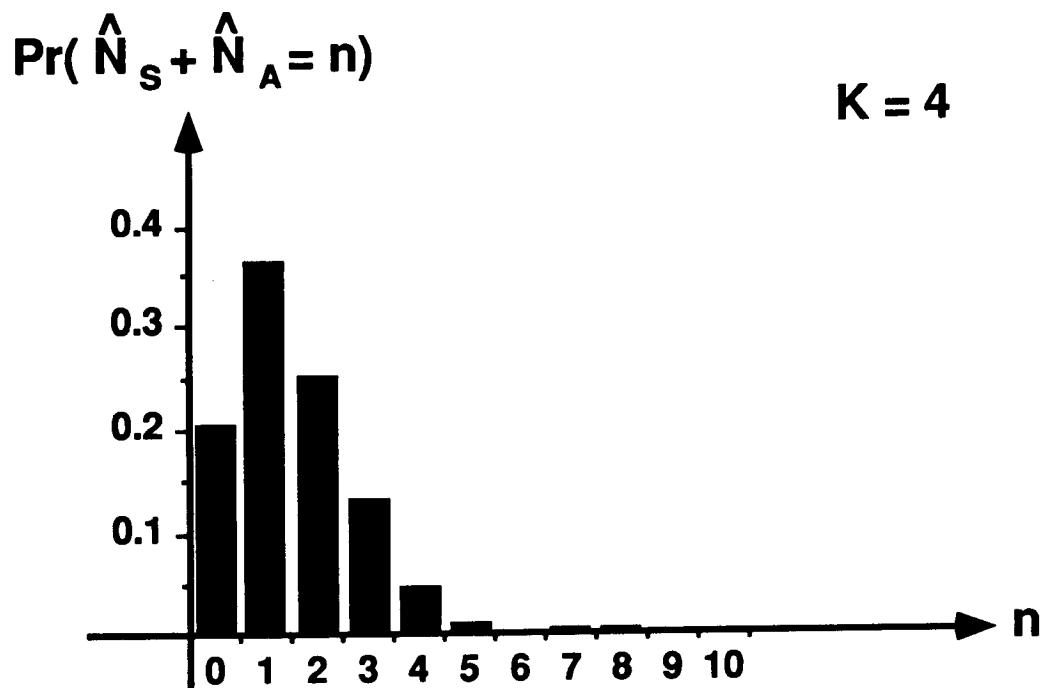
Figure 4: *Signal-plus-apparatus number distribution for the state Eq. 117 when $K = 4$.*

123

QUADRATIC SQUEEZING: AN OVERVIEW[*]

by M. Hillery, D. Yu, and J. Bergou
Dept. of Physics and Astronomy
Hunter College of CUNY
695 Park Ave
New York, NY10021

I. Introduction

The amplitude of the electric field of a mode of the electromagnetic field is not a fixed quantity, there are always quantum mechanical fluctuations. The amplitude, having both a magnitude and a phase, is a complex number and is described by the mode annihilation operator a. It is also possible to characterize the amplitude by its real and imaginary parts which correspond to the Hermitian and anti-Hermitian parts of a,

$$X_1 = \frac{1}{2}(a^+ + a) \qquad\qquad X_2 = \frac{i}{2}(a^+ - a) \ , \qquad\qquad (1.1)$$

respectively. These operators do not commute and, as a result, obey the uncertainty relation (h=1)

$$\Delta X_1 \Delta X_2 \geq \frac{1}{4} \ . \qquad\qquad (1.2)$$

From this relation we see that the amplitude fluctuates within an "error box" in the complex plane whose area is at least 1/4. Coherent states, among them the vacuum state, are minimum uncertainty states with $\Delta X_1 = \Delta X_2 = 1/2$. A squeezed state, squeezed in the X_1 direction, has the property that $\Delta X_1 < 1/2$ (Refs.1-3). A squeezed state need not be a minimum uncertainty state, but those that are can be obtained by applying the squeeze operator

$$S(\zeta) = e^{\zeta^* a^2 - \zeta a^{+2}} \ , \qquad\qquad (1.3)$$

to a coherent state(Ref.1). The phase of the complex parameter ζ determines the

direction of squeezing and its magnitude determines the extent of the squeezing.

Squeezed states are examples of nonclassical states, that is they cannot be described in terms of a nonnegative definite P representation(Ref.3). This means that a field in a squeezed state cannot be modeled as a classical stochastic field. It should be noted that even though a squeezed state is nonclassical it can have a large number of photons. In fact, a highly squeezed state must have a large number of photons(Ref.4). Thus we see that the usual association of large photon number with classical behavior is not correct.

It is possible to generalize the idea of squeezing by looking at fluctuations in variables more complicated than the mode amplitude. The simplest generalization involves variables quadratic, rather than linear, in the amplitude. In the case of a single mode the square of the amplitude, which corresponds to a^2, is one such observable. If one considers two modes with annihilation operators a and b, then products such as ab and a^+b can be considered. At first glance this procedure appears more mathematically than physically inspired. However, fluctuations in these quadratic quantities can be converted into fluctuations of a single mode amplitude by certain nonlinear optical processes after which they can be measured by standard techniques. We shall now disscuss the kinds of higher-order squeezing to which consideration of these quadratic variables leads and the properties they possess.

II. Amplitude-Squared Squeezing

This is perhaps the simplest example of quadratic squeezing, i.e. squeezing in a variable quadratic in the mode amplitudes. It describes the fluctuations in the square of the amplitude of a single mode, a^2 (Refs.5,6). Following the example of standard squeezing we break this variable into its real and imaginary parts

$$Y_1 = \frac{1}{2}(a^{+2} + a^2) \qquad Y_2 = \frac{i}{2}(a^{+2} - a^2) \ . \qquad (2.1)$$

The commutator of these operators is $[Y_1, Y_2] = i(2N+1)$, where $N = a^+a$, and this leads to the uncertainty relation

$$\Delta Y_1 \Delta Y_2 \geq <N + \frac{1}{2}> \ . \qquad (2.2)$$

A state is amplitude-squared squeezed in the Y_1 direction if $(\Delta Y_1)^2 < <N+1/2>$.

States with this property are nonclassical. This follows from the fact that $(\Delta Y_1)^2$ can be written as

$$<:(Y_1 - <Y_1>)^2 :> = (\Delta Y_1)^2 - <N+\frac{1}{2}> \quad , \qquad (2.3)$$

where the double dots indicate normal ordering. For a classical state the normally ordered term is always nonnegative so one can see that the onset of amplitude-squared squeezing corresponds to the onset of nonclassical behavior.

Amplitude-squared squeezing was first disscussed in a paper by Wodkiewicz and Eberly under the name SU(1,1) squeezing (Ref.7). The reason for this name is that commutation relations of the operators Y_1, Y_2, and N are closely related to those of the Lie algebra SU(1,1). In particular this Lie algebra is described by three operators K_1, K_2, and K_3, whose commutation relations are given by

$$[K_1, K_2] = -iK_3 \qquad [K_2, K_3] = iK_1 \qquad [K_3, K_1] = iK_2 \quad . \qquad (2.4)$$

If one makes the identification $K_1 = Y_1/2$, $K_2 = -Y_2/2$ and $K_3 = (N+1/2)/2$, the above commutation relations are satisfied. This means that the representations of SU(1,1) can be used to study higher-order squeezing and this has been done by a number of authors(Refs.8-10).

It is possible to find minimum uncertainty states for amplitude-squared squeezing, i.e. states for which the inequality in Eq.(2.2) is replaced by an equality(Ref.11). This is done by solving the eigenvalue equation

$$(Y_1 + i\lambda Y_2) |\Psi> = \beta |\Psi> \quad , \qquad (2.5)$$

where λ is real and positive, and β is complex. The states $|\Psi>$ which satisfy this equation have the property that

$$(\Delta Y_1)^2 = \lambda <\Psi| N+\frac{1}{2} |\Psi> \qquad (\Delta Y_2)^2 = \frac{1}{\lambda} <\Psi| N+\frac{1}{2} |\Psi> \quad . \qquad (2.6)$$

From these equations it is clear that λ plays the role of a squeezing parameter. If $0 < \lambda < 1$, then Y_1 is squeezed and if $\lambda > 1$, then Y_2 is squeezed. The real and imaginary parts of β are related to the mean values of Y_1 and Y_2, respectively.

A particularly simple subset of these minimum uncertainty states occurs when β

and λ are related. If $\lambda \geq 1$ and $\beta = (\lambda^2 - 1)^{1/2} (m+1/2)$, where m is a nonnegative integer, then the minimum uncertainty states are of the form

$$|\Psi\rangle = C_m(\lambda) \, S(\zeta) \, H_m(\, i\gamma(\lambda) \, a^+) \, |0\rangle \quad . \tag{2.7}$$

Here $C_m(\lambda)$ is a normalization constant, $S(\zeta)$ is a squeeze operator where the squeeze parameter ζ depends on λ, H_m is the mth Hermite polynomial and $\gamma(\lambda) = [(\lambda^2 - 1)^{1/2}/2\lambda]^{1/2}$. The cases m=0 and m=1 correspond to the squeezed vacuum and squeezed one-photon states, respectively. Note that this implies that the squeezed vacuum state is a minimum uncertainty state for both normal squeezing and for amplitude-squared squeezing.

A second kind of minimum uncertainty state is the amplitude-squared squeezed vacuum $|0,\lambda\rangle$. These states satisfy Eq.(2.5) with $\beta=0$ which implies that they have the property that $\langle Y_1 \rangle = \langle Y_2 \rangle = 0$. Such states are superpositions of photon number states whose numbers are multiples of 4.

We now come to the conversion of fluctuations in a^2 into fluctuations of the mode amplitude of a second mode, b. This is accomplished by means of second harmonic generation(Ref.5). If the mode described by a has frequency ω and that described by b has frequency 2ω then the Hamiltonian which corresponds to this process is

$$H = \omega a^+ a + 2\omega b^+ b + k_2(a^{+2}b + a^2 b^+) \quad . \tag{2.8}$$

From this Hamiltonian, using perturbation theory, one can find how fluctuations are transferred from mode a to mode b. First define the slowly varying operators

$$A(t) = e^{i\omega t}a(t) \qquad B(t) = e^{2i\omega t}b(t) \quad , \tag{2.9}$$

and

$$X_{1B}(t) = \frac{1}{2}[\, B^+(t) + B(t)\,] \qquad X_{2B}(t) = \frac{i}{2}[\, B^+(t) - B(t)\,]$$

$$\tag{2.10}$$

$$Y_{1A}(t) = \frac{1}{2}[\, A^+(t)^2 + A(t)^2\,] \qquad Y_{2A}(t) = \frac{i}{2}[\, A^+(t)^2 - A(t)^2\,] \quad .$$

We then find, if the b mode is initially in a coherent state, that after a time t

$$(\Delta X_{1B}(t))^2 = \frac{1}{4} + (k_2 t)^2 [(\Delta Y_{2A})^2 - <N_A + \frac{1}{2}>]$$

$$(\Delta X_{2B}(t))^2 = \frac{1}{4} + (k_2 t)^2 [(\Delta Y_{1A})^2 - <N_A + \frac{1}{2}>] \quad , \tag{2.11}$$

where quantities without a time argument, e.g. $(\Delta Y_{1A})^2$, are assumed to be evaluated at t=0. What these equations tell us is that if the a mode is initially amplitude-squared squeezed in the Y_2 direction then the b mode will become squeezed in the normal sense in the X_1 direction. Similarly, if the a mode is amplitude-squared squeezed in the Y_1 direction the b mode will become squeezed in the X_2 direction. Therefore, the second harmonic generation process converts amplitude-squared squeezing into normal squeezing.

Because normal squeezing can be measured via homodyne detection the preceding results suggests how amplitude-squared squeezing can be detected. One first sends the signal into a frequency doubler and then measures the squeezing of the second harmonic. If it is squeezed, then the original signal was amplitude-squared squeezed.

Finally, let us see how amplitude-squared squeezed states can be produced. The fact that the squeezed vacuum state is also amplitude-squared squeezed shows that a degenerate parametric amplifier can produce amplitude-squared squeezed states. As one of us (D. Yu) has shown, a degenerate parametric oscillator can as well(Ref.12). Well above threshold the field inside the cavity can reach a maximum level of amplitude-squared squeezing given by $(\Delta Y_1)^2 / <N + 1/2> = 1/2$, but just below threshold the amount of amplitude-squared squeezing in the output field can, in principle, be arbitrarily large. The fourth subharmonic generation process, which has been studied in connection with generalized squeezed states(Ref.13), can also produce amplitude-squared squeezing(Ref.6).

III. Sum Squeezing

Sum squeezing, as opposed to amplitude-squared squeezing, is a two mode effect(Ref.14). In fact, amplitude-squared squeezing is the degenerate limit of sum squeezing. Let us consider two modes with annihilation operators a and b and frequencies ω_a and ω_b. The variables involved in sum squeezing are the real and imaginary parts of the product ab, i.e.

$$V_1 = \frac{1}{2} (a^+ b^+ + ab) \qquad V_2 = \frac{i}{2} (a^+ b^+ - ab) \quad . \tag{3.1}$$

129

The commutator of these operators is $[V_1, V_2] = \frac{i}{2} (N_A + N_B + 1)$, where $N_A = a^+a$ and $N_B = b^+b$, which yields the uncertainty relation

$$\Delta V_1 \Delta V_2 \geq \frac{1}{4} < N_A + N_B + 1 > \quad . \qquad (3.2)$$

A state is said to be sum squeezed in the V_1 direction if

$$(\Delta V_1)^2 < \frac{1}{4} < N_A + N_B + 1 > \quad . \qquad (3.3)$$

Such a state is nonclassical.

The commutation relations of the operators V_1, V_2 amd $N_A + N_B + 1$ are also closely related to those of the SU(1,1) Lie algebra. In fact if one sets $K_1 = V_1$, $K_2 = - V_2$ and $K_3 = \frac{1}{2}(N_A + N_B + 1)$ one obtains the SU(1,1) commutation relations given in Eq.(2.4).

The name, sum squeezing, comes from the fact that this kind of squeezing is converted into normal squeezing by the process of sum frequency generation. Sum frequency generation is a three-mode process which is described by the Hamiltonian

$$H = \omega_a a^+a + \omega_b b^+b + \omega_c c^+c + k_s (ca^+b^+ + c^+ab) , \qquad (3.4)$$

where $\omega_c = \omega_a + \omega_b$. As before we define the slowly varying operator $A(t) = e^{i\omega_a t}a(t)$, and similarly for $B(t)$ and $C(t)$. We also define

$$V_1(t) = \frac{1}{2}(A^+B^+ + AB) \qquad X_{C2} = \frac{i}{2}(C^+ - C) \quad . \qquad (3.5)$$

If the c mode is initially in a coherent state then to second order in k_s we find

$$(\Delta X_{C2}(t))^2 = \frac{1}{4} + (k_s t)^2 [(\Delta V_1)^2 - \frac{1}{4} < N_A + N_B + 1 >] , \qquad (3.6)$$

where, as before, quantities without a time argument are evaluated at t=0. Comparing this equation to Eq.(3.3) we see that the c mode will be squeezed in the X_{C2} direction if the a and b modes are sum squeezed in the V_1 direction.

If the a and b modes are uncorrelated, then there is a connection between squeezing in the individual modes and sum squeezing. In particular, if neither mode is

squeezed, then the state is not sum squeezed. If one of the two modes is squeezed and the other is in a coherent state, then the state is sum squeezed. Finally, if both modes are squeezed, then the resulting state may or may not be sum squeezed.

This connection disappears if the modes are correlated. This can be seen by considering the state produced from the vacuum by a parametric amplifier. This system is described by the Hamiltonian

$$H = \omega_a a^+ a + \omega_b b^+ b + g \left(e^{-i\omega_c t} a^+ b^+ + e^{i\omega_c t} ab\right) \quad , \qquad (3.7)$$

where, again, $\omega_c = \omega_a + \omega_b$. This Hamiltonian is an approximation to that in Eq.(3.4) when the c mode is in a highly excited coherent state. Using this Hamiltonian we find that if both the a and b modes are originally in the vacuum state, then

$$(\Delta V_1(t))^2 - \frac{1}{4} < N_A(t) + N_B(t) + 1 > = -\frac{1}{2} \sinh^2(gt) \quad . \qquad (3.8)$$

Therefore, the amount of sum squeezing increases with time and this device is a possible source of sum squeezed light. A further calculation shows that neither of the two modes is squeezed in the normal sense. Therefore, for correlated modes normal squeezing is not a prerequisite for sum squeezing.

IV. Difference Squeezing

Difference squeezing is also a two-mode effect(Ref.14). Its name comes from its close connection to difference-frequency generation. We again describe the modes by annihilation operators a and b , and we assume that $\omega_b > \omega_a$. The observables which describe it are

$$W_1 = \frac{1}{2}(ab^+ + a^+b) \qquad W_2 = \frac{i}{2}(ab^+ - a^+b) \quad . \qquad (4.1)$$

Their commutator is given by

$$[W_1, W_2] = \frac{i}{2}(N_A - N_B) \quad , \qquad (4.2)$$

which yields the uncertainty relation

$$\Delta W_1 \Delta W_2 \geq \frac{1}{4}|<N_A - N_B>| \quad . \qquad (4.3)$$

131

A state is said to be difference squeezed in the W_1 direction if

$$(\Delta W_1)^2 < \frac{1}{4} <N_A - N_B> .$$ (4.4)

Note that for a state to be difference squeezed we must have $<N_A> > <N_B>$.

Difference squeezed states are nonclassical but there is a difference in this regard between them and sum or amplitude-squared squeezed states. For both of the latter, the condition for squeezing and the condition for being nonclassical are the same. For difference squeezing this is not true. A state is nonclassical if

$$(\Delta W_1)^2 < \frac{1}{4} <N_A + N_B> ,$$ (4.5)

which is not the same as the squeezing condition Eq.(4.4). Therefore, difference squeezed states are well within the nonclassical regime.

Difference squeezing is also related to a Lie algebra but this time it is SU(2) instead of SU(1,1). In fact, the operators which describe difference squeezing are those used in the Schwinger representation of the angular momentum operators (Ref.15). The SU(2) Lie algebra consists of three operators J_1, J_2 and J_3 whose commutation relations are

$$[J_k, J_l] = i\epsilon_{klm}J_m ,$$ (4.6)

where all indices run from 1 to 3 and ϵ_{klm} is the completely antisymmetric tensor of rank 3.

If the modes are uncorrelated, then at least one of them must be squeezed for difference squeezing to be present. If the b mode is squeezed and the a mode is in a coherent state $|\alpha>$, the state wil be difference squeezed but only if $|\alpha|^2$ is large enough. A necessary, but not sufficient condition is that $<N_B> < \frac{1}{2}|\alpha|^2$. If the modes are correlated, then it is no longer true that squeezing in the individual modes is required for difference squeezing.

Finally, as might be suspected from the name, difference squeezing is turned into normal squeezing by difference frequency generation. The Hamiltonian describing this process is

$$H = \omega_a a^+ a + \omega_b b^+ b + \omega_c c^+ c + k_d(a^+ b c^+ + a b^+ c) \quad , \qquad (4.7)$$

where $\omega_c = \omega_b - \omega_a$. We define slowly varying A(t), B(t), and C(t) as in the previous section and then set

$$W_1(t) = \frac{1}{2}(A(t)B^+(t) + A^+(t)B(t)) \qquad X_{C2} = \frac{i}{2}(C^+(t) - C(t)) \quad . \qquad (4.8)$$

Using perturbation theory we find that if the c mode is originally in a coherent state, then

$$(\Delta X_{C2}(t))^2 = \frac{1}{4} + (k_d t)^2[(\Delta W_1)^2 - \frac{1}{4} <N_A - N_B>] \quad . \qquad (4.9)$$

This equation shows us that X_{C2} becomes squeezed if W_1 is difference squeezed. Therefore, difference frequency generation can be used to detect difference squeezed light.

V. Amplification of Higher-Order Squeezing

An amplifier consists of a collection of two-level atoms N_1 of which are in their ground states and N_2 of which are in their excited states where N_2 is greater than N_1. We shall assume that we are in the linear regime of this system. An input signal is put into the amplifier at t=0 and emerges at the output at time t. The signal amplitudes at the input and the output are related by $<a(t)> = G <a(0)>$ where G is the amplitude gain. This system was analyzed rather thoroughly by Carusotto(Ref.16).

Hong, Friberg, and Mandel examined the effect of amplification on sub-Poissonian photon statistics and normal squeezing(Ref.17). They found that both of these effects disappear at the output, no matter what the input state is, if the intensity gain, $|G|^2$, is greater than two. The gain $|G|^2 = 2$ is known as the photon cloning limit because one gets two photons out for every one that goes in. This gain has stood as an upper limit for the amplification of nonclassical behavior.

Recently two of us looked at the situation for amplitude-squared squeezing (Ref.18). We found that it can survive amplification for gains slightly greater than two. In particular, amplitude-squared squeezing will be present at the output if

$$|G|^2 < 2 + \frac{1}{<N_0> + 1/2} \quad , \qquad (5.1)$$

133

where $<N_0>$ is the photon number of the input state. Because the right-hand side is greater than two this suggests that there are states which will still be amplitude-squared squeezed at the output if $|G|^2$ is slightly greater than two. Further investigation shows that the amplitude-squared squeezed vacuum, $|0,\lambda>$, with $\lambda<<1$ is such a state. Therefore, the photon cloning limit does not, at least in principle, represent a barrier to nonclassical behavior. It would be of considerable interest to know if there are nonclassical states which can remain nonclassical when they are amplified at gains substantially larger than two.

VI. Conclusion

Quadratic squeezing represents a new class of nonclassical effects. States with this property have fluctuations smaller than is possible for classical light in a variable which is quadratic in mode creation and annihilation operators. As we have seen, quadratic squeezing can be converted into normal squeezing by $\chi^{(2)}$ type nonlinear interactions.

A direction for further investigations into quadratic squeezing is its connection to interferometry. Interferometers, both with and without nonlinear elements, can be described in a natural fashion in terms of the variables which describe quadratic squeezing(Ref.19). This suggests that interferometers can be used to measure quadratic squeeezing and that quadratic squeezed states may be of use in interferometric measurements. We are currently studying these issues.

References

1. D. Stoler, Phys. Rev. D $\underline{1}$, 3217 (1970).
2. H. P. Yuen, Phys. Rev. A $\underline{13}$, 2226 (1976).
3. For a review see D. F. Walls, Nature $\underline{306}$, 141 (1983).
4. M. Hillery, Phys. Rev. A $\underline{39}$, 1556 (1989).
5. M. Hillery, Opt. Commun. $\underline{62}$, 135 (1987).
6. M. Hillery, Phys. Rev. A $\underline{36}$, 3796 (1987).
7. K. Wodkiewicz and J. H. Eberly, J. Opt. Soc. Am. B $\underline{2}$, 458 (1985).
8. C. C. Gerry, Phys. Rev. A $\underline{31}$, 2721 (1985).
9. P. K. Aravind, J. Opt. Soc. Am. B $\underline{5}$, 1545 (1988).
10. V. Buzek, J. Mod. Opt. $\underline{37}$, 303 (1990).
11. J. Bergou, M. Hillery, and D. Yu, Phys. Rev. A $\underline{43}$, 515 (1991).
12. D. Yu, submitted for publication.
13. S. Braunstein and R. McLachlan, Phys. Rev. A $\underline{35}$, 1659 (1987).
14. M. Hillery, Phys. Rev. A $\underline{40}$, 3147 (1989).
15. See, for example, H. M. Nussenzveig, <u>Introduction to Quantum Optics</u> (Gordon and Breach, New York, 1973), P. 219.
16. S. Carusotto, Phys. Rev. A $\underline{11}$, 1629 (1975).
17. C. K. Hong, S. Friberg, and L. Mandel, J. Opt. Soc. Am. B $\underline{2}$, 494 (1985).
18. M. Hillery and D. Yu, submitted for publication.
19. B. Yurke, S. McCall, and J. Klauder, Phys. Rev. A $\underline{33}$, 4033 (1986).

QUANTUM SPATIAL PROPAGATION OF SQUEEZED LIGHT IN A DEGENERATE PARAMETRIC AMPLIFIER*

Ivan H. Deutsch

Department of Physics, University of California Berkeley, California, 94720

John C. Garrison

Lawrence Livermore National Laboratory, University of California, Livermore,, California 94550

Abstract

Differential equations which describe the steady state spatial evolution of nonclassical light are established using standard quantum field theoretic techniques. A Schrodinger equation for the state vector of the optical field is derived using the quantum analog of the slowly varying envelope approximation (SVEA). The steady state solutions are those that satisfy the time independent Schrodinger equation. The resulting eigenvalue problem then leads to the spatial propagation equations. For the degenerate parametric amplifier this method shows that the squeezed state is the ground state of the squeezing Hamiltonian. The magnitude and phase of the squeezing parameter obey nonlinear differential equations coupled by the amplifier gain constant and phase mismatch. The solution to these differential equations is equivalent to one obtained from the classical three wave mixing steady state solution to the parametric amplifier with a nondepleted pump.

1. Introduction

The standard approach in quantum optics for dealing with nonclassical light is to introduce a normal mode expansion for the field. This naturally leads to time evolution equations for the mode amplitudes (creation and annihilation operators) which satisfy the canonical equal time commutation relations. Such an approach is well suited for dealing with systems in optical cavities, such as an optical parametric oscillator, but is not appropriate for open systems such as a parametric amplifier. For the amplifier we are usually interested in the spatial dependence of temporally steady state fields. This problem has been treated for quantum fields either by identifying spatial evolution with temporal evolution for an interaction time set by the effective interaction length [1-4], or through the use of new quantization methods which require nonconventional commutation relations that are generally inconsistent with the fundamental equal time commutators for interacting fields [5-9]. In addition, the problem has recently been studied using the positive-P representation and stochastic differential equations [10]. In this letter we propose an alternative scheme which employs only standard quantum field theoretic techniques, and apply this analysis to the degenerate parametric amplifier (DPA) in

order to study the spatial evolution of squeezed light.

In the classical three wave mixing analysis of the DPA, the positive frequency component of the electric field is written as a slowly varying time independent envelope multiplying a carrier plane wave. Such an ansatz physically represents steady state propagation and leads to spatial differential equations for the envelope. Quantum mechanically, this ansatz cannot hold as an *operator* identity in the Heisenberg picture. Upon closer inspection, we see that the requirement of steady state propagation is enforced through the choice of *state vector* for the field. More precisely, steady state fields are the stationary states of the appropriate Hamiltonian. The resulting eigenvalue problem is then a time independent Schrodinger equation, and leads to spatial differential equations for the functions which parameterize the global state vector. We will apply this technique to the DPA in one dimension with a classical nondepleted pump. The stationary state solutions are squeezed states specified by a set of coupled nonlinear differential equations for the magnitude and phase of the squeezing parameter driven by the coupling constant of the three wave mixing.

2. Steady State Propagation Condition

Using the classical wave mixing analysis as our guide, we formulate the quantum theory in terms of the SVEA. The positive frequency electric field operator is written as an envelope field modulating a carrier plane wave of a given polarization ε. For systems in which the medium has no transverse dependence over the beam diameter and is longitudinally short compared to the Raleigh range, the theory becomes essentially one dimensional so that,

$$E_\omega^{(+)}(x,t) = \varepsilon \sqrt{\frac{2\pi\hbar\omega}{A\, n^2(\omega)}}\, \Psi(z,t)\, e^{i(kz-\omega t)},$$ (1)

where A is the beam area, and $n(\omega)$ is the linear index of refraction. The effective field theory in the SVEA formally resembles a nonrelativistic many body theory for a complex scalar field Ψ [12],

$$[\Psi(z,t),\ \Psi^\dagger(z',t)] = \delta(z-z').$$ (2)

The Hamiltonian (in the Heisenberg picture) can be written as,

$$H = H_c + H_{env} + H_{int}$$ (3a)

$$H_c = \hbar\omega \int d^3x\, \Psi^\dagger \Psi$$ (3b)

138

$$H_{env} = \frac{-i\hbar}{2} \frac{c}{n(\omega)} \int dz \left(\Psi^{\dagger} \frac{\partial \Psi}{\partial z} - \frac{\partial \Psi^{\dagger}}{\partial z} \Psi \right) \tag{3c}$$

$$H_{int} = \frac{i\hbar}{2} \frac{c}{n(\omega)} \int dz \left(\kappa^*(z) e^{-i\omega_p t} \Psi^2(z,t) - \kappa(z) e^{i\omega_p t} \Psi^{\dagger 2}(z,t) \right) \tag{3d}$$

where we have decomposed the "free" field Hamiltonian into the carrier wave Hamiltonian H_c, and the Hamiltonian governing the free (plus linear) evolution of the envelope H_{env}. The effective interaction Hamiltonian for the DPA is given by H_{int} [14] representing the mixing through the nonlinear susceptibility, with pump frequency ω_p. The interaction coupling is determined by

$$\kappa(z) = \frac{1}{2} g_0(z) e^{i\phi(z)}, \tag{4a}$$

$$g_0(z) = \frac{4\pi\omega}{n(\omega)c} |\chi^{(2)}(z)| |\mathcal{E}_P(z)| \tag{4b}$$

$$\phi(z) = -\frac{\pi}{2} + \Delta k\, z + \vartheta(z) \tag{4c}$$

where $g_0(z)$ is the standard power gain coupling constant [13] (allowing for possible z-dependence), Δk is the phase mismatch at the degenerate frequency, and $\vartheta(z)$ is the remaining phase stemming from the pump and $\chi^{(2)}$.

We seek the quantum field state vector corresponding to steady state propagation. Maintaining our close analogy with the classical analysis, we remove the carrier wave oscillation from the dynamics of this state. Quantum mechanically we use the envelope picture (E.P.) originally introduced by Caves [11], in which the dynamics of the operators are dictated by the carrier wave Hamiltonian, and the states evolve by a Schrodinger equation with the Hamiltonian $H_{env} + H_{int}$. If we denote objects in this picture by the superscript (E), then the dynamical equations in this picture are

$$i\hbar \frac{\partial A^{(E)}}{\partial t} = \left[A^{(E)}, H_c^{(E)} \right] \tag{5a}$$

$$i\hbar \frac{\partial |\Phi\rangle^{(E)}}{\partial t} = (H_{env}^{(E)} + H_{int}^{(E)}) |\Phi\rangle^{(E)}. \tag{5b}$$

For steady-state applications there will be exact frequency matching between the carrier frequencies of the various waves which mix through the nonlinear interaction, so that the Hamiltonian in Eq. (5b) will be independent of time. The steady state (ss) solutions are thus identified with the stationary solutions to Eq. (5b),

$$(H_{env}^{(E)} + H_{int}^{(E)}) |\Phi\rangle_{ss}^{(E)} = \lambda |\Phi\rangle_{ss}^{(E)}. \tag{6}$$

139

Henceforth, the labels (E) and (ss) will be omitted. Eq. (6) is the key result of our analysis which we now apply to the parametric amplifier.

3. Propagation Solution to the DPA

It is well known that the output produced during a parametric interaction is a squeezed vacuum state [11]. In an oscillator configuration one can restrict attention solely to a single mode of the cavity (for a doubly degenerate oscillator). In the amplifier configuration under consideration here, we must generalize the squeezing operator to take into account the many modes associated with the envelope field. We define a functional squeezing operator,

$$S[\zeta] \equiv \exp\left\{\frac{1}{2}\int dz\left(\zeta^*(z)\Psi^2(z) - \zeta(z)\Psi^{\dagger 2}(z)\right)\right\}$$

(7)

with z-dependent squeezing parameter $\zeta(z) = r(z)e^{i\theta(z)}$. One can easily show that the Bogoliubov transformation generalizes to

$$\widetilde{\Psi}(z) \equiv S^\dagger[\zeta]\Psi(z)S[\zeta] = \cosh(r(z))\,\Psi(z) - e^{i\theta(z)}\sinh(r(z))\,\Psi^\dagger(z).$$

(8)

The squeezed vacuum,

$$|\{\zeta\}\rangle \equiv S[\zeta]|0\rangle,$$

(9)

satisfies the well known eigenvalue equation [15],

$$\widehat{\Psi}(z)|\{\zeta\}\rangle = 0,$$

(10a)

$$\widehat{\Psi}(z) \equiv S[\zeta]\Psi(z)S^\dagger[\zeta] = \cosh(r(z))\,\Psi(z) + e^{i\theta(z)}\sinh(r(z))\,\Psi^\dagger(z).$$

(10b)

Using the formalism developed in Section 2, we deduce the steady steady solutions by solving the time independent Schrodinger equation (6). We take as our ansatz for the eigenvector a squeezed vacuum state Eq. (9), i.e.

$$(H_{env} + H_{int})|\{\zeta\}\rangle = \lambda|\{\zeta\}\rangle.$$

(11)

Our goal is to prove Eq. (11) and thereby obtain differential equations for the spatial squeezing

parameter $\zeta(z)$. Together, Eqs. (10a) and (11) imply

$$\left[H_{env} + H_{int} , \widehat{\Psi(z)} \right] | \{ \zeta \} \rangle = 0. \tag{12}$$

Substituting Eqs. (3) and (10b) into Eq. (12), using Eq. (8), and the relation (4a) for the polar decomposition of κ gives,

$$\left[\left(\frac{dr}{dz} - \frac{1}{2}g_0 \cos(\theta - \phi) \right) + \frac{i}{2} \left(\frac{d\theta}{dz} \sinh(2r) + g_0 \cosh(2r) \sin(\theta - \phi) \right) \right] \Psi^\dagger |0\rangle = 0. \tag{13}$$

Thus, the eigenvalue condition requires the real and imaginary parts of the coefficient of $\Psi^\dagger$ to vanish, yielding the desired propagation equations:

$$\frac{dr}{dz} = \frac{1}{2}g_0 \cos(\theta - \phi) \tag{14a}$$

$$\frac{d\theta}{dz} = -g_0 \coth(2r) \sin(\theta - \phi). \tag{14b}$$

The solution to (14) produces a relation for the squeezing parameters $\{r(z), \theta(z)\}$ in terms of the experimental parameters $\{g_0(z), \phi(z)\}$. In the next section we give an interpretation of the meaning of these equations and analyze their solutions.

4. Solutions and Interpretation of Propagation Equations

In solving Eqs. (14) we take as our boundary conditions,

$$r(0) = 0 \tag{15a}$$

$$\theta(0) = \phi(0) \tag{15b}$$

to ensure the continuity of the squeezing parameter. In order to get a better understanding of the nature of the equations we examine them for various regimes. Consider first the situation in which the phase of κ, Eq. (4c), is a constant $\phi(z) = \phi_0$ (i.e exact phase matching). With boundary conditions (15), the solution to (14) is immediately seen to be

$$r(z) = \int_0^z dz' \frac{1}{2}g_0(z'), \tag{16a}$$

$$\theta(z) = \phi_0. \tag{16b}$$

141

For a uniform crystal with plane wave pump, this yields the expected result $r_{out} = \frac{1}{2}g_0 L$ (for $z \geq L$), where L is the length of the crystal.

In limit of short crystals, Eqs. (14) can be expanded for small r to yield

$$\left\{ \begin{array}{l} \frac{dr}{dz} = \frac{1}{2}g_0\cos\,(\theta{-}\phi) \\[2mm] \frac{d\theta}{dz} = -\frac{g_0}{2r}\sin(\theta{-}\phi) \end{array} \right\} \Rightarrow \frac{\partial\zeta}{\partial z} = \kappa(z). \tag{17}$$

Thus, in this limit the complex squeezing parameter is just the integral of the interaction coupling constant. Henceforth we consider crystals with uniform nonlinearity and a plane wave pump, so that g_0 is a constant and $\phi(z) = -\frac{\pi}{2} + \Delta kz$. The solution to Eq. (17) for $z \geq L$ is of a familiar form,

$$r_{out} = \frac{1}{2}g_0 L \, \frac{\sin(\Delta kL/2)}{(\Delta kL/2)} \tag{18a}$$

$$\theta_{out} = -\frac{\pi}{2} + \Delta kL/2. \tag{18b}$$

If in addition $\Delta k \ll 1/L$ the amplitude and phase essentially decouple. However, as the phase mismatch increases, the magnitude of the squeezing decreases. Physically, large phase mismatch would cause squeezing along wildly different quadratures as the beam propagates through the crystal, thereby degrading the net squeezing.

For crystals containing many gain lengths, we expect strong sensitivity to the phase mismatch since the nonlinear coupling between r and θ causes rapid oscillations that destroy the magnitude of the squeezing at some value of Δk. To see this we numerically integrate Eq. (14). In presenting the data, we measure all distances in units of the natural length scale $1/g_0$. Fig.(1) shows the magnitude of the squeezing parameter as a function of z for various phase mismatches. Fig. (2) shows the squeezing parameter of downconverted light as function of phase mismatch for various values of the crystal length L, plotted simultaneously with the small r expression, Eq. (18a). For short lengths, Eq. (18a) is an excellent approximation. However, for crystals many gain lengths long (as can be obtained using intense pumps [16]) we see a sharp cutoff in the squeezing at the critical value $\Delta k/g_0$ =1. The sharp transition in output when $\Delta k = g_0$ is also characteristic of the classical three wave mixing solution to the parametric amplifier. This leads us to hypothesize that the solution to Eqs. (14) can be obtained from the classical propagation equations.

The classical solution for the envelope in a DPA is [13]

$$A(z) = \left(\mu(z)A(0) + iv(z)A^*(0)\right)e^{i\Delta kz/2} \tag{19a}$$

$$\mu(z) = \cosh\left(\tfrac{1}{2}gz\right) - i\tfrac{\Delta k}{g}\sinh\left(\tfrac{1}{2}gz\right) \ ; \quad \nu(z) = \sqrt{1-|\mu(z)|^2} = \tfrac{g_0}{g}\sinh\left(\tfrac{1}{2}gz\right) \qquad (19b)$$

$$g = \sqrt{g_0^2 - (\Delta k)^2}. \qquad (19c)$$

If we replace the c-number fields with creation/annihilation operators $A^*(0) \to a^\dagger$, $A(z) \to b$ representing "in" and "out" fields respectively, we recover the solution obtained by Caves and Crouch [5], and Huttner et. al. [6],

$$b = \left(\mu(z)a + i\nu(z)a^\dagger\right)e^{i\Delta kz/2}. \qquad (20)$$

The unitary operator relating a to b, $b = U^\dagger a U$, is a generalized squeezing operator

$$U = R^\dagger\left(\tfrac{1}{2}(\mathrm{Arg}(\mu) + \Delta kz)\right) S\left(-i\sinh^{-1}(\nu)\right), \qquad (21)$$

where S is the standard squeezing operator and R is the phase rotation operator [11]. This unitary operator transforms the vacuum into a squeezed state with squeezing parameter $\zeta = re^{i\theta}$ given by,

$$r(z) = \sinh^{-1}(\nu(z)) \qquad (22a)$$

$$\theta(z) = -\tfrac{\pi}{2} + \mathrm{Arg}(\mu(z)) + \Delta kz. \qquad (22b)$$

Figs. (1) and (2) are now easily understood in terms of limiting cases of (22a). In fact, direct substitution reveals that (22) is indeed the analytic solution to Eq. (14).

To understand the meaning of this result consider the nature of the interaction more carefully. Because we have assumed a classical nondepleted pump, the propagation equations are *linear* in the signal and idler amplitudes . In such a situation one expects the q-number and c-number solutions to be equivalent, i.e., the quantum fluctuations should propagate like a classical signal. This provides a substantial test on our formalism. The successful use of nonconventional commutation relations by previous workers is explained by a combination of good physical intuition and the special linear character of this problem. Indeed, Huttner et. al. showed that for this particular interaction the equal-z commutation relations are consistent with the fundamental equal-t commutators. However, for a general interaction in which the wave mixing equations are truly nonlinear we expect this method to fail. For example, if the pump is treated as a quantum mechanical field, then we find that the equal-z commutation relations are no longer consistent with the fundamental equal-t commutators. Thus, for more complex systems there will be qualitative differences between the classical and quantum propagation solutions. The formalism we have presented here is sufficiently general to handle these situations.

Acknowledgements:

References

* This research was performed under the auspices of the U. S. Department of Energy at the Lawrence Livermore National Laboratory under contract no. W-7405-Eng-48.

1. Shen,Y.R., 1967, Phys Rev. **155**, p. 921.

2. Tucker, J., and Walls, D.F., 1969, Phys. Rev. **178**, p. 2036.

3. Lane, A., Tombesi, P., Carmichael, H.J., and Walls, D.F., 1983, Opt. Com. **48**, p.155.

4. Hong, C.K., and Mandel, L., 1985, Phys. Reav A **31**, p. 2409.

5. Caves, C. M., and Crouch, D.D., 1987, J. Opt. Soc. Am. B **4**, p. 1535.

6. Huttner, B., Serulnik, S., and Ben-Aryeh, Y., 1990, Phys. Rev. A **42**, p. 5594.

7. Imoto, N. in *Proceedings of the 3rd International Symposium on the Foundations of Quantum Mechanics*, Tokyo, 1989, pp. 306-314

8. Yurke, B., Grangier, P., Slusher, R.E., and Potasek, M.J., 1987, Phys. Rev. A **35**, p. 3586.

9. Potesek, M. J., and Yurke, B., 1987, Phys. Rev. A **35**, p. 3974.

10. Drummond, P.D., and Carter, S.J., 1987, J. Opt. Soc. Am. **B4**,1565, p. 6845.; Raymer, M.G., Drummond, P.D., and Carter, S.J., 1991, (unpublished).

11. Caves, C. M. and Schumaker, B. L., 1985 Phys. Rev. A **31**, p. 3068.

12. Deutsch, I.H. and Garrison, J.C., 1991 Phys. Rev. A **43**, p. 2498.

13. Yariv, A., 1989, *Quantum Electronics*, 3rd Ed.John Wiley and Sons, Inc., New York.

14. Hillery, M., and Mlodinow, L., 1984 Phys. Rev. A **30**, p. 1860.

15. Yuen, H., 1976, Phys. Rev. A, **13**, p. 2226.

16. Slusher, R. E., Grangier, P., A LaPorta, Yurke, B., and Potasek, M. J., 1987, Phys. Lett. **59**, p. 2566.

(a)

(b)

(c)
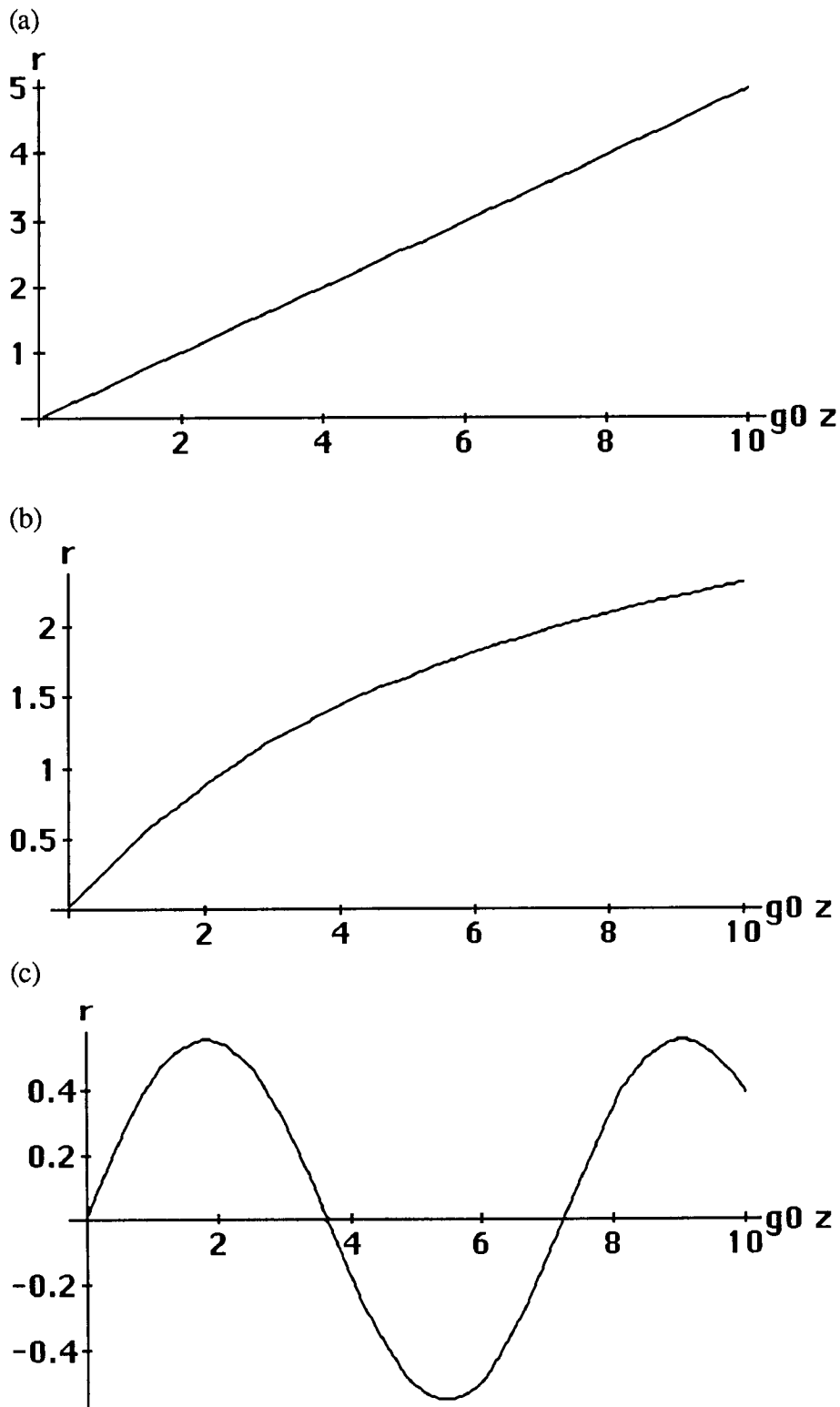
Fig 1. Squeezing magnitude as a function of propagation distance z measured in gain lengths g_0, for different values of phase mismatch Δk: (a) $\Delta k=0.1g_0$, (b) $\Delta k=g_0$, (c) $\Delta k=2g_0$.

145

(a)

(b)

(c)
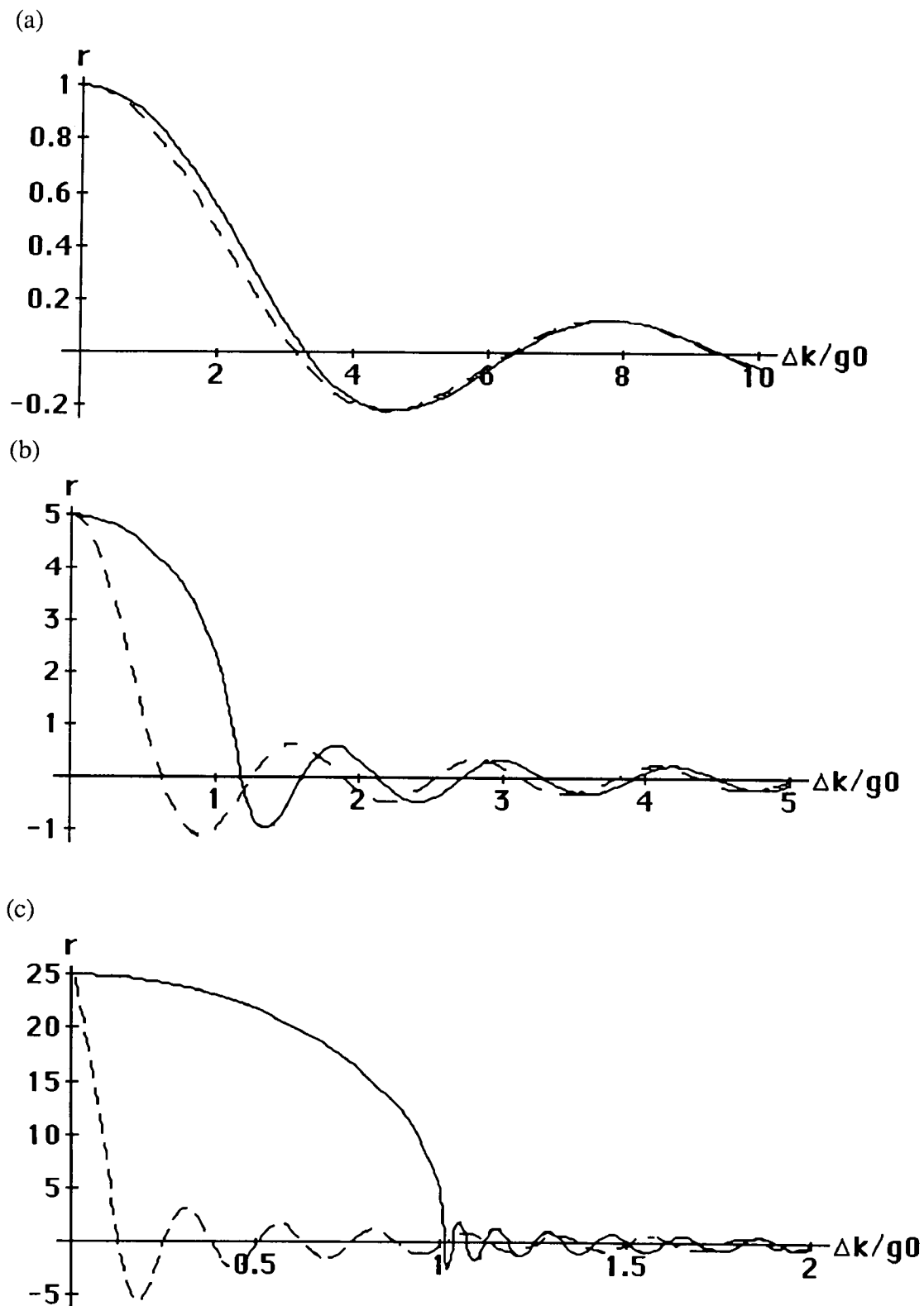
Fig 2. Squeezing at the output face as a function of Δk: (a) $L=2g_0$,(b) $L=10g_0$, (c) $L=50g_0$. The solid curve is the solution to Eq. (14), the dotted curve is given by the asymptotic result Eq. (18a).

SQUEEZED PULSED LIGHT FROM A FIBER RING INTERFEROMETER

K. Bergman and H. A. Haus

Department of Electrical Engineering and Computer Science
and Research Laboratory of Electronics,
Massachusetts Institute of Technology, Cambridge, MA 02139

ABSTRACT

Observation of squeezed noise, 5±0.3 dB below the shot noise level, generated with pulses in a fiber ring interferometer is reported. The interferometric geometry is used to separate the pump pulse from the squeezed vacuum radiation. A portion of the pump is reused as the local oscillator in a homodyne detection. The pump fluctuations are successfully subtracted and shot noise limited performance is achieved at low frequencies (35-85 KHz). A possible utilization of the generated squeezed vacuum in improving a fiber gyro's signal to noise ratio is discussed.

INTRODUCTION

Squeezing in a fiber was first demonstrated by Shelby et al. [1] who showed that the fiber's $\chi^{(3)}$ nonlinearity could be used to shape the field's fluctuations through self phase modulation. The group's experimental results were, however, severely limited by acoustic and thermal noise processes. First, the low Stimulated Brillouin Scattering (SBS) threshold in fibers forced the IBM group to separate their CW pump into 25 frequency components. The second noise source, more difficult to avoid, was the so called GAWBS (Guided Acoustic Wave Brillouin Scattering) excitations [2]. GAWBS is caused by thermal fluctuations that modulate the fiber's refractive index at high frequencies (approximately between 20 MHz and 10 GHz) and thereby scatter acoustic waves which are guided in the forward direction. Because the experiment was performed in a traveling wave geometry, it was necessary to detect the squeezing at high frequencies (50-100 MHz) where the laser noise is negligible. The measurement center frequency was within the frequency range of GAWBS, and only about 12% of noise reduction was thus observed.

To improve upon these earlier results, we used short pulses in a fiber interferometer configuration. Large nonlinear phase shifts of the order of several π are easily achieved with short pulses of high peak power, while the SBS threshold is avoided. The fiber ring geometry is used to separate the pump from the squeezed vacuum fluctuations. Subsequent detection with a balanced detector permitted complete cancellation of the pump fluctuations at frequencies as low as 35-85 KHz. Although the GAWBS noise can be frequency down-converted into the detection "window" when pulses are used [3], it did not seem to prevent the noise reduction in our experiment. The investigation of the down-conversion of GAWBS requires further study.

The experimental results reported in this paper have been recently published [4]. This paper begins with a brief review of the broadband squeezing process in a fiber. Following the approach of Shirasaki and Haus [5], we then show how the pump is separated from the squeezed vacuum when the squeezing is performed within a Mach-Zehnder interferometer. The squeezed vacuum is observed with the aid of a local oscillator derived from the pump. We describe some of the theoretical limitations on the observed squeezing using homodyne detection and a gaussian shaped local oscillator. The experiment and results are then described in detail.

SQUEEZING IN THE NONLINEAR MACH-ZEHNDER

We consider the simple propagation equation for the field operator, $\hat{a}(z)$, in a nonlinear Kerr medium. Assuming no dispersion this equation becomes:

$$\frac{d\hat{a}(z)}{dz} = i\kappa[\hat{a}^+(z)\hat{a}(z)]\hat{a}(z) \tag{1}$$

where κ is the Kerr nonlinearity. The Kerr nonlinearity is calculated as follows,

$$\kappa = \frac{2\pi}{\lambda} n_2 \frac{P_p}{A_{eff}} \tag{2}$$

where λ is the wavelength, n_2 the nonlinear index, P_p the peak power, and A_{eff} the effective coupling area. Equation (1) may be integrated directly, yielding a solution for the field operator, $\hat{a}(z)$, after a propagation distance, L:

$$\hat{a}(L) = e^{i\kappa L\hat{a}^+(0)\hat{a}(0)}\hat{a}(0) \tag{3}$$

The effect of the Kerr medium is to add a nonlinear phase shift proportional to the photon number, propagation distance, and Kerr coefficient. The mean square fluctuations of the field are shaped by this nonlinear process as shown in figure 1. The $\chi^{(3)}$ process couples the amplitude and the phase fluctuations, causing the phase insensitive mean square fluctuations of the incoming field, represented by a circle, to stretch into an ellipse along the amplitude tangents. The area of the resulting squeezed noise ellipse is equal to the area of the initial circle.

Next, we place two equal lengths of Kerr media symmetrically in the two arms of a Mach-Zehnder interferometer, as was analyzed in reference [5]. The input field and its associated fluctuations enter one input port of the interferometer's first beam splitter in figure 2. Into the second, unexcited port enter the zero point fluctuations of the vacuum field. The field's amplitude split coherently in two by the 50/50 beam splitter. The fluctuations add and subtract incoherently.

As each field-half propagates through its Mach-Zehnder arm, it accumulates a nonlinear phase shift (not shown on the phasors in figure 2) and its fluctuation circles are stretched into ellipses. At the second beam splitter, the two half-field amplitudes interfere coherently. Under a linearized first order analysis, the squeezed fluctuations will again add and subtract incoherently. As illustrated with the phasors in figure 2, the original mean

field amplitude emerges from the constructive interference port, and the squeezed vacuum exits from the destructive interference port. The interferometer has made possible this isolation of the squeezed vacuum.

The above explanation for a single frequency phasor (CW pump) also holds for the case of a pulsed pump, as long as dispersion may be neglected. Without dispersion the pulse may be divided into short time segments and each segment analyzed independently. At the output the segments are superimposed to reconstruct the pulse.

DETECTION

The function of homodyne detection is to measure one quadrature of the incoming signal, amplified by the local oscillator. This detection technique is used to observe the phase sensitive fluctuations of the squeezed vacuum signal. If the local oscillator phase is properly adjusted, the squeezed (reduced noise) quadrature is measured. The fluctuations accompanying the pump are completely subtracted by the balanced detection. When the signal arm is blocked, the homodyne detection measures the vacuum state noise. This is a part of the experimental shot noise calibration.

In the Mach-Zehnder squeezing geometry, the exiting pump, shown in figure 2, may be reused as the local oscillator. In this way, the local oscillator pulse shape matches the squeezed vacuum pulse. However, to detect the full pulsed squeezing magnitude a finer matching of the local oscillator phase is required since the squeezing direction as well as magnitude will vary along the pulse duration. Thus, under ideal conditions the local oscillator should be phase shifted in one direction at the pulse center but in a different direction at the pulse wings. Experimentally the local oscillator is shifted by one constant phase leading to a nonideal measured noise reduction magnitude. We have plotted the expected noise reduction for the ideal and single phase adjusted gaussian pulse cases in figure 3 (a). In figure 3(b) we show that for the gaussian pulse case, the amplified noise amplitude is larger than the attenuated noise amplitude for the same peak nonlinear phase level.

EXPERIMENT

The experiment was implemented by replacing the Mach-Zehnder with a fiber ring interferometer, to take advantage of the ring's stability to vibrational and thermal disturbances. Figure 4 is a schematic of the experimental arrangement. A mode-locked $1.3\mu m$ Nd:YAG producing 100 psec pulses at a repetition rate of 100 MHz was used as the pump. This pulse train pump is coupled into the fiber ring reflector composed of 50 m of PM (polarization maintaining) fiber which is spliced to the two pigtails of a 3 dB PM fiber coupler. The coupler's splitting ratio was variable, and was carefully adjusted to 50/50 within 1 part in 500. The pump pulses are thus completely reflected from the ring. A 90/10 beam splitter picks off a portion of the reflected pump to be reused as the local oscillator. The squeezed vacuum signal emerges from the unexcited transmission port of the ring.

The local oscillator and the squeezed signal are then mixed in a 50/50 beam splitter (BS2), and detected with a balanced dual detector receiver. The output difference current is directly fed into a spectrum analyzer. The Power Spectral Density (PSD) reading

corresponds to a measure of the fluctuations magnitude along one quadrature of the squeezed vacuum. The amplified and reduced noise quadratures may now be measured by adjusting the relative phase of the local oscillator and squeezed signal.

The reduced noise will increase with the pulse peak nonlinear phase shift, which can be estimated from the following CW equation,

$$\Phi_{NL} = \frac{2\pi}{\lambda} n_2 L \frac{P_p}{A_{eff}} \tag{4}$$

where n_2 is the nonlinear index, L the fiber length, P_p the pulse peak power, and A_{eff} the effective coupling area. In this experiment, a peak nonlinear phase shift of 1.4 radians corresponds to approximately 100 mW of average power in each ring direction. The PSD measurements were performed at a narrow low frequency window between 39 and 41 KHz. Data was taken with an integration time of 400 msec and a frequency resolution of 2.5 Hz. Before discussing the results, we describe the methods used to calibrate the shot noise level.

IV   SHOT NOISE CALIBRATION

The shot noise level was calibrated in order to confirm that the reduced quadrature fluctuations of the squeezed vacuum dropped below the zero point fluctuations level. Two methods were used. First, direct excitation from the laser was sent through the homodyne detection system and the detector current along with a corresponding PSD level were recorded for a range of input power levels. To cross check this calibration, two white light sources were used to generate detector current levels similar to those obtained with the laser excitation. Again, the PSD levels were recorded along with the current readings for the same range of power levels. The spectrum analyzer's noise floor was measured at -155 dBm/Hz and typical shot noise levels ranged from -120 to -125 dBm/Hz, so that electrical noise was not a factor. The two curves plotted on a dB scale in figure 5 overlapped well with a 45 degree slope. Thus, the laser noise has been successfully subtracted and the detection's response has been shown linear within the measurement current range.

V   EXPERIMENTAL RESULTS

Having accurately established a shot noise level, we proceed with the squeezing measurement. The local oscillator pulse and the squeezed vacuum pulse are aligned to overlap spatially and temporally at the detection beam splitter (BS2). For alignment purposes only, the signal magnitude may be temporarily increased by changing the coupler's splitting ratio. The coupler is adjusted back to 50/50 and the relative phase between the local oscillator and squeezed signal is allowed to drift. While the phase is drifting, PSD measurements are taken continuously with an automated data acquisition system.

The PSD level, a measurement of the squeezed noise will vary from some maximum value to some minimum value corresponding to the amplified and attenuated quadratures of the squeezed vacuum. The resulting histograms from these measurements taken at three separate pump power levels: 60, 85, and 110 mW (in each fiber ring direction) are shown in figure 6 (a), (b), and (c) respectively. In the figure, the black bars are PSD readings taken with the squeezed vacuum arm blocked, and are thus the shot noise calibration for the specific power level. The white bars are a collection of PSD readings taken after the mixing of the local oscillator and squeezed vacuum. The reduced noise level or squeezing magnitude is defined as the distance between the black bars distribution center and the left edge of the white bars distribution. We note that as previously predicted for the case of a gaussian local oscillator, the amplified quadrature noise is larger than the reduced quadrature for the same power level.

In figure 7 we plot the experimental maximum and minimum PSD readings (in dot scatter format) obtained for a collection of power levels, on top of the theoretically predicted limits for the gaussian local oscillator case. The experimental point plot was adjusted horizontally, along the peak nonlinear phase axis for a best fit. This fitting compensates for coupling losses, detector quantum efficiencies, and nonlinear phase estimation.

VI   SQUEEZED VACUUM IN A FIBER GYRO

It has been shown both theoretically [6,7,8], and experimentally [9,10], that the sensitivity of a phase measurement device can be improved with the injection of squeezed vacuum into the unexcited port. Normally, zero point fluctuations enter this unexcited port. We briefly consider the circumstances of utilizing the squeezed vacuum generated by the interferometric fiber ring to improve the performance of a second fiber ring functioning as a fiber gyro. In principle, all of the pump power reflected from the ring may be reused in the gyro.

If the same power levels and fiber lengths that are used in the squeezer ring are also used in the gyro, nonlinear effects in the gyro must be considered. We have explored this issue in detail in a separate paper [11]. Here we shall merely point out that the nonlinearity in the fiber gyro will cause additional squeezing but in an opposite direction. The squeezing that occurs in the gyro will undo some of the squeezing initially injected.

The analysis is shown diagrammatically in figure 8, using a Mach-Zehnder configuration. If the gyro is linear (figure 8(a)), it is clear that the squeezed vacuum should be oriented along the horizontal direction. In this way, at the gyro's output signal port, the reduced quadrature is along the signal direction.

For a nonlinear gyro, the effect of the $\chi^{(3)}$ nonlinearity will be to pull the elliptical locus of fluctuations toward a circular shape, thereby destroying the squeezing. As shown in the inset of figure 8(b), one must prepare the squeezed vacuum to counterbalance some of the effect of the gyro nonlinearity. The gyro's signal to noise ratio improvement will then be diminished, but not destroyed completely. In fact, much of the noise reduction advantages may be regained by properly designing the relative nonlinearity of the gyro and squeezer rings. For example, if we set the squeezer's nonlinear phase at π the ideal noise reduction will be approximately -15 dB. If the gyro's nonlinearity is then half of the squeezer's, the noise improvement will reduce to -6 dB.

VII   CONCLUSIONS

We described the successful observation of squeezed pulsed vacuum, 5 ± 0.3 dB below the shot noise level, generated from a fiber ring interferometer. Noise generated from GAWBS excitations did not appear to damage the squeezing measurements at low frequencies. Further study should determine the exact GAWBS spectra and magnitude for our experimental configuration. If the squeezed vacuum, properly oriented, is injected into a lossless linear interferometer, the interferometer's signal to noise ratio will improve by the noise reduction factor. We considered the utilization of squeezed vacuum in the improvement of the sensitivity of a shot noise limited fiber gyro. In this case the gyro's nonlinearity must be reduced in proportion to the squeezer's nonlinearity.

VIII   ACKNOWLEDGEMENTS

REFERENCES

1. R. M. Shelby, M. D. Levenson, S. H. Perlmutter, R. G. De Voe, and D. F. Walls, *Phys. Rev. Lett.*, **57**, 691, (1986).

2. R. M. Shelby, M. D. Levenson, and P. W. Bayer, *Phys. Rev. B*, **31**, 5244, (1985).

3. R. M. Shelby, P. D. Drummond, and S. J. Carter, *Phys. Rev. A*, **42**, 2966, (1990).

4. K. Bergman and H. A. Haus, *Opt. Lett.*, **16**, 663, (1991).

5. M. Shirasaki and H. A. Haus, *J. Opt. Soc. Am. B*, **7**, 30, (1990).

6. C. M. Caves, *Phys. Rev. D*, **23**, 1693, (1981).

7. R. S. Boudurant and H. J. Shapiro, *Phys. Rev. D*, **30**, 2548, (1984).

8. M. Shirasaki and H. A. Haus, *J. Opt. Soc. Am. B*, **8**, 681, (1991).

9. M. Xiao, L. Wu, and H. J. Kimble, *Phys. Rev. Lett.*, **55**, 2520, (1986).

10. P. Grangier, R. E. Slusher, B. Yurke, and A. LaPorta, *Phys. Rev. Lett.*, **59**, 2153, (1987).

11. H. A. Haus, K. Bergman, and Y. Lai, "Fiber Gyro with Squeezed Radiation," accepted for publication in *J. Opt. Soc. Am. B*, (1991).

drawn with the nonlinear phase shift subtracted
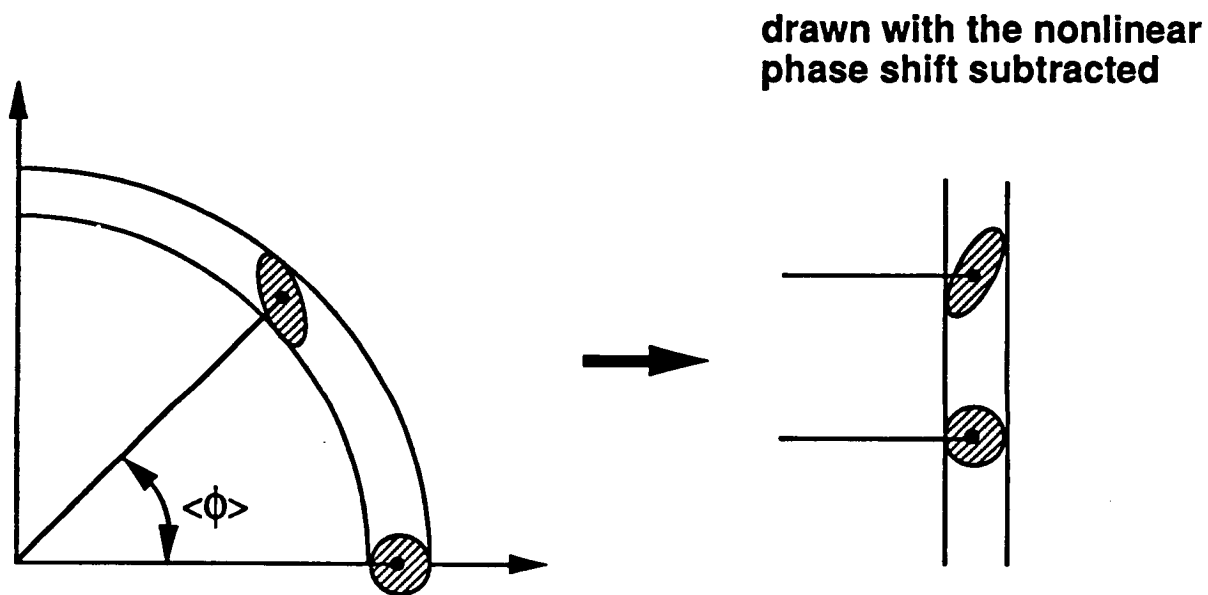
Figure 1   The field's phase insensitive quantum fluctuations are elongated into an ellipse of squeezed noise by the self phase modulation process.
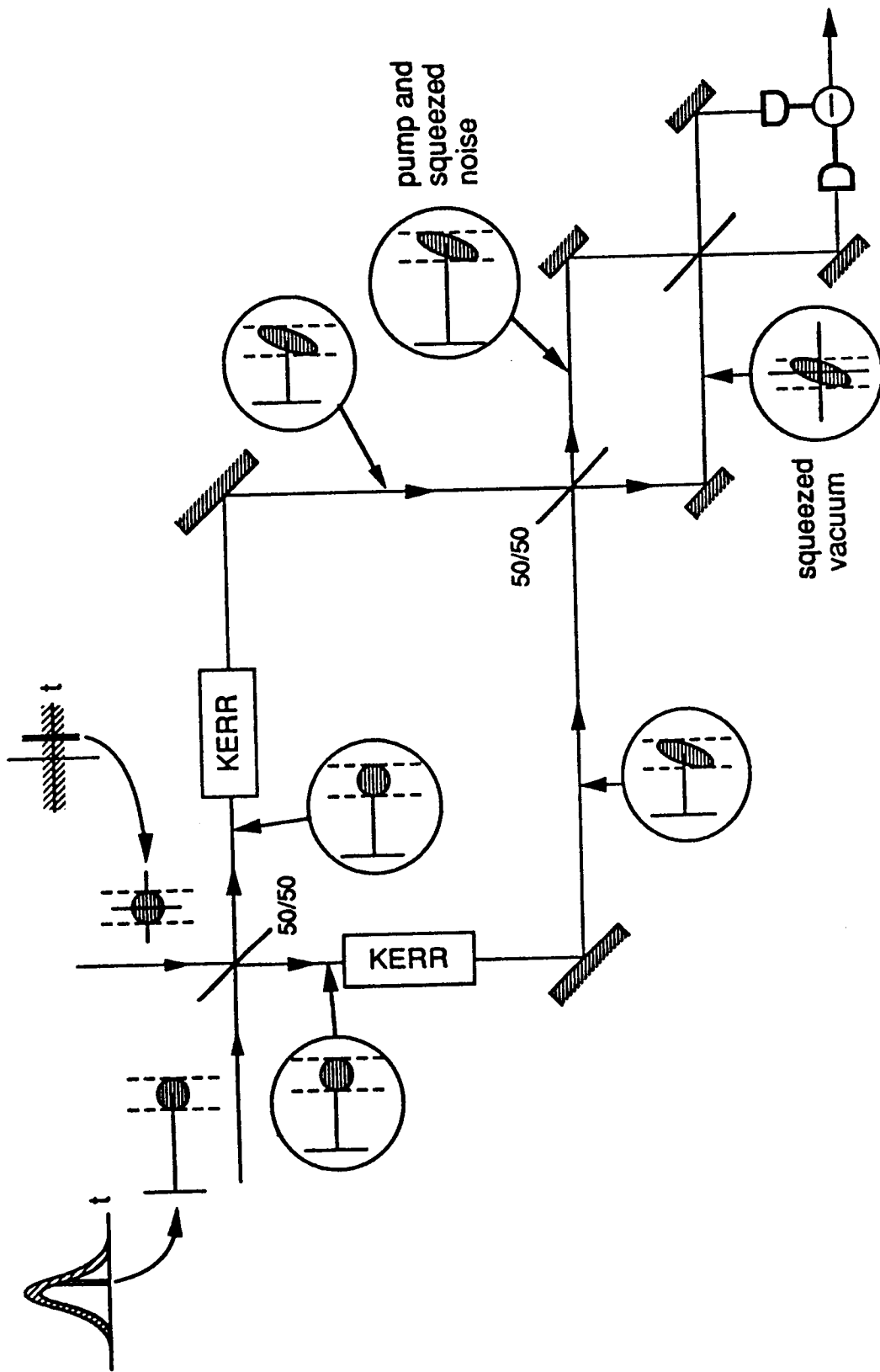
Figure 2   The explanation of squeezing in the Mach-Zehnder interferometric geometry. The pump, separated from the squeezed zero point fluctuations, may be reused as the local oscillator in a homodyne detection.
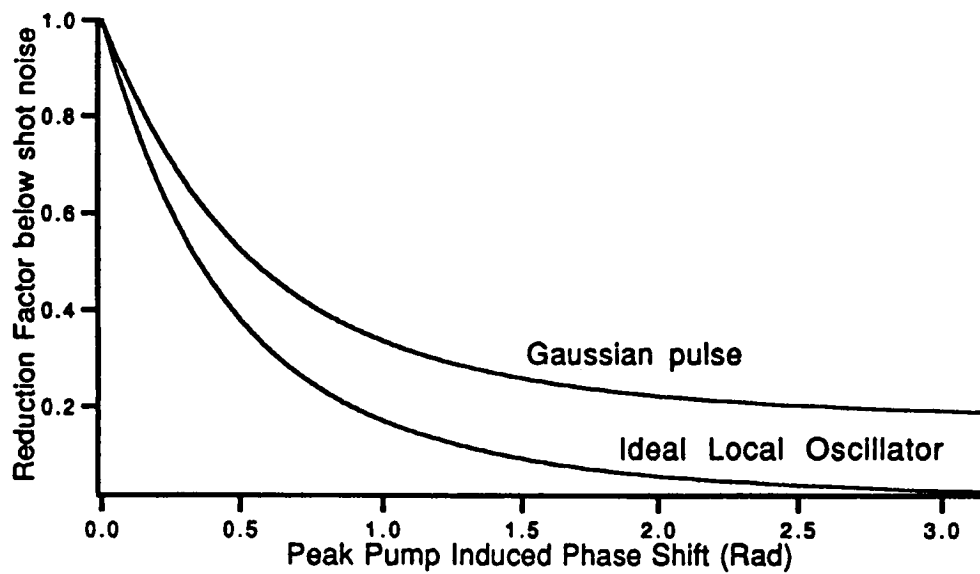
(a)
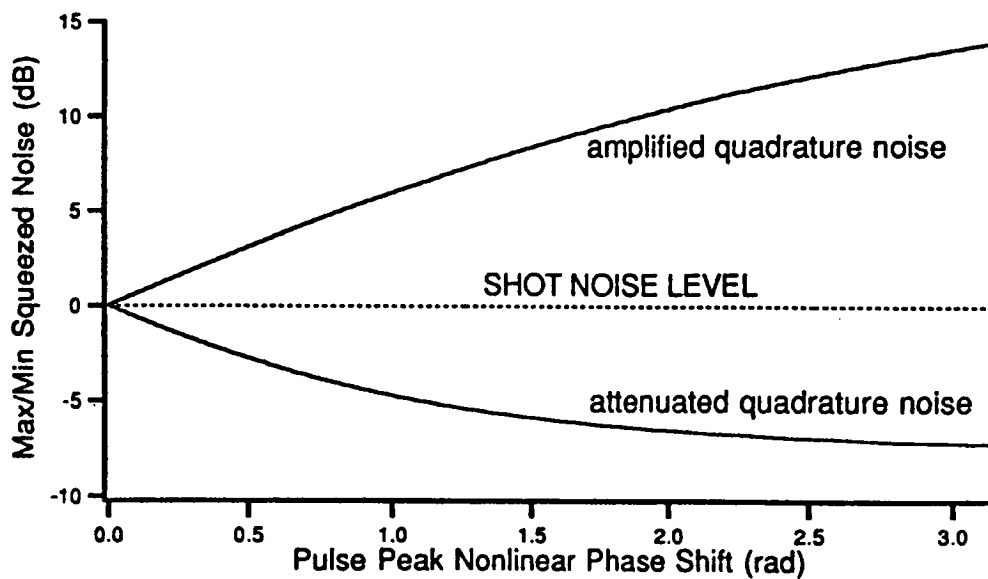
(b)

Figure 3 (a) Expected noise reduction for the ideal and single phase adjusted gaussian pulse cases. (b) Predicted maximum and minimum noise amplitudes for the gaussian local oscillator case, plotted on a dB scale.
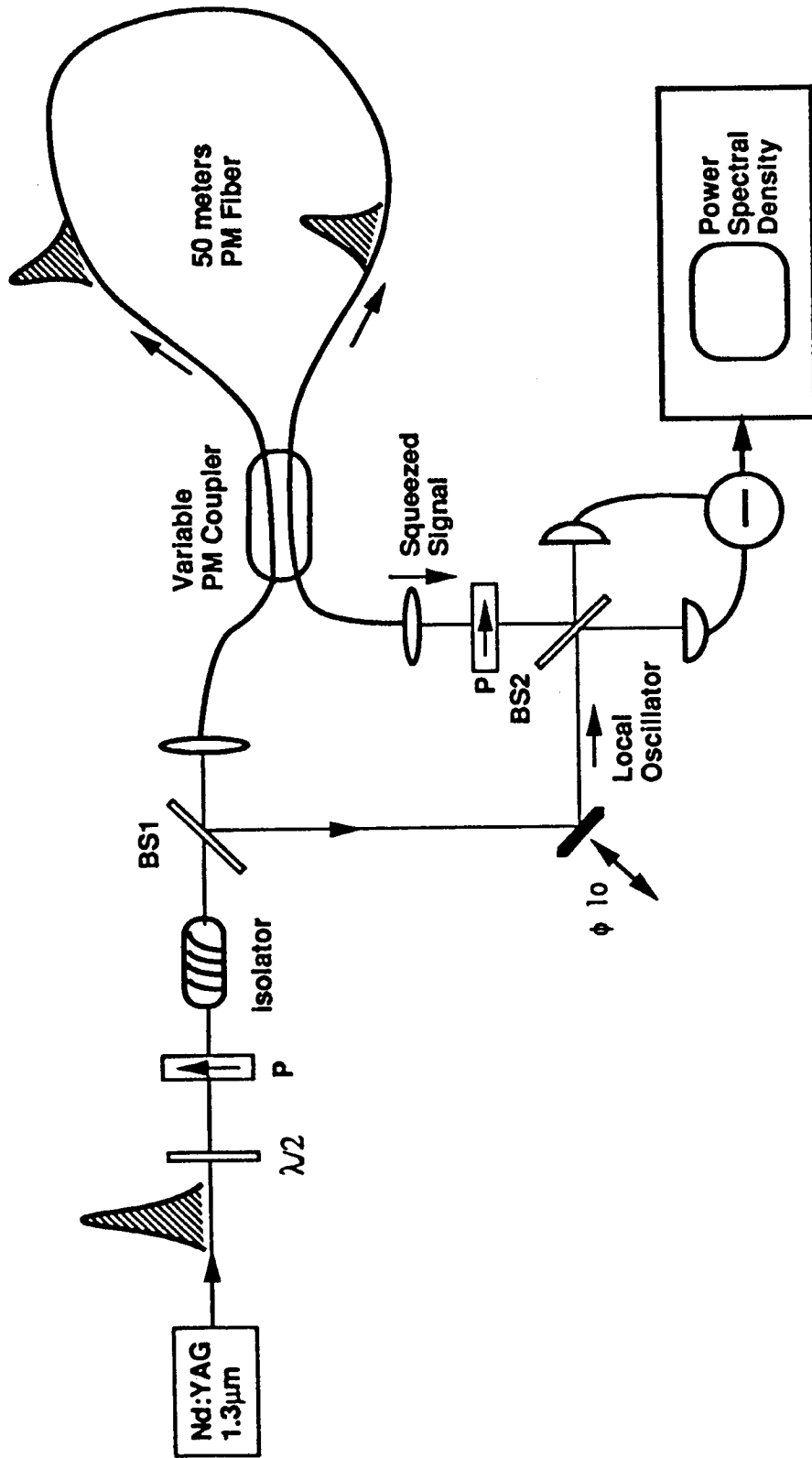
Figure 4   Experimental configuration.
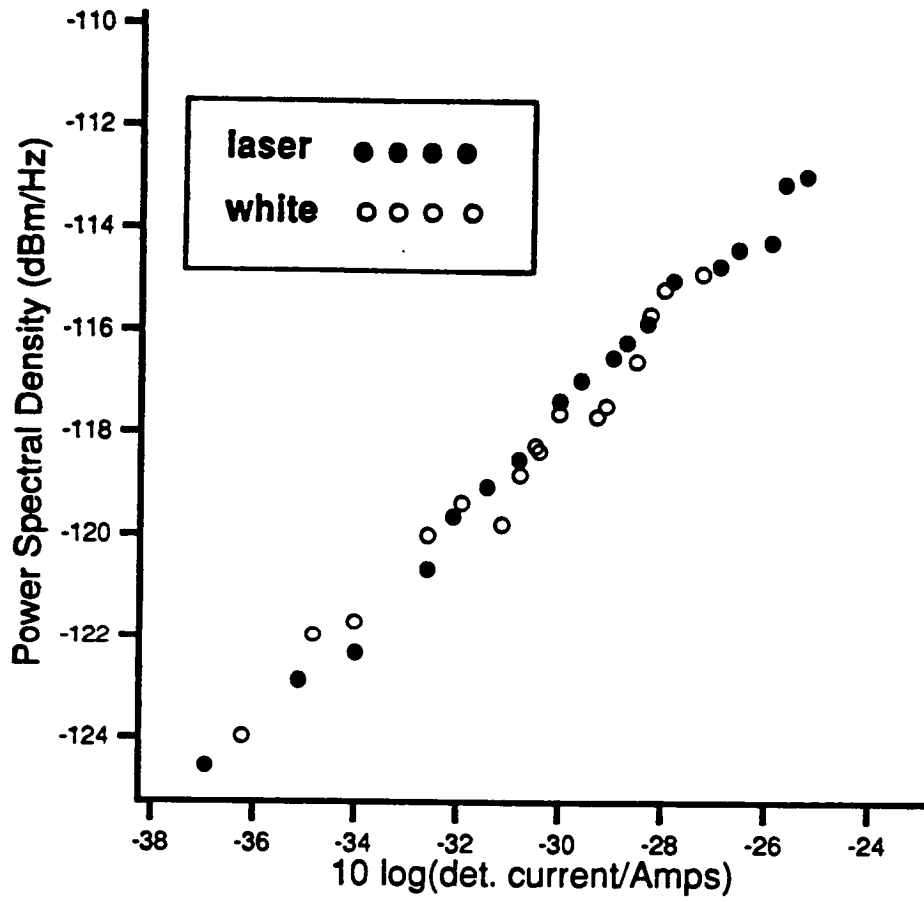
Figure 5   Shot noise calibration using both white light and direct laser excitation.
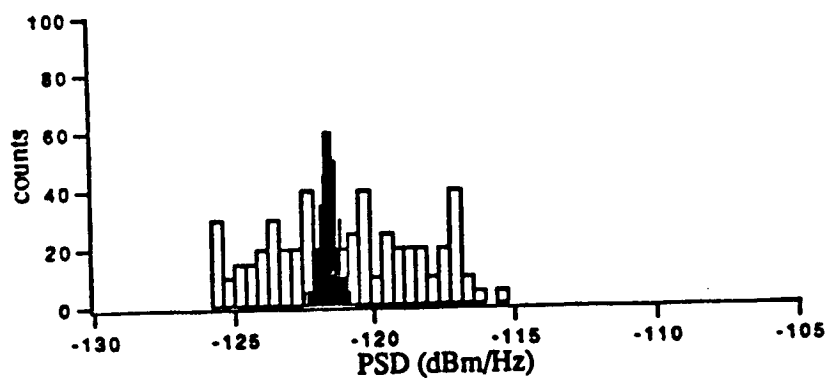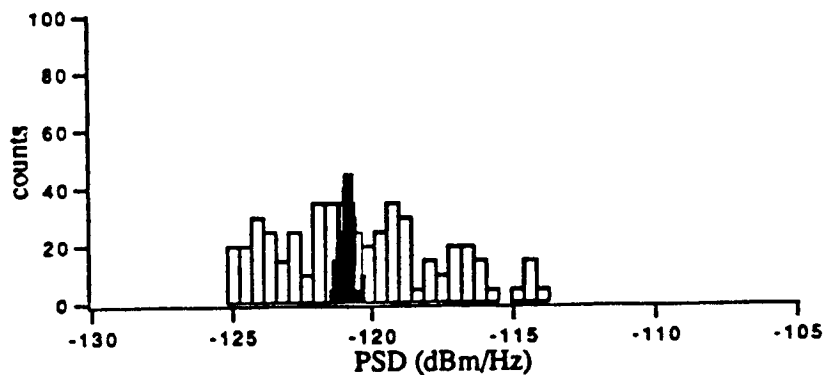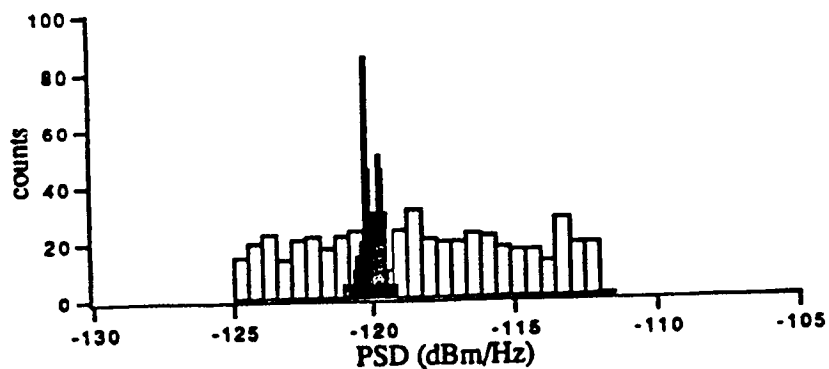
Figure 6 Histograms of PSD readings taken at three separate power levels (a) 60, (b) 85, and (c) 110 mW in each ring direction. The black bars are counts taken with the squeezed signal arm blocked. The white bars are the squeezing PSD measurements.
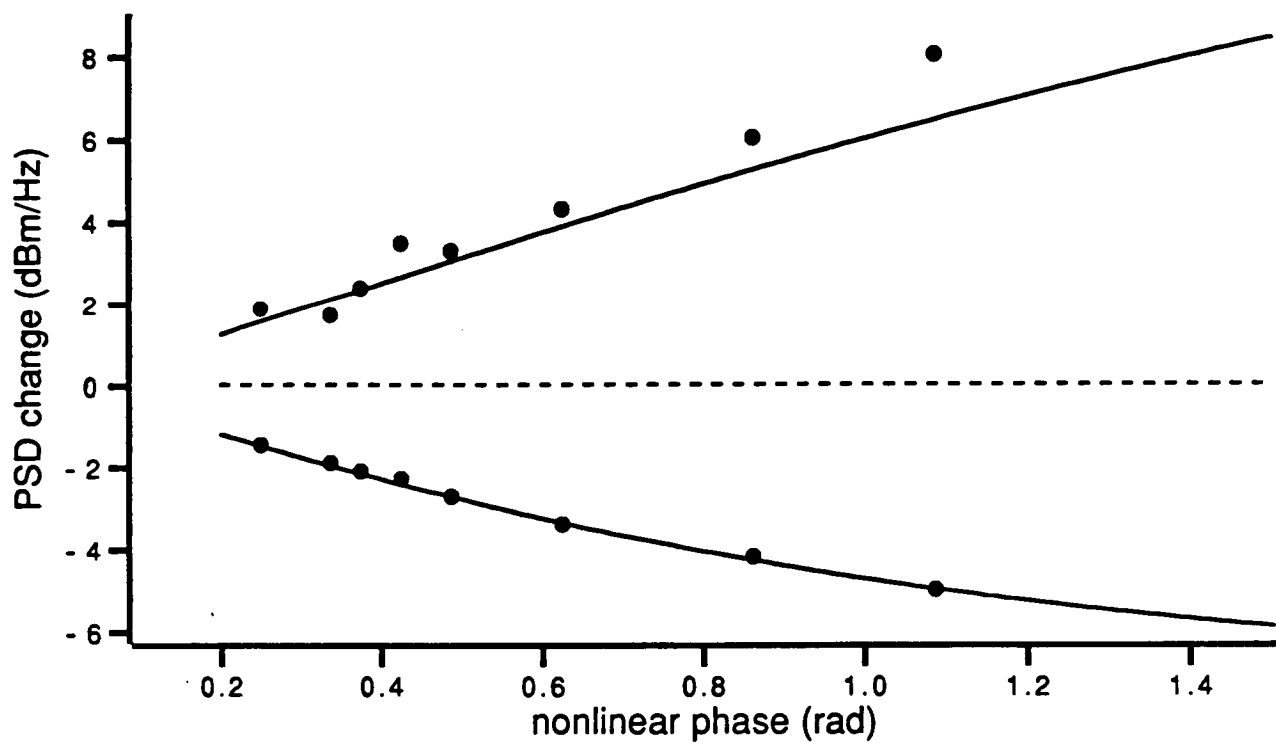
Figure 7   Maximum and minimum values of the PSD readings obtained experimentally (black dots) overlaid on the theoretically predicted curves for the case of a gaussian local oscillator.
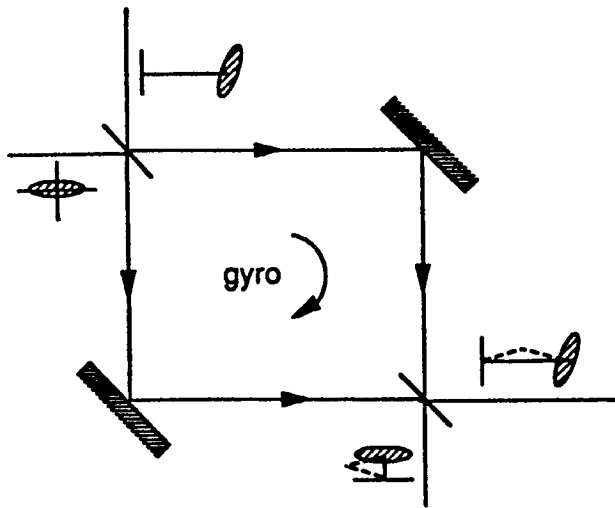
(a)
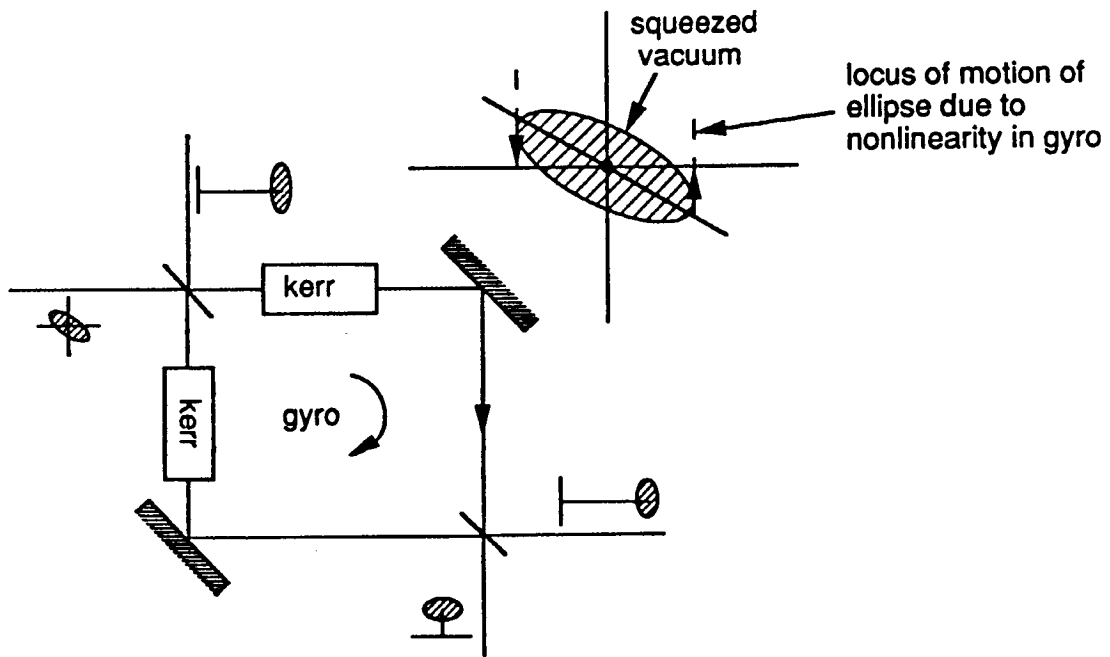
(b)

Figure 8 (a) The linear gyro with squeezed vacuum injected. (b) The nonlinear gyro with phase compensated squeezed vacuum.

EQUILIBRIUM TEMPERATURE OF LASER COOLED ATOMS IN SQUEEZED VACUUM

628/57

14 f,s

Y. Shevy

Applied Physics, California Institute of Technology, 128-95

Pasadena CA-91125

ABSTRACT:

It is shown that by squeezing the vacuum fluctuations of the electromagnetic field the quantum fluctuations of the optical forces exerted on laser cooled two-level atoms, can be dramatically modified. Under certain conditions, this modification in concert with the enhanced average forces can lead to equilibrium temperatures below those attained under normal vacuum fluctuations.

INTRODUCTION:

Laser cooling of atoms in a quasi-resonant standing laser wave has been attracting considerable attention during the past few years[1]. Another exciting subject has been the modification of the statistical properties of the vacuum fluctuations of the electromagnetic field. Reduction of these fluctuations in one quadrature phase of the field by almost an order of magnitude has been already realized in the laboratory. It is well accepted that the minimum equilibrium temperature of laser cooled two level atoms is determined by the interaction with the vacuum fluctuations of the electromagnetic field. This raises the question whether the equilibrium temperature of two level atoms in squeezed vacuum can be lowered below the normal vacuum level and in particular below the so called "Doppler limit" of $K_b T = \hbar \Gamma/2$ for two level atoms.

In the following, the physical origin of the optical forces in a standing laser wave is described and an intuitive model of the effects in a squeezed vacuum is offered, the modified force in squeezed vacuum is presented and compared to the force in a normal vacuum. In order to find the equilibrium temperature the modification of the fluctuations of these forces in squeezed vacuum is calculated. This calculation show, under certain conditions, a dramatic modification of these fluctuations relative to the normal vacuum state. it is found that, *in an intense standing wave*, the reduced fluctuations in concert with the enhanced average cooling force can lead to equilibrium temperatures below those obtained under normal vacuum fluctuations. Moreover, under certain ideal conditions even sub-Doppler temperatures may be reached. In the *running wave* case, however, the temperature can not be lowered below the normal vacuum level. In addition to being of potential use for laser cooling, these results offer an interesting glimpse into the quantum nature of the momentum exchanges between the atoms and the field.

A slowly moving atom (kv<Γ) in a low intensity standing laser light wave experiences a velocity dependent force. This "radiation pressure" force is well understood in terms of absorption and spontaneous emission. As first envisioned by Hänsch and Schawlow[2], the atom experiences an increased absorption of photons from the laser beam which is shifted closer to resonance due to the Doppler effect. This velocity dependent differential absorption can provide a cooling force for laser detuning to the red side of the atomic transition or a heating force for blue detuning. At high intensity, however, stimulated emission can change the sign of the force to a heating force at red detuning and to a cooling force at the blue side of resonance[3-4].
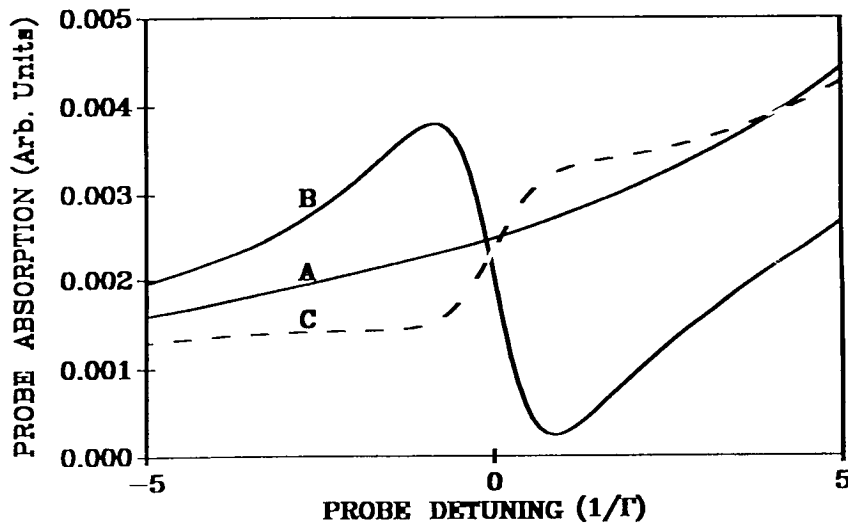
Figure 1: Probe absorption as a function of its detuning from a pump tuned 20Γ to the red of an atomic transition.A)at low pump intensity the probe sees higher absorption at positive detuning closer to the atomic transition B)In normal vacuum at high pump intensity the TWM process is induced leading to less absorption for frequency shifts closer to the atomic transition . C) At the same high intensity as in trace B but in squeezed vacuum the TWM process can change its lineshape leading to an additional cooling force.(Ref. 8 eq. 12 with N =0.1, M=0.33, ϕ= π and Ω=8Γ).

This stimulated force(or "dipole force") has been explained within the framework of the dressed atom model [5] and equivalently as resulting from Two Wave Mixing[6] (TWM). The TWM resonance appears in pump-probe spectra as a dispersive lineshape (as a function of the probe's detuning from the pump). This feature has a width of the excited state decay rate, Γ, and shows decreased absorption at probe detuning from the pump closer to the atomic transition (see figure 1b). In this process the atom absorbs one photon from one wave and emits a photon into the

counter- propagating wave, thus acquiring a momentum kick of $2\hbar k$. This process usually requires high laser intensity ; however, it has been shown to occur at lower intensity when the normal relation between the dipole decay rate Γ_2 and the excited state decay Γ ($\Gamma_2=0.5\ \Gamma$) is modified by the inclusion of phase interrupting events ($\Gamma_2>0.5\ \Gamma$). This effect is due to the appearance of a TWM term at lower order in laser intensity proportional to $[\Gamma_2/\Gamma- 0.5]P$ where P is the saturation parameter. This phenomenon is closely related to the dephasing induced extra resonances in Four Wave Mixing. These resonances , which originally have been studied by Bloembergen and co-workers, are induced whenever the normal decay rates of the the atom are modified. Their relevance to the stimulated force is discussed in more detail in reference 6.

Armed with this insight into the connection between TWM and the stimulated force, it is instructive to find the effect of squeezing on the TWM process. Gardiner[7] has shown that in general squeezing the vacuum fluctuations results in two different decay rates for the two quadratures of the atomic dipole, one of which is larger and the other smaller than the normal $\Gamma/2$ value in ordinary vacuum. Hence, after the decay of the fast decaying quadrature component of the atomic dipole one is left with the slowly decaying component which means that Γ_2 can be much smaller than $0.5\ \Gamma$. One can therefore immediately see that the "extra resonant" TWM process can also be induced in squeezed vacuum. Calculation of the lineshape[8-9] of this process shows that indeed the TWM lineshape becomes phase dependent and can even change to a "dispersive" lineshape with opposite sign (larger absorption closer to the atomic transition) as demonstrated in figure 1c . This indicates that in squeezed vacuum the stimulated force can be induced at low laser intensity . Moreover, it can change sign to provide an additional cooling force instead of heating for red laser detuning from resonance.

THE AVERAGE OPTICAL FORCES IN SQUEEZED VACUUM

The physical system under investigation is a slowly moving two level atom ($k\ v<< \Gamma$) in either a standing or a running wave (a motionless atom is considered in the fluctuations analysis). The atom is embedded in a broad band squeezed light, so that all of the modes coupled to the atoms are squeezed. The bandwidth of the squeezing is broad enough to appear to the atom as a δ correlated squeezed white noise. The correlation functions for the multi-mode squeezed field can then be written as [7]:

$$<b\dagger(t)b(t')> = \Gamma N\delta(t-t')\ ,\qquad <b(t)b\dagger(t')> = \Gamma(N+1)\delta(t-t')\qquad \text{Eq.1}$$

$$<b(t)b(t')>=<b\dagger(t)b\dagger(t')>^* = \Gamma M e^{(-2i\omega_0 t + 2ik\cdot r)}\delta(t-t')$$

Where b,b† are the operators defined in terms of the positive and the negative frequency parts of this field, N and M are the squeezing parameters, N is proportional to the number of photons in the squeezed vacuum, while $M \leq N(N+1)$ signifies the amount of correlation between the sidebands and the equality maximum squeezing. In the following we will choose M to be real and positive .

The Hamiltonian describing the interaction of the atom with the quantized multimode radiation field and a classical coherent field is given in the electric-dipole and rotating-wave approximation by [10]:   Eq.2

$$H = \frac{1}{2}\hbar\omega_0\sigma_{22} + H_{rad} - \left(\mu E_0 e^{-i\omega t}\sigma^\dagger + \sigma\mu^* E_0^* e^{+i\omega t}\right) + \hbar\left(\sigma^\dagger b + b^\dagger\sigma\right)$$

where ω_0 is the atomic resonance frequency, σ_{22} , $\sigma=\sigma_{12}$ and $\sigma^\dagger=\sigma_{21}$ are the atomic operators , μ is the atomic dipole moment , H_0 is the free Hamiltonian of the field, and E_0 is the amplitude of the coherent field. One can then find the master equation for an atom in squeezed vacuum and derive equations of motion for the atomic operators whose expectation value is given by:

$$< \dot{\sigma}_{12} > = - \gamma< \sigma_{12} > - \Gamma M< \sigma_{12} >^* + \Omega< D > \qquad \text{eq.3}$$

$$< \dot{D} > = - \Gamma(2N +1)< D >+ \Gamma - 2[\Omega^*< \sigma_{12} >+\Omega<\sigma_{12} >^*]$$

The average force can now be found by calculating, the expectation value of the atomic variables and subsequently the first order corrections due to the atomic motion [3]. This gives rise to the following expressions[11] for the expectation value of the optical forces acting on the atom in the running<F> and standing wave<Fs> :

$$\langle F \rangle = \frac{\hbar k\Gamma P}{2(2N+1+P)}\left[1+\frac{2(2N+1)\Delta}{\chi(2N+1+P)}\ (\mathbf{k}\cdot\mathbf{v})\right]$$

Eq.4

$$\langle F^s \rangle = - \frac{\alpha\hbar\Lambda P}{\Phi_-(2N+1+P)}\left[1 - \frac{4\chi M\cos(2\phi)P + \Gamma_1^2\Phi_-(2N+1-P) - 2\chi P^2}{\Gamma\chi\Phi_-(2N+1+P)}(\alpha\cdot\mathbf{v})\right]$$

where P is the modified saturation parameter in squeezed vacuum given by $P= 2|\Omega|^2\Phi_-/\chi$, $\Omega=e^{i\phi}\mu E/\hbar$ and the other quantities are defined by: $\Gamma_1=(2N+1)\Gamma$, $\Phi_- = 2N+1 - 2M\cos(2\phi)$, $\chi = |\gamma|^2 - \Gamma^2 M^2$, $\gamma=\Gamma_1/2 - i\Delta$, $\Lambda = \Delta + \Gamma M\sin(2\phi)$, where Δ is the laser detuning from the atomic resonance.

It is instructive to examine the new expression of the force in the standing wave by comparing it to the force in ordinary vacuum. In this limit (N =M=0) the force is reduced to the well known expression of the force (ref.3 eq.18) given by:

$$\langle \vec{F} \rangle = -\alpha \hbar \Delta \, \frac{P}{1+P} \left[1 - \frac{\Gamma^2(1-P) - 2|\gamma|^2 P2}{\Gamma(1+P)2|\gamma|^2} \, \vec{\alpha} \cdot \vec{v} \right] \qquad \text{eq.5}$$

Note that in this limit the first term in the numerator of the velocity dependent part of eq.4 is zero while the other two terms are reduced to those of eq.5. The striking appearance of the additional term in squeezed vacuum is analogous to the result of ref.6. In this case, the introduction of classical phase noise results in the appearance of an extra term $-4|\gamma|2[\Gamma 2/\Gamma - 0.5]P$, $(\Gamma_2=\Gamma/2+\Gamma\phi$ where $\Gamma\phi$ is the rate of the phase interrupting events).This term can give the stimulated force at lower intensity when $\Gamma_2 / \Gamma > 0.5$ as phase noise is added.

Notice that in the case of $\Gamma_2 / \Gamma < 0.5$, this term can also be induced but with opposite sign. This is indeed the case with quadrature squeezing, which can result in either larger or smaller phase noise than the vacuum level.This in turn introduces two different decay rates for the two quadratures of the atomic dipole.One of these, $\Gamma_{2\,x}= \Gamma(N+M+0.5)$, is larger and the other, Γ_2 $_x=\Gamma(N - M+0.5)$, is smaller than the normal $\Gamma_2=\Gamma/2$ value. Therefore, the sign of the extra term in eq.2 $4[|\gamma|2-\Gamma^2 M^2]M \cos(2\phi) P$ can be controlled by the relative phase ϕ of the driving field with respect to the squeezed vacuum. Hence, the stimulated force can not only occur at lower laser intensity, it can change sign to provide an additional cooling force at red laser detuning from resonance.This modification of the force can be further correlated with the TWM lineshape which becomes strongly dependent on the laser phase ϕ and can even change sign as indicated by our intuitive analysis .

Other important modifications of the force in squeezed vacuum are described by the term, $\Delta+\Gamma M \sin 2\phi$. This term gives rise to *a force at zero detuning* as well as strong variations of the force at small detuning ($\Delta<\Gamma M \sin 2\phi$). These effects can be understood by noting that the dephasing induced lineshape of TWM at resonance is absorptive in normal vacuum, but it can be transformed to a dispersive lineshape in squeezed vacuum, giving rise to a force at resonance . In addition it has been shown that the TWM can have sub-natural linewidth at small detuning [7-10]. This indicates that one can obtain arbitrarily large cooling forces at small detuning as the number of photons in the squeezed vacuum N, and therefore the amount of squeezing , is increased. This can be understood by noting that $\Gamma_{2y}=\Gamma (N - M+0.5)$ in the limit of N>>1 becomes arbitrarily

small, $\Gamma_{2y} = \Gamma / 8N$.

In the analytic solution shown above the force is calculated only to first order in velocity (i.e a linear velocity dependence is assumed), this is correct only for small velocities $kv \ll \Gamma$. Numerical solution of the OBE, however, can provide the full velocity dependence of the force. This solution is shown in figure 2 for ordinary (trace A)and squeezed vacuum (trace B) . This figure demonstrates that the stimulated force which gives a heating force in normal vacuum for velocities in the order of $kv < \Gamma/2$ (as expected from the TWM lineshape, fig.1b), can be transformed to a cooling force in squeezed vacuum. The dashed lines in the figure are the results of the spatially averaged analytic solution which show good agreement with the numerical solution at small velocities.
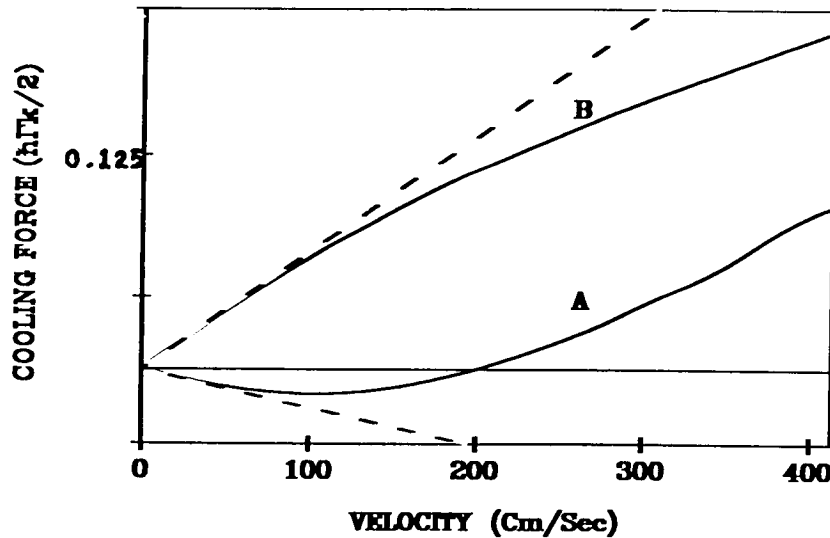
Figure 2: The velocity dependence of the spatially averaged force, in normal vacuum trace A and squeezed vacuum trace B, obtained by numerical solution of the OBE. The dashed lines are the result of the analytic solution. The parameters used for this figure are: $\Delta = -3\Gamma$, $\Omega = 1.36\Gamma$, $\Gamma = 10^7$ Hz and $\lambda = 5890$ A for both traces and N=1., M=$\sqrt{2}$ and $\phi = 0$ for trace B.

Figure 3 demonstrate the interesting dependence of the force on the driving laser phase ϕ (using the analytic solution eq.2 with $kv = \Gamma/2$).This is shown for a constant number of photons in the squeezed vacuum, N=1, but for various values of the squeezing parameter M. Trace A plots the force for thermal light M=0 (i.e no correlation between the sidebands) with no variation on the phase, as expected. Traces B-D , however, show large variations of the force for increasing degree of squeezing up to the maximum value of M, ($M^2 = N[N+1]$). This dependence is due to the different amount of noise that the induced dipole sees at different quadrature phase. Figure 3 also shows that even a modest amount of squeezing induce large effects on the force.

168
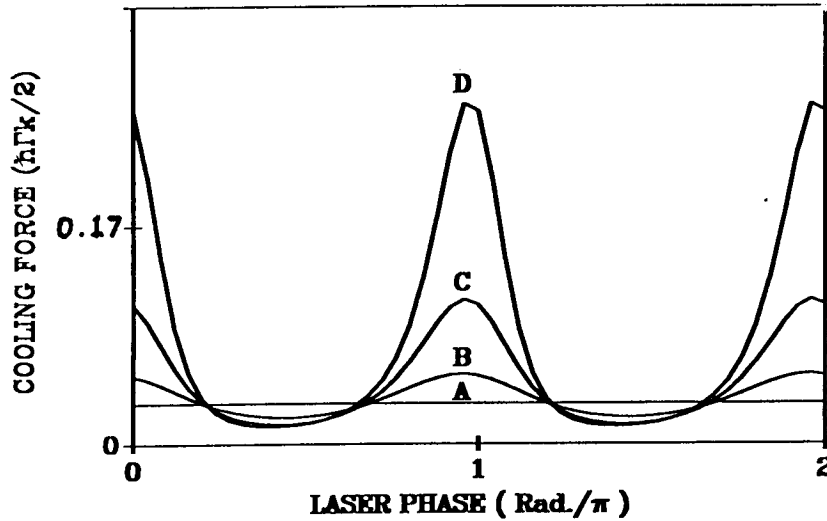
Figure 3: The spatially averaged force as a function of the laser phase ϕ for increasing amount of correlation between the sidebands A)M=0 (thermal light no correlation), B) M=0.5 , C)M=1 and D)M=$\sqrt{2}$ (maximum squeezing). Other common parameters used are: Δ=-3Γ, Ω=1. 5Γ and N=1.

THE QUANTUM FLUCTUATIONS

It was recognized by Einstein [12] as early as 1917 that the fluctuations of the optical force, originating from both spontaneous and induced absorption and emission processes, are important in determining the Maxwellian distribution of the atomic velocity in thermal equilibrium. A simple momentum diffusion process which comes readily to mind is due to the random direction of the spontaneous emission recoils . In addition to this geometrical source of fluctuations one should also consider the fluctuations in the number of photons emitted in a unit time . However, this process can have sub Poisson statistics, as shown by Mandel [13] in resonance fluorescence, and give rise to an anomalous contribution [3,14] which can decrease the momentum spread, as discussed by Cook [14]. An additional momentum diffusion mechanism becomes dominant at high intensities in a standing wave due to fluctuations in the stimulated emission process between the counter-propagating waves [3,14,5]. This photon exchange between the waves, results in a random transfer of $2\hbar k$ units of momentum to the atom. Finally as shown by Gordon and Ashkin [3] an atom even in its ground state can have random recoils due to the zero point vacuum fluctuations.

In the following it will be shown that the dynamics in squeezed vacuum modifies the fluctuations of all of these processes.

We are now interested in finding the force fluctuations on a *stationary* atom which are given by the diffusion constant , 2Dp :

$$2D_p = 2\,\text{Re}\int_0^\infty dt\;[<\vec{F}(0)\,\vec{F}(t)> - <\vec{F}>^2\,]$$

Insertion of $\vec{F}(t) = -\iota\sigma\vec{\nabla}G$ + H.c. for the force (where G is the freely propagating field), using the correlation functions for squeezed vacuum,$<G>=\Omega$ (since$<b>=0$) and the commutation relation $\sigma_{ij}\,\sigma_{kl}=\sigma_{il}\,\delta(j,k)$ for the atomic operators gives :

$$\langle\vec{F}(0)\vec{F}(t)\rangle = \hbar^2\Big[\langle\sigma^\dagger(0)\sigma(t) + \sigma(0)\sigma^\dagger(t)\rangle\,|(\vec{\nabla}\Omega)^2| - \langle\sigma^\dagger(0)\sigma^\dagger(t)\rangle(\vec{\nabla}\Omega)^2 - \langle\sigma(0)\sigma(t)\rangle(\vec{\nabla}\Omega^*)^2\Big]$$

$$+(\hbar k)^2\Big[\,\Gamma N\,\langle\sigma_{11} + \sigma_{22}\rangle + \Gamma\langle\sigma_{22}\rangle\Big]\,\delta(t)$$

Consider first the last terms which depend directly on the quantum fluctuations of the field. These terms in the limit of normal vacuum($N=0$) can be transparently modeled [3] as the random instantaneous emissions of momenta $\hbar k$ at an average rate of $\Gamma<\sigma_{22}>$. In the squeezed vacuum case, this effect is enhanced, by the absorption of squeezed photons $\Gamma N<\sigma_{11}>$ and spontaneous emission $\Gamma N<\sigma_{22}>$ due to the larger number of photons in the squeezed vacuum .

In order to evaluate the remaining terms , which describe the effects of the interaction of the coherent field gradient with the atomic dipole fluctuations,we need to find the integral of the atomic dipole autocorrelation functions which after some algebra leads to the following expression for the diffusion in squeezed vacuum:

$$2D_p = D_0 + \hbar^2\beta^2\frac{\Gamma_1}{2}\frac{P}{(2N+1+P)}[1 + D_1] + \hbar^2\alpha^2\Gamma_1\frac{\Phi_+}{2\Phi_-}\frac{P}{(2N+1+P)}\Big[1 + D_1^s + D_2^s + D_3^s\Big]$$

Where $\alpha=0$, $\beta=k$ in a running wave; and $\alpha=-k\tan(k\,x)$, $\beta=0$ in a standing wave while the other terms are defined by : $\Phi_+ = 2N+1 + 2M\cos(2\phi)$,

$$D_0 = \hbar^2 k^2\frac{\Gamma}{2}\Big[\frac{2N+P}{(2N+1+P)} + 2N\Big] \qquad D_1 = \frac{P}{(2N+1+P)^2}\Big[\frac{\Phi_+}{(2N+1)\Phi_-} - \frac{\Gamma_1\Gamma}{\chi}\Big]$$

and the standing wave terms;

$$D_1^s = \frac{4P}{(2N+1+P)^2 \Phi_- \Phi_+} \left[\frac{(2N+1)\chi}{\Gamma^2} - \frac{\Lambda^2}{\Gamma\Gamma_1}(1+\frac{\Gamma_1^2}{\chi}) \right] \qquad , \qquad D_2^s = \frac{8P^2}{(2N+1+P)^2 \Phi_- \Phi_+} \left[\frac{\chi}{\Gamma^2} - \frac{\Lambda^2}{\Gamma\Gamma_1\Phi_-} \right]$$

$$D_3^s = \frac{4\chi}{\Gamma\Gamma_1 \Phi_- \Phi_+} \frac{P^3}{(2N+1+P)^2} .$$

In the limit of normal vacuum ($N=M=0$) Eq.8 corresponds to the the results of ref.3 eq. 30

$$2D_p = \hbar^2\beta^2\Gamma\frac{P}{2(1+P)}\left[1+\frac{P}{(1+P)^2}\left(1-\frac{\Gamma^2}{|\hbar|^2}\right) \right] + \hbar^2\alpha^2\Gamma\frac{P}{2(1+P)}\left[1+\frac{P}{(1+P)^2}\left(\frac{\Gamma^2}{|\hbar|^2}-3\right) + \frac{2P^2}{(1+P)^2} + \frac{4|\hbar|^2}{\Gamma^2}\frac{P^3}{(1+P)^2} \right]$$

$$+ \hbar^2 k^2 \Gamma \frac{P}{2(1+P)}$$

Let us first examine the terms in the running wave case by associating them with the normal vacuum limit. As we discussed previously spontaneous emission in squeezed vacuum, represented by the diffusion term D_0, gives rise to increased fluctuations as a consequence of the increased number of photons in this state. However, as can be clearly seen, the D_1 induced absorption contribution, even in the normal vacuum limit, can reduce the spread. This term has been shown to originate from sub Poisson statistics of the emitted photons. In fact in the normal vacuum limit D_1 coincides exactly with Mandel's Q parameter [13,14] :

$$Q = \frac{\langle(\Delta n)^2\rangle - \langle n\rangle}{\langle n\rangle}$$

$Q=0$ indicates a variance of $<n>^{1/2}$ in the number of the emitted photons(i.e no correlation between the photons) and negative Q sub-Poisson statistics. Figure 4 plots D_1 as a function of the laser detuning. In squeezed vacuum , with an appropriate phase between the laser and the squeezed vacuum, D_1 can reach a value of -1, whereas in normal vacuum the maximum effect gives $D_1 = -3/4$. This indicates that in squeezed vacuum the photons can be emitted in an orderly manner,thus eliminating this source of fluctuations. Unfortunately, in the traveling wave case, one can not take advantage of this phenomenon due to the increased spontaneous emission term D_0. This is demonstrated in figure 5a, which shows that the equilibrium temperature, given by $KbT = Dp/(-\partial v <F>)$, increases with the amount of squeezing.

We now turn our attention to the more complicated case of the standing wave, as in the

171

running wave case, we still have enhanced fluctuations due to the larger spontaneous emission term, D_0. However, the much larger average cooling force, in conjunction with the smaller fluctuations, of the higher order terms, make it possible to reach temperatures lower than otherwise obtained in normal vacuum. Unfortunately, one can not take full advantage of both of these effects
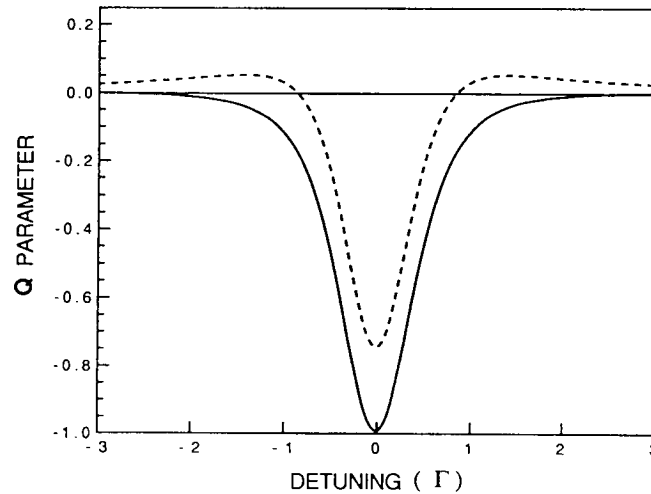
Figure 4: The deviation from Poisson statistics as a function of the laser detuning from resonance.The dashed line shows the maximum effect in normal vacuum , while the solid line indicates that almost no spread in the number of photons emitted in a unit time in squeezed vacuum can be achieved. The parameters used are $\Omega = 0.35\Gamma$ in the normal vacuum while $\Omega = 0.26\Gamma$, $N=2$, $M^2 = N(N+1)$ and $\phi = 0.5\ \pi$ in the squeezed vacuum.
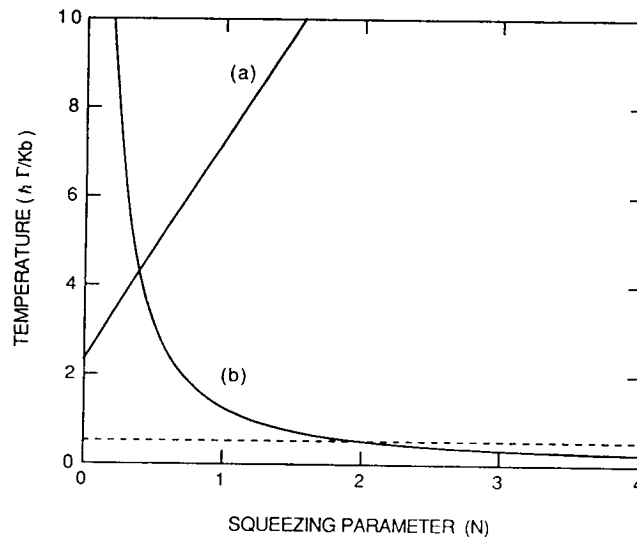
Figure 5: The equilibrium temperature as a function of the squeezing parameter N in: a) running coherent laser cooling wave with $\Delta = 0.5\Gamma$, $\Omega = \Gamma$, $\phi = 0.25\ \pi$. b) a standing wave with $\Delta = 0$, $\Omega = 5\Gamma$, $\phi = 0.6\ \pi$ .The dashed line is the Doppler limit temperature in normal vacuum.

at the same laser phase. Nevertheless, one can choose a particular phase which will minimize the temperature as the squeezing increases. Figure 5b demonstrates the lowering of the equilibrium temperature below the normal vacuum level (N=0) as the amount of squeezing increases.

Moreover, the temperature can be decreased to values slightly below the Doppler limit (which in normal vacuum is achieved at low intensity). Lowering the equilibrium temperature is not the only benefit of squeezing, in the above example, the average force becomes larger than the maximum value in the normal vacuum giving rise to a shorter equilibrium time. Notice, however, that high degree of squeezing is needed in order to reach sub-Doppler temperature, in addition , degradation from ideal squeezing ($M^2 < N(N+1)$) results in a temperatures higher than the Doppler limit. This unfortunately makes the experimental demonstration of this effect rather difficult.

A few words are now in order to get some insight into the modification of the fluctuations in the standing wave case. We first discuss the various terms in the *normal vacuum* case. The most notable difference from the running wave is the appearance of higher order terms in P. These terms were interpreted as resulting from the fluctuations of the dipole force [3,5, 14] and become important at high laser intensity. In particular the P^3 term is the only term that does not saturate at high P. Hence, although one can use the stimulated force in normal vacuum at the blue side of resonance to give a very large average cooling force(with the advantage of very short equilibrium time) the large fluctuations make the equilibrium temperature much higher than the Doppler limit [5].

With regard to the modification of these processes in squeeze vacuum, we begin by comparing the $D_1{}^S$ term to its counterpart in normal vacuum. As discussed in the running wave case, this term can be interpreted as the deviation of the fluctuations from Poisson statistics. We found that the modified $D_1{}^S$ in squeezed vacuum can reach values close to -1. However, the behavior in a standing wave is quite different from the running wave, as is the case in the normal vacuum .

The next term, $D_2{}^S$, is not present in a running wave and we assume that it describes the fluctuations of the lower order stimulated force. In a previous publication [6], it was shown that while the velocity dependent stimulated force does not usually occur at low intensity, the inclusion of phase interrupting events (which increase the dipole decay rate), gives rise to a stimulated force term at lower order in laser intensity. In order to show that this identification is correct and to get some insight into this term $D_2{}^S$ was calculated in normal vacuum but with increased dipole decay $\Gamma_2 = \Gamma/2 + \Gamma_\phi$, where Γ_ϕ is the rate of phase interrupting events, which gives:

$$D_2^S = \frac{2P'^2}{(1+P')^2}\left[\left(\frac{2\Gamma_2}{\Gamma} -1\right)\left(\frac{\Delta}{\Gamma_2}\right)^2 + 2\frac{\Gamma_2}{\Gamma}\right]$$

As can be seen an additional diffusion occurs as phase noise is added , $\Gamma_2 > \Gamma/2$. Note, that when $\Gamma_2 < \Gamma/2$, this term becomes negative. Analogously, $D_2{}^S$ in squeezed vacuum may be associated with the fluctuations of the extra stimulated force in squeezed vacuum (the first term in

the average force in squeezed vacuum , $<F^S>$. Moreover, the fact that one of the dipole's quadrature components can decay at a rate smaller than $\Gamma/2$ suggests that $D_2{}^S$ in squeezed vacuum can become negative, as indeed is the case.

Finally we turn our attention to the highest order term in P , $D_3{}^s$, which is associated with the fluctuations of the normal stimulated force.The modification of this diffusion term is critical for achieving lower temperature at high laser intensity where the stimulated force becomes dominant. Figure 6 shows the spatially averaged total diffusion constant 2Dp, in a high intensity standing wave, as a function of the laser phase, in normal and squeezed vacuum.This comparison demonstrates the dramatically reduced fluctuations in a high intensity standing wave under squeezed vacuum conditions.
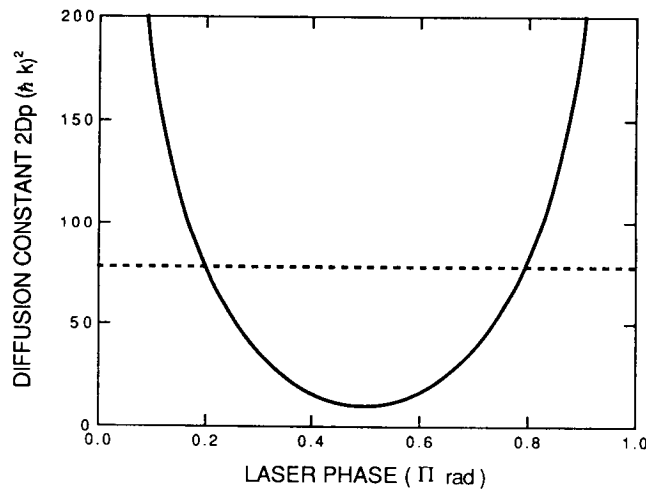
Figure 6: The diffusion constant in a high intensity standing wave as a function of the laser phase in the case of normal vacuum (dashed line) and squeezed vacuum(solid line) .The parameters used are: $\Delta=0$, $\Omega=5\Gamma$, N=5.

As to the experimental verification of these interesting phenomena. Although 90% squeezing has already been achieved in the laboratory, it is important to note, that the calculation presented here is carried out with the assumption that the atom is embedded in squeezed vacuum. In practice, the output of present sources of squeezed light (degenerate parametric oscillators) can couple only to part of the 4π steradians enveloping the atom. A possible solution to this problem has been proposed by Gardiner who suggested coupling the squeezed modes to the atom in a micro cavity. The other important assumption here is that the spectrum of the squeezing is much broader than that of the atomic transition . Theories which include finite bandwidth of squeezing[15] have shown that the essential features due to squeezing are preserved, even for a bandwidth of squeezing only a few times larger than the width of the atomic transition. It should also be noted that it will be interesting to develop the theory with bandwidth of squeezing larger than Γ but smaller than the Mollow sidebands separation . This can introduce the possibility of controlling all three of the

decay rates of the atom and therefore might reduce the problem the diffusion due to of the higher rate of spontaneous emission in a broad band squeezed light [16].

In conclusion, this paper demonstrates a dramatic modification of the quantum fluctuations of the mechanical effects of light on atoms which are also embedded in squeezed vacuum. In the running wave case the temperature can not be lowered below the normal vacuum level. However, in conjunction with the modified average cooling force even sub-Doppler temperatures may be reached, under ideal conditions, for atoms cooled in a standing wave. These interesting results, in addition for being of potential use, offer some insight into the quantum statistics of the photon exchanges between the atom and the field under squeezed vacuum conditions. Further investigation of other schemes of cooling with squeezed light might also be beneficial

REFERENCES:

1) For recent advances in this field see JOSA B November (1989) .

2) T. W. Hansch and A. L. Schawlow, Opt. Commun. 13, 68 (1975).

3) J. P. Gordon and A. Ashkin , Phys. Rev. A21 ,1606 (1980).

4) A. Aspect et al, Phys. Rev. Lett., 57, 1688 (1986).

5) J. Dalibard and C. Cohen-Tannoudji, JOSA B , 2, 1707, (1985)

6) Y. Shevy, Phys. Rev. A 41, 5229, (1990).

7) C. W. Gardiner, Phys. Rev. Lett., 56, 1917, (1986).

8) H. Ritsch and P. Zoller , Opt. Commun. 64, 523 (1987).

9) S. An and M. Sargent III, Phys. Rev. A39 , 3998 (1989).

10) H. J. Carmichael, et al, Phys. Rev. Lett., 58, 2539, (1987).

11) Y. Shevy, Phys. Rev. Lett., 64, 2905 (1990).

12) A. Einstein, Phys. Z.18, 121, (1917).

13) L. Mandel, Optics Lett., 4, 205, (1979).

14) R. J. Cook, Phys. Rev. A 22,1078, (1980); Optics Commun., 35, 347, (1980), S. Stenholm, Phys. Rev. A 27, 2513, (1983).

15) A. S. Parkins and C. W. Gardiner, Phys Rev. A37 , 3867 (1988); H. Ritsche and P.Zoller Phys. Rev. Lett. 61,1098, (1988).

16)A. S. Parkins, Phys. Rev. A 42, 4352, (1990).

17) The magnitude of the force is different from Ref. 11 due to an error by a factor of 5.89

On the Measurement of Time for the Quantum Harmonic Oscillator

Scott R. Shepard
Massachusetts Institute of Technology
Cambridge, MA

Abstract

A generalization of previous treatments of quantum phase[1] is presented. Restrictions on the class of realizable phase statistics are thereby removed, thus permitting "phase wavefunction collapse" (and other advantages). This is accomplished by exciting the auxilary mode of the measurement apparatus in a time-reversed fashion. The mathematical properties of this auxilary mode are studied in the hope that they will lead to an identification of a physical apparatus which can realize the quantum phase measurement.

1. The SG phase statistics

A satisfactory description of the phase of the quantum harmonic oscillator has recently been achieved by considering the realizable measurement[1] of the non-Hermitian Susskind-Glogower (SG) phase operator[2]

$$\widehat{e^{i\phi}} \equiv (\hat{n} + 1)^{-1/2}\hat{a}. \qquad (1)$$

Although it is not Hermitian, the SG operator *does* correspond to a realizable quantum measurement. It's measurement statistics, however, *can not* be calculated from the familiar Hermitian operator rules (e.g. moments calculated via $\langle\psi|(\widehat{e^{i\phi}})^k|\psi\rangle, k = 1, 2, \ldots$ do **not** correspond to the SG operator's realizable measurement statistics). We have demonstrated a variety of ways in which the measurement statistics of the SG operator can be accessed [1],[3]. Perhaps the simplest of these is to form the phase wavefunction

$$\psi(\phi) \equiv \langle\phi|\psi\rangle, \qquad (2)$$

from which the phase probability distribution, $p(\phi) = |\psi(\phi)|^2/2\pi$, and it's associated moments follow directly. This procedure is justified formally by the fact that the infinite energy eigenkets of the SG operator

$$|\phi\rangle \equiv \sum_{n=0}^{\infty} e^{in\phi}|n\rangle \qquad (3)$$

resolve the identity, i.e. $1 = \int_{-\pi}^{\pi} \frac{d\phi}{2\pi}|\phi\rangle\langle\phi|$. This permits the extremely useful phase representation of an arbitrary quantum state:

$$|\psi\rangle = \int_{-\pi}^{\pi} \frac{d\phi}{2\pi}\langle\phi|\psi\rangle|\phi\rangle, \qquad (4)$$

analogous to the familiar number representation of a state:

$$|\psi\rangle = \sum_{n=0}^{\infty} \langle n|\psi\rangle|n\rangle. \qquad (5)$$

The number-ket expansion coefficients, $\psi_n \equiv \langle n|\psi\rangle$, may be viewed as a wavefunction in discrete n-space. The Fourier transform relationship of the number and phase wavefunctions

$$\psi(\phi) = \sum_{n=0}^{\infty} \psi_n e^{-in\phi} \qquad (6)$$

$$\psi_n = \int_{-\pi}^{\pi} \frac{d\phi}{2\pi}\psi(\phi)e^{in\phi} \qquad (7)$$

demonstrates the complementarity of photon number and quantum phase.

Position and momentum are familiar examples of complementary quantities, whose wavefunction representations, $\psi(x) \equiv \langle x|\psi\rangle$ and $\Phi(p) \equiv \langle p|\psi\rangle$, are also related via Fourier transform. Indeed, several relations among ψ_n and $\psi(\phi)$ are reminiscent of those encountered in Schrodinger's wave mechanics. Analogous to the position representation of the momentum operator, $\hat{p} \rightarrow -i\hbar\frac{d}{dx}$, for example, we have a phase representation of the number operator, $\hat{n} \rightarrow i\frac{d}{d\phi}$, viz:

$$\langle\psi|(\hat{n})^k|\psi\rangle = \qquad (8)$$

$$\int_{-\pi}^{\pi} \frac{d\phi}{2\pi}\psi^*(\phi)(i\frac{d}{d\phi})^k\psi(\phi) \qquad (9)$$

177

(where $k = 0, 1, 2...$). These relations yield the correct form of the number/phase uncertainty principle[3]:

$$(\Delta n^2)(\Delta \phi^2) \geq \frac{1}{4}(1 - 2\pi p(\pi))^2. \quad (10)$$

Since we are dealing with a single harmonic oscillator (of frequency ω), phase is related to time ($\phi = \omega t$) in a mod-2π sense, and number is directly related to energy ($\hat{n} = \hat{H}/\hbar\omega - 1/2$). In this sense, the above constitutes a rigorous energy/time uncertainty principle for the quantum harmonic oscillator.

The class of realizable SG phase statistics, however, is restricted (by a Paley-Wiener theorem) due to the fact that $\psi(\phi)$ is a one-sided Fourier series, i.e. this restriction stems from the absence of "negative number states" ($\psi_n = 0 \; \forall n < 0$). One aspect of this restriction is that $\psi(\phi)$ is prohibited from identicaly vanishing over a non-zero interval — thus, delta-functions in phase are not allowed. In as much as we may desire a "wavefunction collapse" view of a phase measurement, the SG statistics appear to be incomplete. This dilema, however, can be resolved by generalizing an alternate route (the product space formalism) to the SG statistics.

Fundamental to the realizable measurement of any non-Hermitian operator is the existance of an auxilary noise source. Zero-point fluctuations from this auxilary mode prevent a simultaneous, perfectly precise, measurement of the non-commuting real and imaginary parts of the non-Hermitian operator (so that the uncertainty principle is not violated). We can study the interaction of our original system of interest (Hilbert space $\mathcal{H}_s$) with this auxilary system (Hilbert space $\mathcal{H}_a$) by working in the product space $\mathcal{H} = \mathcal{H}_s \otimes \mathcal{H}_a$. The *extension* of the SG operator onto $\mathcal{H}$ is [3]

$$\hat{\Gamma} \equiv (\widehat{e^{i\phi}})_s \otimes \hat{V}_a + \hat{V}_s \otimes (\widehat{e^{i\phi}})_a^\dagger, \quad (11)$$

where $\hat{V} \equiv |0\rangle\langle 0|$. This extension has eigenkets (of non-zero eigenvalue), $\hat{\Gamma}|\phi\rangle' = e^{i\phi}|\phi\rangle'$, given by

$$|\phi\rangle' = |0\rangle_s|0\rangle_a + \sum_{n_s=1}^{\infty} e^{in_s\phi}|n_s\rangle|0\rangle_a \quad (12)$$

$$+ \sum_{n_a=1}^{\infty} e^{-in_a\phi}|0\rangle_s|n_a\rangle_a. \quad (13)$$

These reside on a subset, $\mathcal{H}'$, of $\mathcal{H}$ which is defined by the property $n_s n_a = 0$. When the auxilary mode is in the vacuum state ($n_a = 0$), the $\hat{\Gamma}$ measurement yields the SG statistics and their attendant Paley-Wiener restriction.

2. Beyond the SG statistics

We can go *beyond* the SG statistics by exciting the auxilary mode to create an arbitrary state on $\mathcal{H}'$:

$$|\psi\rangle' \equiv \sum_{n_s=0}^{\infty} \psi_{n_s,0}|n_s\rangle_s|0\rangle_a \quad (14)$$

$$+ \sum_{n_a=1}^{\infty} \psi_{0,n_a}|0\rangle_s|n_a\rangle_a. \quad (15)$$

For simplicity, let $N \equiv n_s - n_a$, $\psi_N \equiv \psi_{N,0} (\forall N \geq 0)$, and $\psi_N \equiv \psi_{0,-N} (\forall N < 0)$. The *generalized phase wavefunction*,

$$\psi'(\phi) \equiv {}'\langle\phi|\psi\rangle' = \sum_{N=-\infty}^{\infty} \psi_N e^{-iN\phi}, \quad (16)$$

is a two-sided Fourier series. The the Paley-Wiener restriction is removed and $\psi'(\phi)$ can "collapse" to a delta-function. The fact that the class of $\psi'(\phi)$ is more general than (and includes) the class of $\psi(\phi)$ should prove useful for various optimizations. Indeed, Shapiro[4] has pointed out that error-free communication could *in principle* be achieved by exploiting the newly aquired generality described herein.

Provided that niether of our two modes is purely in the vacuum state, the excitation which creates a state on $\mathcal{H}'$ is not arbitrary in that the $n_s n_a = 0$ property creates an entanglement. Thus, in general, the original system and auxilary modes are not statistically independent on $\mathcal{H}'$, i.e. $|\psi\rangle' \neq |\psi_s\rangle_s|\psi_a\rangle_a$. Denoting the probability that a measurement of $\hat{n}_s$ yields the outcome n by $|\psi_n^s|^2$, we see that $|\psi_n^s|^2 = |\psi_{n,0}|^2 (\forall n \geq 1)$, whereas $|\psi_0^s|^2 = |\psi_{0,0}|^2 + \sum_{n=1}^{\infty} |\psi_{0,n}|^2$ (similarly for

C-3

$|\psi_n^a|^2$). In spite of the lack of statistical independence, we can therefore assign any individual probability distributions for n_s and n_a that we wish, *provided* that

$$|\psi_{0,0}|^2 = (|\psi_0^s|^2 + |\psi_0^a|^2 - 1) \geq 0 \quad (17)$$

is satisfied.

The auxilary mode can be interpreted as a time-reversed mode in the following sense. Consider the case of the auxilary mode being in the vacuum state ($n_a = 0$). Denote the initial state by $|\psi_0\rangle'$. The state (in the Schrodinger picture) after time evolution of an amount τ is

$$|\psi_\tau\rangle' = e^{-i\hat{n}_s\omega\tau}|\psi_0\rangle', \quad (18)$$

so that the relation of the phase representations of the initial and delayed states is simply

$$\psi_\tau'(\phi) = \psi_0'(\phi + \omega\tau) \quad (n_a = 0). \quad (19)$$

Now consider the case of the original system being in the vacuum state ($n_s = 0$). The Schrodinger picture of the delayed version of an initial state $|\psi_0\rangle'$ is

$$|\psi_\tau\rangle' = e^{-i\hat{n}_a\omega\tau}|\psi_0\rangle'. \quad (20)$$

The initial and delayed phase representations for this case are related by

$$\psi_\tau'(\phi) = \psi_0'(\phi - \omega\tau) \quad (n_s = 0). \quad (21)$$

Thus the two modes are time-reversed in that, under time evolution, the $n_a \geq 1$ portion of the generalized phase wavefunction "moves backwards" with respect to the $n_s \geq 1$ portion.

Consistent with the time-reversal property, the auxilary mode serves the topological role of a "negative energy" mode in Hilbert space. The SG operator is a pure lowering operator which **stops** at the vacuum:

$$\widehat{e^{i\phi}}|n\rangle = |n-1\rangle \quad (n \geq 1) \quad (22)$$

$$\widehat{e^{i\phi}}|0\rangle = 0. \quad (23)$$

It cannot lower below the vacuum since we have not allowed negative number (negative energy) states for the quantum harmonic oscillator. It's extension, $\hat{Y}$, however, lowers the original system mode number

$$\hat{Y}|n_s\rangle_s|0\rangle_a = |n_s-1\rangle_s|0\rangle_a \quad (n_s \geq 1), \quad (24)$$

then **continues** through the vacuum

$$\hat{Y}|0\rangle_s|0\rangle_a = |0\rangle_s|1\rangle_a, \quad (25)$$

and raises the auxilary mode number

$$\hat{Y}|0\rangle_s|n_a\rangle_a = |0\rangle_s|n_a + 1\rangle_a. \quad (26)$$

Topologicaly, it is as if $\hat{Y}$ continues to lower below the vacuum into the auxilary ("negative energy") mode. The visualization of this behavioral aspect can be facilitated by simply relabeling the $\mathcal{H}'$ number states according to the value of $N \equiv n_s - n_a$.

The auxilary mode has to be an irrevocable part of the physical apparatus which realizes the quantum phase measurement (so that the uncertainty principle is satisfied and so that the phase wavefunction can collapse). All of the aforementioned mathematical properties must be physicaly realized in the measurement apparatus. These restrictions should prove useful in determining an apparatus which will realize the quantum phase measurement.

3. REFERENCES

1 S. R. Shepard and J. H. Shapiro, OSA'88 Tech. Digest (Opt. Soc. Am., Washington D.C.,1988); see also: J. H. Shapiro, S. R. Shepard, and N. C. Wong, Phys. Rev. Lett. **62**,2377 (1989).

2 L. Susskind and J. Glogower, Physics **1**, 49 (1964).

3 J. H. Shapiro, S. R. Shepard, and N. C. Wong, in *Coherence and Quantum Optics VI*, L. Mandel, E. Wolf, and J. H. Eberly, ed.s (Plenum, NY, 1990); see also: J. H. Shapiro and S. R. Shepard, Phys. Rev. A **43**, (1991).

4 J. H. Shapiro, "Going Through a Quantum Phase", Squeezed States and Uncertainty Relations Workshop, NASA CP- , 1991. (Paper of this compilation).

THE ORIGIN OF NON-CLASSICAL EFFECTS IN A ONE-DIMENSIONAL SUPERPOSITION OF COHERENT STATES

628162

14 ρ_{s}

V. Bužek, P. L. Knight and A. Vidiella Barranco

Optics section, The Blackett Laboratory

Imperial College, London SW7 2BZ, England

Abstract

We investigate the nature of the quantum fluctuations in a light field created by the superposition of coherent fields. We give a physical explanation (in terms of Wigner functions and phase-space interference) why the one-dimensional superposition of coherent states in the direction of the x-quadrature leads to the squeezing of fluctuations in the y-direction, and show that such a superposition can generate the squeezed vacuum and squeezed coherent states.

1 Introduction

The coherent states are always associated with the "most" classical states one can imagine in the framework of quantum theory [1]. In the present Lecture we will study the quantum interference between coherent states and how such interference leads to generation of states whose properties are as far as one can imagine from "classical" states. In particular a one-dimensional superposition of coherent states can exhibit sub-Poissonian photon statistics or squeezing. In our Lecture we will concentrate mainly on squeezing which appears as a consequence of quantum interference between coherent states.

Light squeezing (for recent reviews see [2] as well as topical issues of *JOSA B* [3] and *J. Mod. Opt.* [4]) remains a central topic in quantum optics. Generation of squeezed light has been reported by various groups [5-11] and offers new opportunities for the utilization of light with reduced quadrature noise in interferometry, fiber optics communications and high-precision experiments. Most studies of squeezed states have concentrated on those states generated by quadratic field interaction (e.g. parametric amplification). Recently it has been shown by Wódkiewicz and coworkers [12] that a superposition of two number states (for instance, the vacuum state and the one- or two-photon states) of a single mode electromagnetic field exhibits interesting non-classical properties. In particular, squeezing of the variances of the quadrature operators can be seen (although not necessarily of the quadratic, minimum uncertainty state quality). A superposition of a

finite number of coherent states has also been studied [13-17]. In particular, Hillery [13] has studied the superposition of two coherent states $|\alpha\rangle + |-\alpha\rangle$ (the so-called "even coherent state" [14]) in connection with amplitude-squared squeezing. Yurke and Stoler [15] have shown that such a superposition of coherent states can arise as a consequence of propagation of coherent light through an amplitude-dispersive medium. It has been shown that the even coherent states exhibit ordinary (second order) squeezing as well as fourth order squeezing [16]. In a recent paper, Janszky and Vinogradov [17] extended the idea of superposition of coherent states and investigated the quadrature variances of a continuous one-dimensional superposition of coherent states. They have shown that such a superposition of coherent states can lead to significant reduction of fluctuations in one of the quadratures.

At first sight, the result of Janszky and Vinogradov seems quite remarkable, when reinterpreted in terms of interference in phase space: a superposition of coherent states in the direction of the x-quadrature leads to a suppression in the fluctuations in the y-direction, whereas naively one would expect that the quantum interference relevant to this superposition would modify the fluctuations in the original x-direction.

In the present Lecture we give a physical explanation (in terms of the Wigner function and a phase-space formalism [18-20]) of the origin of this noise suppression and squeezing for a one-dimensional superposition of coherent states. We further demonstrate that a suitable Gaussian superposition of coherent states not only can be squeezed, but is actually a representation of the minimum-uncertainty squeezed vacuum state.

2   Simple example

We start our Lecture with a simple example considering a superposition of two coherent states $|\alpha_1\rangle$ and $|\alpha_2\rangle$

$$|\Psi\rangle = A^{1/2}\{|\alpha_1\rangle + |\alpha_2\rangle\}, \qquad (1)$$

where A is a normalization constant

$$A^{-1} = 2(1 + \mathrm{Re}\langle\alpha_1|\alpha_2\rangle).$$

The coherent state $|\alpha\rangle$ can be obtained by shifting the vacuum state $|0\rangle$ by the displacement operator $\hat{D}(\alpha) = \exp(\alpha\hat{a}^\dagger - \alpha^*\hat{a})$:

$$|\alpha\rangle = \hat{D}(\alpha)|0\rangle,$$

where $\hat{a}^\dagger$ ($\hat{a}$) is the creation (annihilation) operator of a photon.

The density matrix corresponding to the superposition of coherent states (1) is given by the following expression

$$\hat{\rho} = A(|\alpha_1\rangle\langle\alpha_1| + |\alpha_2\rangle\langle\alpha_2| + |\alpha_1\rangle\langle\alpha_2| + |\alpha_2\rangle\langle\alpha_1|), \quad (2)$$

while the density matrix describing statistical mixture of two coherent states $|\alpha_1\rangle$ and $|\alpha_2\rangle$ is

$$\hat{\rho}_M = p_1|\alpha_1\rangle\langle\alpha_1| + p_2|\alpha_2\rangle\langle\alpha_2| \qquad (3)$$

where p_i is the probability to find the system in the state $|\alpha_i\rangle$. These probabilities are normalized to 1.

2.1   Wigner functions

Now we introduce the notion of the Wigner function through the characteristic function $C^{(W)}(\xi)$, which is

associated with the symmetrical order of the bosonic (photon) operators and is given by the relation [21]

$$C^{(W)}(\xi) = \text{Tr}\left[\hat{\rho}\exp(i\xi\hat{a}^\dagger + i\xi^*\hat{a})\right]. \qquad (4)$$

The Wigner function is defined as the Fourier transform of the characteristic function $C^{(W)}(\xi)$:

$$W(\beta) = \pi^{-2}\int d^2\xi \exp[-i(\xi\beta^* + \xi^*\beta)]C^{(W)}(\xi). \quad (5)$$

The Wigner function corresponding to the superposition of two coherent states (1) can be written in the form

$$W(\beta) = A\,(W_1 + W_2 + W_{12}) \qquad (6.a)$$

where

$$W_i = \frac{2}{\pi}\exp(-2|\alpha_i - \beta|^2); \qquad (6.b)$$

and

$$\begin{aligned} W_{12} = \frac{2}{\pi}\exp&\left[-\frac{1}{2}\left(|\alpha_1|^2 + |\alpha_2|^2\right)\right] \\ \times\,\{\exp&\left[\alpha_2\alpha_1^* - 2(\beta - \alpha_2)(\beta^* - \alpha_1^*)\right] \qquad (6.c) \\ +\,\exp&\left[\alpha_1\alpha_2^* - 2(\beta - \alpha_1)(\beta^* - \alpha_2^*)\right]\} \end{aligned}$$

The terms W_i are the Wigner functions corresponding to the coherent states $|\alpha_i\rangle$, while the term W_{12} arises due to the quantum interference between coherent states under consideration.

The Wigner function for the statistical mixture (3) is given by the relation

$$W_M = p_1 W_1 + p_2 W_2 \qquad (7)$$

and it does not contain the term describing the quantum interfence between coherent states.

2.2 Even coherent states

To simplify our task we will suppose that $\alpha_1 = -\alpha_2 = \alpha$, where α is a real parameter. In this case we obtain
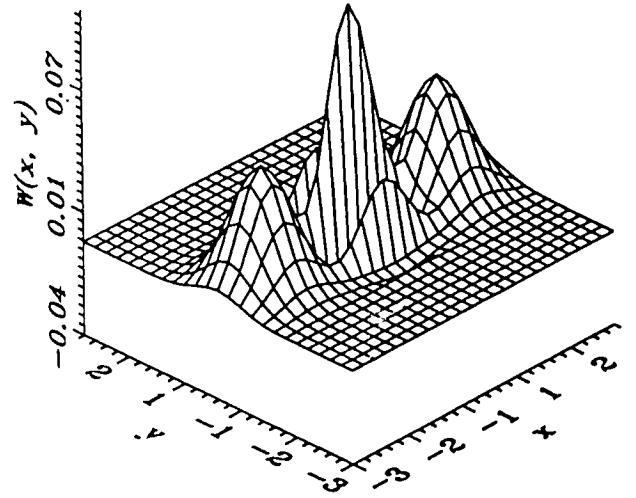
Figure 1: Wigner function corresponding to the even coherent state (8) with $\alpha = 2$. The rôle of the interference term is transparent.

from (1) the following state

$$|\Psi\rangle = A^{1/2}\left\{|\alpha\rangle + |-\alpha\rangle\right\}, \qquad (8)$$

with the normalization constant

$$A^{-1} = 2[1 + \exp(-2\alpha^2)].$$

The state (8) is called [13,14] the even coherent state. The Wigner function corresponding to this state can be found using the general expression (6) and is presented in Figure 1, where $x = \text{Re}\beta$ and $y = \text{Im}\beta$. If we compare this function with the Wigner function (see Figure 2) corresponding to the statistical mixture of states $|\alpha\rangle$ and $|-\alpha\rangle$ described by the density matrix

$$\hat{\rho}_M = \frac{1}{2}\left(|\alpha\rangle\langle\alpha| + |-\alpha\rangle\langle-\alpha|\right) \qquad (9)$$

we can directly observe that the term W_{12} corresponding to the quantum interference between states $|\alpha\rangle$ and $|-\alpha\rangle$ should play an important rôle in statistical properties of superpositions of coherent states.
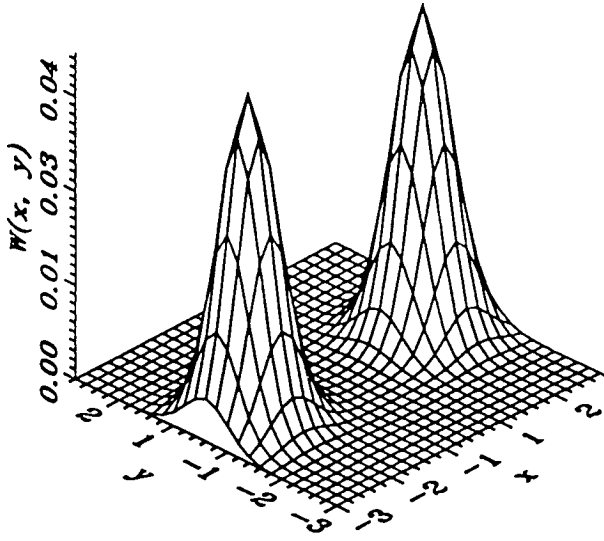
Figure 2: Wigner function corresponding to the statistical mixture (9) with $\alpha = 2$ and $p_1 = p_2 = 1/2$

2.3 Quadrature squeezing

The quadrature operators $\hat{a}_1$ and $\hat{a}_2$ corresponding to the creation and annihilation operators $\hat{a}^\dagger$ and $\hat{a}$ are defined as:

$$\hat{a}_1 = \frac{\hat{a} + \hat{a}^\dagger}{2} \quad ; \quad \hat{a}_2 = \frac{\hat{a} - \hat{a}^\dagger}{2i}. \tag{10}$$

We can easily find that variances of these operators

$$\langle (\Delta \hat{a}_i)^2 \rangle = \langle \hat{a}_i^2 \rangle - \langle \hat{a}_i \rangle^2, \tag{11}$$

in the statistical mixture (9) are:

$$\langle (\Delta \hat{a}_1)^2 \rangle_M = \frac{1}{4} + \alpha^2,$$

and

$$\langle (\Delta \hat{a}_2)^2 \rangle_M = \frac{1}{4}.$$

From above it follows that the fluctuations in the $\hat{a}_1$ quadrature are larger in the case of the statistical mixture compared to the vacuum-state (or the coherent-state) value, which is equal to $1/4$. Fluctuations in $\hat{a}_2$ remain the same for both the statistical mixture (9) as well as for the coherent state $|\alpha\rangle$ (or $|-\alpha\rangle$).
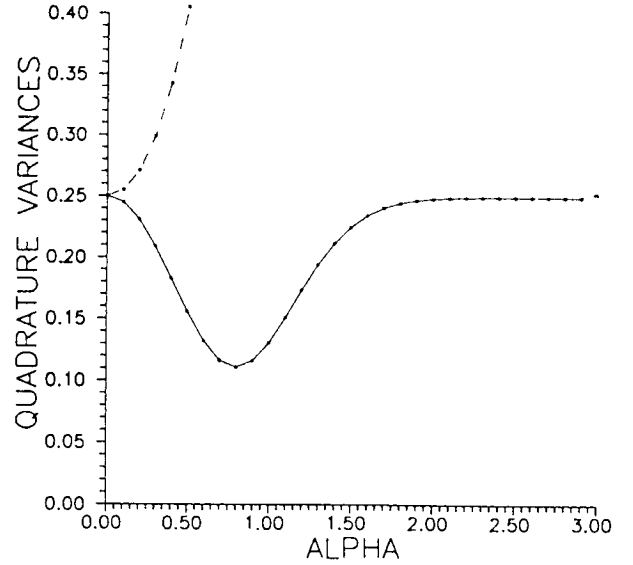
Figure 3: Quadrature variances given by equations (12) versus parameter α. The dashed line corresponds to $\langle (\Delta \hat{a}_1)^2 \rangle$ and the solid line corresponds to $\langle (\Delta \hat{a}_2)^2 \rangle$.

On the other hand, for the even coherent state (8) we find the reduction of fluctuations in $\hat{a}_2$ quadrature (i.e. in the y-direction in the phase space – see Figure 1):

$$\langle (\Delta \hat{a}_2)^2 \rangle = \frac{1}{4} - \frac{\alpha^2 \exp(-2\alpha^2)}{1 + \exp(-2\alpha^2)}. \tag{12.a}$$

Simultaneously fluctuations in $\hat{a}_1$ are enhanced:

$$\langle (\Delta \hat{a}_1)^2 \rangle = \frac{1}{4} + \frac{\alpha^2}{1 + \exp(-2\alpha^2)}. \tag{12.b}$$

Variances $\langle (\Delta \hat{a}_i)^2 \rangle$ versus the parameter α (which is related to the intensity of the even coherent state) are plotted in Figure 3. We see that the maximum reduction in the fluctuations can be obtained for quite small values of α. Reduction of fluctions below the vacuum-state (or coherent-state) level is called quadrature squeezing. From the above it follows that quadrature squeezing can emerge as a consequence of the quantum interference between coherent states. We should note that even coherent states (8) exhibit not only quadrature squeezing, but also higher-order squeezing as well as amplitude squared squeezing [13,16].

184
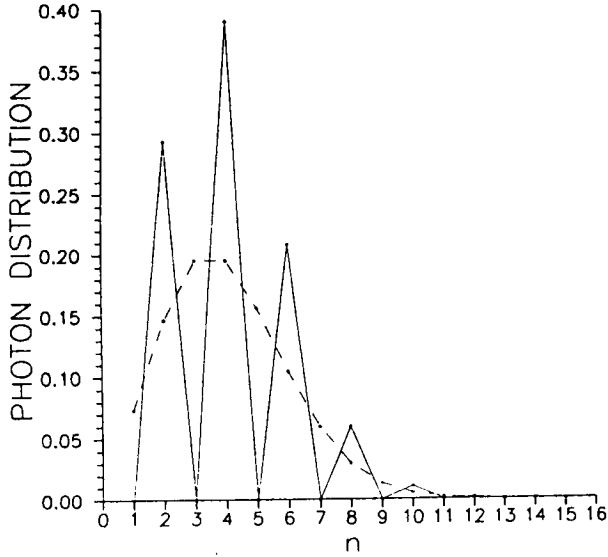
Figure 4: Photon number distribution for a superposition of two coherent states (8) with amplitude $\alpha = 2$. The dashed line is the distribution of the corresponding statistical mixture (9).

2.4 Photon number distribution

Here we discuss briefly properties of the photon number distribution of the statistical mixture (3) as well as the superposition (2) of two coherent states. The photon number distribution is defined as

$$P_n = \langle n|\hat{\rho}|n\rangle. \tag{13}$$

and can be evaluated easily for both the statistical mixture (3)

$$P_n^M = \frac{1}{n!}\left\{p_1|\alpha_1|^{2n}e^{-|\alpha_1|^2} + p_2|\alpha_2|^{2n}e^{-|\alpha_2|^2}\right\} \tag{14}$$

and for the superposition of coherent states (2):

$$P_n = \frac{A}{n!}\left\{|\alpha_1|^{2n}e^{-|\alpha_1|^2} + |\alpha_2|^{2n}e^{-|\alpha_2|^2}\right.$$

$$\left. + [(\alpha_1\alpha_2^*)^n + (\alpha_2\alpha_1^*)^n]\exp[-\frac{1}{2}(|\alpha_1|^2 + |\alpha_2|^2)]\right\} \tag{15}$$

In the case of the statistical mixture the photon number distribution (14) is just the sum of two Poissonian

distributions corresponding to two independent coherent states $|\alpha_1\rangle$ and $|\alpha_2\rangle$. On the other hand, in the case of a superposition of coherent states $|\alpha_1\rangle$ and $|\alpha_2\rangle$ the term corresponding to the quantum interference plays an important rôle. To see this clearly we will assume that $\alpha_1 = -\alpha_2 = \alpha$. In this case the statistical mixture (9) has just the Poissonian photon number distribution

$$P_n^M = \frac{|\alpha|^{2n}}{n!}e^{-|\alpha|^2}. \tag{16}$$

The superposition of coherent states under consideration (i.e. the even coherent state) has the following photon number distribution:

$$P_n = \begin{cases} \frac{2\exp(-|\alpha|^2)}{1+\exp(-|\alpha|^2)} \frac{|\alpha|^{2n}}{n!} & \text{if } n = 2m \\ 0 & \text{if } n=2m+1, \end{cases} \tag{17}$$

The oscillations in P_n are very similar to those in the case of the squeezed vacuum discussed by Schleich and Wheeler [18]. Generally, these oscillations are due to quantum interference in the phase space.

3 Continuous superposition of CS

Now we will discuss the properties of one-dimensional continuous superposition of coherent states. Recently Janszky and Vinogradov [17] defined the continuous superposition $|\xi\rangle$ of coherent states $|\alpha\rangle$ in the following way

$$|\xi\rangle \equiv C_F \int_{-\infty}^{\infty} F(\alpha,\xi)|\alpha\rangle d\alpha, \tag{18}$$

where the coherent state amplitude α is supposed to be real. The normalization constant C_F is defined as:

$$C_F^{-2} = \int\int_{-\infty}^{\infty} F(\alpha,\xi)F(\alpha',\xi)\exp[-(\alpha-\alpha')^2/2]d\alpha d\alpha'. \tag{19}$$

With the superposition state $|\xi\rangle$ given by equation (18) one can find expressions for the mean values of products of the creation $\hat{a}^\dagger$ and the annihilation $\hat{a}$ operators of the field mode in the following form:

$$\langle (\hat{a}^\dagger)^m \hat{a}^n \rangle = \int\int_{-\infty}^{\infty} F(\alpha,\xi)F(\alpha',\xi)$$

$$\times \exp[-(\alpha-\alpha')^2/2]\alpha^m(\alpha')^n d\alpha d\alpha'. \qquad (20)$$

In particular, if $F(\alpha,\xi)$ is taken to be the Gaussian function

$$F(\alpha,\xi) = \exp\left[-\frac{(1-\xi)}{2\xi}\alpha^2\right] \qquad (21)$$

with $\xi \in (0,1)$ and

$$C_F^{-1} = \pi^{-1/2}\frac{(1-\xi^2)^{1/4}}{(2\xi)^{1/2}}, \qquad (22)$$

then one can find for the variances of the quadrature operators $\hat{a}_1$, $\hat{a}_2$ given by eq. (10) the following expressions

$$\langle (\Delta\hat{a}_1)^2 \rangle = \left(\frac{1}{4}\right)\frac{(1+\xi)}{(1-\xi)}; \qquad (23.a)$$

$$\langle (\Delta\hat{a}_2)^2 \rangle = \left(\frac{1}{4}\right)\frac{(1-\xi)}{(1+\xi)}. \qquad (23.b)$$

From this one can conclude that the states $|\xi\rangle$: i) belong to the class of the minimum uncertainty states; ii) the fluctuations in the "second" quadrature are reduced below the shot noise limit.

We see, therefore, that the one-dimensional superposition (with Gaussian distribution) of coherent states leads to states exhibiting a large degree of squeezing (in the limit $\xi \to 1$). We now demonstrate by direct calculations that if $F(\alpha,\xi)$ is the Gaussian function (21), then the state $|\xi\rangle$ is equal to the squeezed vacuum state generated by the action of the squeeze operator $\hat{S}(\hat{a}^\dagger,\hat{a},\xi)$:

$$\hat{S}(\hat{a}^\dagger,\hat{a},\xi) = \exp\left[\frac{r}{2}(\hat{a}^\dagger)^2 - \frac{r}{2}\hat{a}^2\right],$$

$$\xi = \tanh r, \qquad (24)$$

on the vacuum state $|0\rangle$ of the field mode. To do so we decompose the coherent state $|\alpha\rangle$ in equation (18) into number states:

$$|\alpha\rangle = \exp(-\alpha^2/2)\sum_{n=0}^{\infty}\frac{\alpha^n}{\sqrt{(n!)}}|n\rangle,$$

and exchange the order of integration and summation procedures, i.e. we rewrite equation (18) in the form

$$|\xi\rangle = C_F \sum_{n=0}^{\infty}\frac{1}{\sqrt{(n!)}}|n\rangle$$

$$\times \int_{-\infty}^{\infty} d\alpha\, \alpha^n \exp\left[-\frac{1}{2\xi}\alpha^2\right]. \qquad (25)$$

After performing the integration on the r.h.s of equation (25) we find

$$|\xi\rangle = (1-\xi^2)^{1/4}\sum_{n=0}^{\infty}\frac{[(2n)!]^{1/2}}{2^n n!}\xi^n|2n\rangle, \qquad (26)$$

from which it follows that the one-dimensional superposition of coherent states (18) with the distribution function (21) is *identical* to the squeezed vacuum state:

$$|\xi\rangle = C_F \int_{-\infty}^{\infty} F(\alpha,\xi)d\alpha\hat{D}(\alpha)|0\rangle = \hat{S}(\xi)|0\rangle. \qquad (27)$$

We should stress here that the last equation describes the relation between the states, but not between the displacement and the squeeze operators themselves.

3.1 Origin of squeezing

We next provide a physical explanation of the origin of the squeezing generated by such a superposition. We address the question of how the one-dimensional superposition of coherent states in direction of the x-quadrature (corresponding to the operator $\hat{a}_1$) leads to squeezing of the fluctuations in y-direction (associated with the quadrature operator $\hat{a}_2$). To do so we use the Wigner-function phase-space formalism: we define the Wigner function $W(\beta)$ in the following way. First,

we introduce a "generalized" characteristic function $\tilde{C}^{(W)}(\alpha, \alpha', \zeta)$:

$$\tilde{C}^{(W)}(\alpha, \alpha', \zeta) \equiv \langle\alpha'|\hat{D}(\zeta)|\alpha\rangle$$

$$= \exp\left[-\frac{1}{2}|\zeta|^2 + i\zeta\alpha' + i\zeta^*\alpha - \frac{1}{2}(\alpha - \alpha')^2\right], \quad (28)$$

and the "generalized" Wigner function $\tilde{W}(\alpha, \alpha', \beta)$:

$$\tilde{W}(\alpha, \alpha', \beta) = \pi^{-2}\int d^2\zeta$$

$$\times \exp[-i(\zeta^*\beta + \zeta\beta^*)]\tilde{C}^{(W)}(\alpha, \alpha', \zeta) \quad (29)$$

$$= \frac{2}{\pi}\exp\left[\frac{1}{2}(\beta^* - \beta - \alpha' + \alpha)^2\right]$$

$$\times \exp\left[-\frac{1}{2}(\beta + \beta^* - \alpha - \alpha')^2 - \frac{1}{2}(\alpha - \alpha')^2\right].$$

The Wigner function $W(\beta)$ can now be expressed in a very simple form:

$$W(\beta) = C_F^2\int\int_{-\infty}^{\infty} d\alpha\, d\alpha'\, F(\alpha)F(\alpha')\tilde{W}(\alpha, \alpha', \beta). \quad (30)$$

To make our discussion more transparent we will first analyze in detail the simple superposition of two coherent states $|\alpha\rangle$ and $|-\alpha\rangle$ and the vacuum state $|0\rangle$, i.e. we will study the state [17]

$$|\xi\rangle = C_F\left\{|\alpha\rangle + p|0\rangle + |-\alpha\rangle\right\}, \quad (31)$$

which can be obtained from equation (18) with a weight function $F(x) = \delta(x - \alpha) + p\delta(x) + \delta(x + \alpha)$. The normalization constant in this case is given by the relation:

$$C_F^{-2} = 2 + p^2 + 4p\exp(-\alpha^2/2) + 2\exp(-2\alpha^2). \quad (32)$$

One can easily find the variance of the quadrature operator $\hat{a}_2$ for the state (31):

$$\langle(\Delta\hat{a}_2)^2\rangle = \frac{1}{4}\left\{1 - 4C_F^2\alpha^2\right.$$

$$\times[2\exp(-2\alpha^2) + p\exp(-\alpha^2)]\}, \quad (33)$$

from which it follows that a high degree of squeezing (up to 74%) can be obtained for the optimum case, $\alpha = 1.57$ and $p = 1.35$.

The Wigner function of the state (31) can be expressed as the sum of two terms:

$$W(\beta) = W_{cl}(\beta) + W_{quant}(\beta), \quad (34)$$

where

$$W_{cl}(\beta) = \frac{2C_F^2}{\pi}\left\{\exp[-2(x - \alpha)^2 - 2y^2]\right.$$

$$+ \exp[-2(x + \alpha)^2 - 2y^2] + p^2\exp[-2x^2 - 2y^2]\} \quad (35)$$

and

$$W_{quant}(\beta) = \frac{2C_F^2}{\pi}\left\{2\cos(4\alpha y)\exp[-2x^2 - 2y^2]\right.$$

$$+ p\cos(2\alpha y)\left[\exp\left(-2(x - \alpha/2)^2 - 2y^2\right)\right.$$

$$\left.+ \exp\left(-2(x + \alpha/2)^2 - 2y^2\right)\right]\}. \quad (36)$$

The normalization constant C_F in this case is given by equation (32) and $x = \mathrm{Re}\beta$; $y = \mathrm{Im}\beta$. The function $W_{cl}(\beta)$ is equal (up to normalization factors) to the sum of the independent Wigner functions of the vacuum state and two coherent states and can be identified with the Wigner function of the statistical mixture of coherent states and the vacuum state described by the density matrix

$$\hat{\rho}_M = p_1|0\rangle\langle 0| + p_2|\alpha\rangle\langle\alpha| + p_3|-\alpha\rangle\langle-\alpha| \quad (37)$$

with properly chosen parameters p_i.

This function is plotted in Figure 5a, from which it is obvious that $W_{cl}(\beta)$ is positive for any value of x and y. The phase-space contour lines of this function are plotted in Figure 5b. In contrast to the function
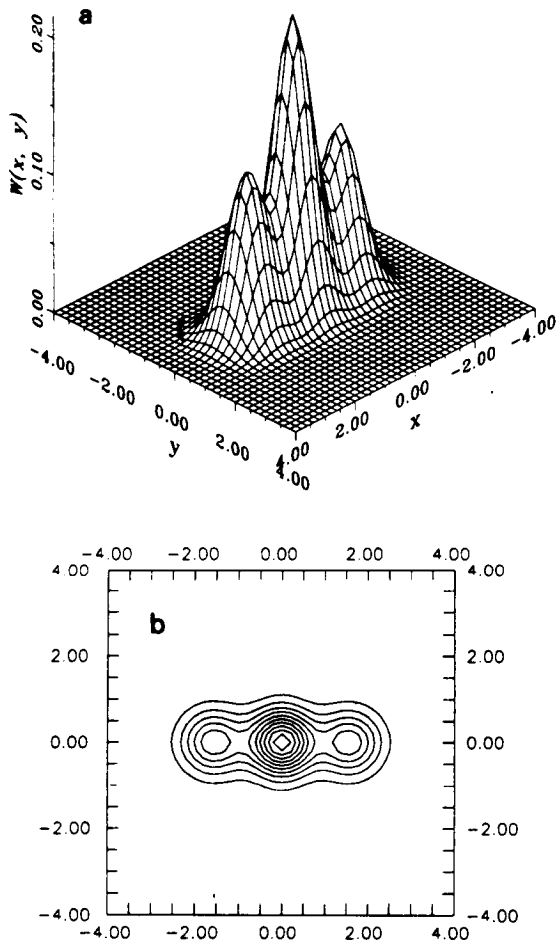
Figure 5: Function $W_{cl}(x, y)$ given by Equation (35) representing the part of the Wigner function of the superposition state (31) is plotted for $\alpha = 1.57$ and $p = 1.35$ (a). In Figure 5b the phase-space contours corresponding to this function are plotted.

$W_{cl}(\beta)$, the function $W_{quant}(\beta)$ can be negative. This function describes in phase-space the quantum interference effects between the states $|\alpha\rangle$, $|-\alpha\rangle$ and $|0\rangle$. The quantum interference is responsible the appearance of the cosine terms in the y-direction, and these oscillating terms are responsible for: 1) negative values of the function $W_{quant}(\beta)$ (see Figure 6a) as well as the total Wigner function $W(\beta)$ (Figure 7a); 2) squeezing of the variance of the quadrature operator in the y-direction, which is clearly seen in Figures 6b and 7b.

This simple example helps us to understand the nature of squeezing in the one-dimensional superposition of coherent states. The squeezing arises as a consequence of quantum interference between the macroscopically distinguishable states. Generally, if more states are involved in the superposition, a higher degree of squeezing (depending on the appropriate shape of the distribution $F(\alpha)$) can be obtained for the same mean value of photons in the mode.

Now we turn our attention to the displacement of the superposition state such that there is a mean field amplitude. We show that a one-dimensional superposition of coherent states with the distribution function $F(\alpha, \xi, \beta)$ centered at a non-zero value of α is equal to the squeezed coherent state. We take for our distribution function $F(\alpha, \xi, \beta)$ the displaced form

$$F(\alpha, \xi, \beta) = \exp\left[-\frac{(1-\xi)}{2\xi}(\alpha - x_0)^2\right], \qquad (38)$$

with the normalization constant C_F given by equation (22) and with a displacement

$$x_0 = \left(\frac{1+\xi}{1-\xi}\right)^{1/2}\beta.$$

In this case from equation (18) we obtain for the state
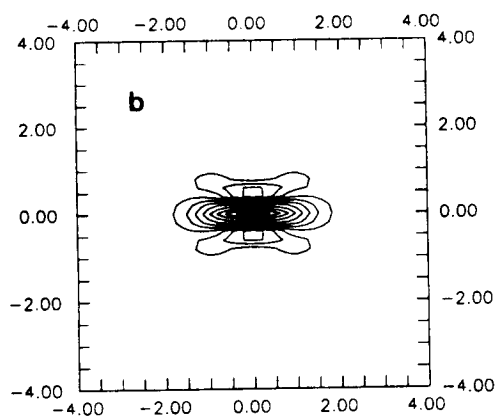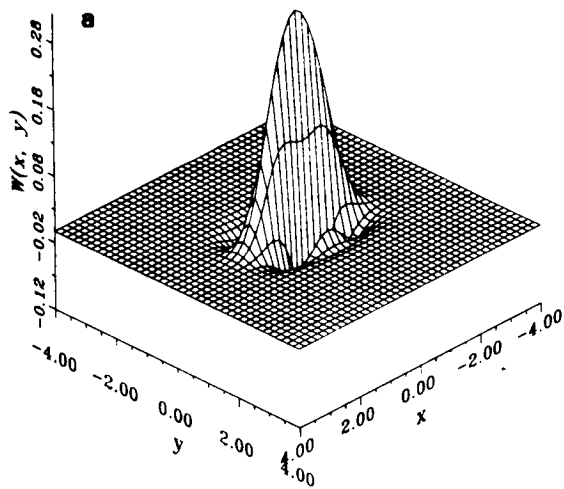
Figure 6: Function $W_{quant}(x,y)$ (36) representing the interference between states in phase space is plotted for $\alpha = 1.57$ and $p = 1.35$ (a). In Figure 6b the phase-space contours corresponding to this function are plotted.
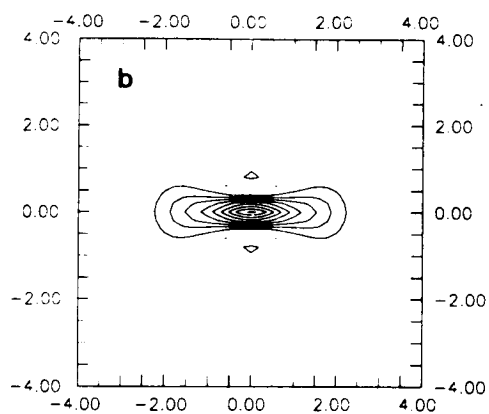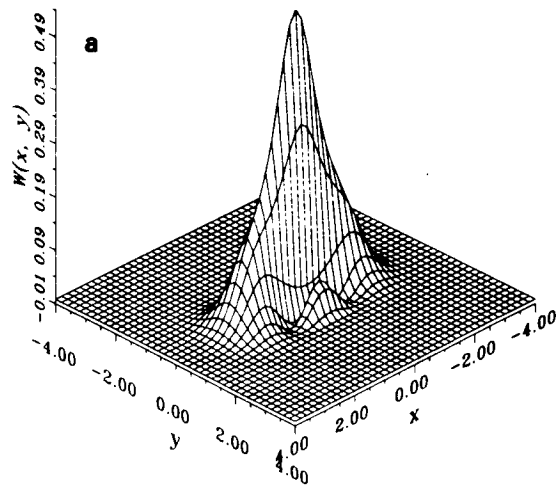
Figure 7: The total Wigner function $W(x,y)$ is plotted for $\alpha = 1.57$ and $p = 1.35$ (a). In Figure 7b the phase-space contours corresponding to this function are plotted.

189

$|\xi\rangle$ the following expression:

$$|\xi\rangle = (1 - \xi^2)^{1/4} \exp\left[-\frac{(1 - \xi)}{2} x_0^2\right]$$

$$\times \sum_{n=0}^{\infty} \sqrt{(n!)} \left[(1 - \xi)x_0\right]^n$$

$$\times \left\{ \sum_{k=0}^{\|n/2\|} \frac{1}{(n - 2k)!k!} \left(\frac{\xi}{2(1 - \xi)^2 x_0^2}\right)^k \right\} |n\rangle, \quad (39)$$

where $\|x\|$ denotes the greatest integer less than or equal to x. Using the new parametrization:

$$\mu = \frac{1}{(1 - \xi^2)^{1/2}} \quad ; \quad \nu = \frac{-\xi}{(1 - \xi^2)^{1/2}}, \quad (40)$$

with $\mu^2 - \nu^2 = 1$ and $|\mu| > |\nu|$, we can rewrite equation (39) in the form:

$$|\xi\rangle = \mu^{-1/2} \exp\left[-\frac{(1 - \nu/\mu)}{2}\beta^2\right]$$

$$\sum_{n=0}^{\infty} \frac{1}{\sqrt{(n!)}} \left(\frac{\nu}{2\mu}\right)^{n/2} H_n(\beta/\sqrt{2\mu\nu})|n\rangle, \quad (41)$$

where $H_n(x)$ is the Hermite polynomial. It is obvious that the last expression obtained describes precisely the squeezed coherent state as defined by Yuen [22], i.e., we have explicitly proved that

$$\hat{S}(\xi)\hat{D}(\beta)|0\rangle = C_F \int_{-\infty}^{\infty} d\alpha \, F(\alpha, \xi, \beta)\hat{D}(\alpha)|0\rangle. \quad (42)$$

In other words, we can construct, through a one-dimensional superposition of coherent states with a properly chosen distribution function, the squeezed coherent state. Obviously, the physical reason for squeezing is the same as for the case of squeezed vacuum state discussed earlier. It is amusing that a superposition of the most classical of field states, the coherent states, can through the action of quantum interference, generate the archetypal nonclassical field states – the squeezed vacuum and the squeezed coherent state.

It can also be shown that the squeezed number state [23] defined as a result of a action of the squeezing operator $\hat{S}(\xi)$ on the number state $|n\rangle$ can be constructed

as a one-dimensional superposition of displaced number states [24], the states obtained through the action of the displacement operator on the number state, that is

$$\hat{S}(\xi)|n\rangle = C_F \int_{-\infty}^{\infty} F(\alpha, \xi)d\alpha\hat{D}(\alpha)|n\rangle, \quad (43)$$

where function $F(\alpha, \xi)$ and the normalization constant C_F are given by the Equations (21) and (22), respectively.

4 Discussion

In our Lecture we discussed the rôle of the quantum interference in the origin of squeezing in the one-dimensional superposition of coherent states. With the aim to make the discussion as clear as possible we started our Lecture with a simple example of superposition of just two coherent states $|\alpha\rangle$ and $|-\alpha\rangle$. Finishing the Lecture we return to this simple example but we take into account the relative phase between the coherent states under consideration, i.e. we will study the following superposition

$$|\Psi\rangle = A^{1/2}\left\{|\alpha\rangle + e^{i\phi}|-\alpha\rangle\right\}, \quad (44)$$

with the normalization constant

$$A^{-1} = 2\left(1 + \cos\phi e^{-2\alpha^2}\right).$$

We will show that the phase ϕ plays a crucial rôle in the character of the quantum interference between coherent states.

First of all we write down the corresponding Wigner function for the state (44). This function can be expressed as a sum of two terms:

$$W(\beta) = W_{cl}(\beta) + W_{quant}(\beta), \quad (45)$$

190
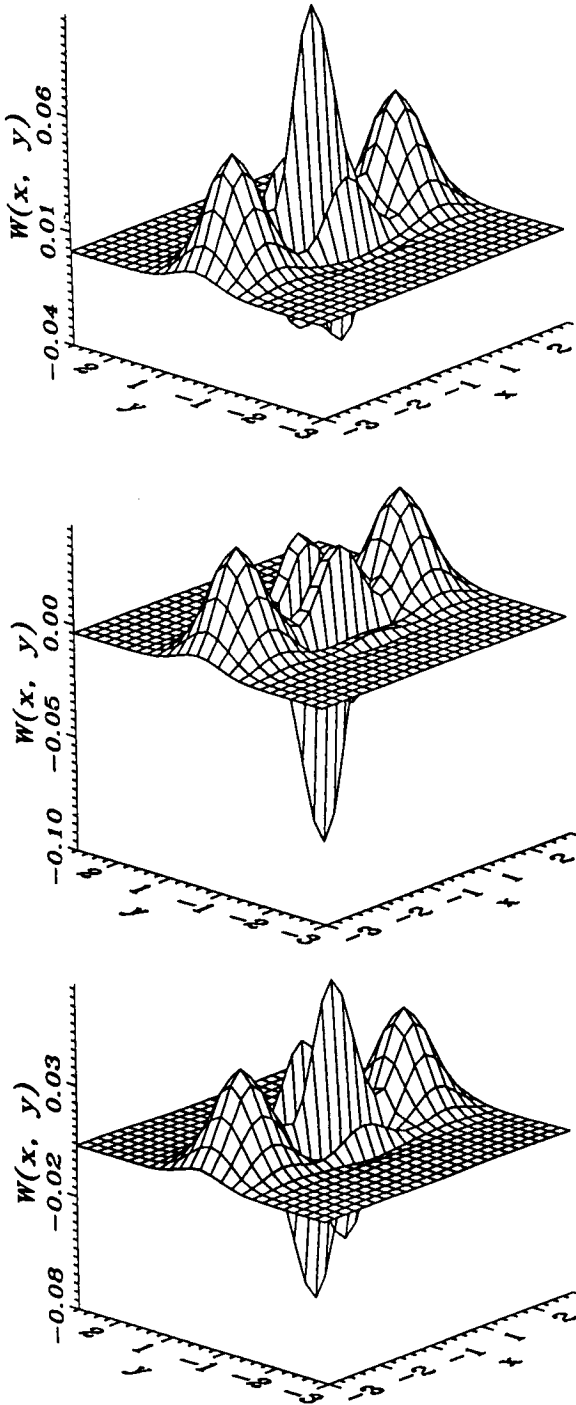
Figure 8: Wigner function corresponding to the super-position (44) of two coherent states with the relative phase ϕ equal to 0 (a); π (b) and $\pi/2$ (c); $\alpha = 2$.

where

$$W_{cl}(\beta) = \frac{4A}{\pi}\left\{e^{-2(x-\alpha)^2-2y^2}\right.$$

$$\left.+e^{-2(x+\alpha)^2-2y^2}\right\} \qquad (46)$$

and

$$W_{quant}(\beta) = \frac{4A}{\pi}\cos(4\alpha y + \phi)e^{-2x^2-2y^2}. \qquad (47)$$

As earlier we use the notation $x = \text{Re}\beta$; $y = \text{Im}\beta$.

To investigate the dependence of the quantum interference on the value of the parameter ϕ we will employ two parameters describing nonclassical properties of light fields. Namely, we will study the Mandel Q parameter, defined as

$$Q = \frac{\langle(\Delta\hat{n})^2\rangle - \langle\hat{n}\rangle}{\langle\hat{n}\rangle} \qquad (48)$$

which is related to the degree of sub-Poissonian photon statistics. In particular, if $Q = 0$ the state has Poissonian photon statistics, while for $Q < 0$ $(Q > 0)$ the state has sub-Poissonian (super-Poissonian) photon statistics. The second parameter we will study is the squeezing parameter

$$S_i = 4\langle(\Delta\hat{a}_i)^2\rangle - 1 \qquad (49)$$

describing the degree of quadrature squeezing. A state is said to be squeezed if S_1 or S_2 is less than zero. In what follows we will suppose three values of ϕ.

1) Let the phase ϕ be equal to zero. In this case the state (44) is equal to the even coherent state (8) and we find

$$Q = \frac{4\alpha^2\exp(-2\alpha^2)}{1-\exp(-4\alpha^2)} > 0; \qquad (50)$$

$$S_1 = \frac{4\alpha^2}{1+\exp(-2\alpha^2)} > 0; \qquad (51)$$

$$S_2 = -\frac{4\alpha^2\exp(-2\alpha^2)}{1+\exp(-2\alpha^2)} < 0, \qquad (52)$$

191

from which it follows that the even coherent state has super-Poissonian photon statistics and simultaneously is squeezed in the $\hat{a}_2$ quadrature.

2) If $\phi = \pi$ then the state (44) is an odd coherent state [14]. This state has sub-Poissonian photon statistics, i.e.

$$Q = -\frac{4\alpha^2 \exp(-2\alpha^2)}{1 - \exp(-4\alpha^2)} < 0; \qquad (53)$$

but is not squeezed

$$S_1 = \frac{4\alpha^2}{1 - \exp(-2\alpha^2)} > 0; \qquad (54)$$

$$S_2 = -\frac{4\alpha^2 \exp(-2\alpha^2)}{1 - \exp(-2\alpha^2)} > 0. \qquad (55)$$

3) Finally, if $\phi = 0$, then the state (44) has Poissonian photon statistics

$$Q = 0, \qquad (56)$$

and simultaneously we can observe squeezing in the $\hat{a}_2$ quadrature

$$S_1 = 4\alpha^2; \qquad (57)$$

$$S_2 = -4\alpha^2 \exp(-4\alpha^2) < 0. \qquad (58)$$

The dependence of the statistical properties of superpositions of coherent states on the value of the relative phase is caused by the character of the quantum interference, that is whether this interference is constructive or destructive in various regions of phase space. This can be clearly seen from Figure 8 in which the Wigner function corresponding to the state (44) is plotted for $\phi = 0; \pi$ and $\pi/2$. We see significant differences in the shape of Wigner functions for various values of ϕ, which is related to the completely different statistical properties of the corresponding states.

5 Conclusion

The main information carried in this Lecture is: **A superposition of the most classical of field states can through the action of quantum interference, generate the archetypal nonclassical field states: the squeezed vacuum and the squeezed coherent state.**

6 REFERENCES

[1] R.LOUDON: *"The Quantum Theory of Light"* (Clarendon, Oxford, 1983).

[2] R.LOUDON and P.L.KNIGHT: *J. Mod. Opt.* **34**, (1987) 709; K.ZAHEER and M.S.ZUBAIRY: in *"Advances in Atomic, Molecular and Optical Physics"*, vol. 28. Edited by D.Bates and B.Bederson (Academic Press, New York, 1990), p.143.

[3] Special issue of *JOSA B* **4** No.10 (1987).

[4] Special issue of *J. Mod. Opt.* **34** No. 6/7 (1987).

[5] R.E.SLUSHER, L.W.HOLLBERG, B.YURKE, J.C. MERTZ and J.F.VALLEY: *Phys. Rev. Lett.* **55**, (1985) 2409.

[6] R.M.Shelby, M.D.Levenson, S.H. Perlmutter, R.G. DeVoe, and D.F. Walls: *Phys. Rev. Lett.* **57**, (1986) 691.

[7] Ling-An Wu, H.J.Kimble, J.L.Hall and H.Wu: *Phys. Rev. Lett.* **57**, (1986) 2520.

[8] M.W.Maeda, P.Kumar and J.H.Shapiro: *Opt. Lett.* **3**, (1986) 161.

[9] S.Machida, Y.Yamamoto and Y.Itaya: *Phys. Rev. Lett.* **58**, (1987) 1000.

[10] A.Heidmann, R.Horowicz, S.Reynaud, E. Giacobino, C.Fabre and G.Gamy: *Phys. Rev. Lett.* **59**, (1987) 2555.

[11] R.Moschovich, B.Yurke, P.G.Kaminsky, A.D.Smith, A.H.Silver, R.W.Simon and M.V. Schneider: *Phys. Rev. Lett.* **65**, (1990) 1419.

[12] K.Wódkiewicz, P.L.Knight, S.J.Buckle and S.M.Barnett: *Phys. Rev. A* **35**, (1987) 2567.

[13] M.Hillery: *Phys. Rev. A* **36**, (1987) 3796; see also K.Vogel and H.Risken: *Phys. Rev. A* **40**, (1990) 2847; W.Schleich, M.Pernigo and Fam Le Kien: *"A nonclassical state from two pseudo-classical states."* to appear in *Phys. Rev. A* (1991); W.Schleich, J.P.Dowling, R.J.Horowicz and S.Varro: in *"New Frontiers in Quantum Electrodynamics and Quantum Optics*, edited by A.Barut (Plenum Press, New York, 1990), p.31.

[14] J.Peřina: *"Quantum Statistics of Linear and Nonlinear Optical Phenomena"* (Reidel, Dordrecht, 1984).

[15] B.Yurke and D.Stoler: *Phys. Rev. Lett.* **57**, (1986) 13.

[16] V.Bužek, I.Jex and Tran Quang: *J. Mod. Opt.* **37**, (1990) 159.

[17] J.Janszky and An.V.Vinogradov: *Phys. Rev. Lett.* **64**, (1990) 2771.

[18] W.P.Schleich and J.A.Wheeler: *JOSA B* **4**, (1987) 1715; W.Schleich, .F.Walls and J.A.Wheeler: *Phys. Rev. A* **38**, (1988) 1177.

[19] W.P.Schleich, R.J.Horowicz and S.Varro: in *"Quantum Optics V"*, edited by J.D.Harvey and D.F.Walls (Berlin, Springer-Verlag, 1989), p.133.

[20] J.P.Dowling, W.P.Schleich and J.A. Wheeler: *Ann. Phys.*, (1990) in press.

[21] W.H.Louisell: *"Quantum Statistical Properties of Radiation"* (Wiley, New York, 1973).

[22] H.P.Yuen: *Phys. Rev. A* **13**, (1976) 2226.

[23] M.S.Kim, F.A.M.deOliveira, and P.L. Knight: *Phys. Rev. A* **40**, (1989) 2494.

[24] F.A.M.deOliveira, M.S.Kim, P.L.Knight, and V.Bužek: *Phys. Rev* **41**, (1990) 2645.

LIMITATIONS ON SQUEEZING AND FORMATION OF THE SUPERPOSITION OF TWO MACROSCOPICALLY DISTINGUISHABLE STATES AT FUNDAMENTAL FREQUENCY IN THE PROCESS OF SECOND HARMONIC GENERATION.

Nikitin S.P., Masalov A.V.
Lebedev Physical Institute

Moscow, USSR

In this paper the results of numerical simulations of quantum state evolution in the process of second harmonic generation (SHG) are discussed. It is shown that at a particular moment of time in the fundamental mode initially coherent state turns into a superposition of two macroscopically distinguishable states. The question if this superposition exhibits quantum interference is analyzed.

To describe the SHG we use the following Hamiltonian:

$$H = \hbar\omega\, a^{\dagger}a + 2\hbar\omega b^{\dagger}b + g\hbar(a^{\dagger}a^{\dagger}b + aab^{\dagger})$$

Here a, $a^{\dagger}$, b, $b^{\dagger}$ are annihilation and creation operators of the fundamental mode and harmonic mode respectively, and g is a coupling constant proportional to the nonlinearity of the medium. The nonlinear interaction is described by the last term in the Hamiltonian. This Hamiltonian corresponds to the case when there is no absorption loss in the medium. The initial quantum state was taken to be a coherent state in the fundamental mode and vacuum state in the harmonic mode.

In our calculations we have used a number-state basis in which a quantum state is just a vector and operators are matrices of c-numbers. Details of our calculations are described in Ref. 1. Earlier similar calculations have been made by Walls and Barakat. It is known that squeezing in the SHG has a minimum. It is shown in Ref. 1 that this minimum appears due to the formation at the fundamental frequency of the superposition of macroscopically distinguishable states. It is the formation of this superposition that is the limiting factor of the largest squeezing achievable in the process.

Fig. 1 represents the dependence of amplitude squeezing in the fundamental mode versus the dimensionless time $\tau = gt\sqrt{2N}$. N is the initial average number of photons in the fundamental mode. Fig 2 represents the quasiprobability distribution for the fundamental mode $Q(\alpha) = \langle \alpha | \rho | \alpha \rangle / \pi$ when this superposition is formed. Here ρ is the density matrix of the quantum state and $|\alpha\rangle$ is a coherent state described by a c-number α. Earlier, in Ref.2 it was shown that superposition of two coherent states can be obtained using Kerr nonlinearity. The SHG process appears to be alternative nonlinear process in which the superposition can be obtained.

The question of the origin of this superposition is discussed in Ref. 1 where this phenomenon is attributed to the instability of the SHG process with respect to the initial harmonic phase which is completely uncertain for the initial vacuum state in the harmonic mode. This instability was illustrated by a classical equation solution where quantum uncertainty of the harmonic state and the fundamental state was imitated by randomized initial conditions distributed by the normal law with the same dispersion as quantum states.

Here we would like to pay more attention to the question of whether the superposition is coherent, that is, a pure quantum state, or whether it is a statistical mixture of two coherent states. In order to answer this question one usually uses simple numerical criteria such as $T = Tr\rho^2$ For a pure state $T = 1$ while for a statistical mixture $T < 1$. The dependence of T versus τ is shown on the Fig. 3. If N=10 the superposition appears at $\tau = 4$. It is clearly seen on Fig. 3 that T at this time is very far from parameter specific to the pure state. So, one can expect that no quantum interference effects could be seen in this state. However, we may check it directly using the density matrix.

To see quantum interference we may consider the function $P(x)=<x|\rho|x>$. Here $|x>$ is an eigenstate of a quadrature operator $x = (a+a^+)/\sqrt{2}$. Experimentally this function $P(x)$ can be obtained using homodyne measurements. It is known that for a coherent state this function is a gaussian. If we calculate this function for a statistical mixture of two coherent states then we get the sum of two gaussians and no quantum interference. For a quantum superposition of two macroscopically distinguishable state this function exhibits an interference pattern. It is therefore interesting to check if the superposition formed in the process of the SHG exhibits quantum interference pattern in $P(x)$.

Fig. 4 represents $P(x)$ calculated from the density matrix of the superposition at $\tau=4$ and N=10. This function obviously exhibits quantum interference, though visibility of the interference pattern is less than for a pure superposition of two coherent states. This result could be explained if we assume that the main portion of the statistical mixture, which in fact the above-mentioned superposition is, is a quantum superposition of two coherent states. Other states which the mixture contains reduce visibility of the interference but can not destroy it completely. Thus the superposition formed in the process of the SHG can exhibit quantum interference though, generally speaking this superposition is a statistical mixture rather than a pure state.

Conclusions

Squeezing in the process of the SHG is limited because of the formation of the superposition of macroscopically distinguishable states at the fundamental frequency. This superposition forms because of the quantum phase uncertainty of the initial harmonic state. Though this superposition is not a pure quantum state, it does exhibit quantum interference in $P(x)$. This fact illustrates that analysis of simple numerical criteria such as $Tr\ \rho^2$ is not enough to decide whether quantum interference appears or not.

REFERENCES:

1 Nikitin S.P.,Masalov A.V.,1991 accepted for publication in Quantum Optics.

2.Yurke B. and Stoler D., 1986, "Generating Quantum Mechanical Superpositions of Macroscopically Distinguishable States via Amplitude Dispersion," Phys. Rev. Lett., 57(1), pp.13-16
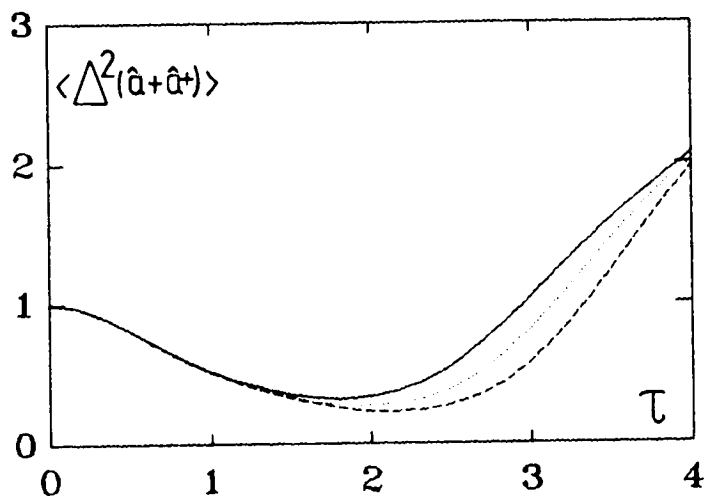
Fig.1 Squuezing in the fundamental mode vs $\tau=gt\sqrt{2N}$. N=10 (solid line) N=20 (dotted line), N=40 (dashed line)
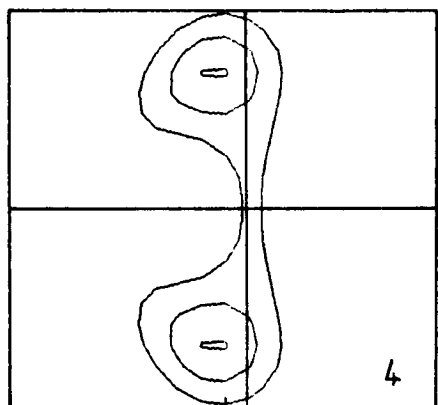
Fig. 2
Quasiprobability $Q(\alpha) = \langle\alpha|\rho|\alpha\rangle/\pi$ for fundamental mode at $\tau=4$; N= 10. Contours at $0.1/\pi$, $0.2/\pi$, $0.3/\pi$.
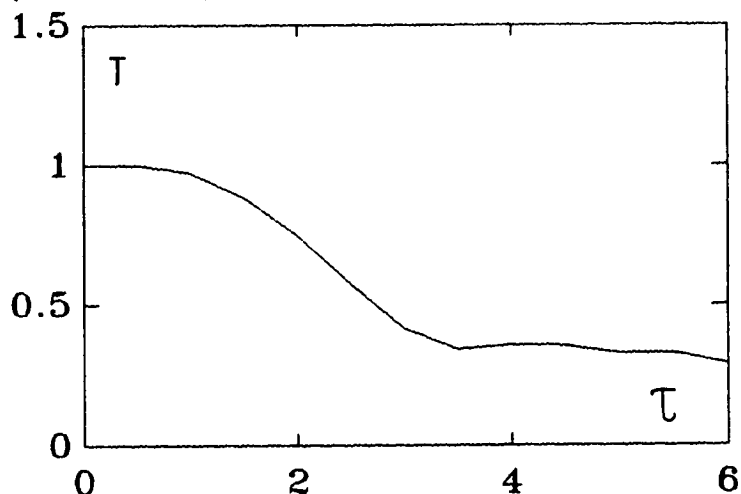
Fig. 3
$T = Tr\rho^2$ versus τ for the fundamental mode. Average photon number N = 10.
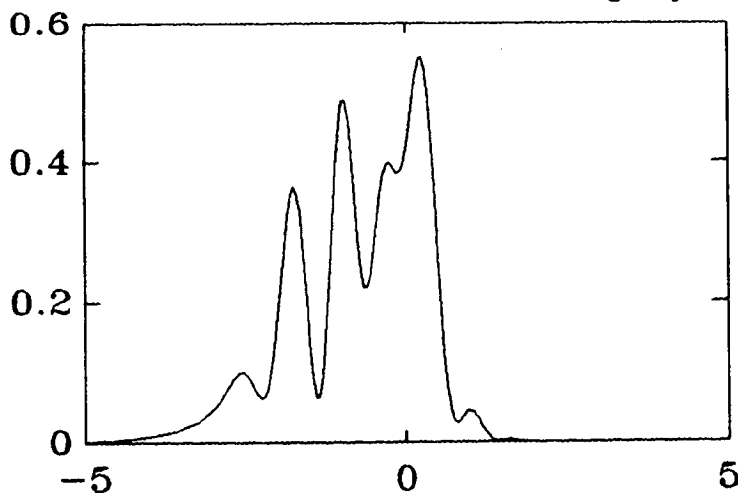
Fig. 4 Quantum interference in $P(x) = \langle x|\rho|x\rangle$ for the fundamental mode at $\tau = 4$. Average photon number N = 10.

197

FIELD QUANTIZATION AND SQUEEZED STATES GENERATION IN RESONATORS WITH TIME-DEPENDENT PARAMETERS

V.V.Dodonov, A.B.Klimov, D.E.Nikonov

Moscow Physics Technical Institute,
16, Gagarin St., Zhukovsky 140160
Lebedev Physics Institute,
53, Leninsky Prospect, Moscow 117924 USSR

The problem of electromagnetic field quantization is usually considered in text-books under the assumption that the field occupies some empty box. The case when the box is filled with a uniform dielectric medium was considered in (Refs.1,2). The quantization of the field in the medium consisting of two uniform dielectrics with different permittivities was studied in (Refs.3-5). The case of an arbitrary inhomogenious dielectric medium was investigated in (Refs.6,7) and especially in (Refs. 8,9). However, in all mentioned papers the properties of the medium were believed time-independent. Here we want to consider the most general case of non-uniform and time-dependent media. Earlier this problem was investigated in (Ref.10), but its authors considered only approximate solutions of the Heisenberg equations for field operators in the case of small polarization of the medium. Our approach differs from that of (Ref.10) and enables to study the case when non-uniform time-dependent dielectric medium is confined in some space region with time-dependent boundaries.

The basis of the subsequent consideration is the system of Maxwell's equations in linear passive time-dependent dielectric and magnetic medium without sources:

$$\text{rot } E = -1/c \; \partial B/\partial t, \qquad \text{rot } H = 1/c \; \partial D/\partial t,$$
$$\text{div } D = 0, \qquad\qquad\qquad \text{div } B = 0,$$
$$D = \varepsilon(r,t)E, \qquad\qquad B = \mu(r,t)H. \qquad (1)$$

Introducing the vector potential according to the relations:

$$B = \text{rot } A, \qquad\qquad E = -1/c \; \partial A/\partial t \qquad (2)$$

and imposing gauge conditions

$$\text{div}(\varepsilon \partial A/\partial t) = 0, \qquad\qquad \varphi = 0 \qquad (3)$$

we can replace the system of the first-order equations (1) with the single second-order one:

$$\text{rot}(1/\mu \; \text{rot}A) = -1/c^2 \; \partial/\partial t(\varepsilon \partial A/\partial t) = 1/c \; \partial D/\partial t. \qquad (4)$$

One can check that the vector equation (4) coincides with the set of Euler's equations

PRECEDING PAGE BLANK NOT FILMED

$$\partial/\partial t \; \partial L/\partial(\partial_T A_\beta) + \partial/\partial x_\alpha \; \partial L/\partial(\partial_\alpha A_\beta) - \partial L/\partial A_\beta = 0 \qquad (5)$$

for the Lagrangian density

$$L = 1/2 \; [\; \epsilon(r,t)(\partial A/\partial t)^2/c^2 - (rot A)^2/\mu(r,t) \;] \qquad (6)$$

in the case of quite arbitrary time and space dependences of the dielectric and magnetic permittivities. Then introducing the canonically conjugated variable

$$P = \partial L/\partial(\partial_T A) = \epsilon(r,t)/c^2 \; \partial A/\partial t = -1/c \; D \qquad (7)$$

one can construct the Hamiltonian density

$$H = P \; \partial A/\partial t - L = 1/2 \; [\; D^2/\epsilon(r,t) + B^2/\mu(r,t) \;] \qquad (8)$$

which leads again to eq.(4). But in the general case the expression (8) is by no means the energy of the system due to possible time-dependences of the coefficients. This fact complicates the quantization procedure. The usual procedure consists in introducing the field expansion over mode functions

$$D(r,t) = \Sigma q_N(t) u_N(r), \qquad B(r,t) = \Sigma p_N(t) v_N(r). \qquad (9)$$

Substituting these expansions into the Hamiltonian density (8) and integrating it over the space variables one gets usually (due to certain orthogonality properties of functions u_N and v_N) a sum of independent oscillator-like Hamiltonians

$$H = \int H(r,t)d^3r = 1/2 \; \Sigma(\mu_N p_N^2 + \eta_N q_N^2). \qquad (10)$$

After this the coefficients p_N and q_N are proclaimed operators satisfying canonical commutation relations, so that the fields become quantized. But this sketch of standard quantization scheme shows distinctly that it can be used only in the case when the solutions of Maxwell's equations can be factorised into the products of two functions: one dependent only of time, and another dependent on space coordinates only. In the general case of non-uniform and time-dependent medium such solutions do not exist, and the usual scheme of quantization is impossible. This means in particular, that we cannot obtain any Hamiltonian and, consequently, any unitary evolution operator. Therefore the Schrodinger picture does not exist in the general case. But the Heisenberg description is still possible. It can be introduced as a generalisation of the approach used earlier by Moore (Ref.11) for the field quantization in the empty space region confined with moving boundaries.

First of all we notice the important property of equation (4): it admits a time-independent scalar product of any two different solutions in the following form:

$$((A,B)) = -1/2 \; i \int d^3r \; \epsilon(r,t)[A\partial B^*/\partial t - B^* \partial A/\partial t]. \qquad (11)$$

It is essential that the dielectric permittivity is a real function, i.e. the medium is assumed lossless. Besides, the vector potential has to turn into zero at the surfaces confining the integration domain. The case of moving boundaries (considered in Ref.11) is included to general situation automatically.

Suppose that before some instant of time (let it be t=0) both the medium and the boundaries were time-independent. Then solutions of (4) could be factorized:

$$A(r,t) = g(r)exp(-i\omega t),\tag{12}$$

$$rot[1/\mu(r)\ rotg] - \omega^2/c^2\ \varepsilon(r)g = 0.\tag{13}$$

The scalar product (11) was proportional to the usual scalar product:

$$((A,B)) = 1/2(\omega_a + \omega_b)exp[i(\omega_b-\omega_a)t](g_b,g_a),\tag{14}$$

$$(g_b,g_a) = \int d^3r\ \varepsilon(r)g_b{}^*g_a.\tag{15}$$

But it is known that solutions of eq.(13) form the complete orthogonal with respect to scalar product (15) set of vector functions. Therefore any real vector field can be decomposed over this set of functions:

$$A(r,t) = \Sigma[a_N g_N(r)exp(-i\omega_N t) + a_N{}^*g_N{}^*(r)exp(i\omega_N t)].\tag{16}$$

Comparing (14) and (15) we can see that the basis functions can be normalised in such way that they will satisfy the relations

$$((A_N,A_M)) = \delta_{NM},\qquad\qquad ((A_N,A_M{}^*)) = 0.\tag{17}$$

After the instant when the properties of the medium became time-dependent the basis functions change their explicit expressions, but the scalar products (17) will not change, and instead of (16) we can write the decomposition

$$A(r,t) = \Sigma[a_N A_N(r,t) + a_N{}^*A_N{}^*(r,t)].\tag{18}$$

Then we proclaim the (time-independent) coefficients of this expansion operators satisfying bosonic commutation relations and thus obtain the quantized field from a classical one.

If in some time the medium will become again time-independent then the physical states will be described with monochromatic mode functions of the type (12), which will not coincide in general with the basis functions of expansion (18). Therefore we will have two different expansions of the field operator: expansion (18) over the states corresponding to the physical photons in remote past and expansion like (16) over the physical states ari-

sing in future. Designating the "physical" states with the super-
script "zero", we can expand each set of basis functions into
a series with respect to another one:

$$A_N = \sum_M [\alpha_{NM} A_M^{(0)} + \beta_{NM} A_M^{(0)*}].$$ (19)

The corresponding expansion of "new" creation and annihilation
operators over the set of "old" ones is as follows:

$$\hat{a}_M^{(0)} = \sum_N [\hat{a}_N \alpha_{NM} + \hat{a}_N^+ \beta_{NM}^*].$$ (20)

The initial state of the quantized field was determined with res-
pect to the set of "old" operators (without the superscript
"zero"). Then using expansion (20) we can calculate all quantum
statistical characteristics of the field in the final state. Tak-
ing into account conditions (17) and the evident properties of
the scalar product (11)

$$((A,B)) = ((B,A))^* = -((B^*,A^*))$$ (21)

one can express the coefficients of expansions (19) or (20) as
follows:

$$\alpha_{NM} = ((A_N, A_M^{(0)})), \qquad \beta_{NM} = ((A_N^*, A_M^{(0)}))^*.$$ (22)

The quantization scheme sketched above can be applied to the
most general situation of an arbitrary space-time nonuniform me-
dium and moving boundaries. However, the explicit calculation of
the mode functions and coefficients of the canonical transforma-
tion (20) can be performed only for rather simple special cases.
The first of them corresponds to the media with factorized elect-
ric and magnetic permittivities:

$$\epsilon(r,t) = \bar{\epsilon}(r)\chi(t), \qquad \mu(r,t) = \bar{\mu}(r)\nu(t)$$ (23)

(the boundaries do not move). Then mode functions can be also
sought for in a factorized form:

$$A(r,t) = g(r)\xi(t) \qquad D(r,t) = \bar{\epsilon}(r)g(r)\eta(t).$$ (24)

Let us demand the function $g(r)$ to satisfy the following equation

$$rot(1/\bar{\mu} \; rotg) = k^2\bar{\epsilon}(r)g, \qquad k = const.$$ (25)

Then eqs.(2) and (4) result in the following ordinary differenti-
al equations for time-dependent factors of the vector potential
and electric displacement:

$$\dot{\eta} = k^2 c\xi/\nu(t) \qquad \dot{\xi} = -c\eta/\chi(t)$$ (26)

Eqs.(26) resemble equations of motion of an oscillator with time-
dependent mass and frequencies. The role of generalized coordi-
nate is played by the electric displacement time-dependent fac-
tor, while the vector potential time-dependent factor plays the

role of generalised momentum. Eqs. (26) can be replaced by the following second-order differential equation:

$$\ddot{\eta} + \gamma(t)\dot{\eta} + \Omega^2(t)\eta = 0, \quad \gamma = \dot{\nu}/\nu, \quad \Omega^2 = k^2c^2/\nu(t)\chi(t). \quad (27)$$

We shall consider the field inside a resonator. Then solutions of eq.(25) can be chosen real vector functions satisfying the orthogonality conditions:

$$\int d^3r \; \varepsilon(r)g_K(r)g_L(r) = k^2\delta_{KL}. \quad (28)$$

Complex solutions of eq.(27) can be normalized as follows:

$$\nu(t) \, [\dot{\eta}\eta^* - \dot{\eta}^*\eta] = -2i. \quad (29)$$

This means that we choose the solution of eq.(27) in the stationary case in the form of

$$\eta_0(t) = (\nu_0\Omega_0)^{-1/2}exp(-i\Omega_0 t). \quad (30)$$

Due to (28) coefficients (22) are not equal to zero only for coinciding indices (intermode interactions are absent), so we can omit the indices. Taking into account eqs.(11),(26),(30) one can represent these coefficients as follows:

$$\alpha = 1/2(\nu_0/\Omega_0)^{1/2}(\Omega_0\eta + i\dot{\eta})exp(i\Omega_0 t) \quad (31)$$

$$\beta = 1/2(\nu_0/\Omega_0)^{1/2}(\Omega_0\eta - i\dot{\eta})exp(i\Omega_0 t). \quad (32)$$

Let us introduce the quadrature components and their variances as follows:

$$\hat{X}_1 = (2)^{-1/2}(\hat{a}_0 + \hat{a}_0^*) \qquad \hat{X}_2 = i(2)^{-1/2}(\hat{a}_0^* - \hat{a}_0) \quad (33)$$

$$\sigma_{IJ} = 1/2\langle\hat{X}_I\hat{X}_J + \hat{X}_J\hat{X}_I\rangle - \langle\hat{X}_I\rangle\langle\hat{X}_J\rangle. \quad (34)$$

Suppose for simplicity that initially the field was in the coherent quantum state. Taking into account eq.(20) one can easily obtain the following expressions:

$$\sigma_{11} = 1/2|\alpha+\beta|^2 = 1/2\nu_0\Omega_0|\eta|^2, \quad (35)$$

$$\sigma_{22} = 1/2|\alpha-\beta|^2 = 1/2\nu_0\Omega_0^{-1}|\dot{\eta}|^2, \quad (36)$$

$$\sigma_{12} = Im(\alpha\beta^*) = 1/2\nu_0 Re(\dot{\eta}\eta^*). \quad (37)$$

We see that time-dependent medium transforms an initially coherent state to a "correlated quantum state" characterized by a nonzero covariance (37) and unequal variances (35) and (36).

This state minimizes the generalized uncertainty relation by Schrodinger and Robertson (Refs.12,13):

$$\sigma_{11}\sigma_{22} - \sigma_{12}^2 \geqslant 1/4 \qquad (38)$$

(*the equality takes place in the case under study due to eq. (29)). For the detailed review of various forms of uncertainty relations see (Ref.14). Properties of correlated and squeezed quantum states were investigated in (Refs.15-19).*

Let us consider as an example the case of a parametric excitation when the properties of the medium harmonically oscillate with twice frequency with respect to some (resonance) mode. This can be achieved, for example, by means of changing the density of the medium. Since the magnetic effects are extremely weak, we can write

$$\Omega^2(t) = \Omega_0^2 \, (1 + \text{æcos}2\Omega_0 t), \qquad \gamma = 0. \qquad (39)$$

We look for the solution of eq.(27) in the form

$$\eta(t) = (\nu_0\Omega_0)^{-1/2} \, [u(t)exp(i\Omega_0 t) + v(t)exp(-i\Omega_0 t)] \qquad (40)$$

with slowly varying time dependent amplitudes. Substituting (39) and (40) into (27) and performing averaging over fast oscillations we arrive at the equations (neglecting the second order derivatives of slowly varying amplitudes)

$$\dot{u} = i\Omega_0 \text{æ} v/4, \qquad\qquad \dot{v} = -i\Omega_0 \text{æ} u/4 \qquad (41)$$

whose solutions are

$$u(t) = cosh(\Omega_0 \text{æ} t/4), \qquad v(t) = -i \, sinh(\Omega_0 \text{æ} t/4). \qquad (42)$$

The variances (35),(36) oscillate with the twice resonance frequency, but their ratio (the so called squeezing coefficient) is confined at every instant between the values

$$exp(-\Omega_0 \text{æ} t) \leqslant \Omega_0^2\sigma_{11}/\sigma_{22} \leqslant exp(\Omega_0 \text{æ} t). \qquad (43)$$

Certain inequalities for the squeezing coefficients can be found for arbitrary time dependence of the frequency in eq.(27). Considering again nonmagnetic medium one can prove the unequalities (Refs.19,20)

$$[(1-R^{1/2})/(1+R^{1/2})]^2 \leqslant \Omega_0^2\sigma_{11}/\sigma_{22} \leqslant [(1+R^{1/2})/(1-R^{1/2})]^2 \qquad (44)$$

where R is the energy reflection coefficient from the effective potential barrier corresponding to eq.(27).

We would like to emphasize once again that we have used the Heisenberg picture for the description of the quantized electromagnetic field. However, since for a factorizable medium (23) Maxwell's equations can be derived from the Hamiltonian (8) or (10), the Schrodinger description is also possible in this case. We shall illustrate it for the most simple case when

$$\nu(t) = 1, \qquad \chi = \chi(ht), \quad \chi(0) = 1. \tag{45}$$

Here h is a characteristic frequency of the medium properties changing. The method used below can be easily applied to a more general case. Let $c = 1$ and the dimensionless time $t_0 = kt$. So (27) results in

$$\ddot{\eta} + \omega^2(\text{æ}t_0)\eta = 0, \tag{46}$$

where
$$\omega^2(\text{æ}t_0) = \omega^2(ht) = 1/\chi(ht), \qquad \text{æ} = h/k. \tag{47}$$

The quantization of a harmonic oscillator with a variable frequency is done by introducing integrals of motion operators (Ref. 17):

$$\hat{a}(t_0) = i(2)^{-1/2} (y(t_0)\hat{\xi} - \dot{y}(t_0)\hat{\eta}), \quad \hat{a}^+(t_0) = [\hat{a}(t_0)]^+. \tag{48}$$

Here $y(t_0)$ is a "ruling solution" of eq.(46) satisfying the time-independent condition

$$\dot{y}(t_0)y^*(t_0) - \dot{y}^*(t_0)y(t_0) = 2i \tag{49}$$

to ensure the following commutation relation

$$[\hat{a}(t_0), \hat{a}^+(t_0)] = 1. \tag{50}$$

We want to stress the difference in signs of right-hand sides of (29) and (49) due to the difference between Heisenberg and Schrodinger pictures. For the integrals of motion to coincide at $t_0 = 0$ with creation and annihilation operators, it is necessary (in accordance with (49)) to choose the initial conditions

$$y(0) = 1, \qquad\qquad \dot{y}(0) = i. \tag{51}$$

After the instant $t_0 = t_F$, when the medium properties stop changing, "new" creation and annihilation operators are to be introduced:

$$\hat{a}_{(0)} = i(2\omega(t_F))^{-1/2} (\hat{\xi} - i\hat{\eta}\omega(t_F)). \tag{52}$$

Then the expansion of "new" operators over "old" ones is

$$\hat{a}_{(0)} = \alpha\hat{a}(t_F) + \beta\hat{a}^+(t_F) \tag{53}$$

and we can get

$$\beta(t_F) = 1/2 (\omega(t_F))^{-1/2} (\omega(t_F)y(t_F) + i\dot{y}(t_F)). \tag{54}$$

Creation and annihilation operators mixing results in a change of occupation numbers in a given mode. Generation of photons from vacuum due to the medium properties change is worth considering. If at $t_0 = 0$ the number of photons was zero then at an instant t_0

>0 *the average number of photons is*

$$\bar{n} = \beta^*(t_0)\beta(t_0). \tag{55}$$

Yablonovitch (Ref.21) stated that photons will have a thermal distribution at a temperature proportional to the rate of the medium properties change , i.e. proportional to h. Then for high photon energies (proportional to k) there will be

$$\bar{n} \sim exp(-const\ k/h). \tag{56}$$

The solution of (39) at a little t_0 can be found for an arbitrary law of change of $\chi(t)$. At $t_0 = 0$ we shall have

$$d/dt_0\ ((\omega)^{1/2}\ \beta) = 1/2\ d\omega((\mathit{æ}t_0))/dt_0 \tag{57}$$

$$\beta \sim t_0/2\ d(\omega(\mathit{æ}t_0))/dt_0 \tag{58}$$

$$t \rightarrow 0$$

$$\bar{n} \sim (t/2\ d(\omega(ht))/dt). \tag{59}$$

For any instant t a decomposition of the solution can be found in the limit $\mathit{æ} \rightarrow 0$ (for high photon frequencies) by means of the method of multy-scale asymptotic decompositions (Ref.22) for an arbitrary law of change:

$$y = (\omega(\mathit{æ}t_0))^{-1/2}\ \{\ exp(is) + \mathit{æ}\ [E(\mathit{æ}t_0)exp(is) +$$

$$+ F(\mathit{æ}t_0)exp(-is)] + \ldots \} \tag{60}$$

where

$$s = 2/\mathit{æ}\ [exp(\mathit{æ}t_0/2) - 1] \tag{61}$$

and functions E and F are determined by

$$F = const$$

$$dE/d(\mathit{æ}t_0) = -i/(4\omega^2)\ d^2\omega/d(\mathit{æ}t_0)^2 + \tag{62}$$

$$+ i3/(8\omega^3)\ [d\omega/d(\mathit{æ}t_0)]^2$$

with initial conditions

$$E(0) + F(0) = 0, \qquad i\ (E(0) - F(0)) = 1/2\ d\omega/d(\mathit{æ}t_0). \tag{63}$$

For the case $\chi = exp(-ht)$, which approximately describes dielectric permittivity falling achievable in experiments (Ref.21), one can find the exact solution — a linear combination of two Hankel's functions $H_0^{(1)}[2/\mathit{æ}\ exp(\mathit{æ}t_0/2)]$ and $H_0^{(2)}[2/\mathit{æ}\ exp(\mathit{æ}t_0/2)]$. Nevertheless an asymptotic decomposition is still more useful and can be expressed in an explicit form:

$$y = exp(-\mathit{æ}t_0/4)exp(is) + \mathit{æ}\ exp(-\mathit{æ}t_0/4)\ \{\ (-i/16) \times$$

$$\times\ [1 + exp(-\mathit{æ}t_0/2)]exp(is) + i/8\ exp(-is)\ \} + \ldots \tag{65}$$

Now we have

$$\beta = i\text{æ}/8 \; [exp(-is) - exp(-\text{æ}t_0/2)exp(is)] \tag{66}$$

and the number of photons

$$\bar{n} = \text{æ}^2/64 \; [1 + exp(-\text{æ}t_0) - 2cos(2s)exp(-\text{æ}t_0/2)] \tag{67}$$

This number oscillates with a growing frequency and a decreasing amplitude and in the limit $t_0 \rightarrow \infty$ tends to a constant

$$\bar{n} \rightarrow h^2/64k^2. $$

As we can see it is not in agreement with the statement (38) from (Ref.21). The energy of photons in the mode is

$$\bar{n}\omega k \rightarrow h^2/64k \; exp(ht/2), \qquad t \rightarrow \infty \tag{69}$$

and it grows without a limit. Also at any time the sum of energies of all modes diverges. This can be explained by the fact that it is impossible to decrease dielectric permittivity to zero for nondispersive media; thus the assumption that it does not depend on a frequency is not valid for high frequencies. In the other limit $\text{æ} = h/k \rightarrow \infty$ we introduce another dimensionless time $t_1 = \text{æ}t_0$. The solution expansion over $\theta = 1/\text{æ}$ (not valid for large t_1) is

$$y = 1 + \theta i t_1/2 + \theta^2/4 \; [t_1 + 1 - expt_1] + \ldots \tag{70}$$

and the first term for the number of photons does not depend on the mode frequency:

$$\beta = exp(t_1/2) - 1 + \theta i/2 \; [t_1 exp(t_1/2) + 1 - expt_1] \tag{71}$$

$$\bar{n} = 1/2 \; [cosh(ht/2) - 1]. \tag{72}$$

Another example of time dependent resonator which can be solved is an empty resonator with a moving ideal wall. Moore (Ref. 11) proposed the following complete orthonormal set of solutions (in the special case of a single space dimension, i.e. confining with the modes with linear polarisation parallel to the wall surface):

$$A_N(x,t) = (4\pi N)^{-1/2}\{exp[-i\pi NR(t-x)] - exp[-i\pi NR(t+x)]\} \tag{73}$$
$$(c = 1).$$

These functions depend on the solution of the functional equation ($L(t)$ is the position of the moving wall, another wall is assumed to be at rest)

$$R(t+L(t)) = R(t-L(t)) +2. \tag{74}$$

An approximate solution of this equation in the case of the small velocities of the wall was found by Moore (Ref.11) and later used in (Refs.23,24). However, that solution is not valid in the case of parametric resonance, when

$$L(t) = L_0[1 + a\,sin(2\Omega_0 t)], \quad |a|<<1, \quad \Omega_0 = \pi/L_0 \qquad (75)$$

(the resonance at the lowest resonator eigenfrequency). The corresponding solution for small values of the percentage modulation was found in (Ref.25):

$$R(\xi) = \xi/L_0 \{1 - a\,sin(2\Omega_0\xi) + a^2[sin^2(\Omega_0\xi) + \\ + 1/4\Omega_0\xi\,sin(2\Omega_0\xi)] + ...\}. \qquad (76)$$

Eqs.(11),(22),(45) result in the following expressions for the transformation coefficients (21):

$$\left.\begin{matrix}\alpha_{NM}\\ \\ \beta_{NM}\end{matrix}\right\} = 1/2\ (M/N)^{1/2} \int_{t/L_0-1}^{t/L_0+1} exp\{i\pi[-NR(L_0 x)\pm Mx]\}dx. \qquad (77)$$

The calculations are rather simple for not very large values of time, when the second-order correction in (76) remains small. Then the following simple formula for variances can be found (Ref.25):

$$\left.\begin{matrix}\sigma_{11}\\ \\ \sigma_{22}\end{matrix}\right\} = 1/2exp(\pm1/2\ \pi aN), \quad N>>1, \quad |aN|<<1 \qquad (78)$$

where N is the number of semiperiods of wall's vibrations. One can check that the maximum squeezing coefficients given by eqs. (43) and (78) coincide for equal values of percentage modulation in two different methods of exciting the field via the parametric resonance.

Now let us consider the long-time asymptotics for the R-function under the condition $\varepsilon/L_0 << 1$, $\varepsilon t >> L_0^2$ for an arbitrary periodic motion of the wall $L(t) = L_0 + \varepsilon f(t)$. We shall choose the solution of eq.(74) in the following form:

$$R(t) = \sum_{N=0}^{\infty} \varepsilon^N R_N(t). \qquad (79)$$

Substituting expansion (79) to eq.(74) we attain

$$\sum_{N=0}^{\infty} \varepsilon^N R_N[t+L_0+\varepsilon f(t)] = \sum_{N=0}^{\infty} \varepsilon^N R_N(t-L_0-\varepsilon f(t)) + 2.$$

Developing both sides of this equation into power series we have

$$\sum_{N=0}^{\infty}\sum_{K=0}^{\infty} \varepsilon^N R_N^{(K)}(t+L_0)\varepsilon^K f^K(t)/K! = \sum_{N=0}^{\infty}\sum_{K=0}^{\infty} \varepsilon^N R_N^{(K)}(t-L_0) \times \\ \times (-1)^K \varepsilon^K f^K(t)/K! + 2.$$

It is convenient to use another summation index $M=N+K$:

$$\sum_{M=0}^{\infty}\sum_{K=0}^{M}\varepsilon^M[R_{M-K}^{(K)}(t+L_0) - (-1)^K R_{M-K}^{(K)}(t-L_0)]f^K(t)/K! = 2.$$

From this equation we obtain the following system of equations for the functions $R_M(t)$ $(M=0,1,\ldots)$:

$$\sum_{K=0}^{M}[R_{M-K}^{(K)}(t+L_0)-(-1)^K R_{M-K}^{(K)}(t-L_0)]f^K(t)/K! = 2\delta_{M0}. \qquad (80)$$

Further we consider the simplest law of motion (75) with $\varepsilon = aL_0$ and the frequency $\omega_0 = Q\Omega_0$. We use the Fourier-transformation method to solve eq.(80):

$$\mathcal{F}(\omega) = \int exp(i\omega t)f(t)dt, \qquad f(t) = \int exp(-i\omega t)\mathcal{F}(\omega)d\omega/2\pi,$$

$$1/2\pi \int exp(iw\tau)dt = \delta(\omega),$$

$$\int exp(i\omega t)f(t+L_0)dt = exp(-i\omega L_0)\mathcal{F}(\omega), \qquad (81)$$

$$\int exp(i\omega t)f^{(N)}(t)dt = (-i\omega)^N \mathcal{F}(\omega).$$

Then we get from (80) the following integral equation:

$$\sum_{N=1}^{M} 1/N! \int d\upsilon(-i\upsilon)^N R_{M-N}(\upsilon) [exp(-i\upsilon L_0)-(-1)^N exp(i\upsilon L_0)] \times$$
$$\times \Phi_{\omega-\upsilon}(sin^N(\omega_0 t)) = 2\pi\delta(\omega)\delta_{M0} \qquad (82)$$

$$\Phi_{\omega}(sin^N \omega_0 t) = \int exp(i\omega t)sin^N(\omega_0 t)dt =$$
$$= 1/(2\pi)^{N-1} \sum_{J=0}^{N} C_N^J (-1)^J \delta(\omega+(N-2J)\omega_0). \qquad (83)$$

Substituting expression (83) to eq.(82) we can easily make integration over υ and arrive at the equation

$$-R_M(\omega)2isin(\omega L_0) = 2\delta_{M0}\delta(\omega) - \sum_{N=1}^{M}\sum_{J=0}^{N}(-1)^{N+J}/2^N C_N^J \times$$
$$\times [\omega+(N-2J)\omega_0]^N R_{M-N}[\omega+(N-2J)\omega_0] \times$$
$$\times [exp(-i\omega L_0)-(-1)^N exp(i\omega L_0)] (-1)^{QN}. \qquad (84)$$

Taking into account the formula for derivatives of δ-function

$$\delta^{(N)}(x) = -N\delta^{(N-1)}(x)/x,$$

one can easily find the expression for $R_0(\omega)$

$$R_0(\omega) = 2\pi\delta'(\omega)/iL_0. \qquad (85)$$

Then making inverse Fourier-transformation we have

$$R_0(t) = t/L_0. \qquad (86)$$

To find the long-time asymptotics we will seek for the solution of eq.(84) in the form of a sum over δ-functions

$$R_M(\omega) = \sum_{K=0}^{M} a_K{}^M \delta^{(M)}(\omega+(M-2K)\omega_0) \qquad (87)$$

This choice corresponds to the representation of the function $R(t)$ in the form of a power series with respect to the parameter $(\varepsilon t/L^2)$ and neglecting terms like $\varepsilon^J t^M$ with $J>N$. Then only terms corresponding to $N=1$ are significant in eq.(84):

$$-R_N(\omega)2i\sin(\omega L_0) = 2\delta_{N0}\delta(\omega) + (-1)^0 \cos(\omega L_0) \times$$

$$\times \; [(\omega+\omega_0)R_{N-1}(\omega+\omega_0) - (\omega-\omega_0)R_{N-1}(\omega-\omega_0)]. \qquad (88)$$

Taking into account the expression for $R_0(\omega)$ (85) we get

$$R_1(\omega) = 2\pi(-1)^0/2L_0 \; \cotan(\omega L_0) \; [(\omega+\omega_0)\delta'(\omega+\omega_0) -$$

$$- (\omega-\omega_0)\delta'(\omega-\omega_0)] = 2\pi(-1)^0 \; [\delta'(\omega+\omega_0) - \delta'(\omega-\omega_0)]/2L_0{}^2. \qquad (89)$$

With respect to expansion (87) we have

$$a_0{}^0 = 2\pi/iL_0, \qquad a_0{}^1 = -a_1{}^1 = 2\pi(-1)^0/2L_0{}^2.$$

Substituting expansion (87) we obtain the following recurrence relation for $N\geqslant 2$

$$a_K{}^N = (-1)^0 i\omega_0/2NL_0 \; [(N-2K-1)a_K{}^{N-1} - (N-2K+1)a_{K-1}{}^{N-1}]. \qquad (90)$$

Let us introduce the notation $a_K{}^{2M} = i\bar{a}_K{}^{2M}$, $\bar{a}_K{}^{2M+1} = a_K{}^{2M+1}$, then

$$N\bar{a}_K{}^N = (-1)^N \alpha[\bar{a}_K{}^{N-1}(N-2K-1) - \bar{a}_{K-1}{}^{N-1}(N-2K+1)],$$
$$\alpha = (-1)^0 \omega_0/2L_0. \qquad (91)$$

Making inverse Fourier-transformation of (87) we get $(N\geqslant 2)$:

$$R_N(t) = 1/2\pi \sum_{K=0}^{N} a_K{}^N \; (it)^N \exp(it(N-2K)\omega_0)$$

Then it is easy to see that we have got the same expression for $R_1(t)$ that was given in eq.(76). Now we consider the sum

$$\Phi(t) = \sum_{N=2}^{\infty} \varepsilon^N R_N(t) = \sum_{N=2}^{\infty} \varepsilon^N(it)^N \sum_{K=0}^{N} a_K{}^N \exp(it\omega_0(N-2K))p^K/2\pi \qquad (92)$$

for $p=1$. Taking into account the evident symmetry condition $\bar{a}_K{}^N = -\bar{a}_{N-K}{}^N$ we obtain

$$\Phi = 2\sum_{N=2}^{\infty} z^N(-1)^n \sum_{K=0}^{n} \bar{a}_K{}^N \sin(\omega_0(N-2K)t)p^K/2\pi, \qquad z = \varepsilon t, \qquad (93)$$

where $n=[N/2]$ and $[\;]$ is the entire part of a number. Taking into account that $(-1)^n = (-1)^{N(N-1)/2}$ we introduce the notation $\Phi = -2ImF$. With the help of the recurrence relation (91) we get the differential equation for the function F

$$\partial F/\partial z = \alpha[p\exp(-i\omega_0 t) - \exp(i\omega_0 t)][z\partial F/\partial z - 2p\partial F/\partial p +$$

210

$$+ (z\alpha/\pi Q)exp(i\omega_0 t)] \qquad (94)$$

with the initial condition $F(z=0,p) = 0$. Its solution is

$$F = -(z\alpha/\pi Q)exp(i\omega_0 t) + \Psi,$$

where Ψ satisfies the equation

$$\partial\Psi/\partial z = \alpha[pexp(-i\omega_0 t) - exp(i\omega_0 t)][z\partial\Psi/\partial z -$$
$$- 2p\partial\Psi/\partial p] + (\alpha/\pi Q)exp(i\omega_0 t). \qquad (95)$$

The particular solution of this equation is as follows:

$$\Psi_0 = -(1/2\pi Q) \, ln[pexp(-i\omega_0 t)/(pexp(-i\omega_0 t) -$$
$$-exp(i\omega_0 t))]. \qquad (96)$$

Then the general solution of eq.(95) is the sum of Ψ_0 and an arbitrary solution of the uniform equation (95) with $b=0$. The uniform equation has the first integral:

$$C = exp(-i\omega_0 t/2) \{zp^{1/2} - 1/2\alpha \, ln[(p^{1/2}exp(-i\omega_0 t/2)-$$
$$-exp(i\omega_0 t/2))/(p^{1/2}exp(-i\omega_0 t/2)+exp(i\omega_0 t/2))]\}.$$

Then we get the general solution of eq.(95) in the form of $\Psi = \Psi_0 + f(C)$, where $f(C)$ is an arbitrary function of the first integral. From the condition $\Psi(z=0) = 0$ we can determine the form of the function f:

$$f(x) = (1/2\pi Q) \, ln\{[1+exp(-2\alpha exp(i\omega_0 t/2)x)]^2/$$
$$/4exp(-2\alpha exp(i\omega_0 t/2)x)\}.$$

After some algebraic transformations we find the function Ψ

$$\Psi = -(1/2\pi Q) \, ln\{4pexp(-i\omega_0 t)exp(-2\alpha z)/[cos(\omega_0 t/2) +$$
$$+ 2isin(\omega_0 t/2)exp(-2\alpha z)]^2\}.$$

Taking into account the first and the second terms of the expansion of $R(t)$ in a set of εt we obtain the final expression:

$$R(t) = t/L_0 - (2/\pi Q) \, Im \, ln[1 + \xi + exp(i\omega_0 t)(1-\xi)], \qquad (97)$$

where a notation $\xi = exp[(-1)^{0+1}\omega_0 \varepsilon t/L_0]$ is introduced. Now we can compute some characteristics of the electromagnetic field in a cavity in the presumption $\varepsilon t/L_0^2 >> 1$, $\varepsilon << L_0$. Let us evaluate the number of photons which will be generated in the resonator with moving walls in the long time limit. For this purpose we must evaluate the integral (77)

$$\beta_{NM} = 1/2 \, (M/N)^{1/2} \int_{N-1}^{N+1} exp[-i\pi((M+N)x+Nf(x))],$$

where the function $f(x)$ is given by (97):

211

$$f(x) = -2/\pi Q \; Im \; ln[1+\xi+exp(i\pi Qx)(1-\xi)].$$

Let us consider the case when $Q=2p$ is an even number, then $\xi \ll 1$. Due to $\varepsilon x/L_0 \ll 1$ we can consider $f(x)$ as a periodical function with the period of oscillations $T=2/Q$. Then

$$\left.\begin{array}{c}\beta_{NM}\\ \alpha_{NM}\end{array}\right\} = (M/N)^{1/2} \sum_{K=0}^{Q-1} exp[-i\pi(N\pm M)2K/Q] \int_{N-1}^{N-1+2/Q} exp[-i\pi \times$$

$$\times \; ((N\pm M)x+Nf(x))]dx. \tag{98}$$

Analyzing the structure of $f(x)$ we can approximate it by three linear functions as follows:

$$f(x) = \begin{array}{ll} -(1-\delta Q)(x-N+1), & N-1 < x < N-1+1/Q-\delta, \\ (1/Q-2\delta)(x-N+1-1/Q)/\delta, & N-1+1/Q-\delta < x < N-1+1/Q+\delta, \\ -(1-\delta Q)(x-N+1-2/Q), & N-1+1/Q+\delta < x < N-1+2/Q, \end{array}$$

$$\delta = 2\xi^{1/2}/\pi q.$$

Then one can easily calculate integrals in (98) and obtain the general expression for the coefficients α_{NM} and β_{NM}

$$\alpha_{NM} = 2(M/N)^{1/2}(-1)^{(N-1)(N-M)}/[\pi(\delta NQ-M)] \; sin[(\delta NQ-M)\pi/Q] \times$$

$$\times \; exp[i\pi(N-M)(Q-1)/Q] \; sin[\pi(N-M)]/sin[\pi(N-M)/Q],$$

$$\beta_{NM} = 2(M/N)^{1/2}(-1)^{(N-1)(N+M)}/[\pi(\delta NQ+M)] \; sin[(\delta NQ+M)\pi/Q] \times$$

$$\times \; exp[i\pi(N+M)(Q-1)/Q] \; sin[\pi(N+M)]/sin[\pi(N+M)/Q]. \tag{99}$$

Hereafter we consider only the main resonance of $Q=2$. After some algebraic transformations we get the following expression for the coefficient $|\beta_{NM}|^2$:

$$|\beta_{NM}|^2 = 4M/(N\pi^2) \; [1-(-1)^M cos(2N\delta\pi)] \; [1+(-1)^{M+N}]/$$

$$/(M+2N\delta)^2. \tag{100}$$

To find the total number of photons in the mode with number M we need to calculate the sum over N. First, let us evaluate the following auxiliary sum:

$$S(z,x) = \sum_{N=1}^{\infty} cos(xN)/[N(z+N)^2], \tag{101}$$

where $x=2\delta\pi \ll 1$ and $z=M/2\delta \gg 1$. Then we have

$$S(z,x) = \int_0^\infty y \sum_{N=1}^{\infty} cos(Nx)exp[-y(z+N)]/N \; dy =$$

$$= 1/z^3 - 1/2 \int_0^\infty y \, exp(-zy)ln(2coshy-2cosx) \; dy. \tag{102}$$

Since $x \ll 1$ and the main region of integration $y \lesssim 1/z \ll 1$, we can expand $coshy$ and $cosx$ into power series of y and x. Thus up to the second order terms we have

$$S(z,x) = 1/z^3 - 1/2 \int_0^\infty y\,exp(-zy)\ln(y^2+x^2)\,dy. \qquad (103)$$

The last integral can be easily evaluated, if one takes into account the inequalities $y \lesssim 1/z << x << 1$. Therefore

$$S(z,x) = -\ln x/z^2 + O(z^{-3}). \qquad (104)$$

The similar sum (see (100))

$$\sum_{N=1}^\infty cos(Nx)/[N(z+N)]\,(-1)^N$$

can be obtained from (102) by means of the replacement $x \to x+\pi$. Then we have in (103) $\ln(4+y^2-x^2) < \ln|x^2|$ for $x<<1$ and $y<<1$, so that the corresponding terms can be omitted. The main contribution to the sum due to the first term (with unity in the numerator) in expression (100) is proportional to

$$S(z,0) = -\int_0^\infty y\,exp(-yz)\ln[1-exp(-y)] \approx \ln z/z^2. \qquad (105)$$

Thus the number of photons generated in the M-th mode is

$$P_M = \sum_{N=1}^\infty |\beta_{MN}|^2 \approx 4[\ln(M/2\delta)-(-1)^M\ln(1/2\delta\pi)]/(M\pi^2). \qquad (106)$$

Since in the considered case $(Q=2)$ $\delta(t)=exp(-\pi\epsilon t/L_0^2)/\pi$, we get the following rate of photon generation for $\epsilon t/L_0^2 >> 1$:

$$dP_M/dt = 4a\Omega_0[1-(-1)^M]/(\pi^2 M). \qquad (107)$$

Here $\Omega_0 = \pi/L_0$ is the main eigenfrequency of the resonator, $a=\epsilon/L_0$ is the dimensionless amplitude of oscillations of the wall (which vibrates at the frequency $2\Omega_0$). Eq. (107) is valid in fact only for not very large numbers of excited modes M (due to limitations arising in approximations made before). Besides, in real situation we should limit the time t by the relaxation time of the resonator τ (due to the dissipation on the walls). Then the maximum number of photons generated in the M-th mode equals approximately

$$P_M^{MAX} \sim 4/(\pi^2 M)\,[2aQ(M)/M + O(\ln(M+1))], \qquad (108)$$

where $Q(M)$ is the quality factor of the resonator's M-th mode. This formula is valid provided $aQ/M >> \ln(M+1)$.

REFERENCES

1. Jauch,J.M., and K.M.Watson, 1948, "Phenomenological Quantum Electrodynamics", Phys.Rev., 74(8), pp. 950-957.
2. Ginzburg,V.L., 1975, "Theoretical Physics and Astrophysics", Nauka, Moscow.
3. Carniglia,C.K., and L.Mandel, 1971, "Quantization of Evanescent Electromagnetic Waves", Phys.Rev. D, 3(2), pp. 280-296.
4. Ujihara,K., 1975, "Quantum Theory of One-Dimensional Optical Cavity with Output Coupling. Field Quantization", Phys.Rev. A,

12(1), pp. 148-158.
5. Abram,I., 1987, "Quantum Theory of Light Propagation: Linear Medium", Phys.Rev. A, 35(11), pp. 4661-4672.
6. Shen,Y.R., 1967, "Quantum Statistics of Nonlinear Optics", Phys.Rev., 155(3), pp. 921-931.
7. Knoll,L., W.Vogel and D.-G.Welsh, 1987, "Action of Passive, Lossless Optical Systems in Quantum Optics", Phys.Rev. A, 36(8), pp. 3803-3818.
8. Drummond,P.D., 1990, "Electromagnetic Quantization in Dispersive Inhomogenious Nonlinear Dielectrics", Phys.Rev. A, 42(11), pp. 6845-6857.
9. Glauber,R.J. and M.Lewenstein, 1991, "Quantum Optics of Dielectric Media", Phys.Rev. A, 43(1), pp. 467-491.
10. Bialynicka-Birula,Z., and I.Bialynicki-Birula, 1987, "Space-Time Description of Squeezing", J.Opt.Soc.Amer. B, 4(10), pp. 621-626.
11. Moore,G.T., 1970, "Quantum Theory of the Electromagnetic Field in a Variable-Length One-Dimensional Cavity", J.Math. Phys., 11(9), pp. 2679-2691.
12. Schrodinger,E., 1930, "Zum Heisenbergschen Unscharfeprinzip", Ber.Kgl.Akad.Wiss., Berlin, pp. 296-303.
13. Robertson,H.P., "A General Formulation of the Uncertainty Principle and Its Classical Interpretation", Phys.Rev., 35(5), p. 667.
14. Dodonov,V.V., and V.I.Man'ko, 1989, "Generalization of the Uncertainty Relations in Quantum Mechanics", Proceedings of the Lebedev Physics Institute, vol. 183, Nova Science, Commack, USA, pp. 3-101.
15. Dodonov,V.V., E.V.Kurmyshev and V.I.Man'ko, 1980, "Generalized Uncertainty Relation and Correlated Coherent States", Phys.Lett. A, 79(2,3), pp. 150-152.
16. Dodonov,V.V., E.V.Kurmyshev and V.I.Man'ko, 1988, "Correlated Coherent States", Proceedings of the Lebedev Physics Institute, vol. 176, Nova Science, Commack, USA, pp. 169-199.
17. Dodonov,V.V., and V.I.Man'ko, 1989, "Invariants and Correlated States of Nonstationary Quantum Systems", Proceedings of the Lebedev Physics Institute, vol. 183, Nova Science, Commack, USA, pp. 103-261.
18. Dodonov,V.V., O.V.Man'ko and V.I.Man'ko, 1988, "Correlated Coherent States and Radiation of Quantum Systems", Proceedings of the Lebedev Physics Institute, vol. 192, Nauka, Moscow, pp. 204-220.
19. Dodonov,V.V., A.B.Klimov and V.I.Man'ko, 1991, "Physical Effects in Correlated Quantum States", Proceedings of the Lebedev Physics Institute, vol. 200, Nauka, Moscow, pp. 56-105.
20. Dodonov,V.V., A.B.Klimov and V.I.Man'ko, 1989, "Photon Number Oscillations in Correlated Light", Phys.Lett. A, 134(4), pp. 211-216.
21. Yablonovitch,E., 1989, "Accelerated Reference Frame for Electromagnetic Waves in a Rapidly Growing Plasma: Unruh-Fulling-DeWitt Radiation and the Nonadiabatic Casimir Effect", Phys.Rev.Lett., 62(15), pp. 1742-1745.
22. Cole,J.D., 1968, "Perturbation Methods in Applied Mathema-

tics", *Waltham (Mass.): Blaisdell Publ. Co.*

23. Sarkar,S., 1988, "The Response of a Quantum Field to Classical Chaos", *J.Phys. A*, 21(4), pp. 971-980.

24. Sarkar,S., 1988, "Moving Mirrors and Nonclassical Light", in *Photons and Quantum Fluctuations*, E.R.Pike and H.Walther, eds., Adam Hilger, Bristol, pp. 151-172.

25. Dodonov,V.V., A.B.Klimov and V.I.Man'ko, 1990, "Generation of Squeezed States in a Resonator with a Moving Wall", *Phys.Lett. A*, 149(4), pp. 225-228.

RADIATION FORCE ON A SINGLE ATOM IN A CAVITY

M. S. Kim
Physics Department, Sogang University,
CPO Box 1142, Seoul, Korea

ABSTRACT

We consider the radiation pressure microscopically. Two perfectly conducting plates are parallelly placed in vacuum. As the vacuum field hits the plates they get pressure from the vacuum. The excessive outside modes of the vacuum field push the plates together, which is known as the Casimir force. We investigate the quantization of the standing wave between the plates to study the interaction between this wave and the atoms on the plates or between the plates. We show that even the vacuum field pushes the atom to place it at nodes of the standing wave.

INTRODUCTION

Casimir showed that when two perfectly conducting plates are parallelly placed in the vacuum they attract each other [1]. Although there has been considerable interest in the Casimir effect within the field of quantum electrodynamics [2a], it was Milonni et al. who introduced the concept of the radiation pressure from the vacuum field to interpret the Casimir effect [3]. When there is a field of a mode separated by a conducting plate the radiation pressure exerted by the field is same both sides. When the distance between the plates is d, the mode separation is proportional to 1/d. Since less number of modes are accommodated between the plates than outside of the plates the excessive outside modes of the vacuum field push the plates together.

Milonni et al. calculate the vacuum radiation pressure intuitively. In this paper we study the vacuum radiation pressure in a microscopical view point. We briefly review previous works on the Casimir effect followed by a classical study of radiation force exerted by standing waves.

Quantum theory has given various applicabilities of the radiation pressure. Laser trapping and cooling and isotope separation have been realized based on radiation pressure. The radiation pressure can increase, decrease or deflect atomic velocities. Different isotopes of the same atom generally have slightly different electronic transition frequencies. The radiation pressure can be tuned to deflect only one kind of isotope in a mixture. Atoms can be slowed down by radiation pressure of counter propagating laser and the velocity distribution of the atoms is narrowed. This process cools down the atomic kinetic energy. Orthogonal pairs of counter—propagating laser beams are used to trap atoms for long periods of time [2b].

We investigate quantization of standing waves between the plates and find the quantum mechanical form of the Maxwell stress tensor. We then check the principle of momentum conservation in quantum physics. When the field interacts with a two—level atom in the cavity the atom is forced to be placed at nodes of the field. We calculated the size of the vacuum force exerted on the atom.

THE CASIMIR FORCE

This section reviews the work of Milonni et al with appropriate extensions. As shown in Fig. 1, the perfectly conducting plates are parallelly placed in the vacuum. We take the z—axis normal to the plates. When the radiation field strikes the plates with the angle of incidence θ, the pressure exerted by the radiation is the force, which is projected on the plate, divided by the area of incidence. Applying Gauss's law we find that the normal component of force per area is the energy per volume of the incident field. The radiation field is totally reflected by the perfectly conducting plates. The field between the plates propagates either to or from the plate so that the photon pressure on the plate is a half the photon energy. Thus the radiation pressure from a mode of the vacuum field is

$$P = \frac{\hbar\omega}{2V}\cos^2\theta \tag{1}$$

where ω is the frequency of the mode and V the quantization volume. When the plates are large enough x— and y—components of the wavevector k take continuous values while $k_z = n\pi/d$, where d is the separation of the plates and n integer. The total outward pressure is the sum of pressure exerted by each mode.

$$P_1 = \frac{\hbar c}{\pi^2 d}\sum\int_0^\infty dk_x\int_0^\infty dk_y\frac{(n\pi/d)^2}{k} \tag{2}$$

where the magnitude of the wavevector

$$k = [k_x^2 + k_y^2 + (n\pi/d)^2]^{\frac{1}{2}}. \tag{3}$$

Considering the modes outside the plates, all the components including the z—component of the wavevector take continuous values so that the total inward pressure is

$$P_2 = \frac{\hbar c}{\pi^3}\int_0^\infty dk_x\int_0^\infty dk_y\int_0^\infty dk_z\frac{k_z^2}{k^2}. \tag{4}$$

The wave vector is now $k = [k_x^2 + k_y^2 + k_z^2]^{\frac{1}{2}}$. The difference between the inward and outward pressure is physically meaningful:

$$P_2 - P_1 = \pi hc/480d^4. \tag{5}$$

The attractive force is inversely—proportional to the fourth order of the separation of the plates. This is the Casimir force in agreement with Power [4].
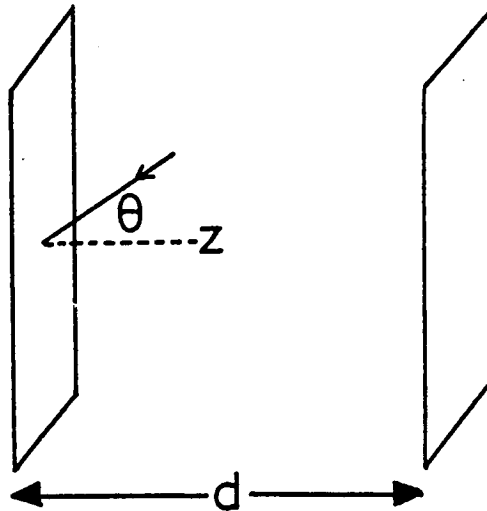
Fig.1 Electromagnetic field incident on one of two perfectly conducting plates separated by distance d.

RADIATION PRESSURE OF CLASSICAL FIELD

We consider the classical field for the quasimicroscopic study of the field—conductor interaction [5]. As shown in Fig.2 the classical electromagnetic field strikes the conducting plate with the angle of incidence θ. Taking the polarization of the electric field on the x—z plane. We write the incident electric field

$$\underline{E} = E_0(x,z,t)\cos\theta\,\underline{x} - E_0(x,z,t)\sin\theta\,\underline{z} \tag{6}$$

and the incident magnetic field

$$H = H_0(x,z,t)\,\underline{y}. \tag{7}$$

The electric field on the x—y plane of the conducting plate is zero thus the x and y components of the electric field is zero while the z—component of the total field on the plate

$$E_z = -2\,E_0(x,z=0,t)\sin\theta. \tag{8}$$

The total magnetic field is then

$$H_y = 2\,H_0(x,0,t). \tag{9}$$

When normal incidence is concerned, $E_z = 0$ and $H_y = 2H_0$. This is obvious from the property of the standing wave that the electric field meets the conducting plate at its node while the magnetic field sees the plate at its peak.

The z—component of the electric field attracts electric charges which causes the surface charge density

$$\epsilon_0 \cdot 2E_0 \sin\theta. \tag{10}$$

In the interior of the conductor there is certain charge flow due to the magnetic field. The current density is

$$\underline{\nabla} \times \underline{H}. \tag{11}$$

The charge and current cause the Lorentz force from the radiation field on the plate. The force per area on charges

$$P_e = -2\epsilon_0 E_0{}^2\sin^2\theta \tag{12}$$

and that on current

$$P_j = \int_0^\infty dz[(\underline{\nabla} \times \underline{H}) \times \underline{B}]_z. \tag{13}$$
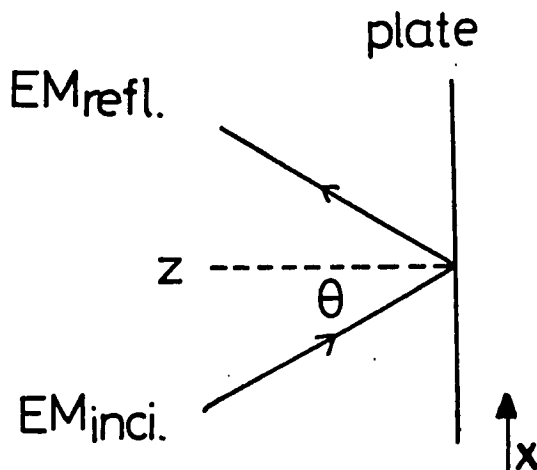
Fig.2 Electromagnetic field reflected by the conducting plate.

The intensity of the current decays exponentially so that

$$P_j = 2\mu_0 H_0{}^2 = 2\epsilon_0 E_0{}^2 \tag{14}$$

where we have used the relation between the electric and the magnetic field which is obtained from the Maxwell equations and $\epsilon_0\mu_0 = 1/c^2$. The total radiation pressure is then

$$P = P_e + P_j = 2\epsilon_0 E_0{}^2 \cos^2\theta. \tag{15}$$

For normal incidence, ie $\theta = 0$, the total radiation pressure is $2\epsilon_0 E_0{}^2$ which is solely from the magnetic field.

The radiation pressure on the conducting plate is the normal component of the Maxwell stress tensor [6]. The normal component of the Maxwell stress tensor is

$$T_{zz} = \frac{1}{2}\epsilon_0(E_x{}^2 + E_y{}^2 - E_z{}^2) + \frac{1}{2}\mu_0(H_x{}^2 + H_y{}^2 - H_z{}^2). \tag{16}$$

Substituting the total field we have in eqs.(8, 9) we find

$$T_{zz} = 2\epsilon_0 E_0{}^2 \cos^2\theta \tag{17}$$

which agrees with the result (15) obtained using the quasimicroscopical interaction theory.

QUANTUM MAXWELL STRESS TENSOR

To simplify the problem we consider normal incidence on the plate. The electric field polarized along the x–axis propagates through the z–axis in fig.2. If the field is a travelling wave the vector potential operator for a mode $\underline{k}$ of frequency ω is known as [7a]

$$\hat{\underline{A}} = \left[\frac{\hbar}{2\epsilon_0 V\omega}\right]^{\frac{1}{2}}\underline{i}\,(\hat{a}e^{-i\omega t + ikz} + \hat{a}^\dagger e^{i\omega t - ikz}) \tag{18}$$

where $\underline{i}$ is the unit vector along the x–axis and the caret is to denote the operator. The operator $\hat{a}$ and $\hat{a}^\dagger$ are respectively the field annihilation and creation operators. The cavity composed of the two parallel conducting plates accommodate standing waves rather than travelling waves. With a similar analogy to find the vector potential in eq.(18) we obtain the vector potential for the standing wave [7b]

$$\hat{\underline{A}} = \left[\frac{\hbar}{\epsilon_0 V\omega}\right]^{\frac{1}{2}}\underline{i}\,\cos kz(\hat{a}e^{-i\omega t} + \hat{a}^\dagger e^{i\omega t}) \tag{19}$$

where $k = n\pi/d$, $n = 1, 3, 5, \cdots$ and d is the length of the cavity. From the one–dimensional potential vector we obtain the electric $\hat{\underline{E}}$ and magnetic $\hat{\underline{B}}$ field operators as

$$\hat{\underline{E}} = -\frac{\partial \hat{A}}{\partial t}\underline{i} = i\left[\frac{\hbar\omega}{\epsilon_0 V}\right]^{\frac{1}{2}}\underline{i}\,\cos kz(\hat{a}e^{-i\omega t} - \hat{a}^\dagger e^{i\omega t}) \tag{20}$$

and

$$\hat{\underline{B}} = \frac{\partial \hat{A}}{\partial z}\underline{i} = -\frac{1}{c}\left[\frac{\hbar\omega}{\epsilon_0 V}\right]^{\frac{1}{2}}\underline{i}\,\sin kz(\hat{a}e^{-i\omega t} + \hat{a}^\dagger e^{i\omega t}) \tag{21}$$

From eq.(16) we may write the Maxwell stress tensor for the quantized field in the cavity.

$$\hat{T}_{zz} = \frac{1}{2}\left(\epsilon_0\hat{E}_x{}^2 + \frac{1}{\mu_0}\hat{B}_y{}^2\right). \tag{22}$$

With the use of eqs.(20, 21)

$$\dot{T}_{zz} = \frac{\hbar\omega}{2V}\{\hat{a}^\dagger\hat{a} + \hat{a}\hat{a}^\dagger - (\hat{a}^\dagger\hat{a}^\dagger e^{2i\omega t} + \hat{a}\hat{a}\, e^{-2i\omega t})\cos 2kz\}. \tag{23}$$

If the number state $|n>$ resides in the cavity the radiation pressure on the conducting plates is

$$P = < \dot{T}_{zz} > = \frac{\hbar\omega}{2V}(n + 1). \tag{24}$$

For the vacuum state, ie $n = 0$, the radiation pressure in eq.(24) becomes $P = \hbar\omega/2V$ which is in agreement with eq.(1) for normal incidence. When the cavity is prepared with the squeezed vacuum the radiation pressure on the cavity wall is

$$P = \frac{\hbar\omega}{2V}(\cosh 2r + \sinh 2r \cos kz \cos 2\omega t) \tag{25}$$

where r is the real squeeze parameter [8]. The second term in the curly bracket fast–oscillates around zero. Taking the time average of the radiation pressure we get

$$P = \frac{\hbar\omega}{2V}\cosh 2r \tag{26}$$

As squeezing gets severe, the radiation pressure increases exponentially. The time average radiation pressure for the coherent state of amplitude α is

$$P = \frac{\hbar\omega}{2V}(\alpha^2 + 1). \tag{27}$$

The momentum density of the electromagnetic field is proportional to the Poynting vector $\hat{\underline{S}}$. While the Poynting vector is clearly defined in classical theory as $\underline{E} \times \underline{H}$, that is not the case in quantum theory because the operator–ordering problem arises. When the Poynting vector is concerned in calculation of the intensity of a field we have the normal ordering of the field operators, ie $\hat{S} \propto \hat{a}^\dagger\hat{a}$ [7]. For the problem in hand we define the Poynting vector with the usual quantum mechanical symmetrization:

$$\hat{S}_z = \frac{1}{2}(\hat{\underline{E}} \times \hat{\underline{H}} - \hat{\underline{H}} \times \hat{\underline{E}}). \tag{28}$$

RADIATION FORCE ON AN ATOM

If a two–level atom is isolated in the cavity composed of two parallel conducting plates the atom is subject to the radiation pressure from the standing wave. To simplify the problem we assume that the field propagation is along the z–axis in Fig.2. We consider the two–level atom with ground state $|g>$ and excited state $|e>$ in interaction with the radiation field of frequency ω. The atom of total mass M has the atomic centre–of mass momentum

$$\hat{\underline{P}} = -i\hbar\underline{\nabla}. \tag{29}$$

The total Hamiltonian of the coupled system is[9]

$$\hat{H} = \hat{H}_{atom}(t) + \hat{H}_{field}(t) + \hat{\underline{P}}(t)^2/2M + \hat{H}_i(t) \tag{30}$$

where under the electric–dipole approximation the interaction Hamiltonian

$$\hat{H}_i(t) = i\hbar g \cos kz \{\hat{a}(t) - \hat{a}^\dagger(t)\}\{\hat{\pi}(t) + \hat{\pi}^\dagger(t)\} \tag{31}$$

with the coupling constant

$$g = e\left[\frac{\omega}{\hbar\epsilon_0 V}\right]^{\frac{1}{2}}\underline{\epsilon}\cdot\underline{D} \tag{32}$$

The operators $\hat{\pi}, \hat{\pi}^\dagger$ are the atomic transition operators.

The radiation force is $d\hat{P}/dt$. Using the Heisenberg equation of motion for

the momentum operator

$$\hat{F}(t) = \frac{\partial \hat{P}(t)}{\partial t} = -\frac{i}{\hbar}[\hat{P}(t), \hat{H}] = -\frac{\partial \hat{H}_i(t)}{\partial z}. \tag{33}$$

To calculate the time–dependent interaction Hamiltonian we need find the time–dependence of operators. With the use of the Heisenberg equation of motion

$$-i\hbar\frac{\partial \hat{a}(t)}{\partial t} = -\hbar\omega g\hat{a}(t) + i\hbar g\cos kz\,\{\hat{\pi}(t) + \hat{\pi}^\dagger(t)\}. \tag{34}$$

The equation is formally integrated to give [7]

$$\hat{a}(t) = e^{-i\omega t}\left[\hat{a} - g\cos kz\int_0^t \{\hat{\pi}(t') + \hat{\pi}^\dagger(t')\}\,e^{i\omega t'}dt'\right] \tag{35}$$

where $\hat{a} = \hat{a}(0)$. Similarly for the transition operator

$$\hat{\pi}(t)=e^{-i\omega_0 t}\left[\hat{\pi}-g\cos kz\int_0^t [2\hat{\pi}^\dagger(t')\hat{\pi}(t')-1][\hat{a}(t')-\hat{a}^\dagger(t')]e^{i\omega t'}dt'\right] \tag{36}$$

where $\hat{\pi} = \hat{\pi}(0)$ and $\hbar\omega_0$ is the energy difference between the excited and the ground states. The operators $\hat{a}(t)$ and $\hat{\pi}(t)$ in eqs.(35, 36) still have integration to carry out. It is not simple to solve the iterative integral equations. For the weak coupling between the field and the atom we calculate the first–order perturbative solution

$$\hat{a}(t) = e^{-i\omega t}(\hat{a} + \alpha\hat{\pi} - \beta\hat{\pi}^\dagger) \tag{37}$$

$$\hat{\pi}(t)=e^{-i\omega_0 t}[\hat{\pi} + (2\hat{\pi}^\dagger\hat{\pi} - 1)(\xi\hat{a} - \zeta\hat{a}^\dagger)] \tag{38}$$

where

$$\alpha = \frac{g\cos kz}{i(\omega_0 - \omega)}\{\exp[-i(\omega_0 - \omega)t] - 1\}$$

$$\beta = \frac{g\cos kz}{i(\omega_0 + \omega)}\{\exp[i(\omega_0 + \omega)t] - 1\}$$

$$\xi = -\frac{g\cos kz}{i(\omega_0 - \omega)}\{\exp[i(\omega_0 - \omega)t] - 1\}$$

$$\zeta = \frac{g\cos kz}{i(\omega_0 + \omega)}\{\exp[i(\omega_0 + \omega)t] - 1\}.$$

We are interested in the radiation force on the atom when the cavity is initially prepared with the vacuum state which is a limiting case of number states. We substitute eqs.(37, 38) and their Hermitian conjugates into eq.(31) to find the radiation force on the atom with the use of eq.(33)

$$\hat{F}(t) = -2\hbar k g^2\sin 2kz\,\{[(2\hat{\pi}^\dagger\hat{\pi} - 1)\hat{a}\hat{a}^\dagger + \hat{\pi}\hat{\pi}^\dagger]A$$
$$+[(2\hat{\pi}^\dagger\hat{\pi} - 1)\hat{a}^\dagger\hat{a} - \hat{\pi}\hat{\pi}^\dagger]B\} \tag{39}$$

where the first term in the curly bracket varies slowly with the parameter

$$A \equiv \frac{1 - \cos(\omega_0 - \omega)t}{\omega_0 - \omega} \tag{40}$$

while the second term varies fast with the parameter

$$B \equiv \frac{1 - \cos(\omega_0 + \omega)t}{\omega_0 + \omega} \tag{41}$$

The second term is so called the counter–rotating term which is often neglected when the field frequency is near resonant with the atomic frequency.

If the field is initially prepared with the number state $|n>$ and the atom in its ground state the radiation force is

$$\hat{F}(t) = 2\hbar k g^2 \sin 2kz \ \{nA + (n+1)B\}. \tag{42}$$

Neglecting the fast oscillating term $(n + 1)B$, which is so called the rotating wave approximation, we write

$$< \hat{F}(t) > = 2n\hbar k g^2 \sin 2kz \ \frac{1 - \cos(\omega_0 - \omega)t}{\omega_0 - \omega}. \tag{43}$$

For the vacuum field, $n = 0$. While the slowly varying contribution is zero, we have the radiation force from the counter—rotating term

$$< \hat{F}(t) > = 2\hbar k g^2 \sin 2kz \ \frac{1 - \cos(\omega_0 + \omega)t}{\omega_0 + \omega}. \tag{44}$$

The time—average force is thus

$$< \hat{F} > = 2\hbar k g^2 \sin 2kz \ \frac{1}{\omega_0 + \omega}. \tag{45}$$

Eq.(47) shows that the time—average force is zero when the electric field is not only at its nodes but also at its peaks. This reflects the fact that the radiation field exerts the force proportional to the gradient of the intensity.

CONCLUSIONS

We have studied the radiation pressure from the field between the conducting plates. We quantized the standing wave and introduced the Maxwell stress tensor in the quantum mechanical form. The Maxwell stress tensor is calculated for the radiation pressure on the plates. For the special case of the vacuum field the radiation pressure shows the Casimir force which pushes the plates together.

When the atom interacts with the travelling wave the time—average radiation force on the atom is zero [10]. The standing wave on the other hand exerts force on the atom to push the atom to a node of the field. Since the force depends on the gradient of the intensity, that is the electric field squared, the force is zero at the nodes and peaks of the field.

ACKNOWLEDGEMENTS

REFERENCES

[1] H.B.G. Casimir, 1948, Proc.Kon.Ned.AKad.Wet. 51, p.793.

[2a] G. Plunien, B. Muller and W. Greiner, 1986, Phys.Rep. 134, p.87.

[2b] S. Stenholm, 1988, Contemp.Phys. 2, P.105.

[3] P.W. Milonni, R.J. Cook and M.E. Goggin, 1988, Phys.Repv.A 38, p.1621.

[4] E.A. Power, 1964, *Introductory Quantum Electrodynamics*, Longmans, London.
[5] M. Planck (translated by M. Masius), 1959, *The Theory of Heat Radiation*, Dover, NY.
[6] J.D. Jackson, 1975, *Classical Electrodynamics*, John Wiley, New York.
[7a] R. Loudon, 1983, *The Quantum Theory of Light*, Clarendon, Oxford.
[7b] R. Loudon and M.S. Kim manuscipt in preparation.
[8] R. Loudon and P.L. Knight, 1987, J.Mod.Opt. 34, p.709.

[9] A. Al–Hilfy and R. Loudon, 1985, Opt.Acta 32, p.995.

   M. Babiker, 1984,J.Phys.B 17, p.4877.

[10] J.P. Gordon, 1973, Phys.Rev.A 8, p.14.

Squeezed light from conventionally pumped multi-level lasers

T.C.Ralph and C.M.Savage

628167

4 pgs

Department of Physics and Theoretical Physics,
Australian National University, Canberra, ACT 2601, Australia

Abstract

We have calculated the amplitude squeezing in the output of several conventionally pumped multi-level lasers. We present results which show that standard laser models can produce significantly squeezed outputs in certain parameter ranges.

Introduction

Production of non-classical light by lasers is an active field both theoretically and experimentally. Sub-Poissonian output has been predicted and observed from lasers in which a regular pumping mechanism reduces the population fluctuations in the lasing levels (Ref.1-4).

Recently we have found that rigorous solutions of conventionally pumped 3 and 4-level lasers predict amplitude squeezing in their output (Ref.5). This is contrary to standard laser theory which predicts Poissonian output far above threshold when the pumping is conventional (Ref.6,7). Our results are in agreement with those of Khazanov et al (Ref.8).

The basic requirement for sub-Poissonian output, without regular pumping, is that the sequence of levels involved in moving an electron from the lower lasing level to the upper lasing level contains at least two steps with approximately equal rates. One of these steps may be the pump itself. Any other rates must be faster. In previous multi-level treatments solutions have been obtained by assuming the pump rate is much slower than all other rates (Ref.6,7). Squeezing will not be seen under these conditions.

We present here results of squeezing spectra calculations for incoherently pumped 3-level and 4-level lasers and a coherently pumped 4-level laser (fig1). The results highlight the basic effect and how it varies between the models. We also discuss a simple statistical model which illustrates the physical mechanism behind the squeezing.
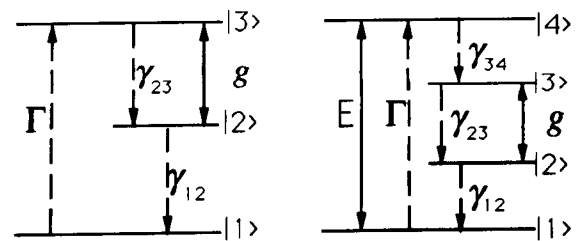
Fig.1 Laser atomic level schemes. Incoherently pumped 3-level on the left and incoherently (E=0) or coherently (Γ=0) 4-level on the right. The γ_{ij} are spontaneous decay rates. g is the dipole coupling strength.

Squeezing Results

Using standard techniques (Ref.6,7) a master equation for the reduced density operator ρ of the atoms and cavity is derived. We solve for the full quantum mechanics of the master equation by transforming it into an equivalent partial differential equation for the generalized P-function of Drummond and Gardiner (Ref.9). We make the usual approximation that the quantum fluctuations are small perturbations on the semiclassical steady state (Ref.2,9,10). The amplitude squeezing spectrum, V, of the laser output field is calculated in the usual way (Ref.10).

In Figure 2 we plot the spectral variance at the zero frequency local minimum of the spectrum as a function of pump rate for the three cases. The full spectra are approximately Lorentzians (in the region shown) with linewidths corresponding to that of the laser cavity. Laser phase diffusion has been ignored. Parameters have been chosen to show maximum squeezing. 0 is perfect squeezing and 1 is the coherent state spectral variance.

Squeezing is improved both by increasing the number of levels with similar rates and by using a coherent pump. The 3-level laser has maximum squeezing of 50% when the spontaneous decay rate γ_{12} is double the pump rate (Γ). The incoherently pumped 4-level laser has maximum squeezing of 66% when $\Gamma = \gamma_{34} = 0.5\gamma_{12}$. The improvement due to the coherent pump is more significant. If $\sqrt{8}E = \gamma_{34} = 0.5\gamma_{12}$, where E is proportional to the coherent field strength, 80% squeezing is predicted.
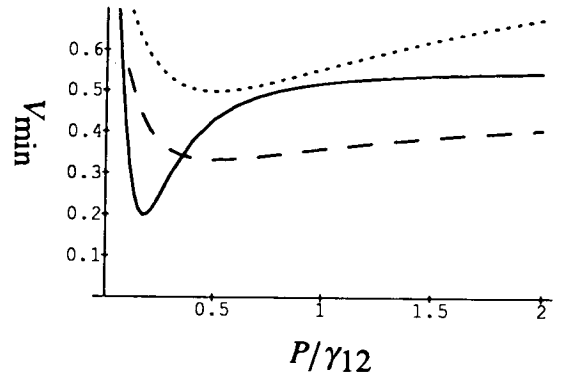
Fig.2 The zero frequency minimum of the amplitude squeezing spectral variance versus pump rate for the incoherently pumped 3-level (dotted line) and 4-level (dashed line) and coherently pumped 4-level (solid line) lasers. For the incoherently pumped case $P=\Gamma$ and for the coherently pumped case $P=E$. Parameters in units of γ_{12} are: $\gamma_{23} = 10^{-6}$, $\gamma_{34} = 0.5$, $\tilde{g} = 1$, $\kappa = 0.01$. κ is the cavity decay rate and $\tilde{g}$ is the scaled dipole coupling constant (Ref.5).

Discussion

The origin of the squeezing can be understood in terms of the temporal behaviour of the electrons in individual atoms[1]. The variance in the time the pump cycle takes to place an electron in the upper lasing level of an individual atom, Δt^2, and the spectral variance at zero frequency, V_{min}, are related by[2]

[1] H.Ritsch, P.Zoller, C.W.Gardiner and D.F.Walls, to be published, (1991).
[2] T.C.Ralph and C.M.Savage, to be published, (1991).

$$V_{\min} \approx \frac{\Delta \bar{n}^2}{\bar{n}} = \frac{\Delta t^2}{(t)^2} \qquad (1)$$

where t is the mean time it takes for the electron to arrive in the upper lasing level, $\Delta \bar{n}$ is the photon number variance of the output and $\bar{n}$ is the mean number of photons. To obtain this result we have assumed the laser is well above threshold and has a strong enough dipole coupling such that the lasing transition time can be considered to have zero variance. Also we assume spontaneous emission out of the upper lasing level is negligible.

The right-hand side of (1) can be evaluated exactly[2]. For an $(r+3)$-level incoherently pumped laser the independence of the noise introduced in each step leads to the following expression

$$V_{\min} \approx \frac{(2/\gamma_L)^2 + (1/\gamma_1)^2 + \dots (1/\gamma_r)^2 + (1/\Gamma)^2}{(2/\gamma_L + 1/\gamma_1 + \dots 1/\gamma_r + 1/\Gamma)^2}$$

where γ_L is the decay rate out of the lower lasing level, Γ is the pump rate and $\gamma_1 \dots \gamma_r$ are the rates of the intermediate steps. The rates are matched for optimum noise reduction when $\Gamma = \gamma_1 = \dots = \gamma_r = 0.5\gamma_L$. The minimum value of $V_{\min}$ is then $1/(r+2)$. If the pump rate is much slower than all the other rates then $V_{\min} \to 1$, ie Poissonian. This is the limit in which previous calculations were carried out.

For a certain range of pump rates a coherent step introduces less noise into the pump cycle than an incoherent step[2]. This leads to superior squeezing in the coherently pumped laser.

Summary
We have presented a brief report of results we have obtained from rigorous solutions of conventionally pumped standard laser models. Contrary to established theory we find amplitude squeezing of the output beam is possible in certain parameter ranges. Physically we find the noise suppression is due to the independence of the noise introduced in the various steps involved in inverting the atoms.

We see no fundamental reason why lasers could not be built which operate in regimes meeting the requirement for squeezing.

References
[1] Y. M. Golubev and I. V. Sokolov, Sov. Phys. JETP **60**, 234 (1984).

[2] M. A. Marte and D. F. Walls, Phys. Rev. A **37**, 1235 (1988).

[3] S. Machida and Y. Yamamoto, Phys. Rev. Lett. **60**, 792 (1988).

[4] W. H. Richardson and R. M. Shelby, Phys. Rev. Lett. **64**, 400 (1990).

[5] T.C.Ralph and C.M.Savage, Opt. Lett, July, (1991).

[6] W. H. Louisell, *Quantum Statistical Properties of Radiation* (Wiley-Interscience, New York, 1973).

[7] H. Haken, *Laser Theory*, in *Encyclopedia of Physics*, **XXX/2c**, ed. S. Flugge (Springer-Verlag, Heidelberg, 1970).

[8] A. M. Khazanov, G. A. Koganov, and E. P. Gordov, Phys. Rev. A **42**, 3065 (1990).

[9] P. D. Drummond and D. F. Walls, Phys. Rev. A **23**, 2563 (1981).

[10] M. D. Reid, Phys. Rev. A **37**, 4792 (1988).

STATISTICAL PROPERTIES OF SQUEEZED BEAMS OF LIGHT GENERATED IN PARAMETRIC INTERACTIONS*

62 8/70

4 Pgs

Reeta Vyas

Department of Physics, University of Arkansas,
Fayetteville, AR 72701

ABSTRACT

Fluctuation properties of squeezed photon beams generated in three wave mixing processes such as second harmonic generation, degenerate and nondegenerate parametric oscillations, and homodyne detection are studied in terms of photon sequences recorded by a photodetector.

Photon number fluctuations and photon number correlations are fundamental properties of a light beam. These properties are different for different light sources and can be used to characterize photon beams. In this short communication we discuss our work on statistical properties of squeezed photon beams generated in three wave interaction processes in terms of counting and waiting time distributions. We summarize some of the interesting results obtained for these systems. Processes that we consider here include second harmonic generation, and degenerate and nondegenerate parametric down conversion (DPO and NDPO). Squeezed state of light have been realized in these systems experimentally (Ref.1). Homodyne statistics when squeezed light produced by the DPO is mixed with coherent light from a local oscillator are also discussed. A dynamical model for these beams is used and photon sequences recorded by a photodetector are calculated.

We use positive-P representation (Ref.2) to map quantum mechanical equations of motion for the annihilation and creation operators onto a set of C-number stochastic equations for the complex field amplitudes. Using simple transformation of field variables it can be shown that the field produced in these processes can be described in terms of independent real Gaussian stochastic processes (Ref.3-4).

We use a generating function technique to obtain the statistics of the photons emitted by these light sources. The generating function $G(s,t,T)$ for the photon statistics measured by a detector with a parameter s is given by (Ref.5)

$$G(s,t,T) = \left\langle e^{-s\eta \int_t^{t+T} I(t')dt'} \right\rangle. \quad (1)$$

Here η is detector efficiency and $I(t)$ is photon flux emitted by the source. Generating function $G(1,t,T)$

is simply the probability of detecting no photon in the time interval t to $t+T$. In order to obtain generating function we express $I(t)$ in terms of the c-number field variables. Statistical averaging is performed by making Karhunen Loéve expansion of the field variables in terms of a set of orthogonal functions. Following the method developed in our earlier investigations (Ref.3) we derive an analytical expression for the generating function $G(s,t,T)$ for the photon statistics. From this generating function various statistical quantities such as factorial moments, photon counting and waiting time distributions can be obtained.

The photon counting distribution $p(m,t,T)$ is the probability of counting m photons in the time interval t to $t+T$. It can be obtained from the generating function by using the relationship

$$p(m,t,T) = \frac{(-1)^m}{m!} \left[\frac{d^m}{ds^m} G(s,t,T) \right]_{s=1}. \quad (2)$$

The waiting time distribution $w(t,T)$ is the probability density for two successive photoelectrons to be separated by the time interval T and it is given by

$$w(t,T = t'-t) = -(\eta I(t))^{-1} \frac{d^2}{dtdt'} G(1,t,t'-t). \quad (3)$$

In the stationary regime these quantities are independent of initial time t. Here we only summarize photon statistics only in the steady state regime. The field from the DPO can be expressed in terms of two independent Gaussian random variables with mean zero and different variances

$$< u_i(t)u_j(t+T) > = \frac{1}{4} \frac{|\kappa \epsilon|}{\lambda_i} \delta_{ij} e^{-\lambda_i T}. \quad (4)$$

Here κ is the mode coupling constant, and ϵ is the dimensionless amplitude of the pump beam incident on the cavity. The decay constants λ_1 and λ_2 are given by

$$\lambda_1 = (\gamma - |\kappa \epsilon|), \qquad \lambda_2 = (\gamma + |\kappa \epsilon|). \quad (5)$$

Here $(1/2\gamma)$ is the cavity lifetime. Below threshold λ_1 and λ_2 are always positive. Using the properties of field variables u_1 and u_2 we obtain the generating function for the DPO as (Ref.3)

$$G(s,T) = Q_1(s,T)Q_2(s,T), \quad (6)$$

where

$$Q_i(s,t,T) = \left[\frac{e^{\lambda_i T}}{[\cosh(z_i T) + f_i(t) \sinh(z_i T)]} \right]^{\ell} , \quad (7)$$

with

$$f_i(t) = \frac{1}{2} \left(\frac{\lambda_i}{z_i} + \frac{z_i}{\lambda_i} \right) , \quad (8)$$

and

$$z_1^2 = \lambda_1^2 + 2s\eta\gamma\kappa\epsilon,$$
$$z_2^2 = \lambda_2^2 - 2s\eta\gamma\kappa\epsilon. \quad (9)$$

Mean photon number inside the cavity is given by

$$\bar{n} = \frac{1}{2} \left(\frac{|\kappa\epsilon|^2}{\gamma^2 - |\kappa\epsilon|^2} \right) . \quad (10)$$

For the DPO ℓ is equal to half. Once the generating function is known photon counting and waiting time distributions are obtained from Eqs. (2) and (3). For small mean photon number and short counting time $p(m,T)$ decreases monotonically.
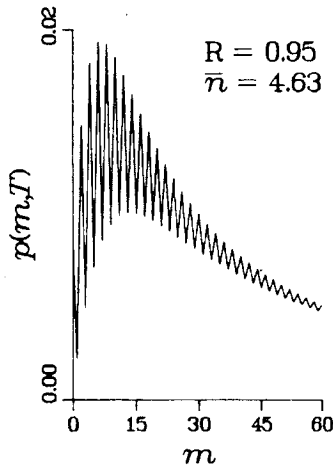
Figure 1a. Photon counting probability distribution for the DPO for $R = 0.95$, unit efficiency, and counting time interval $2\gamma T = 20$.

For long counting times $p(m,T)$ shows sharp even-odd oscillations implying that the probability of detecting odd number of photons is much smaller than the probability of detecting even number of photons. As the mean photon number $\bar{n}$ is increased these even-odd oscillations become smaller. Figure (1a) shows $p(m,T)$ for $R = \kappa\epsilon/\gamma = 0.95$ near threshold corresponding to $\bar{n} = 4.63$. These curves are meaningful only for integer values of m. We see that near threshold even-odd oscillations become less pronounced and

$p(m,T)$ develops a long tail. We have also studied photon statistics for the DPO in the transient regime, that is, during its evolution from vacuum state to the steady state (Ref.4). For small transient time even-odd oscillations in photon counting distributions are even sharper than the even-odd oscillations in the stationary regime.

With the degenerate modes of a parametric oscillator, nondegenerate modes are also present. We consider the nondegenerate modes of parametric oscillator for which two nondegenerate photons have the same frequencies. These fields can be expressed in terms of four real random Gaussian variables. Here we discuss two cases, one in which amplitudes of the two nondegenerate modes are homodyned and second in which intensities of the two modes are added together. For a given pump strength the NDPO the mean photon number is much smaller than the mean photon number for the DPO. Mathematical expression for the generating function for the first case is similar to the generating function for the DPO. Thus $p(m,T)$ for the NDPO also shows even-odd oscillations. However, for the same pump strength, even-odd oscillations in the NDPO are sharper then the oscillations for the DPO. They are centered towards smaller values of m. The difference between the DPO and the NDPO lies mainly in the value of the mean photon number.
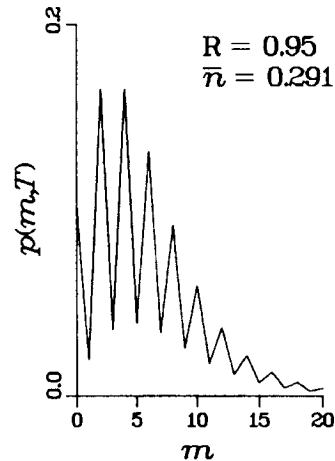
Figure 1b. Photon counting probability distribution for the NDPO for $R = 0.95$, efficiency $\eta = 1$, and counting time interval $2\gamma T = 20$.

The second case that we consider is when intensities of the two modes are added together. In this case the power ℓ appearing in Eq. (7) is one (Ref.6). In this case the expression for $Q_1(s,T)$ is similar to the generating function for thermal light (Ref.5). The counting

distribution for NDPO, however, is very different from that for the thermal light. It shows even-odd oscillations as a function of m whereas such oscillations are not seen for thermal light. Figure (1b) shows even-odd oscillations in $p(m,t)$ for $R = \kappa \epsilon / \gamma = .95$ for the second case.

Next we discuss photon statistics of the fundamental beam from an intracavity second harmonic generation (SHG). Field for this system can be expressed in terms of two real Gaussian random variables and a coherent component (Ref.7). These results are obtained by linearizing the field amplitude equations around the deterministic steady state values. The generating function for the SHG can be written as (Ref.6)

$$G(s,T) = Q_1(s,T)Q_2(s,T)e^{-f(s,T)}. \quad (10)$$

Here

$$f(s,T) = -2s\eta\bar{n}n_0 T \left[\frac{\lambda_1^2}{z_1^2} \left(1 + \frac{2}{(2+\lambda_1 T)} \right) \right.$$
$$\left. - \frac{2s\eta\bar{n}v(z_1)}{z_1^2 \left(1 + \frac{s\eta\bar{n}T}{\lambda_1}\right)} - \frac{2}{(2+\lambda_1 T)\left(1 + \frac{s\eta\bar{n}T}{\lambda_1}\right)} \right], \quad (11)$$

with

$$v(z_1) = \left[\frac{1 + \left(\frac{2+\lambda_1 T}{z_1 T}\right)\tanh(z_1 T/2)}{1 + \frac{z_1}{\lambda_1}\tanh(z_1 T/2)} \right]. \quad (12)$$

Here $Q_1(s,T)$ and $Q_2(s,T)$ are given by equation (7) with $l = 0.5$ and

$$\lambda_1 = (1 + 3\bar{n}), \qquad \lambda_2 = (1 + \bar{n}), \quad (12)$$

For the SHG z_1 and z_2 are given by

$$z_1^2 = \lambda_1^2 - 2s\eta\bar{n},$$
$$z_2^2 = \lambda_2^2 + 2s\eta\bar{n}. \quad (13)$$

Here $\bar{n}$ and n_0 are the average and threshold photon numbers, respectively. From this generating function various statistical quantities of interest can be calculated. Photon sequences in the SHG can be antibunched. Although the antibunching effect is very small riding on an intense coherent background it is clearly reflected in the behavior of the waiting time distribution for the SHG.

Using similar techniques we also obtain the generating function when light from the DPO is homodyned with coherent light from a local oscillator. Depending upon the relative phase between coherent light from the local oscillator and squeezed light from the DPO we can see sub-Poissonian or super-Poissonian

statistics for the homodyned photon beam. Figure (2) shows waiting time distribution when the relative phase is $0°$ and $90°$. We see bunched light when coherent component is added to the unsqueezed component and antibunched light when coherent component is added to the squeezed component.
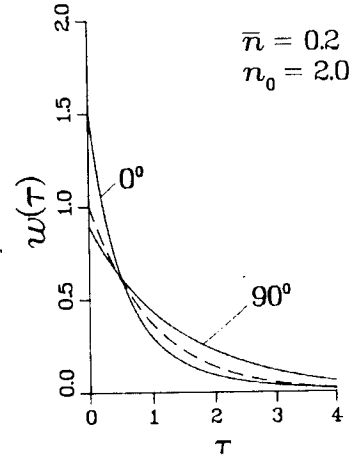
Figure 2. Waiting time distribution for DPO mean photon number $\bar{n} = 0.2$ and local oscillator mean photon number $n_o = 2$. Dashed curve is for coherent light

REFERENCES

* It is a pleasure to acknowledge collaboration with S. Singh and A. L. DeBrito for part of this work. This work was supported in part by grants from Arkansas Science and Technology Authority (ASTA) .

1. Special issue on squeezed states of light, J. Opt. Soc. Am. B4(No. 10) (1988).

2. P. D. Drummond and C. W. Gardiner, J. Phys. 13, 2353 (1980).

3. Reeta Vyas and S. Singh, in *Coherence and Quantum Optics VI*, edited by J.H. Eberly, L. Mandel, and E. Wolf (Plenum, New York, 1990), p. 1189; Opt. Lett. 14, 1110 (1989); Phys. Rev. A 40, 5147 (1989).

4. Reeta Vyas and A. L. DeBrito, Phys. Rev. A 42, 592 (1990); *Nonlinear Dynamics in Optical Systems*, edited by N. B. Abraham, E. M. Garmire and P. Mandel (OSA, Washington, DC, 1991), p. 589.

5. B. E. Saleh, *Photoelectron Statistics* (Springer-Verlag, Berlin, 1973); Reeta Vyas and Surendra Singh, Phys. Rev. A 38, 2423 (1988); H. J. Carmichael, Surendra Singh, Reeta Vyas, and P. R. Rice, Phys. Rev. A 39, 1200 (1989).

6. Reeta Vyas, [to be published].

7. G. S. Holliday and S. Singh, in *Coherence and Quantum Optics VI*, edited by J.H. Eberly, L. Mandel, and E. Wolf (Plenum, New York, 1990), p. 509.

231

NONDESTRUCTIVE MEASUREMENT OF INTENSITY OF OPTICAL FIELDS USING SPONTANEOUS PARAMETRIC DOWN CONVERSION

A.N.Penin, G.Kh.Kitaeva, *)A.V.Sergienko

Department of Physics, Moscow State University,
Moscow 119899, USSR
*)Present address: Department of Physics and Astronomy,
University of Maryland, College Park, MD 20742

Results of nondestructive measurements of intensity (photons per mode) of light from different sources are discussed. The procedure of measurement does not destroy the state of the optical field. The method is based on using the second order nonlinearity of crystal media lacking a center of symmetry and the nonclassical properties of the process of Spontaneous Parametric Down Conversion (SPDC).

The interaction of laser radiation with nonlinear crystal leads to the spontaneous emerging of correlated photons in two modes (ω_1 and ω_2) of the optical field connected by phase matching conditions $\omega_1 + \omega_2 = \omega_L$, $k_1 + k_2 = k_L$. The quantum theory of the parametric amplification process /1-4/ shows that if all initial modes of radiation are in the vacuum state (except the pump radiation), then photon flux after the nonlinear interaction in mode with , for example, frequency ω_1 (Fig.1) is:

$$N_1{}'(t) = \sinh^2(gt) \tag{1}$$

Where $g=(2\pi/h)\chi^{(2)}E_0$, $\chi^{(2)}$ = an effective value of second order susceptibility, and E_0 = amplitude of pump radiation. If we have initial radiation from an external source S producing an intensity $n_2{}^0$ in the mode of frequency ω_2, then after the nonlinear crystal the intensity of radiation in mode of frequency ω_1 is given by:

$$N_1{}'' = (1 + n_2{}^0)\, \sinh^2(gt) \tag{2}$$

Thus the value of the intensity $n_2{}^0$ of the initial radiation can be easily calculated without destruction of initial optical state after two

PRECEDING PAGE BLANK NOT FILMED

measurements of average intensity n_1 of radiation in the parametrically conjugated mode of frequency ω_1:

$$n_2{}^0 = \frac{N_1{}''}{N_1{}'} - 1 \qquad (3)$$

This result is a reflection of the intrinsically quantum character of the SPDC process. The main point of this method is the use of universal properties of electromagnetic vacuum fluctuations, i.e. that the brightness is equal to one photon per mode. This explanation reflects the phenomenological approach in an effective treatment /5/. Detailed quantum description of nondestructive measurement of parameters of optical fields using third-order Kerr nonlinearity was made in /6/. That results could be easily transformed for the case of second order nonlinear susceptibility $\chi^{(2)}$.

The outline of the experimental setup for the nondestructive measurement of intensity of optical fields is shown in Fig.1. The radiation of argon ion laser λ = 488.8 nm interacts with a LiIO$_3$ nonlinear crystal. The scattered (spontaneously generated) radiation of frequency ω_1 is registered by a photomultiplier tube. The radiation from the external source S falls on the crystal in the direction defined by phase matching conditions. The position of the chopper disc divides the process of measurement into two stages: measurement of n_1' and n_1'' values. After the propagation inside the crystal the external radiation of frequency ω_2 can be used for other purposes. In the visible region of the spectrum we can neglect absorption of radiation inside the nonlinear crystal and consider this kind of measurement as nondestructive.

The accuracy of this method improves the closer the brightness of the measured radiation is to the brightness of electromagnetic vacuum fluctuations of the same frequency. It has advantages in measurements of laser radiation and radiation from other bright (high effective temperature) sources of light such as plasmas, high voltage discharges etc.

For our first measurements we used an infrared region of radiation from a high temperature tungsten spiral incandescent lamp as a source of external radiation. In the IR region this thermal radiation has an intensity of about 10^{-2} photons per mode (in the visible region in accordance with Planck formula $N_{therm} \approx 10^{-4}$
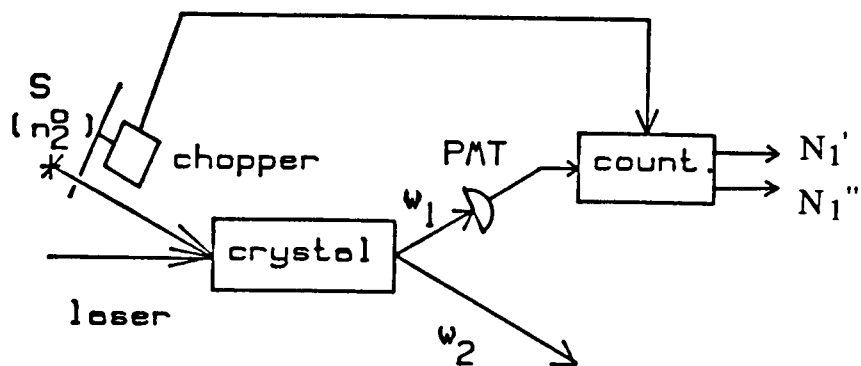
Fig.1. The outline of the experiment for nondestructive measurement of the intensity n_2^0 of light from an external source S.
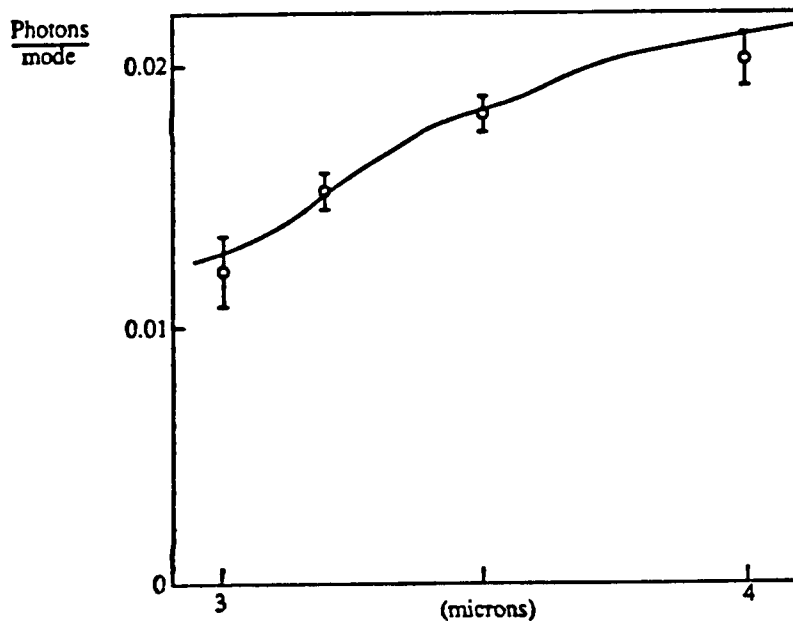
Fig.2. Result of measurement of intensity of thermal radiation source (tungsten spiral incandescent lamp) in the IR region of spectrum. Solid line corresponds to the calculation by Planck formula intensity distribution for the temperature measured by pyrometric technique. All results include correction on crystal absorption coefficient.

photons/mode). The results of measurement are presented in Fig.2. The solid line corresponds to the result calculated by the Planck formula for the temperature measured by a pyrometric technique. The accuracy of these measurements was about 5-20%. Fresnel reflection of radiation on the crystal borders gives an additional source of systematical error in this measurement. This effect could be eliminated by using of a correction coefficient.

The laser (in our case a CW He-Ne laser at $\lambda=3.39$ μ) has a much higher spectral density of radiation (10^6 photons/mode) and can be measured with better accuracy. However, in this case a special procedure of matching external and internal radiation space modes inside the crystal is needed.

The same problem arises in measurements of intensity of second harmonic radiation generated in a KDP crystal by a Nd:YAG pulsed laser. For the radiation at λ =532 nm the measured intensity was $4 \cdot 10^3$ photons/mode.

1.Louisell, W.H., A.Yariv and A.S.Siegman, 1961, "Quantum Fluctuations and Noise in Parametric Processes," Phys.Rev. v.124, p.1646.

2.Mollow, B.R., 1967, "Quantum Statistics of Coupled Oscillator Systems," Phys.Rev. v.162, p.1256.

3.Giallorenzi, T.G., and C.L.Tang, 1968, "Quantum Theory of Spontaneous Parametric Scattering of Intence Light," Phys.Rev. v.166, p.905.

4.Zel'dovich, B.Ya., and D.N.Klyshko,1969, "Statistics of Field in Parametric Luminescence," Sov.Phys.JETP Lett. v.9,p.40.

5.Klyshko, D.N., 1988, Photons and Nonlinear Optics, Gordon and Breach, New York.

6.Yamomoto, Y., and H.A.Haus, 1986, "Preparation, Measurement and Information Capacity of Optical Quantum States," Rev.Mod.Phys. v.58, p.1001.

SHORT-CAVITY SQUEEZING IN BARIUM

D.M. Hope, H-A. Bachor, P.J. Manson and D.E. McClelland
Department of Physics and Theoretical Physics
Faculty of Science
Australian National University
P. O. Box 4, Canberra A.C.T. 2601, Australia

Abstract

Broadband phase sensitive noise and squeezing have been observed experimentally in a system of barium atoms interacting with a single mode of a short optical cavity. Squeezing of 13±3% was observed. A maximum possible squeezing of 45±8% could be inferred for our experimental conditions, after correction for measured loss factors. Noise reductions below the quantum limit were found over a range of detection frequencies 60-170 MHz and were best for high cavity transmission and large optical depths. The amount of squeezing observed is consistent with theoretical predictions from a full quantum-statistical model of the system.

Introduction

The model of the interaction between a cavity mode and an ensemble of two level atoms is of fundamental importance in quantum optics (Ref. 1). Theory (Refs. 2-4) and experiment (Refs. 5-6) indicate that a particularly favorable configuration for squeezing in this model exists where decay rates of the atomic polarization and the cavity mode are approximately matched. To achieve the matching of rates without degrading the cavity finesse the cavity length must generally be reduced to a few millimetres; hence the term 'short-cavity squeezing'. Orozco *et al.* observed 30% squeezing in atomic sodium in this regime (Refs. 5-6). The $J=0 \rightarrow 1$ 553 nm transition of ^{138}Ba is a suitable medium to test detailed theoretical predictions of the dynamics of the cavity-atom interaction. Its simple structure allows us to avoid the complications of optical pre-pumping, necessary to restrict alkali atoms to two-level behaviour.

Experiment

A schematic diagram of the experimental arrangement is shown in Figure 1. A cw ring dye laser supplies 300 mW of light at 553 nm. The laser is frequency stabilized to 1 MHz. The first-
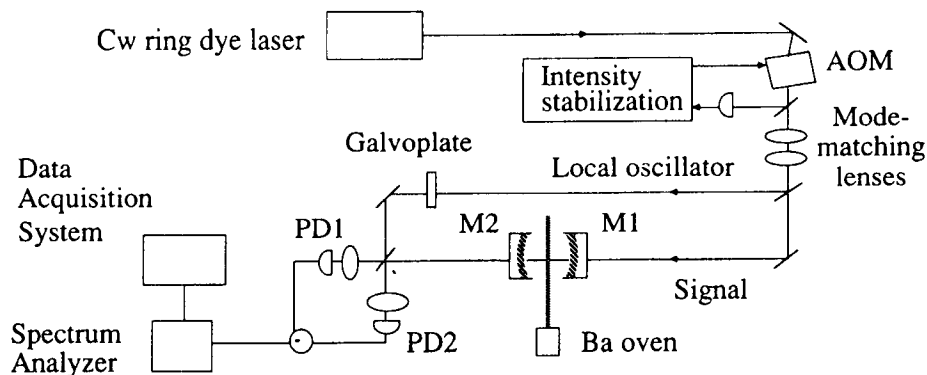
Figure 1. Experimental arrangement

order diffracted beam from an acousto-optic modulator (AOM) passes through a pair of mode-matching lenses and is divided into local osillator and signal beams with a 50% beamsplitter. The AOM serves to isolate the laser from cavity feedback, and is also operated as an intensity stabilizer. The phase of the local oscillator (LO) with respect to the signal beam phase may be varied with a scanning galvoplate, and the LO and cavity output beams are combined on a 50% beamsplitter. The output ports of the beamplitter are focused on to photodiodes PD1 and PD2 in the balanced homodyne detection system. Typically the detector gives 2 dB of quantum noise above amplifier noise at 130 MHz for 1 mA of current. The noise spectrum is displayed on a spectrum analyzer and recorded on a computer.

The optical cavity is comprised of two dielectric mirrors mounted on piezoelectric stacks separated by 4.3 mm. It is held in a stainless steel chamber evacuated to 10^{-6} torr. The input coupler M1 has transmission coefficient T1 < 0.001and a radius of curvature Rz1 of 1 meter. The output coupler M2 has T2 = 0.036 and Rz2 = 2 m. The cavity finesse is measured as F=150 ±10 and the throughput on resonance as 1.3%. The cavity beam waist is calculated to be 92 μm.

A high-density collimated beam of barium is generated and injected perpendicularly to the cavity mode. Optical depths of up to $\alpha_0 l$ =3.5 can be achieved for a beam of diameter 2.3 mm.The FWHM of the absorption peak is 44 MHz for $\alpha_0 l$=3.5, where these values are measured using a monitor beam perpendicular to both cavity axis and atomic beam. The natural linewidth of the atomic line is γ=20MHz. The additional width can be attributed to residual Doppler broadening. We have $\gamma_\perp / \kappa$=0.08 for this experimental configuration, where $\gamma_\perp$ =2γ is the transverse atomic decay rate for purely radiative decay, and κ is the decay rate of the cavity mode.

Results

Figure 2 shows a spectrum analyzer trace with 13±3 % squeezing, after corrections are made for the electronic noise contribution. It was observed for a cavity input intensity of 14 mW, atomic beam optical depth $\alpha_0 l$ = 2.7 and an atomic detuning of 600 MHz below the 553 nm transition. The
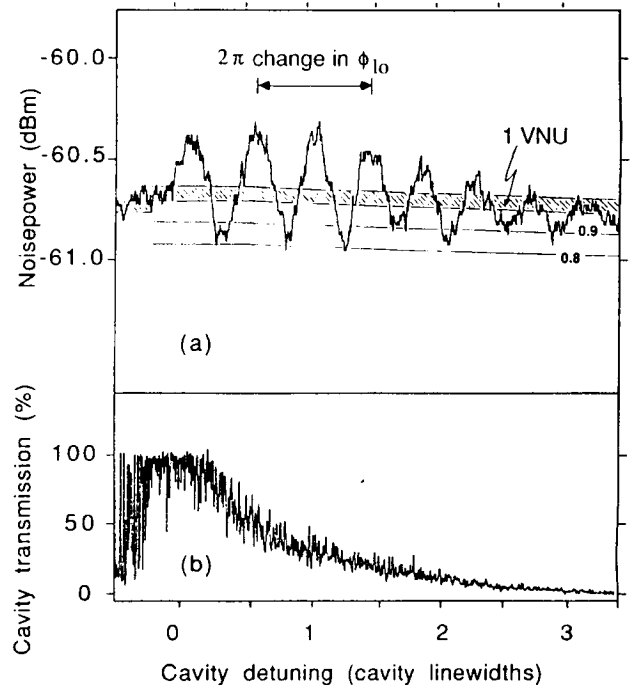
Figure 2. Noise power (a) and cavity transmission (b) recorded for optical depth $\alpha_0 l$=2.7, atomic detuning 600 MHz below the transition, cavity input power 14 mW, detection frequency 147 MHz.

detection frequency was 147 MHz. A 4-second quantum noise recording was taken while scanning the phase of the local oscillator and simultaneously sweeping through the cavity resonance. The modulated signal in Fig. 2a is the noise power. The quantum noise limit (equivalent to 1 Vacuum Noise Unit , or 1 VNU) is given by the center of the solid bar. It is obtained by recording a noise trace with cavity output blocked, under the same experimental conditions. The width of the bar represents the rms fluctuations of the noise trace. The quantum noise limit trace has been corrected for the non-negligible amount of power in the cavity output (0.18 mW compared to 1.1 mW in the LO beam). Figure 2b shows cavity transmission plotted in units of cavity linewidths from the resonance peak.

We see large amounts of phase sensitive noise near the peak of cavity transmission, together with clear reductions below the quantum noise limit, with both noise and squeezing decreasing with the sweep though the cavity. Other data reveal that squeezing exists for a broad range of frequencies 60-170 MHz, and for a bistable cavity. In the bistable regime phase sensitive noise and squeezing are seen predominantly on the upper branch.

238

Figure 3 simulates the experiment, using a plane wave ring-cavity quantum theory of squeezing in optical bistability (Refs. 3-4). The cooperativity, cavity characteristics and atomic detuning are those of the results in Figure 2, within experimental uncertainties; cooperativity $C=\alpha_0 lF/(2\pi) = 64$, atomic detuning $\Delta=(\omega_a-\omega_L)/\gamma_\perp=50$ and $\gamma_\perp/\kappa=0.08$, where ω_a and ω_L are the frequencies of the atomic transition and the signal laser respectively. Other parameters are optimized for best squeezing. Cavity detuning is measured from the peak transmission in units of cavity linewidth and is incremented through the cavity resonance. The parameter corresponding to LO phase is varied at approximately the rate used in the experiment. Trace (a) is the squeezing spectrum plotted on a logarithmic scale against the left vertical axis, where a variance V of unity corresponds to the quantum noise limit and zero corresponds to perfect squeezing. Trace (b) is the intracavity photon number (proportional to cavity transmission), plotted on the right vertical axis and given in units of the saturation intensity on resonance (Ref. 3).

Figure 3 shows good qualitative agreement with experiment. Maximum squeezing is located near the peak of cavity resonance, and the squeezing decreases for decreasing transmission. The best squeezing at these parameters is 55%. Loss factors that reduce the amount of observed squeezing have been measured individually, as follows;
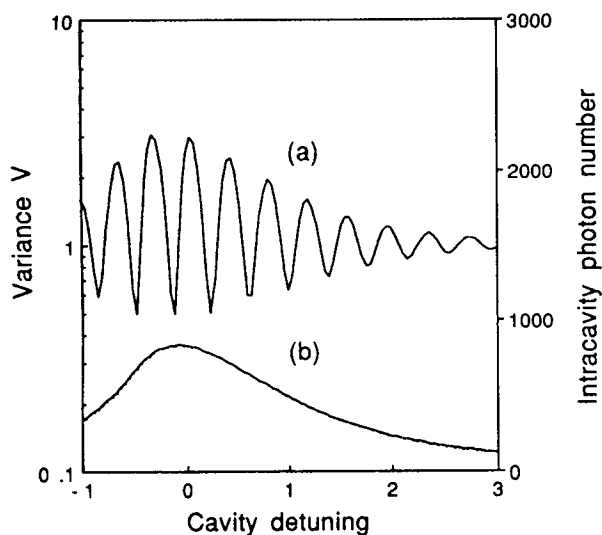
Figure 3: Theoretical modelling of experiment

cavity escape efficiency $\rho = 0.88$, detector quantum efficiency $\alpha=0.65$, mode matching efficiency $\eta^2=0.56$, propagation efficiency $T_0=0.86$, where these quantities are defined as in Refs. 6-7. We calculate that for ideal propagation and detection efficiencies the observed squeezing would equal 45±8%. This is in reasonable agreement with the theoretical prediction of 55%.

Conclusion

It was found that the interaction of a barium beam with a single mode of a short optical cavity generated reductions below the quantum noise limit of 13±3%. We infer that in the absence of loss factors 45±8% squeezing would have been observable. This is consistent with the amount of squeezing (about 55%) predicted from a quantum theory of optical bistability.

References

1. Carmichael, H.J., 1986, "Theory of Quantum Fluctuations in Optical Bistability," in *Frontiers in Quantum Optics*, E.R. Pike and Sarben Sarkar, eds., Bristol, p. 120; and references therein.
2. Castelli, F., Lugiato, L.A., and M. Vadacchino, 1988, "Squeezing in Optical Bistability without Adiabatic Elimination," *Il Nuovo Cimento*, 10 D(2), p. 183.
3. Reid, M.D., 1988, "Quantum Theory of Optical Bistability without Adiabatic Elimination," *Phys. Rev. A*, 37(12), p. 4792.
4. Hope, D.M., McClelland, D.E., and C.M.Savage, 1990, "Squeezed-State Generation in a Spatially Varying Field Mode without Adiabatic Elimination," *Phys. Rev. A*, 41(9), p.5074.
5. Raizen, M.G., Orozco, L.A., Min Xiao, Boyd, T.L., and H.J.Kimble, 1987, "Squeezed-State Generation by the Normal Modes of a Coupled System", *Phys. Rev. Lett.*, 59(2), p. 198.
6. Orozco, L.A., Raizen, M.G., Min Xiao, Brecha, R.J., and H.J. Kimble, 1987, "Squeezed-State Generation in Optical Bistability," *J.Opt. Soc. Am. B*, 4(10), p. 1490.
7. Ling-An Wu, Min Xiao, and H.J. Kimble, 1987, "Squeezed States of Light from an Optical Parametric Oscillator," *J.Opt. Soc. Am. B*, 4(10), p.1465.

AMPLITUDE SQUEEZED LIGHT FROM A LASER

D.L. Hart and T.A.B. Kennedy

School of Physics, Georgia Institute of Technology

Atlanta, GA 30332-0430

I.   Introduction

Intensity squeezed light has been successfully generated using semiconductor lasers with sub-poissonian pumping.[1] Control of the pumping statistics is crucial and is achieved by a large series resistor which regulates the pump current; its sub-poissonian statistics are then transferred to the laser output. The sub-poissonian pumping of other laser systems is not so simple however, and their potential as squeezed state sources is apparently diminished. Here we consider a conventional laser incoherently pumped well above threshold, and allow for pump depletion of the ground state. In this regime subpoissonian photon statistics and squeezed amplitude fluctuations are produced.

II.   Theoretical model

The atomic level scheme for the laser is indicated in fig. 1. We follow the notation of Lax and Louisell,[2] where $\hat{N}_i$ ($i = 0,1,2$) are the atomic population operators and $\hat{n}$ the laser mode photon number operator. The quantum Langevin rate equations are given by

$$\frac{d}{dt}\hat{N}_0 = -w_{20}\hat{N}_0 + \Gamma_1\hat{N}_1 + w_{02}\hat{N}_2 + \hat{G}_0$$

$$\frac{d}{dt}\hat{N}_1 = -(\Gamma_1 + \Pi\hat{n})\hat{N}_1 + (w_{12} + \Pi\hat{n})\hat{N}_2 + \hat{G}_1$$

$$\frac{d}{dt}\hat{N}_2 = w_{20}\hat{N}_0 + \Pi\hat{n}\hat{N}_1 - (\Gamma_2 + \Pi\hat{n})\hat{N}_2 + \hat{G}_2$$

$$\frac{d}{dt}\hat{n} = -\gamma\hat{n} + \Pi\hat{n}(\hat{N}_2 - \hat{N}_1) + \hat{G}_p.$$

Above threshold the mean inversion $D = N_2 - N_1$, is fixed at a constant value independent of pumping.

PRECEDING PAGE BLANK NOT FILMED

The calculation of the quantum noise properties proceeds by linearizing the equations of motion about the semiclassical steady states to calculate the variance σ^2 in photon number, about the steady state mean value n . The Mandel Q-parameter, and amplitude squeezing spectrum normalized to unit shot noise can then be constucted from the mean and variance[3]

$$Q = \frac{\sigma^2 - n}{n}; \quad V(\omega) = 1 + 2Q\frac{1}{1 + (\omega/\gamma)^2}$$

where Q > 0, = 0, and < 0, correspond to superpoissonian, poissonian and subpoissonian photon statistics, respectively, and ω is the spectral offset from the laser frequency. Subpoissonian photon statistics, and concomitant intensity squeezing (V < 1) in the output are signatures of the quantum mechanical nature of the electromagnetic field.

For the case where all spontaneous emission from the excited state goes to ground ($w_{12} = 0$) adiabatic elimination of the atomic fluctuations leads to the equation for photon number fluctuations, for n >> n_s (the saturation photon number), and dropping carets for notational simplicity

$$\frac{d}{dt}\Delta n = -\gamma\Delta n + G(t),$$

where

$$G(t) = \frac{1}{1 + \frac{w_{02}}{\Gamma_1} + \frac{2w_{20}}{\Gamma_1}} G_2 - \frac{\frac{w_{02}}{\Gamma_1} + \frac{2w_{20}}{\Gamma_1}}{1 + \frac{w_{02}}{\Gamma_1} + \frac{2w_{20}}{\Gamma_1}} G_1 + G_p \ .$$

We then find

$$\sigma^2 = n - \frac{\frac{2w_{20}}{\Gamma_1}}{\left(1 + \frac{w_{02}}{\Gamma_1} + \frac{2w_{20}}{\Gamma_1}\right)^2} n + O(n_s)$$

so that the intracavity photon statistics are sub-poissonian, with intensity squeezing (V < 1) in the output. Fig. 2 shows the intensity squeezing at the laser frequency (ω = 0, in the rotating frame of reference), as a function of pump rate, for three different values of the stimulated emission coefficient Π. With increase in Π, the degree of squeezing saturates at around 45% below shot noise level. Analysis of this result indicates that the predicted subpoissonian photon statistics and squeezing are due to a reduction in the role of pump noise and

242

spontaneous emission from the upper atomic level, when w_{20} is increased from the undepleted pump regime (where the photon statistics are poissonian and the output is shot noise limited), towards Γ_1. For larger pump rates these noise terms continue to decrease, and one might expect the degree of squeezing to increase. However spontaneous emission from the lower lasing level, which has little effect on squeezing in the undepleted pump regime provided only that $\Gamma_1 \gg \Gamma_2$, becomes increasingly important as the pump rate is increased (even for $\Gamma_1 \gg \Gamma_2$), and this random noise causes the degree of squeezing to be reduced with yet further increase in pump power. The two opposing tendencies may be seen by inspection of the pump rate dependence of the coefficients of the noise terms in the equation for $G(t)$.

The results presented are consisitent with fully numerical solutions of a three level laser obtained by Ralph and Savage. Note that the squeezing properties of the laser were also recently considered in ref. 5. After our conference presentation we received a preprint by Ritsch et al,[6] which contains closely related results.
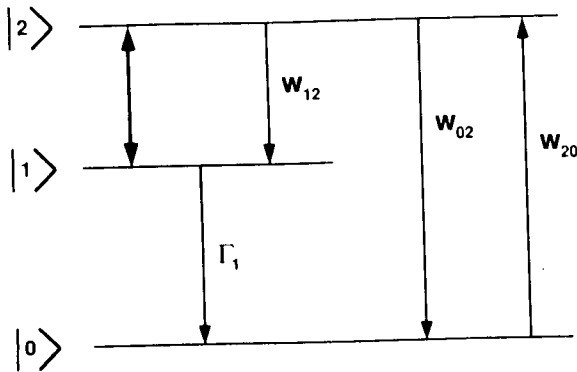
Fig.1: Atomic level scheme
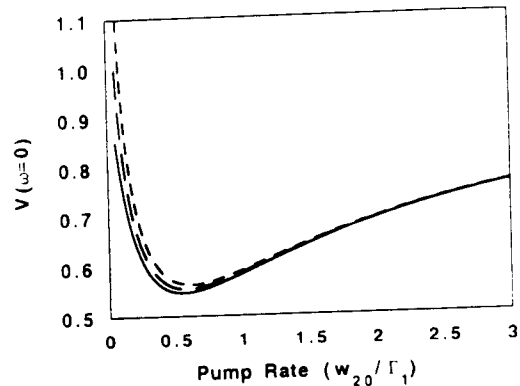
Fig.2: Amplitude squeezing versus pumping

References:

1.   S. Machida, Y. Yamamoto and Y. Itacha, 1987, Phys. Rev. Lett. 58, 1000 .

2.   M. Lax and W.H. Louisell, 1969, Phys. Rev. 185, 568.

3.   T.A.B. Kennedy and D.F. Walls, 1989, Phys. Rev. A40, 6366.

4.   T.C. Ralph and C.M. Savage, private communication.

5.   A.M Khazanov, G. A. Koganov and E.P. Gordov, 1990, Phys. Rev. A 42, 3065.

6.   H. Ritsch, P. Zoller, C.W. Gardiner and D.F. Walls, private communication.

III. Theoretical Developments

SQUEEZED STATES AND PATH INTEGRALS

628176

14 G,

Ingrid Daubechies
AT&T Bell Laboratories
Murray Hill
New Jersey, 07974
and
John R. Klauder
Departments of Physics and Mathematics
University of Florida
Gainesville, FL 32611

ABSTRACT

The continuous-time regularization scheme for defining phase-space path integrals is briefly reviewed as a method to define a quantization procedure that is completely covariant under all smooth canonical coordinate transformations. As an illustration of this method, a limited set of transformations is discussed that have an image in the set of the usual squeezed states. It is noteworthy that even this limited set of transformations offers new possibilities for stationary phase approximations to quantum mechanical propagators.

1. INTRODUCTION

For many years now it has been customary to define path integrals with the aid of coherent states [1]. Such formulations have been developed not only for the canonical coherent states suitable for the Weyl group (i.e., the Heisenberg algebra), but for coherent states based on other groups as well, notably the unitary and orthogonal groups with (in)definite signature, the affine group, etc. However, for the sake of convenience and to focus on the relation with standard squeezed states, attention in this paper will be confined to path integrals constructed with the aid of canonical coherent states. The construction of coherent state path integrals is generally carried out in one of two standard procedures [2]. To illustrate these two procedures let us first introduce a few standard definitions involving coherent states [2]:

$$1 = \int |p, q\rangle \langle p, q| \, dpdq/2\pi,$$

$$H(p, q) = \langle p, q|\mathcal{H}|p, q\rangle,$$

$$H(p_2, q_2; p_1, q_1) = \langle p_2, q_2|\mathcal{H}|p_1, q_1\rangle / \langle p_2, q_2|p_1, q_1\rangle,$$

$$\mathcal{H} = \int h(p, q) \, |p, q\rangle \langle p, q| \, dpdq/2\pi,$$

where $|p, q\rangle$, $(p, q) \in \mathbb{R}^2$, denotes one of a collection of coherent states defined by

$$|p, q\rangle = e^{-iqP} e^{ipQ} |0\rangle, \quad [Q, P] = i, \quad (Q + iP) |0\rangle = 0,$$

all of which are normalized, $\langle p, q | p, q \rangle = 1$. In addition, we have introduced two "symbols" associated with a fairly general operator $\mathcal{H}$, namely H and h as functions on phase space. In terms of these quantities, the propagator form time t' to time $t'' = t' + T$, $T > 0$, is given by either of the two expressions

$$\langle p'', q'' | e^{-i\mathcal{H}T} | p', q' \rangle = \lim_{N \to \infty} \int \cdots \int \times$$

$$\prod_{n=0}^{n=N} \langle p_{n+1}, q_{n+1} | p_n, q_n \rangle \, e^{-i\varepsilon H(p_{n+1}, q_{n+1}; p_n, q_n)} \prod_{n=1}^{n=N} dp_n dq_n / 2\pi.$$

$$\langle p'', q'' | e^{-i\mathcal{H}T} | p', q' \rangle = \lim_{N \to \infty} \int \cdots \int \times$$

$$\prod_{n=0}^{n=N} \langle p_{n+1}, q_{n+1} | p_n, q_n \rangle \prod_{n=1}^{n=N} e^{-i\varepsilon h(p_n, q_n)} dp_n dq_n / 2\pi,$$

where we have introduced the notation $\varepsilon = T/(N+1)$, $p'', q'' = p_{N+1}, q_{N+1}$, and $p', q' = p_0, q_0$. In a formal limit, in which the order of integration and the limit are interchanged and the integrand is evaluated for continuous and differential paths, the formal result emerges, respectively, that

$$\langle p'', q'' | e^{-i\mathcal{H}T} | p', q' \rangle = \mathcal{M} \int e^{i \int [p\dot{q} - H(p, q)] dt} \mathcal{D}p \mathcal{D}q,$$

$$\langle p'', q'' | e^{-i\mathcal{H}T} | p', q' \rangle = \mathcal{M} \int e^{i \int [p\dot{q} - h(p, q)] dt} \mathcal{D}p \mathcal{D}q,$$

where, as conventional, we use a single standard integral sign here to represent a (formal) functional integration. Since, in the general case, $H(p, q) \neq h(p, q)$, we are seemingly led to a paradox, namely that two generally *different* expressions can be given for the *same* quantity. That these two expressions are different is just a dramatic reflection of the very formal nature of such "equations" in the first place; each is correct if interpreted in the manner indicated in the lattice regularized form given above.

In recent years, a very different regularization and formulation of coherent state path integrals has been developed that is both rigorous in construction and does not exhibit the

paradox outlined above [3]. In this formulation, a *continuous-time regularization* scheme is found that takes the form

$$\langle p'', q'' | e^{-i\mathcal{H}T} | p', q' \rangle = \lim_{\nu \to \infty} 2\pi e^{\nu T/2} \int e^{i \int [p(t)dq(t) - h(p(t),q(t))dt]} d\mu_W^\nu (p, q),$$

where μ_W^ν denotes a planar two-dimensional Wiener measure with diffusion constant ν that is pinned so that $p(t'), q(t') = p', q'$ and $p(t''), q(t'') = p'', q''$. Since $p(t)$ and $q(t)$ are (independent) Brownian motion paths, the integral $\int p(t) dq(t)$ is properly understood as a well-defined stochastic integral [4]. In the present form the Ito and Stratonovich formulations yield the same result; however, under coordinate transformations the Stratonovich form is chosen and so it is convenient to adopt the Stratonovich form from the outset. It must be appreciated that the expression above involving the Wiener measure is rigorous and unambiguous; the marvel is that this genuine, i.e., continuous time, path integral formulation actually provides the correct propagator for the Hamiltonian $\mathcal{H}$ provided one adopts the symbol $h(p, q)$ to use as the classical Hamiltonian in the action even though it may, in general, contain a nonzero $\hbar$. In a formal, but nevertheless suggestive language, one may also say that

$$\langle p'', q'' | e^{-i\mathcal{H}T} | p', q' \rangle = \lim_{\nu \to \infty} \mathcal{M} \int e^{i \int [p\dot{q} - h(p,q)]dt} e^{-\frac{1}{2\nu} \int [\dot{p}^2 + \dot{q}^2]dt} \mathcal{D}p\mathcal{D}q,$$

which shows the continuous-time regulatory nature of the indicated expression inasmuch as the ν–dependent factor in the integrand formally goes to unity as $\nu \to \infty$. Although formal in nature, the last equation may be understood as a short hand expression for the former one when it is accepted that the various terms do not have independent meaning but only in combination with one another. Thus they may be recombined into the proper mathematical form at any time. (This is similar to how the "quotient" dy/dx should be understood for the derivative.)

The expression for the propagator given above is not only well defined mathematically, but it also enjoys a covariance under generally time-dependent canonical coordinate transformations. Let two canonical coordinate systems be related according to the equation

$$p\,dq - h(p, q) = \overline{p}\,d\overline{q} + dG(\overline{p}, \overline{q}, t) - k(\overline{p}, \overline{q}, t)$$

that not only holds in the classical case *but for Brownian motion paths* as well thanks to the choice of the Stratonovich rule [4]. Under the same canonical coordinate transformation, the metric on flat space that supports the two-dimensional Brownian motion changes to

$$dp^2 + dq^2 = d\sigma^2(\overline{p}, \overline{q}, t) = A(\overline{p}, \overline{q}, t)\,d\overline{p}\,d\overline{p} + B(\overline{p}, \overline{q}, t)\,d\overline{p}\,d\overline{q} + C(\overline{p}, \overline{q}, t)\,d\overline{q}\,d\overline{q}$$

and as a consequence the propagator takes on the form in the new coordinates, which for convenience we relabel p, q again,

$$\lim_{\nu \to \infty} \mathcal{M} e^{i(G'' - G')} \int e^{i \int [p\dot{q} - k(p,q,t)]dt} e^{-\frac{1}{2\nu} \int [d\sigma^2(p,q,t)/dt^2]dt} \mathcal{D}p \mathcal{D}q$$

This formula expresses —for the first time and after over sixty years of the theory of quantum mechanics—*a fully canonically coordinate covariant formulation of the process of quantization* [5]. This expression clarifies the role of the Schroedinger quantization rule in which coordinates act as multiplication while momenta act as derivatives; this rule of quantization is valid in and only in Cartesian coordinates as often noted, but Cartesian coordinates in *phase space* rather than in p-space and q-space *separately* as commonly stated [6]. Of course, the arena for classical mechanics resides in a symplectic manifold and it does not employ a (Riemannian) metric in its formulation. On the other hand, quantum mechanics has a different and richer basis in which a metric structure appears. Indeed, it is not unreasonable from a classical viewpoint that a metric structure is appended to the classical phase-space manifold, not for purposes of defining the Hamiltonian equations of motion, but rather to keep track of just what physics a given system refers to. For example, an harmonic oscillator (centered at the origin) *appears* as an harmonic oscillator, e.g., with a Hamiltonian given by $\frac{1}{2}\left(ap^2 + 2bpq + cq^2\right)$, $a > 0$, $b > 0$, $ac > b^2$, *only* in Cartesian coordinates in phase space. In *non*-Cartesian coordinates an harmonic oscillator assumes a different form from that indicated. Just what system actually corresponds to an harmonic oscillator (or free particle, or quartic anharmonic oscillator, etc.) is coded into the classical scheme by the implicit use of an auxiliary *flat metric* on the two-dimensional phase space, and its expression in Cartesian coordinates. This same flat metric space actually enters the formulation of the quantization procedure as described in the present article through its use as a carrier for the Brownian motion. Once it is decided which sets of canonical coordinates are the Cartesian ones, so that the expression for a system which represents (say) an harmonic oscillator is unambiguous, then the quantization procedure itself is unambiguous in the approach advocated here. After the well-defined path integral is set up, then one is free to make a variety of coordinate changes within that integral, among which possibly time dependent canonical transformations are to be distinguished. Indeed, one can go so far as to introduce a Hamilton-Jacobi transformation so that the new Hamiltonian vanishes. This puts all the dynamics into the curvilinear coordinate system that is used to track the two-dimensional planar Brownian motion. As a consequence, the overall level of difficulties is conserved, as one would expect to be the case.

It is hard to illustrate this program in its full potential, but it can be shown in a sort of small scale fashion. Indeed, it is *squeezed states* that can be used to provide a limited illustration of this overall program, and it is this "miniature" illustration to which we now

turn our attention. A convenient place to start the investigation is with the kinematics rather than the dynamics, and this in turn can be done simply by looking at the propagator for vanishing Hamiltonian.

2. CHANGE OF VARIABLES IN THE PATH INTEGRAL: CONSTANT ω TRANSFORMATIONS

KINEMATICS

If the Hamiltonian vanishes, or in the limit that $T \to 0$, the "propagator" reduces to the *reproducing kernel*, an integral kernel representing a projection operator onto the relevant subspace of all square integrable functions on phase space as given by

$$\langle p'', q''; 1 | p', q'; 1 \rangle = \lim_{\nu \to \infty} \mathcal{M} \int e^{i \int p\dot{q}dt} e^{-\frac{1}{2\nu} \int (\dot{p}^2 + \dot{q}^2)dt} \mathcal{D}p \mathcal{D}q,$$

which may be explicitly evaluated as

$$\langle p'', q''; 1 | p', q'; 1 \rangle = e^{i\frac{1}{2}(p''+p')(q''-q') - \frac{1}{4}[(p''-p')^2 + (q''-q')^2]}.$$

In these expressions we have added a "1" to the label to emphasize that the coherent states are those based on an harmonic oscillator ground state with a unit angular frequency, $\omega = 1$. In particular, for a general value of ω, the configuration space representation of the coherent states reads

$$\langle x | p, q; \omega \rangle = \left(\frac{\omega}{\pi}\right)^{\frac{1}{4}} e^{-\frac{1}{2}\omega(x-q)^2 + ip(x-q)},$$

and it follows that the overlap of two such states for the same value of ω is given by

$$\langle p'', q''; \omega | p', q'; \omega \rangle = \int \langle p'', q''; \omega | x \rangle \langle x | p', q'; \omega \rangle dx$$

$$= \exp\left\{\frac{i}{2}(p''+p')(q''-q') - \frac{1}{4}\left[\omega^{-1}(p''-p')^2 + \omega(q''-q')^2\right]\right\}.$$

It is clear therefore that the coherent state overlap obeys the identity

$$\langle p'', q''; \omega | p', q'; \omega \rangle = \langle \omega^{-\frac{1}{2}}p'', \omega^{\frac{1}{2}}q''; 1 | \omega^{-\frac{1}{2}}p', \omega^{\frac{1}{2}}q'; 1 \rangle$$

which relates dilation of the angular frequency to a corresponding dilation of the coherent state labels, i.e., an expansion of one phase space coordinate and a contraction of the other.

This relation may be codified another way as well. Let

$$D = \frac{1}{2}(PQ + QP)$$

denote the self-adjoint dilation operator with commutation properties $[Q, D] = iQ$, $[P, D] = -iP$, then it follows that coherent states for different angular frequencies are connected by

$$|p, q; \omega\rangle = e^{i\frac{1}{2}\ln(\omega)D}|\omega^{-\frac{1}{2}}p, \omega^{\frac{1}{2}}q; 1\rangle.$$

Thus the unitary transformation generated by D is nothing other than the squeeze operator relating coherent states and squeezed states, or relating two sets of squeezed states with different squeezing values. In forming the overlap illustrated above, the squeezing operator drops out leading to the indicated relation.

A path integral expression for the coherent state overlap at angular frequency ω can be readily obtained just by a coordinate change of the path integral appropriate for a unit angular frequency. In particular, if one makes the change of integration variables given by

$$p(t) \rightarrow \omega^{-\frac{1}{2}}p(t), \qquad q(t) \rightarrow \omega^{\frac{1}{2}}q(t),$$

then it immediately follows that

$$\langle p'', q''; \omega | p', q'; \omega \rangle = \lim_{\nu \rightarrow \infty} \mathcal{M} \int e^{i\int p\dot{q}dt} e^{-\frac{1}{2\nu}\int(\omega^{-1}\dot{p}^2 + \omega\dot{q}^2)dt} \mathcal{D}p\mathcal{D}q$$

showing quite clearly the connection of the relative scale factor in the two-dimensional Brownian motion and the parametric dependence in the coherent state representation. All this has assumed that ω has been constant throughout; next we take up the case of a time variable ω.

3. CHANGE OF VARIABLES IN THE PATH INTEGRAL: NONCONSTANT ω TRANSFORMATIONS

The overlap of two coherent states for two *different* values of ω is given by

$$\langle p'', q''; \omega'' | p', q'; \omega' \rangle = \int \langle p'', q''; \omega'' | x \rangle \langle x | p', q'; \omega' \rangle dx$$

$$= \frac{\sqrt{2}}{\sqrt{\sqrt{\frac{\omega''}{\omega'}} + \sqrt{\frac{\omega'}{\omega''}}}} \exp\left[i\frac{(p''\omega' + p'\omega'')(q'' - q')}{\omega'' + \omega'} - \frac{(p'' - p')^2}{2(\omega'' + \omega')} - \frac{\omega''\omega'(q'' - q')^2}{2(\omega'' + \omega')}\right].$$

This expression also exhibits an alternative form given by

$$\langle p'', q''; \omega'' | p', q'; \omega' \rangle = \langle \omega''^{-\frac{1}{2}} p'', \omega''^{\frac{1}{2}} q''; 1 | e^{-i\frac{1}{2}\ln\left(\frac{\omega''}{\omega'}\right)D} | \omega'^{-\frac{1}{2}} p', \omega'^{\frac{1}{2}} q'; 1 \rangle$$

$$= \langle \omega''^{-\frac{1}{2}} p'', \omega''^{\frac{1}{2}} q''; 1 | e^{-i\int\frac{d\omega}{2\omega}D} | \omega'^{-\frac{1}{2}} p', \omega'^{\frac{1}{2}} q'; 1 \rangle$$

$$= \langle \omega''^{-\frac{1}{2}} p'', \omega''^{\frac{1}{2}} q''; 1 | e^{-i\int\frac{\dot{\omega}}{2\omega}dt D} | \omega'^{-\frac{1}{2}} p', \omega'^{\frac{1}{2}} q'; 1 \rangle$$

where we have introduced a smooth but otherwise arbitrary function $\omega(t)$, $\quad t' \le t \le t''$, which interpolates between $\omega'' = \omega(t'')$ and $\omega' = \omega(t')$. Of course, this expression holds as well even in the special case that $\omega'' = \omega'$ in which case $\omega(t)$ goes smoothly between equal initial and final values, but is otherwise arbitrary.

In the latter form the overlap of two coherent states for differing angular frequencies has been expressed in terms of the matrix element of a kind of propagator between coherent states of the same angular frequency. But the latter form admits a path integral expression. In particular, it follows that

$$\langle p'', q''; 1 | e^{-i\int\frac{\dot{\omega}}{2\omega}D dt} | p', q'; 1 \rangle$$

$$= \lim_{\nu \to \infty} \mathcal{M} \int e^{i\int[p\dot{q} - \frac{\dot{\omega}}{2\omega}pq]dt} e^{-\frac{1}{2\nu}\int[\dot{p}^2 + \dot{q}^2]dt} \mathcal{D}p\mathcal{D}q.$$

Now, much as was the case earlier when ω was constant, we next make a time-dependent change of variables of the form

$$p(t) \to \omega(t)^{-\frac{1}{2}} p(t),$$
$$q(t) \to \omega(t)^{\frac{1}{2}} q(t),$$

where $\omega'' = \omega(t'')$, $\omega' = \omega(t')$. In making a time-dependent substitution of variables, additional terms will arise in the path integral integrand on the right hand side. In particular, the term

$$\int [p\dot{q} - \tfrac{\dot{\omega}}{2\omega}pq]dt \to \int [p\dot{q}]dt,$$

the formal flat measure remains unchanged,

$$\mathcal{D}p\mathcal{D}q \to \mathcal{D}p\mathcal{D}q,$$

while the all important formal weighting factor

$$e^{-\frac{1}{2\nu}\int[\dot{p}^2 + \dot{q}^2]dt} \to e^{-\frac{1}{2\nu}\int[\omega(t)^{-1}\dot{p}^2 + \omega(t)\dot{q}^2]dt}.$$

Other terms might be contemplated in the exponent of the final expression such as those involving time derivatives of $\omega(t)$; however all of these will be negligible in the limit that $\nu \to \infty$ since they are not as singular as the indicated terms. While we prefer this heuristic characterization of the transformed Wiener process one should bear in mind that only the *coordinate description* of the planar two-dimensional Brownian motion is being changed and the process itself is in no way effected. We are encoding this change of coordinates by means of the change of coordinates of the metric on the plane. (A rigorous analysis of such transformed Wiener processes is in progress by the present authors.) Thus it follows after such a substitution of variables that

$$\langle p'', q''; \omega'' | p', q'; \omega' \rangle = \langle \omega''^{-\frac{1}{2}} p'', \omega''^{\frac{1}{2}} q''; 1 | e^{-i\frac{1}{2}\int \frac{\dot{\omega}}{\omega} D dt} | \omega'^{-\frac{1}{2}} p', \omega'^{\frac{1}{2}} q'; 1 \rangle$$

$$= \lim_{\nu \to \infty} \mathcal{M} \int e^{i \int p\dot{q} dt} e^{-\frac{1}{2\nu} \int [\omega(t)^{-1}\dot{p}^2 + \omega(t)\dot{q}^2] dt} \mathcal{D}p \mathcal{D}q.$$

Consequently, the introduction of a smooth, time-dependent angular frequency that interpolates between the initial and final values in the Wiener measure provides just the right ingredient to yield the overlap between two different coherent states based on two different angular frequencies. This expression yields a simple but nontheless bona fide example of how the classical Hamiltonian — here just $\dot{\omega}(t) p(t) q(t) / 2\omega(t)$ — may be eliminated in favor of a change of coordinates with which to describe the two-dimensional Brownian motion on the phase space plane. Such an elimination additionally involves a change of coordinates at the endpoints, as illustrated in the central equation, but in the case of squeezed states, there is an alternative interpretation involving coherent states based on differing angular frequencies as embodied in the first part of the equation. We now turn our attention to the inclusion of dynamics in this example through the presence of a rather general nonvanishing Hamiltonian.

4. CHANGE OF VARIABLES IN THE PATH INTEGRAL: NONCONSTANT ω TRANSFORMATIONS AND A GENERAL HAMILTONIAN

INTRODUCTION OF GENERAL DYNAMICS

Based on the earlier discussion it is quite straightforward to include a rather general Hamiltonian $h(p,q)$ into the problem. In particular, based on the initial discussion, let us consider

$$\langle p'', q''; 1 | T e^{-i\int [\mathcal{H} + \frac{\dot{\omega}}{2\omega} D] dt} | p', q'; 1 \rangle$$

$$= \lim_{\nu \to \infty} \mathcal{M} \int e^{i \int [p\dot{q} - h(p,q) - \frac{\dot{\omega}}{2\omega} pq] dt} e^{-\frac{1}{2\nu} \int [\dot{p}^2 + \dot{q}^2] dt} \mathcal{D}p \mathcal{D}q$$

which after a change of integration variables becomes

$$\lim_{\nu \to \infty} \mathcal{M} \int e^{i \int [p\dot{q} - k(p,q,t)]dt} e^{-\frac{1}{2\nu} \int [\omega(t)^{-1}\dot{p}^2 + \omega(t)\dot{q}^2]dt} \mathcal{D}p\mathcal{D}q$$

$$= \langle \omega''^{-\frac{1}{2}}p'', \omega''^{\frac{1}{2}}q''; 1| T e^{-i \int [\mathcal{H} + \frac{\dot{\omega}}{2\omega}D]dt} |\omega'^{-\frac{1}{2}}p', \omega'^{\frac{1}{2}}q'; 1\rangle$$

$$= \langle \omega''^{-\frac{1}{2}}p'', \omega''^{\frac{1}{2}}q''; 1| e^{-\frac{i}{2}\ln\omega'' D} T e^{-i \int \mathcal{H}'(t)dt} e^{\frac{i}{2}\ln\omega' D} |\omega'^{-\frac{1}{2}}p', \omega'^{\frac{1}{2}}q'; 1\rangle$$

$$= \langle p'', q''; \omega''| T e^{-i \int \mathcal{H}'(t)dt} |p', q'; \omega'\rangle,$$

where

$$k\left(p\left(t\right), q\left(t\right), t\right) = h\left(\omega\left(t\right)^{-\frac{1}{2}}p\left(t\right), \omega\left(t\right)^{\frac{1}{2}}q\left(t\right)\right),$$

which contains an explicit time dependence from the angular frequency as well as an implicit dependence just from the time dependence of p and q themselves, and in addition where

$$\mathcal{H}'\left(t\right) = e^{i\frac{1}{2}\ln\frac{\omega(t)}{\omega'}D} \mathcal{H} e^{-i\frac{1}{2}\ln\frac{\omega(t)}{\omega'}D}.$$

The basic significance of the preceding equations can be summarized as follows:

$$\langle p'', q''; \omega''| T e^{-i \int \mathcal{H}'(t)dt} |p', q'; \omega'\rangle$$

$$= \langle \omega''^{-\frac{1}{2}}p'', \omega''^{\frac{1}{2}}q''; 1| T e^{-i \int [\mathcal{H} + \frac{\dot{\omega}}{2\omega}D]dt} |\omega'^{-\frac{1}{2}}p', \omega'^{\frac{1}{2}}q'; 1\rangle$$

$$= \left[\lim_{\nu \to \infty} \mathcal{M} \int e^{i \int [p\dot{q} - h(p,q) - \frac{\dot{\omega}}{2\omega}pq]dt} e^{-\frac{1}{2\nu} \int [\dot{p}^2 + \dot{q}^2]dt} \mathcal{D}p\mathcal{D}q \right]_{\substack{p(t)\to\omega(t)^{-\frac{1}{2}}p(t) \\ q(t)\to\omega(t)^{\frac{1}{2}}q(t)}}$$

$$= \lim_{\nu \to \infty} \mathcal{M} \int e^{i \int [p\dot{q} - k(p,q,t)]dt} e^{-\frac{1}{2\nu} \int [\omega(t)^{-1}\dot{p}^2 + \omega(t)\dot{q}^2]dt} \mathcal{D}p\mathcal{D}q.$$

This is the most general form we are able to offer using squeezed states, and it shows, in the first of the equalities, how part of the Hamiltonian can be absorbed quantum mechanically by a change of the fiducial vectors — indeed just like going to the interaction picture in ordinary quantum mechanics, which is then responsible for the introduction of the time-dependent "interaction" picture Hamiltonian $\mathcal{H}'\left(t\right)$. The second pair of equalities just uses the original form of the path integral as modified by a change of variables that effects the end point conditions as well. The final equality just accounts for that very change of variables as requested in the line above.

5. EQUAL END POINT ANGULAR FREQUENCIES

Let us return to the path integrals discussed at the beginning of this article, namely to those for which the initial and final angular frequencies are the same. For the sake of convenience, let us choose that value to be unity, i.e., $\omega'' = \omega' = 1$, and return to the original notation for the coherent states with unit ω, namely that $|p, q\rangle = |p, q; 1\rangle$. However, this time we will retain the option of using a time-dependent angular frequency $\omega(t)$ to interpolate smoothly between the original and final values of unity. In this case the formulas developed above simplify to become

$$\langle p'', q'' | T e^{-i \int \mathcal{H}'(t) dt} | p', q' \rangle$$

$$= \langle p'', q'' | T e^{-i \int [\mathcal{H} + \frac{\dot{\omega}}{2\omega} D] dt} | p', q' \rangle$$

$$= \left[\lim_{\nu \to \infty} \mathcal{M} \int e^{i \int [p\dot{q} - h(p,q) - \frac{\dot{\omega}}{2\omega} pq] dt} e^{-\frac{1}{2\nu} \int [\dot{p}^2 + \dot{q}^2] dt} \mathcal{D}p \mathcal{D}q \right]_{\substack{p(t) \to \omega(t)^{-\frac{1}{2}} p(t) \\ q(t) \to \omega(t)^{\frac{1}{2}} q(t)}}$$

$$= \lim_{\nu \to \infty} \mathcal{M} \int e^{i \int [p\dot{q} - k(p,q,t)] dt} e^{-\frac{1}{2\nu} \int [\omega(t)^{-1} \dot{p}^2 + \omega(t) \dot{q}^2] dt} \mathcal{D}p \mathcal{D}q.$$

With a slight generalization, we can now turn this equation around to read

$$\langle p'', q'' | e^{-i\mathcal{H}T} | p', q' \rangle$$

$$= \lim_{\nu \to \infty} \mathcal{M} \int e^{i \int [p\dot{q} - h(p,q)] dt} e^{-\frac{1}{2\nu} \int [\dot{p}^2 + \dot{q}^2] dt} \mathcal{D}p \mathcal{D}q.$$

$$= \left[\lim_{\nu \to \infty} \mathcal{M} \int e^{i \int [p\dot{q} - h(p,q)] dt} e^{-\frac{1}{2\nu} \int [\dot{p}^2 + \dot{q}^2] dt} \mathcal{D}p \mathcal{D}q \right]_{\substack{p(t) \to \omega(t)^{-\frac{1}{2}} p(t) \\ q(t) \to \omega(t)^{\frac{1}{2}} q(t)}}$$

$$= \lim_{\nu \to \infty} \mathcal{M} \int e^{i \int [p\dot{q} - k(p,q,t) + \frac{\dot{\omega}}{2\omega} pq] dt} e^{-\frac{1}{2\nu} \int [\omega(t)^{-1} \dot{p}^2 + \omega(t) \dot{q}^2] dt} \mathcal{D}p \mathcal{D}q.$$

In this expression the third line holds because it simply corresponds to a change of integration variables that does not have any effect on the values of the boundary labels since $\omega'' = \omega' = 1$. The last line represents, just as before, the consequences of that very change of variables.

256

Now observe that on the *left* side of this equation there is no reference to the function $\omega(t)$, $t' \leq t \leq t''$, $\omega(t'') = \omega(t') = 1$, while on the *right* side of the equation, in the last part of the equation in particular, the function $\omega(t)$ enters in a prominent way. This becomes especially significant when an *approximate* evaluation of the path integral is admitted, such as that which arises from a *stationary phase approximation*. Stationary phase approximations for coherent state path integrals with Wiener measure regularization of the kind considered here have been worked out previously [7] and we do not repeat that discussion here. The point we wish to emphasize, however, is that the choice of the angular frequency $\omega(t)$ *will* enter most probably in the form of the approximate solution, and naturally some expressions will be better approximations to the real answer than other expressions will. Just which will be the best approximation is, of course, not too easy to establish. Perhaps one scheme is to ask that the result be stationary with respect to small changes of the functional form of $\omega(t)$. In practice one might want to let $\omega(t)$ depend on just a few discrete parameters and to seek stationary variations with respect to just these few parameters. This certainly seems easier to do than to ask for an extremal variation with respect to the entire function $\omega(t)$.

One can actually see a miniature working of *this* general kind of procedure in comparing the usual and the Maslov stationary phase approximations to the sharp position propagator; see, e.g., [7]. As given earlier, the configuration-space form of the coherent states given by

$$\langle x|p,q;\omega\rangle = \left(\frac{\omega}{\pi}\right)^{\frac{1}{4}} e^{-\frac{1}{2}\omega(x-q)^2 + ip(x-q)},$$

makes clear that $\lim_{\omega \to \infty} \left(\frac{\omega}{4\pi}\right)^{\frac{1}{4}} \langle x|p,q;\omega\rangle = \delta(x-q)$ which converts the coherent state representation to the sharp position or configuration representation, while $\lim_{\omega \to 0} \left(\frac{1}{4\pi\omega}\right)^{\frac{1}{4}} \langle x|p,q;\omega\rangle = \frac{1}{\sqrt{2\pi}} e^{ip(x-q)}$ which converts it to the dual or momentum representation (up to an unimportant phase factor). These features can also be seen in the relation

$$\langle p'',q'';\omega''|p',q';\omega'\rangle = \int \langle p'',q'';\omega''|x\rangle\langle x|p',q';\omega'\rangle dx$$

$$= \frac{\sqrt{2}}{\sqrt{\sqrt{\frac{\omega''}{\omega'}} + \sqrt{\frac{\omega'}{\omega''}}}} \exp\left[i\frac{(p''\omega' + p'\omega'')(q'' - q')}{\omega'' + \omega'} - \frac{(p'' - p')^2}{2(\omega'' + \omega')} - \frac{\omega''\omega'(q'' - q')^2}{2(\omega'' + \omega')}\right].$$

that gives the overlap of two coherent states based on differing angular frequencies. Consider the limiting situation in which both $\omega'' \to \infty$, $\omega' \to 0$. In that case it follows that

$$\lim_{\substack{\omega'' \to \infty \\ \omega' \to 0}} \left(\frac{\omega''}{16\pi^2\omega'}\right)^{\frac{1}{4}} \langle p'',q'';\omega''|p',q';\omega'\rangle = \frac{1}{\sqrt{2\pi}} e^{ip'(q''-q')}.$$

Thus it should be no surprise that the two standard stationary-phase type approximations are actually contained in the coherent state approach in the form of suitable limits. In a manner of speaking, the usual configuration space approach just involves choosing a constant and very large value of the angular frequency parameter ω (taken to infinity at the end of the calculation) and making a stationary phase approximation to the resulting path integral. On the other hand, the Maslov approach takes the propagator from a sharp configuration initially to a sharp momentum finally, approximates that path integral by a stationary phase approximation, and then returns the end point to configuration space by a Fourier transform. This approach can be approximated in our method by taking an angular frequency history $\omega(t)$ that is initially huge (tending toward infinity) and finally very small (tending toward zero), approximating *that* path integral by a stationary phase approximation, and finally making a change from coherent states based on a very small angular frequency to one based on a huge angular frequency just by the kinematical factor given above. The coherent state approximation developed in particular in reference [7] proceeds in yet another way, namely, starting with a sharp configuration initially, propagating to a coherent state with a finite nonzero value of the angular frequency, i.e., $\omega = O(1)$, approximating *that* path integral by a stationary phase approximation, and then passing from the final coherent state representation to a sharp configuration one. This approach can also be approximated in our scheme by having an $\omega(t)$ that initially is huge, and finally is finite and nonzero [$O(1)$], approximating, in turn, *that* path integral by a stationary phase approximation, and then passing back to a coherent state based on a huge angular frequency at the final point.

6. CONCLUSIONS

In this article we have attempted to show the reader what the authors believe is the "latest" in path integral construction — the state of the art — and illustrate how variable changes can be *rigorously* carried out within the path integral formulation itself. Squeezed coherent states have been used as convenient bases throughout in the illustration of the general program by a "miniature" subprogram involving a fairly limited change of integration variables. The resultant formalism is able to express a path integral in terms of an essentially arbitrary function, the time varying angular frequency, $\omega(t)$, which lends itself to various selections in case an approximation scheme is invoked. By illustrating that the usual and the Maslov approaches are but two small examples of how such an optimization can be used, it becomes clear that there are hidden in these formulas a whole host of differing approximation schemes some of which, in certain applications at least, may well be better than the schemes currently in use. It is left to the future to see just how to exploit the vast number of possibilities that have been opened up here.

REFERENCES

1. Klauder, J.R., 1960, "The Action Option and The Feynman Quantization of Spinor Fields without Anticommuting C-Numbers," *Annals of Physics* 11, p. 123.
2. Klauder, J.R. and B.-S. Skagerstam, 1985, *Coherent States*, World Scientific, Singapore.
3. Daubechies, I. and J.R. Klauder, 1985, "Quantum Mechanical Path Integrals with Wiener Measures for All Polynomial Hamiltonians, II," *J. Math. Phys.* 26, p. 2239.
4. See, e.g., McShane, E.J., 1974, *Stochastic Calculus and Stochastic Models*, Academic Press, New York.
5. Klauder, J.R., 1988, "Quantization *Is* Geometry, After All," *Annals of Physics* 188, p. 120.
6. See, e.g., Dirac, P.A.M., 1956, *The Principles of Quantum Mechanics*, Third Edition, Oxford University Press, Oxford, p. 114.
7. Klauder, J.R., 1987, "Global, Uniform, Asymptotic Wave-Equation Solutions for Large Wave Numbers," *Annals of Physics* 180, p. 108.

SUPERCOHERENT STATES AND PHYSICAL SYSTEMS

62 8183

8 fs

B.W. Fatyga and V. Alan Kostelecký*

*Physics Department, Indiana University
Bloomington, IN 47405, U.S.A.*

Michael Martin Nieto

*Theoretical Division, Los Alamos National Laboratory
University of California, Los Alamos, NM 87545, U.S.A.*

D. Rodney Truax

*Chemistry Department, University of Calgary
Calgary, Alberta, Canada T2N 1N4*

A method is developed for obtaining coherent states of a system admitting a supersymmetry. These states are called supercoherent states. The approach presented in this talk is based on an extension to supergroups of the usual group-theoretic approach. The example of the supersymmetric harmonic oscillator is discussed, thereby illustrating some of the attractive features of the method. Supercoherent states of an electron moving in a constant magnetic field are also described.

1. Introduction

Over the past three decades, the notion of coherent state [1-6] has enjoyed a significant role in diverse areas of physics. Several basic definitions are in use [7]. For example, among the possibilities for the simple harmonic oscillator are the definition as eigenstates of the annihilation operator, the one as states having and preserving minimum uncertainty, and the one via the displacement operator. All these yield the same harmonic-oscillator coherent states, representing a gaussian wavepacket preserving its shape while executing the classical motion.

This talk describes a generalization of the concept of coherent states to that of supercoherent states, relevant for systems admitting one or more supersymmetries. A supersymmetry involves both bosonic and fermionic states, and the

---

* Speaker

corresponding symmetry generators close under a combination of commutation and anticommutation relations into a superalgebra. The additional structure this entails means that the physically appropriate generalization of coherent states to supercoherent states is not immediately apparent.

Our solution to this problem involves a extension to supergroups of a generalized method [6] for ordinary coherent states that is based on Lie groups and involves use of the Baker-Campbell-Hausdorff (BCH) relations [8-13] connecting different group parametrizations. Supergroups can be viewed as extensions of Lie groups with Grassmann-valued parameters. The theory of supergroups considered both as abstract groups and as superanalytic supermanifolds has been developed [14-16], and methods for obtaining BCH relations for supergroups are known [17-19]. A summary of our methods is provided in section 2.

As an example of the method, the supercoherent states for the supersymmetric harmonic oscillator are considered in section 3. The supersymmetry for this case is generated by the super Heisenberg-Weyl algebra, containing the identity and bosonic and fermionic creation and annihilation operators. It is closely related to supersymmetric quantum mechanics [20-29], which is applicable in several physical situations. An example with relevance to the quantum Hall effect is the case of an electron moving in a constant magnetic field [28,29]. This situation is considered in section 4.

The reader is referred to [30], on which this talk is based, for more information about our general construction of supercoherent states, about its relation to other approaches [31-33], and about applications in various physical situations.

2. Method

There is a close connection between group theory and coherent states. To see this for the simple harmonic oscillator, consider the usual approach via the displacement operator D, given by $D(\alpha) = exp(\alpha a^\dagger - \overline{\alpha} a)$. This displaces the annihilation operator a by a complex constant α: $D^{-1}(\alpha) a D(\alpha) = a + \alpha$. The operator D is a unitary element of the harmonic-oscillator symmetry group, called the Heisenberg-Weyl group, for which the associated algebra is $[a, a^\dagger] = 1$. By definition, the coherent state parametrized by α is given by the action of $D(\alpha)$ on the ground state $|0\rangle$. The correct normalization of $|\alpha\rangle$ is fixed by the unitarity of D. The form of $|\alpha\rangle$ can then be explicitly exhibited using the BCH relation $e^A e^B = e^{(A+B+\frac{1}{2}[A,B])}$, valid for any two operators A and B both commuting with $[A, B]$.

For a general system with an arbitrary Lie group G as symmetry group, coherent states can be defined as follows [3,6]. Given a unitary irreducible representation $T(g)$ of G acting in a Hilbert space H, set $|\Psi_0\rangle$ as some given element

in H. The coherent states are then the set $\{|\Psi_g\rangle\} = \{T(g)|\Psi_0\rangle\}$. This definition is parallel to the displacement-operator approach for the harmonic oscillator.

For systems admitting supersymmetry, we extend this method to supergroups using the construction of refs. [14-16]. In this approach, supergroups are defined in analogy with the definition of Lie groups via analytic manifolds, using Grassmann-valued parameters instead of real or complex ones. The resulting supergroup coordinates include both commuting and anticommuting variables. We refer the reader to refs. [14-16] for details of the construction. A summary of the essential points is contained in the paper [30] on which this talk is based.

To find supercoherent states via the group-theoretic method requires the use of unitary supergroup representations. Introduce the supergroup generators B_j, F_α, where the corresponding superalgebra* involves commutators among the B_j and anticommutators among the F_α. Choose a superhermitian basis [31], i.e., set $B_j^\dagger = B_j$ and $F_\alpha^\dagger = -F_\alpha$. Then, a general unitary supergroup element is $T(g) = exp(A_j B_j + \theta_\alpha F_\alpha)$, where A_j is real Grassmann commuting and θ_α is real Grassmann anticommuting.

Supercoherent states are found by applying $T(g)$ to an extremal state in the (super) Hilbert space. To find explicit expressions requires the use of BCH relations for the supergroup. A general method for determining these and specific formulae for some frequently used supergroups may be found in refs. [17-19].

3. The Supersymmetric Harmonic Oscillator

By definition, the hamiltonian H of a supersymmetric quantum-mechanical system [20-23] commutes with N supersymmetry operators Q_j of which it is a quadratic function: $\delta_{jk}H = \{Q_j, Q_k\}$. The superalgebra generated by H and Q_j is called $sqm(N)$. Choosing $N = 2$ gives $sqm(2)$, which appears in several physical contexts [24-29]. Defining $Q = (Q_1 + iQ_2)/\sqrt{2}$ and $Q^\dagger = (Q_1 - iQ_2)/\sqrt{2}$, the superalgebra $sqm(2)$ is $H = \{Q, Q^\dagger\}$, $[H, Q] = [H, Q^\dagger] = 0$.

The supersymmetric quantum harmonic oscillator can be defined in terms of annihilation and creation operators a, $a^\dagger$; b, $b^\dagger$ generating a supersymmetric extension of the usual Heisenberg-Weyl algebra: $[a, a^\dagger] = \{b, b^\dagger\} = I$. The corresponding super Hilbert space is spanned by states $|n, \nu\rangle$, where $n = 0, 1, 2 \ldots$ and $\nu = 0, 1$. States with $\nu = 0$ are called bosonic and those with $\nu = 1$ are called fermionic.

The $sqm(2)$ superalgebra is generated by the oscillator hamiltonian $H = a^\dagger a + b^\dagger b$ and by the supersymmetry operators $Q = ab^\dagger$, $Q^\dagger = a^\dagger b$. It follows from

---

* For an overview of superalgebras, see ref. [34]

$H|n, \nu\rangle = (n + \nu)|n, \nu\rangle$ that $|n, 0\rangle$ and $|n - 1, 1\rangle$ are degenerate states for all n except $n = 0$. The ground state $|0, 0\rangle$ is thus unique. Unbroken supersymmetry, $Q|0, 0\rangle = Q^\dagger|0, 0\rangle = 0$, implies that the ground state has energy eigenvalue zero. The generator $Q^\dagger$ takes bosonic states into fermionic ones, while $Q^\dagger$ takes fermionic states into bosonic ones.

Following the method described in section 2, supercoherent states for the supersymmetric oscillator are given in terms of a unitary representation $T(g)$ of the super Heisenberg-Weyl group. The supergroup element of relevance may be taken as $T(g) = exp(-\bar{A}a + Aa^\dagger + \theta b^\dagger + \bar{\theta}b)$ where A is complex Grassmann commuting and θ is complex Grassmann anticommuting. The necessary BCH relation for the super Heisenberg-Weyl group, needed for explicit calculation of the supercoherent states, is found using Lemma 1 of ref. [17]. The result is

$$T(g) = exp(\frac{1}{2}\theta\bar{\theta} - \frac{1}{2}|A|^2)exp(Aa^\dagger)exp(\theta b^\dagger)exp(-\bar{A}a)exp(\bar{\theta}b) \ . \qquad (3.1)$$

The supercoherent states $|Z\rangle$ are obtained by applying $T(g)$ to the ground state $|0, 0\rangle$. They are given by

$$|Z\rangle = (1 + \frac{1}{2}\theta\bar{\theta})|A, 0\rangle + \theta|A, 1\rangle \ , \qquad (3.2)$$

where for convenience we have defined $|A, \nu\rangle = exp(-|A|^2/2)exp(Aa^\dagger)|0, \nu\rangle$.

The supercoherent states $|Z\rangle$ have the following attractive properties, all of which are natural generalizations of the correesponding features of ordinary harmonic-oscillator coherent states.

- They are defined via a natural extension of the usual displacement operator approach.
- They are eigenstates of the annihilation operators a and b: $a|Z\rangle = A|Z\rangle$, $b|Z\rangle = -\theta|Z\rangle$.
- They maintain the minimum-uncertainty value $\Delta q \Delta p = \frac{1}{2}$ in time.
- They are unity normalized, $\langle Z|Z\rangle = 1$.
- They are not orthogonal and form an (over)complete set. The identity is resolved by $\int |Z\rangle\langle Z|d\bar{\theta}d\theta dA = \pi\mathbf{I}$.
- They yield the usual harmonic-oscillator coherent states $|A\rangle$ when $\theta = 0$.
- They contain as the subset $A = 0$ the usual fermionic coherent states [35] for a single anticommuting fermionic degree of freedom.

4. A Physical Example

The quantum system consisting of a nonrelativistic electron of mass M and charge e moving in a constant uniform magnetic field $\mathbf{B} = B\hat{z}$ provides a physical

realization of supersymmetric quantum mechanics [28,29]. The wavefunctions $e^{-iEt}\psi(\vec{r})$ for this system obey the two-component Pauli equation, which reduces to $H\psi = E\psi$ with $H \equiv \frac{1}{2M}\left[\vec{\sigma} \cdot (\vec{p} - e\vec{A})\right]^2$. The use of cylindrical coordinates is natural, as is the choice of cylindrical gauge $A_x = -\frac{1}{2}By$, $A_y = \frac{1}{2}Bx$. For simplicity, we restrict the analysis to the two-dimensional problem, so that $p_z = 0$.

The explicit realization of the super Heisenberg-Weyl algebra is as follows. Define the dimensionless quantities $\hat{H} = MH/eB$, $\hat{E} = ME/eB$, and introduce the annihilation operators

$$a = \frac{1}{\sqrt{2eB}}e^{i\varphi}\left(\partial_r + \frac{i}{r}\partial_\varphi + \frac{1}{2}eBr\right) \tag{4.1}$$

and

$$b = \begin{bmatrix} 0 & 1 \\ 0 & 0 \end{bmatrix} . \tag{4.2}$$

Then, the Pauli equation takes the manifestly supersymmetric form

$$\hat{H}\psi \equiv (a^\dagger a + b^\dagger b)\psi = \hat{E}\psi . \tag{4.3}$$

All the features of the supersymmetric harmonic oscillator discussed in section 3 are reproduced. Note that the fermion annihilation operator b acts to reverse the electron spin, and therefore the $sqm(2)$ generator Q does also.

Equation (4.3) is equivalent to a confluent hypergeometric equation with two-component solutions labeled by two quantum numbers, one related to the energy eigenvalue $\hat{E}$ and one labeling degenerate eigenstates. The explicit solution is given in our paper [30]. We write $\psi = |n, m; \nu\rangle$, where the upper and lower components of ψ are labeled by $\nu = 0$ and $\nu = 1$, respectively. The operators a and $a^\dagger$ act as canonical lowering and raising operators on the quantum number n, while b and $b^\dagger$ act on ν. To form a complete set, introduce

$$c^\dagger = -\frac{1}{\sqrt{2eB}}e^{i\varphi}\left(\partial_r + \frac{i}{r}\partial_\varphi - \frac{1}{2}eBr\right) , \tag{4.4}$$

acting as a canonical lowering operator on m and satisfying $[c, c^\dagger] = 1$. The full supergroup for this physical system is therefore the product of the super Heisenberg-Weyl group (generated by a, b, and conjugates) with another Heisenberg-Weyl group (generated by c and conjugate).

The supercoherent states can now be constructed via the method of section 2. Their explicit form is quickly found from eq. (3.2) by noting that coherent states with respect to c and $c^\dagger$ are the usual harmonic-oscillator coherent states and that c and $c^\dagger$ commute with all other generators. The result is

$$|Z\rangle = exp(\frac{1}{2}\theta\bar{\theta})exp(-\frac{|A|^2}{2})\,exp(-\frac{|C|^2}{2})\sum_{n,m}\frac{A^n C^m}{\sqrt{n!}\sqrt{m!}}\left(|n, m; 0\rangle + \theta|n, m; 1\rangle\right) . \tag{4.5}$$

These supercoherent states depend on three Grassmann-valued variables, A, C, and θ. It can be shown that all the attractive features of the oscillator supercoherent states discussed in section 3 are reproduced.

The expectation values of the hamiltonian H, $\langle Z|H|Z \rangle = \frac{eB}{M}(A\overline{A} - \theta\overline{\theta})$, and of the magnetic-moment interaction energy $U = -eB\sigma_z/2M$, $\langle Z|U|Z \rangle = -\frac{eB}{2M}(1 + 2\theta\overline{\theta})$, provide insight into the role of the Grassmann-valued variables in Eq. (4.5). The difference $\langle Z|H - U|Z \rangle = \frac{eB}{M}(A\overline{A} + \frac{1}{2})$ represents the energy expectation in the absence of the magnetic moment. It is independent of $\theta\overline{\theta}$ and the value of $A\overline{A}$ is shifted by one half. Since the magnetic moment U distinguishes between eigenstates with $\nu = 0$ and $\nu = 1$, it follows that the term with $\theta\overline{\theta}$ contains the information about the energy splitting between the two sets of eigenstates.

As we have seen, the supersymmetry present in this physical system ensures a group-theoretical and natural incorporation of the electron spin. This feature of supersymmetry is manifest in other physical systems. For instance, one key aspect of atomic and ionic supersymmetry [25] is the natural appearance of the Pauli principle.

Acknowledgments

References

1. For an overview see, for example, J. R. Klauder and B.-S. Skagerstam, *Coherent States* (World Scientific, Singapore, 1985); W.-M. Zhang, D.H. Feng and R. Gilmore, Rev. Mod. Phys. **62**, 867 (1990).
2. E. Schrödinger, Naturwiss. **14**, 664 (1926).
3. J.R. Klauder, Annals of Physics **11**, 123 (1960); J. Math. Phys. **4**, 1055, 1058 (1963).
4. R.J. Glauber, Phys. Rev. **130**, 2529 (1963); Phys. Rev. **131**, 2766 (1964).
5. E.C.G. Sudarshan, Phys. Rev. Lett. **10**, 227 (1963).
6. A. M. Perelomov, Comm. Math. Phys. **26**, 222 (1972); *Generalized Coherent States and Their Applications* (Springer-Verlag, Berlin, 1986).
7. M.M. Nieto, p. 429 in *Coherent States*, ref. [1]; M.M. Nieto and L.M. Simmons, Jr., Phys. Rev. **D20**, 1321 (1979).
8. J. E. Campbell, Proc. London Math. Soc. **28**, 381 (1897).
9. H. F. Baker, *ibid* **34**, 347 (1902); **35**, 333 (1903); **2**, 293 (1905).
10. F. Hausdorff, Ber. Verh. Saechs. Akad. Wiss. Leipzig Math. Phys. Kl. **58**, 19 (1906).

11. R. M. Wilcox, J. Math. Phys. **8**, 962 (1967).
12. B. Mielnik, Ann. Inst. H. Poincaré **A 12**, 215 (1970).
13. R. Gilmore, *Lie Groups, Lie Algebras, and Some of Their Applications* (Wiley, New York, 1974).
14. A. Rogers, J. Math. Phys. **21**, 1352 (1980).
15. A. Rogers, J. Math. Phys. **22**, 443 (1981).
16. A. Rogers, J. Math. Phys. **22**, 939 (1981).
17. V. A. Kostelecký, M. M. Nieto, and D. R. Truax, J. Math. Phys. **27**, 1419 (1986).
18. V. A. Kostelecký and D. R. Truax, J. Math. Phys. **28**, 2480 (1987).
19. B. W. Fatyga, V. A. Kostelecký, and D. R. Truax, J. Math. Phys. **30**, 291 (1989).
20. H. Nicolai, J. Phys. A **9**, 1497 (1976).
21. E. Witten, Nucl. Phys. **B185**, 513 (1981).
22. P. Salomonson and J. W. Van Holten, Nucl. Phys. **B196**, 509 (1982).
23. M. De Crombrugghe and V. Rittenberg, Annals of Physics **151**, 99 (1983).
24. L. F. Urrutia and E. Hernández, Phys. Rev. Lett. **51**, 755 (1983).
25. V. A. Kostelecký and M. M. Nieto, Phys. Rev. Lett. **53**, 2295 (1984); Phys. Rev. **A32** 1293, 3243 (1985); V. A. Kostelecký, M. M. Nieto, and D. R. Truax, Phys. Rev. **A38**, 4413 (1988).
26. B. Freedman and F. Cooper, in V. A. Kostelecký and D. K. Campbell, eds., *Supersymmetry in Physics* (North-Holland, Amsterdam, 1985).
27. V. A. Kostelecký, M. M. Nieto, and D. R. Truax, Phys. Rev. **D32**, 2627 (1985).
28. R. Jackiw, Phys. Rev. D **29**, 2375 (1984).
29. R. J. Hughes, V. A. Kostelecký, and M. M. Nieto, Phys. Lett. B **171** (1986) 226; Phys. Rev. **D34**, 1100 (1986).
30. B.W. Fatyga, V. A. Kostelecký, M. M. Nieto, and D. R. Truax, Phys. Rev. **D43**, 1403 (1991).
31. I. Bars and M. Günaydin, Comm. Math. Phys. **91**, 31 (1983).
32. C. Aragone and F. Zypman, J. Phys. A: Math. Gen. **19**, 2267 (1986).
33. A. B. Balantekin, H. A. Schmitt, and B. R. Barrett, J. Math. Phys. **29**, 1634 (1988).
34. P. Ramond, in V. A. Kostelecký and D.K. Campbell, eds., *Supersymmetry in Physics*, (North-Holland, Amsterdam, 1985).
35. Y. Onuki and T. Kashiwa, Prog. Theor. Phys. **60**, 449 (1978).

SQUEEZED STATES,

TIME-ENERGY UNCERTAINTY RELATION, AND

FEYNMAN'S REST OF THE UNIVERSE

D. Han

National Aeronautics and Space Administration, Goddard Space Flight Center,
Code 936, Greenbelt, Maryland 20771

Y. S. Kim

Department of Physics, University of Maryland, College Park, Maryland 20742

Marilyn E. Noz

Department of Radiology, New York University, New York, New York 10016

Abstract

Two illustrative examples are given for Feynman's rest of the universe. The first example is the two-mode squeezed state of light where no measurement is taken for one of the modes. The second example is the relativistic quark model where no measurement is possible for the time-like separation of quarks confined in a hadron. It is possible to illustrate these examples using the covariant oscillator formalism. It is shown that the lack of symmetry between the position-momentum and time-energy uncertainty relations leads to an increase in entropy when the system is measured in different Lorentz frames.

1. Introduction

In his book on statistical mechanics [1], Feynman makes the following statement on the density matrix. *When we solve a quantum-mechanical problem, what we really do is divide the universe into two parts - the system in which we are interested and the rest of the universe. We then usually act as if the system in which we are interested comprised the entire universe. To motivate the use of density matrices, let us see what happens when we include the part of the universe outside the system.*

The purpose of this paper is to discuss two physical examples of Feynman's rest of the universe. We shall consider first the case of the two-mode squeezed state. In 1987, Yurke and Potasek observed that the failure to make measurements on one of the two modes will lead to non-coherent excitation of the first mode, as in the case of Einstein's calculation of specific heat in the harmonic oscillator model [2]. They observed further that this excitation is just like the thermal excitation of the ground-state harmonic oscillator. From the measurement theoretic point of view, this non-coherent excitation corresponds to an increase in entropy [3].

Let us next consider the quark model in which two quarks are bound together inside a hadron [4]. This system has a time-like separation between quarks as well as a spatial separation between them[5]. While there is no place for the time-separation variable in nonrelativistic quantum

PRECEDING PAGE BLANK NOT FILMED

mechanics, it plays an essential role when observations are made in different Lorentz frames. For this time-like separation, there is a time-energy uncertainty relation. It is of interest to see how this uncertainty relation is combined with the position-momentum to an observer in a different Lorentz frame.

We show in this paper that the longitudinal and time-like excitations in the relativistic quark model are exactly like two photon modes in a two-mode squeezed state [6]. We shall study how the non-measurement of the time-separation variable affects measurements along other coordinates.

In Sec. 2, we study the statistical effect on measurement and density matrices. In Sec. 3, we derive the result of Sec. 3 using the shadow coordinate system commonly used in thermo-field-dynamics [7]. In Sec. 4, the concept of entropy is introduced as a measure of our ignorance [3] [8]. In Sec. 5, the formalism of Sec. 4 is applied to the two-mode squeezed state of light.

The rest of this paper consists of the application of the concept of entropy to the relativistic quantum system in which the time-energy uncertainty relation is coupled covariantly to the position-momentum uncertainty, using the same mathematical formalism developed in Secs. 3, 4, and 5. We start this discussion in Sec. 6 by studying the time-energy uncertainty relation applicable to the time separation variable in the relativistic quark model. In this connection, the covariant harmonic oscillator formalism is presented. In Sec. 7, Lorentz-squeezed hadrons are discussed in terms of the covariant oscillator formalism. Finally, in Sec. 8, we note that the present form of quantum measurement theory does not measure the time separation variable. This incompleteness in measurement leads to an increase in entropy.

2. Statistical Decoherence

In measuring physical quantities, the accuracy of the measuring device is very important. Often, we have to face the situation where the measurement is taken on many different objects. For instance, in the case of the one-dimensional harmonic oscillator, the most general form of normalized solution is

$$\psi(x, t) = e^{-i\omega t/2} \sum_n C_n e^{-in\omega t} \psi_n(x), \tag{2.1}$$

where $\psi_n(x)$ is the solution of the time-independent oscillator equation with the energy level $\omega(n + 1/2)$. The wave function $\psi(x, t)$ is normalized:

$$(\psi(x, t), \psi(x, t)) = \sum_n |C_n|^2 = 1. \tag{2.2}$$

The expectation value $<A> = (\psi(x, t), A\psi(x, t))$ of an operator A(x) can be written as

$$<A> = \sum_n |C_n|^2 (\psi_n(x), A(x)\psi_n(x)) + \sum_{n \neq m} C_m^* C_n e^{i\omega(m-n)t}(\psi_m(x), A(x)\psi_n(x)). \tag{2.3}$$

If we take the ensemble average for many oscillators prepared independently with different initial times, the net effect is same as that of taking the time average, and the second term in the above expression vanishes. As a consequence, the ensemble average is

$$<\bar{A}> = \sum_n |C_n|^2 (\psi_n(x), A(x)\psi_n(x)). \tag{2.4}$$

270

We use the word "mixed" or "non-pure" in order to describe this ensemble average.

It is very convenient to treat this problem if we introduce the density matrix defined as [1] [6]

$$\rho(x, x') = \sum_n |C_n|^2 \psi_n(x)\psi_n^*(x'), \qquad (2.5)$$

and

$$<\bar{A}> = \int dx' \int A(x', x)\rho(x, x')dx, \qquad (2.6)$$

with

$$A(x', x) = \delta(x' - x)A(x).$$

The above expression is then the trace of the matrix $A(x', x)\rho(x, x')$ often written as

$$<\bar{A}> = Tr(\rho A). \qquad (2.7)$$

If $C_n = \delta_{nm}$ for a given value of m, we say that the system is in a pure state. Otherwise, the system is in a mixed state. The information from the interference terms contained in Eq.(2.3) is lost during the process of taking the ensemble average. This information lies in Feynman's rest of the universe.

The best-known example is the thermally excited harmonic oscillator which was used by Einstein in his calculation of the specific heat of a solid. The density matrix takes the form [1] [6]

$$\rho_T(x, x') = \sum_n (1 - e^{-\omega/kT})e^{-n\omega/kT}\psi_n(x)\psi_n^*(x'). \qquad (2.8)$$

In the zero-temperature limit, the system is purely in the ground state. As the temperature increases, $|C_n|^2$ becomes $(1 - e^{-\omega/kT})e^{-n\omega/kT}$, but the above expression does not tell us anything about the phase of C_n. The density matrix does not give any information about the coherence of the system. In Sec. 4, we shall study how this ignorance is translated into entropy.

3. Shadow Coordinates

We discuss in this section a method of deriving the density matrix, without taking the ensemble average, by introducing an auxiliary Hilbert space consisting of $\psi_n(\tilde{x})$ and attach it to C_n [1] [7]. Let us consider the wave function of the form

$$\psi(x, \tilde{x}) = \sum_n (C_n\psi_n(\tilde{x}))\psi_n(x). \qquad (3.1)$$

The auxiliary coordinate $\tilde{x}$ is called the "shadow" coordinate in the literature [7]. It is possible to derive the result of Eq.(2.4) by treating $\psi(x, \tilde{x})$ as a pure-state wave function defined in the total Hilbert space consisting both of $\psi_n(x)$ and $\psi_n(\tilde{x})$. Because of the orthogonality relation for $\psi_n(\tilde{x})$, the expectation value of A(x):

$$<A> = \sum_{n,m} C_m^* C_n(\psi_m(\tilde{x}), \psi_n(\tilde{x}))(\psi_m(x), A(x)\psi_n(x)), \qquad (3.2)$$

271

is the same as the ensemble average $<\bar{A}>$ given in Eq.(2.4). It is possible to obtain the density matrix by integrating $\psi(x, \tilde{x})\psi^*(x', \tilde{x})$ over the $\tilde{x}$ variable:

$$\rho(x, x') = \int \psi(x, \tilde{x})\psi^*(x', \tilde{x})d\tilde{x}. \tag{3.3}$$

The evaluation of this integral leads to the expression for $\rho(x, x')$ given in Eq.(2.5). The shadow coordinate plays the role of taking the ensemble average discussed in Sec. 2.

Let us illustrate this again using the ground-state harmonic oscillator wave function

$$\psi_0(x, \tilde{x}) = \psi_0(x)\psi_0(\tilde{x}) = \left(\frac{1}{\pi}\right)^{1/2} \exp\left\{-\frac{1}{2}(x^2 + \tilde{x}^2)\right\}, \tag{3.4}$$

where x is measured in units of $1/\sqrt{m\omega}$, and let us now make the coordinate transformation:

$$\begin{pmatrix} x' \\ \tilde{x}' \end{pmatrix} = \begin{pmatrix} \cosh\eta & \sinh\eta \\ \sinh\eta & \cosh\eta \end{pmatrix} \begin{pmatrix} x \\ \tilde{x} \end{pmatrix}, \tag{3.5}$$

where

$$\cosh\eta = 1/(1 - e^{-\omega/kT})^{1/2}, \qquad \sinh\eta = e^{-\omega/2kT}/(1 - e^{-\omega/kT})^{1/2}, \tag{3.6}$$

which shares the same mathematics as a Lorentz boost as we shall see in Secs. 7 and 8. Then this coordinate transformation leads to the wave function of the form

$$\psi_T(x, \tilde{x}) = \left[\frac{1}{\pi}\right]^{1/2} \exp\left\{-\frac{1}{4}[(\tanh\frac{\omega}{4kT})(x + \tilde{x})^2 + (\coth\frac{\omega}{4kT})(x - \tilde{x})^2]\right\}. \tag{3.7}$$

The wave function of the two variables can be expanded as [6]

$$\psi_T(x, \tilde{x}) = [1 - \exp(-\omega/kT)]^{1/2} \sum_n \exp(-n\omega/2kT)\psi_n(x)\psi_n(\tilde{x}). \tag{3.8}$$

The evaluation of the density matrix given in Eq.(3.3) with this form of the wave function leads to the density matrix of the form of Eq.(2.8). The same evaluation with the wave function of the form of Eq.(3.7) gives [6]

$$\rho_T(x, x') = \left[\frac{1}{\pi}\tanh\frac{\omega}{2kT}\right]^{1/2} \exp\left\{-\frac{1}{4}\left[(x + x')^2 \tanh\frac{\omega}{2kT} + (x - x')^2 \coth\frac{\omega}{2kT}\right]\right\}. \tag{3.9}$$

Then the probability distribution $\rho_T(x) = \rho_T(x, x)$ becomes

$$\rho_T(x) = \left[\frac{1}{\pi}\tanh\frac{\omega}{2kT}\right]^{1/2} \exp\left\{-\left[\tanh\frac{\omega}{2kT}\right]x^2\right\}. \tag{3.10}$$

This expression is normalized. In the $T = 0$ limit, the probability distribution becomes

$$\rho_0(x) = (1/\pi)^{1/2}\exp(-x^2). \tag{3.11}$$

The increase of temperature broadens the probability distribution. It is possible to carry out the same analysis for the momentum variable. The momentum distribution will also become widespread. The net result is the increase in uncertainty. This increase is due to our ignorance about the shadow coordinate system. Feynman's rest of the universe consists of the shadow coordinate.

4. Entropy and Ignorance

The interpretation in terms of thermal excitation was possible because the expansion coincides with the thermally excited oscillator state. There are, however, cases where the density matrix does not correspond to any state in thermal equilibrium. For instance, if we start from one of the excited harmonic oscillator states [9], the density matrix does not correspond to a thermally excited state. What then will be the variable which measures our ignorance about the second coordinate variable?

The answer to this question is the entropy defined as [8]

$$S = -\sum_n \rho_n \ln(\rho_n). \tag{4.1}$$

In general, the density matrix is Hermitian and can be diagonalized. ρ_n in the above expression is the diagonal element. If the system is in a pure state, the entropy is zero. If the system is not in a pure state, the entropy is positive. This definition of entropy does not depend on the question of whether the system is in thermal equilibrium. The definition given in Eq.(4.1) does not depend on temperature.

On the other hand, the above definition does not exclude a system in thermal equilibrium. In the case of a thermally excited harmonic oscillator, the density matrix of Eq.(2.8) is diagonal and its elements are

$$\rho_n = (1 - e^{-\omega/kT})e^{-n\omega/kT}. \tag{4.2}$$

Thus, according to the definition given in Eq.(4.1),

$$S = \omega/kT(e^{\omega/kT} - 1) - \ln(1 - e^{-\omega/kT}). \tag{4.3}$$

This expression is the same as the one available from textbooks on statistical mechanics.

In Secs. 5 and 8, we shall study the examples which are not thermal excitations, but share the same mathematical formalism. The concept of temperature is convenient but not essential in the examples to be discussed in the following sections.

5. Entropy and Two-Mode Squeezed States of Light

As is well known, the mathematics of harmonic oscillators is the standard language for the photon-number space. The energy level in a given oscillator system corresponds to the number of photons, and the ground state corresponds to the vacuum or zero-photon state. The step-up and step-down operators in the oscillator formalism are given by

$$a^\dagger = \frac{1}{\sqrt{2}}\left(x - \frac{\partial}{\partial x}\right), \qquad a = \frac{1}{\sqrt{2}}\left(x + \frac{\partial}{\partial x}\right), \tag{5.1}$$

respectively. These are now the creation and annihilation operators. Let us consider two sets of these operators: $a^\dagger, a$ and $\tilde{a}^\dagger, \tilde{a}$ for the first and second modes of photons respectively. We are interested in the state of these photons where those created and annihilated by $\tilde{a}^\dagger$ and $\tilde{a}$ are not observed.

We construct the two-mode state by applying to the vacuum state the operator $\exp(-i\eta G)$, where [6] [10]

$$G = -\frac{i}{2}\left(a^\dagger \tilde{a}^\dagger - a\tilde{a}\right),\tag{5.2}$$

where the subscripts 1 and 2 are for photons of the first and second kinds respectively. The two-mode squeezed state constructed from

$$|\eta> = e^{-i\eta G}|0,0>,\tag{5.3}$$

where $|n,\tilde{n}>$ is the state with n photons of the first kind and $\tilde{n}$ for the second kind. According to this definition, $|0,0>$ is the vacuum state. The power-series expansion of the exponential factor leads to

$$|\eta> = (1/\cosh\eta)\sum_n(\tanh\eta)^n|n,n> .\tag{5.4}$$

In order to distinguish the photons of the first and second kinds, we write the above expression as

$$|\eta> = (1/\cosh\eta)\sum_{n,\tilde{n}}(\tanh\eta)^n\delta_{n\tilde{n}}|n,\tilde{n}> .\tag{5.5}$$

The mathematics which led to the above expression is exactly the same as that for the harmonic oscillator with a shadow coordinate given in Sec. 3. From the mathematical point of view, this form is the same as the expansion given in Eq.(2.8), and they become identical if we use the correspondence between T and η given in Eq.(3.6). In terms of the η parameter, an element of the diagonal density matrix is

$$\rho_n = (\tanh\eta)^{2n}/(\cosh\eta)^2,\tag{5.6}$$

which leads to the entropy:

$$S = \ln(\cosh\eta)^2 - (\sinh\eta)^2\ln(\tanh\eta)^2.\tag{5.7}$$

This form of entropy is determined directly from the squeeze parameter η, and it is not necessary to introduce the concept of temperature. The fact is that the measurement or non-measurement of photons of one kind affects the measurement of photons of the other kind. In the present case, the non-measurement of the photon of the second kind increases the degree of ignorance of photons of the first kind, and this degree of ignorance is measured in terms of the entropy. The system of photons of the second kind is Feynman's rest of the world.

There are however special cases where the entropy can be associated with temperature. This is one of those cases. As Yurke and Potasek observed [2], it is possible to define the temperature

C-4

of this system by using the connection between the squeeze parameter and temperature. The temperature T is related to the squeeze parameter by

$$\tanh \eta = e^{-\omega/2kT}. \tag{5.8}$$

If T approaches zero, the squeeze parameter also becomes zero. As the temperature becomes very high, the squeeze parameter becomes very large.

6. Time-energy Uncertainty Relation and Relativistic Quark Model

In order to study the role of the time-energy uncertainty relation in relativistic quantum mechanics and relativistic measurement theory, we consider here a concrete physical example which gives observable effects in high-energy laboratories. Let us consider a hadron consisting of two quarks. If the space-time position of the two quarks is specified by x_a and x_b respectively, the system can be described by the variables:

$$X = (x_a + x_b)/2, \qquad x = (x_a - x_b)/2\sqrt{2}. \tag{6.1}$$

The four-vector X specifies where the hadron is located in space and time, while the variable x measures the space-time separation between the quarks. As for the four-momenta of the quarks p_a and p_b, we can combine them into the total hadronic four-momentum and the momentum-energy separation between the quarks [4]:

$$P = p_a + p_b, \qquad q = \sqrt{2}(p_a - p_b), \tag{6.2}$$

where P is the hadronic four-momentum conjugate to X. The internal momentum-energy separation is conjugate to x.

In the convention of Feynman *et al.* [4], the internal motion of the quarks can be described by the Lorentz-invariant oscillator equation:

$$\frac{1}{2}\left\{ x_\mu^2 - \frac{\partial^2}{\partial x_\mu^2} \right\} \psi(x) = \lambda \psi(x), \tag{6.3}$$

where we use the space-favored metric: $x^\mu = (x, y, z, t)$. The four-dimensional covariant oscillator wave functions are Hermite polynomials multiplied by a Gaussian factor, which dictates the space-time localization property of the wave function. The Gaussian factor takes the form

$$\exp\left\{ -\frac{1}{2}(x^2 + y^2 + z^2 + t^2) \right\}. \tag{6.4}$$

We are accustomed to the polynomial $(x^2 + y^2 + z^2 - t^2)$, but not with $+t^2$. What is the physics of the Gaussian factor of Eq.(6.4)? If the hadron is at rest, it is possible to construct three-dimensional harmonic oscillator wave functions with excited energy levels. This would be a multiplication of the appropriate Laguerre polynomial with the Gaussian factor $\exp\{-(x^2 + y^2 + z^2)/2\}$. As for the time-like separation, Eq.(6.4) contains the factor $\exp(-t^2/2)$. However, unlike the position coordinates, there is no excitation along this axis, since the time variable is a c-number

[5]. The fact that the time-energy uncertainty relation is a c-number relation is well-known and well-established. Figure 1 illustrates these features of the uncertainty relations.
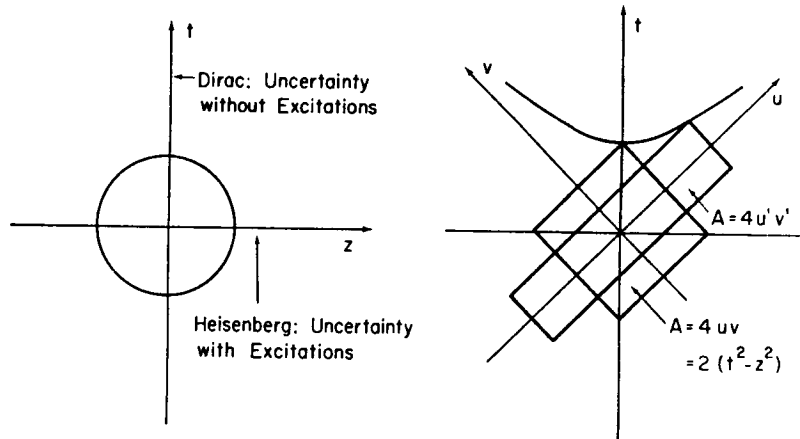
FIG. 1. Quantum mechanics and relativity. The left part of this figure illustrates that the position-momentum uncertainty relation with excitations and the time-energy uncertainty relation without excitations, as the time is a c-number variable. The right part is special relativity. In the light-cone system, it is transparent that the Lorentz boost is a squeeze transformation. One way to combine quantum mechanics with special relativity is to superimpose these two figures, as is done in Fig. 2.

Since the three-dimensional oscillator differential equation is separable in both spherical and Cartesian coordinate systems, $\psi(x, y, z)$ consists of Hermite polynomials of x, y, and z. If the Lorentz boost is made along the z direction, the x and y coordinates are not affected, and can be dropped from the wave function. The wave function of interest can be written as

$$\psi^n(z, t) = \left(\frac{1}{\pi}\right)^{1/4} \exp(-t^2/2)\psi^n(z), \tag{6.5}$$

with

$$\psi^n(z) = \left(\frac{1}{\sqrt{\pi} 2^n n!}\right)^{1/2} H_n(z) \exp(-z^2/2),$$

where $\psi^n(z)$ is for the nth excited oscillator state. The full wave function $\psi^n(z, t)$ is

$$\psi_o^n(z, t) = \left(\frac{1}{\pi 2^n n!}\right)^{1/2} H_n(z) \exp\left\{-\frac{1}{2}\left(z^2 + t^2\right)\right\}. \tag{6.6}$$

The subscript o means that the wave function is for the hadron at rest. The above expression is not Lorentz-invariant, and its localization undergoes a Lorentz squeeze as the hadron moves along the z direction [5].

7. Lorentz-squeezed Oscillator Wave Functions

Let us next consider special relativity and Lorentz transformations. It is important to note that the Lorentz boost is a squeeze transformation in the zt coordinate system if the boost is made along the z axis. In order to see this point, let us use the light-cone variables, which are

276

defined as

$$u = (z + t)/\sqrt{2}, \qquad v = (z - t)/\sqrt{2}. \tag{7.1}$$

The u and v axes are perpendicular to each other. In terms of these variables, the Lorentz boost along the z direction,

$$\begin{pmatrix} z' \\ t' \end{pmatrix} = \begin{pmatrix} \cosh \eta & \sinh \eta \\ \sinh \eta & \cosh \eta \end{pmatrix} \begin{pmatrix} z \\ t \end{pmatrix}, \tag{7.2}$$

takes the simple form

$$u' = e^{\eta} u, \qquad v' = e^{-\eta} v. \tag{7.3}$$

This transformation is illustrated in Fig. 2. This is an area preserving transformation where one side becomes contracted while the other side is expanded in a manner that their product is constant. This is a squeeze transformation.
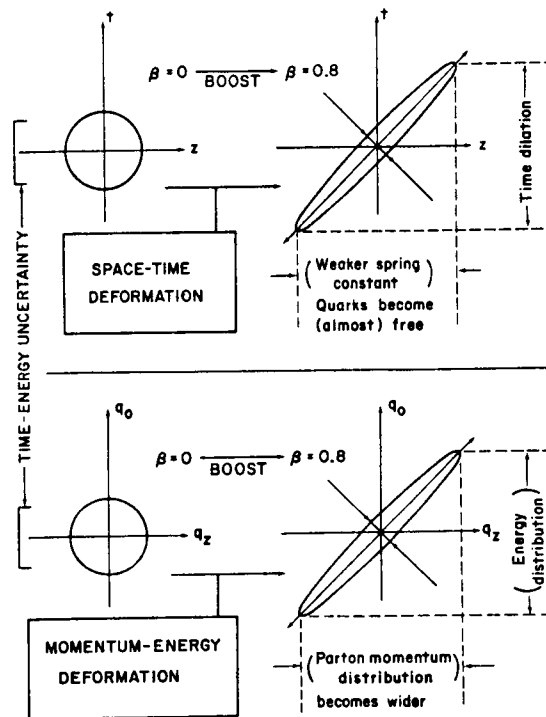
FIG. 2. Lorentz-squeezed space-time and momentum-energy wave functions. This figure is a result of combining quantum mechanics and special relativity described in Fig. 1. The physical significance is that this figure gives a unified picture of the quark model for slow hadrons and the parton model for rapid hadrons. This figure is from Refs. [5] and [6].

In the light-cone coordinate system, the oscillator wave function in the rest frame takes the form

$$\psi_o^n(z,t) = \left[\frac{1}{\pi(n!)2^n}\right]^{1/2} H_n((u+v)/\sqrt{2}) \exp\left\{-\frac{1}{2}(u^2+v^2)\right\}. \tag{7.4}$$

If the system is boosted, the wave function becomes

$$\psi_\eta^n(z,t) = \left[\frac{1}{\pi(n!)2^n}\right]^{1/2} H_n((e^{-\eta}u+e^\eta v)/\sqrt{2}) \exp\left\{-\frac{1}{2}(e^{-2\eta}u^2+e^{2\eta}v^2)\right\}. \tag{7.5}$$

This wave function can be expanded as [5]

$$\psi_\eta^n(z,t) = (1/\cosh\eta)^{n+1} \sum_k (C_{n,k})^{1/2}(\tanh\eta)^k \psi_o^{n+k}(z)\psi_o^n(t), \tag{7.6}$$

where

$$C_{n,k} = (n+k)!/n!k!.$$

Since the space-time localization property is dictated by the Gaussian factor, let us study in detail the ground state with $n = 0$. In this case, the boosted wave function is

$$\psi_\eta(z,t) = \left(\frac{1}{2\pi}\right)^{1/2} \exp\left\{-\frac{1}{2}(e^{-2\eta}u^2+e^{2\eta}v^2)\right\}. \tag{7.7}$$

The quantum space-time distribution of Fig. 1 is squeezed to an ellipse described in the upper half of Fig. 2.

Let us next consider the momentum-energy wave function, which is the Fourier transform of $\psi_\eta(z,t)$:

$$\phi_\eta(q_z,q_o) = \frac{1}{\pi} \int \psi_\eta(z,t) \exp\left\{i(p_z z - p_o t)\right\} dz dt, \tag{7.8}$$

where q_z and q_o are defined in Eq.(6.2). Since the integration measure is invariant under the boost, the evaluation of the integral is straight-forward, and the momentum-energy wave function takes the form

$$\phi_\eta(q_z,q_o) = \left(\frac{1}{\pi}\right)^{1/2} \exp\left\{-\frac{1}{2}(e^{2\eta}q_u^2+e^{-2\eta}q_v^2)\right\}, \tag{7.9}$$

with

$$q_u = (q_z - q_o)/\sqrt{2}, \qquad q_v = (q_z + q_o)/\sqrt{2}.$$

The Lorentz-squeeze property of the momentum-energy wave function is the same as that of the space-time wave function, as is illustrated in the lower half of Fig. 2. The significance of the Lorentz-squeeze property is that it gives observable consequences in high-energy laboratories.

By now the quark model for hadrons is firmly established. The proton consists of three quarks bound together by a oscillator-like force, according to an observer in the Lorentz frame in which the hadron is at rest. On the other hand, to an observer in a moving frame, the wave function appears squeezed. If the frame moves with a speed close to that of light, the hadron appears as a collection of an infinite number of partons [5] [11]. This is called Feynman's parton picture. This phenomenon is now universally observed in high-energy laboratories, and the squeezed picture of Fig. 2 gives an explanation of Feynamn's parton picture.

One of the most uncomfortable aspects of the present discussion is the time-separation variable. Without this variable, it is not possible to perform Lorentz boosts. On the other hand, there is no time-separation variable in any of the existing measurement theories of quantum mechanics. In order to reconcile this difference, we have to conclude that the time-separation exists, but is not a measurable variable. This variable is in Feynman's rest of the universe.

8. Entropy and Lorentz Transformations

Entropy is a measure of our ignorance and is computed from the density matrix, as was noted in Sec. 4. The density matrix is needed when the experimental procedure does not analyze all relevant variables to the maximum extent consistent with quantum mechanics. For the bound state of two particles, the present form of quantum mechanics does not tell us how to measure the time-separation variable, as is illustrated in Fig. 3.
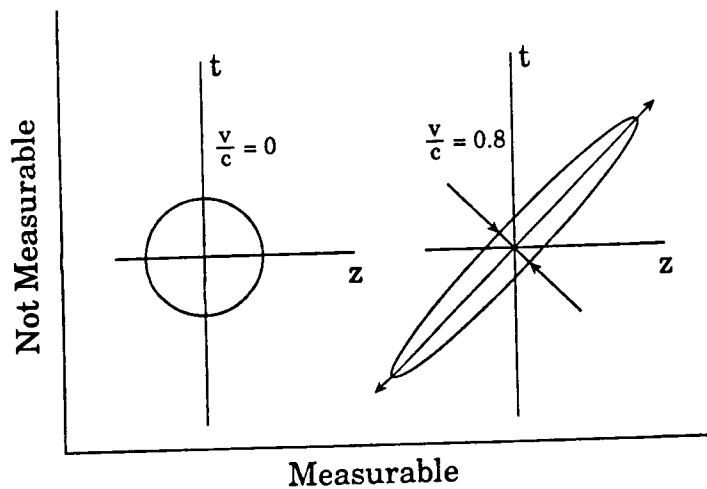
FIG. 3. Localization property in the zt plane. When the hadron is at rest, the Gaussian form is concentrated within a circular region specified by $(z+t)^2+(z-t)^2 = 1$. As the hadron gains speed, the region becomes deformed to $e^{-2\eta}(z+t)^2+e^{2\eta}(z-t)^2 = 1$. Since it is not possible to make measurements along the t direction, we have to deal with information that is less than complete. The time-separation variable lies in Feynman's rest of the universe.

If the time-separation were a measurable variable, the pure-state density matrix would be

$$\rho_\eta^n(z, t; z', t') = \psi_\eta^n(z, t)[\psi_\eta^n(z', t')]^*, \tag{8.1}$$

which satisfies the condition $\rho^2 = \rho$:

$$\rho_\eta^n(z, t; z', t') = \int \rho_\eta^n(z, t; z'', t'')\rho_\eta^n(z'', t''; z', t')dz''dt''. \tag{8.2}$$

This pure-state density matrix is possible only if both the z and t coordinates are measurable space-time variables. On the other hand, there are at present no measurement theories which accommodate the time-separation variable t. Indeed, this time separation variable is the coordinate in the part of the universe outside the system. We do not observe the distribution outside the system. What we do then is to take the trace of the ρ matrix with respect to the t variable. The resulting density matrix is

$$\rho_\eta^n(z, z') = \int \rho_\eta^n(z, t; z', t)dt = \int \psi_\eta^n(z, t)[\psi_\eta^n(z', t)]^*dt$$

$$= (1/\cosh\eta)^{2(n+1)} \sum_k C_{n,k}(\tanh\eta)^{2k}\psi_o^{n+k}(z)[\psi_o^{n+k}(z')]^*. \tag{8.3}$$

The trace of this density matrix is one, but the trace of ρ^2 is less than one, as

$$Tr(\rho^2) = \int \rho_\eta^n(z, z')\rho_\eta^n(z', z)dz'dz$$

$$= (1/\cosh\eta)^{4(n+1)} \sum_k (C_{n,k})^2(\tanh\eta)^{4k}, \tag{8.4}$$

which is less than one. This is due to the fact that we do not know how to deal with the time-like separation which lies in Feynman's rest of the universe. Our knowledge is less than complete.

We can now go back to Sec. 4 on entropy, and write Eq.(4.1) as

$$S = -Tr[\rho\ln(\rho)]. \tag{8.5}$$

If we pretend to know the distribution along the time-like direction and use the pure-state density matrix given in Eq.(8.1), the entropy is zero. However, if we do not know how to deal with the distribution along t, then we should use the density matrix of Eq.(8.3) to calculate the entropy, and the result is

$$S = 2(n + 1)\left\{(\cosh\eta)^2\ln(\cosh\eta) - (\sinh\eta)^2\ln(\sinh\eta)\right\}$$

$$-(1/\cosh\eta)^{2(n+1)} \sum_k [C_{n,k}\ln(C_{n,k})](\tanh\eta)^{2k}. \tag{8.6}$$

In terms of the velocity v of the hadron, where $v/c = \tanh\eta$,

$$S = -(n + 1)\left\{\ln[1 - (v/c)^2] + (v/c)^2\ln\frac{(v/c)^2}{[1 - (v/c)^2]}\right\}$$

$$-[1 - (v/c)^2]^{(n+1)} \sum_k [C_{n,k} \ln(C_{n,k})](v/c)^{2k}. \tag{8.7}$$

Here again, entropy is derived as a measure of ignorance. It does not depend on the question of whether or not the system is in thermal equilibriu m. The expression for S in Eq.(8.7) does not depend on temperature.

It was noted in Sec. 7 that the ground-state wave function occupies an important place in the oscillator formalism, and it will undoubtedly give a simpler and more transparent expression for the entropy. In terms of the z and t variables, the Lorentz-boosted wave function of Eq.(7.7) takes the form

$$\psi_\eta(z,t) = \left(\frac{1}{\pi}\right)^{1/2} \exp\left\{-\frac{1}{4}[e^{-2\eta}(z+t)^2 + e^{2\eta}(z-t)^2]\right\}, \tag{8.8}$$

which can be expanded as

$$\psi_\eta(z,t) = (1/\cosh\eta) \sum_n (\tanh\eta)^n \psi^n(z)\psi^n(t). \tag{8.9}$$

The density matrix is

$$\rho_\eta(z,z') = \left(\frac{1}{\pi\cosh 2\eta}\right)^{1/2} \exp\left\{-\frac{1}{4}[(z+z')^2/\cosh 2\eta + (z-z')^2\cosh 2\eta]\right\}, \tag{8.10}$$

and the entropy becomes

$$S = \ln(\cosh\eta)^2 - (\sinh\eta)^2 \ln(\tanh\eta)^2. \tag{8.11}$$

As a consequence of Eq.(8.10), the quark distribution $\rho(z,z)$ becomes

$$\rho(z) = \left(\frac{1}{\pi\cosh 2\eta}\right)^{1/2} \exp\left(\frac{-z^2}{\cosh 2\eta}\right). \tag{8.12}$$

The width of the distribution becomes $(\cosh 2\eta)^{1/2}$, and becomes wide-spread as the hadronic speed increases. Likewise, the momentum distribution becomes wide-spread [5] [11]. This simultaneous increase in the momentum and position distribution widths is called the parton phenomenon in high-energy physics [11]. The position-momentum uncertainty becomes $\cosh\eta$. This increase in uncertainty is due to our ignorance about the physical but unmeasurable time-separation variable.

For the special case of the ground state, it is possible to convert the entropy into the temperature scale, exactly as we did for the case of two-mode squeezed states in Sec. 5. The squeeze parameter η used in Sec. 5 is now the boost parameter. We can use Eq.(5.8) to establish the correspondence between the temperature and squeeze parameter [12].

References

[1] R. P. Feynman, *Statistical Mechanics* (Benjamin/Cummings, Reading, MA, 1972).

[2] B. Yurke and M. Potasek, Phys. Rev. A **36**, 3464 (1987).

[3] J. Von Neumann, *Mathematical Foundation of Quantum Mechanics* (Princeton Univ. Press, Princeton, 1955).

[4] R. P. Feynman, M. Kislinger, and F. Ravndal, Phys. Rev. D **3**, 2706 (1971).

[5] Y. S. Kim and M. E. Noz, *Theory and Applications of the Poincaré Group* (Reidel, Dordrecht, 1986).

[6] Y. S. Kim and M. E. Noz, *Phase Space Picture of Quantum Mechanics* (World Scientific, Singapore, 1991).

[7] H. Umezawa, H. Matsumoto, and M. Tachiki, *Thermo Field Dynamics and Condensed States* (North-Holland, Amsterdam, 1982).

[8] E. P. Wigner and M. M. Yanase, Proc. National Academy of Sciences (U.S.A.) **49**, 910 (1963).

[9] Y. S. Kim and E. P. Wigner, Phys. Lett. A **147**, 343 (1990).

[10] P. A. M. Dirac, J. Math. Phys. **4**, 901 (1963).

[11] R. P. Feynman, in *High Energy Collisions*, Proceedings of the Third International Conference, Stony Brook, New York, edited by C. N. Yang *et al.* (Gordon and Breach, New York, 1969).

[12] D. Han, Y. S. Kim, and M. E. Noz, Phys. Rev. A **41**, 6233 (1990). Phys. **193**, 255 (1989)

WAVELETS AND THE SQUEEZED STATES OF QUANTUM OPTICS*

628185

14 βs

B. DeFacio
Department of Physics & Astronomy
Missouri University
Columbia, MO 65211

ABSTRACT

Wavelets are new mathematical objects which act as "designer trig functions." To obtain a wavelet, the original function space of finite energy signals is generalized to a phase-space, and the translation operator in the original space has a scale change in the new variable adjoined to the translation. Localization properties in the phase-space can be improved and unconditional bases are obtained for a broad class of function and distribution spaces. Operators in phase space are "almost diagonal" instead of the traditional condition of being diagonal in the original function space. These wavelets are applied to the squeezed states of quantum optics. The scale change required for a quantum wavelet is shown, with Prof. G.M. D'Ariano, to be a Yuen squeeze operator acting on an arbitrary density operator.

1. INTRODUCTION

Wavelets were created in France less than a decade ago[1-5] when J. Morlet[1,4] generalized the phase-space of Gabor[6] by adding a scale change to the frequency (wavenumber) axis for applications to geophysical exploration. Grossmann[2,5] and Meyer[3,5,7] immediately saw the importance of wavelets for mathematical physics and to deep questions in harmonic analysis, respectively. There are a number of review articles[4,5,7-12] available today, each specializing in different aspects of wavelets.

In terms of this paper, which applies wavelets to the squeezed states of quantum optics, two long mathematics papers are the most important. The author is convinced that they will also be the most important for physics, applied mathematics, engineering and industrial problems. The two key papers are those of Daubechies[13], and Frazier and Jawerth.[14] Daubechies[13] first constructed a large family of orthonormal bases of compactly supported wavelets in $L^2(R^n)$. Frazier and Jawerth[14] gave a thorough, complete treatment of **sampled** wavelets which is valid both in the classical function spaces and in the modern distributional spaces.

The approach to squeezed states and quantum optics[15-22] will be through the coherent states.[23-25] The three main approaches to coherent states are those due to Klauder,[23,26-29] to Perelomov,[28] and to Onofrio.[29] The Klauder construction starts with an arbitrary representation of a Lie group G on a complex separable Hilbert space $\mathcal{H}$ and induces a representation of G on itself with $\mathcal{H}$ as a *closed* subspace of $L^2(R^d, d\mu)$ This yields a subrepresentation of the regular representation in the sense of Mackey.[30] It works equally well with states or frames. The approach of Perelomov starts with a "Little vector" and requires a multiplier to add enough structure to force projective representation to be unitary. There is additional subtlety in obtaining an invariant measure on the coset spaces used to reduce G in that G/H_1 can have an invariant measure $d\mu_1$ whereas G/H_2 may not. Thus, the choice of a "Little group" or "stability subgroup" is a sensitive issue in the Perelomov approach. The Onofrio construction yields a holomorphic representation of the Lie group. At

least in simple cases it gives a complexification of the real homogeneous space $M = G/H$, of Perelomov. For additional structure and the proofs see the nice new monograph of Kaiser.[31]

2. SQUEEZED STATES OF QUANTUM OPTICS

The coherent states for each complex number α are generated from the unique, translationally invariant Fock vacuum $\mid 0 >$ using a unitary displacement operator $D(\alpha)$ which is defined below. Let a, a^+ be the Bose destruction and creation operator which satisfy the canonical commutation relations

$$[a, a^+] = 1 \quad ,$$

$$[a, a] = [a^+, a^+] = 0 \quad , \tag{1}$$

and define D as a Weyl-Heisenberg operator,

$$D(\alpha) : = \exp(\alpha a^+ - \alpha^* a) \quad . \tag{2}$$

Then

$$\mid \alpha >= D(\alpha) \mid 0 > \tag{3}$$

is the ordinary coherent state. In terms of an additional complex parameter ζ, the two-photon squeezed states $\mid \zeta, \alpha >$ of Stoler[15] and Yuen[16] can be generated using the squeezing operator $S(\zeta)$

$$S(\zeta) : = \exp(\zeta a^{+2} - \zeta^* a^2) \tag{4}$$

through the action

$$\mid \zeta, \alpha >= S(\zeta) \mid \alpha >$$

$$= S(\zeta)D(\alpha) \mid 0 > \quad . \tag{5}$$

The states generated in Eq. (5) will be called amplitude squeezed states. These coherent states satisfy the **uncertainty principle** but squeeze one side, say time or frequency, exponentially. *Naively*, it would seem that higher order squeezed operators $S^{(k)}, k > 2$, can be defined through the definition

$$S^{(k)}(\zeta) : = \exp(\zeta a^{tk} - \zeta^* a^k) \quad , \tag{6}$$

but a neat paper by Fisher, Nieto and Sundberg[32] has shown the matrix element divergence

$$< 0 \mid S^{(k)}(\zeta) \mid 0 >\to \infty \quad , \tag{7}$$

for all $k > 2$! This can be interpreted as either non-analyticity of the vacuum or as operator domain problems. The task of defining k-photon squeezed wavelets will be relegated to future works. Here a new **quantum** or **operator-valued wavelet** of D'Ariano and the author[33] will be presented. Let $\hat{A}$ be an observable

$$\hat{A} \mid a >= a \mid a > \tag{8}$$

where the states $\mid a >$ give a resolution of the identity

$$1 = \int d\mu(a) \mid a >< a \mid \quad , \tag{9}$$

284

where $d\mu(a)$ is the invariant measure. The generating function of moments of the observable $\hat{A}$ in a state whose density operator is $\hat{\rho}$ is given by

$$< e^{i\alpha\hat{A}} >:= Tr[e^{i\alpha\hat{A}}\hat{\rho}] \quad . \tag{10}$$

The probability distribution function $P(\rho, a)$ is defined as

$$P(\hat{\rho}, a) := Tr\big[|\, a ><a \,|\, \hat{\rho}\big]$$

and is the Fourier transform of the generating function of moments with respect to the measure $d\mu(a)$

$$< e^{i\alpha\hat{A}} >= \int d\mu(a)e^{i\alpha a}P(\hat{\rho}, a) \quad . \tag{11}$$

A filtered Fourier transform with window function $\gamma(a)$ for Eq. (11) can be defined naturally as

$$\left\langle e^{i\alpha\hat{A}} \right\rangle_\gamma := \int d\mu(\theta)e^{i\alpha a}\gamma(a)P(\hat{\rho}, a) \quad . \tag{12}$$

A c-number wavelet transform analogous to Eq. (12) is given by

$$W(\hat{\rho}, \eta, \epsilon) := \frac{1}{|\,\epsilon\,|^{1/2}} \int d\mu(\theta)\chi(\frac{a-\eta}{\epsilon})P(\hat{\rho}, a) \quad . \tag{13}$$

In the next section, additional discussions of wavelets will be given.

3. WAVELETS

For simplicity of exposition, let $f\epsilon L^2(R^1)$ be a real or complex-valued finite energy signal and denote its Fourier transform by $\hat{f}(k)$. In $L^2, \hat{f}$ is guaranteed to exist and by Parseval's theorem $|f|^2 = |\hat{f}|^2$ with proper normalization. Choose conventions s.t.

$$\hat{f}(k) = \int_{-\infty}^{\infty} f(x)e^{2\pi i k \cdot x}dx \quad , \tag{14}$$

and

$$f(x) = \int_{-\infty}^{\infty} \hat{f}(k)e^{-2\pi i k \cdot x}dk \quad . \tag{15}$$

If $supp(\hat{f}) \subset (-1/2, 1/2)$ and $\hat{f}\epsilon L^2(\hat{R}^1)$

$$f(x) = \sum_k \left\{ f(k)\frac{\sin(\pi(x-k)}{\pi(x-k)} \right\} \quad . \tag{16}$$

Inverting Eq. (16) yields

$$\hat{f}(k) = \left\{ \sum_r f(r)e^{2\pi i r k} \right\} \chi_{(-1/2, 1/2)}(r) \quad , \tag{17}$$

where χ_A is the characteristic function of the interval $A \subset R^1$. With discretization the mn^{th} coefficient of f (m,n integers) with "window function" $g(x-nx_0)$, which is one when $(x-nx_0)$ is positive, is given by

$$C_{mn}(f) = \int_{-\infty}^{\infty} e^{2\pi i m k_0 x_0} g(x-nx_0) f(s) dx \quad . \tag{18}$$

Observe that the n-index is a spatial translation of units of x_0 and the m-index is a wave-number translation in units of k_0. The joint appearance of (m,n) indicates that C_{mn} lives in $\hat{Z}^d \otimes Z^d$, a phase-space. The scale change $x \to x/2^\nu$ plays an important role in the Calderón complex interpolation approach. A **dilation** is a translation in x (space) with a scale change in Fourier transform variable k. Calderón[35] published his famous reproducing formula in 1964. The conditions required are the following: (i) Let ψ and φ be radial, smooth $L^2(R^d)$ functions whose Fourier transforms $\hat{\psi}$ and $\hat{\varphi}$ in $L^2(\hat{R}^2)$ with support in a set A,

$$A := supp(\hat{\psi}, \hat{\varphi}) = \left\{ k \mid 0 < C_1 \leq \mid k \mid \leq C_2 < \infty \right\} \quad . \tag{19}$$

(ii) For each $\mid k \mid \neq 0$

$$\sum_{\nu=-\infty}^{\infty} \hat{\varphi}(2^\nu \mid k \mid) \hat{\psi}(2^\nu \mid k \mid) = 1 \quad . \tag{20}$$

Let $f \epsilon L^2(R^d)$ with $\hat{f}(0) = 0$ and then

$$\hat{f}(k) = \sum_\nu \hat{f}(k) \hat{\varphi}(2^\nu \mid k \mid) \hat{\psi}(2^\nu \mid k \mid) \quad . \tag{21}$$

Let

$$g_\nu(k) = \hat{f}(k) \hat{\varphi}(2^\nu \mid k \mid) \tag{22}$$

which implies that rearrangement of Eq. (21) into

$$\sum_s c_s(k) e^{2\pi i 2^\nu k} \tag{23}$$

has an obvious parallel to Eqs. (14-18). Define the quantities

$$\varphi_{\nu,r}(x) := 2^{-\nu/2} \varphi(2^{-\nu} x - r) \quad , \tag{24}$$

$$\psi_{\nu,r}(x) := 2^{-\nu/2} \psi(2^{-\nu} x - r) \quad , \tag{25}$$

$$\varphi_\nu(x) := 2^{-\nu/2} \varphi\left(\frac{x}{2^\nu}\right) \tag{26}$$

and use these with Eq. (23) to obtain

$$c_s(k) = \varphi_k * f(s \cdot 2^k) := <f, \varphi_{k,s}> \quad . \tag{27}$$

Now

$$f(x) = \sum_k \sum_s <f, \varphi_{k,s}> \psi_{k,s}(x) \quad , \tag{28}$$

is a continuous wavelet expansion with wavelet coefficients given by the $c_s(k)$'s of Eq. (27). The mathematical importance of the wavelet expansion over the Fourier method, is that it generalizes to many function and distribution spaces where Fourier analysis is inapplicable. The potential physical importance of wavelet methods is to make possible new formulations and calculations of physical models. For computation or for experimental signal processing the discrete wavelet transform of Frazier-Jawerth called the φ-**transformation** is required. The φ-transform of f is

$$(f, \varphi, \psi) \longrightarrow \sum_k \sum_s <f, \varphi_{k,s}> \psi_{k,s} \tag{29}$$

and holds in general function and distribution spaces. The requirements on the L^2 function which φ must satisfy are:

$$(i) \quad \int_{-\infty}^{\infty} \varphi(x) dx = 0 \quad , \tag{30}$$

$$(ii) \quad \varphi(x) = \varphi_{r,s}(x) = \varphi\left(\frac{x-s}{r}\right) \quad , \tag{31}$$

$$(iii) \quad c_{r,s}(\varphi) = 2\pi \int_{-\infty}^{\infty} |\varphi(k)|^2 \frac{dk}{|k|} < \infty \quad . \tag{32}$$

The *inverse problem* of reconstructing $f(x)$ from coefficients[1,2,4,5,12] can then be reduced to the matrix problem

$$f(x_i) = \left[c_{r,s}(\varphi)\right]^{-1} \left[c_{s,j}(f)\right] \cdot \bar{\psi}\left(\frac{x_i - j}{s}\right) \quad . \tag{33}$$

Observe the correspondence of 2^ν with a scale change and $r(r/s)$ with a spatial translation. A major improvement of wavelets over Fourier methods is apparent from Eq. (16). Whereas, $\hat{f}(k)$ has great *localization* with compact support, $f(x)$ has terrible localization properties in x since as $x \to \infty$

$$\frac{\sin(\pi x)}{\pi x} \longrightarrow \frac{1}{|x|} \quad . \tag{34}$$

The Frazier-Jawerth improvement in localization via the φ-transform is easily seen for $\hat{\psi}(k)\epsilon C_0^r(R)$, where the integration by parts

$$(2\pi i x) \cdot f(x) = -\int_{-\infty}^{\infty} \left(\frac{\partial f}{\partial k}\right)(k) e^{-2\pi i k \cdot x} dk \quad , \tag{35}$$

can be repeated r-times to obtain

$$(2\pi i x)^r f(x) = (-1)^r \int_{-\infty}^{\infty} \left(\frac{\partial^r f}{\partial k^r}\right)(k) e^{-2\pi i k \cdot x} dk \quad . \tag{36}$$

Hence, as $x \to \infty$

$$| f(x) | = 0\left(\frac{1}{| x |^r}\right) \quad . \tag{37}$$

The size of $c_{r,s}(f,\varphi)$ depends largely on f in a neighborhood of the point $\left(0, \frac{s}{2^r}\right)$ with a spread (2^{-r}) and far from this point the coefficient decays as $| x |^{-s}$. The simplest way to obtain wavelets is to decompose the space of interest V_1 into a closed subspace V_0 and its orthogonal complement W_0 according to the direct sum

$$V_1 = V_0 \oplus W_0 \quad , \tag{38}$$

or schematically

$$
\begin{array}{ccc}
 & V_1 & \\
\swarrow & & \searrow \\
V_0 & & W_0
\end{array}
$$
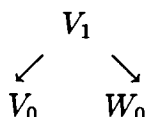
In order to maintain simplicity let V_1 denote either L^2 or ℓ^2. Let φ be a given function in V_1 which satisfies the relation

$$\varphi(x) = \sum_n h(n) 2^{1/2} \varphi(2x - n) \quad , \tag{39}$$

where the set of coefficients $\{h(n)\}_{n=1}^N$ are a collection of constants, called "masking coefficients" and the $2^{1/2}$ factor in front of φ is for L^2 normalization. If V_1 is the closed, linear span of all functions $\{2^{1/2} \cdot \varphi(2x - n)\}$,

$$V_1 = \overline{V_n \{2^{1/2} \varphi(2 \cdot -n\}} \tag{40}$$

and $V_1 \simeq \ell_2$ and is a (useful) special case of Frazier-Jawerth.

Proposition: If the masking coefficients satisfy the condition

$$\sup_n \left\{ \sum_k | h(k - 2n) |^2 \right\} \leq A \tag{41}$$

for $0 < A < \infty$ and $A \epsilon R^1$ then the space V_0 of Eq. (39) is given by

$$V_0 = V_n \varphi(\cdot - n) \tag{42}$$

with $V_0 \simeq \ell_2$ and $V_0 \subset V_1$.

Proof: Any $f(x) \epsilon V_1$ can be expanded in $\varphi(\cdot - n)$'s

$$
\begin{aligned}
f(x) &= \sum_n c_n \varphi(x - n) \\
&= 2^{1/2} \sum_n \sum_m c_n h(m) \varphi(2(x - n) - m) \\
&= 2^{1/2} \sum_n \sum_m c_n h(m) \varphi(2x - m - 2n) \quad .
\end{aligned} \tag{43}
$$

Let

$$k = m + 2n$$

$$f(x) = 2^{1/2} \sum_k b_k \varphi(2x - k) \tag{44}$$

where

$$b_k = \sum_n c_n h(k - 2n) \quad , \tag{45}$$

and take

$$\sum_k | b_k |^2 = \sum_k \left[\sum_n c_n h(k - 2n) \right]^2$$

$$\leq \sum_k \cdot \sum_n | c_n |^2 | h(k - 2n) |^2 \quad . \tag{46}$$

The requirement in Eq. (42) suffices for

$$\sum_k | b_k |^2 \leq A \left(\sum_n | c_n |^2 \right) \quad , \tag{47}$$

for every $\varphi \epsilon V_1$. In the event that $\{h(n)\}_{n=1} \epsilon \ell^2$, eq. (42) is automatically satisfied and V_0 is a closed subspace of V_1.

Question: Does a function $\psi \epsilon V_0^\perp$ exist s.t.

(i) $W_0 = V_0^\perp = \overline{V\psi(\cdot - n)}$ and

(ii) $\{\psi(\cdot - n)\}_{n=1}^\infty$ is an orthonormal basis.

Answer: Yes; Daubechies[13] in L^2, by Frazier and Jawerth[14] in ℓ^2, Besov spaces, Sobolev spaces, bounded mean oscillation (BMO) spaces and Triebel-Lizorkin spaces. Such a function ψ is a **wavelet** and

$$\{2^{\nu/2} \psi(2^\nu \cdot -n) : \nu, n \epsilon Z\} \quad , \tag{48}$$

is an orthonormal basis for $L^2(R)$. This reduces the problem to that of finding a finite set of masking coefficients $\{h(n)\}_{n=1}^N$. The easiest method for finding these coefficients is due to Daubechies in Ref. (13). Assume that the set of non-zero masking coefficients is a finite set and let $\varphi \epsilon L^2$ s.t.

$$\hat{\varphi}(0) = 1 \quad . \tag{49}$$

Given the wavelet expansion

$$\varphi(x) = \sum h(n) 2^{1/2} \varphi(2x - n) \quad ,$$

take its Fourier transform to obtain

$$\hat{\varphi}(k) = \sum h(n) e^{2\pi i n k/2} \varphi(k/2)/2^{1/2}$$

$$=: m(k/2) \varphi(k/2) \quad . \tag{50}$$

It is now necessary to show that

$$\hat{\varphi}(k) = \lim_{N \to \infty} \left\{ \prod_{j=1}^N m(k/2^j) \cdot \hat{\varphi}(k/2^N) \right\}$$

$$= \prod_{j=1}^\infty m(k/2^j) \tag{51}$$
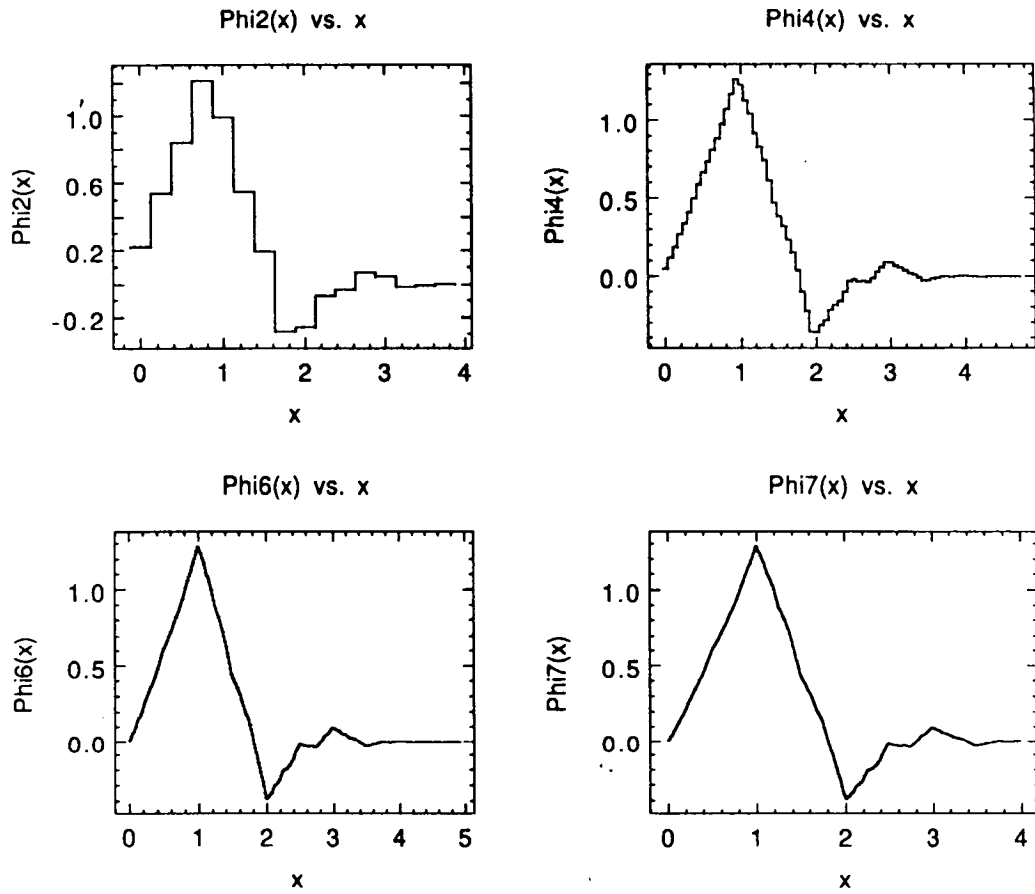
Fig. 1
The second, fourth, sixth and seventh iteration of the Box function for $\varphi(x)$.

makes sense in L^2 (or V_1). This suggests a method of finite approximation providing the masking coefficients are known. Let $\eta_0(x)\epsilon L^2(V_1)$ s.t.

$$\hat{\eta}_0(0) = \int_{-\infty}^{\infty} \eta_0(x)dx = 1 \quad , \tag{52}$$

and iterate

$$\eta_r(x) = \sum_n h(n)2^{1/2}\varphi_{r-1}(2x - n) \quad , \tag{53}$$

to generate φ which is a wavelet, but is not the wavelet ψ of Eq. (25), but rather is that of φ in Eq. (24) instead. In Daubechies nomenclature φ is called a *father wavelet* and if x is identified as a "time" variable the dilations (= scale changes and translations) of φ span V_0 which acts as the high frequency, $k = \omega$, content of the full space V_1. The function φ can be thought of as a "pixel shape" in V_0 as pointed out by Kaiser.[31] Similarly, ψ is called the *mother wavelet* and the dilations of ψ span W_0, which contains the low frequency content of V_1. In Figs. 1, and 2 a mother and father wavelet generated by the choice $\eta_0(x) = b(x)$, the Box function

$$b(x) = \begin{cases} 1, & 1/2 < x < 1/2 \\ 0, & \text{otherwise} \end{cases} \quad . \tag{54}$$

290

Parent Wavelets
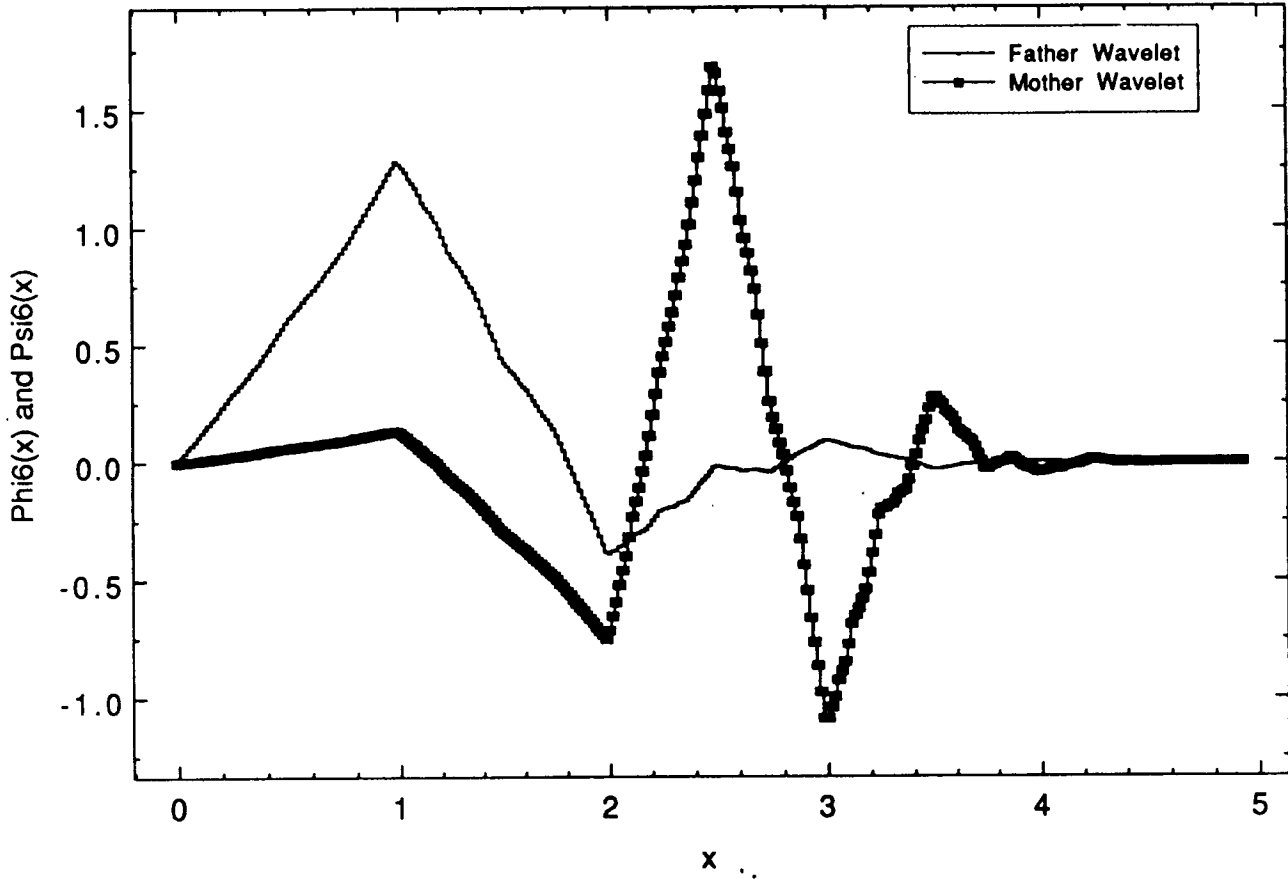
Fig. 2
The father wavelet $\varphi(x)$ and the mother wavelet $\psi(x)$ for η_0 equal to the Box function.

Since $\psi \epsilon W_0 \subset V_1$,

$$\psi(x) = \sum \tilde{h}(n) 2^{1/2} \varphi(2x - n)$$
$$\hat{\psi}(k) = \tilde{m}(k/2) \cdot \hat{\varphi}(k) \tag{55}$$

where $\{\tilde{h}(n)\}_{n=1}^{N}$ is a set of masking coefficients for W_0 and $\tilde{m}(\cdot)$ is a function analogous to $m(\cdot)$ in Eq. (47). Let $\tau = \pi$ be a translation parameter and observe that finding φ and ψ is equivalent to finding two trigonometric polynomials s.t. the 2×2 matrix

$$u(k) = \begin{pmatrix} m(k) & \tilde{m}(k) \\ m(k + \tau) & \tilde{m}(k + \tau) \end{pmatrix} \tag{56}$$

is unitary. It is useful to consider $m(k)$ as a phase function which partitions by translations,

$$|m(k)|^2 + |m(k + \tau)|^2 = 1 \quad . \tag{57}$$

To solve for $|m(k)|^2 = P(|\sin x|^2, |\cos x|^2)$ treat P as the probability of a binomial process with possible outcomes

$$p_1 = |\sin x|^2$$
$$p_2 = |\cos x|^2 \quad . \tag{58}$$

291

Then $m(k)$ is the square root of P. There are many solutions since P is an even, positive polynomial but only one is needed. Then using m, it is straightforward to find $\tilde{m}$. This completes the discussion of simple wavelets.

For mathematical physics, operators and their expectations are the objects of interest. The spectra of operators give infinite dimensional "diagonalizations" in terms of generalized eigenfunctions. In a wavelet basis an operator is "almost diagonal" in a sense discussed next.

Let T be an operator, f a function in a normed space which is in the dense domain of T,

$$T : f \to Tf$$
$$(Tf)(x) = \int K(x,y)f(y)dy \tag{59}$$

s.t.

$$(i) \quad |K(x,y)| \leq \frac{c}{|x-y|} \quad , \tag{60a}$$

and

$$(ii) \quad \left|\frac{\partial K(x,y)}{\partial x}\right| + \left|\frac{\partial K(x,y)}{\partial y}\right| \leq \frac{c}{|x-y|^2} \quad . \tag{60b}$$

Let

$$f(x) = \sum_{j,k} c_{jk}\psi_{jk}(x) \tag{61}$$

where the $\psi_{jk}(x)$'s are a wavelet basis. Then the kernel of T can be written as

$$K(x,y) = \sum_{j,k} e_{jk}\psi_{jk}(x)\bar{\psi}_{jk}(y) \tag{62}$$

where the ψ_{jk}'s satisfy the estimate

$$|\psi_{jk}(x)| < \frac{1}{2^{j/2}}(1 + |2^j \cdot x - k|)^{-1-\epsilon} \quad . \tag{63}$$

In order to prove that K satisfies the conditions (i) and (ii) split the sum according to

$$\sum_{j,k} = \sum_{j<j_0,k} + \sum_{j\geq j_0,k} \tag{64}$$

with j_0 chosen so that

$$2^{j_0} \leq |x-y| \leq 2^{j_0+1} \quad . \tag{65}$$

Using the decomposition of Eq. (64), the estimate of Eq. (63) and geometrical sums, it follows that

$$|K(x,y)| \leq \frac{c}{|x-y|} \quad . \tag{66}$$

The same techniques yield

292

$$\left| \frac{\partial K(x,y)}{\partial x} \right| \leq \frac{c}{|x-y|^2} \quad , \tag{67}$$

and

$$\left| \frac{\partial K(x,y)}{\partial y} \right| \leq \frac{c}{|x-y|^2} \quad . \tag{68}$$

There are several consequences of conditions (i), (ii) and Eq. (63). One is that such operators map $L^p \rightarrow L^p$ for all $1 < p < \infty$, solving deep, old problems. Another is that $\{\psi_{jk}\}$ are an unconditional basis for $L^p, 1 < p < \infty$. The proofs work because of phase-space localization; if two frequencies are well separated their wavelet coefficients are small and if two times are well separated their wavelet coefficients are small. The localization structure in Eq. (64) is the reason that the disadvantages of "almost diagonal" are outweighed by the advantages.

4. WAVELETS FOR SQUEEZED STATES

It is clear that in order to define a wavelet for the squeezed states of quantum optics, it is necessary to define an operator which changes the scale. This has been accomplished in Ref. (33) in a project with G.M. D'Ariano which was initiated at this workshop.

Let $\chi(\cdot)$ be an analytic function of the observable $\hat{A}$ defined s.t.

$$\chi(\hat{A})|a> = a|a> \tag{69}$$

and

$$\chi(\hat{A}) := \int d\mu(a)x|a><a| \quad . \tag{70}$$

This function satisfies the relation

$$<\chi(\hat{a})> = Tr[\chi(\hat{a})\hat{\rho}]$$
$$= \int d\mu(a)\chi(a)P(\hat{\rho},a) \quad . \tag{71}$$

A dilation operator in the Heisenberg picture is defined on an observable $\hat{A}$ as

$$\mathcal{D}_{n\epsilon}(\hat{A}) := \frac{\hat{A}-\eta}{\epsilon} \quad . \tag{72}$$

The time picture is suppressed since no other picture will be used here although Schrödinger picture operators are given in Ref. (17). For some observables, $\hat{A}$, the dilation operator is **unitary** but D'Ariano[21,34] has shown that there are important operators of quantum optics that are **completely positive** maps, abbreviated CP, and are non-unitary. In the unitary case, which is the only case discussed here, all products of operators are preserved and

$$\mathcal{D}_{\eta\epsilon}(\hat{A}) = \chi\{\mathcal{D}_{\eta\epsilon}(\hat{A})\}$$
$$= \chi\left(\frac{\hat{A}-\eta}{\epsilon}\right) \quad . \tag{73}$$

293

Using Eq. (73), the operator-valued wavelet transform can now be written as

$$W(\hat{\rho}; \eta, \epsilon) := \frac{1}{|\epsilon|^{1/2}} Tr\{\mathcal{D}_{\eta\epsilon}(\hat{A})\hat{\rho}\}$$

$$= \frac{1}{|\epsilon|^{1/2}} \left\langle \mathcal{D}_{\eta\epsilon}\big(\chi(\hat{A})\big) \right\rangle \quad . \tag{74}$$

Thus, the dilation operator **squeezes** any state described by a density operator $\hat{\rho}$. In Ref. (34) two examples are presented:

(i) The unitary dilation of one quadrature of the electric field. This case is applicable to a phase sensitive amplification.

(ii) The CP dilation map of the particle number which is applicable to improving noise sensitivity in squeezed light signals.

and analogies of these have been obtained for a quantum wavelet in Ref. (33) with Prof. G.M. D'Ariano.

5. CONCLUSIONS AND OUTLOOK

The scale change part of the wavelet dilation is accomplished by the Yuen[16] squeeze operator. The application of wavelets to quantum optics is an idea with some potential. For example, nonlinear modes and mode-coupling using wavelets should prove useful. The quantum squeezed wavelet with D'Ariano should be a good candidate for highly dispersive biological media. Future work will focus on these ideas.

6. ACKNOWLEDGEMENTS

REFERENCES

1. J. Morlet, G. Ahrens, I. Fourgeau and D. Giard, "Wave Propagation and Sampling Theory," Geophysics **47**, 203-236 (1982).

2. A. Grossmann and J. Morlet, "Decomposition of Hardy Functions into Square-integrable Wavelets of Constant Shape," SIAM J. Math. Anal. **15**, 723-736 (1984).

3. Y. Meyer, "Principle D'incertitude, Bases Hilbertiennes et Algébras D'opérateurs," Séminaire Bourbaki, 1985-1986, nr. 662.

4. J. Morlet, "Sampling Theory and Wave Propagation," NATO ASI Series Volume F1; C.H. Chen, Editor Springer-Verlag, Berlin Heidelberg, 1983.

5. J.M. Combes, A. Grossmann and Ph. Tehamitchian, Editors, **Wavelets Time-Frequency Methods and Phase-Space**, (Springer-Verlag, Berlin and New York, 1989).

6. D. Gabor, "Theory of Communications," J. Inst. Elec. Engr. **93**, 429-457 (1946).

7. Y. Meyer, **Ondelettes et Operateurs**, vols I-III (Herman, Paris, 1990-1).

8. G. Strang, "Wavelets and Dilation Equations, A Brief Introduction," SIAM Rev **31**, 614-627 (1989).

9. C.E. Heil and D.F. Walnut, "Continuous and Discrete Wavelet Transforms," SIAM Rev. **31**, 628-666 (1989).

10. M. Frazier, B. Jawerth and G. Weiss, NSF-CBMS Conference at Auburn University, AL, summer 1989, to be published by SIAM.

11. A. Daubechies, NSF-CBMS Conference at Lowell Unviersity MA, summer 1990, to be published by SIAM.

12. B. DeFacio, C.R. Thompson and G.V. Welland, "Wavelet Version of Fourier Optics," SPIE **1351**, **Digital Image Synthesis and Inverse Optics**, (Soc. Photo-Opt Instr. Engr Bellingham WA, 1990).

13. I. Daubechies, "Orthonormal Basis of Compactly Supported Wavelets," Comm. Pure Appl. Math. **41**, 909-996 (1988).

14. M. Frazier and B. Jawerth, "A Discrete Transform and the Decomposition of Distribution Spaces," J. Funct. Anal. **93**, 134-170 (1990).

15. D. Stoler, "Equivalence Classes of Minimum-Uncertainty Packets II," Phys. Rev. D **4**, 1925-1926 (1971).

16. H.P. Yuen, "Two-photon Coherent States of the Radiation Field," Phys. Rev. A **12**, 2226-2242 (1976).

17. P. Tombesi and E.R. Pike, Editors, **Squeezed and Semi-classical Light** (Plenum, New York, 1989).

18. G. D'Ariano, M. Rasatti and M. Vadacchino, "New Type of Two-photon Squeezed Coherent States," Phys. Rev. D **32**, 1034-1037 (1985).

19. D. Han, Y.S. Kim and M.E. Noz, "Linear Canonical Transformations of Coherent and Squeezed States in the Wigner Phase-space III Two-mode States," Phys. Rev. A **41**, 6233-6244 (1990).

20. R.J. Glauber, "The Quantum Theory of Optical Coherence," Phys. Rev. **130**, 2529-2539 (1963).

21. G.M. D'Ariano, "Number-phase Squeezing Through Non-unitary Scaling," Phys. Rev. A **43**, 2550-2555 (1991).

22. Y.S. Kim and E.P. Wigner, "Canonical Transformations in Quantum Mechanics," Amer. J. Phys. **58**, 439-448 (1990).

23. J.R. Klauder, "The Action Option and a Feynman Quantization of Spinor Fields in Terms of Ordinary C-Numbers," Ann. Phys. (NY) **11**, 123-168 (1968).

24. J.R. Klauder and E.G.C. Sudarshan, **Fundamentals of Quantum Optics** (W.A. Benjamin, New York, 1968).

25. J.R. Klauder and B.-S. Skagerstam, **Coherent States** (World Scientific, Singapore, 1985).

26. J.R. Klauder, "Continuous Representation Theory I," J. Math. Phys. **4**, 1055-1058 (1963).

27. E.W. Aslaksen and J.R. Klauder, "Continuous Representations Using the Affine Group," J. Math Phys **10**, 2267-2276 (1969).

28. A.M. Perelomov, "Coherent States for Arbitrary Lie Group," Commun. Math. Phys. **26**, 222-236 (1972).

29. E. Onofrio, "A Note on Coherent State Representations of Lie Groups," J. Math. Phys. **16**, 1087-1089 (1975).

30. G.W. Mackey, **Induced Representations of Groups and Quantum Mechanics** (W.A. Benjamin, New York, 1968).

31. G. Kaiser, "Quantum Physics, Relativity and Complex Spacetime" (North Holland, Amsterdam, 1991).

32. R.A. Fisher, M.M. Nieto and V.D. Sandberg, "Impossibility of Naively Generalizing Squeezed Coherent States," Phys. Rev. D **29**, 1107-1110 (1984).

33. G.M. D'Ariano and B. DeFacio, "A Quantum Wavelet," (submitted).

34. G.M. D'Ariano, This Proceedings.

35. A. Calderón, "Intermediate Spaces and Interpolation, the Complex Method," Studia Math. **24**, 113-190 (1964).

COHERENT STATES AND
PARASUPERSYMMETRIC QUANTUM MECHANICS

Nathalie DEBERGH

Physique théorique et mathématique,
Institut de Physique au Sart Tilman (B.5), Université de Liège,
B-4000 LIEGE 1 (Belgique)

It is well known (Refs. 1,2) that Parafermi and Parabose statistics are natural extensions of the usual Fermi and Bose ones, enhancing trilinear (anti)commutation relations instead of bilinear ones. Due to this generalization, positive parameters appear : the so-called orders of paraquantization p (= 1,2,3,···) and h_0 (= 1/2,1,3/2,···), respectively, the first value leading in each case to the usual statistics. The superposition of the parabosonic and parafermionic operators gives rise to parasupermultiplets (Refs. 3-5) for which mixed trilinear relations have to be envisaged. In the particular case of quantas of the same order $(p = 2h_0)$, these relations have already been studied (Ref. 6) leading to two (non equivalent) sets : the relative Parabose and the relative Parafermi ones. For the specific values $p = 1 = 2h_0$, these sets reduce to the well known supersymmetry (Refs. 7,8).

Coherent states associated with this last model have been recently put in evidence through the annihilation operator point of view (Ref. 9) and the group theoretical approach or displacement operator context (Refs. 10-12). We propose here to realize the corresponding studies within the new context $p = 2 = 2h_0$, being then directly extended to any order of paraquantization. Even if we have to take account of the two relative sets separately, the arguments are so similar in both cases that we just concentrate on the Parabose set in the following . Within the relations characterizing such a model, it is easy to prove that the operator $A = a + \frac{1}{2} a^\dagger b^{\dagger 2}$ [$a, a^\dagger$ ($b, b^\dagger$) are the usual bosonic (fermionic) annihilation and creation operators] exactly plays the role of a generalized annihilation operator i.e. satisfying the expected commutation relation with the hamiltonian and displaying the right action on the state basis of the Hilbert space (Refs. 13,14). Parasupercoherent states (Refs. 13,14) $|z>$ are then defined as eigenstates of this operator A with eigenvalues being arbitrary complex numbers. The corresponding uncertainty relation is found to be nearly 1 ($\hbar = 1$) .

The group theoretical approach asks for the consideration of a specific representation of the para-operators : the Green-Cusson Ansätze (Refs. 1,15) in which each operator is decomposed into a sum of two other ones related to the usual bosonic scaling operators and the Pauli matrices. By introducing parameters realized through two by two matrices with Grassmannian elements, we are led to the corresponding color supergroups (Ref. 16) and we are thus able to define the associated coherent states by a unitary representation of these groups. Convenient Baker-Campbell-Hausdorff relations (Ref. 12) are of particular interest in this study. Moreover the states obtained in this way are

effective eigenstates of the operator A introduced before. The three usual definitions of ordinary coherent states are thus satisfied in this parasupersymmetric context.

REFERENCES

1. Green, H.S., 1953, "A Generalized Method of Field Quantization", *Phys.Rev.*, **90**, p.270.

2. Ohnuki, Y., and Kamefuchi, S., 1982, *Quantum Field Theory and Parastatistics*, University of Tokyo Press.

3. Beckers, J., and Debergh, N., 1990, "Parastatistics, Supersymmetry and Parasupercoherent States", *J.Math.Phys.*, **31**, p.1513.

4. Beckers, J., and Debergh, N., November 1990, "On Supersymmetric Harmonic Oscillators and Green-Cusson's Ansätze", Preprint Univ.Liège PTM 90/14.

5. Beckers, J., and Debergh, N., 1990, "Parastatistics and Supersymmetry in Quantum Mechanics", *Nucl.Phys.* **B340**, p.767.

6. Greenberg, O.W., and Messiah, A.M.L., 1965, "Selection Rules for Parafields and the Absence of Para Particles in Nature", *Phys.Rev* **B138**, p.1155.

7. Fayet, P., and Ferrara, S., 1985, *Supersymmetry in Physics*, North Holland, Amsterdam.

8. Witten, E., 1982, "Constraints on Supersymmetry Breaking", *Nucl.Phys.* **B202**, p.253.

9. Aragone, C., and Zypman, F., 1986, "Supercoherent States", *J.Phys. A (Math. and Gen.)* **19**, p.2267.

10. Balantekin, A.B., Schmitt, H.A., and Barret, B.R., 1988, "Coherent States for the Harmonic Oscillator Representations of the Orthosymplectic Supergroup OSP (1/2 N, ℝ)", *J.Math. Phys.* **29**, p.1634.

11. Fatyga, B.W., Kostelecky, V.A., Nieto, M.M., and Truax, D.R., 1991, "Supercoherent States", *Phys.Rev.* **D43**, p.1403.

12. Kostelecky, V.A., Nieto, M.M., and Truax, D.R., 1986, "Baker-Campbell-Hausdorff Relations for Supergroups", *J.Math.Phys.* **27**, p.1419.

13. Beckers, J., and Debergh, N., 1989, "On Parasupersymmetric Coherent States", *Mod.Phys. Lett.* **A4**, p.1209.

14. Beckers, J., and Debergh, N., 1989, "Coherent States in Parasupersymmetric Quantum Mechanics", *Mod.Phys.Lett* **A4**, p.2289.

15. Cusson, R.Y., 1969, "Examples of Parastatistics", *Ann.Phys.* **55**, p.22.

16 Rittenberg, V., and Wyler, D., 1978, "Generalized Superalgebras", *Nucl.Phys.***B139**, p.189.

A GAUSSIAN MEASURE OF QUANTUM PHASE NOISE 628188

12 ℓ_{4} s

Wolfgang P. Schleich[*]
Abteilung für Theoretische Physik III, Universität Ulm
Oberer Eselsberg W-7900 Ulm, Germany

and

Jonathan P. Dowling[†]
Weapons Sciences Directorate, AMSMI-RD-WS
U.S. Army Missile Command
Redstone Arsenal, Alabama 35898-5248

ABSTRACT

We study the width of the semiclassical phase distribution of a quantum state in its dependence on the average number of photons $\langle m \rangle$ in this state. As a measure of phase noise, we choose the width $\Delta\varphi$ of the best Gaussian approximation to the dominant peak of this probability curve. For a coherent state this width decreases with the square root of $\langle m \rangle$, whereas for a truncated phase state it decreases linearly with increasing $\langle m \rangle$. For an optimal phase state, $\Delta\varphi$ decreases exponentially — but so does the area "caught" underneath the peak: All the probability is stored in the broad wings of the distribution.

I. INTRODUCTION

The ultimate quantum limit in the goal of optically detecting gravitational waves is to operate a Michelson interferometer with light in a quantum state that minimizes the phase noise at a given mean number of photons (Ref. 1). But what is a good measure for phase noise? Should we consider the inverse peak height of the probability distribution (Ref. 2) — the so-called reciprocal likelihood — or perhaps the second moment of the phase distribution (Ref. 3) or even the periodic measure advocated in Refs. 4 and 5? These are all based on the idea of a phase distribution — but we recall that this in itself is not a trivial construction since the concept of a Hermitian phase operator is not without complications (Ref. 6).

In the present paper we therefore start from the *semiclassical* phase distribution $W_{\varphi}[|\psi\rangle]$ of a quantum state $|\psi\rangle$ (Refs. 7 and 8). We consider states that have a single pronounced maximum of W_{φ} at a phase value that, without loss of generality, we take at $\varphi = 0$. We approximate (Ref. 9) this peak by a Gaussian distribution with an identical height of $W_{\varphi=0}$. The distribution's width $\Delta\varphi$ is determined by the curvature of W_{φ} at $\varphi=0$, together with $W_{\varphi=0}$. The examples of a coherent state $|\psi_{coh}\rangle$ and a truncated phase state $|\psi_{p}\rangle$ will illustrate this scheme: Their widths $\Delta\varphi\,[|\psi_{coh}\rangle]$ and $\Delta\varphi\,[|\psi_{p}\rangle]$ decrease as the *square root* and *linearly* with increasing average photon number $\langle m \rangle$, respectively. In the case of the optimal phase state — the state (Ref. 2) that minimizes the reciprocal likelihood — we find (Ref. 9) even an *exponential* decay for $\Delta\varphi$. However, in contrast to the coherent or the truncated phase state, the area underneath this maximum is not normalized but decays as well (Ref. 10).

---

[*] Also at: Max-Planck-Institut für Quantenoptik, D-8046 Garching bei München, Germany.

[†] National Research Council Associate.

II. FROM PHASE FUNCTIONAL TO GAUSSIAN-APPROXIMATED PHASE DISTRIBUTION

In this section we start from the semiclassical phase amplitude functional $w_\varphi [|\psi\rangle]$ of a quantum state $|\psi\rangle$ and derive a Gaussian approximation to the dominant maximum of this probability curve.

In the semiclassical limit the phase distribution $W_\varphi [|\psi\rangle]$ of a quantum state

$$|\psi\rangle = \mathcal{N} \sum_{m=0}^{\infty} \psi_m |m\rangle \qquad (2.1)$$

represented as a superposition of photon number states $|m\rangle$, with expansion coefficients $\psi_m \equiv \langle m | \psi \rangle$ and the normalization $\mathcal{N}$ such that $\langle \psi | \psi \rangle = 1$, follows from the phase functional

$$w_\varphi \left[|\psi\rangle \right] \equiv \frac{\mathcal{N}}{\sqrt{2\pi}} \sum_{m=o}^{\infty} \psi_m e^{im\varphi} \qquad (2.2a)$$

via

$$W_\varphi \left[|\psi\rangle \right] \equiv \left| w_\varphi \left[|\psi\rangle \right] \right|^2$$

$$= \frac{\mathcal{N}^2}{2\pi} \sum_{m,n=0}^{\infty} \psi_m \psi_n e^{i(m-n)\varphi} . \qquad (2.2b)$$

For the sake of simplicity, we consider in this article only quantum states such that $\psi_m = \psi_m^* \geq 0$. Hence, for the phase value $\varphi = 0$ the terms in the sum of Eq. (2.2b) add constructively, whereas for $\varphi \neq 0$ cancellations occur. This results in a maximum at $\varphi = 0$.

An approximate analytical expression for $W_\varphi [|\psi\rangle]$ in the neighborhood of the origin follows from an expansion of W_φ into a Taylor series around $\varphi = 0$, that is

$$W_\varphi = W_{\varphi=0} + \frac{1}{2} W''_{\varphi=0} \varphi^2 + \cdots$$

$$\equiv W_{\varphi=0} \left\{ 1 + \left[W''_{\varphi=0} / \left(2W_{\varphi=0} \right) \right] \varphi^2 \right\}. \qquad (2.3)$$

Here primes denote differentiation with respect to φ and we have used the property

$$W'_{\varphi=0} = \frac{\mathcal{N}^2}{2\pi} \sum_{m,n=0}^{\infty} i\,(m-n)\psi_m \psi_n = 0,$$

following from Eq. (2.2b). With the help of Eq. (2.3), we arrive at

$$W_\varphi^{(\text{peak})} = \exp\left(\ln W_\varphi \right) \cong W_{\varphi=0} \exp\left[-\left(\frac{\varphi}{\Delta\varphi} \right)^2 \right] \qquad (2.4a)$$

where the width $\Delta\varphi$ of this Gaussian is given by

$$\Delta\varphi^2 \equiv \frac{2 W_{\varphi=0}}{\left| W''_{\varphi=0} \right|}$$

$$= \frac{\left(\displaystyle\sum_{m=0}^{\infty} \psi_m \right)^2}{\left(\displaystyle\sum_{m=0}^{\infty} m^2 \psi_m \right)\left(\displaystyle\sum_{m=0}^{\infty} \psi_m \right) - \left(\displaystyle\sum_{m=0}^{\infty} m \psi_m \right)^2} . \qquad (2.4b)$$

We emphasize that this procedure is valid for any state whose phase probability $W_\varphi [|\psi\rangle]$ enjoys a maximum at $\varphi = 0$.

The area underneath this Gaussian-approximated peak reads as

$$A_{Gauss} \equiv \int_{-\infty}^{\infty} d\varphi \, W_{\varphi=0} \, e^{-(\varphi/\Delta\varphi)^2}$$

$$= \sqrt{\pi} \, \Delta\varphi \, W_{\varphi=0} \, . \tag{2.5}$$

This clearly demonstrates that the Gaussian fit of the peak, Eq. (2.4), is different from the properly normalized Gaussian $G(\varphi) = \pi^{-1/2}$ $(\Delta\varphi)^{-1} \exp[-(\varphi/\Delta\varphi)^2]$. Whereas $W_\varphi^{(peak)}$ is tailored to have a height identical to $W_{\varphi=0}[\,|\psi\rangle]$, the height of G, that is, $\pi^{-1/2}$ $(\Delta\varphi)^{-1}$, adjusts itself to the width of the Gaussian, so as to keep the area normalized.

III. PHASE NOISE AND AVERAGE NUMBER OF PHOTONS

In this section we apply the Gaussian approximation, Eq. (2.4a), in order to discuss the width $\Delta\varphi$, Eq. (2.4b) of the phase distribution of:

(i) a coherent state of large displacement $\alpha \gg 1$,

$$|\psi_{coh}\rangle = (2\pi)^{-1/4} \alpha^{-1/2} \sum_{m=0}^{\infty} e^{-\left(\frac{m-\alpha^2}{2\alpha}\right)^2} |m\rangle \, ,$$

$$\tag{3.1}$$

(ii) a truncated phase state

$$|\psi_p\rangle = \left(m_0+1\right)^{-1/2} \sum_{m=0}^{m_0} |m\rangle \, , \tag{3.2}$$

and

(iii) the optimal phase state

$$|\psi_s\rangle \equiv \mathcal{N} \sum_{m=0}^{m_0} \frac{1}{1+m} |m\rangle \tag{3.3}$$

recently proposed in Ref. 2.

These states are normalized to unity. For a coherent state, Eq. (3.1), we arrive at

$$\langle\psi_{coh}|\psi_{coh}\rangle = (2\pi)^{-1/2} \alpha^{-1} \sum_{m=0}^{\infty} e^{-\left(\frac{m-\alpha^2}{\sqrt{2}\,\alpha}\right)^2}$$

$$\cong \pi^{-1/2} \int_{-\infty}^{\infty} d\bar{m} \, e^{-\bar{m}^2}$$

$$= 1 \tag{3.4}$$

where we have replaced the summation by an integration. For the truncated phase state $|\psi_p\rangle$ we find directly

$$\langle\psi_p|\psi_p\rangle = \left(m_0+1\right)^{-1} \sum_{m=0}^{m_0} 1 = 1 \, ,$$

whereas for the optimal state $|\psi_s\rangle$, Eq. (3.3), the normalization constant $\mathcal{N}$ is given implicitly by

$$\langle\psi_s|\psi_s\rangle = \mathcal{N}^2 \sum_{m=0}^{m_0} (1+m)^{-2}$$

$$= \mathcal{N}^2 \left\{ \sum_{k=1}^{\infty} k^{-2} - \sum_{k=0}^{\infty} \left(m_0+2+k\right)^{-2} \right\} \, ,$$

that is, (Ref. 11)

$$1 = \varkappa^2 \left\{ \frac{\pi^2}{6} - \zeta\left(2; m_o + 2\right) \right\}$$

$$= \varkappa^2 \left\{ \frac{\pi^2}{6} - \frac{1}{m_o + 1} + O\left(m_o^{-2}\right) \right\} . \qquad (3.5)$$

Here,

$$\zeta(s, \upsilon) \equiv \sum_{k=0}^{\infty} (\upsilon + k)^{-s}$$

denotes the generalized Riemann zeta function (Ref. 12).

A. Coherent State

For the coherent state, Eq. (3.1), the expansion coefficients ψ_m read

$$\psi_m = (2\pi)^{-1/4} \, \alpha^{-1/2} \exp\left[-\left(\frac{m - \alpha^2}{2\alpha} \right)^2 \right]$$

---

and the width $\Delta\varphi$, given by Eq. (2.4b) reduces to

$$\Delta\varphi^2 \left[|\psi_{coh}\rangle \right] \equiv$$

$$\frac{\left(\int\limits_{-\infty}^{\infty} dm \, \psi_m \right)^2}{\left(\int\limits_{-\infty}^{\infty} dm \, m^2 \, \psi_m \right) \left(\int\limits_{-\infty}^{\infty} dm \, \psi_m \right) - \left(\int\limits_{-\infty}^{\infty} dm \, m \, \psi_m \right)^2} .$$

$$(3.6)$$

Here, we have once again replaced summations over m by integrations. We evaluate the Gaussian integrals most economically by applying the symmetry of ψ_m with respect to α^2 before performing the integrals. This yields

$$\int\limits_{-\infty}^{\infty} dm \, m^2 \, \psi_m = \int\limits_{-\infty}^{\infty} dm \, (m - \alpha^2)^2 \, \psi_m + 2\alpha^2 \int\limits_{-\infty}^{\infty} dm \, (m - \alpha^2) \, \psi_m + \alpha^4 \int\limits_{-\infty}^{\infty} dm \, \psi_m = \int\limits_{-\infty}^{\infty} dm \, (m - \alpha^2)^2 \, \psi_m + \alpha^4 \int\limits_{-\infty}^{\infty} dm \, \psi_m$$

and

$$\int\limits_{-\infty}^{\infty} dm \, m \, \psi_m = \int\limits_{-\infty}^{\infty} dm \, (m - \alpha^2) \, \psi_m + \alpha^2 \int\limits_{-\infty}^{\infty} dm \, \psi_m = \alpha^2 \int\limits_{-\infty}^{\infty} dm \, \psi_m .$$

This result reduces Eq. (3.6) to

$$\Delta\varphi^2\left[\,|\psi_{coh}\rangle\right] = \frac{\displaystyle\int_{-\infty}^{\infty} dm\,\psi_m}{\displaystyle\int_{-\infty}^{\infty} dm\,(m-\alpha^2)^2\,\psi_m}$$

$$= \frac{\displaystyle\int_{-\infty}^{\infty} dy\,\exp\left[-\left(\frac{y}{2\alpha}\right)^2\right]}{\displaystyle\int_{-\infty}^{\infty} dy\,y^2\,\exp\left[-\left(\frac{y}{2\alpha}\right)^2\right]}$$

$$= \frac{1}{2\alpha^2} \quad . \tag{3.7a}$$

The average number of photons $\langle m \rangle$ follows from the normalization condition, Eq. (3.4), as

$$\langle m \rangle \cong \int_{-\infty}^{\infty} dm\,m\,\psi_m^2$$

$$= \int_{-\infty}^{\infty} dm\left(m-\alpha^2\right)\psi_m^2 + \alpha^2 \int_{-\infty}^{\infty} dm\,\psi_m^2$$

$$= \alpha^2$$

and hence

$$\Delta\varphi\left[\,|\psi_{coh}\rangle\right] \cong \frac{1}{\sqrt{2\langle m\rangle}} \tag{3.7b}$$

for large $\langle m \rangle$. Asymptotically, the width $\Delta\varphi\,[\,|\psi_{coh}\rangle]$ of the phase distribution of a coherent state decreases inversely as the square root of the average photon number.

We now evaluate the area underneath the Gaussian approximation, Eq. (2.5), for the coherent state, Eq. (3.1). The maximum value of the phase distribution reads

$$W_{\varphi=0}\left[\,|\psi_{coh}\rangle\right] = \frac{1}{2\pi}\left(\int_{-\infty}^{\infty} dm\,\psi_m\right)^2$$

$$= \sqrt{\frac{2}{\pi}}\,\alpha$$

$$= \sqrt{\frac{2}{\pi}\,\langle m\rangle} \tag{3.8}$$

and hence the area of the Gaussian is

$$A_{Gauss}\left[\,|\psi_{coh}\rangle\right] = \sqrt{\pi}\cdot\Delta\varphi\left[\,|\psi_{coh}\rangle\right]$$

$$\cdot W_{\varphi=0}\left[\,|\psi_{coh}\rangle\right] = 1 . \tag{3.9}$$

Thus the Gaussian approximation, Eq. (2.4) for a coherent state is properly normalized. Its width $\Delta\varphi\,[\,|\psi_{coh}\rangle]$ decreases linearly with α but its height $W_{\varphi=0}\,[\,|\psi_{coh}\rangle]$ increases linearly with $\alpha \sim \sqrt{\langle m\rangle}$ to leave the area A_{Gauss} constant.

B. Truncated Phase State

We now turn to the discussion of the truncated phase state $|\psi_p\rangle$, Eq. (3.2). According to this equation, the expansion coefficients ψ_m read

$$\psi_m = \begin{cases} 1 , & \text{for } 0 \le m \le m_o \\ 0 , & \text{for } m > m_o \end{cases}$$

which reduces $\Delta\varphi\,[\,|\psi_p\rangle]$ to

$$\Delta\varphi^2\left[\,|\psi_p\rangle\right] = \frac{\left(\displaystyle\sum_{m=0}^{m_o} 1\right)^2}{\left(\displaystyle\sum_{m=0}^{m_o} m^2\right)\left(\displaystyle\sum_{m=0}^{m_o} 1\right) - \left(\displaystyle\sum_{m=0}^{m_o} m\right)^2}$$

$$= \frac{\left(m_o + 1\right)^2}{\frac{1}{6} m_o \left(m_o + 1\right)^2 \left(2 m_o + 1\right) - \frac{1}{4} m_o^2 \left(m_o + 1\right)^2}$$

$$= \frac{12}{m_o\left(m_o + 2\right)}$$

$$= \frac{12}{m_o^2} + O\left(m_o^{-3}\right). \qquad (3.10)$$

Here, we have made use of the summation formulae (Ref. 11)

$$\sum_{m=1}^{m_o} 1 = m_o ,$$

$$\sum_{m=1}^{m_o} m = \frac{1}{2} m_o \left(m_o + 1\right) ,$$

and

$$\sum_{m=1}^{m_o} m^2 = \frac{1}{6} m_o \left(m_o + 1\right)\left(2 m_o + 1\right). \qquad (3.11)$$

When we express m_o in terms of the average number of photons

$$\langle m\rangle = \left(1 + m_o\right)^{-1} \sum_{m=1}^{m_o} m = \frac{1}{2} m_o ,$$

we find

$$\Delta\varphi\left[\,|\psi_p\rangle\right] \cong \frac{\sqrt{3}}{\langle m\rangle} \quad , \qquad (3.12)$$

again for large $\langle m\rangle$. The width $\Delta\varphi\,[\,|\psi_p\rangle]$ of the phase distribution of the truncated phase state decreases linearly with the average photon number $\langle m\rangle$.

The value of W_φ at $\varphi=0$ reads

$$W_{\varphi=0} = (2\pi)^{-1}\left(m_o + 1\right)^{-1}\left(\sum_{m=0}^{m_o} 1\right)^2$$

$$= (2\pi)^{-1}\left(m_o + 1\right)$$

$$\cong \frac{1}{\pi} \langle m\rangle , \qquad (3.13)$$

and yields for the area underneath the Gaussian approximation, Eq. (2.4), of the truncated phase state, Eq. (3.2),

$$A_{Gauss}\left[\,|\psi_p\rangle\right] = \sqrt{\pi} \cdot \Delta\varphi\left[\,|\psi_p\rangle\right] \cdot W_{\varphi=0}\left[\,|\psi_p\rangle\right]$$

$$= \sqrt{\frac{3}{\pi}} \cong 0.98 , \qquad (3.14)$$

i.e., *almost* perfect normalization. Again, we note from Eqs. (3.10) and (3.13) that the width $\Delta\varphi$ decreases with m_o in the same manner as the maximum height $W_{\varphi=0}$ increases — keeping the area A_{Gauss} normalized and, more importantly, keeping it independent of m_o.

C. Optimal Phase State

We conclude our illustration of the Gaussian-approximated phase distribution by applying it to the optimal phase state $|\psi_s\rangle$, Eq. (3.3), which enjoys the expansion coefficients

$$\psi_m = \begin{cases} (1+m)^{-1} & \text{, for } 0 \le m \le m_o \\ \\ 0 & \text{, for } m > m_o . \end{cases}$$

The width $\Delta\varphi\,[\,|\psi_s\rangle]$, Eq. (2.4), then reads

$$\Delta\varphi^2\left[\,|\psi_s\rangle\right] =$$

$$\frac{\left(\displaystyle\sum_{m=0}^{m_o}\frac{1}{1+m}\right)^2}{\left(\displaystyle\sum_{m=0}^{m_o}\frac{m^2}{1+m}\right)\left(\displaystyle\sum_{m=0}^{m_o}\frac{1}{1+m}\right)-\left(\displaystyle\sum_{m=0}^{m_o}\frac{m}{1+m}\right)^2} .$$

When we use the summation formulae, (Ref. 11)

$$f(m_o) \equiv \sum_{m=0}^{m_o}\frac{1}{1+m}$$

$$= C + \ln\left(m_o+1\right) + O\left[\left(m_o+1\right)^{-1}\right], \quad (3.15)$$

where

$$C \equiv \lim_{s\to\infty}\left(\sum_{m=1}^{s}\frac{1}{m}-\ln s\right)$$

$$= 0.577215\ldots$$

is Euler's constant, and from Eq. (3.11)

$$\sum_{m=0}^{m_o}(1+m) = \left(m_o+1\right)+\frac{1}{2}m_o\left(m_o+1\right)$$

$$= \frac{1}{2}\left(m_o+1\right)\left(m_o+2\right),$$

we find

$$\Delta\varphi^2\left[|\psi_s\rangle\right] = f^2(m_o)\left[f(m_o)\sum_{m=0}^{m_o}\frac{(m+1)^2-2(m+1)+1}{m+1} - \left(\sum_{m=0}^{m_o}\frac{m+1-1}{m+1}\right)^2\right]^{-1}$$

$$= f^2(m_o)\left\{\left[\sum_{m=0}^{m_o}(m+1)-2\left(m_o+1\right)+f(m_o)\right]f(m_o)-\left[\left(m_o+1\right)-f(m_o)\right]^2\right\}^{-1}$$

$$= f^2(m_o)\left[\frac{1}{2}\left(m_o+1\right)\left(m_o+2\right)f(m_o)-\left(m_o+1\right)^2\right]^{-1} .$$

In the large m_o limit we arrive at

$$\Delta\varphi^2\left[\,|\psi_s\rangle\right] = \frac{2\,f(m_o)}{\left(m_o+1\right)^2}\left[1+\frac{1}{m_o+1}-\frac{2}{f(m_o)}\right]^{-1}$$

$$= \frac{2\,f(m_o)}{\left(m_o+1\right)^2} + O\left[\left(m_o+1\right)^{-3}\right]$$

and with Eq. (3.15) we then have

$$\Delta\varphi^2\left[\,|\psi_s\rangle\right] \cong \frac{2\left[C+\ln\left(m_o+1\right)\right]}{\left(m_o+1\right)^2}. \qquad (3.16)$$

The average number of photons in this state reads

$$\langle m+1\rangle = \mathcal{N}^2(m_o)\sum_{m=0}^{m_o}\frac{1}{m+1}$$

$$= \mathcal{N}^2(m_o)\left[C+\ln\left(m_o+1\right)+\frac{1}{2\left(m_o+1\right)}+O\left(\frac{1}{m_o^2}\right)\right]$$

$$= \frac{6}{\pi^2}\left[C+\ln\left(m_o+1\right)\right]+O\left[\frac{\ln\left(m_o+1\right)}{m_o+1}\right],$$

$$(3.17a)$$

that is,

$$m_o+1 \cong \gamma^{-1}\exp\left[\frac{\pi^2}{6}\langle m+1\rangle\right], \qquad (3.17b)$$

where we have defined $\gamma \equiv e^C$ in a standard notation. In determining the remainder, we have applied in the last step of Eq. (3.17a) the asymptotic expression for $\mathcal{N}$, Eq. (3.5). With the help of Eqs. (3.17a) and (3.17b), Eq. (3.16) reads

$$\Delta\varphi\left[\,|\psi_s\rangle\right] = \frac{\gamma\pi}{\sqrt{3}}\langle m+1\rangle^{1/2}\,e^{-\frac{\pi^2}{6}\langle m+1\rangle}$$

$$+ O\left[\langle m+1\rangle^{-1/2}\,e^{-\frac{\pi^2}{6}\langle m+1\rangle}\right], \quad (3.18)$$

which shows that the Gaussian-approximated width $\Delta\varphi$ of the phase state $|\psi_s\rangle$ decreases *exponentially* with the average number of photons. The height

$$W_{\varphi=0} = \left(2\pi\,\mathcal{N}^2\right)^{-1}\left[\mathcal{N}^2\sum_{m=0}^{m_o}(1+m)^{-1}\right]^2$$

$$= \left(2\pi\,\mathcal{N}^2\right)^{-1}\langle m+1\rangle^2$$

$$\cong \frac{\pi}{12}\langle m+1\rangle^2 \qquad (3.19)$$

of the distribution increases only *quadratically*. Here, we have also made use of Eq. (3.17a). Hence, the phase probability or area caught underneath the peak,

$$A_{\text{Gauss}}\left[\,|\psi_s\rangle\right] = \frac{\pi^{5/2}\,\gamma}{12\sqrt{3}}\langle m+1\rangle^{5/2}\,e^{-\frac{\pi^2}{6}\langle m+1\rangle} + O\left(\langle m+1\rangle^{3/2}\,e^{-\frac{\pi^2}{6}\langle m+1\rangle}\right),$$

decreases rapidly to zero with increasing average photon number. All the probability is stored in the broad wings of the distribution.

IV. SUMMARY AND OUTLOOK: A NEW VARIATIONAL PROBLEM

In this article we have presented a Gaussian approximation to the maximum of the semiclassical phase distribution of an arbitrary quantum state. We have illustrated this scheme using the example of a coherent state, a truncated phase state, and the intriguing optimal phase state. Our main results are summarized in Table 1. The Gaussian-approximated width $\Delta\varphi\,[\,|\psi_{coh}\rangle]$, Eq. (3.7), of the coherent state $|\psi_{coh}\rangle$ decreases as the square root of the average number of photons, whereas for a truncated phase state $\psi_p\rangle$ the width $\Delta\varphi\,[|\psi_p\rangle]$, Eq. (3.12), decreases linearly with $\langle m\rangle$. In both cases the Gaussian is properly normalized, that is, the probability caught underneath the peak is almost

identical to unity, Eqs. (3.9) and (3.14), and independent of $\langle m\rangle$.

The situation is quite different for the optimal phase state $|\psi_s\rangle$. Here, $\Delta\varphi\,[\,|\psi_s\rangle]$, Eq. (3.18), decreases exponentially with $\langle m\rangle$, but the maximum $W_{\varphi=0}\,[\,|\psi_s\rangle]$, Eq. (3.19), increases only quadratically with $\langle m\rangle$, leading to vanishing probability in the peak. All probability in this case is in the broad wings of the distribution, as is discussed in detail in Ref. 9.

We conclude by noting that the Gaussian approximation might lead to insight into questions such as the existence of a lower bound of $\Delta\varphi$ for a given fixed number of photons $\langle m\rangle$. For that purpose we would like all the probability to reside in the peak, that is, $A_{Gauss}=1$. From Eq. (2.5), we find

$$W_{\varphi=0} = \pi^{-1/2}\,\Delta\varphi^{-1}$$

which, when substituted into Eq. (2.4b), yields

$$\Delta\varphi^3 = \frac{2}{\sqrt{\pi}}\,\left|W''_{\varphi=0}\right|^{-1} = 2\sqrt{\pi}\;\mathcal{K}^{-2}\left[\left(\sum_{m=0}^{\infty}m^2\,\psi_m\right)\left(\sum_{m=0}^{\infty}\psi_m\right)-\left(\sum_{m=0}^{\infty}m\,\psi_m\right)^2\right]^{-1}$$

$$= 4\sqrt{\pi}\;\mathcal{K}^{-2}\left[\sum_{m,n=0}^{\infty}(m-n)^2\,\psi_m\psi_n\right]^{-1} .$$

(4.1)

Two strategies offer themselves: (i) Use appropriate inequalities to rewrite the expression in square brackets in Eq. (4.1) in terms of the average number of photons and its variance. This might lead to a lower bound of $\Delta\varphi$. (ii) Minimize $\Delta\varphi^3$, that is, maximize the expression in square brackets, Eq. (4.1), under the constraint of constant $\langle m\rangle$ and phase state normalized to unity.

REFERENCES

1. Caves, C. M., 1981, "Quantum-mechanical noise in an interferometer," *Phys. Rev. D*, 23 (8), p. 1693.

2. Shapiro, J. H., Shepard, S. R., and Wong, N., 1989, "Ultimate Quantum Limits on Phase Measurement," *Phys. Rev. Lett.*, 62 (20), p. 2377; Shapiro, J. H. and Shepard,

S. R., 1991, "Quantum phase measurement: A system-theory perspective," *Phys. Rev. D*, 43 (7), p. 3795; for a detailed discussion of related problems, see the articles: Shapiro, J. H., Shepard, S. R., and Wong, N., 1989, "A New Number-Phase Uncertainty Principle" and "Coherent Phase States and Squeezed Phase States," in *Quantum Optics VI*, J. H. Eberly, L. Mandel, and E. Wolf, eds., Plenum, New York, p. 1071 and 1077; Shapiro, J. H., "Going Through a Quantum Phase," *Workshop on Squeezed States and Uncertainty Relations*, NASA CP-____ , 1991. (Paper ____ of this compilation).

3. Summy, G. S. and Pegg, D. T., 1990, "Phase Optimized Quantum States of Light," *Opt. Commun.* 77 (1), p. 75.

4. Bandilla, A. and Paul, H., 1969, "Laser-Verstärker und Phasenunschärfe," *Ann. Phys.* (Leipzig), 23 (7), p. 323; Paul, H., 1966, "Ein Beitrag Zur Quantentheorie der Optischen Kohärenz," *Fortschr. Phys.*, 14, p. 141.

5. Bandilla, A., Paul, H., and Ritze, W. R., "Realistic Quantum States of Light with Minimum Phase Uncertainty," to be published.

6. For a review, see: Pegg, D. and Barnett, S., 1986, "Phase in quantum optics," *J. Phys. A*, 19, p. 3849.

7. Schleich, W., Horowicz, R. J., and Varro, S., 1989, "Bifurcation in the phase probability distribution of a highly squeezed state," *Phys. Rev. A*, 40 (12), p. 7405; also, 1989, "A Bifurcation in Squeezed State Physics: But How?" in *Quantum Optics V*, D. F. Walls and J. Harvey, eds., Springer, Heidelberg; Schleich, W. P., Dowling, J. P., Horowicz, R. J., and Varro, S., 1990, "Asymptotology in Quantum Optics," in *New Frontiers in QED and Quantum Optics*, A. O. Barut, ed., Plenum Press, New York.

8. The phase distribution resulting from the newly proposed phase operator [Pegg, D.T. and Barnett, S. M., 1988, "Unitary Phase Operator in Quantum Mechanics," *Europhys. Lett.*, 6 (6), p. 483; 1989, "Phase properties of the quantized single-mode electromagnetic field," *Phys. Rev. A*, 39 (4), p. 1665.] yields results identical to those obtained from semiclassical quantum mechanics, as in Ref. 7.

9. Schleich, W. P., Dowling, J. P. and Horowicz, R. J., 1991, "Exponential decrease in phase uncertainty," *Phys. Rev. A*, to be published.

10. Similar results have been reported by Caves, C. M., Lane, A. S., and Braunstein, S. L., "Maximum-Likelihood Statistics of Multiple Quantum Phase Measurements," *Workshop on Squeezed States and Uncertainty Relations*, NASA CP-_____, 1991. (Paper ____ of this compilation). Moreover, simulations of a sequence of phase measurements based on the scheme of Ref. 2 have been reported by, Caves, C. M., Lane, A. S., and Braunstein, A. S., 1991, "Maximum-likelihood Statistics of Multiple Phase Measurements," *Proceedings of NATO Advanced Research Workshop on Quantum Measurements in Optics*, Cortina d'Ampezzo, 1991, P. Tombesi and D. F. Walls, eds., Plenum Press, New York.

11. Hansen, E. R., 1975, *A Table of Series and Products*, Prentice-Hall, Englewood Cliffs.

12. Magnus, W., Oberhettinger, F., and Soni, R. P., 1966, *Formulas and Theorems for the Special Functions*, Springer Verlag, Heidelberg.

Table 1. Gaussian approximation $W_\varphi = W_{\varphi=0} \exp[-(\varphi/\Delta\varphi)^2]$ for dominant maximum of the phase distribution $W_\varphi = (2\pi)^{-1} \mathcal{N}^2 \left| \Sigma_{m=0}^{\infty} \psi_m \exp(im\varphi) \right|^2$ for a coherent state $|\psi_{coh}\rangle$, a truncated phase state $|\psi_p\rangle$ and an optimal phase state $|\psi_s\rangle$.

	Coherent State	Truncated Phase State	Optimal Phase State
Width = $\Delta\varphi$	$2^{-1/2} \langle m\rangle^{-1/2}$	$\sqrt{3} \langle m\rangle^{-1}$	$(\gamma\pi/\sqrt{3}) \langle m+1\rangle^{1/2} \exp[-\pi^2 \langle m+1\rangle/6]$
Maximum = $W_{\varphi=0}$	$\sqrt{2/\pi} \langle m\rangle^{1/2}$	$\pi^{-1} \langle m\rangle$	$\dfrac{\pi}{12} \langle m+1\rangle^2$
Area = $\sqrt{4} \, \Delta\varphi \, W_{\varphi=0}$	1	$\sqrt{3/\pi} = 0.98$	$\dfrac{\pi}{12}^{5/2} \dfrac{\gamma}{\sqrt{3}} \langle m+1\rangle^{5/2} \exp[-\pi^2 \langle m+1\rangle/6]$ $\rightarrow 0$ $(m \rightarrow \infty)$

IDEAL PHOTON NUMBER AMPLIFIER AND DUPLICATOR

G. M. D'Ariano

Dipartimento di Fisica 'Alessandro Volta', via Bassi 6, I-27100 Pavia, Italy

ABSTRACT: The photon number-amplification and number-duplication mechanisms are analyzed in the ideal case. The search for unitary evolutions leads to consider also a number-deamplification mechanism, the symmetry between amplification and deamplification being broken by the integer-valued nature of the number operator. Both transformations—amplification and duplication—need an auxiliary field which, in the case of amplification, turns out to be amplified in the inverse way. Input-output energy conservation is accounted for using a classical pump or through frequency-conversion of the fields. Ignoring one of the fields is equivalent to consider the amplifier as an open system involving entropy production. The Hamiltonians of the ideal devices are given and compared with those of realistic systems.

1. INTRODUCTION

Squeezing and amplification are two intimately related concepts. A scaling of the quantum fluctuations $\langle \Delta \hat{O}^2 \rangle \rightarrow G^2 \langle \Delta \hat{O}^2 \rangle$, independently on the state of the field, corresponds to the amplification of the fluctuating observable $\hat{O} \rightarrow G\hat{O}$. Such kind of ideal quantum amplification rescales all the moments of $\hat{O}$ simultaneously, leaving the signal-to-noise ratio (SNR) unchanged when detecting $\hat{O}$.

Ideal quantum amplifiers are key-devices in quantum optical applications, where, depending on the particular circumstances, one would possibly change the levels of both signal and fluctuations without degrading the SNR. For example, in local-area network (LAN) communications, strongly subpoissonian fields with limited average number of photons are needed to exploit the ultimate channel capacity of the field (which is constrained in the total power and the bandwidth). On the other hand, a large signal is preferred just before the detection stage, in order to minimize all the subsequent sources of disturbance. In both cases an ideal photon number-amplifier ($\hat{O} \equiv \hat{n}$) would allow to change signal and fluctuations as desired, leading to significant improvements of the network performance.

Another point which should be considered in any quantum amplification process is the role played by the Heisenberg principle in defining the ideal behaviour of the amplifier. In fact, the amplification of the observable $\hat{O}$ affects the statistics of the observables which do not commute with $\hat{O}$. For a couple of conjugated variables $(\hat{O}_1, \hat{O}_2)$, analogous to the momentum and the

PRECEDING PAGE BLANK NOT FILMED

position of a particle, the quantum fluctuations are constrained by the uncertainty relation

$$\langle \Delta \hat{O}_1^2 \rangle \langle \Delta \hat{O}_2^2 \rangle \geq \frac{1}{4} \langle [\hat{O}_1, \hat{O}_2] \rangle^2 \, , \tag{1}$$

according to which, when the $\hat{O}_1$ fluctuations are rescaled as $\langle \Delta \hat{O}_1^2 \rangle \rightarrow G^2 \langle \Delta \hat{O}_1^2 \rangle$, the corresponding $\hat{O}_2$ fluctuations become $G^{-2} \langle \Delta \hat{O}_2^2 \rangle$ or larger. An ideal $\hat{O}_1$ amplifier, namely an amplifier performing at best, should preserve the minimum uncertainty product and, as a consequence, it should simultaneously attain the two opposite amplifications

$$\hat{O}_1 \rightarrow G\hat{O}_1 \, , \quad \hat{O}_2 \rightarrow G^{-1}\hat{O}_2 \, . \tag{2}$$

Depending on the conjugated pair $(\hat{O}_1, \hat{O}_2)$ one has different kind of amplifiers and related different kind of squeezing. For example, when the conjugated variables are two quadrature of a field mode $(\hat{a}_1, \hat{a}_2)$—$\hat{a}_1 + i\hat{a}_2 = a$ being the annihilation operator—the rescaling (2) defines the phase sensitive linear amplifier (PSA). The ideal PSA (essentially a parametric amplifier) preserves the homodyne SNR$= \langle \hat{a}_1 \rangle / \sqrt{\langle \Delta \hat{a}_1^2 \rangle}$ and produces the squeezing in a quadrature of the field. In this case the transformation (2) is realized by the Yuen's[1] unitary evolution $\hat{U}^\dagger a \hat{U} = \mu a + \nu a^\dagger$, with $\mu = (G + G^{-1})/2$ and $\nu = (G - G^{-1})/2$, $\hat{U}$ representing the usual squeezing operator.

The photon number-amplifier (PNA) is another example of ideal amplifier, which would transform ideally $\hat{n}$ into $G\hat{n}$, preserving the direct detection SNR and the number-phase uncertainty product. The corresponding kind of squeezing is the number-phase squeezing[2] (or amplitude squeezing), in which the quantum noise is shared between the number $\hat{n}$ and the phase $\hat{\Phi}$. This kind of amplifier is a relatively new concept and is probably not simple to realize concretely: it has been proposed by Yuen[3-5], who also suggested physically viable approximate schemes based on resonance fluorescence. PNA's would be particularly useful in direct-detection receiver and transceiver in a LAN environment, where, as already mentioned, number states are preferred to coherent or squeezed states, in order to achieve the ultimate channel capacity of the field. Furthermore, a PNA (but also a PSA) can be used to realize a lossless optical tap, which, in a LAN would enable a very large number of users to obtain the same performance as the first user.[6]

In this paper the number-phase amplification mechanism is analyzed in detail, in order to find physical schemes for an ideal PNA. It is shown that, due to the peculiar role of the two conjugated variables $(\hat{n}, \hat{\Phi})$ in the Fock representation, the requirement of a unitary transformation leads to consider a second field in addition to the amplified one, the two fields being inversely amplified by the transformation. Input-output energy conservation can be accounted for either by adding a suited classical pump or by locking the frequencies of the two fields, attaining simultaneously number-amplification and frequency-conversion. The obvious constraint of integer gain G (preserving the integer-valued nature of $\hat{n}$) must be relaxed, to consider the deamplification case: as a consequence, the abstract amplifying transformation $|n\rangle \rightarrow |Gn\rangle$ is replaced by $|n\rangle \rightarrow |[Gn] + n_0\rangle$, $[x]$ denoting the integer part of x, and n_0 being a constant as a function of n and depending on the input state of the other field. The general Schrödinger evolution of the two fields is

$$\hat{U}_{(G^{-1})}|n, m\rangle = |[Gn] + G\langle G^{-1}m\rangle, [G^{-1}m] + G^{-1}\langle Gn\rangle\rangle \, , \tag{3}$$

$\langle x \rangle = x - [x]$ denoting the fractional part of x and the gain G being restricted to be either integer or the inverse of an integer. Eq.(3) can be attained by means of a unitary transformation involving a classical pump operating at the frequency $\Omega = G^{-1}\omega_a - \omega_b$, ω_a and ω_b being the frequencies of the G-amplified and G-deamplified fields respectively. In the case of simultaneous amplification/frequency-conversion one has the resonance condition $\omega_b = G^{-1}\omega_a$, and the two fields are intertwined in (3) in order to preserve the total input energy $E = (n + G^{-1}m)\omega_a$.

In Sect.2 I derive the transformation (3) and the related Hamiltonian. Apart from the eventual classical pump, the ideal PNA in the present framework is a four-port nonlinear device (see Fig.1). However, it can be regarded as a two port device by fixing one input port state (for example,
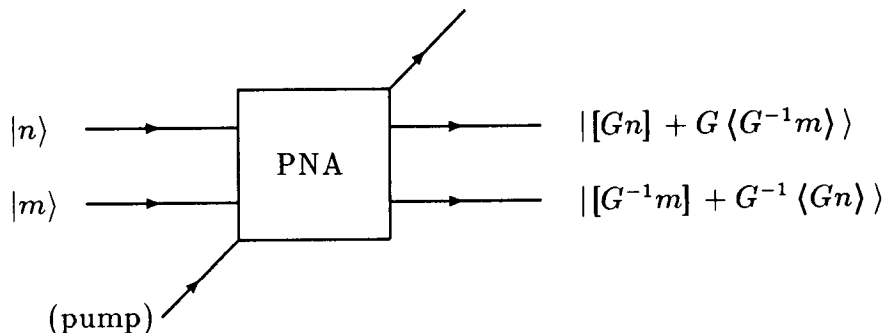
Figure 1: Scheme of the ideal PNA.

using the vacuum) or by totally ignoring one field. In the last case the PNA should be regarded as an open quantum system which changes the entropy of the input state of the field: the particular case of coherent inputs will be examined in this respect.

In Sect.3 another device analogous to the PNA is analyzed, namely the ideal photon number-duplicator (PND). Instead of amplifying the number of photons, the ideal PND produces two copies of the same input state for eigenstates of the number operator. Such a device would be extremely useful in LAN applications, because it provides a convenient realization of the quantum nondemolition measurement of the photon number, beside itself realizing lossless optical taps superior to the amplifier tap[6] (both applications make possible sharing of information in a LAN). Arguments related to unitarity—similar to those used for the ideal PNA—lead to the need of a third auxiliary field, whereas input-output energy conservation can be taken into account either by means of a classical pump or through frequency-conversion, in a way completely analogous to the case of the ideal PNA.

In the last section I make some preliminary comparisons between the Hamiltonians of the ideal devices and those of realistic systems, focusing attention on the gain-2 amplifier, in some respects very similar to the duplicating device.

2. IDEAL PHOTON NUMBER-AMPLIFIER

2.1 *The unitary transformation*
In the Heisenberg picture the ideal PNA corresponds to a multiplication of the number operator $\hat{n}$ by the amplification factor G

$$\hat{n} \longrightarrow G\hat{n} . \tag{4}$$

The requirement of an ideal—i.e. minimum-uncertainty preserving—behaviour reflects on the Heisenberg transformations for the phase operator $\hat{\Phi}$, which should be the inverse of (4), namely

$$\hat{\Phi} \longrightarrow G^{-1}\hat{\Phi} \, . \tag{5}$$

For highly excited states (i.e. states approximately orthogonal to the vacuum $|0\rangle$) and for small phase uncertainties $\langle\Delta\hat{\Phi}^2\rangle \ll 1$ the following simple definition for the phase can be adopted[7]

$$\hat{E}_{\pm} = e^{\mp i\hat{\Phi}} \, , \tag{6}$$

$\hat{E}_{\pm}$ denoting the shift operators $\hat{E}_- = (a^{\dagger}a + 1)^{-1/2}a$, $\hat{E}_+ = (\hat{E}_-)^{\dagger}$ ($\hat{E}_{\pm}|n\rangle = |n \pm 1\rangle$). Eq.(6) shows how the integer-valued nature of $\hat{n}$ reflects on the phase operator $\hat{\Phi}$: the amplification (5) can simply be attained for $G^{-1} = r$ integer, raising the shift operators to the power r, whereas, for the number operator, preservation of its integer-valued nature requires G itself to be integer. For noninteger G, the transformation (4) can be substituted with the following

$$\hat{n} \longrightarrow [G\hat{n}] \, , \tag{7}$$

which coincides with (4) for integer G. For the moment, I focus attention on the deamplification case ($G^{-1} = r$ integer), the integer-G case being naturally contained in the following framework.

Denoting by $\mathcal{S}_H^{(r)}$ the Heisenberg transformation corresponding to Eqs.(7) and (5), for integer $G^{-1} = r$ one has

$$\mathcal{S}_H^{(r)}(\hat{E}_{\pm}) = (\hat{E}_{\pm})^r \, , \tag{8}$$

$(\hat{E}_{\pm})^r$ now being represented on the Fock space as follows:

$$(\hat{E}_{\pm})^r|n\rangle = |n \pm r\rangle \, . \tag{9}$$

From Eqs.(8) and (9) it turns out that the $\mathcal{S}_H^{(r)}$ acting on a generic operator $\hat{O}$ has the general form

$$\mathcal{S}_H^{(r)}(\hat{O}) = \sum_{\lambda=0}^{r-1}(\hat{S}_{\lambda}^{(r)})^{\dagger}\hat{O}\hat{S}_{\lambda}^{(r)} \, , \quad \hat{S}_{\lambda}^{(r)} = e^{i\phi_{\lambda}}\sum_{n=0}^{\infty}|n\rangle\langle nr + \lambda| \, , \tag{10}$$

and the phase factors, being totally ineffective in the action (10), will be dropped in the following. One can check that the Heisenberg transformation (8) attains the number-amplification (7)

$$\mathcal{S}_H^{(r)}(\hat{n}) = [\hat{n}/r] \, , \tag{11}$$

and, formally, $\mathcal{S}_H^{(r)}$ achieves the phase amplification (5) according to Eq.(6). The transformation (8) is not unitary and, as a consequence, there is no Hamiltonian producing it. The operators $\hat{S}_{\lambda}^{(r)}$ in the definition of the map (10) satisfy the following relations

$$\sum_{\lambda=0}^{r-1}(\hat{S}_{\lambda}^{(r)})^{\dagger}\hat{S}_{\lambda}^{(r)} = 1 \, , \tag{12}$$

$$\hat{S}_{\lambda}^{(r)}(\hat{S}_{\mu}^{(r)})^{\dagger} = \delta_{\lambda\mu} \, , \tag{13}$$

$$\hat{S}_{\lambda}^{(r)}\hat{S}_{\mu}^{(s)} = \hat{S}_{\lambda s + \mu}^{(rs)} \, . \tag{14}$$

Despite the map $\mathcal{S}_H^{(r)}$ is not unitary, the completeness relation (12) and the orthogonality conditions (13) allow one to recover a unitary evolution on an enlarged quantum system. I postpone for the moment the construction of the corresponding unitary evolution and the related Hamiltonians, to continue the discussion on the properties of the map.

Eq.(14) leads to semigroup composition of the maps $\mathcal{S}_H^{(r)}$

$$\mathcal{S}_H^{(r)}\mathcal{S}_H^{(s)} = \mathcal{S}_H^{(rs)} \tag{15}$$

corresponding to the amplification of PNA's in series. On the other hand, as a consequence of the completeness and orthogonality relations (12) and (13), $\mathcal{S}_H^{(r)}$ preserves the operator products and the adjoint operation, thus transforming consistently the whole operator algebra. When applied on the particle operator a the transformation $\mathcal{S}_H^{(r)}$ gives the result

$$\mathcal{S}_H^{(r)}(a) = \sum_{n=1}^\infty |n-1\rangle\sqrt{[n/r]}\langle n| = \left[\frac{(1+[\hat{n}/r])\hat{n}!}{(\hat{n}+r)!}\right]^{1/2} a^r \equiv a_{(r)} , \tag{16}$$

and for the creation operator one has $\mathcal{S}_H^{(r)}(a^\dagger) = a_{(r)}^\dagger$. Eq.(16) shows that the transformed particle operator $\mathcal{S}_H^{(r)}(a)$ coincides with the r-boson operator $a_{(r)}$ introduced by Brandt and Greenberg:[10] $a_{(r)}$ and $a_{(r)}^\dagger$ annihilate and create r photons simultaneously and satisfy the commutation relations $[a_{(r)}, a_{(r)}^\dagger] = 1$, $[\hat{n}, a_{(r)}] = -ra_{(r)}$. The preservation of the operator product implies that the transformation $\mathcal{S}_H^{(r)}$ applied to a generic operator $\hat{O} = \hat{O}(a, a^\dagger)$ (Hermitian analytic function of a and $a^\dagger$) can simply be obtained substituting a and $a^\dagger$ with $a_{(r)}$ and $a_{(r)}^\dagger$, i.e. $\mathcal{S}_H^{(r)}(\hat{O}) = \hat{O}(a_{(r)}, a_{(r)}^\dagger)$. Therefore, $\mathcal{S}_H^{(r)}$ corresponds to the construction of the r-photon observables of D'Ariano.[11,12]

The completeness and orthogonality relations (12) and (13) are preserved by similarity transformations

$$\hat{S}_\lambda^{(r)\prime} = \hat{V}\hat{S}_\lambda^{(r)}\hat{W} , \tag{17}$$

$\hat{V}$ and $\hat{W}$ being unitary operators. A general transformation (17), however, would destroy, the ideal behaviour of the PNA: the only similarity transformations which preserve the Heisenberg evolutions (7) and (5) are the permutations of the λ's

$$\hat{S}_\lambda^{(r)\prime} = \hat{P}\hat{S}_\lambda^{(r)} = \hat{S}_{P(\lambda)}^{(r)} , \tag{18}$$

where $\hat{P}$ denotes the operator representing a permutation of the λ's, namely $\hat{P}|nr + \lambda\rangle = |nr + P(\lambda)\rangle$.

I return now to the construction of the unitary evolution corresponding to $\mathcal{S}_H^{(r)}$. From the definition (10) and the completeness relation (12) it follows that $\mathcal{S}_H^{(r)}$ is a *completely positive map* (shortly CP map):[8,9] this is physically relevant, because the subdynamics of the open systems are CP maps, the set of CP maps being closed under partial trace. Here I recall that a unit-preserving CP map has the general form $\mathcal{T}(\hat{O}) = \sum_\alpha \hat{V}_\alpha^\dagger \hat{O}\hat{V}_\alpha$, where $\sum_\alpha \hat{V}_\alpha^\dagger \hat{V}_\alpha = 1$. The space of the unit-preserving CP maps is closed under: i) convex combination $\sum_i p_i \mathcal{T}_i$; ii) composition $\mathcal{T}_1\mathcal{T}_2$; iii) tensor product $\mathcal{T}_1 \otimes \mathcal{T}_2$; iv) partial trace: namely, if $\mathcal{T}$ is CP on $\mathcal{F}_1 \otimes \mathcal{F}_2$ and $\hat{\mu}$ is a

density operator on $\mathcal{F}_2$, then $\mathcal{T}_1(\hat{O}) = \text{Tr}_2[\hat{\mu}\mathcal{T}(\hat{O} \otimes \hat{1})]$ is CP on $\mathcal{F}_1$. The last point means that if we have a unitary evolution in a closed system and if subdynamics on a (open) subsystem can be defined—i.e. partial trace on the subsystem degrees of freedom—then these subdynamics are CP maps. However, the converse is not true in general (namely not every CP map corresponds to a unitary evolution on an enlarged system) and the additional orthogonality constraints (13) are essential in guaranteeing also the converse assertion.

The unitary evolution corresponding to $\mathcal{S}_H^{(r)}$ can be constructed by using two different photon fields in the amplification process and considering the following operator $\hat{U}_{(r)}$ acting on the Fock space of the composite system $\mathcal{F} \otimes \mathcal{F}$

$$\hat{U}_{(r)} = \sum_{\lambda=0}^{r-1} \hat{S}_\lambda^{(r)} \otimes (\hat{R}_\lambda^{(r)})^\dagger \, , \tag{19}$$

where $\hat{R}_\lambda^{(r)}$ are similar to $\hat{S}_\lambda^{(r)}$ in the sense of Eq.(17). $\hat{U}_{(r)}$-unitarity follows from Eqs.(12), (13) and (17). The subdynamics of the first photon field correspond to $\mathcal{S}_H^{(r)}$:

$$\langle \hat{U}_{(r)}^\dagger \hat{O}_1 \hat{U}_{(r)} \rangle = \text{Tr}\left[(\hat{\rho}_1 \otimes \hat{\rho}_2)\hat{U}_{(r)}^\dagger(\hat{O}_1 \otimes \hat{1})\hat{U}_{(r)}\right] = \text{Tr}_1\left[\hat{\rho}_1 \mathcal{S}_H^{(r)}(\hat{O}_1)\right] \, , \tag{20}$$

where the uncorrelated pair of states $(\hat{\rho}_1 \otimes \hat{\rho}_2)$ has been considered as the input of the amplifier. The semigroup property (14) reflects on the composition law for the operators $\hat{U}_{(r)}$

$$\hat{U}_{(r)}\hat{U}_{(s)} \simeq_P \hat{U}_{(rs)} \, , \tag{21}$$

the symbol $\simeq_P$ denoting similarity under permutations (18).

Among all operators $\hat{U}_{(r)}$ the case of $\hat{R}_\lambda^{(r)} = \hat{S}_\lambda^{(r)}$ is particularly interesting, because the second field undergoes the transposed transformation of $\mathcal{S}_H^{(r)}$

$$\hat{U}_{(r)} = \sum_{\lambda=0}^{r-1} \hat{S}_\lambda^{(r)} \otimes (\hat{S}_\lambda^{(r)})^\dagger \, . \tag{22}$$

One should notice, however, that $\langle \hat{U}_{(r)}^\dagger \hat{O}_2 \hat{U}_{(r)} \rangle$ depends on the first input state $\hat{\rho}_1$ in general. In fact, the action of the operator $\hat{U}_{(r)}$ in Eq.(22) on a number eigenstate is

$$\hat{U}_{(r)}|n, m\rangle = |[n/r], mr + \langle n/r \rangle\rangle \, , \tag{23}$$

and the second field undergoes an exact number-amplification only if the first field is in a r-photon state, (namely it contains only number of photons multiple of r), in particular if it is in the vacuum state. Eq.(23) can be rewritten in the following more symmetrical form

$$\hat{U}_{(G^{-1})}|n, m\rangle = |[Gn] + G\langle G^{-1}m \rangle, [G^{-1}m] + G^{-1}\langle Gn \rangle\rangle \, , \tag{24}$$

which coincides with Eq.(23) for $G^{-1} = r$ integer, whereas, for G integer, corresponds to (23) but with the roles of the two fields interchanged, as a consequence of the identity $\hat{U}_{(G)}^\dagger = \hat{U}_{(G)}^{-1} = \hat{U}_{(G^{-1})}$ (notice that Eq.(24) leads to integer valued number of photons only if either G or G^{-1} is integer).

2.2 *The Hamiltonian*

I consider the operator $\hat{U}_{(G^{-1})}$ in Eq.(23) only for the case $G^{-1} = r$ integer, the integer-G case $\hat{U}_{(G)}$ corresponding to the inverse operator $\hat{U}^{\dagger}_{(G^{-1})}$. I denote by $a^{\dagger}$ and $b^{\dagger}$ the particle operators of the two fields, namely

$$|n, m\rangle = \frac{(a^{\dagger})^n}{\sqrt{n!}} \frac{(b^{\dagger})^m}{\sqrt{m!}} |0, 0\rangle . \tag{25}$$

Comparing the transformation (24) with the action of the multiboson operator of Eq. (16)

$$a^{\dagger}_{(r)}|n\rangle = \sqrt{[n/r] + 1}|n + r\rangle , \tag{26}$$

one can see that the ideal amplification (23) can be attained by interchanging $a^{\dagger}$ with $b^{\dagger}_{(r)}$ and then permuting $a^{\dagger}$ with $b^{\dagger}$ modes. The operator permuting $a^{\dagger}$ and $b^{\dagger}$ (apart from a sign) has the form

$$\hat{V} = \exp\left[\frac{\pi}{2}\left(a^{\dagger}b - b^{\dagger}a\right)\right] \tag{27}$$

and, as a consequence, the operator $\hat{U}_{(r)}$ is given by

$$\hat{U}_{(r)} = \exp\left[\frac{\pi}{2}\left(a^{\dagger}b - b^{\dagger}a\right)\right] \exp\left[-\frac{\pi}{2}\left(a^{\dagger}_{(r)}b - b^{\dagger}a_{(r)}\right)\right] . \tag{28}$$

The representation (23) of the operator $\hat{U}_{(r)}$ in Eq. (28) can directly be checked using Eqs.(25) and (26). From Eq.(28) one can see that, apart from a permutation of the form (27) (which could be attained by means of beam splitters), the ideal PNA is described by an interaction Hamiltonian in the Dirac picture

$$\hat{H}^D_I = -ik\left(a^{\dagger}_{(r)}b - b^{\dagger}a_{(r)}\right) , \tag{29}$$

and an interaction length L given by

$$kL = \frac{\pi}{2} , \tag{30}$$

k being the interaction coupling per unit length. Using Eq.(16) the Hamiltonian (29) can be rewritten in terms of the a and b particle operators

$$\hat{H}^D_I = -ik\left((a^{\dagger})^r f_{(r)}(a^{\dagger}a)b - b^{\dagger}f_{(r)}(a^{\dagger}a)a^r\right) , \tag{31}$$

$$f_{(r)}(a^{\dagger}a) = \left[\frac{1 + [a^{\dagger}a/r]}{(a^{\dagger}a + 1)\ldots(a^{\dagger}a + r)}\right]^{1/2} .$$

Regarding the energy conservation during the amplification process, one can now thinks to the four-port device as a globally inelastic process in the time domain (Dirac picture), with the free Hamiltonian

$$\hat{H}_0 = \omega_a a^{\dagger}a + \omega_b b^{\dagger}b . \tag{32}$$

317

The interaction Hamiltonian $\hat{H}_I^p$ has the form (29) when in the Schrödinger picture reads

$$\hat{H}_I = -ik\left(a_{(r)}^\dagger b e^{-i\Omega t} - b^\dagger a_{(r)} e^{i\Omega t}\right) \tag{33}$$

with $\Omega = r\omega_a - \omega_b$. As for the usual parametric frequency-converter the phase factor oscillating at frequency Ω can be attained by considering an additional classical (i.e. highly excited) pumping field. On the other hand, also the first permuting operator in (28) requires a classical pump (at frequency $\Omega' = \omega_a - \omega_b$) and it can be attained by means of beam splitters if $\omega_a = \omega_b$, otherwise it corresponds to a parametric frequency-converter.

The case $\omega_b = r\omega_a$ requires no pump at the second step in (28). In this case, the second operator in (28) can be reviewed as a PNA/frequency-converter (PNAFC) described by the equations

$$|n\rangle \rightarrow \left|[G^{-1}m] + G^{-1}\langle Gn\rangle\right\rangle, \qquad (\omega = \omega_a),$$

$$\tag{34}$$

$$|m\rangle \rightarrow \left|[Gn] + G\langle G^{-1}m\rangle\right\rangle, \qquad (\omega = \omega_b = r\omega_a),$$

The PNAFC conserves the total input-output energy $E = (n + rm)\omega_a$, as it follows from Eq.(34). On the other hand, for $\omega_b = r\omega_a$ the first permuting operator in Eq.(28) needs a pump at frequency $\Omega' = (r-1)\omega_a$ and represents now a parametric frequency-converter (FC) intertwining the two amplified modes. In this fashion the ideal PNA can be viewed as the cascade of an ideal PNAFC (an energy preserving four-port device) followed by an ideal FC (a four port device with pump).

2.3 *The PNA as an open system: the amplification entropy*

In practical applications it is useful to consider the ideal PNA as a two-port device, actually ignoring not only the pumping field, but also one of the two amplified fields. This description is equivalent to consider the PNA as an open quantum system, which no longer preserves both the energy and the entropy of the input field. However, the amplification and the deamplification cases now become quite different. This follows from the unitary transformation (24) where, despite the apparent symmetrical roles of the two fields, the state of the amplified one depends on the state of the other, whereas the deamplified field is always independent on the amplified one. This strange unilateral dependence is due to the integer-valued nature of $\hat{n}$, that breaks the symmetry between amplification and deamplification. In the following I examine the two cases separately.

The number-amplification—ignoring the deamplified field—corresponds to the partial trace

$$\langle \hat{O}_2 \rangle = \text{Tr}\left[(\hat{\rho}_1 \otimes \hat{\rho}_2)\hat{U}_{(r)}^\dagger(\hat{1} \otimes \hat{O}_2)\hat{U}_{(r)}\right] = \text{Tr}_2\left(\hat{\rho}_2 \sum_{\lambda=0}^{r-1} (\hat{V}_\lambda^{(r)})^\dagger \hat{O}_2 \hat{V}_\lambda^{(r)}\right), \tag{35}$$

where

$$\hat{V}_\lambda^{(r)} = \left\{\text{Tr}_1\left[\hat{\rho}_1(\hat{S}_\lambda^{(r)})^\dagger \hat{S}_\lambda^{(r)}\right]\right\}^{1/2} (\hat{S}_\lambda^{(r)})^\dagger. \tag{36}$$

Therefore, the amplification corresponds to the CP map

$$\mathcal{S}_H^{(1/r)}(\hat{O}) = \sum_{\lambda=0}^{r-1} (\hat{V}_\lambda^{(r)})^\dagger \hat{O} \hat{V}_\lambda^{(r)}, \tag{37}$$

which, due to the form of operators $\hat{V}_\lambda^{(r)}$ in Eq.(36), depends on the state $\hat{\rho}_1$ of the other field, (namely on the 'temperature' of the PNA). The case of $\hat{\rho}_1$ equal to the vacuum state ('zero temperature') is particularly simple

$$\mathcal{S}_H^{(1/r)}(\hat{O}) = (\hat{V}_0^{(r)})^\dagger \hat{O} \hat{V}_0^{(r)} , \quad \hat{V}_0^{(r)} \equiv (\hat{S}_0^{(r)})^\dagger = \sum_{n=0}^{\infty} |rn\rangle\langle n| , \tag{38}$$

and corresponds to the exact number-amplification

$$\mathcal{S}_H^{(1/r)}(f(\hat{n})) = f(r\hat{n}) . \tag{39}$$

In the Schrödinger picture one has

$$\mathcal{S}_S^{(1/r)}(\hat{\rho}) = \hat{V}_0^{(r)} \hat{\rho} (\hat{V}_0^{(r)})^\dagger . \tag{40}$$

Despite the evolution (40) is not unitary (it is only an isometry), it preserves the Newmann-Shannon entropy

$$S(\hat{\rho}) = -\mathrm{Tr}\hat{\rho}\log\hat{\rho} . \tag{41}$$

The entropy conservation follows from the orthogonality conditions (13) which imply that $(\hat{V}_0^{(r)})^\dagger \hat{V}_0^{(r)} = 1$ (but $\hat{V}_0^{(r)}(\hat{V}_0^{(r)})^\dagger \neq 1$). Thus, the physical picture of the abstract number-amplification $|n\rangle \rightarrow |rn\rangle$ corresponds to an ideal PNA operating with the auxiliary field in the vacuum (namely a PNA at zero temperature). As long as the number-amplification is attained exactly, no entropy change of the field occurs.
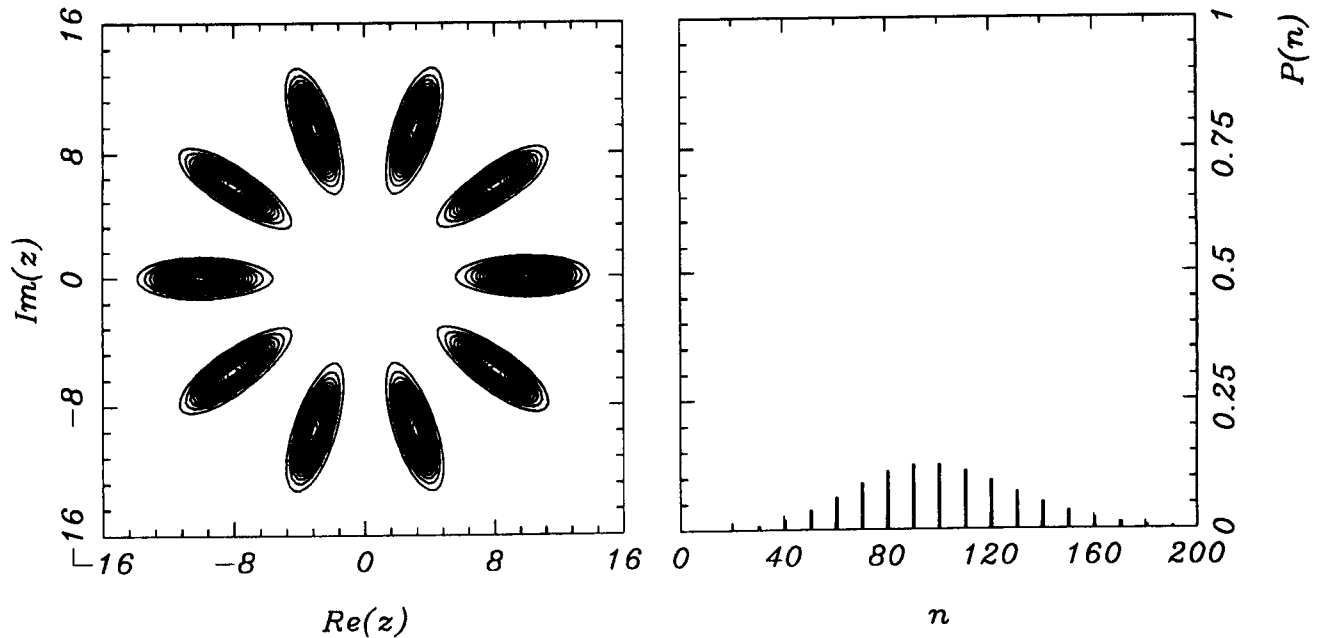

Figure 2: Q-function and number distribution of a coherent state having $\langle \hat{n} \rangle = 10$ photons after number-amplification with $G = 10$. The final moments are $\langle \hat{n} \rangle = 100$ and $\langle \Delta \hat{n}^2 \rangle^{1/2} = 31.52$.

319

In Fig.2 the effect of exact number-amplification on an input coherent state is illustrated in both the Q-function and number representations. The amplified coherent state

$$|\alpha\rangle_{(r)} = e^{-\frac{1}{2}|\alpha|^2} \sum_{n=0}^{\infty} \frac{\alpha^n}{\sqrt{n!}} |rn\rangle \qquad (42)$$

has a Poisson distribution of multiples of r photons. In the phase space the exact number-amplification corresponds to a symmetrical split of the quantum distribution into r identical replicas having fluctuations enhanced in the number and reduced in the phase (the quantum distribution becomes longer in the radial direction and narrower in the tangential one).

I now examine the case of number-deamplification. Ignoring the amplified field corresponds to the partial trace

$$\langle \hat{O}_1 \rangle = \mathrm{Tr} \left[(\hat{\rho}_1 \otimes \hat{\rho}_2) \hat{U}_{(r)}^{\dagger} (\hat{O}_1 \otimes \hat{1}) \hat{U}_{(r)} \right] = \mathrm{Tr}_1 \left(\hat{\rho}_1 \sum_{\lambda=0}^{r-1} (\hat{S}_{\lambda}^{(r)})^{\dagger} \hat{O}_1 \hat{S}_{\lambda}^{(r)} \right) . \qquad (43)$$

The deamplification thus corresponds to the CP map (10)

$$\mathcal{S}_H^{(r)}(\hat{O}) = \sum_{\lambda=0}^{r-1} (\hat{S}_{\lambda}^{(r)})^{\dagger} \hat{O} \hat{S}_{\lambda}^{(r)} , \qquad (44)$$

and is totally independent on the state of the amplified field. In the Schrödinger picture one has

$$\mathcal{S}_S^{(r)}(\hat{\rho}) = \sum_{\lambda=0}^{r-1} \hat{S}_{\lambda}^{(r)} \hat{\rho} (\hat{S}_{\lambda}^{(r)})^{\dagger} , \qquad (45)$$

namely, the number-deamplification corresponds to an isometric evolution which does not preserve the entropy (41) in general. The entropy change depends only on the gain $G^{-1} = r$ and on the input state of the deamplified field (and not on the other field). It is worth noticing that the entropy during deamplification can either increase or decrease as a function of r. As the photon number-deamplification leads to the vacuum state for $r = G^{-1} \to \infty$, the entropy is asymptotically a decreasing function of r for large r. On the other hand, the evolution (45) would in general transform a pure state into a mixed one (the only state which are left pure being the number eigenstates and the r-photon states), and thus leads to an increase of entropy in this case. Therefore, when a pure state is number-deamplified, the entropy exhibits at least one maximum as a function of the inverse gain r. In Fig.3 the Newmann-Shannon entropy (41) is plotted as a function of r, for two different input coherent states. One can see that for small average number of input photons the entropy has only one maximum, whereas for intense input fields several maxima appear and local very low minima can occur (corresponding to almost pure states). As a rule, for coherent inputs the maxima are located approximately at $r \simeq |\alpha|^2/l$—$|\alpha|^2$ being the average number of input photons and $l = 1, 2, \ldots$—the maxima weakening for increasing l and the entropy S being always smaller than $\log 2$, which is the entropy of two pure states mixing.

In Fig.4 the Q-function and the number distribution of a strongly deamplified coherent state are reported, in order to illustrate the number-phase squeezing related to number-deamplification. In a fashion which is exactly the opposite of that depicted in Fig.2 the number-deamplification leads to spreading in the phase and narrowing in the number, thus converting highly excited
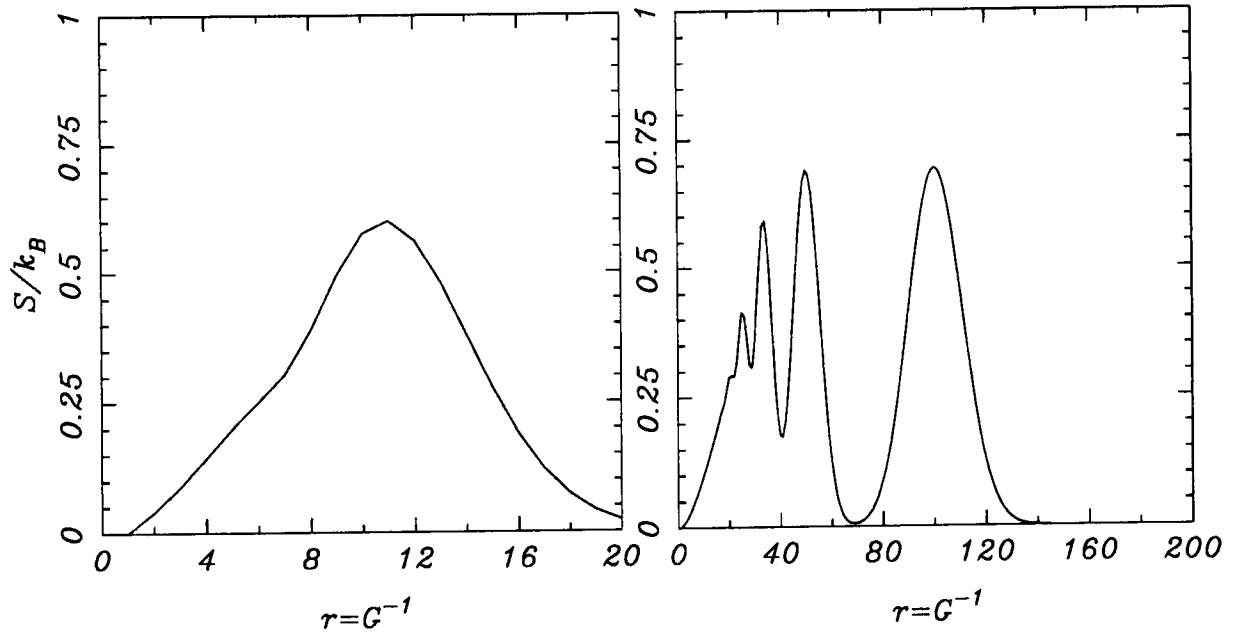
Figure 3: Deamplification Newmann-Shannon entropy versus the inverse gain $r = G^{-1}$ for a coherent state with $\langle \hat{n} \rangle = 10$ photons (figure on the left) and $\langle \hat{n} \rangle = 100$ photons.

states into nearly Fock states. Asymptotic evaluations[12] for $G \to 0$, keeping constant the average number of output photons, leads to $\langle \hat{n} \rangle \sim G|\alpha|^2$ and $\langle \Delta \hat{n}^2 \rangle \sim G^2 |\alpha|^2$. Therefore, the gain G corresponds to the Fano factor $F = \langle \hat{n} \rangle / \langle \Delta \hat{n}^2 \rangle$ of the output distribution, as long as the input state is excited before amplification in order to keep constant the intensity at the output: in this way the PNA works as a device converting coherent states in nearly-number eigenstates.

3. IDEAL PHOTON NUMBER-DUPLICATOR

A photon number-duplicator (PND) is a device which, upon acting on a input field in a certain number eigenstate, produces two output fields both of which are in the same number eigenstate as the input. Such a device can be realized in principle, whereas a 'cloning' device producing multiple copies of a (generally not orthogonal) input set of states would violate unitarity.[4,13] For the ideal PNA the unitary transformation has been obtained starting from the amplifying CP map defined by the relation

$$\mathcal{S}_H^{(r)}(\hat{E}_\pm) = (\hat{E}_\pm)^r \ . \tag{46}$$

The case of the ideal PND can be obtained in strict analogy with Eq.(46) by means of the duplicating CP map

$$\mathcal{S}_H(\hat{E}_\pm) = \hat{E}_\pm \otimes \hat{E}_\pm \ . \tag{47}$$

The general transformation attaining the duplication of the shift operators (47) has the form

$$\mathcal{S}_H(\hat{O}) = \sum_{\lambda=-\infty}^{\infty} \hat{S}_\lambda^\dagger \hat{O} \hat{S}_\lambda \ , \tag{48}$$

321
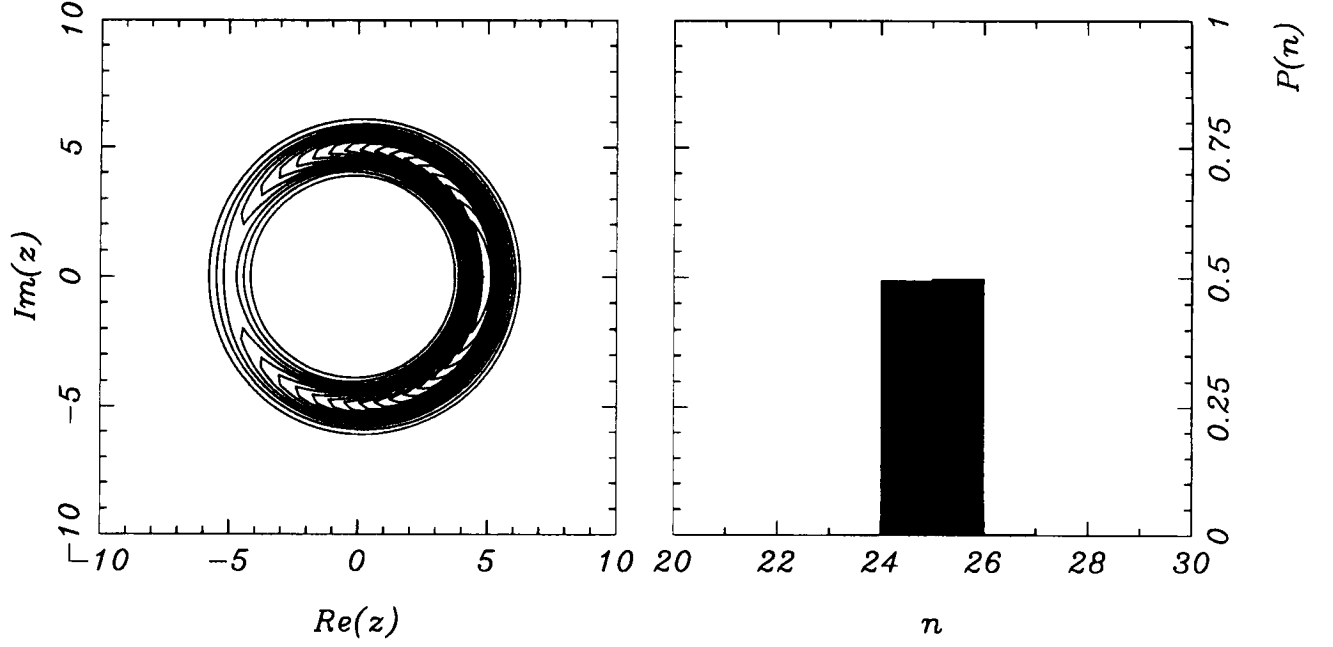
Figure 4: Q-function and number distribution of a coherent state having $\langle \hat{n} \rangle = 5000$ photons, after strong number-deamplification $G = .005$. The final moments are $\langle \hat{n} \rangle = 25$ and $\langle \Delta \hat{n}^2 \rangle^{1/2} = 1.16$.

where the nonunitary operators $\hat{S}_\lambda$ ($\hat{S}_\lambda : \mathcal{F} \otimes \mathcal{F} \to \mathcal{F}$) are given by

$$\hat{S}_\lambda = \sum_{n,m=0}^{\infty} \delta_{m,n+\lambda} |\min\{n,m\}\rangle\langle m,n| \,, \tag{49}$$

and satisfy the orthogonality and completeness relations

$$\hat{S}_\lambda \hat{S}_\mu^\dagger = \delta_{\lambda\mu} \hat{1} \,, \tag{50}$$

$$\sum_{\lambda=-\infty}^{\infty} \hat{S}_\lambda^\dagger \hat{S}_\lambda = \hat{1} \otimes \hat{1} \,. \tag{51}$$

By adding a third photon field we can write a unitary operator $\hat{U}$ ($\hat{U} : \mathcal{F} \otimes \mathcal{F} \otimes \mathcal{F} \to \mathcal{F} \otimes \mathcal{F} \otimes \mathcal{F}$) as follows

$$\hat{U} = \sum_{\lambda=-\infty}^{\infty} \hat{S}_\lambda \otimes \hat{S}_\lambda^\dagger = \sum_{\lambda=-\infty}^{\infty} \sum_{n_1,n_2,m_1,m_2=0}^{\infty} \delta_{\{m_l\},\{n_l+\lambda\}} \times$$
$$|\min\{n_1,m_1\}\rangle\langle\min\{n_2,m_2\}| \otimes |n_2\rangle\langle n_1| \otimes |m_2\rangle\langle m_1| \,. \tag{52}$$

The operator $\hat{U}$ is involutive (i.e. $\hat{U}^2 = 1$) and produces the intertwining

$$\hat{U}(\hat{E}_\pm \otimes \hat{1} \otimes \hat{1})\hat{U} = \hat{1} \otimes \hat{E}_\pm \otimes \hat{E}_\pm \,,$$

$$\hat{U}(\hat{1} \otimes \hat{E}_\pm \otimes \hat{E}_\pm)\hat{U} = \hat{E}_\pm \otimes \hat{1} \otimes \hat{1} \,, \tag{53}$$

which corresponds to the Fock representation

$$\hat{U}|l,m,n\rangle = \begin{cases} |m,l,l+n-m\rangle & n \geq m \,, \\ |m,l-n+m,l\rangle & n \leq m \,. \end{cases} \tag{54}$$

322

In particular, one has $\hat{U}|l,n,n\rangle = |n,l,l\rangle$, and for the practically interesting case of the second and third fields in the vacuum state one obtains

$$\hat{U}|n,0,0\rangle = |0,n,n\rangle \,, \tag{55}$$

which is the required duplication. The scheme of the ideal PND is depicted in Fig.(5). As the ideal PNA corresponds to intertwining the one-particle operator $a^\dagger$ with the r-particle operator $b^\dagger_{(r)}$, the PND performs a change between the one-mode operator $a^\dagger$ and the two-mode operator $b^\dagger_{(1,1)}$

$$b^\dagger_{(1,1)} = b^\dagger c^\dagger \left(\max\{b^\dagger b, c^\dagger c\} + 1\right)^{-1/2} \,, \tag{56}$$

which satisfies the commutation relations $[b_{(1,1)}, b^\dagger_{(1,1)}] = 1$ and $[b^\dagger b + c^\dagger c, b_{(1,1)}] = -2b_{(1,1)}$. It follows that the Hamiltonian in the Dirac picture is

$$\hat{H}^D_I = -ik\left(a^\dagger b_{(1,1)} - b^\dagger_{(1,1)} a\right) \,, \tag{57}$$

with the same interaction length as in (30). Conservation of energy now requires a classical pump at frequency $\Omega = \omega_a - \omega_b - \omega_c$, apart from the case of frequency matching $\omega_a = \omega_b + \omega_c$, which preserves the input energy $E = \omega_a l + \omega_b m + \omega_c n$. The PND described in the present context is more precisely a PNDFC (frequency-converter): in order to keep the frequency constant during the duplication one can choose $\omega_b = \omega_c$ and put a parametric frequency-converter acting on the input field a.

In conclusion of this section I remark that the ideal PND produces the same effect of a gain-2 PNA when the total number of photons of the two replica outputs is detected. In fact, one has

$$_{(1,1)}\langle\alpha|f(b^\dagger b + c^\dagger c)|\alpha\rangle_{(1,1)} = {}_{(2)}\langle\alpha|f(a^\dagger a)|\alpha\rangle_{(2)} = \langle\alpha|f(2a^\dagger a)|\alpha\rangle \,, \tag{58}$$

where

$$|\alpha\rangle_{(2)} = \sum_{n=0}^\infty \alpha_n|2n\rangle \tag{59}$$

denotes the gain-2 PNA output state and

$$|\alpha\rangle_{(1,1)} = \sum_{n=0}^\infty \alpha_n|n,n\rangle \tag{60}$$

the PND output state corresponding to input

$$|\alpha\rangle = \sum_{n=0}^\infty \alpha_n|n\rangle \,, \quad \sum_{n=0}^\infty |\alpha_n|^2 = 1 \,. \tag{61}$$

Moreover, one has

$$_{(1,1)}\langle\alpha|f(b^\dagger b)|\alpha\rangle_{(1,1)} = {}_{(1,1)}\langle\alpha|f(c^\dagger c)|\alpha\rangle_{(1,1)} = \langle\alpha|f(a^\dagger a)|\alpha\rangle \,, \tag{62}$$
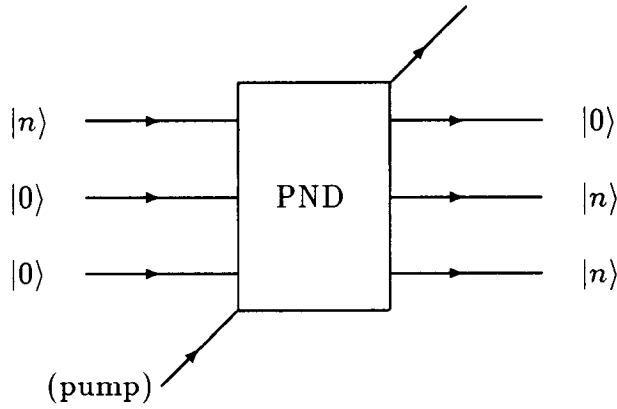
Figure 5: Scheme of the ideal PND.

and the SNR in detecting $b^\dagger b$, $c^\dagger c$ (or their sum) remains the same as at the input of the PND: in this sense the PND can be regarded an ideal amplifier.

4. COMPARISON WITH REAL SYSTEMS

The Hamiltonians (31) and (57) are quite complicated, due to the presence of an interaction strength which depends on the input number of photons of one field. For high average number of photons $\langle a^\dagger a \rangle \gg r$ the interaction strength in (31) behaves asymptotically as follows

$$f_{(r)}(a^\dagger a) \sim \left(a^\dagger a \right)^{-\frac{1}{2}(r-1)} . \tag{63}$$

Alternatively, one can look directly at the asymptotic behaviour of the multiboson operator $a^\dagger_{(r)}$:

$$a^\dagger_{(r)} = \left\{ \frac{[a^\dagger a/r](\hat{n}-r)!}{\hat{n}!} \right\}^{1/2} (a^\dagger)^r =$$

$$[a^\dagger a/r]^{1/2}(\hat{n}-r+1)^{-1/2}r^{\frac{1}{2}}\kappa_r(\hat{\Phi})a^\dagger \sim \kappa_r(\hat{\Phi})a^\dagger , \tag{64}$$

where $\kappa_r(\hat{\Phi})$ denotes the function of the phase

$$\kappa_r(\hat{\Phi}) = r^{-\frac{1}{2}}e^{-i(r-1)\hat{\Phi}} . \tag{65}$$

Taking into account also the pumping field, the phase-number amplifier would require a medium with a $\chi^{(2)}$ susceptibility and an interaction Hamiltonian of the form

$$\hat{H}_I \sim \lambda\kappa_r(\hat{\Phi}_a)a^\dagger bc + \text{h.c.} , \tag{66}$$

c denoting the annihilator of the pumping field. From Eq.(66) it follows that in order to attain phase-number amplification one should use a $\chi^{(2)}$ medium having polarization which depends on the phase of the field according to (65) only in a limited frequency range. The amplifier gain r is involved only in the phase factor (65), and the interaction length has to be tuned at the complete conversion value $L = \pi/[2\lambda I_c^{1/2}]$, I_c being the average power flux of the (classical undepleted)

pump, and $\lambda \propto \chi^{(2)}$. For $r = 2$ one has $\kappa_2(\hat{\Phi}) = 2^{-\frac{1}{2}} e^{-i\hat{\Phi}} = (2\hat{n})^{-\frac{1}{2}} a^{\dagger}$. This case is approximated by the usual degenerate four-wave mixing medium having Hamiltonian

$$\hat{H}_I \propto \chi^{(3)} (a^{\dagger})^2 bc + \text{h.c.} . \tag{67}$$

For $\lambda \propto \chi^{(3)} I_a^{1/2}$ this medium attains gain-2 number amplification approximately in the average values.

The ideal PND is quite similar to the gain-2 ideal PNA, the main difference being that the field in the phase-dependent frequency range now splits into the two nondegenerate modes bearing the replica-states (actually one can analogously define G-'multiplicator' devices, which then compares to gain-G PNA's). When operating on two vacuua as in Fig.5, one can substitute the function $\max\{b^{\dagger}b, c^{\dagger}c\}$ in the Hamiltonian with either $b^{\dagger}b$ or $c^{\dagger}c$, without changing the output.

In conclusion, some remarks are in order, regarding the possibility of attaining the amplifying CP maps (37) and (44) through interaction with atomic—instead of electromagnetic—fields. In this case the nonunitary operators in Eqs.(37) and (44) should be regarded as partial trace of the interaction over the atomic degrees of freedom. The relations (12-14) have no faithful representation on a finite-dimensional Hilbert space, and one cannot realize them using atoms with a finite number of levels. However, some similarities can be recognized between this case and the PNA mechanism. For example, in the *high-Q micromaser Fock state generation*, the role of the auxiliary field is played by an inverted two-level atom entering the cavity with a well defined velocity:[14] the nonunitary reduction of the signal field is obtained by means of nonselective measurements of the atomic variables. The CP map experimented by the electromagnetic field is

$$\mathcal{S}_S^{(r)}(\hat{\rho}) = \sum_{\alpha=0}^{r-1} \hat{V}_\alpha^{(r)} \hat{\rho} (\hat{V}_\alpha^{(r)})^{\dagger} , \tag{68}$$

$$\hat{V}_\alpha^{\dagger} = \langle \alpha | \exp \left(-i \hat{H}_I^P t \right) | \uparrow \rangle , \tag{69}$$

where $r = 2$, $\hat{H}_I^P$ denotes the usual Jaynes-Cummings Hamiltonian, and $| \uparrow \rangle$ represents the inverted state of the atom. As a matter of fact, the high-Q micromaser works as a 'number-phase squeezer' (in this fashion the micromaser is a sort of PNA and the successive atomic passages correspond to gain-2 open PNA's in series). One should notice, however, that the number-phase squeezing in the micromaser strongly depends on the initial state of the field (which should have less photons then the asymptotic 'trapping' state), and this feature does not depend on the particular form of the interaction Hamiltonian $\hat{H}_I^P$, as long as a finite number of the atomic levels is concerned.

5. ACKNOWLEDGMENTS

6. REFERENCES

1 H. P. Yuen, Phys. Rev. A**13** 2226 (1976)

2 Y. Yamamoto, S. Machida, N. Imoto, M. Kitagawa and G. Björk, J. Opt. Soc. Am. B **4** 1645 (1987)

3 H. P. Yuen, Phys. Rev. Lett. **56** 2176 (1986)

4 H. P. Yuen, Phys. Lett. A**113** 405 (1986)

5 H. P. Yuen, Opt. Lett. **12** 789 (1987)

6 H. P. Yuen, in *Quantum Aspects of Optical Communications*, Ed. by C. Bendjaballah, O. Hirota and S. Reynaud, Lecture Notes in Physics **378**, Springer, Berlin-New York (1991) (in press)

7 Strictly speaking, according to Eq.(6) $\hat{\Phi}$ is not Hermitian ($\hat{E}_\pm$ are not unitary); one should use the Hermitian operators $\sin\hat{\Phi}$ and $\cos\hat{\Phi}$. However, for states approximately orthogonal to the vacuum and for small phase uncertainties (such that $\sin\hat{\Phi} \sim \hat{\Phi}$), $\hat{\Phi}$ is approximately Hermitian: the asymptotic commutation relation $[\hat{n}, \hat{\Phi}] \sim i$ holds, assuring that $(\hat{n}, \hat{\Phi})$ can be treated as a conjugated pair (see R. Loudon *The Quantum Theory of Light*, Clarendon Press, Oxford (1983)

8 K. Kraus *States, effects and Operations*, Lecture Notes in Physics **190**, Springer (1983)

9 G. Lindblad in *Quantum Aspects of Optical Communications*, Ed. by C. Bendjaballah, O. Hirota and S. Reynaud, Lecture Notes in Physics **378**, Springer, Berlin-New York (1991) (in press)

10 R. A. Brandt and O. W. Greenberg J. Math. Phys. **10** 1168 (1969)

11 G. M. D'Ariano and N. Sterpi Phys. Rev. A **39** 1860 (1989)

12 G. M. D'Ariano Phys. Rev. A **41** 2636 (1990)

13 W. K. Wootters, W. H. Zurek, Nature **299** 802 (1982)

14 P. Filipowicz, J. Javanainen, and P. Meystre, J. Opt. Soc. Am. B **3**, 906 (1986)

DECOHERENCE IN QUANTUM MECHANICS AND QUANTUM COSMOLOGY

James B. Hartle
Department of Physics, University of California
Santa Barbara, CA 93106

ABSTRACT

In the search for a theory of the initial condition of the universe, quantum mechanics must be applied to the universe as a whole. For this the "Copenhagen interpretations" of quantum mechanics are insufficiently general. Characteristically these interpretations assumed that there was a division of the universe into "observers" and "observed", that the outcomes of "measurements" were the primary focus of scientific statement, and, in effect, posited the existence outside of quantum mechanics of the quasiclassical domain of familiar experience. However, in a theory of the whole thing there can be no fundamental division into observers and observed. Measurements and observers cannot be fundamental notions in a theory that seeks to describe the early universe where neither existed. In a unified theory of cosmology there is no fundamental basis for a separate classical physics. Copenhagen quantum mechanics must, therefore, be generalized to apply to cosmology.

This talk sketched a quantum mechanics for closed systems adequate for cosmology developed in joint work with Murray Gell-Mann.[1,2,3] This framework is an extension and clarification of that of Everett[4] and builds on several aspects of the post-Everett development. It builds especially the work of Zeh[5], Zurek[6], Joos and Zeh[7], and others on the interactions of quantum system with the larger universe and on the ideas of Griffiths[9], Omnès[10], and others on the requirements for consistent probabilities for histories.

Three forms of information are necessary for prediction in the quantum mechanics of a closed system. In an approximation in which quantum spacetime is ignored, these are the Hamiltonian, the initial density matrix of the universe, and the information specifying particular histories. The most general objective of quantum theory is the prediction of the probabilities of the individual histories in a set of alternative histories for the universe. However, the characteristic feature of a quantum theory is that not every set of histories that may be described can be assigned probabilities because of quantum interference. Probabilities can be assigned only to sets of histories for which there is negligible interference between the individual histories in the set as a consequence of the initial density matrix of the universe and the Hamiltonian governing its dynamics. Such sets of histories are said to decohere.

Histories described at an arbitrarily fine-grained level do not decohere; some coarse graining is necessary for decoherence. Coarse-graining was described in the talk and the decoherence functional that measures the level of decoherence for sets of alternative coarse-grained histories was introduced. Mechanisms for decoherence were reviewed in simple models. Habitual decoherence was argued to be widespread in the universe for coarse-grained histories defined by certain quasiclassical variables.

A quasiclassical domain is roughly a set of alternative coarse-grained histories that is as refined as possible consistent with decoherence and has individual branches that are defined by quantities that are similar from one time to the next correlated in time mostly according to classical deterministic laws. The problem of precisely defining quasiclassical domains was discussed. The question of whether or not the universe exhibits a quasiclassical domain like the one of familiar experience is a calculable one in quantum cosmology given a suitably precise definition, the Hamiltonian of the elementary particles and the initial density matrix of the universe. In particular, the variables that describe classical physics and the form of its phenomenological equations of motion should be deriv-

able from that Hamiltonian and the initial condition.[10]

A measurement situation is one in which a variable becomes correlated with a quasiclassical operator of the "quasiclassical domain". The theory of measurements in quantum mechanics was discussed from this point of view. The recovery of the Copenhagen formulation of quantum mechanics as an approximation to the more general framework appropriate in measurement situations was described. An "observer" (or information gathering and utilizing system, IGUS) was treated as a complex adaptive system that evolves to utilize the relative predictability of a "quasiclassical domain".

The talk concluded that resolution of many of the problems of interpretation presented by quantum mechanics is not to be found within the theory *in general* but rather through an examination of the universe's initial condition and the emergent features that it, together with the Hamiltonian of the elementary particles, implies. Quantum mechanics may be best and most fundamentally understood in the context of quantum cosmology.

Acknowledgement

References

1. Gell-Mann, M. and J.B. Hartle (1990) "Quantum Mechanics in the Light of Quantum Cosmology" in *Complexity, Entropy and the Physics of Information, Santa Fe Institute Studies in the Sciences of Complexity*, Volume VIII, edited by W. Zurek, Addison Wesley, Reading or in (1991) *Proceedings of the 3rd International Symposium on the Fundations of Quantum Mechanics in the Light of New Technology*, edited by S. Kobayashi, H. Ezawa, Y. Murayama, S. Nomura, Physical Society of Japan, Tokyo.

2. See, e.g. Hartle, J.B. (1991) "The Quantum Mechanics of Cosmology" in *Quantum Cosmology and Baby Universes: Proceedings of the 1989 Jerusalem Winter School*, eds. S. Coleman, J.B. Hartle, T. Piran, and S. Weinberg World Scientific, Singapore.

3. Gell-Mann, M. and J.B. Hartle (1990) "Alternative Decohering Histories in Quantum Mechanics", to appear in the *Proceedings of the International Conference on High Energy Physics*, Singapore, August (1990).

4. Everett, H. (1957) *Rev. Mod. Phys.*, **29**, 454.

5. Zeh, H.D. (1971) *Found. Phys.*, **1**, 69.

6. Zurek, W. (1981) *Phys. Rev. D*, **24**, 1516; (1982) *ibid.*, **26**, 1862.

7. Joos, E. and H.D. Zeh (1985) *Zeit. Phys.*, **B59**, 223.

8. Griffiths, R. (1984) *J. Stat. Phys.*, **36**, 219.

9. Omnès, R. (1988) *J. Stat. Phys.*, **53**, 893; (1988) *ibid.*, **53**, 933; (1988) *ibid.*, **53**, 957; (1989) *ibid.*, **57**, 357.

10. Gell-Mann, M. and J.B. Hartle (1991) "Classical Equations for Quantum Systems". Preprint UCSBTH91-15.

SQUEEZED STATES IN THE THEORY OF PRIMORDIAL GRAVITATIONAL WAVES

Leonid P. Grishchuk*

JILA, University of Colorado, Boulder, CO 80309-0440

and

Sternberg Astronomical Institute, Moscow University, 119899 Moscow, V-234, USSR

ABSTRACT

It is shown that squeezed states of primordial gravitational waves are inevitably produced in the course of cosmological evolution. The theory of squeezed gravitons is very similar to the theory of squeezed light. Squeeze parameters and statistical properties of the expected relic gravity-wave radiation are described.

INTRODUCTION

Squeezed quantum states of light have been successfully generated and detected under laboratory conditions. It is known how much skill and effort by our experimentalist colleagues it requires to achieve even a modest amount of squeezing, that is, to obtain the squeeze parameter r of order of 1. The main purpose of my talk is to show that, in the cosmos, squeezed quantum states of gravitational waves are produced inevitably and with a much much larger amount of squeezing, simply as a result of expansion of the Universe.

In the context of gravity-wave research, the notion of squeezed quantum states has been often referred to. However, what was always meant was the squeezing of a quantized vibrational mode of a detecting device that could be implemented for a better detection of a classical gravitational wave. For instance, it was shown (Ref. 1) that the performance of a laser interferometer gravity-wave detector can be improved by using squeezed light. In another paper (Ref. 2) it was argued that any detector-oscillator can be specially "prepared" in a squeezed state and used for gravity-wave detection during some interval of time before the thermal noise destroys squeezing and degrades the detector's sensitivity.

However, it is the squeezing of the gravitational waves themselves that will be discussed in my talk today. I will show that the production of squeezed relic gravitational waves is an inescapable consequence of the variability of cosmological gravitational field and the existence of zero-point quantum fluctuations.

The mathematical theories of relic graviton production and squeezing of light are very similar. To make this similarity especially transparent, I will begin by presenting Einstein's general relativity in the form of a traditional field theory, such as the theory of classical electromagnetic fields. Those of you who may feel uncomfortable, or even intimidated, with the notion of curved space-time, will, perhaps, find it easier to deal with the concept of a gravitational field given in the usual flat Minkowski space-time. (More details about this "field-theoretical" formulation of general relativity are presented in Ref. 3; it is important to emphasize that we are dealing with a different mathematical formulation of general-

---

relativity, not with some alternate physical theory, see Ref. 4.) This approach leads to manifestly nonlinear field equations. In contrast to quantum optics based on the laws of linear electrodynamics, in the case of a gravitational field one does not need any material medium in order to couple a "pump" field with the "signal" waves; for gravity this is achieved automatically due to the nonlinearity of the gravitational field itself. As is often done, we will present the total gravitational field in the form of an approximate sum of a large "classical" contribution and a small quantized perturbation. This approach will be applied to the cosmological gravitational field of the expanding Universe acting upon zero-point quantum fluctuations of the gravitational waves. I hate to call the variable gravitational field of the expanding Universe –the most grandiose and magnificent phenomenon we are aware of – just a "pump" field, but, technically speaking, it plays precisely this role. As a result, the initial vacuum state of gravitational waves will evolve into a strongly squeezed vacuum state with very specific statistical properties.

We will discuss the expected characteristics of the relic gravity-wave background radiation and the problem of its detection.

FIELD-THEORETICAL APPROACH TO GENERAL RELATIVITY

A gravitational field is fully described by a symmetric second-rank tensor $h_{\mu\nu}$ (note that the gravitational field variables have just one extra index as compared with the electromagnetic 4-vector potential A_μ, not a big difference!). For writing down the Lagrangian of the gravitational field it is convenient to use also an additional set of variables: the tensor field $P^\alpha{}_{\mu\nu}$, symmetric with respect to the last two indices. However, $P^\alpha{}_{\mu\nu}$ is not a new physical field but rather a combination of the first derivatives of $h_{\mu\nu}$, as follows from the field equations.

Gravitational field potentials $h_{\mu\nu}(x,y,z,t)$ are mathematically treated as components of one of many physical fields immersed in the ordinary Minkowski space-time:

$$d\sigma^2 = c^2 dt^2 - dx^2 - dy^2 - dz^2 . \tag{1}$$

The metric tensor of Minkowski space-time will be denoted by $\gamma_{\mu\nu}$. With respect to this metric tensor all covariant differentiations (denoted by the symbol ";") and lowerings or raisings of indices are to be performed. In the Lorentzian coordinates, like the ones implied in eq. (1) and which we will be using in practical calculations below, $\gamma_{\mu\nu}$ acquires especially simple values: $\gamma_{00} = 1$, $\gamma_{11} = \gamma_{22} = \gamma_{33} = -1$, with the rest of $\gamma_{\mu\nu}$ being equal to zero.

The gravitational part of the total action $S = S^g + S^m$ is

$$S^g = -\frac{1}{2c\kappa} \int d^4x \, L^g , \quad \kappa = \frac{8\pi G}{c^4}$$

where the gravitational Lagrangian L^g has the form

$$L^g = (-\gamma)^{1/2} \left[h^{\mu\nu}{}_{;\alpha} P^\alpha{}_{\mu\nu} - (h^{\mu\nu} + \gamma^{\mu\nu}) \left(P^\alpha{}_{\mu\beta} P^\beta{}_{\nu\alpha} - \frac{1}{3} P^\sigma{}_{\sigma\mu} P^\rho{}_{\rho\nu} \right) \right] .$$

The nongravitational sources and fields and their interaction with the gravitational field are described by

$$S^m = \frac{1}{c} \int d^4x \, L^m .$$

The energy-momentum tensor $t_{\mu\nu}$ of the gravitational field itself and the energy-momentum tensor $\tau_{\mu\nu}$ of the nongravitational matter and fields interacting with gravity are defined in the usual manner:

$$\kappa t_{\mu\nu} = -\frac{1}{\sqrt{-\gamma}} \frac{\delta L^g}{\delta \gamma^{\mu\nu}} \quad , \quad \tau_{\mu\nu} = \frac{2}{\sqrt{-\gamma}} \frac{\delta L^m}{\delta \gamma^{\mu\nu}} .$$

The precise expression for $\kappa t_{\mu\nu}$ is as follows:

$$\kappa t_{\mu\nu} = P^\alpha{}_{\mu\beta} P^\beta{}_{\nu\alpha} - \frac{1}{2}\gamma_{\mu\nu}\gamma^{\sigma\rho} P^\alpha{}_{\sigma\beta} P^\beta{}_{\rho\alpha} - \frac{1}{3}\left(P_\mu P_\nu - \frac{1}{2}\gamma_{\mu\nu} P_\sigma P^\sigma \right) + Q_{\mu\nu} \tag{2}$$

where $P_\mu \equiv P^\alpha{}_{\alpha\mu}$, $Q_{\mu\nu} \equiv Q^\alpha{}_{\mu\nu;\alpha}$ and

$$Q^\tau{}_{\mu\nu} \equiv \frac{1}{2} P^\sigma{}_{\alpha\beta} \left[\gamma_{\mu\nu} h^{\alpha\beta}\delta^\tau_\sigma + \gamma^{\tau\alpha}\left(\gamma_{\sigma\mu}h^\beta_\nu + \gamma_{\sigma\nu}h^\beta_\mu\right) - h^{\tau\beta}\left(\delta^\alpha_\mu\gamma_{\sigma\nu} + \delta^\alpha_\nu\gamma_{\sigma\mu}\right) - \delta^\tau_\sigma\left(\delta^\alpha_\mu h^\beta_\nu + \delta^\alpha_\nu h^\beta_\mu\right) \right] .$$

By varying the action S with respect to $h^{\mu\nu}$ and $P^\alpha{}_{\mu\nu}$ one can derive the following gravitational field equations:

$$h_{\mu\nu}{}^{,\alpha}{}_{,\alpha} + \gamma_{\mu\nu}\, h^{\alpha\beta}{}_{,\alpha,\beta} - h^\alpha{}_{\nu,\alpha,\mu} - h^\alpha{}_{\mu,\alpha,\nu} = \frac{16\pi G}{c^4}\left(t_{\mu\nu} + \tau_{\mu\nu}\right) \tag{3}$$

where the comma means an ordinary derivative ($_{,\alpha} = \partial/\partial x^\alpha$) and $\gamma_{\mu\nu}$ is assumed to be in the simplest form corresponding to eq. (1). For reference purposes we will also write down the relationship between the first derivatives of $h_{\mu\nu}$ and $P^\alpha{}_{\mu\nu}$:

$$-h^{\mu\nu}{}_{;\rho} - \frac{1}{2}h^{\mu\nu}\gamma^{\alpha\beta}\,\gamma_{\alpha\beta,\rho} + (\gamma^{\mu\alpha} + h^{\mu\alpha})\,P^\nu{}_{\alpha\rho} + (\gamma^{\nu\alpha} + h^{\nu\alpha})\,P^\mu{}_{\alpha\rho} - \frac{1}{3}P_\alpha\left[(\gamma^{\mu\alpha} + h^{\mu\alpha})\,\delta^\nu_\rho + (\gamma^{\nu\alpha} + h^{\nu\alpha})\,\delta^\mu_\rho\right] = 0.$$

The theory possesses a gauge freedom quite similar to the gauge freedom of classical electrodynamics. One can apply the gauge transformations to the gravitational variables $h_{\mu\nu}$ and matter variables without changing the field equations. At the expense of the gauge freedom one can impose some gauge conditions which are normally used for diminishing the number of variables and simplifying the field equations.

The transition to the usual "geometrical" formulation of general relativity is established by introducing the new functions $g_{\mu\nu}$ according to the rule

$$\sqrt{-g}\, g^{\mu\nu} = \sqrt{-\gamma}\,\left(\gamma^{\mu\nu} + h^{\mu\nu}\right) \tag{4}$$

and by identifying the $g_{\mu\nu}$ with the metric tensor of the curved space-time: $ds^2 = g_{\alpha\beta}dx^\alpha dx^\beta$.

GRAVITATIONAL FIELD OF THE EXPANDING UNIVERSE

Let us apply the developed formalism for description of the gravitational field of the homogeneous isotropic Universe. From our new point of view this is just a specific gravitational field $h_{\mu\nu}(t,x,y,z)$ given in Minkowski space-time (1). Let us take the nonvanishing gravitational potentials in the form

$$h_{00} = a^3(t) - 1 \quad , \qquad h_{11} = h_{22} = h_{33} = 1 - a(t) \tag{5}$$

where $a(t)$ is, as yet unspecified, function of time. One can calculate the gravitational energy-momentum tensor $t_{\mu\nu}$, eq. (2), and find that the nonvanishing components of $\kappa t_{\mu\nu}$ are

$$\kappa t_{00} = -\frac{3\ddot{a}}{2a}(a^2 - 1) - 3\dot{a}^2$$

$$\kappa t_{11} = \kappa t_{22} = \kappa t_{33} = -\frac{\ddot{a}}{2a}(3a^3 - a^2 + a - 3) - \dot{a}^2(3a - 1) \tag{6}$$

where the dot means the time derivative (for simplicity we choose the units where the velocity of light $c = 1$).

The nongravitational sources are assumed to be in the form of hydrodynamical matter with the Lagrangian

$$L^m = \frac{1}{2}\sqrt{-g}\,\left[\epsilon + 3p - (\epsilon + p)g_{\mu\nu}\,u^\mu\,u^\nu\right]$$

where $g_{\mu\nu}$ is defined by eq. (4). One can find the nonvanishing components of the energy-momentum tensor $\tau_{\mu\nu}$:

$$\tau_{00} = \epsilon + \frac{3}{4}(a^2 - 1)(\epsilon - p)$$

$$\tau_{11} = \tau_{22} = \tau_{33} = p - \frac{1}{4}(a^2 - 1)(\epsilon - p)\,. \tag{7}$$

By substituting expressions (5), (6), and (7) into the field equations (3) one can derive equations governing the function $a(t)$ and, hence, the gravitational field (5):

$$\frac{\ddot{a}}{a} = -\frac{4\pi G}{3}(\epsilon + 3p), \qquad \left(\frac{\dot{a}}{a}\right)^2 = \frac{8\pi G}{3}\epsilon\,.$$

(In "geometrical" language, these are, of course, the Einstein equations for a spatially flat cosmological model: $ds^2 = dt^2 - a^2(t)\,(dx^2 + dy^2 + dz^2)$.) By specifying the relationship between ϵ and p ("the equation of state") one can solve these equations and find a concrete function $a(t)$.

AMPLIFICATION OF GRAVITATIONAL WAVES

Gravitational field (5) is just a main term of a more complicated and realistic cosmological gravitational field which includes the gravity-wave perturbations. Let us present the total field $h_{\mu\nu}$ in the form

$$h_{\mu\nu} = h_{\mu\nu}^{(0)} + h_{\mu\nu}^{(1)}(t, x, y, z)\,, \tag{8}$$

where $h_{\mu\nu}^{(0)}$ is given by eq. (5). At the expense of gauge freedom one can always satisfy the conditions $h^{(1)\mu\nu}{}_{,\nu} = 0$. Moreover, in the case of gravitational waves, the perturbations of ϵ, p, and u^α are equal to zero and one can, in addition, satisfy the requirements $h_{o\mu}^{(1)} = 0$, $h_{\mu\nu}^{(1)}\gamma^{\mu\nu} = 0$, so that one is left with only two independent polarization components (designated by a = 1, 2) of $h_{\mu\nu}^{(1)}$. For a wave with the wave vector **n** one can write down the nonzero components of the field:

$$h_{ij}^{(1)}(t, x, y, z) = \left(\mu_n^a(t)e^{i\mathbf{n}\mathbf{x}} + \mu_n^{a*}(t)e^{-i\mathbf{n}\mathbf{x}}\right)p_{ij}^a; \tag{9}$$

where the constant polarization tensors p_{ij}^a fulfill the conditions $p_{ik}^a n^k = 0$, $p_i^a i = 0$.

Now one should substitute (8) into the field equations (3) and linearize them with respect to $h_{ij}^{(1)}$. It is clear that the left-hand side of eq. (3) is simply the usual D'Alembert differential operator applied to $h_{ij}^{(1)}$. At the same time, the right-hand side of eq. (3) will contain the products of $h_{\mu\nu}^{(0)}$ and $h_{\mu\nu}^{(1)}$ since all the nonlinearities are collected there.

For a given perturbation with the wave vector $\mathbf{n}$ and for each of the two polarization components, the field equations reduce to a single equation for the time-dependent function $\mu(t)$ (indices n and a are omitted):

$$\ddot{\mu} + n^2\mu = \left[\frac{n^2(a^2-1)}{a^2} + \frac{\ddot{a}}{a} + \left(\frac{\dot{a}}{a}\right)^2\right]\mu - \frac{\dot{a}}{a}\dot{\mu} \tag{10}$$

where $n^2 = n^{1^2} + n^{2^2} + n^{3^2}$. If there is no "pump" field (5), that is $a(t) = 1$, the right-hand side of eq. (10) vanishes. It is worth noting that in the gravitational case, in contrast to electrodynamics, there is not any dimensional coupling constant between the "pump" and "wave" fields, the strength of the coupling is regulated by the rate of variability of the "pump" field.

It is convenient to introduce a new time coordinate η related to t by $d\eta = a(t)^{-1}dt$, and to denote the η-time derivative by prime. Equation (10) gets an especially simple form (Ref. 5):

$$\mu'' + \left(n^2 - \frac{a''}{a}\right)\mu = 0 \tag{11}$$

which makes it possible to treat the problem as a problem for a parametrically excited oscillator. The notion of squeezing appears quite naturally.

SQUEEZED VACUUM STATES OF RELIC GRAVITONS

In some cosmologically interesting and realistic situations, the function a''/a goes asymptotically to zero for $\eta \to -\infty$ and $\eta \to +\infty$. In the asymptotic regions $\eta \to -\infty$ and $\eta \to +\infty$, solutions to eq. (11) are very simple: $\mu(\eta) \sim e^{\pm in\eta}$ The general complex solution to eq. (11) can be presented in the form

$$\mu(\eta) = a\xi(\eta) + b^+\xi^*(\eta) \tag{12}$$

where $\xi(\eta)$ and $\xi^*(\eta)$ are complex-conjugated normalized base functions. The same general solution can be decomposed over other base functions $\chi(\eta)$ and $\chi^*(\eta)$:

$$\mu(\eta) = c\chi(\eta) + d^+\chi^*(\eta) \,. \tag{13}$$

One can choose the base functions in such a way that

$$\xi(\eta) \to \frac{1}{\sqrt{2n}}e^{-in\eta} \quad \text{for} \quad \eta \to -\infty$$

and

$$\chi(\eta) \to \frac{1}{\sqrt{2n}}e^{-in\eta} \quad \text{for} \quad \eta \to +\infty \,.$$

Since (12) and (13) describe the same solution, their coefficients are related:

$$a = uc + vd^+ \,, \quad b^+ = v^*c + u^*d^+ \,, \tag{14}$$

where $|u|^2 - |v|^2 = 1$.

For a quantized field, the coefficients a, b^+, c, d^+ have the meaning of the creation and annihilation operators and the relations (14) are called the Bogoliubov transformations.

Complex numbers u, v can be parameterized by the three real numbers r, θ, φ, $r \geq 0$:

$$u = e^{-i\theta}\, chr\ , \quad v = -e^{i(\theta + 2\varphi)}shr\ . \tag{15}$$

The transformations (14) can also be presented in the form:

$$a = R^+ S^+ c S R, \qquad b^+ = R^+ S^+ d^+ S R\ , \tag{16}$$

where $S(r, \varphi)$ and $R(\theta)$ are unitary operators:

$$
\begin{aligned}
S(r, \varphi) &= \exp[r(e^{-2i\varphi}cd - e^{2i\varphi}c^+ d^+)] \\
R(\theta) &= \exp[-i\theta c^+ c - i\theta d^+ d]\ .
\end{aligned}
$$

In the theory of squeezed quantum states, the operator $S(r, \varphi)$ is called the two-mode squeeze operator, the operator $R(\theta)$ is the two-mode rotation operator, r is the squeeze parameter and φ is the squeeze angle (see, for instance, Ref. 6).

As a result of evolution, the two-mode vacuum state $|0, 0\rangle$ transforms into a two-mode squeezed vacuum state:

$$|SS\rangle_2 = S(r, \varphi)|0, 0\rangle\ .$$

The two modes under discussion are two waves with the same frequency but propagating in opposite directions. In the field of quantum optics, one is usually interested in the temporal fluctuations of the light field, so that the spatial distribution of the field is not always important. However, in cosmology, we need to know the complete space-time distribution of the gravity-wave field. For this aim we augment the time-dependent functions $\mu(\eta)$ with the spatial functions $U(\mathbf{x})$. For every n-mode contribution and a given polarization component, one has:

$$h_{\mathbf{n}} = \mu_{n,1}\, U_{\mathbf{n},1} + \mu_{n,2} U_{\mathbf{n},2}\ .$$

One can work, for example, with complex functions $U_{\mathbf{n},1} = K\, e^{i\mathbf{n}\mathbf{x}}$, $U_{\mathbf{n},2} = K\, e^{-i\mathbf{n}\mathbf{x}}$ (and complex conjugated μ: $\mu_{n,2} = \mu_{n,1}^*$) or with real functions $U_{\mathbf{n},1} = K\cos \mathbf{n}\mathbf{x}$, $U_{\mathbf{n},2} = K\sin \mathbf{n}\mathbf{x}$ (and real μ), where K is a normalization constant. Classically, this corresponds to the decomposition of the field over traveling or standing waves. For the field operators, one writes

$$h_{\mathbf{n}} = \left(a\xi + b^+ \xi^*\right) K\, e^{i\mathbf{n}\mathbf{x}} + \left(a^+ \xi^* + b\xi\right) K\, e^{-i\mathbf{n}\mathbf{x}}\ ,$$

in the first case, and

$$h_{\mathbf{n}} = \left(b_1\xi + b_1^+ \xi^*\right)\sqrt{2}K\cos \mathbf{n}\mathbf{x} + \left(b_2\xi + b_2^+ \xi^*\right)\sqrt{2}K\sin \mathbf{n}\mathbf{x}\ , \tag{17}$$

in the second case. Transition between the two descriptions is fulfilled by the transformation

$$\frac{a + b}{\sqrt{2}} = b_1\ , \quad \frac{i(a - b)}{\sqrt{2}} = b_2\ . \tag{18}$$

In terms of the theory of squeezed states, it means that, in the second case, one will be dealing with a pair of one-mode squeezed states instead of a single two-mode state. Indeed, under the transformation

(18) the two-mode squeeze operator factorizes into a product of the two one-mode squeeze operators $S_1(r, \varphi)$, so that instead of (16) one will have

$$b_1 = R_1^+ S_1^+ c_1 S_1 R_1$$

where $S_1(r, \varphi)$ is the one-mode squeeze operator

$$S_1(r, \varphi) = \exp\left[\frac{r}{2}(e^{-2i\varphi}c_1^2 - e^{2i\varphi}c_1^{+2}\right]$$

and $R_1(\theta)$ is the one-mode rotation operator

$$R_1(\theta) = \exp(-i\theta c_1^+ c_1) .$$

The operator b_2 transforms in precisely the same manner and is associated with the other squeezed mode.

As a result of evolution, the one-mode vacuum state transforms into a one-mode squeezed state.

In what follows, we will base our analysis on the representation (17) and on the one-mode squeezed states. The annihilation and creation operators will be denoted by b and b^+.

The classical equations of motion (11) can be derived from the Hamiltonian

$$H = \frac{1}{2}\left[p^2 + \frac{a'}{a}(\mu p + p\mu) + n^2\mu^2\right]$$

where p is the momentum, canonically conjugated to the coordinate μ, $p = \mu' - \frac{a'}{a}\mu$. In a standard manner, by introducing the annihilation and creation operators b, b^+:

$$b = \sqrt{\frac{n}{2}}\left(\mu + i\frac{p}{n}\right) , \quad b^+ = \sqrt{\frac{n}{2}}\left(\mu - i\frac{p}{n}\right) ,$$

one can present the Hamiltonian in the form

$$H = nb^+ b + \sigma(\eta)b^{+^2} + \sigma^*(\eta)b^2 \tag{19}$$

where the coupling function $\sigma(\eta)$ is $\sigma(\eta) = ia'/2a$, and the Planck constant $\hbar = 1$. Note that the Hamiltonian (19) belongs to the class of Hamiltonians that characterize a number of physical processes (Ref. 7). However, in most of them the function $\sigma(t)$ has a specific form $\sigma(t) = \sigma e^{-2i\omega t}$ where σ is a constant, albeit in our case $\sigma(\eta)$ is a more general function of time.

The Heisenberg equations of motion, following from this Hamiltonian, have the form

$$i\frac{db}{d\eta} = nb + i\frac{a'}{a}b^+ , \quad -i\frac{db^+}{d\eta} = nb^+ - i\frac{a'}{a}b .$$

Their solution is

$$b(\eta) = u(\eta)b_0 + v(\eta)b_0^+ , \quad b^+(\eta) = u^*(\eta)b_0^+ + v^*(\eta)b_0 ,$$

where b_0, b_0^+ are the initial values of $b(\eta)$, $b^+(\eta)$ (Schrödinger operators) and the complex functions $u(\eta)$ and $v(\eta)$ satisfy the equations

$$iu' = nu + i\frac{a'}{a}v^* , \quad -iv^{*\prime} = nv^* - i\frac{a'}{a}u, \quad u(0) = 1, \quad v(0) = 0 . \tag{20}$$

It follows from these equations that $u + v^*$ satisfies the equation identical to eq. (11):

$$(u + v^*)'' + (n^2 - \frac{a''}{a})(u + v^*) = 0 .$$

As for the function $u - v^*$, it can be found from the relation

$$-in(u - v^*) = (u + v^*)' - \frac{a'}{a}(u + v^*) .$$

By substituting eq. (15) into eq. (20) one can find equations for the time-dependent parameters $r(\eta)$, $\theta(\eta)$, $\varphi(\eta)$:

$$
\begin{aligned}
r' &= -\frac{a'}{a}\cos 2\varphi \\
\theta' &= n - \frac{a'}{a}\sin 2\varphi\, thr \\
\varphi' &= -n - \frac{a'}{a}\sin 2\varphi\, cth2r .
\end{aligned}
\tag{21}
$$

Solutions to these equations determine the precise form of evolution of the initial vacuum state into a one-mode squeezed vacuum state. Statistical properties of the final state depend on the numerical values of r and φ in a well-known way (see, for instance, Refs. 6,7).

A possible way of calculating $r(\eta)$ and $\varphi(\eta)$ (Ref. 8) for a given gravitational field $a(\eta)$ relies on the observation that the complex function $B(\eta)$, where

$$\left(\frac{u - v^*}{u + v^*}\right)^* \equiv \frac{chr + e^{2i\varphi}shr}{chr - e^{2i\varphi}shr} = \frac{2}{n}B(\eta) , \tag{22}$$

satisfies the equation

$$B' = i\frac{n^2}{2} - 2\frac{a'}{a}B - 2iB^2$$

with the solution

$$B(\eta) = -\frac{i}{2}\frac{(\mu/a)'}{\mu/a}$$

where $\mu(\eta)$ obeys eq. (11). The properly chosen solutions to eq. (11) define $B(\eta)$ and allow one to find $r(\eta)$ and $\varphi(\eta)$ from eq. (22). The meaning of the function $B(\eta)$ is that it determines the Gaussian wave function $\Psi(\mu, \eta) \sim \exp(-B(\eta)\mu^2)$ which is a solution to the Schrödinger equation in the coordinate representation.

The parameters $r(\eta)$, $\varphi(\eta)$ can be calculated (Ref. 8) for a cosmological model which includes three sequential stages of expansion: inflationary ($a(t) \sim e^{H_o t}$), radiation-dominated ($a(t) \sim t^{1/2}$) and matter-dominated ($a(t) \sim t^{2/3}$). It can be shown that the present-day values of the squeeze parameter r range from $r \approx 1$, for frequencies $\nu \approx 10^8$ Hz, up to $r \approx 120$, for frequencies $\nu \approx 10^{-18}$ Hz. In the

frequency interval $\nu \approx 10^{-1} - 10^{-3}$ Hz, accessible for the planned Laser Interferometer Gravitational-Wave Observatory in Space (Ref. 9), the squeeze parameter r reaches large values of order 40-50.

As for the parameter $\varphi(\eta)$, it can be shown to have the form $\varphi \approx -n\eta + \varphi_0$, where φ_0 is a constant. This behaviour can already be envisaged from eq. (21) for φ', since, in the asymptotic region $\eta \to +\infty$, one has $|\frac{a'}{a}| \ll n$ and $cth2r \approx 1$.

RELIC GRAVITONS: A STOCHASTIC COLLECTION OF STANDING WAVES

As we see, the $\cos \mathbf{nx}$ and $\sin \mathbf{nx}$ modes in the representation (17), evolve into a strongly squeezed vacuum state. The mean number of quanta $\langle N \rangle$ and its variance $\langle (\Delta N)^2 \rangle$ are determined by the squeeze parameter r:

$$\langle N \rangle = sh^2 r, \quad \langle (\Delta N)^2 \rangle = \frac{1}{2} sh^2 2r .$$

The mean values of $\hat{\mu}$ and $\hat{p}$ are equal to zero, but their variances do not vanish:

$$\langle (\Delta \hat{\mu})^2 \rangle = \frac{1}{2n}(ch2r - sh2r \cos 2\varphi), \quad \langle (\Delta \hat{p})^2 \rangle = \frac{n}{2}(ch2r + sh2r \cos 2\varphi).$$

In order to relate the rigorous quantum-mechanical treatment, described above, with the notions of random classical waves, one can use the Wigner function formalism. It allows one to derive the distributions of the random variables A and ϕ entering the classical expression for μ:

$$\mu = A \sin(-n\eta + \phi) . \tag{23}$$

It can be shown (see Ref. 8) that, in the limit of large r, the Gaussian distribution for ϕ is very narrow, like a δ-function. It is concentrated near the values

$$\phi = \varphi_0 + \pi \ell \tag{24}$$

where φ_0 is a constant, the same for all unit vectors $\mathbf{n}/n$, and $\ell = 0, \pm 1, \ldots$.

A similar conclusion can be reached in a simpler, though perhaps less rigorous way. Let us consider the ratio $\langle (\Delta \hat{\mu})^2 \rangle / \langle (\Delta \hat{p})^2 \rangle$. For large r, this number is approximated by

$$\langle (\Delta \hat{\mu})^2 \rangle / \langle (\Delta \hat{p})^2 \rangle \approx \frac{1}{n^2} \, tg^2 \varphi .$$

For a classical expression (23), this ratio corresponds to the number $n^{-2} \, tg^2(-n\eta + \phi)$. From their comparison, and taking into account the fact that $\varphi \approx -n\eta + \varphi_0$, one can derive eq. (24). The very small variance of the phase, $\Delta \phi$, is, of course, consistent with the large variance of the number of quanta, $\langle (\Delta N)^2 \rangle$.

The negligibly small variance of the phase distribution leads to an important result: every pair of $\cos \mathbf{nx}$, $\sin \mathbf{nx}$ modes forms together a standing wave. Indeed, let us consider a given $\mathbf{n}$. The corresponding terms, contributing to the total wave-field $h(\eta, x, y, z)$, can be written in the general form:

$$h_{\mathbf{n}} = A_1 \sin(-n\eta + \phi_1) \cos \mathbf{nx} + A_2 \sin(-n\eta + \phi_2) \sin \mathbf{nx} . \tag{25}$$

The amplitudes A_1 and A_2 are taken from a broad Gaussian distribution and are, in general, different. However, the phases ϕ_1 and ϕ_2 are taken from a very narrow Gaussian distribution and are essentially fixed and equal up to $\pm\pi$. Because of that, expression (25) can be written as a product of a function of time and a function of spatial coordinates:

$$h_{\mathbf{n}} = \pm\sin(-n\eta + \varphi_0)(A_1\cos\mathbf{nx} \pm A_2\sin\mathbf{nx}) . \tag{26}$$

In other words, expression (26) describes a standing wave. A characteristic feature of a standing wave pattern is that the field vanishes all over the space at every half of the period. The randomness of the wave-field is displayed in its spatial functions $A_1\cos\mathbf{nx} \pm A_2\sin\mathbf{nx}$. This is why we say that the relic gravitational waves are present now in the cosmos in the form of a stochastic collection of standing waves.

The total field $h(\eta,\mathbf{x})$ is obtained by summing over all n-mode contributions (26). Of course, the total field loses the property of vanishing at some moments of time, because the various $\sin(-n\eta + \varphi_0)$ factors have different arguments. However, the difference in the arguments is not random, but deterministic. For instance, if at some moment of time $\eta = \eta_0$ the component $h_n(\eta,\mathbf{x})$ vanishes, the same will be true for all other components $h_m(\eta,\mathbf{x})$, where $m = n(1 + k/\ell)$ and k/ℓ is an arbitrary rational number. Hopefully, this property can somehow be used in a specific strategy of observational discrimination of relic gravitational waves from stochastic gravitational waves of a different origin. I think that the inevitable "squeezing" of relic gravitational waves (and other primordial fluctuations of quantum-mechanical origin) can manifest itself in a variety of circumstances, not all of which are foreseeable at the moment.

References

1. Caves, C.M., 1981, *Phys. Rev. D* 23, p. 1693.

2. Grishchuk, L.P., and M.V. Sazhin, 1983, *Zh. Eksp. Teor. Fiz.* 84, p. 1937 (*Sov. Phys. JETP*, 1983, 57, p. 1128).

3. Grishchuk, L.P., A.N. Petrov, and A.D. Popova, 1984, *Commun. Math. Phys.* 94, p. 379; Grishchuk, L.P., and A.N. Petrov, 1987, *Zh. Eksp. Teor. Fiz.* 92, p. 9 (*Sov. Phys. JETP*, 1987, 65, p. 5); Grishchuk, L.P., and A.N. Petrov, 1986, *Pis'ma Astron. Zh.* 12, p. 429 (*Sov. Astron. Lett.*, 1986, 12, p. 179).

4. Grishchuk, L.P., 1990, *Usp. Fiz. Nauk* 160, p. 147 (*Sov. Phys. Usp.*, 1990, 33, p. 669).

5. Grishchuk, L.P., 1974, *Zh. Eksp. Teor. Fiz.* 67, p. 825 (*Sov. Phys. JETP*, 1974, 40, p. 409); Grishchuk, L.P., 1988, *Usp. Fiz. Nauk* 156, p. 297 (*Sov. Phys. Usp.*, 1988, 31, p. 940).

6. Schumacher, B.L., 1986, *Phys. Rep.* 135, p. 317; Yuen, H.P., 1976, *Phys. Rev. A* 13, p. 2226.

7. See special issues: 1987, *J. Opt. Soc. Am.* 84(10); 1987, *J. Mod. Opt.* 34(6,7).

8. Grishchuk, L.P., and Yu.V. Sidorov, 1990, *Phys. Rev. D* 42, p. 3413; Grishchuk, L.P., and Yu.V. Sidorov, 1989, *Class. Quantum Grav.* 6, p. L161.

9. Faller, J.E., P.L. Bender, J.L. Hall, D. Hils, R.T. Stebbins, and M.A. Vincent, 1989, *Adv. Space Res.* 9, p. 107.

SQUEEZED STATES: A GEOMETRIC FRAMEWORK[*]

S. T. Ali[a], J. A. Brooke[b]. J.-P. Gazeau[c]

[a] Department of Mathematics and Statistics
Concordia University
Montreal, Canada H4B 1R6

[b] Department of Mathematics
Florida Atlantic University
Boca Raton, FL 33431, USA
and
University of Saskatchewan
Saskatoon, Canada S7N 0W0

[c] Laboratoire de Physique Théorique et Mathématique
Université Paris 7, F–75251 Paris Cedex 05, France

ABSTRACT

A general definition of squeezed states is proposed and its main features are illustrated through a discussion of the standard optical coherent states represented by "Gaussian pure states" (Ref. 1).

The set–up involves representations of groups on Hilbert spaces over homogeneous spaces of the group, and relies upon the construction of a square integrable (coherent state) group representation modulo a subgroup (Ref. 2). This construction depends upon a choice of a Borel section which has a certain permissible arbitrariness in its selection; this freedom is attributable to a squeezing of the defining coherent states of the representation, and corresponds in this way to a sort of gauging.

AN EXAMPLE: GAUSSIAN PURE STATES

Gaussian pure states (GPS's), as defined by Schumaker (Ref. 3) and elaborated by Simon, Sudarshan and Mukunda (Ref. 1), are functions:

$$\psi(\vec{x}) = (\text{const}) \exp[P(\vec{x})] \qquad (1)$$

where $\vec{x} \in \mathbb{R}^n$ and $P(\vec{x})$ is a quadratic polynomial in $\vec{x}$ with complex coefficients:

$$P(\vec{x}) = -i/2 \ \vec{x}Z\vec{x} + i\vec{w} \cdot \vec{x} + w_0 \qquad (2)$$

with Z a symmetric ($Z^t = Z$) complex $n \times n$ matrix, $\vec{w} \in \mathbb{C}^n$, $w_0 \in \mathbb{C}$, and where, if $Z = V - iU$ is the decomposition into real and imaginary parts, then U is positive definite ($U > 0$).

Let G denote the semi–direct product of the Weyl–Heisenberg group $H(2n + 1)$ with the symplectic group $Sp(2n;\mathbb{R})$ of symplectic linear maps of $\mathbb{R}^{2n}$.

$$G = H(2n + 1) \oslash Sp(2n;\mathbb{R}). \qquad (3)$$

Multiplication in G is as follows:

$$g_1 g_2 = (c_1 c_2 \exp[i\Omega(Q_1, s_1 Q_2)/2], Q_1 + s_1 Q_2, s_1 s_2) \qquad (4)$$

where $g = (c, Q, s)$ denotes a general element of G; $(c, Q) \in H(2n + 1)$ where $|c| = 1$, $Q \in \mathbb{R}^{2n}$; $s \in Sp(2n;\mathbb{R})$; Ω is the symplectic structure on $\mathbb{R}^{2n}$ defined for $Q_r = (\vec{q}_r, \vec{p}_r)$, $r = 1,2$, by

$$\Omega(Q_1, Q_2) = \vec{p}_1 \cdot \vec{q}_2 - \vec{p}_2 \cdot \vec{q}_1.$$

Let $U(g)$, $g \in G$, denote the irreducible unitary representation of G on the Hilbert

space $\mathcal{H} = L^2(\mathbb{R}^n)$ whose restrictions to $H(2n+1)$ and $Sp(2n;\mathbb{R})$ are:

$$[U(c,Q)\psi](\vec{x}) = c \ \exp[i(\vec{p}\cdot\vec{x} - \vec{p}\cdot\vec{q}/2)]\psi(\vec{x} - \vec{q}) \tag{5}$$

and

$$[U(s)\psi](\vec{x}) = (2\pi)^{-n/2}(\det A)^{-1/2}$$
$$\times \int_{\mathbb{R}^n} \exp[iS(\vec{x},\vec{k})]\hat\psi(\vec{k})d\vec{k} \tag{6}$$

where

$$S(\vec{x},\vec{k}) = -1/2\vec{x}CA^{-1}\vec{x} + \vec{k}A^{-1}\vec{x} + 1/2\vec{k}A^{-1}B\vec{k},$$

$\hat\psi$ is the Fourier transform of ψ, and we assume $\det A \neq 0$ if $s = \begin{bmatrix} A & B \\ C & D \end{bmatrix} \in Sp(2n;\mathbb{R})$. Actually, U defines a double–valued representation of $Sp(2n;\mathbb{R})$, i.e., a representation of the metaplectic group, but this subtlety will be ignored here.

Some facts (see Refs. 1 and 4):

(i) Let $\psi_0 = \pi^{-n/4}\exp[-\vec{x}\cdot\vec{x}/2]$ be the special GPS with $U = I_n$, $V = O_n$, $\vec{w} = \vec{0}$, $w_0 = o$, and suppose ψ is any GPS. Then $\psi = (\text{const})U(g)\psi_0$ for some $g \in G$; moreover if $g' \in G$ also satisfies this condition then $g' = gk_0$ for some $k_0 \in K_0$:

$$K_0 = Sp(2n;\mathbb{R}) \cap O(2n;\mathbb{R}) \cong U(n) \tag{7}$$

which is a maximal compact subgroup of $Sp(2n;\mathbb{R})$, and conversely.

(ii) $Sp(2n;\mathbb{R})$ has a "block Iwasawa" decomposition:

$$Sp(2n;\mathbb{R}) = \bar{N}AK_0 \tag{8}$$

where $\quad \bar{N} = \left\{ \begin{bmatrix} I_n & O \\ -V & I_n \end{bmatrix} : V^t = V \right\},$

$$A = \left\{ \begin{bmatrix} \Delta & O_n \\ O_n & \Delta^{-1} \end{bmatrix} : \Delta^t = \Delta > 0 \right\},$$

$$K_0 = \left\{ \begin{bmatrix} a & b \\ -b & a \end{bmatrix} : a^t a + b^t b = I_n, \quad a^t b = b^t a \right\}.$$

Moreover, defining $U = \Delta^{-2}$ and

$$s(U,V) = \begin{bmatrix} I_n & O_n \\ -V & I_n \end{bmatrix} \begin{bmatrix} U^{-1/2} & O_n \\ O_n & U^{1/2} \end{bmatrix},$$

we have for $\psi \in \mathcal{H}$:

$$[U(s(U,V))\psi](\vec{x}) =$$
$$(\det U)^{1/4}\exp[i\vec{x}V\vec{x}/2]\psi(U^{1/2}\vec{x}) \tag{9}$$

and if $\psi = \psi_0$ in (i), $Z = V - iU$ then:

$$[U(s(U,V))\psi_0](\vec{x}) =$$
$$\pi^{-n/4}(\det U)^{1/4}\exp[-i\vec{x}Z\vec{x}/2] \tag{10}$$

(iii) A maximal compact subgroup K of G is:

$$K = U(1) \times K_0 \cong U(1) \times U(n) \tag{11}$$

where $U(1) = \{(c,O) \in H(2n+1)\}$, and with the same meaning for $U(1)$ define also:

$$H = U(1) \times Sp(2n;\mathbb{R}). \tag{12}$$

By Y we mean the homogeneous space:

$$Y = H/K \approx Sp(2n;\mathbb{R})/K_0 \tag{13}$$

which may be regarded as the set of positive symplectic matrices; these are uniquely expressible in the form $s(U,V)^{-1^t}s(U,V)^{-1}$ thereby establishing an identification of Y with the collection of GPS's centered at $Q = (\vec{0},\vec{0}) \in \mathbb{R}^{2n}$. By X we mean the homogeneous space:

$$X = G/H \approx \mathbb{R}^{2n} \tag{14}$$

the identification being through the map sending $(c,Q,s) \in G$ to $Q \in \mathbb{R}^{2n}$. In this way X inherits

the symplectic structure Ω which happens therefore to be G–invariant.

SQUEEZED COHERENT STATES

The theory of square integrable representations modulo a subgroup (Ref. 2) is immediately applicable in the present situation, and together with the notion of squeezing, to be outlined below, provides a convenient picture of GPS's. In what follows, a general discussion (example of which is the case of GPS's, same notation) will be given.

Let H be a closed subgroup of a Lie group G. Let $X = G/H$ and suppose $d\nu(x)$ is a left G–invariant measure on X (in general, $d\nu$ need only be quasi–invariant); let $\beta{:}X \rightarrow G$ denote a Borel section. Now suppose $U(g)$, $g \in G$, is an irreducible unitary representation on $\mathscr{H}$, and suppose there exists an admissible vector $\eta \in \mathscr{H}$ such that, as a weak integral:

$$\int_X | \eta_{\beta,x}> <\eta_{\beta,x}| \, d\nu(x) = A_\beta \qquad (15)$$

defines a bounded, positive operator A_β with (possibly unbounded) inverse; $\eta_{\beta,x}$ denotes the vector $U(\beta(x))\eta$ (example: notation as before with $\eta = \psi_0$, $x = Q$, $\beta(x) = (1,Q,I)$, $d\nu(x) = \Omega_Q \wedge \Omega_Q \wedge \cdots \wedge \Omega_Q$ (n factors), A_β is a multiple of the identity on $\mathscr{H}$). In this case U is square integrable mod (H,β), and $\{\eta_{\beta,x}\}$ is a family of coherent states for U.

Let K be a closed subgroup of H of k's:

$$U(k)\eta = \rho(k)\eta \qquad (16)$$

where ρ is a 1–dimensional unitary representation of K ($|\rho(k)| = 1$). Let $\gamma{:}Y = H/K \rightarrow H$ denote a Borel section, and define:

$$\sigma{:}X \times Y \rightarrow G, \quad \sigma(x,y) = \beta(x)\gamma(y) \qquad (17)$$

For fixed $y \in Y$, $\sigma(\cdot,y){:}X \rightarrow G$ is a Borel section and letting $\eta_{\sigma(\cdot,y),x} = U(\sigma(x,y))\eta$ it is easy to verify that U is square integrable mod $(H,\sigma(\cdot,y))$ for each $y \in Y$; in fact:

$$\int_X | \eta_{\sigma(\cdot,y),x}> <\eta_{\sigma(\cdot,y)x}| \, d\nu(x) = A_{\sigma(\cdot,y)} \qquad (18)$$

defines a bounded, positive invertible operator (which coincides with A_β here). The collection $\{\eta_{\sigma(\cdot,y),x}\}$, for y fixed, is a family of squeezed coherent states associated to $\{\eta_{\beta,x}\}$; one interprets $U(\gamma(y))$ as the squeezing operator defining a change of section $\beta(\cdot) \rightarrow \beta(\cdot)\gamma(y)$ (example: $k = (c,O,k_0)$, $\rho(k) = c$, $y = Z = V - iU$, $\gamma(y) = (1,O,s(U,V))$).

In this manner, squeezing in its general setting is describable in terms of changes of Borel section of the associated coherent state representation. Details of this general construction with examples will appear elsewhere.

REFERENCES

1. Simon, R.A., E. C. G. Sudarshan, and N. Mukunda, 1988, "Gaussian pure states in quantum mechanics and the symplectic group," Phys. Rev. A 37, pp 3028–3038.

2. Ali, S.T., J.–P. Antoine, and J.–P. Gazeau, 1991, to appear, "Square Integrability of Group Representations on Homogeneous Spaces I & II," Ann. Inst. H. Poincaré A.

3. Schumaker, B.L., 1986, Phys. Reports 135, 317.

4. Folland, G. B., 1989, Harmonic Analysis in Phase Space, Annals of Math. Studies #122, Princeton U. Press, Princeton.

Wormholes and Negative Energy from the Gravitationally Squeezed Vacuum

David Hochberg

Department of Physics and Astronomy, Vanderbilt University

Nashville, TN 37235

ABSTRACT

Minkowski-signature wormhole solutions of the Einstein field equations require the existence of negative energy density in the vicinity of their throats. In this note, we point out that the gravitational interaction automatically generates squeezed vacuum states of matter, which by thier nature, entail negative energy and thus provide a natural source for maintaining this class of wormholes.

1. Introduction

Wormholes are handles in the spacetime topology linking widely seperated regions of the Universe. Major insights have been made in the past few years in understanding general properties and physical consequences of Minkowski-signature wormholes [1-3]. A key aspect of wormholes discovered in [1] has to do with the type of matter and energy needed to thread the wormhole throat: it must violate the weak energy hypothesis. Although no known form of classical matter violates this energy condition, the squeezed vacuum does, and moreover, the coupling of matter to gravity leads automatically to the production of squeezed vacuum states [4]. The negative energy of the squeezed vacuum can be understood in simple terms. Consider a single mode oscillator. Its vacuum state is represented in phase space (from the Wigner distribution) by a circle centered at the origin. The squeezed vacuum state, by contrast, leads to an elliptical region. As this ellipse rotates (with the angular frequency of the mode), its periodic profile exhibits quantum fluctuations both larger and smaller than the uniform profile characteristic of the unsqueezed vacuum state. In field theory, the energy of the unsqueezed vacuum gets renormalized to zero. Thus, any state having lower fluctuations than the ordinary vacuum must have a negative (renormalized) energy.

2. Quantized scalar in a uniform gravitational field

We make these concepts explicit by showing that the interaction between matter and gravity leads to a squeeze operator acting on the Fock space of particle states, which includes the vacuum. We consider a scalar under the influence of a uniform background gravitational field. From the equivalence principle, this can be handled by transforming to a uniformly accelerating frame (i.e., Rindler space). Take the background field pointing in the x-direction. The transformation from Minkowski (t, x) to Rindler (T, X) is $x = X \cosh(T)$ and $t = X \sinh(T)$, and the scalar equation to be solved is

$$\Box \Phi + m^2 \Phi = 0. \tag{1}$$

The normalized solution is given by

$$\Phi_{k_\perp, j}(T, X; \mathbf{x}_\perp) = \pi^{-1}[\sinh(\pi j)]^{1/2} K_{ij}((m^2 + \mathbf{k}_\perp^2)^{1/2} X) e^{-ijT} e^{i\mathbf{k}_\perp \cdot \mathbf{x}_\perp}, \tag{2}$$

PRECEDING PAGE BLANK NOT FILMED

where K is a modified Bessel function of imaginary order, m is the scalar mass, $\mathbf{k}_\perp = (k_y, k_z)$ refers to the transverse momentum and $j \geq 0$. Contrast these Rindler modes with the familiar plane wave solutions of (1) for Minkowski space:

$$U_{\mathbf{k}} = \frac{e^{i(\mathbf{k} \cdot \mathbf{x} - \omega_{\mathbf{k}} t)}}{(2\pi)^{3/2} \sqrt{2\omega_{\mathbf{k}}}}, \tag{3}$$

where $\omega_{\mathbf{k}} = (m^2 + \mathbf{k}^2)^{1/2}$. The complete solution of (1) in Rindler or Minkowski space can be expanded in terms of the sets (2) and (3), respectively. The expansion coefficients become, after canonical quantization, operators satisfying the algebras $[\bar{a}(j, \mathbf{k}_\perp), \bar{a}^\dagger(j', \mathbf{p}_\perp)] = \delta(j, j')\delta(\mathbf{k}_\perp - \mathbf{p}_\perp)$ and $[a(\mathbf{k}), a^\dagger(\mathbf{k})] = \delta(\mathbf{k} - \mathbf{p})$ The Rindler and Minkowski vacua are defined by $\bar{a}|\bar{0}> = 0$ and $a|0> = 0$. Completeness of the two sets of modes (2) and (3) leads to nontrivial relations among the Minkowski and Rindler creation/annihilation operators:

$$a(\mathbf{k}) = \int dj\, d^2\mathbf{p}_\perp \, \alpha(j, \mathbf{p}_\perp | \mathbf{k})\bar{a}(j, \mathbf{p}_\perp) + \beta^*(j, \mathbf{p}_\perp | \mathbf{k})\bar{a}^\dagger(j, \mathbf{p}_\perp), \tag{4}$$

together with the Hermitian conjugate. The Bogolyubov coefficients in (4) are computed from the inner product and measure the overlap between the Rindler and Minkowski modes: $\alpha = (\Phi_{\mathbf{k}_\perp, j} | U_{\mathbf{p}})$ and $\beta = -(\Phi_{\mathbf{k}_\perp, j} | U_{\mathbf{p}}^*)$. A most important consequence of (4) is the *inequivalence* of the vacuum states $|\bar{0}>$ and $|0>$, and the Fock spaces built up from them. This inequivalence shows up physically as squeezing.

3. The Squeezed Vacuum

The free Hamiltonian for a massive scalar in Minkowski space is

$$H = \int d^3\mathbf{k} \, \omega_{\mathbf{k}} \, a^\dagger(\mathbf{k})a(\mathbf{k}), \tag{5}$$

where $\omega_{\mathbf{k}} = (m^2 + \mathbf{k}^2)^{1/2}$. From the point of view of the Rindler modes, (5) is a quasiparticle hamiltonian, and so the canonical transformation in (4) allows one to derive the exact interaction hamiltonian acting on Rindler states. One can also start from the exact Rindler hamiltonian, which has the same <u>form</u> as (5) when expressed in terms of the Rindler operators, and applying (4) leads to the exact Minkowski interaction hamiltonian. Since the intermediate momentum integrations are easier to carry out in the Minkowski picture, we derive the squeeze operator for Rindler states, but the equivalence principle guarantees the existence of an identical operator (expressed in Minkowski momenta) acting on the Minkowski modes. Using (4) and performing the intermediate integrations over the Minkowski momenta yields [4] $H = H_o + H'$ where

$$H_o = \int dj\, d^2\mathbf{p}_\perp \, \omega_{\mathbf{p}_\perp} h_1(j) \, \bar{a}^\dagger(j, \mathbf{p}_\perp)\bar{a}(j, \mathbf{p}_\perp), \tag{6}$$

and

$$H' = \int dj\, dj'\, d^2\mathbf{p}_\perp \, \omega_{\mathbf{p}_\perp} \left(h_2(j, j')[\bar{a}(j', \mathbf{p}_\perp)\bar{a}(j, -\mathbf{p}_\perp) + \bar{a}^\dagger(j', \mathbf{p}_\perp)\bar{a}^\dagger(j, -\mathbf{p}_\perp)] \right.$$

$$+h_1(j,j')\theta(j-j') + \theta(j'-j)\bar{a}^\dagger(j,\mathbf{p}_\perp)\bar{a}(j',\mathbf{p}_\perp)\Big) , \tag{7}$$

where

$$h_1(j,j') = \frac{\cosh[\pi(j+j')/2](1+(j-j')^2)^{-1}}{2\pi[\sinh(\pi j)\sinh(\pi j')]^{1/2}}, \text{ and } h_2(j,j') = \frac{-e^{-pi(j-j')/2}(1+(j+j')^2)^{-1}}{4\pi[\sinh(\pi j)\sinh(\pi j')]^{1/2}}, \tag{8}$$

are functions computed from the Bogolyubov coefficients [4]. We begin to see the operator structure characteristic of squeezing. To make this precise, consider the Schrödinger equation for a state of the scalar formulated in terms of the interaction picture. The above splitting of the Hamiltonian suggests writing the full time evolution operator as $U = U^\circ U'$ where $U^\circ(T) = e^{-iH_\circ T}$. The interaction Hamiltonian in the interaction picture is computed from $H_I'(T) = U^{\circ\dagger}(T) H' U^\circ(T)$ [4]. Then, the state of the scalar at any time T is simply given by

$$|\Phi(T)>_I = \mathcal{T} exp\left(-i/\hbar \int_{T_o}^T H_I'(T')dT'\right)|\Phi(T_o)>, \tag{9}$$

where the time evolution operator is a (multi-mode) squeeze operator, by virtue of (6) and (7). This is the main result. If we now identify the initial state with the Rindler vacuum, $|\Phi(T_o)>=|\bar{0}>$, the final state is precisely the gravitationally squeezed vacuum. Since every quantum field is equivalent to an infinite collection of (coupled) harmonic oscillators, it should come as no surprise that the evolution operator for Φ is just a multi-mode generalization of the single mode squeeze operator. If we specialize to two scalar modes having equal but opposite values of the transverse momentum and with $j = j'$, then the evolution operator in (9) reduces to

$$S(z) = exp\left(\frac{-i}{2}[z\bar{a}(j,\mathbf{p}_\perp)\bar{a}(j,-\mathbf{p}_\perp) - z^\star\bar{a}^\dagger(j,\mathbf{p}_\perp)\bar{a}^\dagger(j,-\mathbf{p}_\perp)]\right), \tag{10}$$

where $z = i\frac{h_2(j)}{h_1(j)}[e^{-2i\omega\mathbf{p}_\perp h_1(j)T} - 1]$ is the squeeze parameter for these modes. Apart from the bounded T-dependent factor, we see that appreciable squeezing obtains for $j \to 0$. Expressing j back in terms of physical quantities, we have $j = \frac{4\pi r_s}{\lambda}$, where λ is the mode wavlength and r_s is the Schwarzschild radius of the equivalent gravitational mass giving rise to the constant acceleration at the point r_s [4]. Thus, the interaction between matter and gravity leads to squeezed states of matter, and these provide a natural source of negative energy for supporting wormholes in Lorentzian spacetime.

1. M.S. Morris and K.S. Thorne, Am. J. Phys. **56** (1988) 395.

2. M. Visser, Phys. Rev. D39 (1989) 3182; Nucl. Phys. B328 (1989) 203; Phys. Lett B242 (1990) 24; Phys. Rev. D41 (1990) 1116; *ibid* D43 (1991) 402.

3. D. Hochberg, Phys. Lett. B**251** (1990) 349.

4. D. Hochberg and T.W. Kephart, *Lorentzian Wormholes from the Gravitationally Squeezed Vacuum*, VAND-TH-91-1 (April 1991).

Exact Solution of a Quantum Forced Time-Dependent Harmonic Oscillator

Kyu Hwang Yeon
Department of Physics, Chungbuk National University
Cheong Ju, Chungbuk 360-763, Korea

Thomas F. George
Departments of Chemistry and Physics & Astronomy, 239 Fronczak Hall
State University of New York at Buffalo, Buffalo, New York 14260, USA

Chung In Um
Department of Physics, College of Science
Korea University, Seoul 136-701, Korea

The Schrödinger equation is used to exactly evaluate the propagator, wave function, energy expectation values, uncertainty values and coherent state for a harmonic oscillator with a time-dependent frequency and an external driving time-dependent force. These quantities represent the solution of the classical equation of motion for the time-dependent harmonic oscillator.

I. Introduction

It is well known that an exact solution of the Schrödinger equation is possible only for special cases. For this reason, approximate methods are needed. Exact solutions provide important tests for these approximate methods and for various models of physical phenomena. In general, the solution of the Schrödinger equation for explicit time-dependent systems has met with limited success because of analytical difficulties, although progress has been made during the past three decades.[1-5] Camiz et al[6] have obtained the wave functions of a time-dependent harmonic oscillator perturbed by an inverse quadratic potential, using the Schrödinger formalism and a generating function. Further, Khandekar and Lawande[7] have evaluated the exact propagator and wave function for a time-dependent harmonic oscillator, both with and without an inverse quadratic potential, using Feynman path integrals. In addition, Jannussis et al[8] have calculated the propagator for several quantum mechanical systems with friction.

In a previous paper,[9] we have evaluated the propagator, wave function, energy expectation values, uncertainty values and transition amplitudes for a quantum damped driven harmonic oscillator by using path integral methods. Also, we have obtained the coherent state for the damped harmonic oscillator[10] and calculated the propagator for coupled driven harmonic oscillators.[11]

In this paper we discuss the exact quantum theory of a forced harmonic oscillator with a time-dependent frequency. In Sec. II we evaluate the propagator using the Schrödinger equation and path integral methods, and in Sec. III we calculate the wave functions using the propagator. In Sec. IV we define the energy operator and calculate energy expectation values. In Sec. V we obtain the uncertainty values. In Sec. IV we determine the coherent state and its properties. Finally, in Sec. VII we present results and a discussion.

II. Propagator

We consider a system whose classical Hamiltonian is of the form

$$H = \frac{1}{2M} p^2 + \frac{M}{2} \omega^2(t) x^2 - f(t)x \quad , \tag{2.1}$$

where x is a canonical coordinate, p is its conjugate momentum, $\omega(t)$ is a frequency as a function of time, M is a positive real mass, and $f(t)$ is an external driving force. The Lagrangian corresponding to the Hamiltonian (2.1) is

$$L = \frac{1}{2} M\dot{x}^2 - \frac{1}{2} M\omega^2(t)x^2 + f(t)x \quad . \tag{2.2}$$

Here, the Hamiltonian H and Lagrangian L depend on time. The classical equation of motion for our system is

$$\frac{d^2}{dt^2} x + \omega^2(t)x = \frac{1}{M} f(t) \quad . \tag{2.3}$$

For the case where $\omega(t) = \omega_0$ (constant), the solution of Eq. (2.3) represents harmonic motion; otherwise, it is difficult to evaluate the exact solution.

The path integral formulation of Feynman provides an alternate approach to solving dynamical problems in quantum mechanics.[12] In this approach, the usual Schrödinger equation is replaced by the integral equation

$$\psi(x,t) = \int dx' \, K(x,t;x't') \, \psi(x',t') \qquad (t > t') \tag{2.4}$$

with the initial condition $\psi(x,t) = \psi(x',t)$. Here, $\psi(x,t)$ is a wave function and $K(x,t; x',t')$ is a propagator. The propagator $K(x,t; x',t')$ is defined by the path integral[12]

$$K(x,t; x',t') = \lim \int_{(x',t')}^{(x,t)} \prod_{j=1}^{N-1} dx_j \, \exp[\frac{i}{\hbar} S(x,t; x',t')] \quad , \tag{2.5}$$

where the integration is over all possible paths from the point (x',t') to the point (x,t), and $S(x,t; x',t')$ is the action defined as

$$S(x,t; x',t') = \int_{t'}^{t} d\tau \ L(\dot{x},x,\tau) \ . \tag{2.6}$$

For a short time interval ϵ, substitution of Eqs. (2.2) and (2.6) into Eq. (2.5) gives the normalizing factor A_j and the usual Schrödinger equation:

$$A_j = (2i\pi\epsilon\hbar/M)^{\frac{1}{2}} \tag{2.7}$$

$$i\hbar \frac{\partial}{\partial t} \psi = - \frac{\hbar^2}{2M} \frac{\partial^2}{\partial x^2} \psi + \frac{1}{2} M\omega^2(t) x^2 \psi - f(t) x \psi \ . \tag{2.8}$$

Since $K(x,t; x't')$ can be thought of as a function of the variables (x,t) or of (x',t'), it is a special wave function, and it satisfies Eq. (2.8):

$$i\hbar \frac{\partial}{\partial t} K(x,t; x',t') = - \frac{\hbar^2}{2M} \frac{\partial^2}{\partial x^2} K(x,t;x',t') + \frac{1}{2} M\omega^2(t) x^2 K(x,t; x',t')$$

$$- f(t) x K(x,t;x',t'), \quad (t > t') \tag{2.9}$$

$$- i\hbar \frac{\partial}{\partial t'} K(x,t;x',t') = - \frac{\hbar^2}{2M} \frac{\partial^2}{\partial x'^2} K(x,t; x't') + \frac{1}{2} M\omega(t') x'^2$$

$$\times K(x,t;x',t') - f(t') x' K(x,t;x',t') \ ,$$

$$(t' > t) \ . \tag{2.10}$$

Because the Lagrangian is quadratic, the propagator has the form[12,13]

$$K(x,t; x't') = \exp[a(t,t')x^2 + b(t,t')xx' + c(t,t')x'^2 + g(t,t')x$$

$$+ h(t,t')x' + d(t,t')] \ , \tag{2.11}$$

where from Eqs. (2.9) and (2.10) we can easily deduce that the coefficient of the third and higher powers in x is zero.

Substituting Eq. (2.11) into Eqs. (2.9) and (2.10), we obtain the differential equations

$$\frac{d}{dt} a - \frac{2i\hbar}{M} a^2 + \frac{M}{2i\hbar} \omega^2(t) \tag{2.12}$$

$$\frac{d}{dt} (bx'+g) - \frac{2i\hbar}{M} a(bx'+g) + \frac{1}{\hbar} f(t) \tag{2.13}$$

$$\frac{d}{dt} (cx'^2+hx'+d) - \frac{i\hbar}{M} a + \frac{i\hbar}{2M} (bx'+g)^2 \tag{2.14}$$

$$\frac{d}{dt'} c - \frac{2\hbar}{Mi} c^2 + \frac{iM}{2\hbar} \omega(t')^2 \tag{2.15}$$

$$\frac{d}{dt'} (bx+h) - \frac{2\hbar}{Mi} c (bx+h) + \frac{f(t')}{i\hbar} \tag{2.16}$$

$$\frac{d}{dt'} (ax^2+gx+d) - \frac{\hbar}{2iM} (bx+h)^2 + \frac{\hbar}{Mi} c \quad . \tag{2.17}$$

Equations (2.12) and (2.15) are nonlinear equations. For the case where $\omega(t) - \omega_o$, a solution is easily found, but in other cases it is difficult to find an exact solution. If $q(t)$ obeys the differential equation

$$\frac{d^2}{dt^2} q(t) + \omega^2(t) q(t) - 0 \quad , \tag{2.18}$$

then the solutions of Eqs. (2.12)-(2.14) are

$$a(t) - \frac{iM}{2\hbar} \frac{\dot{q}(t)}{q(t)} \tag{2.19}$$

$$b(t)x' + g(t) - \frac{i}{\hbar} \frac{1}{q} [\int^t ds \, f(s)q(s) + b_o] \tag{2.20}$$

$$c(t)x'^2 + h(t)x' + d(t) - \ln q^{-\frac{1}{2}} + \frac{b_o^2}{2iM\hbar} \int^t \frac{ds}{q(s)^2} + \frac{b_o}{iM\hbar} \int^t \frac{ds}{q(s)^2}$$

$$\times \int^s dp \, f(p)q(p) + \frac{1}{2i\hbar M} \int^t \frac{ds}{q(s)^2} \int^s dp \, f(p)q(p) \int^s dr \, f(r)q(r) + d_o \quad , \tag{2.21}$$

where b_o and d_o are constants of integration and do not depend on t, and the solutions of Eqs. (2.15)-(2.17) are

$$c(t') - \frac{M}{2i\hbar} \frac{\dot{q}(t')}{q(t')} \tag{2.22}$$

$$b(t')x + h(t') - \frac{1}{i\hbar q} [\int^{t'} ds \, f(s)q(s) + b_o'] \tag{2.23}$$

$$a(t')x^2 + g(t')x + d(t') - \ln q(t')^{-\frac{1}{2}} + \frac{ib_0'^2}{2\not{h}M}\int^{t'}\frac{ds}{q(s)^2} + \frac{ib_0'}{M\not{h}}\int^t\frac{ds}{q(s)^2}$$

$$\times \int^s dp\, f(p)q(p) + \frac{1}{2iM\not{h}}\int^{t'}\frac{ds}{q(s)^2}\int^s dp\, f(p)q(p)\int^s dr\, f(r)q(r) + d_0' \quad , \qquad (2.24)$$

where b_0' and d_0' are constants of integration and independent of t'. Since only t is a variable in Eqs. (2.19)-(2.21), we have suppressed t' in $a(t,t')$, $b(t,t')$, etc., and we have similarly suppressed t in Eqs. (2.22)-(2.24).

In polar form we may write

$$q(t) - \eta(t)e^{i\gamma(t)} \quad , \qquad (2.25)$$

where $\eta(t)$ and $\gamma(t)$ are real quantities. From Eqs. (2.18) and (2.25) we note that

$$\ddot{\eta}(t) - \eta(t)\dot{\gamma}^2(t) + \omega^2(t)\,\eta(t) - 0 \qquad (2.26)$$

$$2\dot{\eta}(t)\dot{\gamma}(t) + \eta(t)\ddot{\gamma}(t) - 0 \qquad (2.27)$$

$$\eta^2(t)\dot{\gamma}(t) - \Omega \qquad (2.27')$$

where the constant Ω is a time-variant quantity. From Eqs. (2.26) and (2.27), we find another form for the solution of Eq. (2.18) as

$$q(t) - \eta(t)\sin(\gamma-\gamma') \qquad (2.28)$$

$$q(t') - \eta(t')\sin(\gamma-\gamma') \quad , \qquad (2.29)$$

where $\gamma - \gamma(t)$ and $\gamma' - \gamma(t')$.

Substitution of Eq. (2.28) into Eqs. (2.19) and (2.21) gives

$$a(t) - \frac{iM}{2\not{h}}\left[\frac{\dot{\eta}}{\eta} + \dot{\gamma}\cot(\gamma-\gamma')\right] \qquad (2.30)$$

$$b(t)x' + g(t) - \frac{ib_0}{\not{h}\eta\sin(\gamma-\gamma)} + \frac{1}{\not{h}\eta\sin(\gamma-\gamma')}\int^t ds\, \eta(s)f(s)\sin[\gamma(s)-\gamma'] \qquad (2.31)$$

$$c(t)x'^2 + h(t)x' + d(t) - \ln[\eta^{-\frac{1}{2}}\sin^{-\frac{1}{2}}(\gamma-\gamma')] + \frac{ib_0^2}{2\not{h}\Omega M}\cot(\gamma-\gamma')$$

$$+ \frac{b_o}{i\hbar\Omega M \sin(\gamma-\gamma')} \int^t ds \, f(s)\eta(s) \sin[\gamma(s)-\gamma')]$$

$$+ \frac{1}{2i\hbar\Omega M \sin(\gamma-\gamma')} \int^t ds \int^t dp \, f(s)f(p)\eta(s)\eta(p)$$

$$\times \sin[\gamma(s)-\gamma']\sin[\gamma(p)-\gamma'] \tag{2.32}$$

Furthermore, substitution of Eq. (2.29) into Eqs. (2.22) and (2.24) gives

$$c(t') - \frac{iM}{2\hbar} [- \frac{\dot{\eta}'}{\eta'} + \dot{\gamma}' \cot(\gamma-\gamma')] \tag{2.33}$$

$$b(t')x + h(t') - \frac{b_o'}{i\hbar\eta' \sin(\gamma-\gamma')} + \frac{1}{i\hbar\eta \sin(\gamma-\gamma')} \int^{t'} ds \, f(s)\eta(s)\sin[\gamma-\gamma(s)] \tag{2.34}$$

$$a(t')x^2 + g(t')x + d(t') - \ln[\eta'^{-\frac{1}{2}} \sin^{-\frac{1}{2}}(\gamma-\gamma')] + \frac{ib_o'^2}{2\hbar\Omega M} \cot(\gamma-\gamma')$$

$$- \frac{ib_o'}{\hbar\Omega M \sin(\gamma-\gamma')} \int^{t'} ds \, f(s)\eta(s) \sin[\gamma-\gamma(s)]$$

$$+ \frac{1}{2i\Omega\hbar M \sin(\gamma-\gamma')} \int^{t'} ds \int^{t'} dp \, f(s)f(p)\eta(s)\eta(p)$$

$$\times \sin[\gamma(s)-\gamma]\sin[\gamma(p)-\gamma] \quad . \tag{2.35}$$

From Eqs. (2.31), (2.32), (2.34) and (2.35), we deduce that the constants b_o and b_o' are given as

$$b_o - -M\dot{\gamma}'\eta'x' \tag{2.36}$$

$$b_o' - M\dot{\gamma}\eta x \quad . \tag{2.37}$$

Also, from the normalization condition,

$$d_0 - \ln(\frac{M}{2\pi\hbar})^{\frac{1}{2}} \quad . \tag{2.38}$$

From Eqs. (2.30)-(2.37) and (2.27'), we find that

$$a(t,t') = \frac{iM}{2\hbar}\left[\frac{\dot{\eta}}{\eta} + \dot{\gamma}\cot(\gamma-\gamma')\right] \tag{2.39}$$

$$c(t,t') = \frac{iM}{2\hbar}\left[-\frac{\dot{\eta}'}{\eta'} + \dot{\gamma}'\cot(\gamma-\gamma')\right] \tag{2.40}$$

$$b(t,t') = -\frac{iM}{\hbar}\frac{\sqrt{\dot{\gamma}\dot{\gamma}'}}{\sin(\gamma-\gamma')} \tag{2.41}$$

$$g(t,t') = \frac{i}{\hbar}\frac{\sqrt{\dot{\gamma}}}{\sin(\gamma-\gamma')}\int_{t'}^{t}ds\,\frac{f(s)}{\sqrt{\dot{\gamma}(s)}}\sin[\gamma(s)-\gamma] \tag{2.42}$$

$$h(t,t') = \frac{i}{\hbar}\frac{\sqrt{\dot{\gamma}'}}{\sin(\gamma-\gamma')}\int_{t'}^{t}ds\,\frac{f(s)}{\sqrt{\dot{\gamma}(s)}}\sin[\gamma-\gamma(s)] \tag{2.43}$$

$$d(t,t') = -\frac{1}{2M\hbar}\frac{1}{\sin(\gamma-\gamma')}\int_{t'}^{t}ds\,\frac{f(s)}{\sqrt{\dot{\gamma}(s)}}\sin[\gamma-\gamma(s)]\int_{t'}^{t}dp\,\frac{f(p)}{\sqrt{\dot{\gamma}(p)}}$$

$$\times\,\sin[\gamma(p)-\gamma'] \tag{2.44}$$

Inserting Eqs. (2.39)-(2.44) in Eq. (2.11), we obtain the propagator for the forced time-dependent harmonic oscillator as

$$K(x,t;x't') = \left[\frac{M\,(\dot{\gamma}'\dot{\gamma})^{\frac{1}{2}}}{2\pi i\hbar\,\sin(\gamma-\gamma')}\right]$$

$$\times\,\exp\left[\frac{iM}{2\hbar}\left(\frac{\dot{\eta}}{\eta}x^2 - \frac{\dot{\eta}'}{\eta'}x'^2\right)\right]$$

$$\times\,\exp\left\{\frac{i\,M}{2\hbar\,\sin(\gamma-\gamma')}\left[(\dot{\gamma}x^2 + \dot{\gamma}'x'^2)\cos(\gamma-\gamma') - 2\sqrt{\dot{\gamma}\dot{\gamma}'}\,xx'\right.\right.$$

$$+\frac{2\sqrt{\dot{\gamma}}}{M}x\int_{t'}^{t}ds\,\frac{f(s)}{\sqrt{\dot{\gamma}(s)}}\sin[\gamma(s)-\gamma']$$

$$+\frac{2\sqrt{\dot{\gamma}'}}{M}x'\int_{t'}^{t}ds\,\frac{f(s)}{\sqrt{\dot{\gamma}(s)}}\sin[\gamma-\gamma(s)]$$

$$\left.\left.-\frac{1}{M^2}\int_{t'}^{t}ds\,\frac{f(s)}{\sqrt{\dot{\gamma}(s)}}\sin[\gamma-\gamma(s)]\int_{t'}^{t}dp\,\frac{f(p)}{\sqrt{\dot{\gamma}(p)}}\sin[\gamma(p)-\gamma']\right]\right\}\,,$$

$$\tag{2.45}$$

where the unprimed and the primed variables denote the quantities which are functions of time t and t', respectively. It may be easily verified that for the case where $\omega(t)$ is a real positive constant ω_o, we have $\eta(t) = 1$ and $\gamma(t) = \omega_o t$,

and the propagator of Eq. (2.45) reduces to the usual expression for a forced harmonic oscillator.[12]

III. Wave function

We now rewrite the propagator in another form in order to derive the wave function:

$$
K(x,t: x't') = \left[\frac{M\ (\dot{\gamma}'\dot{\gamma})^{1/2}}{2\pi i \hbar\ \sin(\gamma-\gamma')}\right]^{1/2}
$$

$$
\times \exp\left[\frac{iM}{2\hbar}\left\{\left[\frac{\dot{\eta}}{\eta}\ x^2 + \frac{2}{M}\overline{\sqrt{\dot{\gamma}}}\ x\int^t ds\ \frac{f(s)}{\sqrt{\dot{\gamma}(s)}}\ \cos[\gamma-\gamma(s)]\right]\right.\right.
$$

$$
\left.\left.- \left[\frac{\dot{\eta}'}{\eta'}\ x'^2 + \frac{2}{M}\overline{\sqrt{\dot{\gamma}'}}\ x'\int^{t'} ds\ \frac{f(s)}{\sqrt{\dot{\gamma}(s)}}\ \cos[\gamma'-\gamma(s)]\right]\right\}\right]
$$

$$
\times \exp\left[\frac{iM}{2\hbar}\cot(\gamma-\gamma')\left\{\left[\overline{\sqrt{\dot{\gamma}}}\ x - \frac{1}{M}\int^t ds\ \frac{f(s)}{\sqrt{\dot{\gamma}(s)}}\ \sin[\gamma-\gamma(s)]\right]^2\right.\right.
$$

$$
\left. + \left[\overline{\sqrt{\dot{\gamma}'}}\ x' - \frac{1}{M}\int^{t'} ds\ \frac{f(s)}{\sqrt{\dot{\gamma}(s)}}\ \sin[\gamma'-\gamma(s)]\right]^2\right\}
$$

$$
- \frac{iM}{\hbar}\ \frac{1}{\sin(\gamma-\gamma')}\left\{\left[\overline{\sqrt{\dot{\gamma}}}\ x - \frac{1}{M}\int^t ds\ \frac{f(s)}{\sqrt{\dot{\gamma}(s)}}\ \sin[\gamma-\gamma(s)]\right]\right.
$$

$$
\left.\left. \times \left[\overline{\sqrt{\dot{\gamma}'}}x' - \frac{1}{M}\int^{t'} ds\ \frac{f(s)}{\sqrt{\dot{\gamma}(s)}}\ \sin[\gamma'-\gamma(s)]\right]\right\}\right]
$$

$$
\times \exp\left[\frac{1}{2\hbar M}\left\{\cot(\gamma-\gamma')\left[\int^t ds\ \frac{f(s)}{\sqrt{\dot{\gamma}(s)}}\ \sin[\gamma-\gamma(s)]\right]^2\right.\right.
$$

$$
+ \cot(\gamma-\gamma')\left[\int^{t'} dp\ \frac{f(p)}{\sqrt{\dot{\gamma}(p)}}\ \sin[\gamma'-\gamma(p)]\right]^2
$$

$$
+ \frac{2}{\sin(\gamma-\gamma')}\int^t ds\ \sin(\gamma-\gamma_s)\int^{t'} dp\ \frac{f(p)}{\sqrt{\dot{\gamma}(p)}}\ \sin[\gamma'-\gamma(p)]
$$

$$
- \frac{1}{\sin(\gamma-\gamma')}\int^t_{t'} ds\ \frac{f(s)}{\sqrt{\dot{\gamma}(s)}}\ \sin[\gamma-\gamma(s)]\int^t_{t'} dp\ \frac{f(p)}{\sqrt{\dot{\gamma}(p)}}
$$

$$
\left.\left. \times \sin[\gamma(p)-\gamma']\right\}\right] \tag{3.1}
$$

$$- \left(\frac{M}{\pi\hbar}\right)^{\frac{1}{2}} (\dot{\gamma}')^{\frac{1}{2}}(\dot{\gamma})^{\frac{1}{2}} \frac{e^{-i(\gamma-\gamma')}}{1 - e^{-2i(\gamma-\gamma')}}$$

$$\times \exp\left[\frac{iM}{2\hbar}\left\{\left[\frac{\dot{\eta}}{\eta} x^2 + \frac{2}{M} \sqrt{\dot{\gamma}} x \int^t ds \frac{f(s)}{\sqrt{\dot{\gamma}(s)}} \cos[\gamma-\gamma(s)]\right]\right.\right.$$

$$\left.\left. - \left[\frac{\dot{\eta}'}{\eta'} x'^2 + \frac{2}{M} \sqrt{\dot{\gamma}'} x' \int^t ds \frac{f(s)}{\sqrt{\dot{\gamma}(s)}} \cos[\gamma'-\gamma(s)]\right]\right\}\right]$$

$$\times \exp\left[\frac{M}{2\hbar}\left\{\left[\sqrt{\dot{\gamma}} x - \frac{1}{M} \int^t ds \frac{f(s)}{\sqrt{\dot{\gamma}(s)}} \sin[\gamma-\gamma(s)]\right]^2\right.\right.$$

$$\left.\left. + \left[\sqrt{\dot{\gamma}'}x' - \frac{1}{M} \int^{t'} ds \frac{f(s)}{\sqrt{\dot{\gamma}(s)}} \sin[\gamma'-\gamma(s)]\right]^2\right\}\right]$$

$$\times \exp\left[\frac{-M}{\hbar[1-e^{-2i(\gamma-\gamma')}]}\left\{\left[\sqrt{\dot{\gamma}} x - \frac{1}{M} \int^t ds \frac{f(s)}{\sqrt{\dot{\gamma}(s)}} \sin[\gamma-\gamma(s)]\right]^2\right.\right.$$

$$+ \left[\sqrt{\dot{\gamma}'}x' - \frac{1}{M} \int^{t'} ds \frac{f(s)}{\sqrt{\dot{\gamma}(s)}} \sin[(\gamma-\gamma(s)]\right]^2$$

$$- 2\left[\sqrt{\dot{\gamma}} x - \frac{1}{M} \int^t ds \frac{f(s)}{\sqrt{\dot{\gamma}(s)}} \sin[\gamma-\gamma(s)]\right]\left[\sqrt{\dot{\gamma}'}x'\right.$$

$$\left.\left. - \frac{1}{M} \int^{t'} ds \frac{f(s)}{\sqrt{\dot{\gamma}(s)}} \sin[\gamma'-\gamma(s)]\right]\right\}\right] e^{-i\theta(t)}e^{i\theta(t')} \quad , \tag{3.2}$$

where

$$\theta(t') - \theta(t) = \frac{1}{2\hbar M} \left\{\cot(\gamma-\gamma')\left[\int^t ds \frac{f(s)}{\sqrt{\dot{\gamma}(s)}} \sin[\gamma-\gamma(s)]\right]^2\right.$$

$$+ \cot(\gamma-\gamma')\left[\int^{t'} ds \frac{f(s)}{\sqrt{\dot{\gamma}(s)}} \sin[\gamma'-\gamma(s)]\right]^2 + 2 \frac{1}{\sin(\gamma-\gamma')}$$

$$\times \int^t ds \frac{f(s)}{\sqrt{\dot{\gamma}(s)}} \sin[\gamma-\gamma(s)] \int^{t'} dp \frac{f(p)}{\sqrt{\dot{\gamma}(p)}} \sin[\gamma'-\gamma(p)]$$

$$\left. - \int^t_{t'} ds \frac{f(s)}{\sqrt{\dot{\gamma}(s)}} \sin[\gamma-\gamma(s)] \int^t_{t'} dp \frac{f(p)}{\sqrt{\dot{\gamma}(p)}} \sin[\gamma(p)-\gamma']\right. \quad . \tag{3.3}$$

Let us introduce Mehler's formula,[14]

355

$$\frac{\exp[-(X^2+Y^2-2XY)/(1-Z^2)]}{\sqrt{1-Z^2}} = e^{-(X^2+Y^2)} \sum_{n=0}^{\infty} \frac{Z^n}{2^n n!} H_n(X) H_n(Y) \tag{3.4}$$

where

$$X = \sqrt{\tfrac{\bar{M}}{\hbar}} \left[\sqrt{\dot{\bar{\gamma}}} \, x + \frac{1}{M} \int_0^t ds \, \frac{f(s)}{\sqrt{\dot{\gamma}(s)}} \sin[\gamma-\gamma(s)] \right] \tag{3.5}$$

$$Y = \sqrt{\tfrac{\bar{M}}{\hbar}} \left[\sqrt{\dot{\bar{\gamma}}'} \, x' - \frac{1}{M} \int^{t'} ds \, \frac{f(s)}{\sqrt{\dot{\gamma}(s)}} \sin[\gamma'-\gamma(s)] \right] \quad . \tag{3.6}$$

$$Z = e^{-i(\gamma-\gamma')} \tag{3.7}$$

Substituting Eqs. (3.4)-(3.7) in Eq. (3.2), we obtain

$$K(x,t;\, x',t) = \sum_{n=0}^{\infty} \psi_n^*(x,t) \, \psi_n(x',t') \quad , \tag{3.8}$$

where

$$\psi_n(x,t) = \left[\frac{1}{2^n n!} \left(\frac{M\dot{\gamma}}{\pi\hbar} \right)^{1/2} \right]^{1/2} \exp\left\{ \frac{iM}{2\hbar} \left[\frac{\dot{\eta}}{\eta} \, x^2 - \frac{2}{M} \sqrt{\dot{\bar{\gamma}}} \, \ddot{x} \int^t ds \, \frac{f(s)}{\sqrt{\dot{\gamma}(s)}} \cos[\gamma-\gamma(s)] \right] \right\}$$

$$\times \exp\left\{ \frac{M}{2\hbar} \left[\sqrt{\dot{\bar{\gamma}}} \, x - \frac{1}{M} \int^t ds \, \frac{f(s)}{\sqrt{\dot{\gamma}(s)}} \sin[\gamma-\gamma(s)] \right]^2 \right\}$$

$$\times H_n \left\{ \sqrt{\frac{M\dot{\gamma}}{\hbar}} \left[x - \frac{1}{M\sqrt{\dot{\gamma}}} \int^t ds \, \frac{f(s)}{\sqrt{\dot{\gamma}(s)}} \sin[\gamma-\gamma(s)] \right] \right\}$$

$$\times \, e^{i[\theta(t)-(n+\frac{1}{2})\gamma(t)]} \quad . \tag{3.9}$$

Moreover, we may write

$$\psi_n(x,t) = \exp\{i[\theta(t) - (n+\tfrac{1}{2})\gamma(t)]\} \, \phi_n(x,t) \quad , \tag{3.10}$$

where

$$\phi_n(x,t) = \left[\frac{1}{2^n n!} \left(\frac{M\dot{\gamma}}{\pi\hbar} \right)^{1/2} \right]^{1/2} \exp\left\{ \frac{iM}{2\hbar} \left[\frac{\dot{\eta}}{\eta} \, x - \frac{2}{M} \sqrt{\dot{\bar{\gamma}}} \, x \int^t ds \, \frac{f(s)}{\sqrt{\dot{\gamma}(s)}} \cos[\gamma-\gamma(s)] \right] \right\}$$

$$\times \exp\left\{\frac{M}{2\hbar}\left[\dot{\bar{\gamma}} \; x - \frac{1}{M} \int^{t} ds \; \frac{f(s)}{\sqrt{\dot{\gamma}(s)}} \sin[\gamma-\gamma(s)]\right]^2\right\}$$

$$\times \; H_n\left[\sqrt{\frac{\bar{M}}{\hbar}}\left\{\dot{\bar{\gamma}}x - \frac{1}{M} \int^{t} ds \; \frac{f(s)}{\sqrt{\dot{\gamma}(s)}} \sin[\gamma-\gamma(s)]\right\}\right] \quad . \tag{3.11}$$

In Eq. (3.10), the wave function $\psi_n(x,t)$ is merely a unitary transformation of $\phi_n(x,t)$, and thus $\phi_n(x,t)$ satisfies all the properties associated with $\psi_n(x,t)$:

$$\int dx \; \psi_n^* \psi_n - \langle m|n \rangle - \int dx \; \phi_n^* \phi_n - \delta_{m,n} \quad . \tag{3.12}$$

The expectation value of a given operator O is

$$\langle m|O|n \rangle - \int dx \; \psi_n^* \; O\psi_n - \int dx \; \phi_n^* O\phi_n \quad . \tag{3.13}$$

IV. Energy expectation values

For the forced time-dependent harmonic oscillator system, both the Hamiltonian and Lagrangian have the units of energy but depend on time. We must therefore find a time-invariant energy operator. If $\beta(t)$ is a particular solution of Eq. (2.3), we have

$$\frac{d^2}{dt^2} (x-\beta) + \omega^2(t) (x-\beta) - 0 \quad , \tag{4.1}$$

and from Eqs. (2.26) and (2.27') we note that

$$\ddot{\eta} + \omega^2(t) \; \eta - \Omega^2/\eta^3 \quad . \tag{4.2}$$

From Eqs. (4.1) and (4.2), we get the following expression for the energy:

$$E - \frac{1}{2M} (\eta p - M\dot{\eta}x)^2 + (M\dot{\eta}x - \eta p)(\beta\dot{\eta}-\eta\dot{\beta}) + \frac{M}{2}(\beta\dot{\eta}-\eta\dot{\beta})^2 + \frac{M}{2} \Omega^2(\frac{x-\beta}{\eta})^2 \quad . \tag{4.3}$$

Because Eq. (4.3) is time invariant, we can use it for the quantum mechanical energy operator,

$$E_{op} - -\frac{\hbar^2\eta^2}{2M} \frac{\partial^2}{\partial x^2} + \frac{M}{2}(\dot{\eta}^2+\eta\dot{\gamma}^2)x^2 - \frac{\eta\dot{\eta}}{2} (2x\frac{\partial}{\partial x} + 1)$$

$$+ (\beta\dot{\eta}-\eta\dot{\beta})(i\hbar\frac{\partial}{\partial x} + M\dot{\eta}x) + M\eta\dot{\gamma}^2\beta x + \frac{M}{2} \eta\dot{\gamma}^2\beta^2 + \frac{M}{2}(\beta\dot{\eta}-\eta\dot{\beta})^2 \quad . \tag{4.4}$$

Equation (3.11) now simplifies to the expression

$$\phi_n(x,t) = \left(\frac{\delta}{2^n n! \sqrt{\pi}}\right)^{\frac{1}{2}} e^{i\mu x^2 + i\lambda x} e^{-\frac{1}{2}\delta^2(x-\beta)^2} H_n[\delta(x-\beta)]$$

$$= \left(\frac{\delta}{2^n n! \sqrt{\pi}}\right)^{\frac{1}{2}} e^{Ax^2 + Bx} H_n[\delta(x-\beta)] \quad , \tag{4.5}$$

where

$$\delta = (M\gamma/\hbar)^{\frac{1}{2}} \tag{4.6}$$

$$\mu(t) = \frac{M}{2\hbar} \frac{\dot{\eta}}{\eta} \tag{4.7}$$

$$\lambda(t) = \frac{1}{\hbar} \sqrt{\dot{\gamma}} \int^t ds \frac{f(s)}{\sqrt{\dot{\gamma}(s)}} \cos[\gamma - \gamma(s)] \tag{4.8}$$

$$\beta(t) = \frac{1}{M\sqrt{\dot{\gamma}}} \int^t ds \frac{f(s)}{\sqrt{\dot{\gamma}(s)}} \sin[\gamma - \gamma(s)] \tag{4.9}$$

$$A = i\mu - \delta^2/2 \tag{4.10}$$

$$B = i\lambda + \beta\delta^2 \quad . \tag{4.11}$$

Here, $\beta(t)$ is a particular solution of Eq. (2.3).

In order to evaluate the energy expectation $E_{m,n} = \langle m|E_{op}|n\rangle$, we perform the following calculations:

$$x|n\rangle = \frac{1}{\sqrt{2}\delta} [\sqrt{n+1}|n+1\rangle + \sqrt{n}|n-1\rangle] \tag{4.12}$$

$$x^2|n\rangle = \frac{1}{2\delta^2} [\sqrt{(n+2)(n+1)}|n+2\rangle + (2n+1)|n\rangle + \sqrt{n(n-1)}|n-2\rangle] \tag{4.13}$$

$$p|n\rangle = \frac{\hbar A}{i\delta} 2(n+1)|n\rangle + \frac{\hbar}{i} B|n\rangle + \frac{\hbar}{i}(\delta + \frac{A}{\delta}) \sqrt{2n}|n-1\rangle \tag{4.14}$$

$$p^2|n\rangle = -\hbar^2 [\frac{2A^2}{\delta^2} \sqrt{(n+2)(n+1)}|n+2\rangle + 2\sqrt{2} \frac{AB}{\delta} \sqrt{n+1}|n\rangle + 2(A+\frac{A^2}{\delta^2})(2n+1)|n\rangle$$

$$+ 2\sqrt{2} \frac{AB}{\delta} + \delta B)\sqrt{n}|n-1\rangle + 2(\frac{A^2}{\delta^2}+2A+\delta^2)\sqrt{n(n-1)}|n\rangle] \tag{4.15}$$

$$xp|n\rangle = \frac{\hbar}{i}\{\frac{A}{\delta^2}\sqrt{(n+2)(n+1)}|n+2\rangle + \frac{B}{\sqrt{2}\delta}\sqrt{n+1}|n+1\rangle + [\frac{A}{\delta^2}(2n+1)+n]|n\rangle$$

$$+ \frac{B}{\sqrt{2}\delta}\sqrt{n}|n-1\rangle + (\frac{A}{\delta^2}+1)\sqrt{n(n+1)}|n-2\rangle\} \tag{4.16}$$

$$px|n\rangle = xp|n\rangle + |n\rangle \quad . \tag{4.17}$$

Substituting Eqs. (4.6)-(4.17) into Eq. (4.4), we directly obtain the energy expectation values as

$$E_{n,n} = E_n = \frac{\hbar}{2}(\eta^2\dot{\gamma})(2n+1)$$

$$= \Omega\hbar(n+\frac{1}{2}) \quad . \tag{4.18}$$

This energy expectation value is a time-invariant quantity.

V. Uncertainty values

The uncertainty product defined as

$$(\Delta x\Delta p)_{m,n} = \{[(\langle m|x^2|n\rangle - \langle m|x|n\rangle^2)^*(\langle m|x^2|n\rangle - \langle m|x|n\rangle^2)]^{\frac{1}{2}}$$

$$\times [(\langle m|p^2|n\rangle - \langle m|p|n\rangle^2)^*(\langle m|p^2|n\rangle - \langle m|p|n\rangle^2)]^{\frac{1}{2}}\}^{\frac{1}{2}} \quad . \tag{5.1}$$

Inserting Eqs. (4.12)-(4.15) into Eq. (5.1), we obtain

$$(\Delta x\Delta p)_{n,n} = (1 + \frac{\dot{\eta}^2}{\dot{\gamma}^2\eta^2})^{\frac{1}{2}}(n+\frac{1}{2})\hbar \tag{5.2}$$

$$(\Delta x\Delta p)_{n+2,n} = (1 + \frac{\dot{\eta}^2}{\dot{\gamma}^2\eta^2})^{\frac{1}{2}}\sqrt{(n+2)(n+1)}\hbar \tag{5.3}$$

$$(\Delta x\Delta p)_{n,n+2} = (1 + \frac{\dot{\eta}^2}{\dot{\gamma}^2\eta^2})^{\frac{1}{2}}\sqrt{n(n-1)}\hbar \quad . \tag{5.4}$$

VI. Coherent states of the time-dependent harmonic oscillator

First, we construct the creation operator $a^\dagger$ and destruction operator a. For a forced time-dependent harmonic oscillator, it is not possible to construct a and $a^\dagger$, but we can construct a and $a^\dagger$ for the time dependent harmonic oscillator. From Eqs. (4.12) and (4.14), we obtain

$$a^\dagger = (\frac{M\dot{\gamma}}{2\hbar})^{1/2} [(1 + \frac{\dot{\eta}}{\eta\dot{\gamma}}) x - i\frac{p}{M\dot{\gamma}}] \tag{6.1}$$

$$a = (\frac{M\dot{\gamma}}{2\hbar})^{1/2} [(1 - i\frac{\dot{\eta}}{\eta\dot{\gamma}}) x + i\frac{p}{M\dot{\gamma}}] \tag{6.2}$$

From Eqs. (6.1) and (6.2), we can represent (x,p) in terms of $(a^\dagger, a)$ as

$$x = (\frac{\hbar}{2M\dot{\gamma}})^{1/2} (a^\dagger + a) \tag{6.3}$$

$$p = (\frac{\hbar M\dot{\gamma}}{2})^{1/2} [(\frac{\dot{\eta}}{\eta\dot{\gamma}} + i) a^\dagger + (\frac{\dot{\eta}}{\eta\dot{\gamma}} - i)a] \quad . \tag{6.4}$$

Also from Eqs. (6.1) and (6.2), if $[x,p] = i\hbar$ we see that

$$[a^\dagger, a] = 1 \quad . \tag{6.5}$$

Conversely, from Eqs. (6.3) and (6.4), if $[a^\dagger, a] = 1$ we note that $[x,p] = i\hbar$.

The coherent state can be defined by the eigenstate of the nonhermitian operator a,[15]

$$a|\alpha> = \alpha|\alpha> \quad . \tag{6.6}$$

Let us find the coordinate representation of the coherent state. From Eqs. (6.2) and (6.3), we have

$$(\frac{M\dot{\gamma}}{2\hbar})^{1/2} [(1 - i\frac{\dot{\eta}}{\eta\dot{\gamma}}) x + \frac{\hbar}{M\dot{\gamma}} \frac{\partial}{\partial x'}] <x'|\alpha> = \alpha<x'|\alpha> \quad . \tag{6.7}$$

We solve this equation and change the variable x' into x for convenience,

$$<x|\alpha> = N \exp [\frac{M\dot{\gamma}}{2\hbar}(-1 + i\frac{\dot{\eta}}{\eta\dot{\gamma}}) x^2 + (\frac{2M\dot{\gamma}}{\hbar})^{1/2} \alpha x] \quad . \tag{6.8}$$

We choose the constant of integration N such that

$$\int dx \ |<x|\alpha>|^2 = 1 \quad . \tag{6.9}$$

Then, we find the eigenvector of the operator a in the coordinate representation $|x>$ as

$$\langle x|\alpha\rangle = (\frac{M\dot{\gamma}}{\pi\hbar})^{\frac{1}{2}} \exp[\frac{M\dot{\gamma}}{2\hbar}(-1 + i\frac{\dot{n}}{\eta\gamma}) x^2 + (\frac{2M\dot{\gamma}}{\hbar})^{\frac{1}{2}} \alpha x - \frac{1}{2}|\alpha|^2 - \frac{1}{2}\alpha^2] \quad . \qquad (6.10)$$

Next, we show that a coherent state is a minimum uncertainty state. From Eqs. (6.3), (6.4) and (6.6) and their adjoints, we evaluate the expectation values of x, p, x^2 and p^2 in the state $|\alpha\rangle$:

$$\langle\alpha|x|\alpha\rangle = (\frac{\hbar}{2M\dot{\gamma}})^{\frac{1}{2}} (\alpha^* + \alpha) \qquad (6.11)$$

$$\langle\alpha|p|\alpha\rangle = (\frac{M\hbar\dot{\gamma}}{2})^{\frac{1}{2}} [(\frac{i}{\eta\dot{\gamma}} + 1)\alpha^* + (\frac{i}{\eta\dot{\gamma}} - 1)\alpha] \qquad (6.12)$$

$$\langle\alpha|x^2|\alpha\rangle = \frac{\hbar}{2M\dot{\gamma}} \langle\alpha|a^{+2} + a^2 + aa^+ + a^+a|\alpha\rangle$$

$$= \frac{\hbar}{2M\dot{\gamma}} (\alpha^{*2} + \alpha^2 + 2\alpha\alpha^* + 1) \qquad (6.13)$$

$$\langle\alpha|p^2|\alpha\rangle = \frac{\hbar M\dot{\gamma}}{2} \{(\frac{\dot{n}}{\eta\dot{\gamma}} + 1)^2 \alpha^{*2} + (\frac{\dot{n}}{\eta\dot{\gamma}} - 1)^2\alpha^2$$

$$+ [(\frac{\dot{n}}{\eta\dot{\gamma}})^2 + 1](2\alpha\alpha^* + 1)\} \quad . \qquad (6.14)$$

The uncertainty value is

$$\Delta x\Delta p = [(\langle\alpha|x^2|\alpha\rangle - \langle\alpha|x|\alpha\rangle)(\langle\alpha|p^2|\alpha\rangle - \langle\alpha|p|\alpha\rangle)]^{\frac{1}{2}}$$

$$= \hbar/2 [1 + (\frac{\dot{n}}{\eta\dot{\gamma}})^2]^{\frac{1}{2}} \quad , \qquad (6.15)$$

which is the minimum value allowed by Eq. (5.2).

VII. Results and discussion

In the previous sections, we have obtained the propagator, wave function, energy expectation values, uncertainty values and coherent state for a quantum forced time-dependent harmonic oscillator. These quantities represent the solution of the classical equation of motion for the time-dependent harmonic oscillator. If we set f(t) equal to zero, then our solution is correct for the time-dependent harmonic oscillator. Setting $\omega(t) = \omega_o$ gives results for the forced harmonic

oscillator. For the case where $f(t) = 0$ and $\omega(t) = \omega_o$, our results are those of the simple harmonic oscillator.

For the explicit time-dependent system, we need to consider the quantum mechanical operator. In our work, the Hamiltonian, Lagrangian and mechanical energy have the units of energy, but these are not time invariant. Yet, in order to solve macroscopic physical problems, we use time-invariant operators. For this reason, we have derived the energy operator from the classical equation of motion and used it to calculate energy expectation values. Our energy operator is similar to the Ermakov-Lewis invariant operator.[1,2] Our quantum energy expectation vlaues are time-independent quantities, and our uncertainty values are consistent with Heisenberg's uncertainty principle. Yet, our uncertainty values are time dependent, in contrast to those of time-independent systems.

Since it is not possible to construct a coherent state for the forced time-dependent harmonic oscillator, we have constructed it for the time-dependent harmonic oscillator. In general, the coherent state is a minimum uncertainty state, which is also true for our system.

Time-dependent systems are observed in various physical experiments. Two general types of such systems are: that which is formed through its own environmental conditions, and that which is formed when external forces are added. In regard to the second type, various experiments are being carried out to see how an applied, time-dependent electric, magnetic or other field can alter the physical properties of materials such as semiconductors and superconductors. Experiments show that a system becomes time dependent when a time-dependent electric or magnetic field (such as a.c.) is applied. However, obtaining the quantum mechanical solution by a direct method is not easy mathematically. One way of obtaining a solution is to use the propagator method as indicated in this paper, where the relevant equations are those of a time-dependent harmonic oscillator.

Our results, which are exact for one dimension, can be extended to two or more dimensions, and they can also be applied to time-dependent macroscopic systems. One example of an extension to two dimensions would be to solve the motion of a quantum electron in a time-dependent magnetic field.

References

1. H. R. Lewis, Jr., Phys. Rev. Lett. $\underline{18}$, 510, 636 (1967).

2. H. R. Lewis, Jr., J. Math. Phys. $\underline{9}$, 1976 (1968).

3. P. G. L. Leach, J. Math. Phys. $\underline{10}$, 1902 (1977).

4. J. R. Burgan, M. R. Felx, E. Fijalkow and A. Munier, Phys. Lett. A $\underline{74}$, 11 (1979).

5. J. G. Hartly and J. R. Ray, Phys. Rev. A $\underline{24}$, 2873 (1981).

6. P. Camiz, A. Gerardi, C. Marchioro, E. Presutti and E. Scacciatelli, J. Math. Phys. $\underline{12}$, 2040 (1971).

7. D. C. Khandekar and S. V. Lawande, J. Math. Phys. $\underline{16}$, 384 (1975).

8. A. D. Jannussis, C. N. Brodimas and A. Streclas, Phys. Lett. A $\underline{74}$, 6 (1979).

9. C. I. Um, K. H. Yeon and W. H. Kahng, J. Phys. A $\underline{20}$, 611 (1987).

10. K. H. Yeon, C. I. Um and T. F. George, Phys. Rev. A $\underline{36}$, 5287 (1987).

11. K. H. Yeon, C. I. Um, W. H. Kahng and T. F. George, Phys. Rev. A $\underline{38}$, 6224 (1988).

12. R. P. Feynman and A. R. Hibbs, *Quantum Mechanics and Path Integrals* (McGraw-Hill, New York, 1965).

13. G. J. Papadopoulous, Phys. Rev. D $\underline{11}$, 2870 (1975).

14. A. Erdelyi, *Higher Transcendental Functions*, Vol. 2 (McGraw-Hill, New York, 1953), p. 194.

15. W. H. Louisell, *Quantum Statistical Properties of Radiation* (Wiley, New York, 1973).

Nonclassical Depth of a Quantum State*

628197

4 pr

Ching Tsung Lee

Department of Physics, Alabama A & M University, Normal, Alabama 35762

A measure is defined for how nonclassical a quantum state is, with values ranging from 0 to 1. When it is applied to the photon-number states, the calculated value is 1, the maximum possible. For squeezed states, it is a monotonically increasing function of the squeeze parameter with values varying from 0 to 1/2. The physical meaning of the nonclassical depth is found to be just the number of thermal photons necessary to ruin the nonclassical nature of the quantum state.

In the coherent-state description of radiation fields, initiated by Glauber (Ref. 1) and Sudarshan (Ref. 2) in 1963, there are P and Q representations corresponding to the normal and antinormal ordering, respectively, of the creation and annihilation operators. Their distribution, or quasi-distribution, functions in the complex plane are related to each other through the following convolution transform (Ref. 3):

$$Q(z) = \int \frac{d^2 w}{\pi} e^{-|z-w|^2} P(w),$$ (1)

where z and w are complex variables. We can introduce a continuous parameter τ and define a general distribution function as

$$R(z, \tau) = \frac{1}{\tau} \int \frac{d^2 w}{\pi} \exp\left(-\frac{1}{\tau}|z - w|^2\right) P(w).$$ (2)

We shall call $R(z, \tau)$ the R function from now on. The original P and Q functions are two limiting cases of the R function with $\tau = 0$ and 1, respectively.

Our motivation for introducing the τ parameter is to define a measure of how nonclassical quantum states are. It is well known that the origin of the nonclassical effects is that the P functions of all pure quantum states are singular and not positive definite, as shown by Hillery (Ref. 4); hence it is called quasi-distribution function. On the other hand, the Q function is always a positive definite regular function. The smoothing effect of the convolution transform of Eq. (2) is enhanced as τ increases. If τ is large enough so that the R function becomes acceptable as a classical distribution function, *i.e.*, it is a positive definite regular function, then we say that the smoothing operation is complete. Let C denote the set of all the τ that will complete the smoothing of the P function of a quantum state and let the greatest lower bound, or infimum, of all the τ in C be denoted by

$$\tau_m \equiv \inf_{\tau \in C} (\tau).$$ (3)

We propose to adopt τ_m as the nonclassical depth of the quantum state.

According to this definition, we have $\tau_m = 0$ for an arbitrary coherent state $|\alpha\rangle$ since its P function is of the form of a delta function, $\pi \delta^2(z - \alpha)$. On the other hand, for $\tau = 1$ we have $R(z, 1) = Q(z)$, which is always acceptable as a classical distribution function for any quantum state; hence, 1 is an upper bound for τ_m. Therefore, we can specify the range of τ_m to be

$$0 \leq \tau_m \leq 1.$$ (4)

We shall try this definition on two of the most familiar types of nonclassical radiation states: the photon-number (Fock) states and the squeezed states.

For a photon-number state $|n\rangle$, we obtain

$$R_n(z,\tau) = \frac{1}{\tau}\left(-\frac{1-\tau}{\tau}\right)^n \exp\left(-\frac{|z|^2}{\tau}\right) L_n\left(\frac{|z|^2}{\tau(1-\tau)}\right),$$

(5)

where L_n is the Laguerre polynomial. From Eq. (5), we see that, for $0 < \tau < 1$, $R_n(z,\tau)$ is not positive definite since the Laguerre polynomial has n real positive roots. However, for $\tau \geq 1$, the argument of the Laguerre polynomial is negative and $R_n(z,\tau)$ becomes positive definite. So we have $\tau_m = 1$, which reconfirms our belief that the photon-number states are the most nonclassical quantum states.

For the squeezed state generated from the vacuum state by the well-known squeeze operator $S(\zeta)$ with the complex parameter $\zeta \equiv re^{i\theta}$, we obtain the Gaussian function

$$R_\zeta(z,\tau) = \frac{(\operatorname{sech} r)}{\sqrt{D}} \exp\left\{-\frac{1}{D}[ax^2 + 2bxy + bx^2]\right\}$$

(6)

with

$$a = \tau + (1-\tau)\tanh^2 r - \cos\theta \tanh r, \qquad b = \sin\theta \tanh r,$$
$$c = \tau + (1-\tau)\tanh^2 r + \cos\theta \tanh r, \qquad D = \tau^2 - (1-\tau)^2 \tanh^2 r.$$

(7)

For $R_\zeta(z,\tau)$ to be normalizable we must have

$$ac - b^2 > 0 \quad \text{and} \quad D > 0.$$

(8)

Both conditions lead to the same conclusion that

$$\tau_m = \tanh r/(1 + \tanh r).$$

(9)

This nonclassical depth can be expressed as a function of the squeeze parameter, $s \equiv e^r$, as follows:

$$\tau_m(s) = (s^2 - 1)/2s^2.$$

(10)

From Eq. (10) we see that τ_m is a monotonically increasing function of s; it varies from 0 to 1/2 as s varies from 1 to ∞.

In the first example, τ_m is determined by the requirement that $R_n(z,\tau)$ be positive definite; while in the second example, it is determined by the condition that $R_\zeta(z,\tau)$ be normalizable. Is there a more systematic way to determine τ_m? To answer this question, we need to study more examples.

As a by-product of such calculations, we will also obtain new expressions for the P functions as follows:

$$P(z) = \lim_{\tau \to 0} R(z,\tau).$$

(11)

Since the P function of a quantum state is typically highly singular, it is usually very difficulty to visualize in its original form. Now we can visualize it as the limit of the regular R function as $\tau \to 0$.

On the other hand, we consider the superposition of two quantum states with $P_1(z)$ and $P_2(z)$ as their P functions. According to Glauber (Ref. 5) the P function for the superposed state is the convolution product of $P_1(z)$ and $P_2(z)$; namely,

$$P_{su}(z) = \int \frac{d^2z}{\pi} P_1(z-w)P_2(w) \tag{12}$$

It is well known that the P function for a single-mode thermal radiation is (Ref. 5)

$$P_{th}(z) = \frac{1}{\langle n_{th} \rangle} \exp\left(-|z|^2/\langle n_{th} \rangle\right), \tag{13}$$

where $\langle n_{th} \rangle \equiv \left(e^{\hbar\omega/kT} - 1\right)^{-1}$ is the *average photon number* in the thermal radiation.

We now consider the superposition of the thermal radiation with an arbitrary state of single-mode radiation with $P(z)$ as its P function. Then the P function of this quantum state with thermal noise can be expressed as

$$P_{su}(z) = \frac{1}{\langle n_{th} \rangle} \int \frac{d^2w}{\pi} \exp\left(-|z-w|^2/\langle n_{th} \rangle\right) P(w) \tag{14}$$

Comparing Eqs. (1) and (14) we see that the superposed P function, $P_{su}(z)$, is identical to the Q function when $\langle n_{th} \rangle = 1$. The implication of this coincidence can be stated as follows: *One thermal photon is always sufficient to destroy whatever nonclassical effects any single-mode radiation might have.*

The R function for the superposed state of Eq. (14) can be obtained as

$$R_{su}(z, \tau) = \frac{1}{\tau + \langle n_{th} \rangle} \int \frac{d^2w}{\pi} \exp\left[-|z-w|^2/(\tau + \langle n_{th} \rangle)\right] P(w). \tag{15}$$

Therefore, we have

$$\tau_m^{th} = \tau_m - \langle n_{th} \rangle; \tag{16}$$

which means that the reduction in the nonclassical depth of a quantum state in the presence of thermal noise is exactly equal to the average number of thermal photons present. This also gives the following physical meaning to the nonclassical depth we have defined previously: *The nonclassical depth of a quantum state is the minimum number of thermal photons necessary to destroy any of its nonclassical characteristics.*

We have previously calculated the nonclassical depth of a Fock state to be exactly 1, so it takes one thermal photon to ruin the nonclassical nature of a Fock state. We have also calculated the nonclassical depth of a squeezed state to varies from 0 to 1/2 as s varies from 1 to ∞; so it never takes more than 1/2 of a thermal photon to ruin a squeezed state.

---

1. Glauber, R. J., 1963, "Photon Correlations," Phys. Rev. Lett., 10(3), p. 84.
2. Sudarshan, E. C. G., 1963, "Equivalence of Semiclassical and Quantum mechanical Descriptions of Statistical Light Beams," Phys. Rev. Lett., 10(7), p. 277.
3. Cahill, K. E., and Glauber, R. J., 1969, "Density Operators and Quasiprobability Distributions," Phys. Rev., 177(5), p. 1882.
4. Hillery, M., 1985, "Classical Pure States Are Coherent States," Phys. Lett., 111A(8,9), p. 409.
5. Glauber, R. J., 1963, "Coherent and Incoherent States of the Radiation Field," Phys. Rev., 131(6), p. 2766.

TOWARDS A WAVE THEORY OF CHARGED BEAM TRANSPORT: A COLLECTION OF THOUGHTS

G. Dattoli, C. Mari, and A. Torre
ENEA - Area INN, Dip. Sviluppo Tecnologie di Punta,
P.O. Box 65 - 00044 Frascati, Rome, Italy

ABSTRACT

In this paper we formulate in a rigorous way a wave theory of charged beam linear transport. The Wigner distribution function is introduced and provides the link with classical mechanics. Finally the Von-Neumann equation is shown to coincide with the Liouville equation for the linear transport.

INTRODUCTION

A formal "quantum" theory of charged beam transport has been recently proposed. (Ref. 1) Within such a context the possibility of viewing the beam emittance as a kind of quantization constant has been considered on the basis of some strong conceptual similarities existing with the so-called "quantum" theory of light rays. (Ref. 2)

The proposed quantization procedure (described in some detail below) cannot be thought as fully satisfactory and in particular the role played by the "beam wave function" (b.w.f.) and its link with classical dynamics have not ben thoroughly investigated and clarified.

In this paper we develop, in a more rigorous way, the fundamental steps towards a "quantum" theory of beam transport through linear elements, showing the relation with classical mechanics and discussing the connections with the Liouville equation which describes the time evolution of non-interacting classical ensembles. We will show that classical dynamics and the Courant-Snyder theory (Ref. 3) can be recovered by using the formalism of the Wigner phase-space function, (Ref. 4) which therefore can be seen as the natural framework to study the evolution of charged beam transport through linear magnetic systems.

The paper is organized as follows. In Sect. 1 we review some aspects of symplectic mechanics (Ref. 5) and introduce some definitions which will be useful in Sect. 2 where the "quantum" theory of charged linear transport will be completely developed in terms of the Wigner phase-space function. Some comments and final remarks on the "quantum" theory of nonlinear charged transport conclude this paper.

1. SYMPLECTIC MECHANICS OF QUADRATIC HAMILTONIANS

The most general time dependent quadratic Hamiltonian in one degree of freedom can be written as

$$H = \frac{1}{2}a(t)q^2 + \frac{1}{2}b(t)p^2 + c(t)qp \tag{1.1}$$

or in a matrix form as

$$H = \frac{1}{2}\underline{z}^T \hat{H} \underline{z} \tag{1.2}$$

where

$$\underline{z} = \begin{pmatrix} q \\ p \end{pmatrix}, \quad \hat{H}_0 = \begin{pmatrix} a(t) & c(t) \\ c(t) & b(t) \end{pmatrix} \tag{1.3}$$

and the superscript "T" denotes transpose.

The equations of motion for the vector $\underline{z}$ are obtained from the Poisson Brackets (P.B.) with the Hamiltonian (1.1). The relevant rules are easily derived. It is quite straightforward to realize that

$$\{\underline{z}, \underline{z}^T\} = \hat{S} = \begin{pmatrix} 0 & 1 \\ -1 & 0 \end{pmatrix} \tag{1.4a}$$

and that

$$\{\underline{z}, \underline{z}^T \hat{B} \underline{z}\} = 2\hat{S}\hat{B}\underline{z} \quad {}^* \tag{1.4b}$$

where $\hat{S}$ is the unit symplectic matrix in two dimensions. According to the above rules the equations of motion of $\underline{z}$ are easily written, namely,

$$\dot{\underline{z}} = \{\underline{z}, \underline{z}^T \hat{H} \underline{z}\} = \hat{S}\hat{H}\underline{z} \tag{1.5}$$

and therefore immediately integrated, thus yielding

$$\underline{z}(t) = \hat{U}(t)\underline{z}(0) \tag{1.6}$$

where

---

* Note that $\{\underline{z}^T, \underline{z}\} = 0$ and therefore the above product cannot be, strictly speaking, considered a conventional P.B. In the case that the second term in the $\{,\}$-product is a scalar function [as in Eq. (1.4b)] then the $\{,\}$ is a conventional P.B.

$$\hat{U}(t) = \left\{ \exp\left[\hat{S} \int_0^t \hat{H}(t')dt' \right] \right\}_+ \qquad (1.7)$$

and $\{,\}_+$ denotes time ordering for the classical evolution operator which is necessary when the commutator $[\hat{S}\hat{H}(t), \hat{S}\hat{H}(t')]$ is different from zero.

The above formalism is particularly useful to introduce the fluctuation tensor and its dynamical features, namely, let us pose

$$\hat{\Sigma}(t) = \langle \underline{z}(t)\underline{z}^T(t) \rangle - \langle \underline{z} \rangle \langle \underline{z}^T \rangle \qquad (1.8)$$

where $\langle , \rangle$ denotes ensemble average.

In a matrix form we recover the usual expression

$$\hat{\Sigma}(t) = \begin{pmatrix} \sigma_q^2 & \sigma_{pq}^2 \\ \sigma_{pq}^2 & \sigma_p^2 \end{pmatrix} \qquad (1.9)$$

The equation of motion of $\hat{\Sigma}$ follows from Eq. (1.5) and reads

$$\frac{d}{dt}\hat{\Sigma}(t) = \hat{V}\hat{\Sigma} + \hat{\Sigma}\hat{V}^T \qquad (1.10)$$

where $\hat{V} = \hat{S}\hat{H}$, and can be immediately integrated in terms of the above evolution operator $\hat{U}$ thus getting

$$\hat{\Sigma}(t) = \hat{U}(t)\hat{\Sigma}(0)\hat{U}^T(t) \qquad (1.11)$$

Within this formalism it is easy to recover the well-known quadratic invariant of Courant-Snyder, namely, let us write the most general quadratic (time dependent) expression in $\underline{z}$

$$I = \underline{z}^T \hat{T}(t)\underline{z} \qquad (1.12)$$

where

$$\hat{T}(t) = \begin{pmatrix} \gamma & \alpha \\ \alpha & \beta \end{pmatrix} \qquad (1.13)$$

Then we impose that I is a "time-dependent" invariant, i.e.,

$$\frac{dI}{dt} \equiv \frac{\partial I}{\partial t} + \{I, H\} = 0 \qquad (1.14)$$

thus obtaining the following equations specifying α, β, γ

$$\begin{cases} \dot{\beta} = -2b\alpha + 2c\beta & \beta(0) = \beta_0 \\ \dot{\gamma} = 2a\alpha - 2c\gamma & \gamma(0) = \gamma_0 \\ \dot{\alpha} = a\beta - \beta\gamma & \alpha(0) = \alpha_0 \end{cases} \qquad (1.15)$$

from which it is easy to verify that

$$\beta\gamma = 1 + \alpha^2 \qquad (1.16)$$

The Courant-Snyder invariant reads explicitly as

$$I = \gamma q^2 + 2\alpha pq + \beta p^2 \qquad (1.17)$$

and it is widely used in the theory of linear transport.

2. TOWARDS A QUANTIZED THEORY

In the previous section we introduced the necessary background to derive a kind of uncertainty principle in the theory of linear transport. From Eq. (1.11) we get the relevant result

$$\det \hat{\Sigma}(t) = \det \hat{\Sigma}(0) \qquad (2.1)$$

i.e., $\det \hat{\Sigma}$ is an invariant quantity and the emittance A of the system

$$A(t) = [<q^2><p^2> - <qp>^2]^{1/2} \qquad (2.2)$$

is preserved in time.

Furthermore this means that

$$\sigma_q \sigma_p \geq A$$

which represents a kind of uncertainty principle in the canonical variables q, p and can be used as the starting point of our quantization procedure.

The rules are simple, the beam momentum is replaced by an operator specified by

$$p = \frac{A}{i} \frac{\partial}{\partial q} \qquad (2.3)$$

where A is the beam reduced emittance and the following rule of commutation is also assumed:

$$[p, q] = -iA \qquad (2.4)$$

A "Hamiltonian" operator is finally associated to the longitudinal coordinate of propagation s

$$\hat{H} = i\hbar \frac{\partial}{\partial s} \qquad (2.5)$$

so that the "Schrödinger" equation for a beam passing through a quadrupole of strength $k(s)$ reads

$$i\hbar \frac{\partial}{\partial s} \psi(q,s) = \left[-\frac{\hbar^2}{2} \frac{\partial^2}{\partial q^2} + \frac{1}{2} k(s) q^2 \right] \psi(q,s) \qquad (2.6)$$

where $\psi(q,s)$ denotes the beam wave function (b.w.f.). Clearly the b.w.f. $\psi(q,s)$ must be related in some way to the "classical" beam distribution $\rho(q,p,s)$ satisfying the Liouville equation for the time evolution of an ensemble of single-particle systems. The link is not obvious since ψ depends only on q and eventually on s while p is a function of q,p and s. The answer is given by the Wigner distribution function which is defined as follows:

$$W(q,p,s) = \frac{1}{\pi} \int_{-\infty}^{+\infty} dy\, \psi^* \left(q + \frac{1}{2} y, s \right) \psi \left(q - \frac{1}{2} y, s \right) e^{ipy/\hbar} \qquad (2.7)$$

and satisfies the Von-Neumann equation for a generic potential $V(q)$ (Ref. 6)

$$i \left[\frac{\partial}{\partial s} + p \frac{\partial}{\partial q} \right] W(q,p,s) = \hbar^{-1} \left[V \left(q + \frac{i}{2} \hbar \frac{\partial}{\partial p} \right) - V \left(q - \frac{i}{2} \hbar \frac{\partial}{\partial p} \right) \right] W(q,p,s) \qquad (2.8)$$

In the above-considered case of propagation through a quadrupole of strength $k(s)$ i.e., for an elastic potential $V(q) = \frac{1}{2} k(s) q^2$, the Von-Nuemann equation reduces to

$$\frac{\partial}{\partial s} W(q,p;s) = - \left[p \frac{\partial}{\partial q} - k(s) q \frac{\partial}{\partial p} \right] W(q,p;s) \qquad (2.9)$$

which is equivalent to the Liouville classical equation. In this simple case we can identify the classical distribution density ρ with the Wigner distribution function W thus providing a completely consistent quantization scheme. Within this framework the physically meaningful quantity is not $|\psi(q,s)|^2 dq$ but $W(q,p;s) dq dp$ which ensures the consistency of our procedure.

As a simple exercise it is straightforward to see that

$$W(q,p;s) = \frac{1}{(2\pi)(A/2)} \exp\left[-\frac{1}{2} \frac{\gamma(s)q^2 + 2\alpha(s)qp + \beta(s)p^2}{(A/2)}\right] \qquad (2.10)$$

is a solution of (2.9) if and only if the "time-dependent" parameters (α,β,γ) satisfy the following system of differential equations:

$$\begin{cases} \beta' = -2\alpha \\ \alpha' = k(s)\beta - \gamma \\ \gamma' = 2k(s)\alpha \end{cases} \qquad (2.11)$$

which are the well-known equations defining the evolution of the Twiss parameters in quadrupole lenses [see Eq. (1.15)].

3. CONCLUDING REMARKS

The extension of the developed theory to the case of nonlinear transport of charged beams is not straightforward and the problems involved can be illustrated in a simple example.

A sextupole term introduces, in the single-particle Hamiltonian, a contribution of the type

$$V(q,s) = \frac{\lambda(s)}{3} q^3 \qquad (3.1)$$

Inserting the above potential in the Von-Neumann equation (2.8) we easily get the following evolution equation for the Wigner distribution function:

$$\frac{\partial}{\partial s} W(q,p;s) = -\underbrace{\left[p\frac{\partial}{\partial q} - \lambda(s)q^2\frac{\partial}{\partial p}\right]}_{\hat{L}} W(q,p;s)$$

$$-\frac{\lambda(s)}{12} A^2 \frac{\partial^3}{\partial p^3} W(q,p;s) \qquad (3.2)$$

where $\hat{L}$ denotes the Liouville operator associated to the potential (3.1) and given by $\hat{L} = -p\frac{\partial}{\partial q} + \lambda q^2\frac{\partial}{\partial p}$. The extra term in Eq. (3.2) is a purely "quantum" contribution and it is not present in the classical Liouville equation for $\rho(q,p;s)$. From this point of view W and ρ cannot be identified and since they coincide in the limit $A \to 0$, ρ may be viewed as the "classical" counterpart of the Wigner distribution function W.

REFERENCES

1. Dattoli, G., Gallerano, G.P., Mari, C., Torre, A., and Richetta, M., "Twiss Parameters and Evolution of Quantum Harmonic Oscillator States," accepted for publication in <u>Il Nuovo Cimento</u>.
   Fedele, R., Miele, A., and Ricciardi, G., 1989, <u>Thermal Wave Model behind the Envelope Equation for the Final Focus in a Linear Collider</u>, INFN Report IFUP-TH 11/89.

2. Gloge, D., and Marcuse, D., 1969, <u>JOSA</u>, 59, p. 1629.

3. Courant, E., and Snyder, H., 1958, <u>Ann. Phys.</u>, 3, p. 1.

4. Wigner, E.P., 1932, <u>Phys. Rev. A</u>, 40, p. 749.
   Han, D., Kim, Y.S., and Noz, M.E., 1988, <u>Phys. Rev. A</u>, 37, p. 807; 1989, <u>Phys. Rev. A</u>, 40, p. 902 and 1990, <u>Phys. Rev. A</u>, 41, p. 6233.

5. Dattoli, G., Mari, C., and Torre, A., 1991, <u>Il Nuovo Cimento B</u>, 2, p. 201.

6. Carruthers, P., and Zachariasen, F., 1983, <u>Rev. Mod. Phys.</u>, 55, p. 245.

Entropic uncertainty relation at finite temperature

Sumiyoshi Abe[a] and Norikazu Suzuki[b]

(a) Institute for Theoretical Physics, University of Erlangen-Nürnberg, W-8520 Erlangen, Germany
(b) Max-Planck-Institute for Nuclear Physics, W-6900 Heidelberg, Germany
and Department of Physics, College of Science and Technology, Nihon University, Tokyo 101, Japan

The uncertainty relation associated with the measurements of a generic noncommutative pair of observables (A, B) in a normalized state $|\psi\rangle$ is usually expressed as

$$\Delta A \cdot \Delta B \geq \frac{1}{2} |\langle \psi | [A, B] | \psi \rangle|. \tag{1}$$

For a canonically conjugate pair, the position and momentum of a particle (X, P), this equation gives the original Heisenberg uncertainty relation $\Delta X \cdot \Delta P \geq \frac{1}{2}, (\hbar \equiv 1)$. On the other hand, if the commutator $[A, B]$ remains as a q-number, the r.h.s. depends on the state $|\psi\rangle$ and can be made arbitrarily small. For example, if $|\psi\rangle$ is chosen as an eigenstate of A, then Eq.(1) becomes trivial and no information can be extracted on ΔB. Thus this formulation of the uncertainty principle has no practical meanings in general.

To improve the situation, the information-theoretic formulation of the uncertainty principle has been repeatedly studied in the recent literature. Deutsch[1] and Partovi[2] discussed that the sum of entropies,

$$U[A, B : \psi] = S_A[\psi] + S_B[\psi], \tag{2}$$

has an irreducible lower bound independent of the choice of $|\psi\rangle$. Here, the information entropy associated with the measurement of A is defined by

$$S_A[\psi] = -\mathsf{S}_\alpha |\langle \alpha | \psi \rangle|^2 \ln |\langle \alpha | \psi \rangle|^2, \quad (A|\alpha\rangle = \alpha |\alpha\rangle), \tag{3}$$

where S_α stands for the summation (integration) over the discrete (continuous) spectra. This is a quantity dependent on the choice of the representation $|\alpha\rangle$ in general and is not expressed as a quantum mechanical expectation value of a certain operator.

Prior to the authors of Refs.[1, 2], Bialynicki-Birula and Mycielski[3] discussed the sum (2) for the pair (X, P) and proved the optimal relation

$$U[X, P : \psi] \geq 1 + \ln \pi. \tag{4}$$

Here we discuss that how much information loses when a particle is in equilibrium with the thermal reservoir of temperature $T(= 1/\beta)$[4]. The universal temperature correction to the r.h.s. of Eq.(4) is determined.

For this purpose, it is convenient to employ the framework of *thermo field dynamics* (TFD) formulated by Takahashi and Umezawa[5]. This formulation of finite-temperature $(T \neq 0)$ quantum theory utilizes the doubled Hilbert space $\mathcal{H} \otimes \tilde{\mathcal{H}}$[6], the *normal* operator (A) acting on the objective space $\mathcal{H}$ and its corresponding *tildian* operator $(\tilde{A})$ on the fictitious space $\tilde{\mathcal{H}}$.

A thermal state $|\psi, \tilde{\psi}; \beta\rangle$ in $\mathcal{H} \otimes \tilde{\mathcal{H}}$ is not a physical state. The physical probability density associated with the measurement of the normal operator A is given by the reduced one

$$\rho_R(\alpha) = \mathsf{S}_{\tilde{\alpha}} |\langle \alpha, \tilde{\alpha} | \psi, \tilde{\psi}; \beta \rangle|^2, \tag{5}$$

where $|\alpha, \tilde{\alpha}\rangle$ is the complete eigenbasis of A and $\tilde{A}$. With this quantity, we define the information entropy at $T \neq 0$ as follows:

$$S_A[\psi, \tilde{\psi}; \beta] = -\mathsf{S}_\alpha \rho_R(\alpha) \ln \rho_R(\alpha). \tag{6}$$

Now we wish to find the stationary value of the functional

$$U[X, P : \psi, \tilde{\psi}; \beta] = S_X[\psi, \tilde{\psi}; \beta] + S_P[\psi, \tilde{\psi}; \beta], \tag{7}$$

at given T. In what follows, we propose a variational approach.

We are not concerned with the whole system including the tildian but only with the reduced one. Therefore, the minimum value of the functional U at given T can be determined completely within the reduced subsystem. This philosophy should be also respected by the variational operation itself. The operation proposed here is as follows:

$$|\psi, \tilde{\psi}; \beta\rangle \rightarrow |\psi, \tilde{\psi}; \beta\rangle + \epsilon|\xi, \tilde{\psi}; \beta\rangle, \tag{8}$$

where ϵ and ξ denote an infinitesimal variation parameter and an arbitrary deformation of the $\mathcal{H}$ component, respectively. Under this operation, the functional U of the normalized thermal state $|\psi, \tilde{\psi}; \beta\rangle$ varies as

$$U[X, P : \psi, \tilde{\psi}; \beta] \rightarrow U[X, P : \psi, \tilde{\psi}; \beta] + \epsilon\Gamma + o(\epsilon^2), \tag{9}$$

$$\Gamma \equiv [\int dx \rho_R(x) \ln \rho_R(x) + \int dp \rho_R(p) \ln \rho_R(p)]\langle \psi, \tilde{\psi}; \beta | \xi, \tilde{\psi}; \beta\rangle$$
$$- \int \int dx \, d\tilde{x} \ln [\rho_R(x)]\langle \psi, \tilde{\psi}; \beta | x, \tilde{x}\rangle\langle x, \tilde{x} | \xi, \tilde{\psi}; \beta\rangle - \int \int dp \, d\tilde{p} \ln [\rho_R(p)]\langle \psi, \tilde{\psi}; \beta | p, \tilde{p}\rangle\langle p, \tilde{p} | \xi, \tilde{\psi}; \beta\rangle. \tag{10}$$

We do not know how to solve generally the equation $\Gamma = 0$ with respect to the unknown state $|\psi, \tilde{\psi}; \beta\rangle$. Here, instead, we examine the thermal coherent state (TCS)[7], which is the oscillator coherent state at $T \neq 0$. This is based on the following viewpoints; (i) the information entropy is the measure of uncertainty, and (ii) at $T = 0$, the coherent state saturates the Heisenberg uncertainty ($\Delta X \cdot \Delta P = \frac{1}{2}$).

Let us consider a harmonic oscillator with a frequency ω in TFD. The thermal vacuum state is generated from the $T = 0$ Fock vacuum state $|0, \tilde{0}\rangle$ by the Bogoliubov transformation

$$|0(\beta)\rangle = \exp(-iG)|0, \tilde{0}\rangle, \quad -iG(\beta) = \theta(\beta)(a^\dagger \tilde{a}^\dagger - \tilde{a}a), \tag{11}$$

$$\cosh \theta(\beta) = [1 - \exp(-\beta\omega)]^{-1/2}, \tag{12}$$

provided that the creation and annihilation operators satisfy $[a, a^\dagger] = [\tilde{a}, \tilde{a}^\dagger] = 1$, $[a, \tilde{a}] = 0$, and so on. With this state, the TCS is defined as follows:

$$|z, \tilde{z}; \beta\rangle = \exp[za^\dagger(\beta) - z^*a(\beta) + \tilde{z}^*\tilde{a}^\dagger(\beta) - \tilde{z}\tilde{a}(\beta)]|0(\beta)\rangle, \tag{13}$$

$$a(\beta)|z, \tilde{z}; \beta\rangle = z|z, \tilde{z}; \beta\rangle, \quad \tilde{a}(\beta)|z, \tilde{z}; \beta\rangle = \tilde{z}^*|z, \tilde{z}; \beta\rangle, \tag{14}$$

where the operators at $T \neq 0$ are given by

$$a(\beta) = \exp(-iG)a\exp(iG) = a\cosh\theta(\beta) - \tilde{a}^\dagger \sinh\theta(\beta), \tag{15a}$$

$$\tilde{a}(\beta) = \exp(-iG)\tilde{a}\exp(iG) = \tilde{a}\cosh\theta(\beta) - a^\dagger \sinh\theta(\beta), \tag{15b}$$

and so on. The self-tildian condition[7] states $z = \tilde{z}$.

One can find that the TCS actually gives the desired result $\Gamma^{TCS} = 0$, and, therefore, Eq.(9) becomes

$$U[X, P : z, \tilde{z}; \beta] \rightarrow 1 + \ln \pi + \ln[\cosh 2\theta(\beta)] + o(\epsilon^2). \tag{16}$$

Thus we have the thermal information-entropic uncertainty relation[4]

$$U[X, P : \psi, \tilde{\psi}; \beta] \geq 1 + \ln \pi + \ln[\cosh 2\theta(\beta)]. \tag{17}$$

The third term in the r.h.s. determines the minimum loss of measurement information due to the thermal disturbance effects.

The Heisenberg uncertainty relation at $T \neq 0$ can be derived from Eq.(17). To see this, let us find the maximum value of the concave entropy functional S_X with fixing the variance $\langle (X - \langle X\rangle)^2\rangle = (\Delta X)^2$. ($\langle \cdot \rangle$ denotes the expectation value with respect to the normalized probability density $\rho_R(x)/\langle \psi, \tilde{\psi}; \beta | \psi, \tilde{\psi}; \beta\rangle$.) This is just the constrained variational problem characterized by the functional

$$\Phi[\psi, \tilde{\psi}; \beta] = S_X[\psi, \tilde{\psi}; \beta] - \lambda[\langle (X - \langle X\rangle)^2\rangle - (\Delta X)^2], \tag{18}$$

where λ is Lagrange's multiplier. Applying again the variational operation (8), we can find the maximum value

$$S_X{}^{max}[\psi, \tilde{\psi}; \beta] = \frac{1}{2} \ln [2\pi e(\Delta X)^2]. \tag{19}$$

Therefore we have an inequality

$$S_X[\psi, \tilde{\psi}; \beta] \leq \frac{1}{2} \ln [2\pi e(\Delta X)^2]. \tag{20}$$

Repeating a similar discussion for the momentum P, we also get

$$S_P[\psi, \tilde{\psi}; \beta] \leq \frac{1}{2} \ln \left[2\pi e (\Delta P)^2 \right]. \tag{21}$$

The combination of Eqs.(20) and (21) leads to

$$2(\Delta P)^2 \geq \exp\left(-1 - \ln \pi + 2S_P[\psi, \tilde{\psi}; \beta]\right)$$

$$\geq \exp\left(1 + \ln \pi + 2\ln\left\{\cosh[2\theta(\beta)]\right\} - 2S_X[\psi, \tilde{\psi}; \beta]\right) \tag{22}$$

$$\geq \frac{1}{2}\cosh^2[2\theta(\beta)](\Delta X)^{-2}.$$

Thus we obtain the thermal Heisenberg uncertainty relation

$$\Delta X \cdot \Delta P \geq \frac{1}{2}\cosh\left[2\theta(\beta)\right]. \tag{23}$$

We have used Eq.(17) in the second inequality of Eq.(22). This shows that the information-entropic uncertainty relation is *stronger* than Heisenberg uncertainty relation[3].

Finally, we comment on squeezing of the thermal uncertainty relation. The thermal squeezed state is defined by

$$|z, \tilde{z} : \eta, \tilde{\eta}; \beta\rangle = \exp\left[za^\dagger(\beta) - z^*a(\beta) + \tilde{z}^*\tilde{a}^\dagger(\beta) - \tilde{z}\tilde{a}(\beta)\right]$$

$$\times \exp\left[\frac{1}{2}\{\eta a^{\dagger 2}(\beta) - \eta^* a^2(\beta) + \tilde{\eta}^*\tilde{a}^{\dagger 2}(\beta) - \tilde{\eta}\tilde{a}^2(\beta)\}\right]|0(\beta)\rangle. \tag{24}$$

Straightforward calculation gives

$$S_X[z, \tilde{z} : \eta, \tilde{\eta}; \beta] = \frac{1}{2}(1 + \ln \pi + \ln\left\{\cosh\left[2\theta(\beta)\right]\right\} + \ln\left[\cosh\left(2r\right) + \sinh\left(2r\right)\cos\left(\varphi\right)\right]), \tag{25a}$$

$$S_P[z, \tilde{z} : \eta, \tilde{\eta}; \beta] = \frac{1}{2}(1 + \ln \pi + \ln\left\{\cosh\left[2\theta(\beta)\right]\right\} + \ln\left[\cosh\left(2r\right) - \sinh\left(2r\right)\cos\left(\varphi\right)\right]), \tag{25b}$$

$$U[X, P : z, \tilde{z} : \eta, \tilde{\eta}; \beta] = 1 + \ln \pi + \ln\left\{\cosh\left[2\theta(\beta)\right]\right\} + \ln\left[1 + \sinh^2(2r)\sin^2(\varphi)\right]^{\frac{1}{2}}, \tag{26}$$

$$\Delta X = \left\{\frac{1}{2}\cosh\left[2\theta(\beta)\right](\cosh\left(2r\right) + \sinh\left(2r\right)\cos\left(\varphi\right))\right\}^{\frac{1}{2}}, \tag{27a}$$

$$\Delta P = \left\{\frac{1}{2}\cosh\left[2\theta(\beta)\right](\cosh\left(2r\right) - \sinh\left(2r\right)\cos\left(\varphi\right))\right\}^{\frac{1}{2}}, \tag{27b}$$

$$\Delta X \cdot \Delta P = \frac{1}{2}\cosh\left[2\theta(\beta)\right](1 + \sinh^2(2r)\sin^2(\varphi))^{\frac{1}{2}}, \tag{28}$$

where we have employed the self-tildian condition for a squeeze factor (i.e., $\eta = \tilde{\eta}$), and $\eta \equiv r\exp(i\varphi)$. These results describe how the thermal disturbance effects in S_X or S_P (ΔX or ΔP) can be suppressed by squeezing with keeping $U = S_X + S_P$ ($\Delta X \cdot \Delta P$) its minimum value.

REFERENCES

1. D. Deutsch, *Phys. Rev. Lett.* **50** (1983), 631.
2. M. H. Partovi, *Phys. Rev. Lett.* **50** (1983), 1883.
3. I. Bialynicki-Birula & J. Mycielski, *Commun. Math. Phys.* **44** (1975), 129; see also H. Everett III, in *The Many-worlds Interpretation of Quantum Mechanics*, edited by B. S. De Witt & N. Graham (Princeton University Press, Princeton, NJ, 1973).
4. S. Abe & N. Suzuki, *Phys. Rev.* **A41** (1990), 4608.
5. Y. Takahashi & H. Umezawa, *Collect. Phenom.* **2** (1975), 55.
6. I. Ojima, *Ann. Phys. (N.Y.)* **137** (1981), 1.
7. A. Mann, M. Revzen, K. Nakamura, H. Umezawa & Y. Yamanaka, *J. Math. Phys.* **30** (1989), 2883.

THE HAMILTONIAN STRUCTURE OF DIRAC'S EQUATION IN TENSOR FORM AND ITS FERMI QUANTIZATION

Frank Reifler and Randall Morris
Government Electronic Systems Division
General Electric Company
Moorestown, NJ 08057

628201

$4/9s$

ABSTRACT

Currently there is some interest in studying the tensor forms of the Dirac equation to elucidate the possibility of the constrained tensor fields admitting Fermi quantization. In this paper, we demonstrate that the bispinor and tensor Hamiltonian systems have equivalent Fermi quantizations. Although the tensor Hamiltonian system is noncanonical, representing the tensor Poisson brackets as commutators for the Heisenberg operators directly leads to Fermi quantization without the use of bispinors.

I. CLASSICAL DERIVATION

We apply the double covering map from bispinors to their tensor equivalents. This map[1], an extension of Cartan's spinor map [Ref. 4], maps the bispinor ψ to a constrained set of SL(2,C) x U(1) gauge potentials A_α^K and a complex scalar field ρ, where $\alpha = 0, 1, 2, 3$ is a Lorentz index and $K = 0, 1, 2, 3$. Since the Lie algebra of SL(2, C) is regarded as the complexification of the Lie algebra of SU(2), the gauge potentials A_j^α for $j = 1, 2, 3$ are complex, while the U(1) gauge potential A_0^α is real. A_α^K and ρ satisfy the following constraint:

$$A_\alpha^K A_{K\beta} = -|\rho|^2 g_{\alpha\beta} \qquad (1)$$

where K is contracted using the SU(2) × U(1) Killing metric and $g_{\alpha\beta}$ is the space-time metric.

With this constraint, the Dirac bispinor Lagrangian comes from the following Yang-Mills tensor Lagrangian L, in the limit of a large Yang-Mills coupling constant g:

---

[1] The Cartan map [Refs. 1, 2] maps the bispinor ψ to a triplet of complex antisymmetric tensors $F_j^{\alpha\beta}$ (where $j = 1,2,3$) of Carmeli class G [Ref. 3]. Such $F_j^{\alpha\beta}$ can be expressed as $F_j^{\alpha\beta} = \rho(A_0^\alpha A_j^\beta - A_j^\alpha A_0^\beta + i\varepsilon_{jkm}A_k^\alpha A_m^\beta)$ where ρ is a complex scalar and A_K^α for $K = 0,1,2,3$ are SL(2,C) × U(1) gauge potentials satisfying (1). (ε_{jkm} for j, k, m = 1, 2, 3 is the permutation symbol.)

$$L = -\tfrac{1}{4} \text{Re} \, [A_K^{\alpha\beta} \, A_{\alpha\beta}^K] + (\overline{D_\alpha \rho}) \, (D^\alpha \rho) - \frac{g^2}{2} \, |\rho + 2m|^4 \qquad (2)$$

where m denotes mass. D_α denotes the Yang-Mills covariant derivative with connection coefficients A_α^K, and $A_{\alpha\beta}^K$ is the Yang-Mills curvature tensor associated with the gauge potentials A_α^K. The indices are contracted using the Killing metric as well as the space-time metric. All bispinor observables can be derived from L using Yang-Mills formulas. Although previous authors [Refs. 5, 2] derived the tensor form of the Dirac Lagrangian, they did not put it in the gauge symmetric Yang-Mills form (2).

The Dirac equation can be derived from the Lagrangian L by ascribing to the Yang-Mills field A_α^K a large self-coupling constant g. To be consistent with observation, the fields A_α^K and ρ must couple more weakly (by the factor 1/g) with other fields. In particular, Einstein's equation becomes $G_{\alpha\beta} = kT_{\alpha\beta}$ where $G_{\alpha\beta}$ is the Einstein tensor, k is the gravitation constant, and $T_{\alpha\beta}$ is the energy-momentum tensor derived from the Lagrangian L. In the limit of large self-coupling g (neglecting terms in $T_{\alpha\beta}$ not containing g) we have $T_{\alpha\beta} = g \, T'_{\alpha\beta}$ where $T'_{\alpha\beta}$ is exactly the usual Dirac energy-momentum tensor [Ref. 5]. Hence $k' = kg$ is the observed gravitational constant, not k. Note also that in the Lagrangian L, the observed mass is $m' = mg$, not m. Then, as g tends to infinity, the Lagrangian kL is independent of g. In this limit, which we henceforth assume, we have:

$$\underset{g \to \infty}{\text{Lim}} \; k \, L = k' \, L' \qquad (3)$$

where L' is exactly equal to Dirac's bispinor Lagrangian [Ref. 5]. Thus, as previously stated, Dirac's bispinor Lagrangian is a limiting case of the Yang-Mills Lagrangian (2), in which the self-coupling constant g tends to infinity.

II. FERMI QUANTIZATION

We quantize A_α^K and ρ by defining the classical Hamiltonian to be: (Let $S \subset R^3$ be a large cube.)

PRECEDING PAGE BLANK NOT FILMED

$$H = \int_S T^{oo} \, d\mathbf{x} \qquad (4)$$

where $T^{\alpha\beta}$ is the energy-momentum tensor derived from the fermion tensor Lagrangian (3). We make a classical change of variables that simplifies H. The resulting Hamiltonian equations are then formulated as Heisenberg operator equations.

Because the SL(2, C) × U(1) gauge group is not compact, H is not bounded from below. This has the consequence that any quantization of the fields A_α^K and ρ must obey the exclusion principle; otherwise fermions descend forever to lower energy states.

By the Cartan map [Refs. 1, 5] the energy-momentum tensor has an expansion of the form:

$$T^{\alpha\beta}(\mathbf{x},t) = \sum_p \sum_q T_{pq}^{\alpha\beta}(\mathbf{x}) \, a_{pq}(t) \qquad (5)$$

where the sum is over all pairs of fermion modes p and q, and where $T_{pq}^{\alpha\beta}(\mathbf{x})$ are fixed functions of $\mathbf{x} \, \varepsilon \, S$, and $a_{pq}(t)$ are complex functions of time t satisfying $a_{pq} = \overline{a}_{qp}$. The bimodal expansion (5) is irreducible because it cannot be expressed in tensor terms as a sum over products of single modes, as is the case with bosons. The Hamiltonian (4) can be written in terms of the amplitudes $a_{pq}(t)$ as follows:

$$H = \sum_p \omega_p \, a_{pp} \qquad (6)$$

where ω_p is the frequency of the mode p. Note that for simplicity, the amplitudes $a_{pq}(t)$ are defined to be consistent with the hole theory.

The classical Hamiltonian equations (which are equivalent to the constrained Euler-Lagrange equations for A_α^K and ρ) are given by:

$$\frac{da_{pq}}{dt} = \{a_{pq}, H\} \qquad (7)$$

where the Poisson brackets { , } are defined for the classical amplitudes $a_{pq}(t)$ as follows:

$$\{a_{pq}, a_{p'q'}\} = -i \, (a_{pq'} \, \delta_{p'q} - a_{p'q} \, \delta_{pq'}) \qquad (8)$$

where δ_{pq} equals one if p = q and zero otherwise.

Formulas (6), (7), and (8) are noncanonical tensor Hamiltonian equations which cannot be formulated as canonical equations in tensor terms. Nevertheless, they are easily quantized by replacing the classical amplitudes $a_{pq}(t)$ with Heisenberg operators, denoted as $\hat{a}_{pq}(t)$, and the Poisson brackets (8) with (equal time)

commutators [,] as follows:

$$[\hat{a}_{pq}, \hat{a}_{p'q'}] = \hat{a}_{pq'} \, \delta_{p'q} - \hat{a}_{p'q} \, \delta_{pq'} \qquad (9)$$

The Heisenberg equations become:

$$\frac{d\hat{a}_{pq}}{dt} = -i \, [\hat{a}_{pq}, \hat{H}] \qquad (10)$$

where $\hat{H}$ is the operator version of the Hamiltonian (6).

To further simplify these equations, we attempt to factor $\hat{a}_{pq}(t)$ into a product of operators:

$$\hat{a}_{pq}(t) = \hat{c}_p^\dagger(t) \, \hat{c}_q(t) \qquad (11)$$

where the dagger (†) signifies adjoint. Since they do not occur explicitly in the Hamiltonian $\hat{H}$, the new operators $\hat{c}_p(t)$ a priori could satisfy *any* relations consistent with the commutation relations (9). We exploit this arbitrariness in order to satisfy the exclusion principle, previously discussed. At time t we define:

$$\hat{c}_p^\dagger \, \hat{c}_q + \hat{c}_q \hat{c}_p^\dagger = \delta_{pq} \qquad (12)$$

All other equal time anti-commutators of $\hat{c}_p(t)$ are defined to be zero. Formulas (11) and (12) are consistent with the commutation relations (9) as required.

It is clear that equations (9), (10), (11), and (12), while derived from the tensor Hamiltonian equations, are equivalent to Fermi quantization via bispinors. Thus, the tensor Lagrangian (3) leads to Fermi quantization without the use of bispinors.

Again, without the use of bispinors, we may extend the tensor Lagrangian (3) to include the electromagnetic field. Quantization is straight forward due to the fact that the interaction term is a function of the fermion amplitudes $a_{pq}(t)$, as well as boson amplitudes $b_n(t)$.

III. QUANTUM GRAVITY

Spinor structure can be defined on a noncompact space-time manifold M by specifying, at each point $x \varepsilon M$, a set of Pauli spin-half matrices $\sigma_{AB'}^\alpha(x)$ satisfying [Ref. 3]:

$$\sigma_{AB'}^\alpha \sigma^{\beta AB'} = g^{\alpha\beta} \qquad (13)$$

Formula (13) has a topological as well as a metric consequence. The topological consequence of (13) is that M must be parallelizable [Ref. 6]. The metric consequence is that $g_{\alpha\beta}$ is constrained as in formula (1). Since, for noncompact parallelizable space-times for-

mulas (1) and (13) are equivalent, spinor structure is nothing but an indirect way of constraining the metric $g_{\alpha\beta}$ on such space-times. However, the tensor fields A_α^K and ρ satisfying the constraint (1) are more general than (13), since they can be defined on general space-times.

Formula (13) presents a dilemma [Ref. 7] for quantizing both gravity and the Dirac field, since the definition of the Pauli matrices $\sigma_{AB'}^\alpha$ depends on the gravitational field $g_{\alpha\beta}$. The problem is resolved by identifying the degrees of freedom in the constraint (1) as follows.

Consider a *fixed* metric $\tilde{g}_{\alpha\beta}$ on M and define Pauli matrices $\tilde{\sigma}_{AB'}^\alpha$ with respect to $\tilde{g}_{\alpha\beta}$. The metric $g_{\alpha\beta}$ on M is expressed by:

$$g_{\alpha\beta} = \tilde{g}_{\alpha\beta} + h_{\alpha\beta} \tag{14}$$

We also express the gauge potentials A_α^K by:

$$A_\alpha^K = f_\alpha^\beta \, \tilde{A}_\beta^K \tag{15}$$

where $\tilde{A}_\alpha^K$ satisfies the constraint (1) with respect to the fixed metric $\tilde{g}_{\alpha\beta}$. The dynamical fields are then $\tilde{A}_\alpha^K$, ρ, and $h_{\alpha\beta}$ provided that the matrix $f = f_\alpha^\beta$ can be uniquely solved as a function of $h_{\alpha\beta}$. Since $\tilde{A}_\alpha^K$ and ρ have bispinor coordinates with respect to the *fixed* spinor structure on M, the fields $\tilde{A}_\alpha^K$, ρ, and $h_{\alpha\beta}$ can be quantized as in Section II.

It remains to solve for the matrix f in formula (15) using the constraint (1). Since

$$\tilde{A}_\alpha^K \tilde{A}_{K\beta} = -|\rho|^2 \, \tilde{g}_{\alpha\beta} \tag{16}$$

formulas (14) and (15) give:

$$\tilde{g}_{\gamma\sigma} \, f_\alpha^\gamma \, f_\beta^\sigma = \tilde{g}_{\alpha\beta} + h_{\alpha\beta} \tag{17}$$

The solution of (17) is given by:

$$f = \sum_{n=0}^\infty C_n^{1/2} \, h^n \tag{18}$$

where C_n^m denote the binomial coefficients, and the matrix h is defined by:

$$h = h_\alpha^\beta = \tilde{g}^{\beta\gamma} \, h_{\gamma\alpha} \tag{19}$$

where $\tilde{g}^{\alpha\beta}$ is the inverse matrix of $\tilde{g}_{\alpha\beta}$.

For the power series (18) to converge, the eigenvalues of h must lie within the unit circle. This restricts the validity of quantum gravity to small fluctuations of $g_{\alpha\beta}$

about the fixed metric $\tilde{g}_{\alpha\beta}$.

IV. CONCLUSIONS

In this paper we have adhered to the program of first defining all fields, Bose and Fermi, as classical tensor fields, and then quantizing them using Hamilton equations and Poisson brackets. From this vantage point, the Dirac equation becomes a classical tensor equation on the same level as the electromagnetic and gravitation tensor equations. Fermions, photons, and gravitons are obtained by quantizing the degrees of freedom allowed by the tensor constraint (1). We have shown in Section III that the constraint (1) implies that we cannot, in general, separate fermion and graviton degrees of freedom, except when the power series (18) converges.

We also found that the fermion degrees of freedom require the use of noncanonical Hamilton equations (6), (7), and (8). Since the free Dirac tensor equation is completely *integrable*, we have shown that current usage of only canonical Hamilton equations is too restrictive for quantizing integrable tensor fields.

REFERENCES

1. Reifler, F. and R. Morris, 1986, "A Gauge Symmetric Approach to Fierz Identities," *J. Math. Phys.*, 27(11), pp. 2803-2806.

2. Zhelnorovich, V. A., 1990, "Complex Vector Triplets in the Spinor Theory in Minkowski Space," *Proc. Acad. of Sciences of USSR*, 311 (3), pp. 590-593.

3. Carmeli, M., Kh. Huleihil, and E. Leibowitz, 1989, "Gauge Fields," *World Scientific*, Singapore, pp. 21 and 40.

4. Cartan, E., 1981, *The Theory of Spinors*, Dover, New York, p. 41.

5. Takahashi, Y., 1983, "The Fierz Identities—A Passage Between Spinors and Tensors," *J. Math. Phys.*, 24(7), pp. 1783-1790.

6. Geroch, R., 1968, "Spinor Structure of Space-times in General Relativity I," *J. Math. Phys.*, 9 (11), pp. 1739-1744.

7. Ashtekar, A. and R. Geroch, 1974, "Quantum Theory of Gravitation," *Rep. Prog. Phys.*, 37, pp. 1211-1256.

REPORT DOCUMENTATION PAGE		Form Approved OMB No. 0704-0188

Public reporting burden for this collection of information is estimated to average 1 hour per response, including the time for reviewing instructions, searching existing data sources, gathering and maintaining the data needed, and completing and reviewing the collection of information. Send comments regarding this burden estimate or any other aspect of this collection of information, including suggestions for reducing this burden, to Washington Headquarters Services, Directorate for Information Operations and Reports, 1215 Jefferson Davis Highway, Suite 1204, Arlington, VA 22202-4302, and to the Office of Management and Budget, Paperwork Reduction Project (0704-0188), Washington, DC 20503.

1. AGENCY USE ONLY *(Leave blank)*	2. REPORT DATE February 1992	3. REPORT TYPE AND DATES COVERED Conference Publication

4. TITLE AND SUBTITLE Workshop on Squeezed States and Uncertainty Relations	5. FUNDING NUMBERS C·NAS5-30376

6. AUTHOR(S)
D. Han, Y. S. Kim, and W. W. Zachary, Editors

7. PERFORMING ORGANIZATION NAME(S) AND ADDRESS(ES) NASA Goddard Space Flight Center Greenbelt, Maryland 20771	8. PERFORMING ORGANIZATION REPORT NUMBER 92B00024

9. SPONSORING/MONITORING AGENCY NAME(S) AND ADDRESS(ES) National Aeronautics and Space Administration Washington, DC 20546-0001	10. SPONSORING/MONITORING AGENCY REPORT NUMBER NASA CP-3135 Code 936

11. SUPPLEMENTARY NOTES
D. Han, NASA-GSFC, Greenbelt, Maryland, 20771
Y. S. Kim, Dept. of Physics, University of Maryland, College Park, Maryland 20742
W. W. Zachary, COMSERC, Howard University, Washington, D.C. 20059

12a. DISTRIBUTION/AVAILABILITY STATEMENT Unclassified–Unlimited Subject Category 74	12b. DISTRIBUTION CODE

13. ABSTRACT *(Maximum 200 words)*

This conference publication contains the proceedings of a workshop on squeezed states and uncertainty relations held at the University of Maryland, College Park, Maryland, on March 28–30, 1991.

Squeezed states were predicted theoretically in the 1970s. They became a physical reality during the period 1985–1988. Efforts are being made to produce more efficient squeezed-state lasers. More refined theoretical tools are being developed for this new physical phenomenon. One of the pressing questions during the 1990s will be: What should we do with squeezed states? This is the main question we wanted to address in this workshop.

There are many who say that the potential for industrial applications is enormous, as the history of the conventional laser suggests. All those who worked so hard to produce squeezed states of light are continuing their efforts to construct more efficient squeezed-state lasers. Quite naturally, they are looking for new experiments using these lasers. The physical basis of squeezed states is the uncertainty relation in Fock space, which is also the basis for the creation and annihilation of particles in quantum field theory. Indeed, squeezed states provide a unique opportunity for field theoreticians to develop a measurement theory for quantum field theory.

14. SUBJECT TERMS Squeezed States, Quantum Optics, Uncertainty Relations, Poincare Group	15. NUMBER OF PAGES 400
	16. PRICE CODE A17

17. SECURITY CLASSIFICATION OF REPORT Unclassified	18. SECURITY CLASSIFICATION OF THIS PAGE Unclassified	19. SECURITY CLASSIFICATION OF ABSTRACT Unclassified	20. LIMITATION OF ABSTRACT UL

NSN 7540-01-280-5500

Standard Form 298(Rev. 2-89)
Prescribed by ANSI Std. Z39-18
298-102

NASA-Langley, 1992